Physics of Nearby Galaxies

Nature or Nurture ?

XXVIIth Rencontre de Moriond
XIIth Moriond Astrophysics Meetings
Les Arcs, Savoie, France - March 15-22-1992

Physics of Nearby Galaxies
Nature of Nurture ?
Series : Moriond Astrophysics Meetings

ISBN 2-86332-124-2

EDITIONS FRONTIERES
B. P. 33
91192 Gif-sur-Yvette Cedex - France

Printed in Singapore by Fong & Sons Printers Pte Ltd

Proceedings of the XXVIIth RENCONTRE DE MORIOND
XIIth Moriond Astrophysics Meetings
Les Arcs, Savoie, France March 15-22, 1992

Physics of Nearby Galaxies
Nature or Nurture ?

edited by

Trinh Xuan Thuan
Chantal Balkowski
Jean Tran Thanh Van

EDITIONS
FRONTIERES

The Astrophysics Session of the XXVIIth Rencontre de Moriond

Physics of Nearby Galaxies
Nature or Nurture ?

was organized by :

Trinh Xuan Thuan	*(Charlottesville)*
Balkowski C.	*(Meudon)*
Tran Thanh Van J.	*(Orsay)*

with the collaboration :

Athanassoula E.	*(Marseille)*
Audouze J.	*(Paris)*
Cesarsky C.	*(Saclay)*
de Vaucouleurs G.	*(Austin)*
Dennefeld M.	*(Paris)*
Larson R.	*(New-Haven)*
Lequeux J.	*(Paris)*
Léna P.	*(Meudon)*
Renzini A.	*(Bologne)*
Rowan-Robinson M.	*(London)*
Sancisi R.	*(Groningen)*
Trümper J.	*(Garching)*
van den Bergh S.	*(Victoria)*

CONTENTS

FOREWORD

There is relatively less empty space between the galaxies in a rich cluster than between the stars of a globular cluster: the ratio of the average separation between objects to their size in a rich cluster of galaxies is about 5 while it is about 100 000 in a globular cluster. Thus it is evident (although that realization only really came in the last 2 decades) that the properties of a galaxy cannot be properly discussed without taking into account the interaction with its environment.

A galaxy cannot be thought of any longer as a separate entity whose properties were "genetically" determined at birth, which evolves afterwards in splendid isolation. There can be no doubt now that a galaxy is the product of both nature and nurture. It is the task of the astrophysicist who wishes to understand the evolution and formation of galaxies to disentangle the galaxian "genetic" properties from those which were fashioned by environmental interactions.

With the many new exciting observational results on galaxies from such instruments as the ESO New Technology telescope and of such space telescopes as Hubble and Rosat, and the ever more sophisticated computer simulations of galaxy formation and evolution, we wanted to gather together leading researchers in a beautiful place to think about the respective roles of nature vs nurture in shaping galaxian properties.

One of the ways of accomplishing this purpose is to compare the properties of distant galaxies, seen in their youth, whose properties are mainly due to nature, to the properties of nearby galaxies, seen in their maturity whose properties have been fashioned by both nature and nurture. As there have been, of late, many conferences on the subject of distant galaxies, we wished to concentrate the workshop exclusively on the properties of nearby galaxies. The latter offer also the advantages of large fluxes and high spatial resolution, permitting detailed studies which are not possible for distant galaxies.

With these considerations in mind, we have organized a 6-day workshop in the spectacular setting of Les Arcs, in the French Alps, barely 2 months after the end of the winter Olympic Games. The workshop was attended by 50 participants, from 12 countries, with a mixture of observational astronomers, theorists and instrument builders.

These proceedings contain in camera-ready form the papers that were presented during the meeting. They are organized as follows : Part I discusses the art of classifying galaxies. Part II deals with multi-wavelength observations of galaxies along the Hubble sequence. Part III is concerned with the extension of the Hubble sequence to dwarf and low surface brightness galaxies, active galactic nuclei and starbursts. Parts IV and V discuss the environmental influences on galaxian properties. Part VI discusses the impact of future instruments on the observations of nearby galaxies and Part VII is concerned with theories

the Hubble sequence.

The workshop also included a very interesting joint scientific session with the particle physicists attending the concurrent workshop on "Electroweak interactions and unified theories", during which Ken Freeman reviewed the Dark Matter problem in galaxies and its search.

The success of this most productive, yet friendly and relaxed Rencontre de Moriond is due to the flawless local organisation of J. Tran Thanh Van and his team. We wish to thank particularly Valérie Demailly, Jacqueline Plancy and Joëlle Raguideau.

We gratefully acknowledge the financial support of the Centre National de la Recherche Scientifique, the Commissariat à l'Energie Atomique, the Observatoire de Paris and the Ministère de la Recherche et de l'Espace.

TRINH XUAN THUAN CHANTAL BALKOWSKI

AVANT-PROPOS

Il y a relativement moins d'espace entre les galaxies d'un amas qu'entre les étoiles d'un amas globulaire : le rapport de la séparation moyenne entre objets à leur taille est environ 5 dans un amas riche de galaxies alors qu'il est de l'ordre de 100 000 dans un amas stellaire globulaire. Il est donc bien évident (bien que l'importance de ce point n'ait été prise en compte que dans les deux dernières décennies) que les propriétés d'une galaxie ne peuvent être discutées correctement qu'en prenant en considération son interaction avec l'environnement.

Une galaxie ne peut plus être considérée comme une entité en elle-même, dont les propriétés sont déterminées une fois pour toutes par des processus "génétiques" au moment de sa formation et qui évolue ensuite dans un splendide isolement. Aujourd'hui, il ne subsiste plus de doute qu'une galaxie est le produit à la fois de l'inné et de l'acquis. C'est à l'astrophysicien qui désire comprendre l'origine et la formation des galaxies, de séparer le "génétique" de "l'environnement".

Stimulés par la moisson extraordinaire d'observations de galaxies provenant d'instruments tel que le Télescope à Nouvelle Technologie de l'ESO, ou de télescopes spatiaux comme Hubble et Rosat, et par les simulations numériques de plus en plus sophistiquées sur la formation et l'évolution des galaxies, nous avons voulu rassembler dans un cadre agréable les experts du sujet pour tenter de définir la part relative de l'inné et de l'acquis dans les galaxies.

Une approche possible du problème consiste à comparer les propriétés "innées" des galaxies lointaines vues dans leur jeunesse, à celles "acquises" des galaxies proches observées dans leur maturité. Récemment de nombreux colloques sur les galaxies lointaines ont eu lieu. C'est pourquoi nous avons voulu consacrer cette Rencontre de Moriond aux galaxies proches. Elles sont en effet plus brillantes, offrent plus de résolution spatiale et permettent des études détaillées impossibles à réaliser sur les galaxies lointaines.

A la suite de ces réflexions, nous avons organisé un colloque de 6 jours dans le cadre grandiose des Arcs, dans les Alpes Françaises, deux mois à peine après les Jeux Olympiques d'hiver. Le colloque a réuni 50 participants venant de 12 pays, mêlant observateurs, théoriciens et instrumentalistes.

Le présent volume contient les communications présentées lors du colloque. Elles sont classées dans l'ordre suivant : le chapitre I a pour sujet l'art de classifier les galaxies ; le chapitre II rassemble les observations des galaxies de la séquence de Hubble dans les différents domaines du spectre électromagnétique ; le chapitre III généralise la séquence de Hubble aux galaxies naines, à celles de faible brillance de surface, aux galaxies avec un noyau actif et à celles avec des flambées d'étoiles ; les chapitres IV et V traitent des effets

d'environnement sur les galaxies ; le chapitre VI discute de l'impact qu'auront les instruments futurs sur l'observation des galaxies proches ; enfin, le chapitre VII présente les théories sur l'origine de la séquence de Hubble.

Une session conjointe a également eu lieu avec des physiciens des particules qui assistaient en même temps à leur propre colloque sur les interactions électrofaibles et les théories d'unification. Au cours de cette session, Ken Freeman a présenté une revue sur le problème de la Masse Noire dans les galaxies.

Le succès et l'animation de cette Rencontre de Moriond, l'ambiance amicale et détendue, doivent beaucoup à la perfection de l'organisation sur place, menée par J. Tran Thanh Van et son équipe. Nous tenons à remercier tout particulièrement Valérie Demailly, Jacqueline Plancy et Joëlle Raguideau.

Enfin, nos remerciements vont au Centre National de la Recherche Scientifique, au Commissariat à l'Energie Atomique, à l'Observatoire de Paris et au Ministère de la Recherche et de l'Espace pour leur aide financière.

TRINH XUAN THUAN CHANTAL BALKOWSKI

I - MORPHOLOGICAL CLASSIFICATION

2

THE MORPHOLOGICAL CLASSIFICATION OF GALAXIES

Ronald Buta
University of Alabama
Box 870324, Tuscaloosa, AL 35487

ABSTRACT
Much of what is known about galaxies began with a simple classification of their forms as seen on direct blue-light plates. This classification continues to be useful at a time when galaxies have never been better understood. The reason for this is that morphology contains information on the dynamics and evolution of galaxies in spite of the fact that the features dominating the appearance may include only a small fraction of the total mass. In this article I briefly review the important classification systems in use today and highlight classification as an art having significant discriminating ability and at the same time serious limitations. I also summarize recent developments in this field from a morphologist's point of view.

1. INTRODUCTION

Galaxy classification is one of those enjoyable aspects of galaxy research that few of us consider ourselves specialists in. Most of us obtain the morphological information we require from the large catalogues or lists provided by a few respected "morphologists", and

rarely attempt to improve on those types by re-inspecting the galaxies ourselves or by carrying out an imaging survey. Though we may on occasion question a catalogue type in individual cases, especially if better image material becomes available, published morphological types provide an important starting point for most extragalactic research. This is as true today as it was 66 years ago when Hubble published his famous classification system.

There can be little doubt now that *nature* and *nurture* play a role in determining the morphology of galaxies. The main questions are to what degree have each of these processes influenced present-day morphology, and how do we recognize these influences. Morphology alone cannot answer these questions, so a confrontation between theory and observation is essential. It is thus fitting to begin this conference with a review of the morphological classification of galaxies, since this provides the background for the nature vs. nurture controversy. Due to space limitations, the discussions are necessarily brief.

2. REVIEW OF CLASSIFICATION SYSTEMS

Though the nomenclature was very simplistic, the morphological classification of galaxies can be traced back to the time of the Herschels (1781–1847), whose telescopes were large enough to allow visual recognition of distinct differences in the large-scale characteristics of the so-called "white nebulae". Different degrees of central concentration, apparent flattening, and mottling were clearly distinguishable. More complex structure was seen in a few of the brighter cases, but it was Lord Rosse who, in 1845, added the attribute "spiral" to some members of the Herschels' white nebulae. This is when morphology began to get interesting.

The advent of photography in astronomy at the end of the 19th century firmly established the reality of the spiral morphology. Photography also provided a greater appreciation of the complexity and range of galaxy morphology that must have proved almost daunting to anyone wishing to understand how the different forms are related to one another, if at all. As the number of good quality images grew in the first part of the 20th century, different classification schemes were naturally attempted. An excellent review of the steps which led to the recognition of the main types is provided by Sandage[45], who gives all of the early references as well as references to a number of classification systems which fell into early dis-use. Examples of most of the main types were already known by 1920.

The classification systems in use today are all in some way related to that described

in Hubble's[34] paper. This system, which originally included only ellipticals, spirals, and irregulars, focused on a few basic characteristics and ordered galaxies in a manner that was eventually found to correlate with some basic measured parameters. The sequence was best defined for spirals since three classification criteria were available: the relative strength of the bulge, the openness of the arms, and the degree of resolution of the arms. Van den Bergh[62] commented that the firm establishment and later addition of the S0 class by Hubble[35] destroyed the "simple beauty" of the original system. It is interesting also that in spite of a great deal of recent research, there have been no firm correlations found between ellipticity and other properties of E galaxies, leaving the value of this criterion as part of the "sequence" in doubt (e.g., Tremaine[59]). The later division of irregulars into two subclasses, "Irr I" and "Irr II", was proposed by Holmberg[33].

Hubble's final revision to his system is illustrated and described by Sandage[44]. No other classification system has ever been so beautifully illustrated. This was complemented recently by the *Atlas of Galaxies Useful for the Cosmological Distance Scale* by Sandage and Bedke[46], and by the published "mini-atlases" of Dressler and Sandage[27], Sandage and Brucato[48], Sandage, Binggeli, and Tammann[50] and the *Revised Shapley-Ames Catalogue*[49] (=RSA).

De Vaucouleurs[18),19),20] presented a personal revision of Hubble's system that provides a better description of what a galaxy looks like without being too complicated. The system uses the concept of a classification volume, rather than a simple multi-pronged "tuning fork", and is recognized mainly for its addition of stages *later* than Sc, called Sd and Sm, and for the notation (SA, SAB, and SB) used to denote continuity of the bar characteristic. These revisions to Hubble's system have been largely accepted by most astronomers. The Sm class is particularly important because it recognized the Magellanic Clouds not simply as "irregulars" but as very late spirals with no spheroidal component[25),43].

The classification system proposed by Morgan[40] (see also Morgan, Kayser, and White[41]) was designed as a means of tying galaxy morphology to the then current ideas of stellar populations. The degree of central concentration was used to define a one-dimensional spectral classification system (population group) based on form alone. Secondary dimensions, defined by the "form family" and the tilt index, tied the system in an indirect way to Hubble's system. Morgan also introduced some types not recognized fully by Hubble. The best known of these was the cD class, although its discovery is claimed by Vorontsov-Velyaminov[67]. The Morgan system has recently been used in a

study of the spiral-to-elliptical galaxy ratio in two nearby galaxy clusters[70]. However, it has not been used in any recent major catalogues.

One limitation of Hubble's system was recognized by van den Bergh[60),61)], who demonstrated the existence of luminosity effects on the contrast and development of spiral arms. He assigned not only modified Hubble types to galaxies, but also luminosity classes symbolized in a manner similar to stellar luminosity classes. The luminosity classes were originally applied to Sb, Sc, and Irr galaxies, but the latter objects, lacking spiral structure, had to have their luminosity classes estimated from surface brightness alone. Van den Bergh's modified Hubble system was later drastically changed; he disagreed with Hubble's placement of S0's in the "transition region" between ellipticals and spirals for reasons related to flattening and bulge-to-disk ratio. He instead proposed placing S0's in a sequence parallel to spirals[62] (RDDO system). The two sequences use bulge to disk ratio as a classification criterion, and he identified transition cases between S0's and normal spirals which appeared to be spirals with little star formation in the arms. These were given the term "anemics", and were assumed to be gas-poor.

Because the RDDO system builds around the expected evolutionary scenario in clusters that stripping can deplete spirals of the gas needed for ongoing star formation, nurture is explicit: galaxies which may once have been spirals evolved to a completely different type called S0's owing to an interaction with the cluster environment. S0's may not be born, but are made by this interaction. This is a controversy that has not yet been resolved. A primary problem, noted by Burstein[9)], is that there are as yet no known examples of S0c galaxies, i.e., galaxies of the S0 type which have a bulge-to-disk ratio as small as those seen in many Sc galaxies. Another problem, noted by van den Bergh[64)], is that the S0 class is a mixed bag of possibly unrelated types of objects.

Vorontsov-Velyaminov[67)], referring to his work on the Morphological Catalogue of Galaxies (MCG) in the 1960's, has held steadfastly to the view that galaxy morphology is too complicated to be represented adequately by any of the available Hubble or Hubble-like systems. He developed in the MCG a purely descriptive classification with symbols geared to almost every detail of morphology. This makes for a complex symbolism but is still useful because it allows the isolation of specific categories of objects that the broad Hubble classes do not adequately represent.

3. CLASSIFICATION AS AN ART

It is one thing to know the various classification systems, but quite another to apply these to real galaxies. As an art, galaxy classification has many stringent requirements as well as limitations. For instance, a system is usually defined by a set of standards or prototypes as they appear on a selected type of image material. Thus, reproducibility and consistency will depend on different observers using similar material to classify other objects. For Hubble's system, this image material included prime focus and other *blue-light* plates taken with 1.5-5m class telescopes. In general, telescope focal length and ratio, image resolution, and the depth of exposure, in addition to the characteristics of a given galaxy itself, all play a role in determining what information is available for classification.

However, there are important problems, such as high inclination, and the fact that large-scale plates or digital images, ideal for classification, are available for less than 15% of the ≈25,000 galaxies having a standard isophotal diameter $\geq 1'$. This means that *for most galaxies, morphology is judged from small-scale sky survey plates, prints, and films.* The pitfall of the sky survey images, in addition to the much smaller image scale than is typical of Cass or prime focus large reflector images, is frequent overexposure, making it difficult to see the crucial inner regions where high surface brightness bars, rings, lenses, etc., may be present. Distinguishing E and S0 galaxies on such image material, for example, can be difficult[48]. On the other hand, the pitfall of large reflector plates in the past has often been underexposure, causing very low surface brightness disks, rings, arms, etc. to be completely missed. (In fields with significant galactic extinction, these same details can still be lost even on deep SRC-J plates.) Thus, *it is important when using published morphological types to know where the types came from and their limitations.*

The standard Hubble classification system can also simply be difficult to apply to certain kinds of galaxies. Some of the worst offenders can be early-type ringed, barred galaxies, where the bulge can be relatively small in spite of the fact that a spiral pattern is tightly wrapped and not highly resolved[44),15]. Particularly interesting and important in my view also are what Vorontsov-Velyaminov[67] calls "double or triple stage spirals", which refers to those spirals which exhibit distinct sets of spiral structure on different scales. The use of one pattern could lead to a different type from the other. A good example is NGC 3504 in the Hubble atlas, where a well-resolved oval and bar dust lanes lead to a classification of Sb in the RSA, but a fainter, larger, and smooth outer pseudoring with almost zero pitch angle would clearly warrant a type of Sa. De Vaucouleurs[20]

compromises on a type of Sab for this one. The classification of galaxies with hierarchical spiral structure is an interesting problem hardly discussed in the literature, but this kind of structure plays a selective role in the application of Hubble's system[44].

Perhaps the most serious problem with galaxy classification is that it is still largely a subjective visual exercise. The human eye is very good at pattern recognition, and is capable of integrating the information in an image quite quickly. However, a morphological type is not a measured quantity even if it is coded on a numerical scale. De Vaucouleurs[23] emphasized that in spite of the subjective nature of classification, such classification is a time-honored tradition in astronomy that has been largely successful. This has been recently demonstrated very definitively by the extensive analysis of published type (T) and luminosity (L) classifications that provided the coded types given in the *Third Reference Catalogue of Bright Galaxies*[26] (=RC3). From this analysis, which is based mainly on sky survey (PSS or SRC-J) classifications, the average uncertainty in both of these parameters is $\approx$0.9 step, where one step represents a difference such as Sb to Sbc, Sa to Sab, etc. Classifications based on large-scale reflector plates, or for large face-on galaxies based on sky survey images, are generally considerably better than this.

4. TYPE CORRELATIONS

Several studies have quantified two aspects of the spiral sequence that determine the Hubble classification: the bulge to disk ratio and the pitch angle of the arms. Kennicutt[37] showed that objectively measured pitch angles correlate on average with RSA type, but with a large scatter; a rough correlation of pitch angle with Morgan concentration class was also found. Simien and de Vaucouleurs[57] used bulge/disk decompositions to illustrate how the bulge-to-total luminosity ratio varies with Hubble type. A smooth variation with type was found, but most importantly, this study found no support for van den Bergh's belief that S0's form a sequence parallel to spirals. The bulge contribution for S0's is generally intermediate between pure spheroidal systems and spirals, thus supporting Hubble's placement of S0's as transitions between E's and S0's.

The above correlations are expected because they underlie the classification system. But what really makes the Hubble system important are the correlations with other parameters that were not part of the system. It has been known for a long time that Hubble types, especially de Vaucouleurs revised Hubble types, also correlate very closely with objective measures of color, surface brightness, and HI content[22),11]. Late-type galaxies

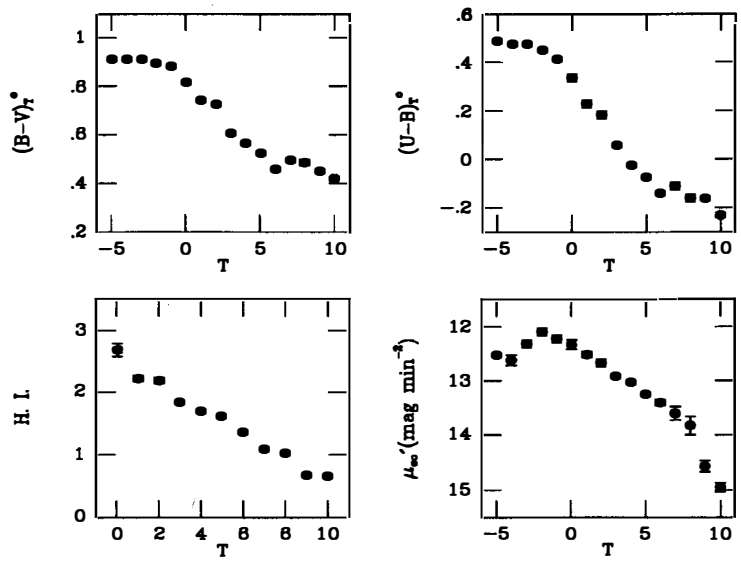

Figure 1: Dependence of several photometric parameters on the coded numerical stage in de Vaucouleurs system. The top two panels illustrate the correlations for colors, while the lower panels show the correlations for hydrogen index H. I. and mean effective surface brightness μ'_{eo}, all as defined and corrected in the introduction to RC3.

are bluer, have more hydrogen, and generally lower surface brightnesses than early-type galaxies. Intermediate types have intermediate properties between these extremes. These correlations are illustrated with new RC3 data and revised galactic extinction and tilt corrections in Figure 1. They are remarkable, at least for spirals, S0's, and irregulars, and they suggest that the revised Hubble sequence has physical significance[21]. Possible scenarios for the origin of the Hubble sequence are discussed by Larson in this volume.

5. RECENT DEVELOPMENTS IN CLASSIFICATION AND MORPHOLOGY

Recent developments in this field have been concerned with (1) new major catalogues of standard Hubble types; (2) slight modifications to existing classification systems; (3) the identification of new types of galaxies and improved understanding of older types; (4) identification of the major orbit resonances in grand design spirals and ringed galaxies; (5) widespread application of electronic detectors with high quantum efficiency to large numbers of galaxies of many types, and over a wide range of passbands; and (6) computer classification.

Major catalogues with morphological data continue to be produced. These are

summarized in reviews by Corwin[17] and Buta[13]. The RC3 combined several of these catalogues and other smaller lists into the largest database of Hubble morphological type information ever compiled. The 17,700 types given in this catalogue are based solely on photographic sources and are on the classification system of de Vaucouleurs[19]. Other major catalogues include the Virgo Cluster Catalogue[5] and the RSA; these give types on Hubble's revised system[44], with additions and revisions, some described below.

No major new classification systems have been proposed since 1976, though modifications to existing systems have been suggested. For example, Kormendy[38] suggested that *lenses* be distinguished from rings using their own notation within the framework of the de Vaucouleurs revised Hubble system. He suggested denoting inner lenses by (l) and outer lenses by (L) in the same classification positions where inner and outer rings would be specified. Kormendy also suggested a different approach to morphology, the idea of characterizing galaxies in terms of a small number of "distinct components" (bars, rings, etc.) rather than a large number of morphological "cells". The objective of the approach is to make deductions concerning secular evolution from the ways these components might be expected to interact (see Table 1 of Kormendy[39]). Kormendy suggested that such an approach leads to the possible conclusion that bars are not permanent features of galaxies but may evolve under certain circumstances to a lens. Whether this evolution actually takes place or not is still uncertain.

Another revision to the classification systems is the recognition of "dusty E's." The misclassification of these objects as S0's is a noteworthy problem of catalogues emphasized by Ebneter, Djorgovski, and Davis[28] (and references therein; =EDD). The presence of such "features" in a type of galaxy which was by definition featureless led EDD to suggest a more physical classification of E's is now warranted. A lovely montage and catalogue of dust-lane ellipticals is provided by Bertola[3].

Sandage and Brucato[48] pointed out that the original classes called Irr I and Irr II in the Hubble Atlas are not satisfactory because they combine widely differing objects into the same bin, namely "Irr". To distinguish galaxies which are not E, S0, or S but which have an amorphous appearance to the unresolved light, sometimes with imbedded resolved stars, they proposed the term "amorphous" galaxies. Sandage and Brucato emphasize that these objects are similar to, but not precisely like, the Irr II's in the Hubble Atlas, and that some similar objects classified as I0 by de Vaucouleurs may be peculiar spirals or S0's. One of the hallmarks of the amorphous class is a well-developed early-type absorption spectrum spread throughout the disk.

In the case of spirals, many aspects of the "grand design" and "flocculent" spiral morphologies have now been quantified[31]. These are aspects of spiral structure morphology that are not directly built into Hubble classifications. Flocculent galaxies lack bimodal symmetry and have a spiral-like structure composed only of small pieces of arms. Grand design galaxies generally have a two-armed structure and the arms are longer and more continuous than in flocculent galaxies. To account for these differences and for combinations of the two pattern types in many galaxies, Elmegreen and Elmegreen[30] proposed a system of 10–12 "arm classes" or AC's to highlight a systematic orderliness of spiral arms. The AC's are not exactly the same as van den Bergh luminosity classes because they emphasize symmetry and arm length, rather than arm contrast.

The identification of the locations of specific dynamical orbital resonances in spiral galaxies has seen much progress in recent years. Research has focussed on two classes of objects: grand design spirals by the Elmegreens, and ringed galaxies by myself. The paper by Elmegreen and Elmegreen[29] summarizes how to recognize the primary orbit resonances in a relatively typical grand design spiral, NGC 1566. For this purpose, purely *morphological methods* guided by expectations from spiral structure theory are used. The features considered are spiral arm kinks, gaps, spurs, bifurcations, endpoints to star formation ridges, dust-lane crossover points, interarm star formation, and the ends of a weak bar. If consistency can be found between the positions of these features and those inferred for specific resonances from a rotation curve, then the pattern speed of the wave can be derived with reasonable confidence. However, even in an extreme grand design case like NGC 1566, the resonance features are very weak. It takes a great deal of tenacity, for example, for the reader to study and identify clearly all of the features summarized in Table 1 of Elmegreen and Elmegreen[29].

Ringed galaxies refer to normal galaxies classified in the de Vaucouleurs revised Hubble system with the symbols (R)SB(r), (R′)SB(rs), (R′)SAB(s), (R)SAB(r,nr) etc., that is, objects which have inner, outer, or nuclear rings or pseudorings. These rings are believed to define the locations of specific orbital resonances with a bar or oval, and if correct they are much more obvious optical features with a direct link to resonances than some of the features seen in the best grand design spirals. Thus, they provide a promising way of indirectly estimating pattern speeds of bars and ovals, of which very little is known. At the moment, there is a great deal of evidence that the outer rings and pseudorings of SB and SAB galaxies trace the location of the outer Lindblad resonance, or OLR. This follows from statistics of their shapes and orientations with respect to

bars[10], from their relative sizes with respect to inner rings[2] and most of all from their morphology[15]. The *Catalogue of Southern Ringed Galaxies*[12] is designed specifically to understand the link between rings and resonances, and has been the basis for the studies of Buta[10] and Buta and Crocker[15].

A number of interesting findings have been made concerning cluster galaxies. A photometric study of brightest cluster members, or "BCM's", including gE, D, and cD types (Schombert[51),52),53]) has led to a refined and quantitative classification of these galaxies based on luminosity profile shapes. Schombert has noted that the characteristic extended envelopes of cD galaxies are generally fainter than 10% of the night sky brightness and are not readily seen on PSS prints. Thus, the rather shallow luminosity profiles of cD's is what led to their recognition, in addition to their central location in clusters. It is the existence of a true extended envelope that distinguishes the cD from the D class.

As emphasized by Sandage and Binggeli[47] (=SB), the Virgo Cluster contains galaxies of virtually every known morphological type. Of particular interest has been the identification in Virgo of dwarf S0, or dS0 galaxies, which morphologically are like S0's but which are of considerably lower luminosity and surface brightness than normal S0's (see also Binggeli and Cameron[4]). Most of the galaxies in Virgo fainter than $B \approx 14$ appear to be dwarf E, or dE, systems. SB emphasize that the "great void" in luminosity below Sa, Sb, and Sc types is real - there are no convincing cases of dSa, for example. This confirms that the Hubble sequence is largely defined by giant galaxies. However, although no examples of dSa or dSb were found in Virgo, a promising example was found by van den Bergh[63] in the compact, apparent elliptical galaxy NGC 3928, a member of the Ursa Major Cloud of galaxies.

The luminosity class system of van den Bergh has been extended to classes V-VI and VI by Corwin (see introduction to RC3) to allow for a greater range of apparent surface brightnesses seen among dwarf and late-type galaxies on the SRC-J sky survey. The RSA luminosity class system was also refined by SB to allow for a greater apparent range of surface brightnesses seen among Im galaxies in the Virgo Cluster. Among the galaxies classified as Im V by SB are "huge" Im types having significant diameters (up to 10 kpc) and peak central surface brightnesses less than 10% of night sky in blue light. These are accompanied by similar huge dE systems. The data from a variety of sources of luminosity classes have been compared and combined in RC3[24].

Van den Bergh, Pierce, and Tully[65] (=BPT) have discussed the classification of 231 Virgo Cluster galaxies from CCD images. They propose a revision to the classifica-

tion system of van den Bergh[62] to include Sd and Sm types, and demonstrate that the accuracy of luminosity classification is improved on digital images ($\sigma(M_T^B) \approx 0.7$ mag) compared to classifications based on photographic plates published in the RSA ($\sigma(M_T^B) \approx 1$ mag). Of particular interest in this work was the identification of a possible new class of galaxies, called "Virgo types." These galaxies have fuzzy outer regions and active star formation in their bulges or inner disk regions, and constitute 43% of 88 Virgo cluster spirals. In contrast, BPT find that the Ursa Major cluster includes only 2 "Virgo types" out of 35 spirals, suggesting real differences. BPT suggest that the early "Virgo types" represent a mild form of the Butcher-Oemler effect that persists at zero redshift.

In a study of the HI and optical properties of cluster galaxies, Bothun, Schommer, and Sullivan[6] identified a class of *red*, HI-rich, low surface brightness spirals. A sample of these objects is compiled by Schommer and Bothun[54], and two extreme examples of the class, NGC 3883 and UGC 542, were studied by van der Hulst et al[66]. The types of these galaxies range from Sa to Sc in Schommer and Bothun[54], and NGC 3883 is quite distinctive for its size and appearance in Abell 1367. Van der Hulst et al[66] interpret these galaxies in terms of a threshold HI surface density for star formation and possible interrupted star formation activity or an altered IMF.

An important serendipitous finding from a study of a field of the Virgo Cluster was an object dubbed "Malin 1"[7]. This galaxy appears small enough on PSS prints that it did not make inclusion into the UGC[42]. However, on amplified deep IIIa-J plates, Malin 1 shows an extended, low surface brightness disk surrounding a small bright core. The object is not a member of the Virgo Cluster (it is $\approx$ 20 times as distant) and is now recognized as a new class of giant, HI rich, low surface brightness disk galaxies the likes of which had not been appreciated before. The properties of Malin 1 are further summarized and described by Impey and Bothun[36], and a second example of the class was reported by Bothun et al[8]. These objects are now interpreted as disk galaxies whose HI surface density is so low that they evolve only slowly.

The study of interacting galaxies has led to the recognition of several new morphologies. Polar ring galaxies[69] are believed to be cases where a small satellite has been disrupted into a polar orbit around an S0. Hoag-type ringed galaxies[55] may be related cases where the central object is an E0 system. X-galaxies are edge-on S0's displaying a distinct X-shape across the center that may also be related to polar ring galaxies[68]. "Ocular" galaxies are interacting galaxies displaying an "oval-apex structure resembling an eye"[32]. The latter objects are particularly interesting, because they represent a type

of bar not distinguished within the Hubble system. A key feature is a double arm on one side, as illustrated in Figure 1 of Elmegreen et al[32].

Of particular interest to students of spiral structure is the discovery of a leading spiral arm in the interacting galaxy NGC 4622[16]. The arm was first noticed by Byrd on a well-known commercially available photograph published in Shu[56]. The galaxy is of type SA(r)ab and shows two major outer arms that wind clockwise, but inside the inner ring a single arm winding in the opposite sense is present. Since the "discovery" photograph was taken in blue light, Buta, Crocker, and Byrd[15] (=BCB) re-observed the galaxy in the Cousins I-band to test whether the arm is stellar or an artifact of dust. The leading arm was found to be a clear feature in the galaxy's old disk population. The fact that only a single leading arm is observed in this case, rather than two, is strong evidence that the arm was generated by a tidal interaction, as discussed in detail by BCB.

The widespread use of high quality CCD's, especially the large format TEK CCD's at KPNO and CTIO, has greatly increased the number of large-scale images available for classifying galaxies. What is particularly important is that a typical modern CCD can provide in a short amount of time images that are deeper in limiting surface brightness than the SRC-J sky survey, and yet still provide detailed information on the central regions of galaxies. Thus, they bypass the main problems of direct prime focus or Schmidt plates and have the potential of adding greatly to our knowledge of morphology. It is also clear that recent advances in infrared detectors make the development of a classification system in the 1–3 μ wavelength range a real possibility. The advantages of using near infrared images to type galaxies are their increased sensitivity to the dominant old stellar populations, which tends to enhance the visibility of features such as bars and bulges. The young component of galaxies which dominates blue light images for many spirals as well as dust will be less prominent and therefore not important for typing purposes. The number of "cells" required to classify galaxies should therefore decrease somewhat. However, going to the infrared will not change the pitch angle of spiral arms or the relative sense of the Hubble sequence. What is clear is that the number of "non-barred" galaxies will probably decrease, as can be gathered just from a comparison of images on the ESO-B and ESO-R sky survey charts.

Finally, in the future some catalogues of galaxies will probably include automatic classification[1),58]. This is an approach still under development, owing to the difficulty of defining some aspects of morphology, but once a satisfactory methodology is achieved, it has the potential of providing more consistent classifications than might be achieved

visually.

6. CONCLUSIONS

One of the sobering realizations of recent years has been the discovery that a large fraction of the matter in galaxies is unseen. As discussed by Freeman (this conference), the evidence for this dark matter is overwhelming, and we are forced to conclude that most of what we see in galaxy morphology may only be like *icing on a cake.* However, this icing makes galaxies more interesting than they might otherwise be and it offers a lot for understanding galaxy structure and evolution. It seems clear that external influences can drive morphology in a variety of different ways, from gas stripping, accretion, and mergers, to tidally generated bars and spiral structure. Natural formation of bars and spiral patterns can probably also occur, and the influence of the orbital resonances of these non-axisymmetric disturbances can add further complexity to what we see. Morphological classification has many limitations and can only be used as a guide to understanding the underlying dynamics. However, even though it can be misleading, classification is still alive and well in the 1990's, as evidenced by the publication of the RC3. Now, for the rest of a conference like this, we have to weigh the evidence for nature vs. nurture in influencing galaxy structure and evolution.

REFERENCES

1. Accomazi, A., Delfini, D., Kurtz, M. J., and Mussio, P., 1992, in *Morphological and Physical Classification of Galaxies*, G. Busarello, M. Capaccioli, and G. Longo, eds., (New York: Kluwer), p. 459.
2. Athanassoula, E., Bosma, A., Creze, M., and Schwarz, M. P., 1982, *Astron. Astrophys.*, **107**, 101.
3. Bertola, F., 1987, in *Structure and Dynamics of Elliptical Galaxies, I.A.U. Symposium No. 127*, T. de Zeeuw, ed.,(Dordrecht: Reidel), p. 135.
4. Binggeli, B. and Cameron, L. M., 1991, *Astron. and Astrophys.*, **252**, 27.
5. Binggeli, B., Sandage, A., and Tammann, G. A., 1985, *Astron. J.*, **90**, 1681.
6. Bothun, G. D., Schommer, R. A., and Sullivan, W. T., 1982, *Astron. J.*, **87**, 731.
7. Bothun, G. D., Impey, C. D., Malin, D. F., and Mould, J. R., 1987, *Astron. J.*, **94**, 23.
8. Bothun, G. D., Schombert, J. M., Impey, C. D., and Schneider, S. E., 1990, *Astrophys. J.*, **360**, 427.
9. Burstein, D., 1979, *Astrophys. J.*, **234**, 435.
10. Buta, R., 1986, *Astrophys. J.*, **61**, 609.
11. Buta, R., 1989, *The World of Galaxies*, H. G. Corwin and L. Bottinelli, eds., (New York: Springer-Verlag), p. 29.
12. Buta, R., 1991, in *Dynamics of Galaxies and Their Molecular Cloud Distributions, I.A.U. Symposium No. 146*, F. Combes and F. Casoli, eds., (Dordrecht: Kluwer), p. 251.

13. Buta, R., 1992, in *Morphological and Physical Classification of Galaxies*, G. Busarello, M. Capaccioli, and G. Longo, eds., (New York: Kluwer), p. 1.
14. Buta, R. and Crocker, D. A., 1991, *Astron. J.*, **102**, 1715.
15. Buta, R., Crocker, D. A., and Byrd, G. G., 1992, *Astron. J.*, **103**, 1526.
16. Byrd, G. G., Thomasson, M., Donner, K. J., Sundelius, B., Huang, T.-Y., and Valtonen, M. J., 1989, *Cel. Mech.*, **45**, 31.
17. Corwin, H., 1989, *The World of Galaxies*, H. G. Corwin and L. Bottinelli, eds., (New York: Springer), p. 1.
18. de Vaucouleurs, G., 1956, *Mem. Commonwealth Obs.*, **Ser. 3**, No. 13.
19. de Vaucouleurs, G., 1959, *Handbuch der Physik*, **53**, 275.
20. de Vaucouleurs, G., 1963, *Astrophys. J. Suppl.*, **8**, 31.
21. de Vaucouleurs, G., 1974, in *Formation and Dynamics of Galaxies*, J. R. Shakeshaft, Ed. (Dordrecht: Reidel), p. 1.
22. de Vaucouleurs, G., 1977, in *The Evolution of Galaxies and Stellar Populations*, B. M. Tinsley and R. B. Larson, eds. (New Haven: Yale University Press), p. 43.
23. de Vaucouleurs, G., 1979, *Astrophys. J.*, **227**, 380.
24. de Vaucouleurs, G. and Odewahn, S. C., 1992, in preparation.
25. de Vaucouleurs, G. and Freeman, K. C., 1973, *Vistas in Astron.*, **14**, 163.
26. de Vaucouleurs, G., de Vaucouleurs, A., Corwin, H. G., Buta, R., Paturel, G., and Fouqué, P., 1991, *Third Reference Catalogue of Bright Galaxies*, (New York: Springer-Verlag) - "RC3".
27. Dressler, A. and Sandage, A., 1978, *Pub. Astron. Soc. Pacific*, **90**, 5.
28. Ebneter, K., Djorgovski, S., and Davis, M., 1988, *Astron. J.*, **95**, 422.
29. Elmegreen, B. G. and Elmegreen, D. M., 1990, *Astrophys. J.*, **355**, 52.
30. Elmegreen, D. M. and Elmegreen, B. G., 1982, *M.N.R.A.S.*, **201**, 1021.
31. Elmegreen, D. M. and Elmegreen, B. G., 1984, *Astrophys. J. Suppl.*, **54**, 127.
32. Elmegreen, D. M., Sundin, M., Elmegreen, B., and Sundelius, B., 1991, *Astron. Astrophys.*, **244**, 52.
33. Holmberg, E., 1950, *Medd. Lunds Astron. Obs.*, Ser. II, No. 128.
34. Hubble, E., 1926, *Astrophys. J.*, **64**, 321.
35. Hubble, E., 1936, *The Realm of the Nebulae* (New Haven: Yale University Press)
36. Impey, C. and Bothun, G., 1989, *Astrophys. J.*, **341**, 89.
37. Kennicutt, R. C., 1981, *Astron. J.*, **86**, 1847.
38. Kormendy, J., 1979, *Astrophys. J.*, **227**, 714.
39. Kormendy, J., 1981, in *The Structure and Evolution of Normal Galaxies*, S. M. Fall and D. Lynden-Bell, eds., (Cambridge: Cambridge University Press), p. 85.
40. Morgan, W. W., 1958, *Pub. Astron. Soc. Pac.*, **70**, 364.
41. Morgan, W. W., Kayser, S., and White, R. A., 1975, *Astrophys. J.*, **199**, 545.
42. Nilson, P., 1973, *Uppsala General Catalogue of Galaxies*, Upp. Obs. Ann., Vol.6.
43. Odewahn, S., 1989, PhD Thesis, University of Texas.
44. Sandage, A., 1961, *The Hubble Atlas of Galaxies*, Carnegie Inst. of Wash. Publ. No. 618, Washington, D.C.
45. Sandage, A., 1975, *Galaxies and the Universe, Stars and Stellar Systems Vol. IX*, A. Sandage, M. Sandage, and J. Kristian, eds., (Chicago: Univ. of Chicago Press), p. 1.
46. Sandage, A. and Bedke, J., 1988, *Atlas of Galaxies Useful for the Cosmological Distance Scale*, NASA.
47. Sandage, A. and Binggeli, B., 1984, *Astron. J.*, **89**, 919.
48. Sandage, A. and Brucato, R., 1979, *Astrophys. J.*, **84**, 472.
49. Sandage, A. and Tammann, G. A., 1981, *A Revised Shapley-Ames Catalog of Bright Galaxies*, Carnegie Inst. of Wash. Publ. No. 635, Washington, D.C. - "RSA".

50. Sandage, A., Binggeli, B., and Tammann, G. A., 1985, *Astron. J.*, **90**, 395.
51. Schombert, J. M., 1986, *Astrophys. J. Suppl.*, **60**, 603.
52. Schombert, J. M., 1987, *Astrophys. J. Suppl.*, **64**, 643.
53. Schombert, J. M., 1988, *Astrophys. J.*, **328**, 475.
54. Schommer, R. A. and Bothun, G. D., 1983, *Astron. J.*, **88**, 577.
55. Schweizer, F., Ford, W. K., Jedrzejewski, R., and Giovanelli, R., 1987, *Astrophys. J.*, **320**, 454.
56. Shu. F. H., 1982, *The Physical Universe: An Introduction to Astronomy* (Mill Valley: Univ. Sci. Books).
57. Simien, F. and de Vaucouleurs, G., 1986, *Astrophys. J.*, **302**, 564.
58. Thonnat, M., 1989, *The World of Galaxies*, H. G. Corwin and L. Bottinelli, eds., (New York: Springer), 53.
59. Tremaine, S., 1987, in *Structure and Dynamics of Elliptical Galaxies, I.A.U. Symposium No. 127*, T. de Zeeuw, Ed., (Dordrecht: Reidel), p. 367.
60. van den Bergh, S., 1960a, *Astrophys. J.*, **131**, 215.
61. van den Bergh, S., 1960b, *Astrophys. J.*, **131**, 558.
62. van den Bergh, S., 1976, *Astrophys. J.*, **206**, 883.
63. van den Bergh, S., 1980, *Pub. Astron. Soc. Pacific*, **92**, 409.
64. van den Bergh, S., 1990, *Astrophys. J.*, **348**, 57.
65. van den Bergh, S., Pierce, M., and Tully, R. B., 1990, *Astrophys. J.*, **359**, 4.
66. van der Hulst, J. M., Skillman, E. D., Kennicutt, R. C., and Bothun, G. D., 1987, *Astron. Astrophys.*, **177**, 63.
67. Vorontsov-Velyaminov, B. A., 1987, *Extragalactic Astronomy* (New York: Horwood Publ.)
68. Whitmore, B. C. and Bell, M., 1988, *Astrophys. J.*, **324**, 741.
69. Whitmore, B. C., Lucas, R., McElroy, D. B., Steiman-Cameron, T.-Y., Sackett, P. D., and Olling, R. P., 1990, *Astron. J.*, **100**, 1489.
70. Wirth, A. and Gallagher, J. S., 1980, *Astrophys. J.*, **242**, 469.

BOLOMETRIC HUBBLE TYPES FOR GALAXIES

Barry F. Madore
NASA/IPAC Extragalactic Database
Jet Propulsion Laboratory
California Institute of Technology

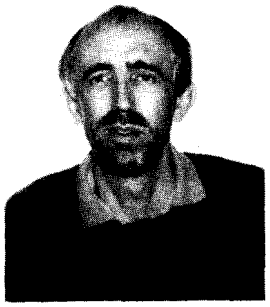

ABSTRACT

A multi-wavelength project is being undertaken to establish *Bolometric Hubble Types* for galaxies. The first step in this process involves collecting and standardizing images of galaxies culled from the archives of ground-based and space-based missions, covering diverse parts of the electromagnetic spectrum. Simultaneously with the collection of data we are beginning to use Neural Network software en route to a multi-dimensional mapping of the morphological components of galaxies into the standard Hubble Types. This step involves using data already compiled by and available from the *NASA/IPAC Extragalactic Database*. We then plan to generalize the process of machine-aided classification to extend the optical paradigm into the other wavelength domains. Having distilled the essential information from each wavelength-specific study into wavelength-dependent morphological bins, we then plan to re-apply Neural Networks to produce a *Bolometric Hubble Type.*

1. INTRODUCTION

There are a number of reasons, both scientific and logistical, to believe that the time is right for a new look at galaxy classification. The human expertise is being lost. The number of galaxies being imaged is exploding. The typing scheme needs to be extended to other wavelengths. And finally, the whole question of the ultimate meaning of a morphological type (be it derived in the optical, the radio, or the infrared) needs to be addressed and reconciled with the results from more quantitative, global measurements. The approach discussed here for the first time is aimed at addressing each of these questions, en route to establishing a wavelength-independent ***Bolometric Hubble Type*** (see Figure 1).

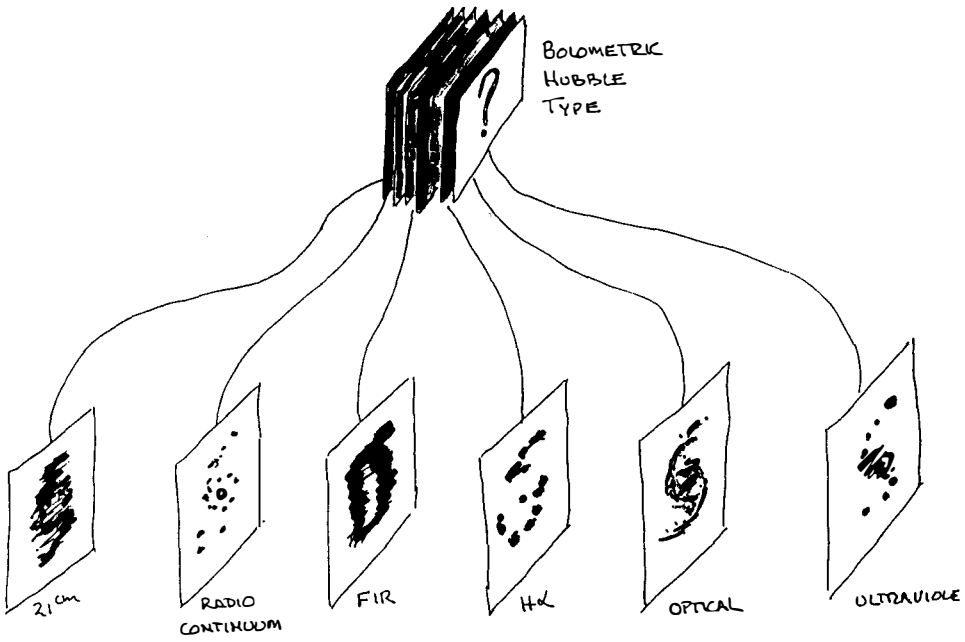

Figure 1. – Schematic Constituents of a Bolometric Hubble Type. The classifications resulting from the morphology apparent at each distinct wavelength (lower panels) give rise to "a morphological data cube" (top), which then becomes the input matrix to be trained upon, and classified by, the final application of neural networks to the data set. Each step is a distillation of much more extensive information; the ultimate goal being a compact characterization of the galaxy that is wavelength independent, and by supposition, physically meaningful.

2. THE CLASSIFICATION PARADOX

On top of the avalanche of multi-wavelength data drawn from space and ground-based telescopes, which is confronting all extragalactic astronomers, there is also a deeper problem surfacing which has yet to be fully appreciated by practitioners in the field of galaxy morphology: There is a paradoxical relation between the classification and the quantification of galaxy properties. An enormous variety of forms, structures and sub-structures comprise the optical 'families', the 'stages' and the 'types' of galaxies (presently) found in the Universe. Much of this beauty and complexity (spiral arms, rings, and bursting nuclei, *etc.*) is a reflection of present-day star formation patterns, superimposed on long-lived relics of past star-formation activity (bulges and exponential disks, *etc.*) and/or global instabilities (bars, oval distortions, lenses, and grand-design spirals, *etc.*). And yet, despite this varied past history and the patently complex present, attempts at using global properties (see Brosche 1973; Whitmore 1984), extracted from quantitative measures (*e.g.,* colors, maximum rotation rates, absolute magnitudes, *etc.*) all fail to show spiral galaxies to be anything more than "form" (*e.g.,* absolute magnitude or absolute radius) and "scale" (*e.g.,* color or bulge-to-disk ratio); simple beyond all measure. All at once we have qualitative complexity and diversity co-existing in the optical images of objects that are quantitatively described equally well by any two of the many apparently lock-step parameters, no one of which is any more revealing than the next.

Ostensibly a galaxy is the cumulative sum of its past star-formation history. How is it then that the temporal and spatial integrals of that star-formation history are apparently so decoupled from their obviously changing and spectacularly varied instantaneous, contemporary star-formation morphologies? For example, can anyone cite a global property such as scale length, color or absolute magnitude that would unequivocally tell you that a galaxy has a central bar or not? Or take something as innocuous as the *Tully-Fisher* relation, the incredibly tight relation between absolute magnitude and maximum rotational velocity has a dispersion of less than 0.4 mag (for a very recent discussion and calibration see Freedman 1990). It is independent testimony to the absurd simplicity of these systems (where the scatter, such that there is, correlates convincingly with nothing as yet observed). And still the variety in the optical appearance of these same galaxies cries out for understanding, and too it seems to argue for a depth of complexity that should influence and/or result from deeper global diversity; but none has been found! Perhaps all of this is an inappropriate conflict between aesthetics and cold hard facts; but it is still an unresolved and intriguing aspect of extragalactic astronomy that we are exploring. And we feel that the process outlined below will shed light upon this issue.

3. NEW APPROACHES TO CLASSIFICATION

Artificial Intelligence (unjustifiably but understandably) has not yet gained a very good reputation in the scientific community as a whole, largely because of media hype and over-extended and premature commercial ventures – always promising much, but delivering little. But honest *AI* is in fact good, solid, computer science. Within most progressive computer science departments *AI* has undergone significant development, and although they are not yet familiar tools to most astronomers, *Expert Systems* abound in the real world; serious applications are in fact meeting with commercial success. And in fact two recent applications can be found in an astronomical setting: their use in real-time compensation for seeing in active optics (Angel 1990; Sandler 1991) and their use in automatically distinguishing between (but not classifying) stars and galaxies in *Palomar Observatory Sky Survey* (POSS) scans (Odewahn 1991). The time is ripe for astronomers to become even more familiar with these tools and take advantage of them for their own scientific purposes. Galaxy classification is a natural point of departure.

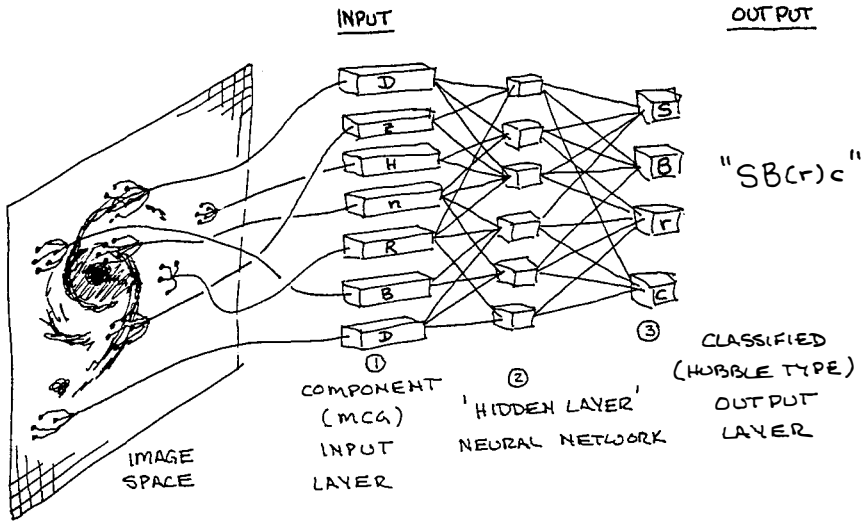

Figure 2. – *Conceptual Schematic of the Application of a Neural Network to Galaxy Classification.* To the left, the galaxy image is seen as an array of grey-scale pixels. An observer (human in the first instance, a machine in later implementations decomposes the image and tabulates the constituent components of the galaxy in the manner described in the *Morphological Catalogue of Galaxies.* These component elements are used as input (1), for training the network (2), to map from *MCG-style* descriptors to standard, optical Hubble Types upon output (3). Once trained the Neural Net can be applied to any such input data gathered from any arbitrary wavelength.

We are presently developing a number of very specific and measured applications of Neural Nets to galaxy classification, *en route to a much more exciting goal.* In the first instance, we are bringing together and compiling morphological data, uniquely available through the *NASA/IPAC Extragalactic Database*, and interfacing it with images from the infrared *IRAS* mission and the (more limited set of) ultraviolet *Astro-D* mission images, for comparison with our own (unpublished and still on-going) all-sky CCD imaging survey of the 10,000 brightest galaxies (the so-called Mega-Galaxy Project). The long-term goals are: (1) To apply these results and algorithms for galaxy recognition and classification to the digitized version of the POSS (examples of which are available now at the *Space Telescope Science Institute* and from *European Southern Observatory*) (2) To supply the Two Micron All-Sky Survey (2MASS) project with an efficient algorithm for typing the galaxies to be found by them in their near-infrared (and especially near the Galactic plane), and (3) To explore the wavelength dependence of Hubble type in anticipation of actually seeing galaxies with the *Hubble Space Telescope* in their earlier incarnations viewed in their short-wavelength rest-frame colors.

For a number of reasons the optical paradigm of galaxy classification has not migrated much beyond the blue and visual wavelengths. One small foray into the (photographic) near-infrared has been made by Elmegreen (1981), while some further thoughts and discussion of the potential here has been raised by Bothun (1990). Of course, the lack of comprehensive surveys at UV or infrared wavelengths is, in part, to blame for a corresponding lack in activity, but even when adequately large samples are available the immediate tendency of this generation of astronomers is not to classify the new wavelength images on their own merits but rather to merely cite the optical classification, as if it had some ultimate precedence. For instance, detailed and reasonably high-resolution 21cm interferometric maps of the neutral hydrogen HI distribution in spiral galaxies have been available for some time, but the most that has ever been done with them in a morphological context is to characterize the radial density distribution (as being flat, centrally depressed, or peaked). Similarly the *IRAS Large Galaxy Catalog* (Rice *et al.* 1988) is an impressive compilation untouched by classifiers. Hα photographs, UV images and radio continuum maps of galaxies all continue to be published, correlated and dissected, but never have they been systematically compiled and/or classified.

4. SUMMARY

We are only just beginning this multi-wavelength task. And, our purpose goes beyond just archiving; our program is designed to extract new information from a synthesis of existing catalogs and digital data. With this proposal we would like to begin extending the classification methodology (so successful in the optical) out into other diverse wavelengths where major surveys are coming to completion and/or will soon be available. However, rather than relying solely on human intervention and decision making, we plan to use Neural Networks to accomplish this first goal (Figure 2). This said, the ultimate aim of our program is to construct *Bolometric Hubble Types*: a system of classification of galaxies which has no direct reference to a specific wavelength region, but one that nevertheless is a type that depends on and reflects the distribution of luminous stars and gas in a galaxy as viewed from a variety of wavelengths. A *Bolometric Hubble Type*, we believe, would be more representative of what a galaxy is in its totality. Therefore, the *Bolometric Hubble Type* should be the proper interface to theory, correlating more readily with physical quantities such as total luminosity, scale length, angular momentum distribution, *etc.*, as those quantities become available. Moreover, the *Bolometric Hubble Type* will, by its definition, provide observers and theorists alike with galaxy sub-samples that are selected by their similarity over a wide range of attributes, rather than being grouped, as they are at present, by a detector-driven slice at 4500Å.

References:

Angel, J.R.P. *et al.* 1990, *Nature*, **348**, 221.

Bothun, G. D. 1990 *Evolution of the Universe of Galaxies*, ed. R. Kron, pg. 55.

Brosche, P. 1973, *Astron. Ap.*, **23**, 234.

Elmegreen, D. 1981, *Ap. J. Suppl.*, **47**, 229.

Freedman, W. L. 1990, *Ap.J.*, **355**, L35.

Odewahn, S. *et al.*, 1991, Univ. Minnesota preprint

Rice, W. *et al.* 1988, *IRAS Large Galaxy Catalog Ap.J. Suppl.*, **68**, 91.

Sandler, D. *et al.* 1991, *Nature*, **351**, 300.

Whitmore, B. C. 1984, *Ap. J.*, **278**, 61.

NASA/IPAC EXTRAGALACTIC DATABASE

The NED Team*
Presented by Barry F. Madore
NASA/IPAC Extragalactic Database
Jet Propulsion Laboratory
California Institute of Technology

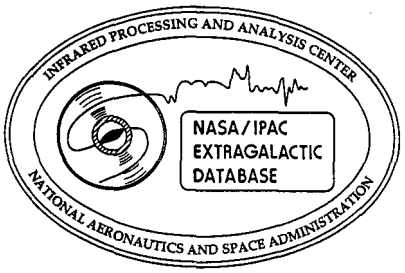

ABSTRACT

A brief historical introduction of the NASA/IPAC Extragalactic Database is given, followed by an overview of the operational status as of May 1992.

* The NED Team:
George Helou, Barry F. Madore,
Marion Schmitz, Harold G. Corwin, Jr.
Xiuqin Wu, Judy Bennett, Cheryl Lague

1. THE PAST

Extragalactic research is one of the fastest-growing sub-disciplines within astronomy and astrophysics. In response to that growth, and in direct aid of that research, the *NASA/IPAC Extragalactic Database* (NED) was created by Helou and Madore. From conception to funding the NED Team moved swiftly to establish the first version of the extragalactic database which was verified and loaded within the first year of full operations; it consisted of 54,000 objects culled mostly from major published galaxy catalogs. Within 18 months end-to-end software prototypes had been written, fully integrated and tested. The system consisted of a database management system (DBMS) seamlessly connected to a user-friendly interface which incorporated a very high-level, customized, extragalactic name interepreter. "Experimental Operations" of NED, available to the astronomical community over the electronic (SPAN and Internet) networks, were inaugurated with the summer 1990 meeting of the American Astronomical Society in Albuquerque, New Mexico, and within six months of that date NED was averaging 600 user-logins per month.

2. THE PRESENT

As NED becomes an everyday tool for astronomers it is changing the way that extragalactic research is being done around the United States and around the world. As news of this service moves throughout the community the interactive sessions continue to grow. And they have been growing at an accelerated pace, with the doubling time for the number of sessions currently being about six months (see Figure 1 for a plot of recent statistics). In the first quarter of 1992 NED serviced over 6,000 interactive user sessions. And this statistic does not include batch requests, a feature added in mid-1991 to ease the interactive load on the system and on the users. This service allows large jobs to be submitted remotely, processed automatically and deposited into an anonymous ftp account for retrieval by the user at their convenience after automatic notification by the NED system.

While the vast majority of NED users are from the USA (with the *Space Telescope Science Institute* being our most frequent regular patron), almost all major astronomical centers are in regular contact with the database. Almost daily usage is seen from the Netherlands, Italy, Canada and Australia, with requests often originating from such far-flung places as Japan, Korea, Finland, Sweden, Israel, South Africa, Chile, Brazil and indirectly from our colleagues in Russia.

Between May 1991 and February 1992 a major expenditure of NED manpower was dedicated to migrating the database from the IM/DM system running on a CYBER to a SYBASE system on a UNIX platform. During 1992 a commercial user interface will be tested for the next major release of NED which will be capable of supporting multiple windows, data-table scrolling, line graphics, and eventually digital images.

NED is a continuously evolving, real-time research archive built around known extragalactic objects. Recent inclusions to our list of searchable objects cover all wavelengths, and (in addition to the major optical galaxy catalogs) they include the *Greenbank 5GHz Catalogs*, the *IRAS Faint Source Catalog*, the *Abell Clusters*, the *Einstein Extended Medium Sensitivity Survey*, *Case Galaxies*, *QSO Absorption-Line Systems*, *KISO Ultraviolet Excess Galaxies*, and Zwicky's *Catalogue of Compact and Post-Eruptive Galaxies*. NED supports searches by names and aliases, and by location, with total sky coverage. Filters on object types are being implemented as a new service. As of 1992, NED contained over 400,000 names for 200,000 objects. To this we can add nearly a quarter million citations linked to 15,000 bibliographic references. NED also provides on-line access to nearly 5,000 abstracts of articles (from the AJ, ApJ, A&Ap, MNRAS and PASP) pertaining to extragalactic astronomy; and this number of abstracts is increasing by about 1,200 per year. Both *Nature* and the *IAU Circulars* have been recently added to the list of periodicals being scanned by NED on a regular basis. Finally, the titles and abstracts of recently published theses pertaining to extragalactic research are being provided as yet another NED service.

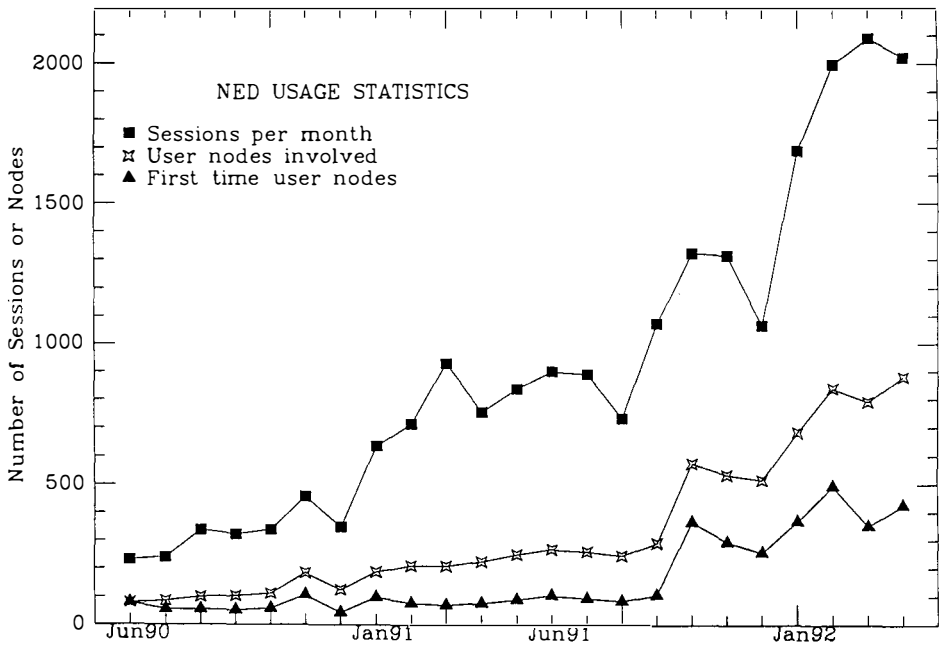

Figure 1. – Growth of NED usage as measured by interactive sessions registered each month since its opening to the public in June of 1990.

3. THE FUTURE

Of vital concern to NED and its ever-widening user community is the need to maintain existing functions while at the same time increasing the breadth of the NED services. We are currently moving on two major fronts to broaden the NED services: introducing detailed, referenced data, and sample-generating capabilities using filters on object attributes. The first data with detailed pointers back to the original literature will be positions and redshifts as measured at any wavelength (at present NED displays only one (referenced) optical position and one high-quality (unreferenced) redshift). Next, we will be making available total continuum flux densities (radio, x-ray, optical magnitudes and colors, etc) and total line fluxes (HI, CO, Hα, etc.). Morphology and classification frames are also well into the prototyping stages. Finally, we are scoping the implementation of data pointers to other types of observed data, (such as rotation curves, HI diameters, etc) as well as derived quantities (such as virial mass, cluster membership, distances, etc.)

This research was supported by the Jet Propulsion Laboratory, California Institute of Technology, under the sponsorship of the National Aeronautics and Space Administration's Office of Space Science and Applications.

ADDENDUM: HOW TO ACCESS AND USE NED

Access to NED is provided over INTERNET or SPAN. A VT100 terminal or VT100 emulation software is needed at the user's home terminal. On INTERNET, a connection to NED may be set up with the command `telnet ned.ipac.caltech.edu` (absolute address as of this writing is `134.4.10.118`). From a node on SPAN, use the command `set host IPAC` (absolute address is 5.857). Once connected and prompted for a "login", respond with `NED`; no password is needed. From this point on the system is self-documenting, especially through use of the `HELP` utilities and the "control-H" key. First-time users may want to read the `TUTORIAL` offered in the first screen. Regular users are encouraged to read the NED `NEWS` occasionally as it is changed regularly, reflecting additions to the NED database and its complement of tools and features.

II- PROPERTIES ALONG THE HUBBLE SEQUENCE

1) GASEOUS CONTENT

GAS AROUND GALAXIES. EPISODIC INFALL?

Renzo Sancisi
Kapteyn Astronomical Institute
University of Groningen
The Netherlands

The structure and kinematics of neutral hydrogen around spiral galaxies are discussed and circumstantial evidence for gas infall is presented. On the basis of their HI morphology spiral galaxies can be assigned to one of the following categories:

I) multiple systems in strong tidal interaction,
II) systems interacting with small gas-rich companions,
III) isolated spirals, with peculiar HI structures,
IV) isolated galaxies, normal, regular.

The multiple interacting systems may end up in major mergers. Those with gas-rich satellites and those with peculiar HI are galaxies which may be accreting lumps of gas now or have done it in the recent past. Among the one hundred galaxies studied in detail about twenty such cases have been found.

For elliptical galaxies accretion and merger processes are thought to play an important role, although there is disagreement as to the merger rate and the fraction of mass accreted. Supporting observational evidence comes from the presence, in some ellipticals, of HI gas, of counter-rotating cores and of outer shells. In SO galaxies the polar rings are regarded as possible results of accretion.

For spirals the observational picture is less clear and there is less hope of finding supporting evidence as the HI layer may have wiped out all traces of past gas infall. Furthermore, stringent limits are set on the accretion of satellites by using the thinness and coldness of galactic disks and the conclusion is that only a few percent of their mass has been accreted (Toth and Ostriker, 1992).

Here we discuss some results of a search for traces of gas infall onto spiral galaxies. The search has been carried out on existing HI line observations. Maps of the distribution and kinematics of neutral hydrogen exist now for a large number of spiral galaxies. We have examined about one hundred field spirals with observations of good quality and have recognized four principal types of systems with different HI morphologies and kinematics:

I) Multiple systems (typically 2 to 4 members of comparable mass) in strong tidal interaction, characterized by the well-known HI tails and bridges. They represent about one quarter of the sample examined. Well-known examples are M81–M82–NGC3077, NGC4631–4656–4627, NGC4038–4039 (Antennae) and NGC3623–3627–3628 (Leo group).

II) Galaxies with one or a few gas-rich dwarf companions, showing signs of weak tidal interaction (HI bridges, partial disruption of the companion). Examples are NGC3359, NGC4565, NGC4694. The companions have masses of a few percent or less as compared to the main galaxy. The cases of the Magellanic Clouds–Galaxy and of NGC5194–5195 (M51), where the companions are more massive, may be regarded as intermediate between categories I and II.

III) Galaxies with peculiar, irregular HI structures in their outer parts. These structures are often similar to those found near systems in strong interaction, but there are no visible companions to have caused them. Examples are NGC1023, M101, NGC628, NGC3067, NGC262.

IV) Normal, regular systems. These include the spirals with warps, with lopsided disks, and the SO's with HI rings. They form about one half of the sample examined.

It is obvious that the sample used here is not complete in any sense and has all sorts of biases. It is simply the collection of objects with the best HI data observed with the Westerbork radio telescope and the VLA in the course of the past 20 years. The present tentative classification based on HI morphology and kinematics serves to identify the

main characteristics of the galaxies surveyed and to study the main phenomena. It is clear that a large number of systems, about half in the present sample, are interacting now or show anomalies suggestive of past interactions. Actually, it is likely that the number of apparently "normal" systems in the present sample will decrease as higher sensitivity observations become available and fainter HI features are revealed, and that the number of "peculiar" cases in group III will increase.

The strongly interacting systems of our group I may end up in mergers as seen in various recent computer simulations (see e.g. Barnes, 1990). Here we draw attention to the systems of groups II and III. These are disk galaxies only moderately perturbed by the interaction with the dwarf companions or by the events which caused the anomalous structures observed in their outer parts. The two groups may, in fact, be showing similar phenomena and represent, respectively, less and more advanced stages in the process of accretion. The material is added in the outer parts and contributes to the formation and evolution of the disk. The peculiar HI structures seen now are not necessarily always fresh gas falling in from outside. They may represent, instead, material drawn out of the disk by a past interaction with a companion, before this was swallowed up. In either case, whether it is truly new gas of extragalactic origin or old, pulled out and temporarily refrigerated disk gas, it should have relatively low metal abundances.

The HI masses of the dwarf companions and of the observed peculiar features are in the range from 1×10^7 $M_\odot$ to 5×10^8 $M_\odot$ and the M_H/L values are of order 1 or larger. Their total masses, mainly dark matter, may be a factor ten larger. The time scales for the accretion may be of the order of 10^9 yr, as implied by the orbital periods in the outer parts of those galaxies. The accretion rate may be as low as 0.02 $M_\odot$/yr for the gas alone and may reach up to as much as 1 $M_\odot$/yr if optimistic estimates including stars and dark matter are made. As to the known difficulties, in particular the disk heating and a too high X-ray luminosity in the case of high accretion rates, there is, perhaps, a way out. In fact the satellites may not be hitting the disk from all directions with velocities of order 100 km/s, as assumed in Toth and Ostriker's calculations, The observations of NGC3359, NGC4565, NGC5907 and of some other spiral galaxies show that the companions have positions and velocities consistent with their being located close to the principal plane of the main galaxy and corotating with it. This suggests that they are gently coming in in the outer parts of the disks with low infall velocities, probably of order 10 km/s, and are not causing much trouble to the inner stellar disk.

In this picture the process of gas acquisition and disk formation in spiral galaxies would not take place in the form of a continuous drizzle of small gas clouds but would consist of episodic infall of large lumps of gas. The examples mentioned above indicate that some accretion does probably take place. But the frequency of such events is not

known and the time scales and masses are quite uncertain. It is conceivable, however, that such accretion has been more frequent in the past. Ten to one hundred such events as described here would be necessary over the Hubble time to account for the present gas content of spirals.

Also for some ellipticals similar observational evidence has emerged. There are, for instance, the well-known gas-rich systems like NGC1052, 4278 and 5128. But a more striking case, where the accretion seems to be taking place now, is that of the giant elliptical NGC4472 with the nearby dwarf irregular UGC7636, tidally disturbed and stripped of its gas, and the HI cloud of a few 10^7 $M_\odot$ found between them (Sancisi *et al.* 1987; see also Thuan, this volume).

REFERENCES

Barnes, J. 1990, in Dynamics and Interactions of Galaxies, ed. R. Wielen, Springer-Verlag: Berlin, p. 186

Sancisi, R., Thonnard, N., and Ekers, R.D. 1987, ApJ, 315, L39

Toth, G., and Ostriker, J.P. 1992, ApJ, 389, 5

THE MOLECULAR CONTENT

Françoise Combes
Radioastronomie Millimétrique, DEMIRM,
Observatoire de Meudon, F-92 190 Meudon, FRANCE

ABSTRACT

The molecular component, traced by the CO molecule, represents most of the interstellar medium mass within the optical disk of spiral galaxies. Its radial distribution is quite complementary to the HI gas, the latter being dominant in the outer parts. Since the H_2 gas is cold, it is a good tracer of fine structures and density waves in galaxies, such as the spiral arms, bars and rings. While the atomic gas is stripped in clusters, no such effect has been observed for the molecular gas.

From a recent IRAM survey of 100 nearby galaxies, it is shown that interacting galaxies have more H_2 gas than unperturbed galaxies, while they have comparable HI gas. We propose that tidal interactions trigger gas infall of diffuse ionized gas from the outer regions of galaxies towards the disk and center, where it condenses into neutral gas.

1. IMPORTANCE OF THE H_2 COMPONENT

The molecular component represents a significant part of the interstellar medium of galaxies; inside the optical disk, it is even the dominant component. The radial distributions of the HI and H_2 gas are not correlated at all, in our own Galaxy as well as in nearby galaxies (fig. 1). For example, the H_2 to HI surface density ratio varies from 30 in the center to 1 in the outer parts of NGC 6946 (Tacconi & Young 1986). The H_2 component is correlated with the far-infrared radiation, the radio-continuum, and Hα emission. Stars are formed out of molecular clouds, and the H_2 gas is the key to understand star-formation and evolution of galaxies.

Unfortunately, the H_2 molecule is not observable directly in the radio range because of its symmetry (it has no dipole moment). The best tracer of H_2 is CO: it is the most abundant molecule after H_2, and due to its small dipole moment it is excited by collisions with H_2 at low density, typically $n(H_2) = 10^3\ cm^{-3}$. It thus traces all giant molecular clouds, while higher-moment molecules like HCN or CS for example, trace densities larger than $10^5\ cm^{-3}$.

Large millimeter-wave telescopes (Onsala 20m, IRAM 30m, Nobeyama 45m) provide a spatial resolution as high as 12" (IRAM in the CO(2-1) line), and interferometers (Caltech 3x10m, BIMA 5x6m, NRO 5x10m, IRAM 4x15m) up to 2" in the CO(1-0) line. Considerable progress has therefore been possible during the last decade.

As we know the H_2 molecular distribution only through the CO molecule, we need to establish a precise conversion ratio H_2/CO. The often used "standard" ratio has been determined in the Milky-Way, and is based on the assumption of virialized clouds, with average physical conditions that I now describe.

2. THE H_2/CO CONVERSION RATIO

The main problem in the interpretation of the CO line is the optical thickness. The ^{12}CO(1-0) line in the Milky-Way molecular clouds is always highly optically thick (τ>10). This is well established from the observation of the isotopic molecule ^{13}CO.

However, if we assume that molecular clouds are self-gravitating and nearly virialized, then the internal line-width reflects the cloud mass. The observational data, when observing the CO line, are the antenna temperature T_b and the half-power width of the profile Δv. Let us call I(CO) the integrated CO emission $I(CO) = \int T_b\, dv$, which can also be considered as the CO flux. We can define a CO luminosity, which is the CO integrated emission summed over the emitting area: $L(CO) = D^2 \int I(CO)\, d\Omega = \pi R^2\, T_b\, \Delta v$. From the virial hypothesis, $\Delta v = (GM/R)^{1/2}$ and the cloud mass is $M = L(CO)\, (4\rho/3\pi G)^{1/2} T_b^{-1}$, if ρ is the average volumic density of the clouds.

The mass to luminosity ratio is therefore $M/L \propto \rho^{1/2}/T_b$.

The H_2/CO conversion ratio (or M/L ratio) can be considered almost constant, since any telescope beam averages over a large quantity of molecular clouds; statistically all clouds can be considered as identical, with an average density and temperature. Also, due to collisionnal excitation, the antenna temperature increases in denser regions where the line excitation is higher, keeping $\rho^{1/2}/T_b$ in the same range. The molecular mass is then directly proportional to the CO emission, as if it were optically thin.

The H_2/CO conversion ratio has been determined empirically in the Milky Way, by several independent methods. One of them is to obtain in the solar neighbourhood the ratio between the optically thin ^{13}CO emission and optical

extinction Av (Dickman 1978); another one is to observe γ-rays, produced on large scales by the interaction between cosmic rays and the nucleons of the ISM (Strong et al 1988). The presently adopted value gives $N(H_2) = 2.3\ 10^{20} I(CO)$ mol cm^{-2}, and the numerical value 2.3 can be in fact between 1 and 5. The main factors that can make the H_2/CO ratio vary is the high excitation of the gas (M82 is such an example), the fraction of dense gas (Solomon et al 1992) and the metallicity; it is for instance 6 times higher in the LMC (Cohen et al 1988) and 20 times higher in the SMC (Rubio et al 1991).

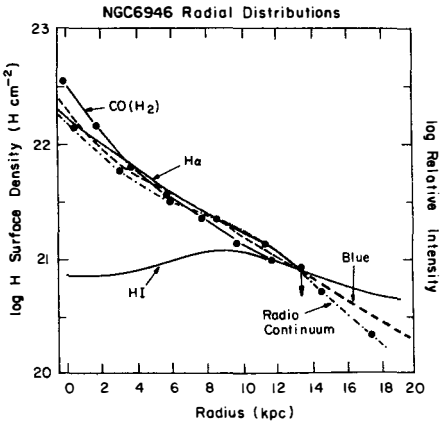

Figure 1: Comparison of the radial distributions of $CO(H_2)$, HI, Hα, blue and radio-continuum in NGC 6946 (from Tacconi & Young 1986).

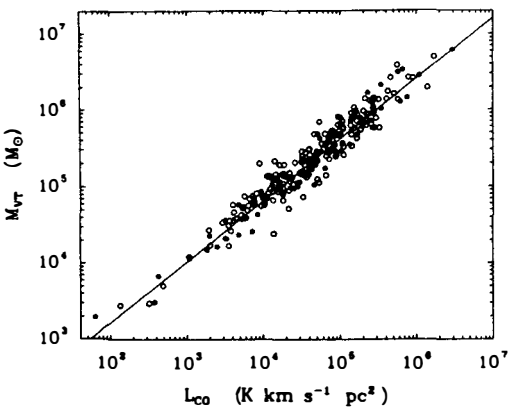

Figure 2: Virial cloud mass versus CO luminosity (Solomon et al 1987).

Are clouds in virial equilibrium?

The molecular component, in contrast to the HI gas, is observed in a very clumpy structure. Most of the molecular mass is comprised in large clouds (the GMC or Giant Molecular Clouds), since the mass spectrum of clouds is a power law of slope larger than -2 : $N(m) \propto m^{-1.5}$ (see e.g. Solomon & Rivolo 1989). Observed characteristics of clouds at various scales obey relations that support the virial hypothesis.

Cloud sizes and internal linewidths are linked by the relation: σ (km/s) = $r(pc)^{1/2}$ (Solomon et al 1987), and the mass M is proportional to the square of size (M in R^2, i.e. constant column densities for all-scales). These relations imply that the density at one given scale is inversely proportional to this scale (ρ in R^{-1}). The virial hypothesis receives observational support, since it is found that the virial mass (computed from the line-width) is highly correlated to the CO luminosity in a

galactic survey (fig. 2). However the relation is not linear, $M_{vir} \propto L(CO)^{0.8}$, which implies that the H_2/CO conversion ratio varies with the cloud mass as $m^{-1/4}$, i.e. by a factor 10 for the dynamical range observed (m=10^3 to 10^7 $M_\odot$). Since several scales are averaged out in a single beam, the empirical conversion ratio is valid for an average over the entire mass spectrum.

In external galaxies with normal metallicity, no observation is incompatible with molecular clouds being of the same nature as those of the Milky Way. In M33, Wilson & Scoville (1990) have been able with the Caltech interferometer to statistically study the sizes of clouds: the same size-linewidth and $L(CO)/M_{vir}$ relations are derived. In the Magellanic Clouds however, strong departures from the $L(CO)/M_{vir}$ relation are observed (Rubio et al 1992, fig. 3).

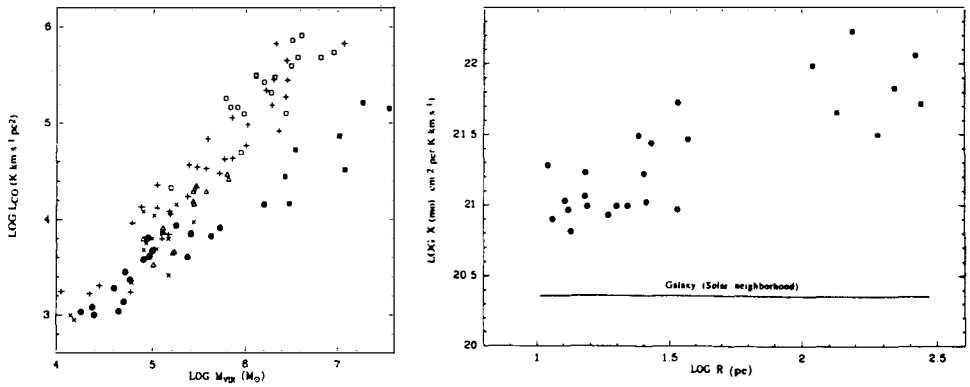

Figure 3: a) The CO(1-0) luminosity as a function of the virial mass M_{vir} for SMC (filled symbols) and Galactic clouds (open symbols); b) The H_2/CO conversion ratio in function of cloud sizes in the SMC (from Rubio et al 1992).

Molecular clouds therefore seem to be self-gravitating, and supported by their internal turbulence. At small scale, this turbulence is maintained by the star-formation energy (stellar winds, expanding HII regions, supernovae..), and at large-scale, the rotational energy of the galaxy is progressively dissipated in disordered motions, by viscous shear (Fleck 1981), or gravitational viscosity (Jog & Ostriker 1988).

3. RINGS, BARS AND SPIRAL STRUCTURE

Radial Distributions and Rings

In comparison to the HI gas, the molecular component is much more concentrated to the optical disk. However, there exist peaked distribution (example NGC 6946), as well as depletions in the center (M31, M81). Nuclear rings have frequently been discovered (Sofue 1991, fig. 4). These rings correspond in barred galaxies to the HII rings (Hα hot spots); they are from 200pc to a few kpc in diameter.

The depletions in the center could be explained by gas consumption by star-formation. This is the case for the Andromeda galaxy, where no gas (HI, HII, H_2) exists in the center, which consists only of an old stellar population.

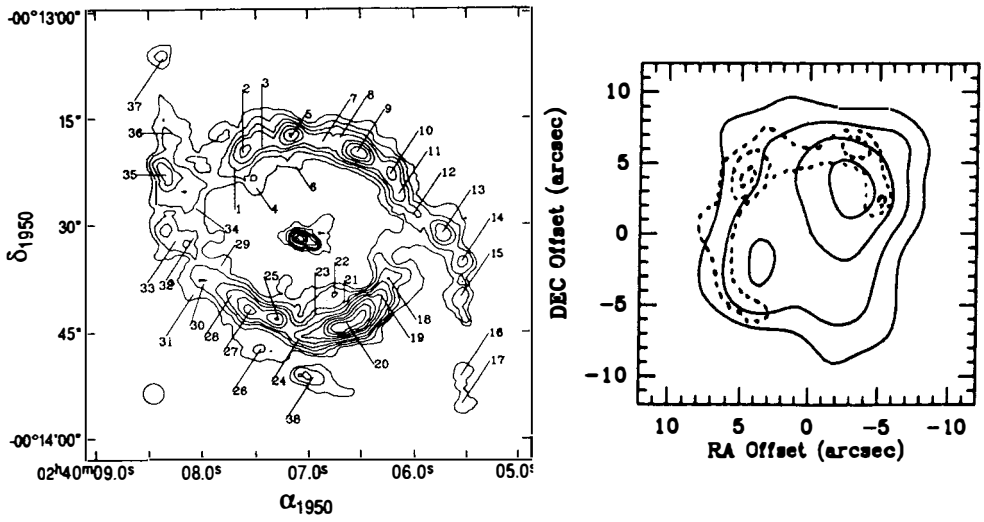

Figure 4: a) CO map of the NGC 1068 center (Planesas et al 1991); b) CO contours in the center of NGC 4314 (filled), compared with radiocontinuum contours (dashed) (Combes et al 1992).

Nuclear rings are usually located at the turn-over of the rotation curve: this has been the justification for the viscous torques mechanism (Lesch et al 1990): inside the turn-over, there is no shear (rigid-body rotation), and no viscous torques. However, the turn-over point corresponds also to the inner Lindblad resonance, when there is a bar in the galaxy. Gravitational torques are then very efficient to drive the disk gas towards the ILR (Combes 1991).

Recently, we mapped in CO with the Nobeyama interferometer the nuclear ring in NGC 4314 (Combes et al 1992, fig. 4). The molecular ring is located inside the ring of continuum emission, which traces the recent star formation. We suggest that the molecular ring is evolving slowly, reducing its radius due to dynamical friction exerted by the background stars on the giant molecular clouds.

Bars

When a galaxy is strongly barred (SB), the CO emission is highly concentrated towards the center, and also aligned along the bar (NGC 1097, Gerin et al 1988; M83, Handa et al 1991; NGC 1365, Sandquist et al 1992). More precisely, when interferometric resolution is available, CO emission is seen associated with the characteristic dust lanes.

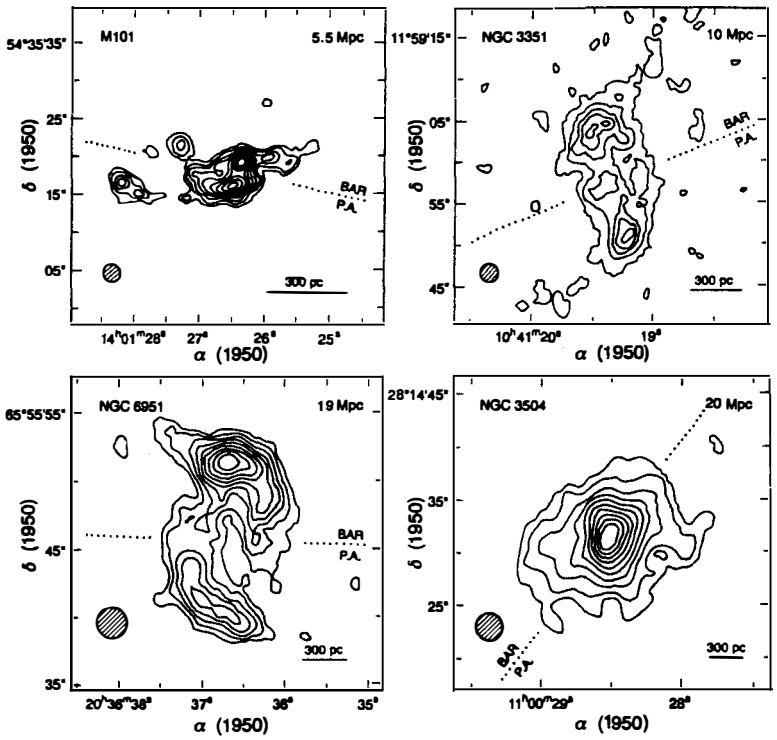

Figure 5: Interferometric CO maps of the centers of M101, NGC 3351, NGC 6951 and NGC 3504 (from Kenney 1991). The large-scale stellar bars are 2-3 larger than the size of each frame and have position angles indicated by the dotted lines. The peaks of CO emission occur where dust lanes intersect rings near inner Lindblad resonance.

Molecular bars have been very frequently discovered in non-barred galaxies, or galaxies of the intermediate-type when there is only an oval distortion. The H_2 gas is such a cold component (with velocity dispersion down to 4km/s) that it reveals strong and thin bars, even in spiral galaxies that were not suspected optically to be barred: NGC 6946 (Ball et al 1984; Ishizuki et al 1990a), IC 342 (Lo et al 1984, Ishizuki et al 1990b); M101 (Kenney 1991a).

A suggested possibility is that the molecular gas is so abundant in the center of galaxies, that it becomes self-gravitating and unstable to its own bar formation. However, the observed molecular bars until now always appear to trace a large-scale potential; they sometimes appear in the center perpendicular to the main bar, due to the presence of two inner Lindblad resonances (Kenney 1991b; Devereux et al 1992, fig. 5).

Spiral Structure

It has been established for a long time that star-formation is enhanced in spiral arms. Then it is necessary to precise the relationship between the density-wave, the formation of giant molecular clouds, and star-formation. Are the arms brighter in the blue because the density wave triggers star formation, or because more molecular clouds are formed in the arms?

Spiral structure has been resolved by mm-wave instruments only since 1986. A lot of work has been devoted to the prototype grand-design spiral M51, and some other nearby galaxies listed in Table 1. Some discrepancies have arisen about the position of molecular arms in M51, but this can simply due to the observational method. While single-dishes are sensitive to all spatial frequencies of the signal, interferometers only see contrasted emission and fail to detect the signal extended in their primary beam. In M51, about 20% of the emission only is detected, and addition of short spacings are essential (Lo et al 1991).

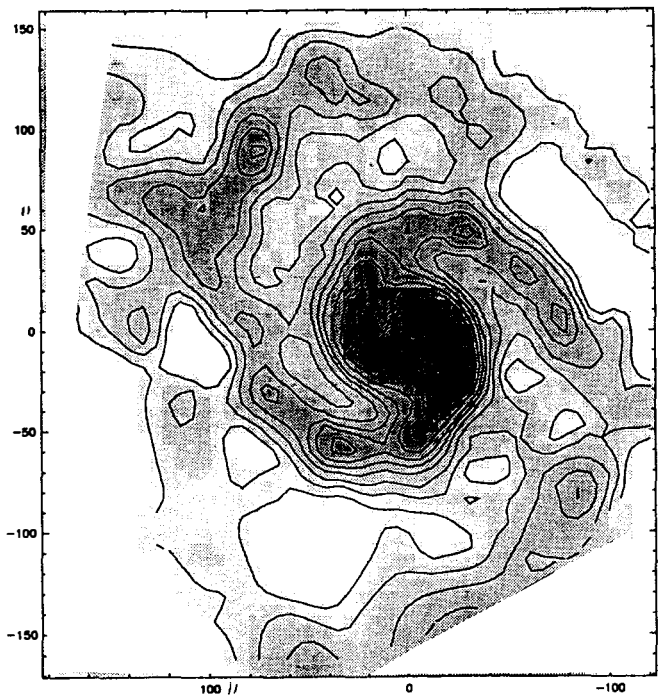

Figure 6: The M51 CO(2-1) map carried out at the IRAM 30m with 12" resolution (from Garcia-Burillo et al 1992).

The spiral structure in molecular clouds is highly contrasted: the ratio of the arm to the interarm emissions vary from 2 in the center to 12 in the outer parts (Garcia-Burillo & Guélin 1991; fig. 6). This can be explained by the longer time spent between two arms in the outer parts, and by the larger amount of molecular gas in the center. The contrast is higher than in the near-infrared (stellar component) and the HI; this can be due only to the lower velocity dispersion of the molecular clouds.

Table 1: Galaxies where spiral structure is resolved

Name	Arm Class	D Mpc	θ "	size pc	Bar?	$M(H_2)$ 10^8 $M_\odot$	Ref
M31	-	0.7	7	23	Y	2.5	1
M33	5	0.8	7	26	N	?	2
M81	12	3.3	12	200	N	3.5	3
M83	9	3.7	16	280	Y	50	4
IC342	9	4.6	2	50	Y	52	5
N6946	9	5	4	100	Y	23	6
M101	9	5.5	2	220	Y	33	7
M51	12	9.6	4	190	Y	130	8

The arm class is from Elmegreen & Elmegreen (1984)
θ is the highest resolution obtained for each galaxy, which corresponds to the given size in pc.
References: (1) Vogel et al 1987; Ichikawa et al 1987; Casoli & Combes 1988; Dame et al 1991 (2) Wilson & Scoville 1989, 1990 (3) Brouillet et al 1991 (4) Wiklind et al 1990; Handa et al 1991 (5) Lo et al 1984; Eckart et al 1990; Ishizuki et al 1990b; Rydbeck et al 1991 (6) Ball et al 1985; Casoli et al 1990; Ishizuki et al 1990a (7) Kenney et al 1991; Kenney 1991a,b (8) Lo et al 1987, Rand & Kulkarni 1990; Tosaki et al 1991; Garcia-Burillo et al 1992

In M51, the CO ridges (seen with the interferometers) are associated with the thin dust lanes, and with the non-thermal radio-continuum emission, in the concave parts inside the arms. On the contrary, the HI is found downstream, with the thermal continuum and the HII regions. This has been interpreted in terms of HI formation by destruction of molecular clouds and H_2 photodissociation due to star formation in the arms (Vogel et al 1988).

But only the high contrasted CO structures are shifted with respect to other tracers of star-formation. Most of the molecular mass is distributed in a broad spiral arms, coincident with the optical arm. In other galaxies as well, the CO arms are completely coincident with the HI and HII arms (NGC 6946, Casoli et al 1990; M83, Wiklind et al 1990).

4. GLOBAL CONTENT

Morphological type

There is no evidence of the total molecular mass to vary along the Hubble sequence. The $M(H_2)/L_B$ is constant from Sa to Sc, then the CO luminosity decreases somewhat with respect to L_B, but this could be due to a metallicity decrease. As for the $M(H_2)/M(HI)$ ratio, it decreases from 4 for Sa to 0.2 for Sd/Sm, but this is essentially due to the well-known larger percentage of HI mass for late-type galaxies. When the total gas mass is considered (H2 + HI), then M_{gas}/M_{dyn} increases slightly along the Hubble sequence (Young & Scoville 1991). The surface density of gas over the optical area is in average $17 M_\odot$ pc^{-2} within a factor 2.

Influence of the environment

While HI gas is deficient in cluster spiral galaxies, no deficiency has been observed in the molecular component. The H_2 gas is likely to be much less sensitive to ram pressure because of its larger column density, and also its central distribution makes it more bound to the galaxy. For this, tidal stripping too is expected to be much less efficient. The Virgo spirals have been surveyed by Kenney & Young (1988), and some Coma spirals by Casoli et al (1991) without any evidence of H_2 deficiency.

The molecular content does depend however on the environment, in the sense that interacting and merging galaxies have a higher molecular mass than normal isolated galaxies. This result has been derived from a survey of a hundred galaxies carried out at the IRAM 30m telescope (Braine et al 1992), and from the existing data in the litterature (Young et al 1989; Solomon & Sage 1988; Tinney et al 1990).

The sample of the IRAM survey includes all spiral galaxies with $B_T < 12$ mag, with heliocentric velocities between 500 and 1700kms (i.e. between about 7 and 24 Mpc), and with declinations limitations. We observed simultaneoulsy in the CO(1-0) and CO(2-1) lines 9-points maps in the center of the galaxies, and major or minor-axis cuts. The beam of the telescope is 23" and 12" respectively in the two CO lines. 81 galaxies of the sample have been observed and 60 detected (Braine et al 1992).

We classed the galaxies either as Disturbed (presumably interacting now or in the recent past), Close (cluster or near neighbor but without optical signs of interaction or disturbance), or Isolated. The environment was determined through inspection of Palomar Sky Survey plates. The relative population fractions of the three classes are 28% D, 42% C and 29% I.

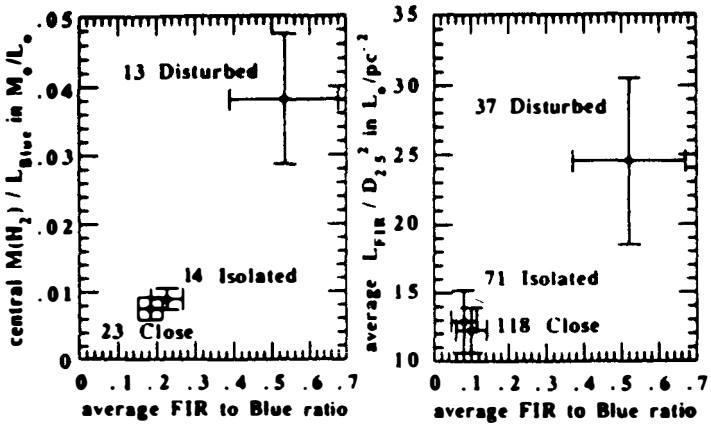

Figure 7: a) Central H_2 versus FIR, both normalized to the blue luminosity, for the IRAM sample; b) FIR surface brightness versus FIR to blue light ratio for a larger sample, classed by interaction type (from Braine & Combes 1992).

We confirm that the CO emission does not highly depend on morphological type, neither the CO(2-1)/CO(1-0) line ratio. The most striking result is that Disturbed galaxies have more CO emission that the two other classes, in absolute measure as well as relative to the blue luminosity or dynamical mass (to get rid of size effects). Fig. 7 shows that D galaxies have 4 times more CO emission, normalized to the blue luminosity. This result is valid for the CO(1-0) line as well as the CO(2-1) line (Braine & Combes 1992).

Since this result concerns only the central parts of galaxies, we compared our results with previous studies, classifiying the galaxies in the same way (D, C, I). Similar results are obtained: Disturbed galaxies have stronger normalized CO emission compared to Isolated and Close.

We have only divided our galaxies into three environment classes but a continuous index would be preferable to avoid averaging and discrete effects. Since Disturbed galaxies have also a higher FIR to blue luminosity ratio, and a higher FIR luminosity to optical area ratio (or average FIR surface brightness) (fig. 7), we will use the latter as our "interaction indicators". Fig. 8 shows the total H_2 mass surface density versus the FIR surface brightness. We can see that the CO emission increases linearly over two orders of magnitude.

Excitation of the gas, and the H_2-CO conversion ratio

The above H_2 masses were computed using the standard factor to convert the CO luminosity to a molecular mass. We know that this ratio will vary as $\rho^{1/2}/T_b$, or $n(H_2)^{1/2}/T_b$ (cf §2). Several observational clues confirm now that the average density $n(H_2)$ of molecular clouds is not lower in interacting galaxies and mergers. Density is traced by molecules like CS and HCN with high dipole moments and lines from these molecules have been observed with similar ratios with respect to the CO(1-0) line than in the Milky Way (Sage et al 1990).

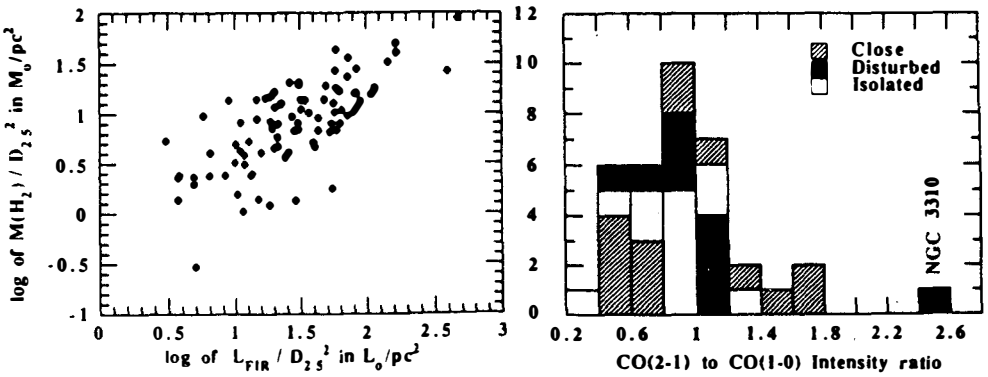

Figure 8: The normalized H_2 content versus an indicator of interaction, FIR surface brightness (Braine & Combes 1992).

Figure 9: Histogram of CO line ratios for the IRAM sample, divided into interaction classes.

In parallel, brightness temperatures T_b appear to be comparable to those of the Milky Way clouds. Our CO(1-0) and CO(2-1) survey in nearby galaxies reveals that the excitation of the CO gas is remarkably similar from one galaxy to the other and in particular that it varies little with the interaction type of the galaxy. The histogram of the CO line ratios is shown in fig. 9. The clustering of the ratios about a mean of 0.9 is a strong indication that much of the gas is thermalized and optically thick. The excitation temperature of the clouds is around 15K. These physical conditions have also been found for more active starbursts (Casoli et al 1988; Solomon et al 1990; Radford et al 1991).

The only observational data that make us suspect that the CO to H_2 conversion ratio is not the same in IRAS luminous galaxies and mergers is that mergers generally have a lower ^{13}CO to ^{12}CO intensity ratio (Casoli et al 1992a). Observation of $C^{18}O$ in the merger NGC 3256 means that the low ^{13}CO to ^{12}CO ratio (four times lower than usual) is not caused by a change in optical depth (Casoli et al. 1992b). On the contrary, the abnormally low ^{13}CO emission may be the result of a tidally-triggered infall of a large quantity of unprocessed gas from the outer parts of the disk. ^{13}CO is indeed a secondary element generated in stars of intermediate-mass and thus has not had time to enrich the ISM (e.g. Langer & Penzias 1990; Sage et al. 1991).

If merging systems do contain unprocessed gas, the H_2/CO conversion factor would be higher in merging and interacting galaxies, and the latter will have even more H_2 masses than the normal isolated galaxies.

Given that our sample does not contain such extreme mergers, we adopt the standard ratio, and deduce that **interacting galaxies have more H_2 masses.** This increase in H_2 mass could only be due to the transformation of HI into H_2, without increasing the total gas mass; to test this hypothesis, we plot now the HI content in function of interaction indicator (fig. 10). The absence of correlation reveals that the HI is not different in interacting galaxies. The increase in H_2 cannot be accounted for by a decrease in HI, and thus the total gas masses increase in interacting galaxies.

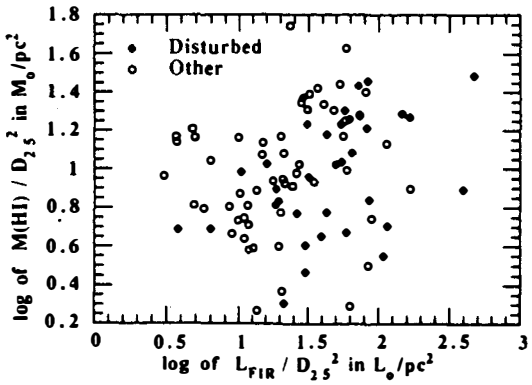

Figure 10: Same as fig. 8, but for the HI content.

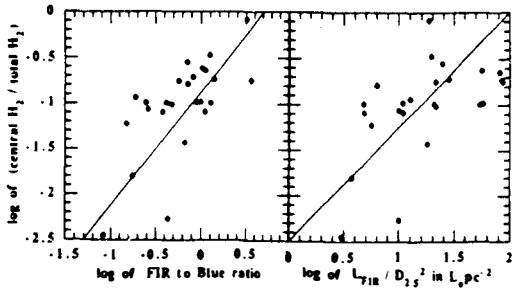

Figure 11: The degree of concentration of the H_2 gas (central H_2/total H_2) versus two interaction indicators, FIR to blue and FIR surface brightness. Lines are power-laws of slope 1.25 (Braine & Combes 1992).

For the galaxies of our sample, where we have the central H_2 content, that are also included in other samples observed with a larger beam, we investigated the ratio of the central to global H_2 content as a function of the interaction indicators. Fig. 11 shows that there is more H_2 gas concentration in disturbed galaxies. An increase of the surface density of H_2 has also been observed in ultraluminous IRAS objects (Scoville et al 1991; Okumura et al 1991).

Where does the excess gas come from?

Disturbed galaxies have more molecular gas than isolated or unperturbed galaxies. This is true both in an absolute sense, per unit blue luminosity, and per unit dynamical mass. Unless the disturbed galaxies were different from the others even before being perturbed, we must account for this new gas.

The need to bring gas inwards from outside the disk is even more crucial in extreme starbursting galaxies such as Arp 220 or Mkn 231. Their H_2 masses are about a factor 10 higher than those of almost any two isolated spiral galaxies. This implies that the majority of the gas in these mergers must come from outside the thin disk because the disks alone simply do not contain this much gas.

Several less direct but independent observations indicate that large reservoirs of unobserved gas exist. A "thick disk" of ionized gas with $n = 1cm^{-3}$ and $500 < T_e < 1000$ was proposed by Israel & Mahoney (1990) to explain the free-free absorption they observed at 57.5MHz. HI searches (Lo & Sargent 1979) have not detected HI gas at large radii but HI emission is several orders of magnitude less sensitive than absorption line searches. Petitjean & Bergeron (1990) and Bergeron & Boissé (1991) find MgII and Lyman α absorption in positions more than 100 kpc from the nucleus of some absorbing galaxies and deduce gas column densities of about 10^{20} cm^{-2}. Observational evidence for gas reservoirs of 10^{10} - 10^{11} M_0 therefore exists.

Theoretical arguments also point to the existence of gas reservoirs or continuous infall. Binney (1991) proposed that accretion of material (possibly dwarf galaxies) onto a massive primary galaxy could explain the frequent occurrence of warps. A second argument is that the gas consumption timescale due to star formation in spiral galaxies is of the order of a few 10^9 years and even less in starbursting systems (Larson 1987) so accretion or infall of fresh gas is probably required to replenish the disk. A third argument is given by the maintenance of spiral structure (Toomre 1990). The spiral wave transfers gas from the disk towards the center or the inner Lindblad resonance. If the dissipative medium disappears, the spiral structure will be washed away on the timescale of a rotation period.

In the outer parts of galaxies, outside the HI disk, gas must be in ionised form at temperatures 10^3-10^4 K. The main energy source for these outer regions is heating by absorption of UV from QSO (Heisler & Ostriker 1988). This keeps the gas from condensing in the absence of a perturbation. Once a perturbation causes the density to increase, the near-equilibrium state is pushed towards net cooling.

The gas is not pressure-supported, and must be rotating around the galactic center in a thick plane. Viscous torques are negligible at such a distance to produce a slow infall (Lynden-Bell & Pringle 1974). Only a violent non-axisymmetry such as that due to an interacting companion could produce the gravitational torques necessary for the gas to lose its angular-momentum. The time-scales of gas infall is of the order of the rotation period, i.e. 10^9 yrs at 50kpc

(Combes 1991). Simulations of interacting and merging galaxies (Barnes 1989; Barnes & Hernquist 1991) have shown that a high amount of interstellar gas can infall towards the central merging systems by gravitational torques.

The gas does not accumulate in the HI phase, since the time-scale to transform HI into H_2 during cloud-cloud collisions is only of the order of 10^6 yrs (e.g. Smith 1980). This can explain why the average HI surface density remains relatively constant in interacting galaxies. In the ultraluminous IRAS galaxies, there is however a tendency for the normalized HI content to decrease (Mirabel & Sanders 1989; Martin et al 1991). This could be interpreted as a shortage of gas from the outer parts.

5. CONCLUSIONS

The global H_2 content of spiral galaxies does not vary significantly with morphological type, nor with the presence of a bar or spiral structure. Interacting galaxies have more H_2 gas, while keeping their average HI surface density constant. The H_2 gas is also more concentrated in Disturbed galaxies. Only in extreme interacting systems and mergers, does the HI content begin to decrease. We propose that galaxies are surrounded by large gas reservoirs in the form of highly ionised medium. During galaxy interactions, this gas is driven towards the center, where it cools down and condenses onto the disk.

REFERENCES

Ball R., Sargent A.I., Scoville N.Z., Lo K.Y., Scott S.: 1985, ApJ 298, L21
Barnes J. E.: 1989 Nature 338, 123
Barnes J.E., Hernquist L.: 1991, ApJ 370, L65
Bergeron, J., Boissé, P. 1991, A&A 243, 344.
Binney, J. 1991, in Dynamics of Disk Galaxies, ed. B. Sundelius (Göteborg, Sweden) page 297.
Braine, J., Combes, F., Casoli, F. et al. 1992, A&A in press (Paper I)
Braine, J., Combes, F. 1992, A&A submitted (Paper II and III)
Brouillet N., Baudry A., Combes F., Kaufman M., Bash F.: 1991, A&A 242, 35
Casoli F., Boisse P., Combes F., Dupraz C.: 1991, A&A 249, 359
Casoli F., Combes F.: 1988 A&A 198, 43
Casoli F., Combes F., Dupraz C. et al. : 1988 A&A 192, L17
Casoli F., Clausset F., Viallefond F., Combes F., Boulanger F.: 1990, A&A 233, 357
Casoli, F., Dupraz, C. & Combes, F. 1992a, A&A in press
Casoli, F., Dupraz, C. & Combes, F. 1992b, A&A in press
Cohen, R.S., Dame, T.M., Garay, G. et al. 1988, ApJ 311, L95.
Combes, F. 1991, in IAU 146 Dynamics of Galaxies and their Molecular Cloud Distributions, eds. F. Combes and F. Casoli, Kluwer p. 255.
Combes F., Gerin M., Nakai N., Kawabe R., Shaw M.A. 1992: A&A in press
Dame T.M., Koper E., Israel F., Thaddeus P.: 1991 in "Dynamics of Galaxies and their Molecular Cloud Distributions", ed. F. Combes & F. Casoli, Kluwer, IAU 146, page 23
Devereux N. A., Kenney J.D.P., Young J.S. 1992, AJ 103, 784
Dickman R.L. 1978: ApJS 37, 407
Dickman, R.L., Snell, R.L., Schloerb, F.P. 1986, ApJ 309, 326.
Eckart A., Downes D., Genzel R., Harris A.I., Jaffe D.T., Wild W.: 1990 ApJ 348, 434
Elmegreen D.M., Elmegreen B.G.: 1984 ApJS 54, 127
Fleck R.C.: 1981, ApJ 246, L151
Garcia-Burillo S., Guelin M., Cernicharo J. 1992: A&A in press

Garcia-Burillo S., Guélin M.: 1991, in "Dynamics of Galaxies and their Molecular Cloud Distributions", ed. F. Combes & F. Casoli, Kluwer, IAU 146, page 67
Gerin M., Nakai N., Combes F.: 1988, A&A 203, 44
Handa T., Sofue Y., Nakai N.: 1991 in "Dynamics of Galaxies and their Molecular Cloud Distributions", ed. F. Combes & F. Casoli, Kluwer, IAU 146, page 156
Heisler, J., Ostriker, J.P. 1988, ApJ 332, 543.
Ichikawa T., Nakano M., Tanaka Y.D.: 1987 I.A.U. 115, Star Forming Regions, eds M. Peimbert & J. Jugaku , page 622
Ishizuki S., Kawabe R., Ishiguro M., Okumura S.K., Morita K-I., Chikada Y., Kasuga T, Doi M.: 1990a ApJ 355, 436
Ishizuki S., Kawabe R., Ishiguro M., Okumura S.K., Morita K-I., Chikada Y., & Kasuga T: 1990b Nature 344, 224
Israel, F.P., Mahoney, M.J. 1990, ApJ 352, 30.
Jog C., Ostriker J.P.: 1988, ApJ 337, 1035
Kenney J.D. and Young J. S. 1988, ApJS 66, 261
Kenney J.D., Scoville N.Z., Wilson C.D.: 1991, ApJ 366, 432
Kenney J.D. 1991a: in "Dynamics of Galaxies and their Molecular Cloud Distributions", ed. F. Combes & F. Casoli, Kluwer, IAU 146, page 265
Kenney J.D. 1991b: in "Dynamics of disk galaxies", ed B. Sundelius,p. 171
Langer, W.D., Penzias, A.A., 1990 ApJ 357, 477.
Larson, R.B. 1987, in Starbursts and Galaxy Evolution, eds. T.X. Thuan, T. Montmerle, and J. Tran Thanh van (Editions Frontières: Gif sur Yvette) page 467.
Lesch H. et al.: 1990, MNRAS 242, 194
Lo K.Y., et al: 1984, ApJ 282, L59
Lo K.Y., Ball R., Masson C.R., Phillips T.G., Scott S., Woody D.P.: 1987, ApJ 317, L63
Lo K.Y., Adler D.S., Allen R.J., Plante R., Wright M.C.H., Rydbeck G.: 1991 in "Dynamics of Galaxies and their Molecular Cloud Distributions", ed. F. Combes & F. Casoli, Kluwer, IAU 146, page 81
Lo K. Y., Sargent, W.L.W. 1979, ApJ 227, 756.
Lynden-Bell D., Pringle J.E.: 1974 MNRAS 168, 603
Martin, J.-M., Bottinelli, L., Dennefeld, M., Gougenheim, L. 1991, A&A 245, 393.
Mirabel I.F., Sanders D.B.: 1989, ApJ 340, L53
Okumura, S.F., Kawabe, R., Ishiguro, M. et al. 1991, in IAU 146, page 425.
Petitjean, P., Bergeron, J. 1990, A&A 231, 309.
Planesas P., Scoville N.Z., Myers S.T.: 1991 ApJ 369, 364
Radford S.J.E., Solomon P.M., Downes D.: 1991 ApJ 368, L15
Rand R.J., Kulkarni S.R.: 1990, ApJ 349, L43
Rubio, M., Garay, G., Montani, J., Thaddeus, P. 1991, ApJ 368, 173.
Rubio M., Lequeux J., Boulanger F. 1992, A&A in press
Rydbeck G., Hjalmarson A., Wiklind T., Olofsson H., Rydbeck O.E.H.: 1991, in "Dynamics of Galaxies and their Molecular Cloud Distributions", ed. F. Combes & F. Casoli, Kluwer, IAU 146, page 59
Sandquist Aa., Elfhag T., Jörsäter S., Lindblad P.O.: 1992, preprint
Sage L.J, Shore S.N., Solomon P.M.: 1990 ApJ 351, 422
Sage, L.J., Mauersberger, R., Henkel, C. 1991, A&A 249, 31.
Scoville N.Z., Sargent A.I., Sanders D.B., Soifer B.T.: 1991 ApJ 366, L5
Sofue Y., 1991 in "Dynamics of Galaxies and their Molecular Cloud Distributions", ed. F. Combes & F. Casoli, Kluwer, IAU 146, page 287
Solomon, P.M., Rivolo, A.R., Barrett, J.W. & Yahil, A. 1987, ApJ 319, 730.
Solomon P. M., Sage L. J. 1988, ApJ 613, 334
Solomon P.M., Rivolo A.R.: 1989, ApJ 339, 919
Solomon P.M., Radford S.J.E., Downes D.: 1990 ApJ 348, L53
Solomon P.M., Downes D., Radford S.J.E.: 1992 ApJ 387, L55
Smith J.: 1980 ApJ 238, 842
Strong, A.W., Bloemen, J.B.G.M., Lebrun, F., et al. 1988, A&A 207, 1.
Tacconi L., Young J.S. (1986) ApJ 322, 681

Tinney, C.G., Scoville, N.Z., Sanders, D.B., Soifer, B.T. 1990, ApJ 362, 473
Toomre, A. in Dynamics and Interactions of Galaxies, ed Wielen, R., 1990 (Springer-Verlag: Berlin) page 292.
Tosaki T., Kawabe R., Ishiguro M., Okumura K., Morita K-I, Kasuga T., Ishizuki S.: 1991, in "Dynamics of Galaxies and their Molecular Cloud Distributions", ed. F. Combes & F. Casoli, Kluwer, IAU 146, page 79
Vogel S.N., Boulanger F., Ball R: 1987, ApJ 321, L145
Vogel S.N., Kulkarni S.R., Scoville N.Z.: 1988, Nature 334, 402
Wiklind T., Rydbeck G., Hjalmarson A., Bergman P.: 1990, A&A 232, L11
Wilson C.D., Scoville N.Z.: 1989, ApJ 347, 743
Wilson C.D., Scoville N.Z.: 1990, ApJ 363, 435
Young, J. S., Scoville, N. Z. 1991, ARAA 29, 581.
Young, J. S., Xie, S., Kenney, J. D. P., Rice, W. L. 1989, ApJS 70, 699

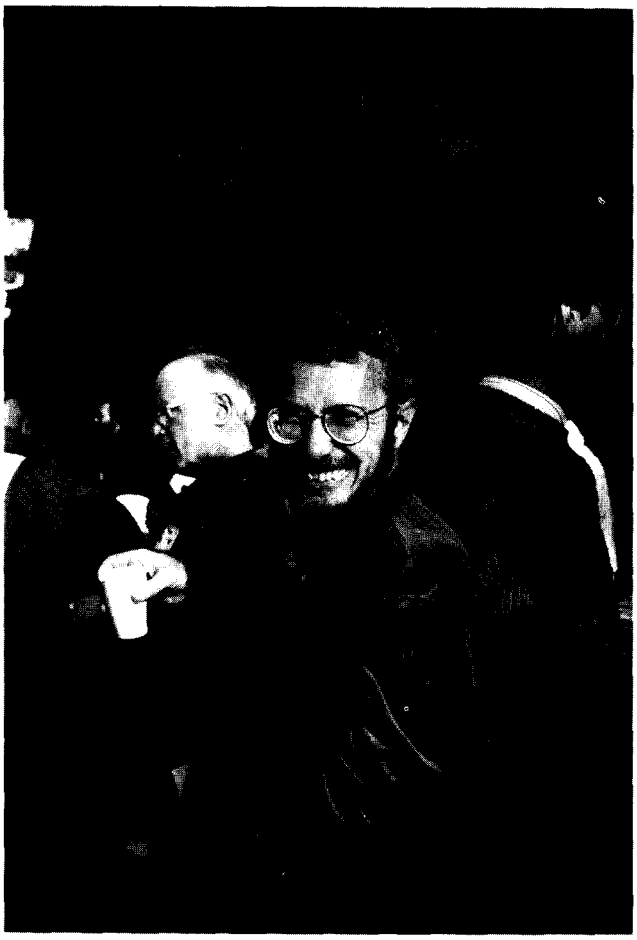

X-RAY EMISSION FROM GALAXIES

Craig L. Sarazin
Astronomy Department, University of Virginia
Box 3818, Charlottesville, VA 22903-0818 U.S.A.

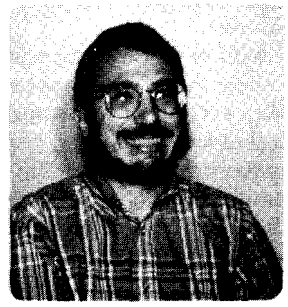

ABSTRACT

The X-ray properties of galaxies are reviewed. The nature of the dominant X-ray emission processes for galaxies varies along the Hubble sequence. In late-type galaxies, the X-ray emission is dominated by a stellar component; most of the X-rays come from high mass binary stars and supernova remnants. By contrast, the X-ray emission from early-type galaxies (ellipticals and S0s) is dominated by emission from hot interstellar gas. The discovery of this hot gas in ellipticals resolved the long-standing question of the fate of gas produced by normal stellar mass loss. Of particular interest in X-rays are the very large D or cD galaxies located at the centers of many clusters of galaxies. X-ray observations show that large amounts of initially hot gas are cooling onto many of these galaxies. Typical cooling rates are $\sim$100 $M_\odot$/yr. New ROSAT high resolution X-ray images are presented for the two cD galaxies located at the centers of the cooling flow clusters A2029 and 2A0335+096. These high resolution images show that the X-ray emission from the cooling flow region comes primarily from filamentary structures. The high densities associated with these X-ray filaments indicate that they cannot be in hydrostatic equilibrium. Other forces such as rotation, turbulence, and particularly magnetic fields may play an important role in these systems.

1. Introduction

Observations with the *Einstein* X-ray Observatory showed that all types of galaxies produce significant amounts of X-ray emission. The first half of this paper (§ 2,3) gives a very brief review of the X-ray properties of "normal" galaxies. "Normal" here is taken to mean galaxies which are not dominated by an active nucleus, and which are not located in the central regions of a rich cluster of galaxies. In the second half of this paper (§ 4–7), I will present some new results from ROSAT observations of the luminous D and cD galaxies which are located at the centers of rich clusters. These galaxies are at the centers of X-ray "cooling flows". There are several recent reviews of cooling flows[1][2].

The *Einstein* Observatory measurements showed that most normal galaxies have X-ray luminosities in the range $L_X \approx 10^{38} - 10^{42}$ ergs/s. (I assume $H_o = 50$ km s^{-1} Mpc^{-1} and $q_o = 1/2$ throughout this paper.) Generally, this is a small fraction of the bolometric luminosity of galaxies. However, this emission is still of considerable interest, because X-ray observations of galaxies can provide important information on the interstellar medium and the stellar population in galaxies.

The gravitational potential wells of galaxies correspond to velocity dispersions which are typically ~300 km/sec. If these gravitational potential energies are translated into thermal energies per particle, they correspond to temperatures on the order of $10^6 - 10^7$ K. In fact, all galaxian systems (individual galaxies, groups of galaxies, and rich clusters of galaxies) have gravitational potentials corresponding to characteristic temperatures in the range $10^6 - 10^8$ K. This implies that any volume–filling thermal plasma which is in dynamical equilibrium will have a temperature on this order. For a thermal plasma with a temperature of this order, the dominant emission is in the X-ray band. Thus, X-ray observations provide information on the volume–filling component of the interstellar medium. This component is also likely to provide the dominant pressure in the interstellar medium on the largest scales.

The other major source of X-ray emission in galaxies is associated with their stellar population. Very luminous X-ray emission is produced by accretion processes in binary stars containing compact objects. In many cases, these compact objects are the result of the stellar evolution of very massive stars. There is also a contribution to the X-ray emission from our own galaxy which is associated with lower mass X-ray binary stars. Thus, X-ray emission provides unique information on the binary component of the stellar composition of galaxies. X-ray observations of galaxies also provide information on the most massive stars in the galaxy (either single or multiple); these stars produce supernovae and supernova remnants, which are also important sources of X-ray radiation. Because massive stars are short–lived, X-ray emission may be useful diagnostic of recent star formation.

There are a number of excellent reviews and comprehensive catalogs of the X-ray properties of normal galaxies. Fabbiano[3] gives a thorough review of the observed X-ray properties of normal galaxies. I have written a more theoretical review of X-ray emission from elliptical galaxies[4]. Roberts *et al.*[5] give a catalog of X-ray properties of early-type galaxies (ellipticals and S0s). This catalog also includes measurements of these galaxies in other spectral regimes, and lists evidence that the galaxies contain cooler interstellar matter. A comprehensive catalog of all the *Einstein* observations of normal galaxies is given by Fabbiano *et al.*[6]. A catalog of the X-ray spectra of normal galaxies observed with the *Einstein* observatory is given by Kim *et al.*[7]. The *Einstein* Observatory had rather limited spectral resolution and a narrow bandwidth. More detailed X-ray spectra

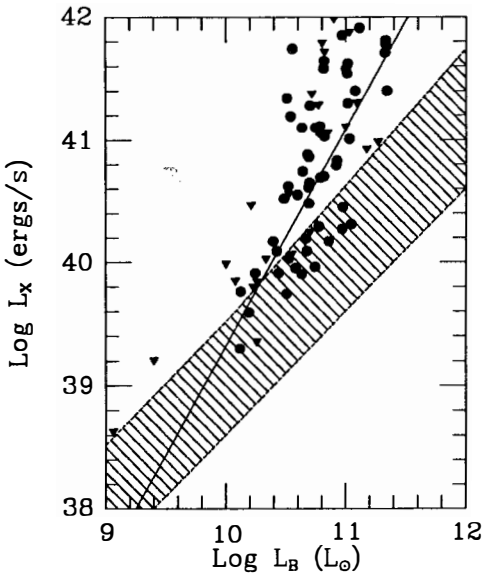

FIG. 1—The correlation of X-ray and optical luminosities of early-type galaxies[10]. The filled circles are detections, and the inverted triangles are upper limits. The solid line is the best-fit correlation. The hatched area gives the range of estimated stellar X-ray luminosities[4].

of a few bright, normal galaxies covering a wider bandwidth have been observed with the Ginga satellite[8].

2. X-Rays from Normal Elliptical and S0 Galaxies

Normal elliptical and S0 galaxies are very luminous X-ray sources, with typical X-ray luminosities of $L_X \sim 10^{39} - 10^{42}$ ergs/sec[9][10]. This applies to ellipticals and S0s which are not located near the centers of rich clusters of galaxies. At present, we do not know whether individual elliptical galaxies in clusters of galaxies are individual X-ray sources.

Elliptical galaxies produce extended, soft X-ray emission. There is a very strong, non-linear correlation between their optical and X-ray luminosities. Fig. 1 shows the correlation between the X-ray and optical luminosities of a sample of elliptical and S0 galaxies. The filled circles are detections, while the arrows mark upper limits on the X-ray luminosity. This X-ray—optical correlation is roughly of the form $L_X \propto L_B^2$. Because of the non-linear dependence of X-ray luminosity on optical luminosity, this correlation is unlikely to be the result of a flux limited sample. On the other hand, uncertainties in the distance can strongly affect the correlation. Note also that there is a considerable dispersion around this correlation.

Detailed observations with the *Einstein* Observatory were made primarily for the brighter X-ray ellipticals and S0s. At least for these brighter X-ray ellipticals and S0s, it seems clear that the X-ray emission is thermal emission from hot interstellar gas. The temperature of this gas is $T \approx 10^7$ K. From the X-ray surface brightness observed in ellipticals, we deduce that the interstellar gas density varies with radius roughly as $\rho_{gas} \propto r^{-3/2}$. When the inferred gas density is integrated over the entire image of an elliptical,

gas masses are found to be in the range $M_{gas} \sim 10^9 - 10^{11} M_\odot$. Unfortunately, the observed gas density distribution leads to a mass which diverges rapidly at large radii. Because of the X-ray background, the X-ray surface brightness of ellipticals is poorly determined at large radii. Thus, the total gas masses are relatively uncertain. If the observed gas masses are compared with the mass of stars in the elliptical galaxy (assuming a reasonable stellar mass–to–light ratio), the proportion of gas mass to stellar mass is typically $M_{gas}/M_* \approx 0.02$.

The discovery of this X-ray emission from elliptical galaxies has resolved one of the long-standing mysteries about early-type galaxies. The stars in these galaxies must be losing mass at a significant rate, through red giant winds and planetary nebulae. However, very little cool interstellar gas is seen in most of these galaxies. It now appears that in isolated elliptical galaxies, the gas from stellar mass loss is not removed from the galaxies, but is stored as hot interstellar gas. The source of the hot X-ray emitting gas is simply this normal stellar mass loss. For the stellar population in elliptical and S0 galaxies, the expected rate of stellar mass loss is on the order of $\dot{M}_* \approx 1 M_\odot$/year in a large elliptical galaxy.

Why is it that the interstellar gas in elliptical galaxies is hot, while the interstellar gas in spiral galaxies is for the most part relatively cool? There are several important heating processes associated with stellar mass loss in elliptical galaxies. First of all, stars in elliptical galaxies move about on random orbits. In contrast, stars in spiral galaxies move together in circular motion in the disk. As a result, the relative velocities between nearby stars in elliptical galaxies are much larger than those between nearby stars in spiral galaxies. When gas is lost from a star in an elliptical galaxy, it will tend to collide with gas either sitting in the galaxy or gas which was shed from another star in the galaxy. Because of the high relative velocities of stars in elliptical galaxies, gas which is lost from the stars in these galaxies will collide at high velocity and be shocked to high temperatures. If the kinetic energy associated with the motions of stars in these galaxies is thermalized, it results in gas temperature on the order of 10^7 K. A second source of heating of the gas which is associated with its ejection from stars comes from Type Ia supernovae. These supernovae eject gas with tremendous amounts of kinetic energy. However, only a small proportion of the gas is ejected in this fashion. When the large kinetic energy associated with this ejected gas is diluted by the larger proportion of gas which is ejected by more tranquil processes, the net temperature which is produced is still typically greater than 10^7 K.

For the brighter X-ray elliptical galaxies for which we have the most detailed information, the inferred gas densities imply rather short cooling times. Typically, The cooling time t_{cool} is less than 10^{10} yr over the entire observed galaxy. This suggests that the gas is able to cool everywhere within the lifetime of the galaxy. Theoretical models of the evolution of galaxies indicate that when the gas is able to cool throughout the galaxy, it rapidly approaches a steady-state cooling configuration. In steady–state cooling, the rate of stellar mass loss is balanced by the cooling. The source of gas and heat associated with stellar mass loss equals the loss of hot gas and the loss of thermal energy through cooling. This cooling occurs through radiative emission of the X-rays, which we use to detect the gas. Steady-state cooling models for the hot gas in elliptical galaxies provide a reasonable fit to the observed X-ray luminosities, temperatures and surface brightness profiles of the brighter X-ray ellipticals.

As noted before, there is a considerable dispersion in the correlation between X-ray and optical luminosities of ellipticals and S0 galaxies (Fig. 1). The detailed studies of

elliptical galaxies with the *Einstein* Observatory were mainly confined to the brighter X-ray galaxies. There is a considerable uncertainty as to the origin of the X-ray emission in the fainter X-ray galaxies, and the nature of the interstellar gas in these systems. First of all, it is uncertain whether the X-ray emission from these galaxies is due to hot interstellar gas or to stellar X-ray binaries. Because of the late-type stellar population in elliptical galaxies, any stellar X-ray sources are probably low mass X-ray binaries (LMXRBs). The stellar evolution of LMXRBs is poorly understood, and it is very difficult to predict what contribution they might make to elliptical galaxies. Most estimates of the stellar contribution to the X-ray emission from ellipticals and S0s have been based on extrapolations from the X-ray emission of nearby spiral bulges. Unfortunately, there is a considerable range in these estimates[9][10]. Fig. 1 illustrates the range in the expected stellar X-ray contribution. The banded area shows the full range of stellar X-ray luminosities extrapolated for ellipticals from the literature.

Because LMXRBs have hard X-ray spectra, while hot interstellar gas must have a much softer X-ray spectrum, X-ray spectra of fainter elliptical and S0 galaxies should allow us to decide whether they are dominated by hot interstellar gas or LMXRBs. Such spectra should become available with the launch of ASTRO D next year.

Whatever the source of the X-ray emission in the faintest X-ray ellipticals, why is it that they are so much fainter than the brighter galaxies? One suggestion is that these galaxies have not yet reached steady-state cooling[11]. In non-steady-state models, the heat input from stellar mass loss goes into heating and inflating the gas in the galaxy, rather than directly into X-ray emission from the gas. Another possible explanation for the weakness of X-ray emission in these galaxies is that they have been stripped of much of their hot interstellar gas. White and Sarazin[12] suggested that ram pressure stripping of gas from elliptical galaxies lowers their X-ray luminosities significantly. The fainter elliptical galaxies tend to have more neighboring galaxies, which suggests that they are located in denser regions having denser intergalactic gas. This intergalactic gas could strip the interstellar gas from the galaxies. In any case, one certainly expects this process to apply to the elliptical galaxies located near the centers of rich clusters of galaxies.

3. X-Ray Emission from Spiral Galaxies

At least for the later Hubble–type spiral galaxies, the X-ray emission is believed to be dominated by stellar sources. In the nearest spiral galaxy to our own (Andromeda – M31), the X-ray emission has been nearly fully resolved into individual stellar sources[13] . In somewhat more distant spiral galaxies, the X-ray emission cannot be resolved completely, but it has a spatial distribution which suggests that it is stellar in origin, and is particularly correlated with high mass stars.

In our own galaxy, the X-ray emission is dominated by binary X-ray stars. There are two important classes of such X-ray binaries. First, there are the high mass X-ray binary stars (HMXRB). These are associated with very massive stars. In our galaxy, they are found predominantly in the spiral arms and within the disk of our galaxy. However, there is also a much more broadly distributed set of stellar X-ray sources. These are the so-called low mass X-ray binary stars (LMXRB). These LMXRBs are located in globular clusters and in the bulge of our galaxy; some are also found in the disk. The origin and stellar evolution of the HMXRBs is fairly well understood, at least in our own galaxy. On the other hand, we have a much poorer understanding of the LMXRBs. Another stellar source of X-rays which is associated with predominantly high mass stars are supernovae and particularly supernova remnants.

All of these stellar X-ray components produce rather hard X-ray spectra. For this reason, it is not surprising that the integrated X-ray spectra of spiral galaxies are hard[7]. By contrast, X-ray bright elliptical and S0 galaxies mainly have soft X-ray spectra. These spectra are consistent with emission from thermal gas at a temperature of about ten million degrees, which is the expected temperature of gas in hydrostatic equilibrium in these galaxies.

There are several other possible components to the X-ray emission from spiral galaxies. In most of the spirals which have been observed, these components would appear to be considerably weaker. First, many types of individual stars produce coronal X-ray emission. However, the integrated stellar coronal emission from spiral galaxies is appears to be relatively weak[14]. Second, diffuse hot interstellar gas might be an important contributor to the X-ray emission from spirals. In fact, at the time when the *Einstein* Observatory was launched, it was thought that large amounts of supernova-heated, hot interstellar gas would produce copious X-ray emission from spiral galaxies. Very little of this interstellar emission has been detected[15]. Both stellar coronae and hot interstellar gas would produce relatively soft X-ray emission. The hard X-ray spectra observed from spiral galaxies are an indication that these two components are not of great importance.

In late-type spiral galaxies, there is a rather good correlation between the X-ray luminosity and the blue optical luminosity, the radio luminosity, and particularly the far infrared luminosity[16]. All three of these longer wavelength diagnostics are believed to point to regions of current star formation. The correlation between current indicators of star formation and X-ray emission suggests that the X-ray emission from spiral galaxies is mainly from HMXRBs and supernova remnants.

4. D and cD Galaxies in Cooling Flow Clusters

Observations with the *Einstein* X-ray Observatory showed that large quantities of gas are cooling below X-ray emitting temperatures at the centers of many clusters of galaxies (see[1][2] for a recent review). The signatures of "cooling flow" clusters are centrally peaked X-ray morphologies[17] and X-ray spectral line emission from the cooling gas over a range of temperatures[18][19]. Typical cooling rates are $\dot{M}_c \sim 100\,M_\odot\,\mathrm{yr}^{-1}$, and the gas appears to cool over a wide range of radii, extending to $r_c \sim 200$ kpc[20][21]. Generally, it is thought that this indicates that the gas is inhomogeneous, with denser clumps of gas cooling more rapidly than lower density diffuse gas[1]. X-ray spectra of cooling flows also imply that they are inhomogeneous[19]. Physically large, dense clumps of gas would fall rapidly in to the nucleus of the central galaxy, and might be broken apart by hydrodynamic forces. This suggests that the clumps in the intracluster gas are rather small, with typical sizes of $\sim$10 pc[22]. In fact, the *Einstein* X-ray images of cooling flows are generally fairly smooth, which suggested that the inhomogeneities had not been spatially resolved (or that the gas is actually homogeneous).

The key question concerning these cooling flow is: what becomes of the cooling gas? X-ray spectra follow the cooling gas to about 3×10^6 K. Far UV observations of A2199 with ROSAT's Wide Field Camera[23] and optical coronal line observations[24][25] may trace the gas as it cools further to $\sim 10^5$ K. Cooling flows often show strong optical line emission from gas at $\sim 10^4$ K, although this gas is probably not excited directly by cooling[26]. In several cooling flow clusters, much cooler atomic and molecular gas and dust have been detected[27][28][29][30][31][32]. While it is tempting to think of all this material as part of a cooling cascade which originated as hot gas, the detailed connection between the cool and

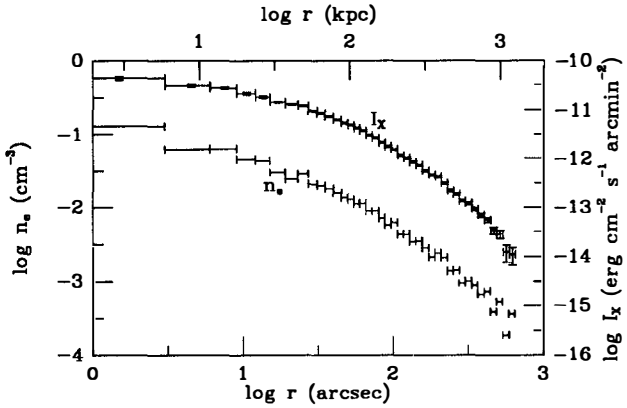

FIG. 2—The ROSAT HRI X-ray surface brightness and derived electron density for A2029. The upper curve gives the azimuthally averaged X-ray surface brightness in the ROSAT band of 0.1 – 2.4 keV as incident at the Earth, corrected for absorption. The scale I_X is given on the right–hand axis. The vertical error bars give the 1 σ errors. The radial error bars show the widths of the annuli used to derive I_X. The lower curve gives the derived electron number density; the scale is given on the left–hand axis. The lower axis gives the radial scale in seconds of arc, while the upper axis gives the scale in kpc.

hot gas is unclear. In any case, not enough cold material has been detected to equal the accumulated mass of cooling gas over a cluster lifetime.

A recent reanalysis of the *Einstein* Solid State Spectrometer (SSS) data for many cluster cooling flows indicates that they have large amounts of excess soft X-ray absorption[33]. If this material is associated with the cooling flow, then $10^{10} - 10^{12}\ M_\odot$ of cold gas may be present in these systems. This is the only positive, direct evidence we have for a possible final repository of the cooling gas.

Low mass star formation has also been suggested to be the ultimate repository of most of the cooling gas[34][35]. Very bright D or cD galaxies are always found at the centers of cooling flows. Many have unusually blue colors in their central regions $r \lesssim 20$ kpc, indicative of recent star formation[32]. However, if this star formation has the same initial mass function as that in the disk of our galaxy, it consumes typically $\lesssim 1\%$ of the cooling gas.

Bob O'Connell (University of Virginia), Brian McNamara (Kapteyn Institute), and I are involved in a project to use the High Resolution Imager (HRI) on ROSAT to obtain images of the central regions of cooling flows. The object of this study is to determine the physical state of the X-ray emitting gas, and its relation to cooler material (cooler gas and star formation). In the next two sections, the initial results for the first two clusters will be discussed.

5. ROSAT Observations of A2029

Abell 2029 (A2029) is a richness class II, Bautz-Morgan class I cluster with a redshift of $z = 0.0767$. The cluster's central cD galaxy (UGC 9752 = IC 1101) is located at the peak of the X-ray image. Although all of the other cooling flows we observed have strong optical line emission and most have regions of star formation, A2029 was included as a "null test": although the *Einstein* X-ray imaging and spectroscopic observations suggest

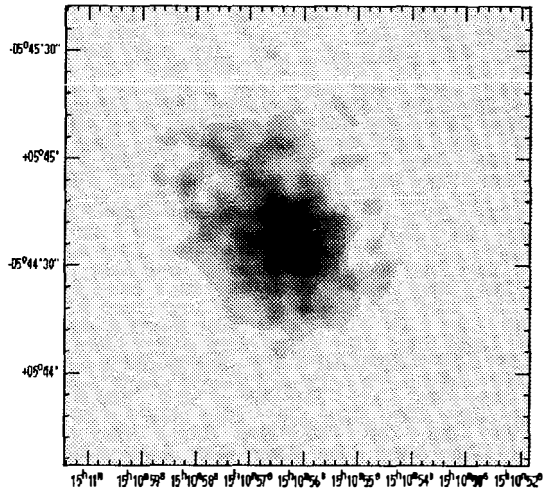

FIG. 3—The ROSAT HRI X-ray image of the cooling flow region at the center of A2029. The image covers an area of 128 × 128 arcsec, or 251 × 251 kpc at the assumed distance. The image was smoothed with a gaussian with $\sigma = 2$ arcsec.

that it is a cooling flow, it shows no evidence for optical line emission or blue stellar colors[36], and its identification as a cooling flow has occasionally been questioned. A2029 was observed for 17,614 seconds on 25 July, 1990 with the High Resolution Imager (HRI) on ROSAT. This observation was made during the Pre-measurement, Calibration, and Verification (PCV) phase of operations, prior to the start of the ROSAT All Sky Survey and about seven months prior to the beginning of normal pointed mode guest observer observations. The observations and analysis are described in more detail elsewhere[37].

The X-ray centroid is R.A. = $15^h10^m56.1^s$ and Dec. = $5°44'38''$ (J2000), which is within $2''$ of the optical center of the cD galaxy at R.A. = $15^h10^m56.2^s$ and Dec. = $5°44'39.5''$. However, we caution that there is a possible systematic uncertainty in ROSAT HRI positions of as much as $10''$.

The azimuthally averaged X-ray surface brightness distribution of the cluster is shown in Fig. 2 with 1 σ errors. In the outer regions of the image ($r \gtrsim 2$ arcmin ≈ 250 kpc), the X-ray surface brightness declines roughly as $I_X \propto r^{-2.65}$. This is fairly typical for rich clusters, and corresponds to $\beta \approx 0.61$ in the isothermal model[17], The central surface brightness rises to value which is $\gtrsim 30$ times the value at the core radius (estimated from the isothermal model). This central peaking of the X-ray surface brightness is the main X-ray diagnostic of a cooling flow. If the gas were roughly isothermal in the center, the X-ray surface brightness would be nearly constant within the cluster core ($r \lesssim 100'' \approx 200$ kpc).

We determined the X-ray emissivity of the gas by a deprojection of the X-ray surface brightness into spherical shells, each of constant emissivity (Fig. 2). A crude but useful boundary to the cooling flow region is given by the "cooling radius" r_c, defined as the radius where the cooling time equals the age of the cluster. For an assumed age of 10^{10} years, we find $r_c \approx 116'' = 228$ kpc and a total cooling rate within this radius of $\dot{M}_c \approx 370\,M_\odot\,\mathrm{yr}^{-1}$. These values are in excellent (but probably somewhat fortuitous) agreement with the values of $r_c \approx 226$ kpc and $\dot{M}_c \approx 366\,M_\odot\,\mathrm{yr}^{-1}$. derived from the *Einstein* IPC image[38]. In the innermost annulus in Fig. 2, the cooling time is very short

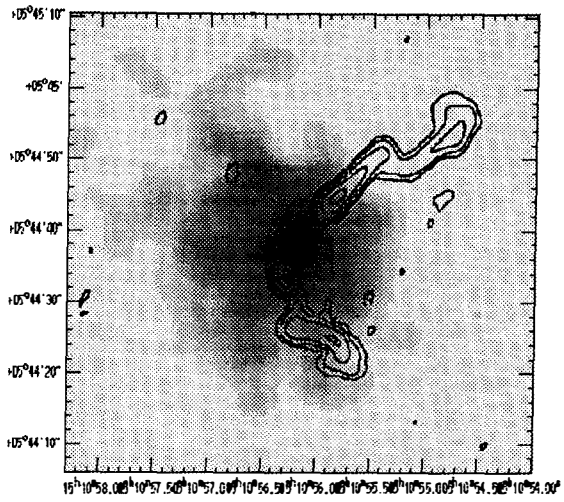

FIG. 4—The 1.5 GHz radio contour map of the WAT radio source[39] is superimposed on the ROSAT HRI X-ray image of the inner 64 × 64 arcsec.

$t_{cool} \lesssim 3 \times 10^8$ years. A2029 is indeed a cooling flow, despite the lack of optical anomalies associated with cool gas or recent star formation.

Fig. 3 shows the ROSAT HRI X-ray image of the cooling flow region at the center of the cluster. The global X-ray morphology is elongated, with the major axis at a position angle of about 35°. The emission from the cooling flow region lacks mirror symmetry; more emission is found to the northeast and southeast compared to the southwest and northwest, respectively.

The most remarkable features in the X-ray image are the inhomogeneities within the inner ~30 arcsec. There, the emission is dominated by a number of filaments. There are three bright arms extending northeast, east, and southwest from the X-ray centroid. The northeast arm has a depression in its surface brightness at $r \approx 6''$. Further to the northeast, there are two filaments which appear to form a loop. Two filaments extend directly south from the X-ray centroid, with a gap between them. The western most of these "legs" curves to form another loop, similar to the northeast loop. Although projection effects undoubtedly complicate the morphology, the structure may be characterized as radial filaments extending from the center that curve to form loop structures at larger radii.

The central cD in this cluster hosts a Wide–Angle–Tail (WAT) radio source, which contains a nuclear point source, and two oppositely directed jets. In Fig. 4, the 1.5 GHz radio contour map[39] is shown superimposed on the X-ray image of the inner cooling flow. Two broad radio jets emerge from the nuclear radio source (marked by a cross), then disrupt $10 - 15''$ from the nucleus.

Several mechanisms have been suggested to decollimate WAT radio sources. The radio jets in WATs may be disrupted when they collide with inhomogeneities in the intracluster gas[40]. Based on the *Einstein* HRI image of A2029, Sumi argued that the jets in A2029 disrupt when they encounter X-ray emitting clouds. However, we do not find any clear evidence for stronger X-ray emission at the point where the jets disrupt (Fig. 4). There is a region of brighter X-ray emission near the point where the southeast jet disrupts, but the northwest jet fades and changes direction in a region of low X-ray brightness.

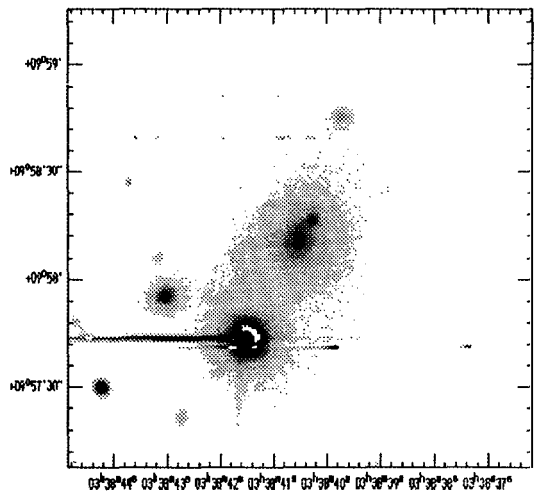

FIG. 5—An optical V band CCD image of the central regions of the 2A0335+096 cluster. The image covers an area of 128″ × 128″. The central D galaxy is at the center of the image, with the companion nucleus about 6″ to the NW. The extremely bright object to the SE of the D galaxy is a foreground star. Two other cluster galaxies are located to the ENE of this star, and to the NW of the D galaxy near the top of the image.

6. ROSAT Observations of 2A0335+096

The cluster 2A0335+096 was detected as an X-ray source by the *Ariel V* satellite[41], and was later identified with a compact Zwicky cluster at $z = 0.035$[42]. An EXOSAT image of the cluster, combined with an IPC image and a Solid State Spectrometer (SSS) spectrum from *Einstein*, showed that the cluster contained a cooling flow with a total cooling rate of $\dot{M} \approx 100 - 200\, M_\odot\ \mathrm{yr}^{-1}$ within $r \lesssim 200$ kpc[43][33]. Centered in the cluster is a D galaxy with an extended envelope[44]. Fig. 5 shows a V band CCD image of the central region[32]. The central galaxy has a nearby (∼6″), relatively bright companion nucleus to the NW. Two other bright cluster galaxies are located about 40″ to the NNW and ESE. (The bright star, V ≈ 12, located 30″ from the D galaxy causes serious problems for most optical studies of the central regions of the cluster.)

2A0335+096 exhibits many of the most intriguing aspects of cooling flow clusters: low energy X-ray line emission, optical line emission, evidence for dust, neutral hydrogen, soft X-ray absorption, and perhaps blue stellar colors suggesting recent star formation. These properties might all result from a cascade produced by the cooling of the intracluster gas, or alternatively, might indicate that a recent merger has occurred. The cluster was observed for 13,883 seconds during 10–14 February, 1991 with the High Resolution Imager (HRI) on ROSAT. The X-ray observations and analysis are described in more detail elsewhere[45]. The ROSAT HRI image of the central region of the cooling flow is shown in Fig. 6. Overall, the X-ray image is elongated at a position angle of about 145°, which corresponds to the direction from the central D galaxy to its companion.

The X-ray emission from the central regions of the cooling flow exhibits considerable structure. The brightest feature is a point source to the NW of the center; comparison to Fig. 5 shows that this corresponds to the position of the companion nucleus. There

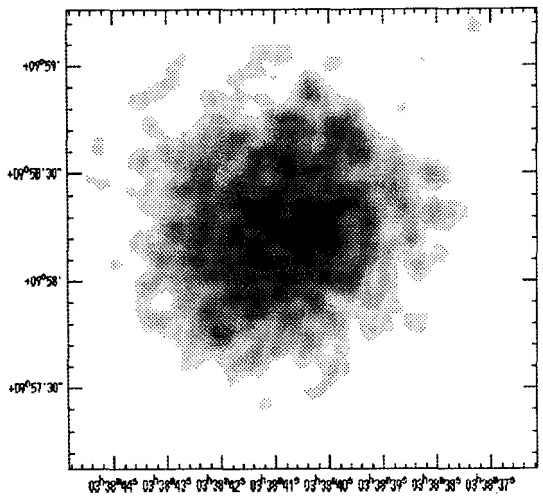

FIG. 6—The ROSAT HRI X-ray image of the central cooling flow region at the center of A2029. The image shows the central 128″ × 128″ (251 × 251 kpc) of the cluster, and was smoothed with a Gaussian ($\sigma = 2''$) which corresponds roughly with ROSAT's point-spread-function. The image covers the same region as Fig. 5.

is a bright bar of X-ray emission running from NE to SE below the point source. The central D galaxy is apparently located at the SE end of this bright bar. Just beneath this bright bar is a parallel linear feature of reduced X-ray brightness. There is a triangular region of bright X-ray emission below this dark X-ray lane. There are loops of enhanced X-ray emission to the W and E of the bright lane, and a filament of X-ray emission which extends to the north of the bright lane, ending near the position of the cluster galaxy at the top of Fig. 5.

There is a significant hole in the X-ray emission to the SE of the cluster center which is barely visible in Fig. 6. This hole occurs at the position of the bright galaxy at the left of Fig. 5. If this association is not coincidental, it would imply that this galaxy is in front of the cooling flow. To produce the observed reduction in surface brightness, this galaxy must contain X-ray absorbing gas with a column density of $N_H \gtrsim 5 \times 10^{21}$ cm^{-2}, or a total mass of $\gtrsim 10^9\ M_\odot$.

Romanishin and Hintzen[44] discovered an extensive filamentary Hα emission line system in the central regions of this cluster, which envelopes both central galaxies. There is a relatively narrow "disk" of emission in the nucleus of the D galaxy which extends $\sim 4''$ NW towards the companion nucleus. The Hα emission peaks on the secondary nucleus. All of this is embedded in a wider, $\sim 30''$ long "bar" of line emission, which is slightly offset but also extends to the NW. A recent spectrum of this region[46] shows that the inner disk and outer bar are kinematically distinct; they appear to rotate in opposite directions. Both the disk and bar are also turbulent, with $\sigma \sim 100\,\mathrm{km\,s^{-1}}$.

In Fig. 7, the contours of Hα surface brightness are shown superimposed on the X-ray image of the cooling flow region. There are a number of interesting correspondences between the optical line and X-ray emission. In general, the X-ray emission is elongated in the same direction as the optical line emission bar. The companion nucleus is a very bright source of both Hα emission and X-ray emission. A gap in the Hα emission bar

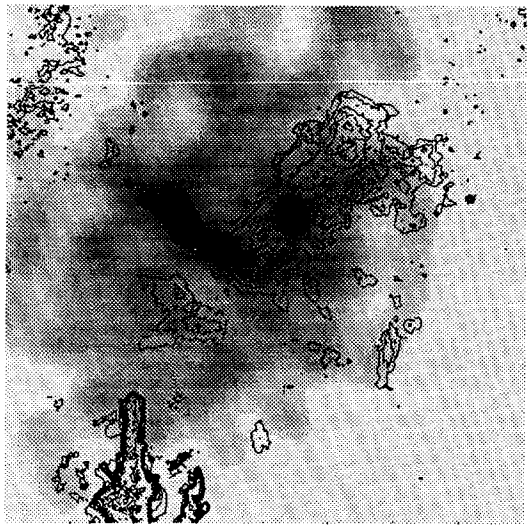

FIG. 7—The contours of the Hα emission line intensity[44] are shown superimposed on the X-ray image of the center of the cooling flow. The cross marks the position of D galaxy nucleus. The bright point source of Hα and X-ray emission corresponds to the companion nucleus.

below the D nucleus corresponds to the dark lane in the X-ray image. Below this gap there is a triangular region of Hα emission which is similar to a triangular region in the X-ray. There are filaments of Hα which correspond to both the east and west loops in the X-ray image. However, there is no Hα feature associated with the very bright X-ray bar. A comparison of Fig. 7 with the V-band image (Fig. 5) does not reveal any continuum feature corresponding to the dark lane seen in the X-ray and the Hα image. This indicates that this lane is not the result of absorption from dust and cool gas. There appears to be a real deficit in optical line and X-ray emission in this region.

7. Discussion

It is initially unclear whether the structures in the X-ray image arise from local excess absorption or emission. Photoabsorption primarily eliminates soft X-rays. If the structures in Figs. 3 and 6 are due to absorption, then the darker regions would have harder spectra than the brighter regions. The ROSAT HRI was designed to provide high spatial resolution without any spectral resolution. However, it does appear to have a very coarse spectral resolution (L. David, S. Murray, and M. Zombeck, private communication). We used this resolution to compare the hardness of the X-ray features. With one exception, the darker features all apparently have softer X-ray spectra than the brighter features. (The exception was the SE hole in 2A0335+096 [Fig. 6]). Thus, the X-ray structures are unlikely to be due to absorption.

The X-ray filaments in 2A0335+096 and A2029 probably require support from forces beyond the pressure of the ambient gas. The surface brightness of the filaments is typically $I_X \approx 3\times10^{-11}$ ergs cm^{-2} s^{-1} arcmin^{-2} in the ROSAT band (0.1–2.4 keV). If the filaments have dimensions along the line of sight which are comparable to their narrower transverse dimensions, then they contain gas with a density $n_e \gtrsim 0.1\,\mathrm{cm}^{-3}$, which is typically 2 to

4 times the average density in this region. Such dense regions cannot be supported in hydrostatic equilibrium, and should fall into the center of the cluster on a free-fall time scale ($\sim 10^8$ yr). Because the total mass in the filaments is large ($\gtrsim 10^{11}\,M_\odot$), and the cooling time in the ambient gas is longer than the free–fall time, it is unlikely that the filaments could be resupplied if they really fell into the galaxy center so quickly.

This suggests that other forces may help to support and maintain the filaments. Possibilities include magnetic forces, turbulence and rotation[37][45]. Inflow and cooling of intracluster magnetic fields should generate very strong magnetic fields in cooling flows[47]. Magnetic pressures are expected to equal gas pressure within the inner cooling flow regions. Recent radio observations have confirmed the presence of such strong fields in cluster cooling flows through Faraday rotation measurements[48]. In several cases, the Faraday rotation shows a filamentary structure; these filaments may be related to the X-ray emitting filaments. Radio polarization studies of A2029 and 2A0335+096 would be useful to study the relationship of the X-ray emitting filaments, magnetic fields, and Faraday rotation. Hα spectroscopy suggests that rotation and turbulence may also play an important role in the dynamics of the cooling flow gas.

In 2A0335+096, there are several spatial correlations between the X-ray and optical emission line filaments. This suggests that the Hα emission is a direct result of the cooling of the X-ray emitting gas. A surprising result is the coincidence of the bright optical line and X-ray emission peaks at the position of the companion nucleus. Since D galaxies at the centers of clusters often have significant orbital velocities[49], it is possible that the companion nucleus will be more nearly at rest relative to the intracluster gas than the D galaxy. Then, the cooling gas may be focussed onto the companion rather than the D galaxy. Alternatively, the companion nucleus may contain an AGN, although optical spectroscopy of the companion nucleus suggests otherwise[46]. Or, the companion galaxy may be a gas rich system merging with the D galaxy. Optical spectroscopy of the Hα and the galaxies is needed to understand the kinematics of the gas and galaxies.

8. Conclusion

The X-ray emission from normal spiral galaxies is apparently mainly due to binary stars and supernovae remnants. It is particularly associated with the youngest, most massive stars. On the other hand, the X-ray emission from normal elliptical and S0 galaxies is due to hot interstellar gas. At least in relatively isolated ellipticals and S0s, it appears that most of the gas generated by normal stellar mass loss is accumulated as hot interstellar gas at about 10^7 K.

The very optically bright D and cD galaxies at the centers of many clusters of galaxies are particularly luminous X-ray sources. Observations with the *Einstein* Observatory showed that many of these galaxies are accreting large amounts of cooling gas. This gas comes from the hot intracluster medium present in these rich clusters. Typically, $M_{cool} \sim 100\,M_\odot$/yr is cooling onto these galaxies.

New ROSAT high resolution X-ray images for two cooling flow galaxies were presented. These are the large cD and D galaxies at the centers of the clusters A2029 and 2A0335+096. These high resolution X-ray images show a considerable amount of structure in the X-ray emission from the cooling flow. Much of the X-ray emission appears to arise from filamentary structures. Because of the high densities associated with these filamentary structures, they cannot be in hydrostatic equilibrium with the ambient gas in the gravitational field of the cluster and the central galaxy. Assuming that these filaments

are not very short lived, other forces must act to support them. Such forces might include rotation, turbulence, and magnetic fields. Recent radio observations and theoretical models show that magnetic fields must be dynamically important in the central regions of cooling flows.

A comparison of the X-ray and Hα images of 2A0335+096 demonstrates a good deal of correspondence. This is consistent with the idea that the optical emission line gas originated as cooling, X-ray emitting gas.

These new ROSAT observations suggest that the gas at the centers of cooling flow clusters of galaxies is in a more complex dynamical state than had been previously assumed. Some simple conclusions about the gas in galaxies which were based on assuming that this gas was homogeneous and in equilibrium are now called into question. For example, the assumption of hydrostatic equilibrium has been used to determine the mass distributions in the central cD and D galaxies from the distribution of hot gas. These high resolution X-ray images do not support the assumption of smooth hydrostatic equilibrium. The structures which are seen in these X-ray images are located in the densest central cooling flow regions. We do not yet know whether the intracluster gas on large scales is smooth and homogeneous or also has a filamentary structure. If would be difficult to detect structures similar to those seen in these observations at larger distances in clusters. The lower X-ray surface brightness in the outer parts of clusters means that there are too few photons to detect small structures. Thus, we have no evidence at present that the gas on large scales in clusters is inhomogeneous. On the other hand, we have no convincing evidence that it is homogeneous. If the gas in the general intracluster medium is inhomogeneous and filamentary, it will be difficult to use the distribution of this gas to determine the mass profiles of clusters at large distances. Similarly, it will be difficult to apply the Zeldovich–Sunyaev effect to determine the distances to these clusters.

I would like to thank Chantal Balkowski and Trinh Thuan for organizing such a delightful and interesting meeting. This work was supported by NASA Astrophysical Theory Program grant NAGW–2376 and NASA ROSAT grants NAG 5–1577 and NAG 5–1891.

9. References

[1] Fabian, A. C., Nulsen, P. E., & Canizares, C. R. 1991, A&ARev, 2, 191.
[2] Sarazin, C L. 1992, in Frontiers of X-ray Astronomy, ed. by Y. Tanaka and K. Koyama, (Universal Academy: Tokyo), in press
[3] Fabbiano, G. 1989, ARAA, 27, 87
[4] Sarazin, C L. 1990, in The Interstellar Medium in Galaxies, ed. H. A. Thronson, Jr. and J. M. Shull, (Kluwer: Amsterdam), 201
[5] Roberts, M., Hogg, D., Bregman, J., Forman, W., & Jones, C. 1991, ApJS, 75, 751
[6] Fabbiano, G., Kim, D.-W., & Trinchieri, G. 1992, ApJS, in press
[7] Kim, D.-W., Fabbiano, G., & Trinchieri, G. 1992, ApJS, in press
[8] Awaki, H., Koyama, K., Kunieda, H., Takano, S., Tawara, Y., & Ohashi, T. 1991, ApJ, 366, 88
[9] Forman, W., Jones, C., & Tucker, W. 1985, ApJ, 293, 102
[10] Trinchieri, G., Fabbiano, G., & Canizares, C. R. 1986, ApJ, 310, 637
[11] D'Ercole, A., Renzini, A., Ciotti, L., & Pellegrini, S. 1989, ApJ, 341, L9
[12] White, R. E. III, & Sarazin, C. L. 1991, ApJ, 367, 476

[13] Trinchieri, G., & Fabbiano, G. 1991, ApJ, 382, 82
[14] Helfand, D. J., & Caillault, J.-P. 1982, ApJ, 253, 760
[15] Cox, D. P., & McCammon, D. 1986, ApJ, 304, 657
[16] Fabbiano, G., Gioia, I. M., & Trinchieri, G. 1988, ApJ, 324, 749
[17] Jones, C. & Forman, W. 1984, ApJ, 276, 38
[18] Mushotzky, R. F. 1984, PhyScr, T7, 157
[19] Canizares, C. R., Markert, T. H., & Donahue, M. E. 1988, in Cooling Flows in Clusters and Galaxies, ed. A. C. Fabian, (Dordrecht: Kluwer), 63
[20] Thomas, P. A., Fabian, A. C., & Nulsen, P. E. J. 1987, MNRAS, 228, 973
[21] White, R. E. III & Sarazin, C. L. 1987, ApJ, 318, 612
[22] Nulsen, P. E. 1986, MNRAS, 221, 377
[23] Pounds, K. 1992, in Frontiers of X-ray Astronomy, ed. Y. Tanaka and K. Koyama (Universal Academy: Tokyo), in press
[24] Anton, K., Wagner, S., & Appenzeller, I. 1991, A&A, 246, L51
[25] Hu, E. 1992, private communication
[26] Heckman, T. M., Baum, S. A., van Breugel, W. J., & McCarthy, P. 1989, ApJ, 338, 48
[27] Lazareff, B., Castets, A., Kim, D., & Jura, M. 1989, ApJ, 336, L13
[28] Mirabel, I., Sanders, D., & Kazes, I. 1989, ApJ, 340, L9
[29] Bregman, J. N., McNamara, B. R., & O'Connell, R. W. 1990, ApJ, 351, 406
[30] McNamara, B. R., Bregman, J. N., & O'Connell, R. W. 1990, ApJ, 360, 20
[31] Jaffe, W. 1992, in Clusters and Superclusters of Galaxies, ed. A. C. Fabian, (Dordrecht: Kluwer), in press
[32] McNamara, B. R. & O'Connell, R. W. 1992, ApJ, in press
[33] White, D. A., Fabian, A. C., Johnstone, R. M., Mushotzky, R. F., & Arnaud, K. A. 1991, MNRAS, 252, 72
[34] Fabian, A. C., Nulsen, P. E., & Canizares, C. R. 1982, MNRAS, 201, 933
[35] Sarazin, C. L. & O'Connell, R. W. 1983, ApJ, 268, 552
[36] McNamara, B. R. & O'Connell, R. W. 1989, AJ, 98, 2018
[37] Sarazin, C. L., O'Connell, R. W., & McNamara, B. R. 1992, ApJ, 389, L59
[38] Arnaud, K. A. 1989, preprint
[39] Sumi, D. M., Norman, M. L., & Smarr, L. L. 1988, in Cooling Flows in Clusters and Galaxies, ed. A. C. Fabian, (Dordrecht: Kluwer), 257
[40] Sumi, D. 1992, preprint
[41] Cooke, B., et al. 1978, MNRAS, 182, 489
[42] Schwartz, D. A., Schwarz, J., and & Tucker, W. H. 1980, ApJ, 238, L59
[43] Singh, K. P., Westergaard, N. J., & Schnopper, H. W. 1988, ApJ, 331, 672
[44] Romanishin, W., & Hintzen, P. 1988, ApJ, 324, L17
[45] Sarazin, C. L., O'Connell, R. W., & McNamara, B. R. 1992, ApJ, submitted
[46] Gelderman, R., Whittle, D. M, and Sarazin, C. L. 1992, in preparation
[47] Soker, N. & Sarazin, C. L. 1990, ApJ, 348, 73
[48] Ge, J.-P. 1991, Ph.D. thesis, New Mexico Institute of Mining and Technology
[49] Zabludoff, A. I., Huchra, J. P., & Geller, M. J. 1990, ApJS, 74, 1

X-RAY EMISSION OF GALAXIES; ROSAT LATEST RESULTS

Wolfgang Pietsch
Max Planck Institut für extraterrestrische Physik
D-8046 Garching, Federal Rep. of Germany

ABSTRACT

First results of pointed and All Sky Survey observations of galaxies with the X-ray observatory satellite ***ROSAT*** are reported. Survey correlations with IRAS galaxies led to the detection of spiral galaxies with X-ray luminosities of up to 10^{43} erg s^{-1} . During observations of the Magellanic Clouds and the Andromeda galaxy new super-soft X-ray sources have been detected. This new class of luminous X-ray sources may help to solve the millisecond pulsar progenitor problem. Due to the improved sensitivity and longer observation times of ***ROSAT*** new X-ray point sources have been resolved in several nearby galaxies. The diffuse emission of the LMC that was already reported by ***EINSTEIN*** has been been mapped in detail. It shows a lot of fine structure and temperatures around 5×10^6 K. The improved low energy response of ***ROSAT*** led to the discovery of 10^6 K gas from the spiral galaxy M101 and the halo of the starburst galaxy NGC 253. No diffuse emission was detected from the halo of the edge-on spiral galaxy NGC 5907.

1. INTRODUCTION

More than 10 years after the observations with the *EINSTEIN* satellite a comprehensive analysis of normal galaxies is collected in ***An X-Ray Catalog and Atlas of Galaxies***[1] and ***The X-Ray Spectra of Galaxies***[2),3)]. The catalog consists of 493 galaxies, 238 of which are detected, for 212 upper limits are given, some are at the edge of the field of view or confused with other X-ray sources. Spectral parameters are presented for 43 galaxies and X-ray colors for 127 galaxies. Detailed analysis of individual galaxies have added important information to our knowledge of the X-ray emission of normal galaxies. Some galaxies were detected with enough resolution and sensitivity to study their X-ray morphology, spectra and individual sources within the galaxy. Comparison with infrared, optical, and radio data gave further information. For a recent review see [4)]. Detailed descriptions of the *EINSTEIN* view of the local group galaxies LMC, SMC and M31 are given in [5),6),7)] and references therein.

The *EINSTEIN* observations have shown that normal galaxies of all morphological types are spatially extended sources of X-ray emission with luminosities in the range of $\sim 10^{38}$ erg s^{-1} to 10^{42} erg s^{-1} with spirals only reaching a few 10^{41} erg s^{-1} . On average for spiral galaxies the X-ray spectra are harder than for ellipticals. This is explained by the commonly accepted view that the X-ray emission of spirals is dominated by accreting binaries and supernova remnants (SNR) while a hot interstellar medium is present in ellipticals. However also some spirals show a very soft component in their spectra. This may manifest that an extended gaseous component is also present in some spirals as has been resolved in the starburst galaxies NGC 253 and M82.

In the following I will report on X-ray observations with the Röntgen Observatory SATellite (***ROSAT***)[8)] during it's calibration and verification phase, during the ***ROSAT*** All Sky Survey (RASS) and on first pointed observations of galaxies. They were devoted to the local group galaxies LMC, SMC, and M31. Further observations were planed to search for the hot interstellar medium or hot halo gas with temperatures of $\sim 10^6$ K in the face-on respectively edge-on spirals M101 and NGC 5907 and in the starburst galaxy NGC 253.

The ***ROSAT*** X-ray telescope consists of 4 nested Wolter type I mirrors[9)]. The ***ROSAT*** design reduces mirror scattering to a minimum. This leads to high-contrast images that are essentially free of non-X-ray background and allow to directly map the diffuse sky background. For all observations reported a position sensitive proportional counter (PSPC) [10)] was the focal plane instrument in use. The PSPC covers the energy range $0.1 - 2.4$ keV and has a field of view of 57 arcmin radius. The on axis resolution is limited by the PSPC to 25 arcsec and degrades for off axis angles larger than 20 arcmin due to the telescope blur, the energy resolution is 45% FWHM at 1 keV. With respect to *EINSTEIN* the main improvements are collecting area, spatial and energy resolution, lower intrinsic background and especially the highly improved low energy response in the $0.1 - 0.4$ keV band.

Before *ROSAT* all sky X-ray surveys have been performed by collimated photon counters aboard the *UHURU*[11], *Ariel-5*[12),13)], and *HEAO-1*[14] satellites detecting some 970 sources. During the *EINSTEIN* and *EXOSAT* missions that carried pointed X-ray telescopes about 5,000 sources have been looked at. The RASS is the first all sky survey in X-rays by means of a true imaging telescope. It is a factor of hundred more sensitive than *HEAO-1*, allows much higher angular resolution, and source positions are determined to $\sim$ 30 arcsec or better depending on source strength. During the RASS *ROSAT* scanned the sky with constant speed on great circles perpendicular to the sun direction covering all the sky within half a year starting July 30, 1990. The PSPC was the focal plane instrument in use. The angular resolution of the *ROSAT* telescope/PSPC system in survey mode is about 1 arcmin, if all the photons accumulated for a source at different PSPC off axis angles are used. The typical exposure in the ecliptic plane is 400 sec adding up to 50,000 sec at the north ecliptic pole. Due to the position close to the south ecliptic pole the LMC region got a rather deep exposure during the RASS.

For the analysis of *ROSAT* data a Standard Analysis Software System (SASS)[15] has been developed at the Max Planck Institut für extraterestrische Physik (MPE).

2. RASS OBSERVATIONS OF GALAXIES

During the first processing of the RASS with SASS X-ray data have been accumulated in 2 degree wide strips that pass through the ecliptic poles. On strip typically was ready for processing every two days during the survey. Fields with 17 degree radius around the ecliptic poles, where the strips strongly overlap have been processed separately. The data have been analysed using source detection algorithms. Sources have been checked for variability and extend. Information on the energy spectra was achieved by fitting Raymond-Smith thermal plasma and power low spectra to the brighter sources; for the fainter ones only hardness ratios have been determined. About 60,000 sources have been detected during this first processing. RASS sources have been correlated with with a special version of the SIMBAD catalog at MPE and with so-called 'user-supplied' catalogs[16].

The nearby galaxy group at MPE provided a galaxy catalog to SASS containing $\sim$ 30,000 entries from the UGC[17], RC2[18], RSA[19], ESO[20], and Tully[21] catalogs. Cross-correlation of this catalog with the RASS detected sources yields of about 600 identifications, $\sim$ 150 of which are AGN. Detailed analysis of this sample of RASS galaxies is in progress.

Another catalog correlated contained $\sim$ 15,000 extragalactic infrared sources selected from the *IRAS* Point Source Catalog via statistical classification[22]. 244 of the *IRAS* galaxies are positionally coincident with RASS sources; 222 have optical counterparts identified by comparison with the NASA/IPAC Extragalactic Database. The sample of X-ray emitting *IRAS* galaxies contains infrared luminous nearby galaxies, spirals and ellipticals, Seyfert galaxies, and QSOs. More than half of the sample are

galaxies with active nuclei which only make up 6% in the unselected sample of *IRAS* galaxies. The number of X-ray selected ellipticals ($\sim$ 3%) is enhanced by a factor of more than 3. Figure 1 shows a histogram of the sources versus the X-ray luminosity for the subgroups. The interesting result is the discovery of spiral galaxies with X-ray luminosities of up to 2×10^{44}erg s^{-1} , more than a factor of 10 above the highest luminosities quoted for spirals from *EINSTEIN* observations. Follow up optical observations showed that a few of these spiral galaxies with very high X-ray luminosity (up to a few times 10^{43}erg s^{-1}) are misclassified Seyfert galaxies or AGN; most of them however are *ROSAT* detected X-ray luminous narrow emission line galaxies. These may hide an AGN nucleus that is not detected in the optical regime[23].

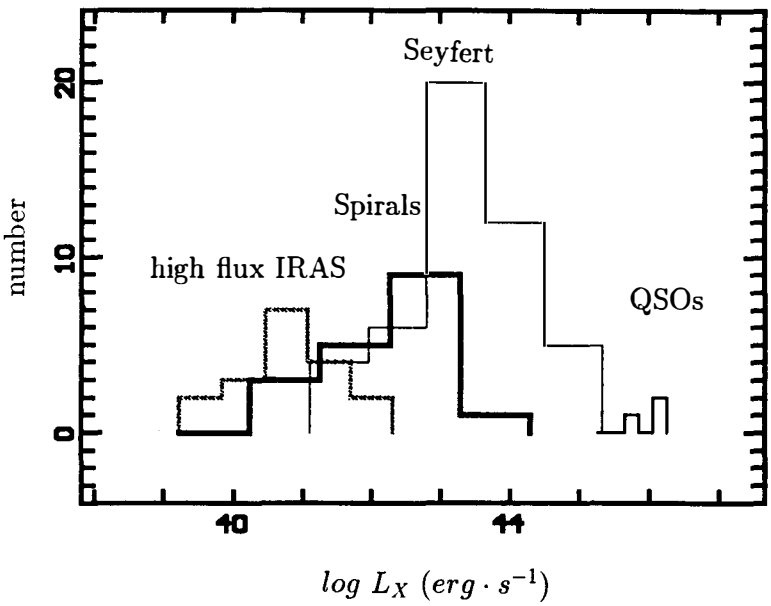

Fig. 1. X-ray luminosity for RASS detected *IRAS* galaxies (Fig. 14 of [22])

The first RASS processing did only cover 97% of the sky. The way the source detection was done has inhibited the detection of sources in a few percent of the sky. In a second processing run of the RASS SASS will bin photons in slightly overlapping images similar to optical plate surveys, allowing a 100% detection capability. The images will take the full RASS exposure of that region of the sky (including the remaining 3% of the sky, that have been filled by follow up survey observations) and therefore the source flux limit will decrease. This will increase the number of galaxy detections since most of the galaxies are found at the detection limit of the survey.

The investigations of the RASS reported above are using the final output of the SASS source detection programs that have been correlated with 'user defined' catalogs. Individual galaxies however can also be analysed by starting from the information collected for each individual photon of the survey. Image processing and source detection is the done using the This technic has been applied to RASS data of local group galaxies. In the following paragraph RASS and *ROSAT* pointed observations are reported.

3. LOCAL GROUP GALAXIES

In the small irregular metal deficient companions of the Galaxy, the Magellanic Clouds (MCs), before the *EINSTEIN* observations only a few persistent and some transient very bright X-ray binaries had been detected by collimated detector systems aboard satellites like *UHURU*, *Ariel-V*, and *HEAO-1*. The giant early type spiral galaxy M31, the most massive galaxy in the local group, was just detected as an unresolved faint source.

For the *EINSTEIN* imaging telescope the local group galaxies were close enough to offer the possibility for a detailed study of bright X-ray sources. These consist of X-ray binaries of population I (young) and II (older, within or outside of globular clusters), SNRs, and probably also cataclysmic variables. *EINSTEIN* observations of the MCs were sensitive enough to detect extremely soft X-ray binaries and diffuse emission. More than 100 sources have been reported in the LMC area[24),5)] and more than 70 in the SMC area[25),26),27),6)]. In the field of M31 *EINSTEIN* discovered 117 sources with a limiting sensitivity of $\sim 10^{37}$ erg s^{-1} [28),29),7)]. The M31 bulge region has been resolved into individual sources with the *EINSTEIN* High Resolution Imager (HRI). The variety of possible optical counterparts[30)] includes globular clusters, faint blue stars, small M31 companion galaxies, foreground stars and background galaxies and AGN. The largest number of identified sources are globular clusters ($\sim$ 20) and the globular cluster sources seem to be more luminous than in the Galaxy. There has been the discussion, if this means that the M31 globular cluster X-ray sources are really more luminous or if there are more globular cluster sources and *EINSTEIN* was just only observing the high luminosity tail of these X-ray sources. For two of the sources time variability was detected within the *EINSTEIN* observations[31)].

In the following I will discuss first *ROSAT* results on these local group galaxies. For a more detailed summary of the first *ROSAT* MC observations see [32)].

3.1 The Large Magellanic Cloud (LMC)

The first target observed by *ROSAT* starting from 16 June 1990 was the central region of the LMC around the bright X-ray binary LMC X−1. A mosaic of observations covering an area of $\sim$ 8 square degrees with exposure times ranging from 1,000 to 20,000 seconds was searched for discrete sources and diffuse emission[33)]. From the 45 sources

detected 15 were not known before. Sources could be grouped as foreground stars, or SNRs from there spectral hardness. Several sources were classified as extended. Follow up optical observations of these sources add 7 new SNR identifications to the 27 SNRs discovered by *EINSTEIN* in the LMC[34].

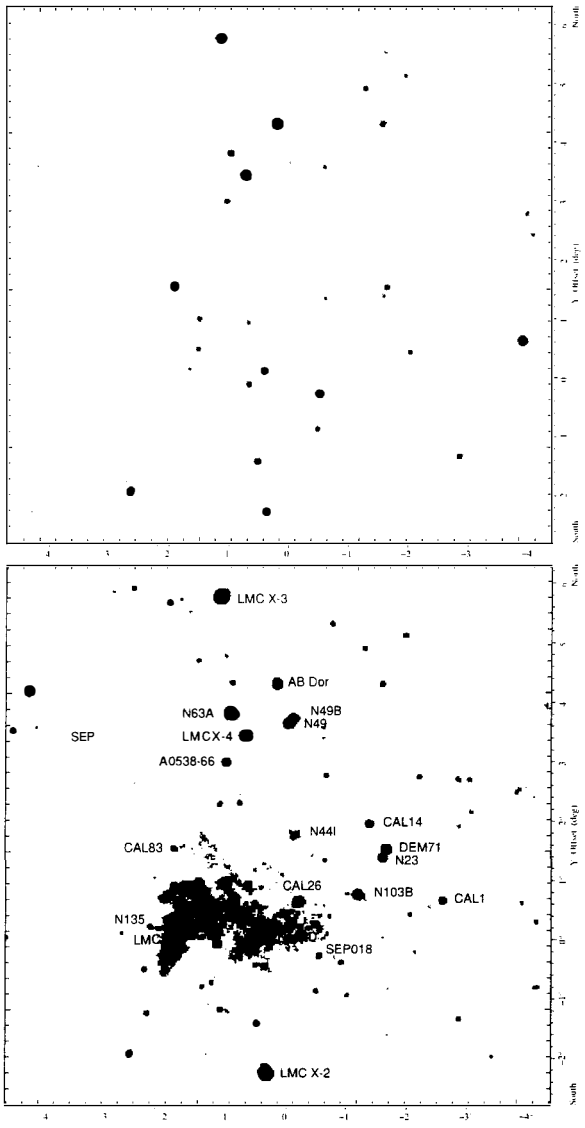

Fig. 2. *ROSAT* all sky survey image of the LMC in the energy range 0.1−0.4 keV (above) and 0.4−2.4 keV (below). Some source identifications and the position of the SEP are indicated. In the hard image highly structured diffuse emission is visible.

As pointed out above due to the proximity to the south ecliptic pole (SEP) the LMC got a long exposure during the RASS spread over several months. In the exposure corrected RASS images in the energy range 0.1–0.4 keV and 0.4–2.4 keV (fig. 2) some well known bright LMC sources, X-ray binaries and SNRs are indicated as well as the bright galactic RS CVn star AB Dor and the SEP region. The X-ray binary LMC X–4 was followed for more than 50 days and the observations indicate that the length of the 30 day cycle is decreasing with time[35]. The Be type LMC transient A0538-66[36] was active during the survey, the *EXOSAT* detected LMC transient EXO053109-6609.2[37),38] however was inactive. Supernova 1987A was neither detected in the deep pointed nor in the RASS observations.

In the soft RASS image no structured diffuse emission is visible. Since LMC radiation is strongly absorbed by the galactic foreground N_H the diffuse emission in this energy band is dominated by the flat diffuse foreground emission of our own galaxy. In the hard RASS image structured diffuse emission from the LMC is seen even further out than in the pointed observations. The *EINSTEIN* LMC survey already revealed this diffuse component. The lower intrinsic background, lower mirror scattering, as well as the higher spatial and spectral resolution of the ROSAT PSPC however allowed to image this LMC diffuse emission in unprecedented detail during pointing and RASS. The brightest regions are east of LMC X–1 and in the star forming region 30 Doradus. The bulk of the diffuse emission has a temperature of $(3-7)\times 10^6$ K (fig. 3). The diffuse emission shows structure down to the angular resolution of the instrument. In the 30 Doradus area the raw ROSAT PSPC images are very similar to the maximum-entropy map deconvolved from the *EINSTEIN* observations[39].

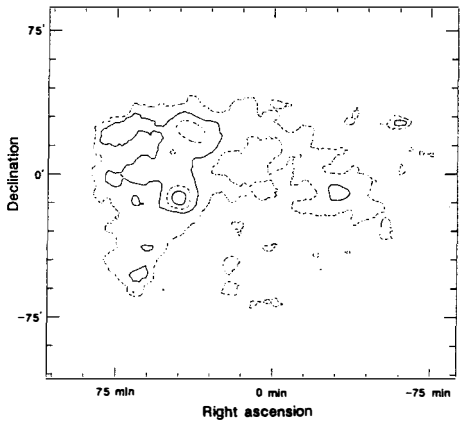

Fig. 3. Temperature map of the diffuse LMC emission; contours are at 4.5, 5.8, 6.7, and 10 million K (Fig. 3 of [33]).

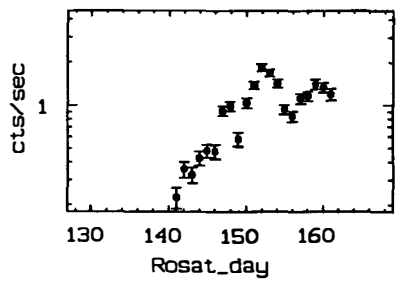

Fig. 4. X-ray light curve for the super-soft X-ray transient SEP018 detected in the RASS (Fig. 9 of [42])

ESO colour images of the LMC in visible light correlate strongly with diffuse features in the ROSAT images. H II emission in the optical corresponds to bright knots in X-rays. The bright X-ray region to the northeast of LMC X−1 has been attributed to the blow-out of the hot supergiant bubble LMC 2. The detailed structure of the X-ray emission however suggests that the diffuse emission extends much further than the actual superbubble.

Two rather bright sources stand out in the pointed observations due to their unusually soft X-ray spectra and essentially no X-ray emission above 0.5 keV, the *EINSTEIN* low mass X-ray binary CAL 83[40] and the *ROSAT* detected transient RX J05278-6954. This source was 6 times brighter than CAL 83 and well within the range of the *EINSTEIN* survey. The X-ray spectra resemble black-body spectra with a temperature of 20−40 eV and N_H values that clearly indicate a LMC membership[41]. They radiate at or even above the Eddington limit for a $1.4M_\odot$ object at the distance of the LMC. An additional bright transient of this class of super-soft X-ray sources (SEP018, see fig. 2) turned on during the RASS (fig. 4)[42] and was neither detected by *EINSTEIN* nor in the pointed observation. The nature of these sources will be discussed in section 5.

3.2 The Small Magellanic Cloud (SMC)

During the RASS the SMC has been homogeneously covered at a similar depth as during the *EINSTEIN* raster scan of the SMC area[25]. In a field of (8 × 8 square degrees 41 sources have been detected, 15 of which could be identified with *EINSTEIN* sources[43].

Body and wing of the SMC are covered by a raster of deep pointed *ROSAT* observations. In a preliminary analysis of part of these observation ∼ 100 sources are detected, 38 of which could be identified with detections from the *EINSTEIN* deep pointings[32),6)]. In overlapping areas the number of *ROSAT* sources is higher by at least a factor of 2. Many of the faint unidentified sources are expected to be not associated with the SMC but background objects.

Two hard transients have been detected, SMC X−2 not reported since its *SAS 3* discovery in 1977[44] and the new *ROSAT* source RX J0049.1-7251. Three super-soft X-ray sources are detected, two of which were known from *EINSTEIN* observations and proposed identifications are the planetary nebula PN 67 and a low mass X-ray binary. The new *ROSAT* super-soft X-ray source RX J0048.3-7332 is identified with the symbiotic star SMC 3 in the SMC cluster NGC 269, that is in outburst since 1981[45].

EINSTEIN observations led to the identification of 11 SNRs in the SMC. The prominent ones were detected in the RASS and further SNRs or candidates have been found in the pointed observations. Within the giant H II region N 66 two proposed SNRs[46] are detected in a pointed observation and there is even one more *ROSAT* SNR candidate (i.e. showing extended emission) within N 66.

3.3 The Andromeda galaxy M31

ROSAT observed M31 in 6 deep pointings in July 1991. More than 250 sources have been found with the SASS processing. Spectra and time variability of individual sources are studied. Optical identifications are searched for using CCD images complete to magn 22.2 in B, V and R and to 20.9 in I [47] and for SNR identifications [SII] and H_α CCD images.

So far more than 20 globular cluster sources(10 of which were not detected with *EINSTEIN*), 5 SNR, 14 foreground stars, and 2 background galaxies have been optically identified. A strong transient shows up in the pointed observations, that was not detected with *EINSTEIN* and in RASS images made 6 month earlier. Fig. 5a shows spectrum and time variability of one of the brightest globular cluster sources, the light curve of which indicates a 16 hour periodicity. If interpreted as orbital period such a long period system should, according to theory, not be able to survive in a globular cluster. Fig. 5b shows an unidentified object. Its spectrum requires two-temperature thermal line emission and its light curve shows large outbursts. From the PSPC observation alone, without any optical information, this source can be classified as a foreground flare star.

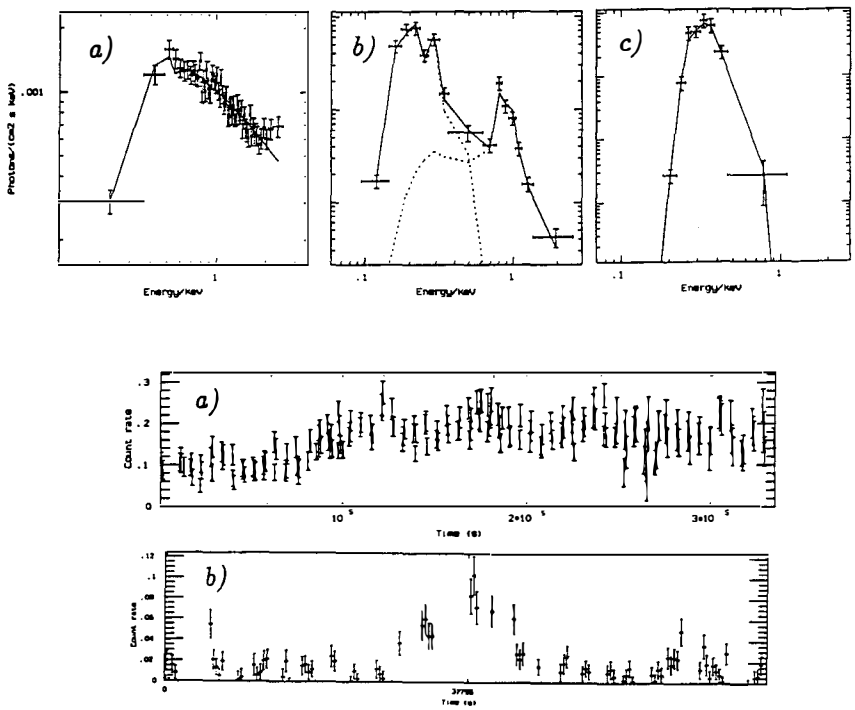

Fig. 5. X-ray spectra and light curves of sources in the M31 field. a) bright globular cluster source; b) foreground flare star; c) M31 super-soft X-ray source

The most important finding in the *ROSAT* observations of M31 to date is the discovery of several super-soft X-ray sources; the spectrum of the brightest of them is shown in fig. 5c. The absorption identifies the source as M31 member and the spectral parameters are similar to CAL 83 (see above). The spectra of these sources is so soft, that only a few percent of the total luminosity is detectable due to the absorption along the line-of-sight and inside M31. We therefore only see the most luminous of those super-soft X-ray sources in M31 and the discovery of several may imply that there are hundreds in M31.

4. SEARCH FOR MILLION K GAS IN GALAXIES

The existence of a few times 10^6 K gas in galaxies has been proposed by theorists. It should originate from SNRs in the galaxies and make up part of the galaxies interstellar medium and via galactic fountains fill the halo of galaxies (e.g. [48),49),50),51),52)]). RASS and *ROSAT* pointed shadowing observations detected the hot interstellar medium in the galaxy[53)]; hot interstellar gas in the LMC was reported above. Searches with *EINSTEIN* in edge-on galaxies[54)] and in the large face-on galaxy M101[55)] could only derive upper limits for hot gas emission. Extended emission of gas of these temperatures in galaxies outside the local group has only been reported from *EINSTEIN* observations of the starburst galaxies M82[56),57)] and NGC 253[57),58)].

The improved low energy sensitivity, spectral and spatial resolution, and the low intrinsic background capability of the *ROSAT* telescope/PSPC combination with respect to *EINSTEIN* are the ideal combination for a new search for hot gas in galaxies. We selected face-on and edge-on galaxies and the starburst galaxy NGC 253 for our investigation that stand out for low foreground N_H ($< 1.5 \times 10^{20}$ cm^{-2}) and are not too distant to be resolved by *ROSAT* . Here I report preliminary results on NGC 253, M101 and the edge-on galaxy NGC 5907.

4.1 The edge-on starburst galaxy NGC 253

To search for 10^6 K gas we analysed a 12 ksec *ROSAT* observation of NGC 253 in three energy bands (fig. 6). The medium and hard band resemble all the features reported in the *EINSTEIN* IPC and HRI observations[57),58)]. The PSPC clearly resolves the *EINSTEIN* HRI detected sources no. 1, 2, and 5. Source no. 4, 3, and 6 were not active. Source no. 7 and 8 may be confused by the bright emission region originating from the galaxy center. On the other hand we detect several new pointlike sources. This indicates that a great fraction of the extremely bright X-ray binaries are transients. The plume and the inner 10 arcmin of the disk are not resolved. The diffuse emission reported by *EINSTEIN* in the north-western halo region is resolved in filamentary structure in the *ROSAT* medium energy band image.

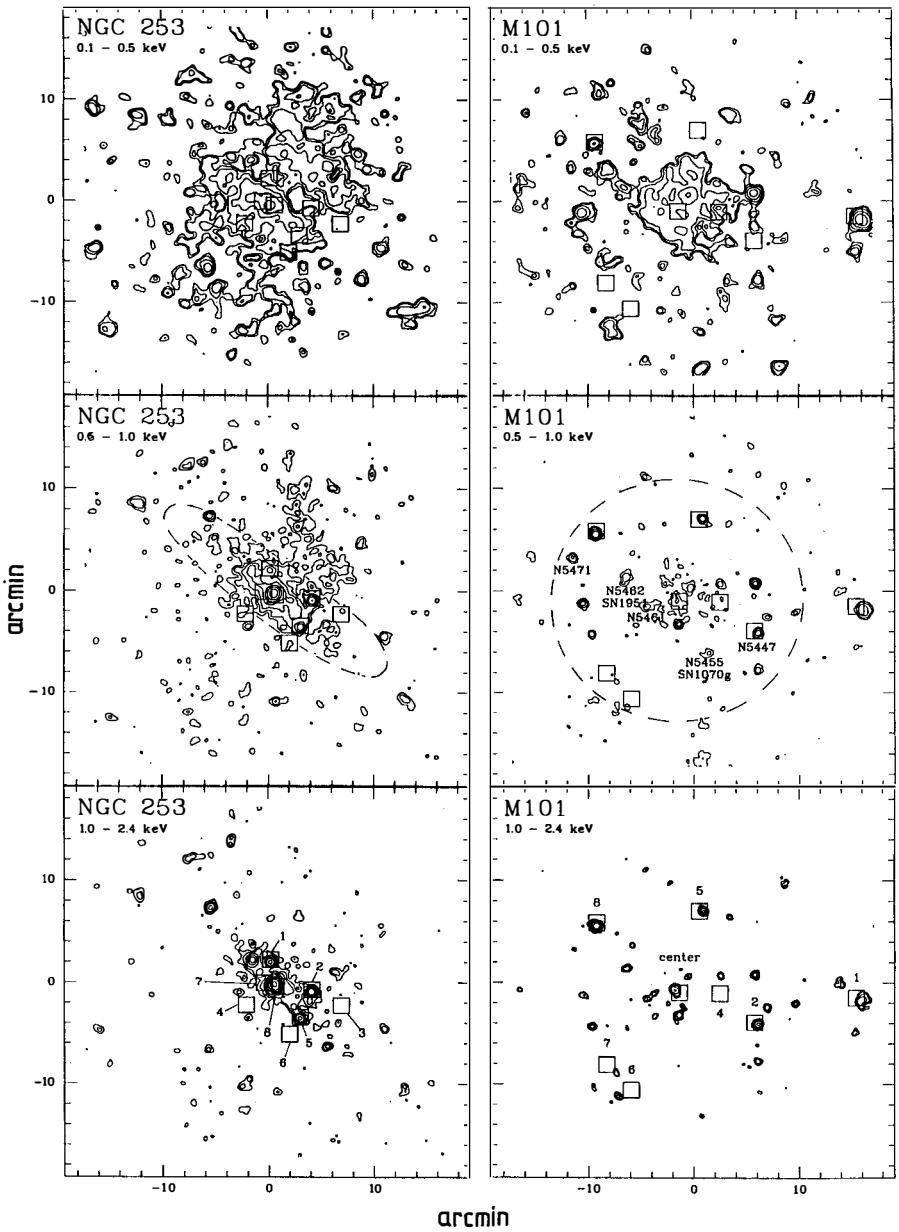

Fig. 6. Contour plots for the soft, medium, and hard *ROSAT* band for NGC 253 and M101. The images have been smoothed with a Gaussian filter with the FWHM of the PSPC point response function, however have not been exposure corrected. Contours are 2, 3, 5, 9, 17, ... σ above background. In the medium energy image the dashed ellipse gives the optical D_{25} contour taken from[21]. H II region and historical supernova sites are indicated for M101. *EINSTEIN* detected sources[58),60)] are given as squares; the *EINSTEIN* source no. is added in the hard image.

The most striking new *ROSAT* results come from the soft energy band image. There, compared to the harder energy band images, we do not only see unresolved emission from an even larger area of the inner disk of the galaxy ($\sim$ 15 arcmin diameter), that is by far less peaked to the galaxy center. We resolve several super-soft pointlike X-ray sources further out in the disk of NGC 253 that may be of the same class as reported for LMC, SMC, and M31. The eye-catching feature however is that the soft emission is more extended perpendicular to the disk ($>$ 13 arcmin in both directions) than in the disk. This has to be explained by hot gas that is filling the halo of NGC 253. The gas is not distributed homogeneously. In the south-east it seems to emanate from the entire inner disk area and to reach further out in the wings than from the center area. In the north-west in a area parallel to the plane of the galaxy with a projected distance from the plane of between 1 and 4 arcmin the soft radiation is strongly reduced or totally absent. This can be easily explained knowing that the north-western part of NGC 253 is closer to us than the south-east. Soft X-rays emitted close to the inner disk in the north-west are therefore absorbed within the spiral arms of NGC 253 lying in the line of sight (the absorbing column needed is a few times $10^{20}\mathrm{cm}^{-2}$).

If one assumes that the hot halo gas is driven out with constant speed by a super-wind originating from the starburst[59] one can calculate from the extent of the hot gas an age for the starburst of $\sim 3 \times 10^7$ years (using a NGC 253 distance of 3 Mpc and $v_{gas} = 400$ km sec^{-1}) fitting nicely to other age determinations.

4.2 The face-on giant spiral M101

ROSAT PSPC images of M101 integrated over 34.5 ksec in the soft, medium, and hard energy band are shown in fig. 6. As reported above *EINSTEIN* observations failed to detect diffuse emission[56]. *EINSTEIN* detected 10 sources in the field and emission from the galaxy center[60]. We do not detect *EINSTEIN* source no. 4, 6, and 7. On the other hand we detect several new hard and medium hard sources. Some may be identified with the H II regions NGC 5455, NGC 5461, NGC 5462, and NGC 5471. We also detect sources close to the location of historical supernovae (SN1951 and SN1970g).

The important new *ROSAT* result on M101 however also comes from the soft image. Again we discover several super-soft pointlike X-ray sources. Moreover we detect extended diffuse emission in the inner part of the disk ($\sim$ 10 arcmin diameter) that seems to follow outward the spiral arms. Detailed analysis can only be done after careful exposure correction[61]. The natural interpretation of this emission is 10^6 K gas. Since the galaxy is seen face-on it is not possible to decide from the X-ray observations if the gas is confined within the disk or located in the halo of M101.

4.3 The edge-on spiral NGC 5907

The low foreground N_H edge-on spiral NGC 5907 has been observed by *ROSAT* for 19.1 ksec. More than seven pointlike sources have been resolved. Again we searched in

the soft energy band image for hot gas of similar temperatures as in the NGC 253 halo or in M101, however with no success. The surface brightness of the NGC 5907 halo emission in the soft energy band therefore has to be lower by at least a factor of a few.

5. CONCLUSIONS

Here I only want to elaborate on two topics: Super-Soft X-ray sources (SSX) as a new class of X-ray binaries and the *ROSAT* detection of diffuse emission in galaxies.

After the detection by *EINSTEIN* SSX have been identified as a new class of X-ray binaries by the *ROSAT* observations. They have not only been detected in the MCs but also in M31 and there is even one candidate identified within the Galaxy[62]. That we do not detect more of them in our galaxy is easily explained by the severe extinction and the incompleteness of previous X-ray surveys in the soft energy band. The super-soft sources in NGC 253 and M101 may add further candidates. Several models have been proposed to explain the nature and soft spectra of these sources. One model puts a compact object with supercritical accretion into a cocoon of surrounding material. The extremely soft spectrum could be produced by Compton scattering within that cloud[63]. A second explanation proposed is accretion of a white dwarf with steady nuclear burning on the surface, a kind of persistent nova[64]. This new class of SSX detected in external galaxies and mostly hidden behind the interstellar medium in our galaxy provide accretion powered compact X-ray sources that as a class were not taken into account before *ROSAT*. The inclusion of these sources as progenitors to millisecond pulsars may help to solve the millisecond pulsar birthrate problem[65]

The detection of resolved diffuse emission of 10^6 K gas in nearby galaxies by *ROSAT* opens a new field for investigations of nearby galaxies. At the moment *ROSAT* data for only a few galaxies have been analysed. The detection of gas of this temperatures for the starburst galaxy NGC 253 will allow to constrain parameters for the starbust (e.g. duration, mass ejected by the superwind). The investigation of additional suitable galaxies that are already observed or scheduled for observation by *ROSAT* will help to constrain filling factors and/or halo origin of hot gas emission. The *ROSAT* PSPC instrument will be for quite some time the only instrument to do this kind of research.

The results reported above are just a first glance on *ROSAT* observations of galaxies. It is clear from these first observations that *ROSAT* due to its sensitivity, spatial and spectral resolution, and low intrinsic background will strongly widen the X-ray view on galaxies.

I would like to thank many colleagues at the Max Planck Institut für Extraterrestrische Physik who worked on *ROSAT* hardware and software. The help of K. Dennerl, J. Engelhauser, and W. Voges preparing the LMC survey images and of A. Jain prepared M31 source spectra and light curves is acknowledged.

REFERENCES

1. Fabbiano, G., Kim, D.-W., and Trinchieri, G. 1992, *Astrophys. J. Suppl.* 80, 531
2. Kim, D.-W., Fabbiano, G., and Trinchieri, G. 1992, *Astrophys. J. Suppl.* 80, 645
3. Kim, D.-W., Fabbiano, G., and Trinchieri, G. 1992, *Astrophys. J.* 393, 134
4. Fabbiano, G. 1989, *Ann. Rev. Astr. Astrophys.* 27, 87
5. Wang, Q., Hamilton, T., Helfand, D.J., and Wu, X. 1991, *Astrophys. J.* 374, 475
6. Wang, Q., and Wu, X. 1992, *Astrophys. J. Suppl.* 78, 391
7. Trinchieri, G., and Fabbiano, G. 1991, *Astrophys. J.* 382, 82
8. Trümper, J. 1983, *Adv. Sp. Res.* 2, 241
9. Aschenbach, B. 1988, *Appl. Optics* 27, 1404
10. Pfeffermann, E., Briel, U.G., Hippmann, H., Kettenring, G., Metzner, G., Predehl, P., Reger, G., Stephan, K.H., Zombeck, M.V., Chappell, J., and Murray, S.S. 1988, *Proc. SPIE* 733, 519
11. Forman, W., Jones, C., Cominsky, L., Julien, P., Murray, S., Peters, G., Tananbaum, H., and Giacconi, R. 1978, *Astrophys. J. Suppl.* 38, 357
12. Warwick, R.S., Marshall, N., Fraser, G.W., Watson, M.G., Lawrence, A., Page, C.G., Pounds, K.A., Ricketts, M.J., Sims, M.R., and Smith, A. 1981, *Mon. Not. R. astr. Soc.* 197, 865
13. McHardy, I.M., Lawrence, A., Pye, J.P., and Pounds, K.A. 1981, *Mon. Not. R. astr. Soc.* 197, 893
14. Wood, K.S., Meekins, J.F., Yentis, D.J., Smathers, H.W., McNutt, D.P., Bleach, R.D., Byram, E.T., Chubb, T.A., and Friedman, H. 1984, *Astrophys. J. Suppl.* 56, 507
15. Voges, W., Gruber,R., Paul, J., Bickert, K., Bohnet, A., Bursik, J., Dennerl, K., Englhauser, J., Hartner, G., Jennert, W., Köhler, H., and Rosso, C. 1992, Proc. *'European ISY meeting: "Space Science with particular emphasis on High Energy Astrophysics" Symposium'*, Munich
16. Voges, W. 1992, Proc. *'European ISY meeting: "Space Science with particular emphasis on High Energy Astropysics" Symposium'*, Munich
17. Nilson, P. 1973, *Acta Univ. Uppsala* Ser. V, Vol. 1
18. de Vaucouleurs, G., de Vaucouleurs, A., and Corwin, H.G., Jr. 1976, *The Second Reference Catalogue of Bright Galaxies* (Austin: University of Texas Press)
19. Sandage, A., and Tammann, G. 1981, *The Revised Shapley-Ames Catalog of Bright Galaxies* (Washington, DC: Carnegie Institution)
20. Lauberts, A. 1982, *ESO/Uppsala Survey of the ESO(B) Atlas* (European Southern Observatory)
21. Tully, R.B. 1988, *Nearby Galaxies Catalog* (Cambridge: Cambridge University Press)
22. Boller, Th., Meurs, E.J.A., Brinkmann, W., Fink, H., Zimmermann, U., and Adorf, H.-M. 1992, *Astron. Astrophys.* 261, 57
23. Boller, Th., private communication
24. Long, K.S., Helfand, D.J., and Grabelsky, D.A. 1981, *Astrophys. J.* 248, 925
25. Seward, F.D., and Mitchell, M. 1981, *Astrophys. J.* 243, 736
26. Inoue, H., Koyama, K., and Tanaka, Y. 1983, *Supernova Remnants and their X-Ray Emission*, eds. J. Danziger and P. Gorenstein, p. 535
27. Bruhweiler, F.C., Klinglesmith III, D.A., Gull, T.R., and Sofia, S. 1987, *Astrophys. J.* 317, 152
28. Van Speybroeck, L., Epstein, A., Forman, W., Giacconi, R., Jones, C., Liller, W., and Smarr, L. 1979, *Astrophys. J. (Letters)* 234, L45
29. Long, K.S., and van Speybroeck, L.P. 1983, in *Accretion Driven Stellar X-Ray Sources*, eds. W.H.G. Lewin and E.P.J. van den Heuvel (Cambridge: Cambridge University Press), 117
30. Crampton, D., Cowley, A.P., Hutchings, J.B. Schade, D.J., and van Speybroeck, L.P. 1984, *Astrophys. J.* 284, 663
31. Collura, A., Reale, F., and Peres, G. 1990, *Astrophys. J.* 356, 119

32. Pietsch, W., and Kahabka, P. 1992, in *Lecture Notes in Physics: 'New Aspects of Magellanic Cloud Research'*, eds. B. Baschek, G. Klare, and J. Lequeux, in press
33. Trümper, J., Hasinger, G., Aschenbach, B., Bräuninger, H., Briel, U.G., Burkert, W., Fink, H., Pfeffermann, E., Pietsch, W., Predehl, P., Schmitt, J.H.M.M., Voges, W., Zimmermann, U., and Beuermann, K. 1991, *Nature* 349, 579
34. Aschenbach, B., private communication
35. Dennerl, K., Kürster, M., Pietsch, W., and Voges, W. 1992, in *Lecture Notes in Physics: 'New Aspects of Magellanic Cloud Research'*, eds. B. Baschek, G. Klare, and J. Lequeux, in press
36. Skinner, G.K. 1980, *Nature* 288, 141
37. Pakull, M., Brunner, H., Pietsch, W., Staubert, A., Beuermann, K., van der Klis, M., and Bonnet-Bidaud, J.M. 1985, *Space Sci. Rev.* 40, 379
38. Pietsch, W., Dennerl, K., and Rosso, C. (1989): Proc. 23rd ESLAB Symp. on Two-Topics in X-ray Astronomy, Bologna, ESA SP-296, 573
39. Wang, Q., and Helfand, D.J. 1991, *Astrophys. J.* 370, 541
40. Smale, A.P., Corbet, R.H.D., Charles, P.A., Ilovaisky, S.A., Mason, K.O., Motch, C., Mukai, K., Naylor, T., van der Klis, M., and van Paradijs, J. 1988, *Mon. Not. R. astr. Soc.* 233, 51
41. Greiner, J., Hasinger, G., and Kahabka, P. 1991, *Astron. Astrophys. (Letters)* 246, L17
42. Schaeidt, S., Hasinger, G., and Trümper, J. 1991, in *X-ray Emission from Active Galactic Nuclei and the Cosmic X-ray Background*, eds. W. Brinkmann and J. Trümper (MPE Garching), MPE report 235, p. 191
43. Kahabka, P., and Pietsch, W. 1992, in *Lecture Notes in Physics: 'New Aspects of Magellanic Cloud Research'*, eds. B. Baschek, G. Klare, and J. Lequeux, in press
44. Clark, G., Doxsey, Li, F., Jernigan, J.G., and van Paradijs, J. 1978, *Astrophys. J. (Letters)* 221, L37
45. Morgan, D.H. 1992, *Symbiotic stars in the Magellanic Clouds*, Edinburgh Astronomy Preprint Nr. 10
46. Ye, T., and Turtle, A.J. 1991, *Mon. Not. R. astr. Soc.* 249, 722
47. Magnier, E.A., Lewin, W.H.G., van Paradijs, J., Trümper, J., Jain, A., and Pietsch, W. 1992, *Astron. Astrophys.* in press
48. Spitzer, L. 1956, *Astrophys. J.* 124, 20
49. Cox, D.P., and Smith, B.W. 1974, *Astrophys. J. (Letters)* 189, L105
50. Bregman, J.N. 1980, *Astrophys. J.* 236, 577
51. Bregman, J.N. 1980, *Astrophys. J.* 237, 681
52. Corbelli, E., and Salpeter, E.E. 1988, *Astrophys. J.* 326, 551
53. Snowdon, S.L., private communication
54. Bregman, J.N., and Glassgold, A.E. 1982, *Astrophys. J.* 263, 564
55. McCammon, D., and Sanders, W.T. 1984, *Astrophys. J.* 287, 167
56. Watson, M.G., Stanger, V., and Griffiths, R.E. 1984, *Astrophys. J.* 286, 144
57. Fabbiano, G. 1988, *Astrophys. J.* 330, 672
58. Fabiano, G., and Trinchieri, G. 1984, *Astrophys. J.* 286, 491
59. Heckman, T.M., Armus, L., and Miley, G.K. 1990, *Astrophys. J. Suppl.* 74, 833
60. Trinchieri, G., Fabbiano, G., and Romaine, S. 1990, *Astrophys. J.* 356, 110
61. Snowdon, S. et al., in preparation
62. Motch, Ch., private communication
63. Ross, R.R. 1979, *Astrophys. J.* 233, 334
64. van den Heuvel, E.P.J., Bhattacharya, B., Nomoto, K., and Rappaport, S.A. 1992, *Astron. Astrophys.* in press
65. Kulkarni, S.R., and Narayan, R. 1988, *Astrophys. J.* 335, 755

II- PROPERTIES ALONG THE HUBBLE SEQUENCE

2) STAR FORMATION AND DUST

OBSERVABLE MANIFESTATIONS OF ACTIVITY IN NORMAL SPIRAL GALAXIES

Giuseppe Gavazzi

Osservatorio di Brera, Milano, Italy

ABSTRACT: multifrequency observations of 874 spiral galaxies are analyzed with the aim of isolating few relevant parameters which govern their disk activity. It is shown that quite accurate predictions can be made if estimates of their old stellar component, of their present star formation rate (SFR), and informations on their environment are available.

INTRODUCTION

High spatial resolution observations of several nearby galaxies became recently available at various frequencies. The most obvious example, yet anomalous in many respects, is M31 (see radio continuum map in Walterbos, 1986; 21 cm line map in Unwin, 1980; FIR maps in Walterbos and Schwering, 1987; CO map in Dame et al, 1991; H_α distribution in Pellet et al, 1978 and X-ray study in Trinchieri and Fabbiano, 1991), but other galaxies have been analyzed at several frequencies (see for example FIR-radio comparisons in Bicay and Helou, 1990 and in Fitt, et al, 1992). Any attempt to produce a realistic and sufficiently sophisticated model of galaxy evolution will have to face with this fast growing observational material spanning 10 orders of magnitude in frequency. This is an ambitious and difficult task due to the complex relationships and feedback mechanisms which regulate the various manifestations of activity in galaxies. In fact dramatic galaxy-to-galaxy differences are observed, and even within galaxies, unexpected local peculiarities are found, which remain unexplained by most models. Actually, our understanding of galaxies is still in the pre-Darwinian phase, where a clear definition of *species* has still to be identified (see the controversy on the meaning of galaxy morphological classification which has been emphasized at this meeting). Obviously it is not the purpose of this paper to produce any detailed and universal explanation (we refer the reader to the work of Kennicutt, 1990 and of Mas-Hesse and Kunth, 1991). We will limit our investigation to a much simpler, although realistic approach. We will attempt to show that the available *integrated over the galaxy* multifrequency data can constrain models of galaxy evolution. This "low resolution" approach is certainly simplistic, since it does not account for the infinite variety of small, yet important details mentioned above, but will unable us to use larger data samples.

When we say "model of evolution" we mean a model which describes reasonably well the observed behavior of galaxies in the local Universe ($z < 0.1$), without any pretention to explore the early cosmological phases which gave birth to galaxies nor the dependence of galaxy properties on redshift.

In the remainder we will focus only on normal spiral galaxies. Consequently we will not account for any of the nuclear phenomena which originate in active galactic nuclei and in radio galaxies, considering only the low-level type of activity which takes place in quiescent disks and arms of galaxies.

A schematic framework on which the following analysis is based is illustrated in Fig. 1, where, ordered as a function of the frequency *window* used in the observations (vertical axis) some observable (circled) are connected by lines which represent causality relations and feedback mechanisms.

Neutral atomic hydrogen (21 cm line) is assumed to be the primordial reservoir of matter which "fuels" the star formation processes in galaxies via the collapse of molecular H2 clouds (see reviews on H2 in Young, 1990 and in Kenney, 1990). Stellar evolution provides the observed variety of stars (in the proper *melange* of types and with the proper life-times). The most abundant, slowly evolving, "boring", red stars are assumed to account for most of the mass in galaxies (therefore regulating the mass-dependent processes such as rotational properties etc. Dark matter might in fact do most of this job). They contribute to the near IR emission. More interesting to us is the minority of young, massive, rapidly evolving stars (mostly observed in the UV spectrum). Their UV photons ionize the surrounding gas, making HII regions visible (for example via emission of Balmer lines), heat the dust, producing strong far infrared flux

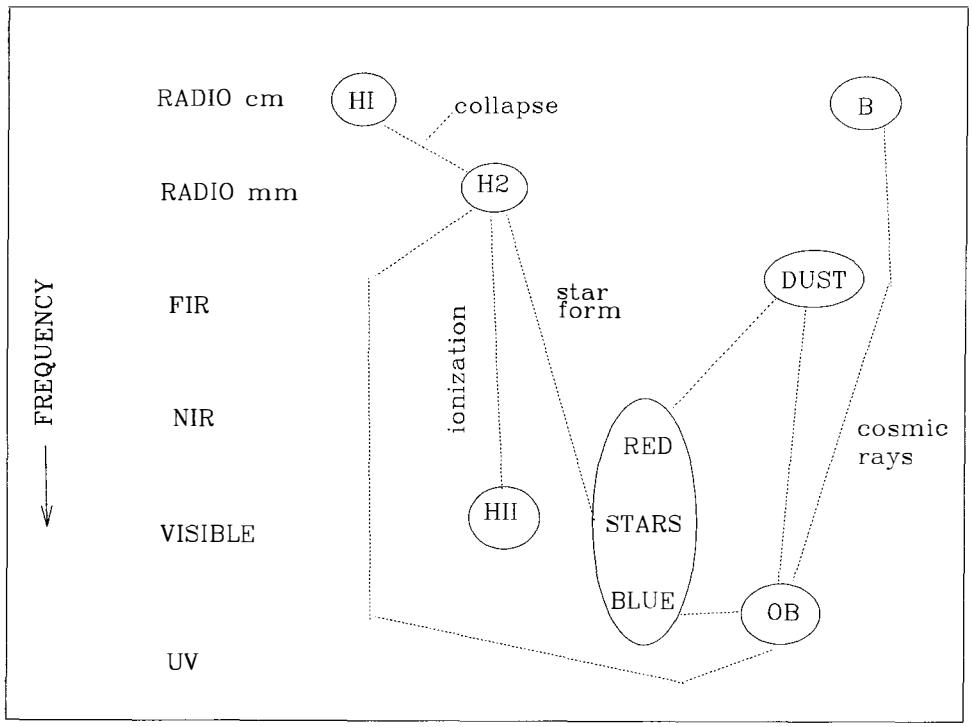

Fig. 1: Schematic model of the feedback processes which take place in galaxy disks and their observability.

and contribute, with frequent Supernova explosions to inject relativistic particles in preexisting magnetic fields, producing synchrotron emission (centimetric radio emission). The role of supernova might be relevant also in the process of cloud collapse and the magnetic field structure should have some important role in determining the shape and size of the molecular clouds (thus regulating the FIR temperature of the clouds themselves). The scheme, although quite naive, is already enough complicated for pretending to constraint it observationally. In the remainder we will focus on the simple question: is it possible to isolate few parameters which will enable us to make reliable predictions on the activity in disk galaxies?

1: THE SAMPLE

The sample used in the following analysis is based on all CGCG (Zwicky et al, 1963-1968) galaxies ($m_p \leq 15.7$) in 9 nearby clusters of galaxies: A262 (Perseus supercluster), Cancer region, A1367, A1656 (Coma Supercluster), Virgo cluster (limited to $m_p \leq 14.5$), A2147, A2151, A2197, A2199 (Hercules supercluster). In addition to the cluster galaxies, the sample includes all CGCG galaxies in the Coma *wall* between $11^h30^m < \alpha < 13^h30^m$; $18° < \delta < 32°$ which we use as a reference sample of non-cluster objects. The total number of galaxies is 1758, about

equally distributed in the cluster and reference samples. Of these, 874 are spirals. We have collected as much information as possible from the literature on these galaxies and devoted to them extensive observational campaigns in order to accumulate homogeneous information including the following photometric measurements:

- radio continuum (mostly at 1.4 GHz), possibly also at 0.6 GHz.
- 21cm line.
- deepest available FIR data in four bands, from the IRAS all sky survey (generally obtained from the Faint Object Catalogue).
- Near IR H, J and K band measurements (from aperture photometry).
- visible V,B,U photometry (from aperture and CCD measurements)
- measurements of the integrated H_α+[NII] line equivalent width.

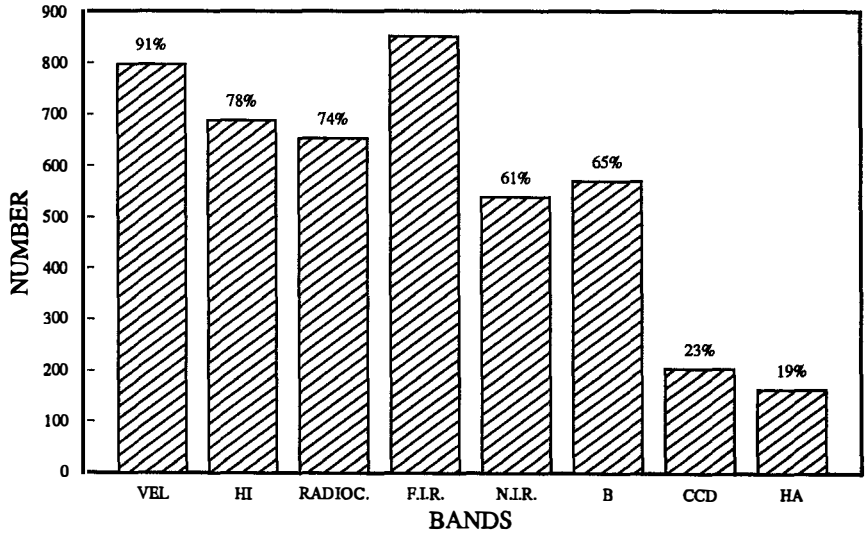

Fig. 2: State of completion of the survey of 874 spiral galaxies (march 92).

The database includes detections as well as upper limits (typically in the radio continuum and line and in the FIR). In addition to the photometric information, general properties have been determined or collected from the literature such as: UGC (Nilson, 1973), NGC and IC names (from RC3, de Vaucouleurs et al, 1991), accurate coordinates (with 2 arcsec accuracy), morphological types (generally from the UGC or redetermined if large scale plate material was available), recessional velocities and other miscellaneous information. We tried to keep track of the references on each of these measurements. Individual aperture measurements are transformed into total or isophotal magnitudes and corrections are applied according to well defined criteria (RC3). Magnitudes have typical uncertainties of 0.1 mag. Distance dependent quantities are computed assuming $H_0 = 100$ Km $s^{-1} Mpc^{-1}$. The transformed quantities constitute a database of 1758 entries, each with 70 fields.

Since here we are interested only in disk galaxies we will focus on galaxies of morphological

type later than Sa (874 objects). Fig. 2 gives the present (march 1992) status of completion of the survey in some relevant bands. Except for the radio continuum and FIR (where magnitude limited samples were observed) the survey does not yet match any completeness criterion. Nevertheless from Fig. 2 it appears that we are dealing with one of the largest samples of galaxies with homogeneous and accurate (integrated) photometrical measurements at many frequencies, which can be used for statistical purposes. The database has never been published as such, since it is continuously evolving, but it can be made available in computer readable form upon request to the author and will be maintained and updated.

2: THE FIRST ORDER DEPENDENCE: GALAXY LUMINOSITY

It has been stressed by many authors (e.g. Kennicutt, 1990, Gavazzi, 1991) that galaxies obey to a scaling law such that "bigger galaxies emit more of everything". Examples of such a law are given in Fig. 3 (a,b,c) where the luminosity in the Radio Continuum, 21 cm line (in solar masses) and FIR luminosities are plotted against absolute (photographic) magnitude. The relations shown are little more than trends, given the tremendous scatter of the data. Nevertheless these trends (indicating an almost direct proportionality) have important implications. The major implication is a negative one: one should never accomplish analyses based on luminosity-luminosity plots since these relations are dominated by the scaling law which hides other more interesting dependencies.

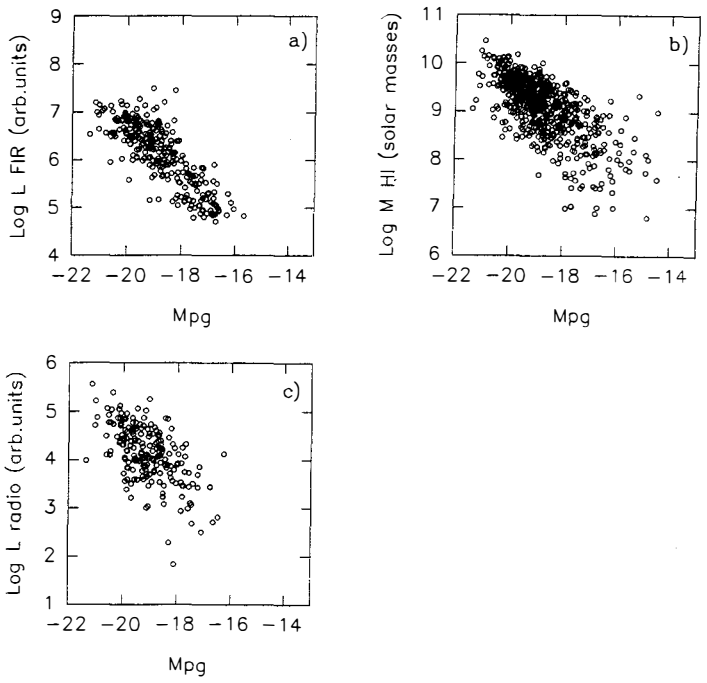

Fig. 3: Three examples of the nearly direct proportionality between luminosities in various bands and absolute magnitude. a) FIR, b) Neutral Hydrogen mass, c) radio continuum.

On the contrary, given the near proportionality observed, it is natural to produce normalized quantities, such as radio (or FIR) "excess" over the light, obtained by dividing the radio (FIR) flux by the flux emitted in some optical or infrared band. These adimensional quantities have the additional advantage of being distance independent. Gavazzi, Boselli and Kennicutt, (1991) illustrate that IR H band must be preferred to optical V band measurements, to perform a proper normalization, but either do a good job. Fig. 4 further illustrates this point.

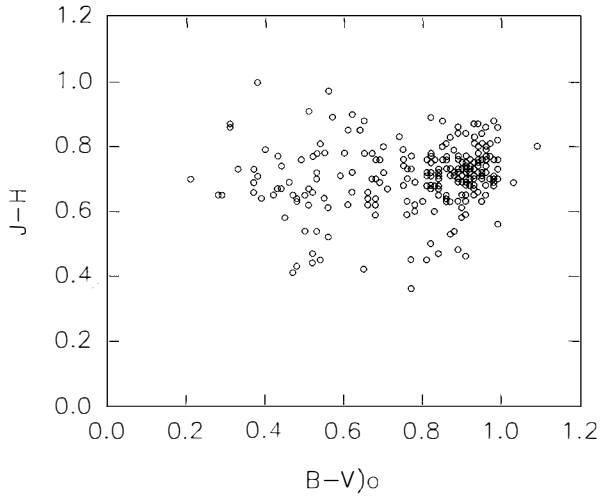

Fig. 4: The relation between the color index B-V and the infrared J-H for E+S0+S.

Here J-H color indices are plotted versus B-V for our total sample of E+S0+S. It is apparent that the interval in J-H is about half the interval in B-V. This indicates that galaxies have very similar IR properties, in spite of their variety of morphological types and of their star formation histories. This implies that galaxies of different types are dominated by the same type of cold stars (K giants), therefore measurements sensitive to low temperatures (typically few thousands degrees) are better probes of their total stellar content.

Accordingly, we use Radio/H and FIR/H flux ratios in the following.

The result of this section can be equivalently rephrased as: the overall galaxy luminosity L_H is the first order parameter regulating many forms of activity (L_ν) in galaxy disks:

$$L_\nu \propto L_H^\alpha \quad \text{with } \alpha \simeq 1 \tag{1}$$

The problem now is that of determining the second order parameter which "modulates" α.

3: THE SECOND ORDER DEPENDENCE: THE PRESENT STAR FORMATION RATE

The second point we would like to discuss is what our integrated data tell us on the dependence of the radio continuum and FIR emission on the star content of disk galaxies. Let us take a look to typical "overall" spectra of two galaxies in our sample with extremely different nuclear properties (Fig. 5).

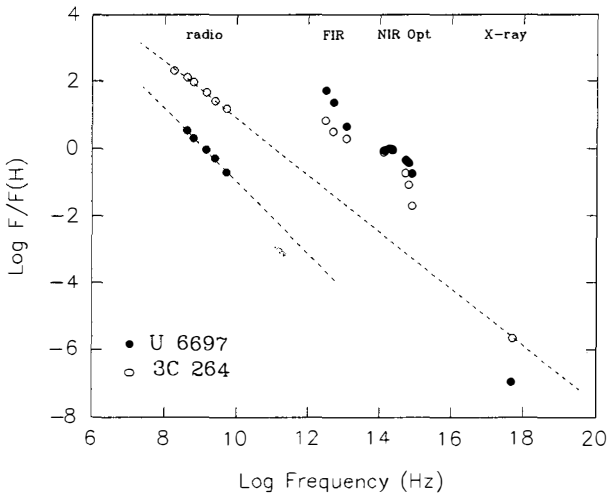

Fig. 5: Overall spectra (from radio to X-ray) of the irregular galaxy U6697 and of the radio galaxy 3C264.

The data represent fluxes normalized to the H band flux of one Irregular (UGC 6697) and one radio galaxy (3C 264 = NGC 3862). The difference in their optical colors is evident in V, B, U compared to H. The FIR emissivity of UGC 6697 is much higher than that of the Elliptical. The 5 points in the radio of both galaxies are nicely fitted by a power law (of slope $\sim$-0.8): a firm signature of non-thermal synchrotron processes (notice that in the radio galaxy the same power law fits the X-ray measurement). However in the case of 3C 264 the emission originates in the nucleus, in UGC 6697 it is a genuine disk emission (see Gavazzi et al. at this meeting). Nothing is known on the radio continuum in the millimeter and submillimeter bands. The data in the FIR can be fitted by thermal laws at two temperatures (one around 25 K and one slightly hotter). The NIR measurements (J, H, K) and the visible data (V, B, U) can be fitted by thermal distributions around 3000 K and 6000 K respectively. They represent the cold and the relatively hotter stellar components.

If one puts together many such spectra, grouped for example in classes of constant B-V color index, one obtains diagrams like those illustrated in Fig. 6. The scatter is tremendous in each band: as we already noticed galaxies have large "individualities". However one can discern a tendency for decreasing FIR and radio continuum emission with increasing color index (going from blue to redder galaxies). This becomes much more convincing when averages are taken within color classes, as plotted in Fig. 7. Although qualitatively, the above argument illustrates that indeed the present color of the stellar population governs the emissivity in the FIR and

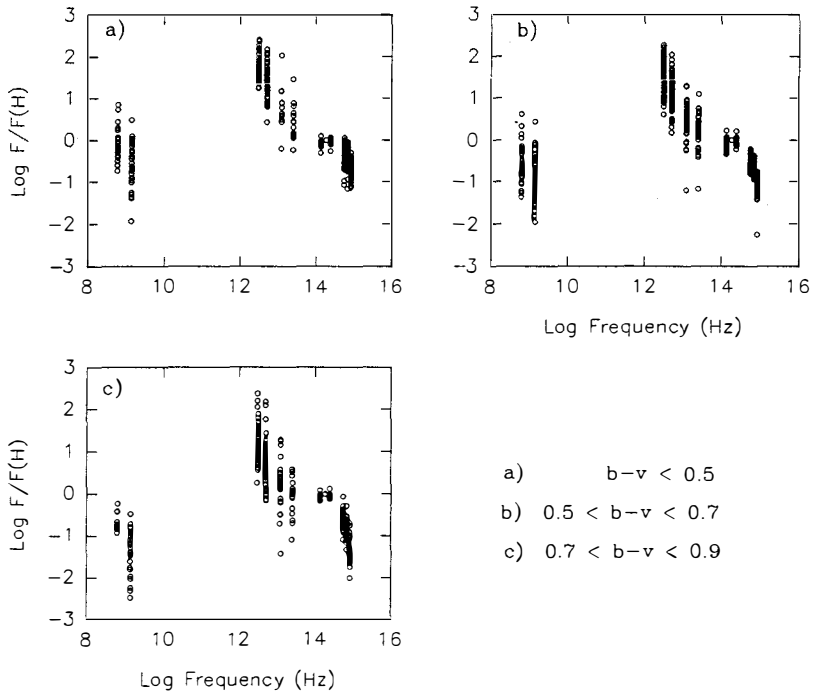

Fig. 6: Overall spectra of spiral galaxies grouped in classes of B-V color index.

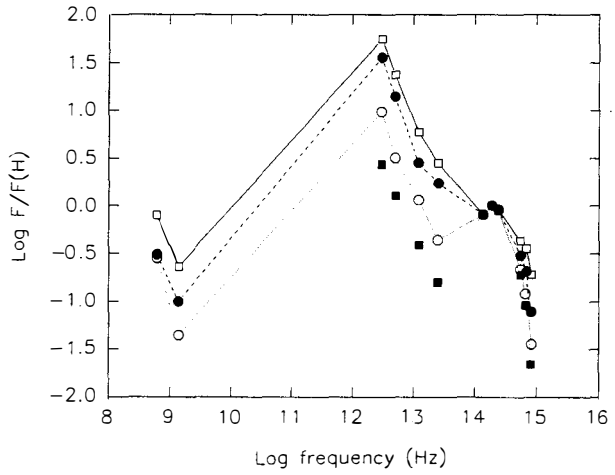

Fig. 7: Average overall spectra of galaxies of increasing B-V color: B-V<0.5 (open squares); 0.5<B-V<0.7 (filled circles); 0.7<B-V<0.9 (open circles); B-V>0.9 (Filled squares).

radio continuum bands. Further evidence is obtained by plotting the FIR/V and Radio/V flux ratios as a function of U-B)o (Fig. 8 a and b respectively).

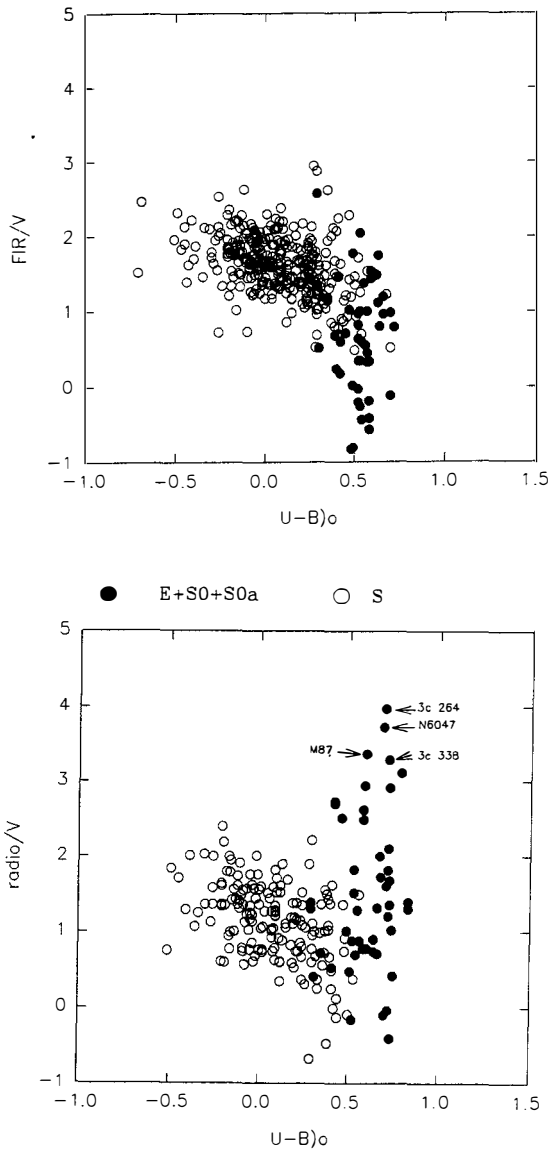

Fig. 8: Relation between FIR/V (a) or Radio/V (b) and U-B separately for Spirals and E+S0s. Some luminous radio galaxies are indicated.

In these diagrams we have included all morphological classes, from E to Spirals to emphasize that in the radio continuum there is a difference between galaxies dominated by a diffuse disk (spirals) and galaxies with strong nuclear sources (radio galaxies). While there is a clear trend

with U-B)o for the former, E+SOs do not follow any trend, showing a four order of magnitude scatter (along with a small range in color) which must be attributed to their unrelated nuclear activity. The same is not true in the FIR/V vs. U-B)o diagram, which shows more continuity between the two morphological classes. In this plot the few points higher than normal are associated with interacting Spiral+Spiral systems.

Color indices however are not the best available indicators of the star formation rate in galaxies, or at least not of the present star formation rate. This parameter is better quantified by the emissivity in the H_α line.

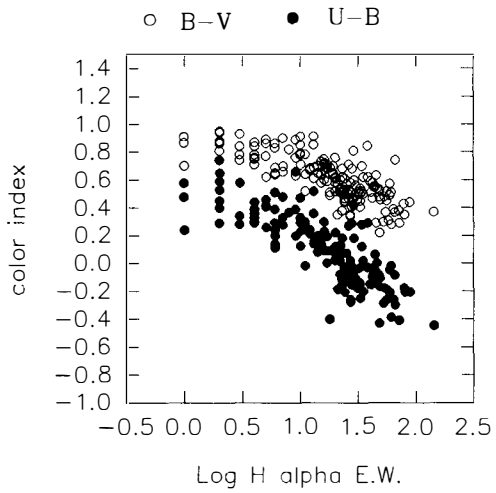

Fig. 9: Relations between H_α E.W. and B-V or U-B color indices.

Fig. 9 shows that color indices and H_α equivalent width (E.W.) are indeed non- linearly correlated (see Kennicutt and Kent, 1983). The strongest indication that both radio continuum and FIR emission are proportional to the present star formation rate is derived from Fig. 10, where the Radio/H and FIR/H flux ratios are plotted against H_α E.W. The radio correlates with H_α with a slope of one, while a slightly flatter slope is derived for FIR. This indicates that synchrotron emission can be taken as a direct indicator of the current star formation rate, or equivalently that sources of cosmic-ray electrons are identified with supernovae. This evidence was first discovered by Lequeux, (1971) and further investigated by Klein, (1982); Condon et al, (1982); Kennicutt, (1983), Gavazzi and Jaffe, (1986) and Gavazzi, Boselli and Kennicutt, (1991). FIR emission, on the contrary, comes from two components: one associated with massive star formation, another with the general radiation field (see also Helou, 1986; Deveroux and Eales, 1989; Mas-Hesse, 1992 and Thuan at this meeting, who has shown clearly that the contribution from the general radiation field increases in galaxies of earlier type). In conclusion we have established that in second approximation α in equation 1 is linearly related to the SFR for radio continuum luminosity and with a somewhat milder slope for FIR luminosity. In other words, quite accurate predictions can be made on radio continuum and FIR luminosities of disk galaxies given their H band luminosity (old stellar population) and estimates of the present SFR.

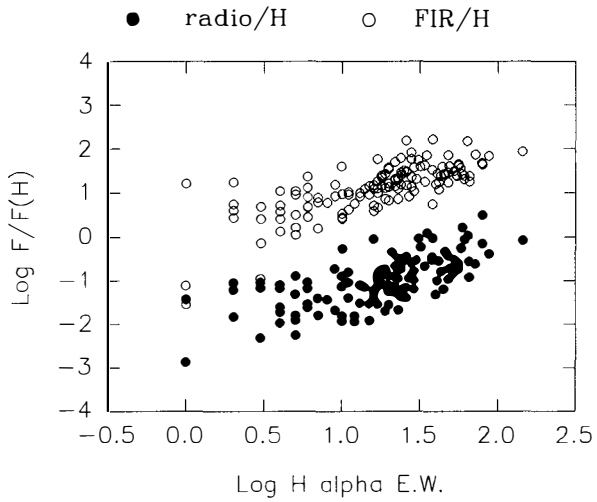

Fig. 10: The dependence of Radio/H and FIR/H on H_α E.W.

4: THE THIRD ORDER DEPENDENCE: THE INFLUENCE OF THE ENVIRONMENT

It is not the scope of the present work to discuss the dependence of galaxy properties on the environment, which has been covered by Balkowski at this meeting. However we would like to point out briefly some evidence which has relevant implications on the subject we are discussing.

We ask ourself the question: what fraction of galaxies surveyed in the radio continuum and FIR has a certain Radio/optical (FIR/optical) ratio and is this fraction similar in isolated and cluster galaxies? The question can be answered by constructing fractional luminosity functions, a statistical tool which allows us to take into account detections as well as upper limits (see Hummel, 1981).

The FIR/optical and Radio/optical luminosity functions are shown in Fig. 11 and 12 respectively (in this case we are forced to use the optical photographic magnitude to perform the normalization, since only this measurement is available for all surveyed galaxies). The 9 panel figures allow us to compare the luminosity functions of each cluster (and for the 9 clusters put together) with that of the reference sample of isolated objects in the Coma Supercluster region (solid line). It is immediately apparent that the FIR luminosity functions are not dissimilar one another, indicating that the FIR/optical ratio is strongly gaussian (in other words that FIR is almost proportional to optical, as we have already seen in Section 2). The only difference among cluster and isolated objects is that some clusters (typically: Coma, A2147 and Cancer) have a fraction of galaxies at high FIR/optical ratio (Log $FIR/m_p = 4.2$) marginally lower than the corresponding isolated galaxies. In other words the high FIR/optical ratios are missing in

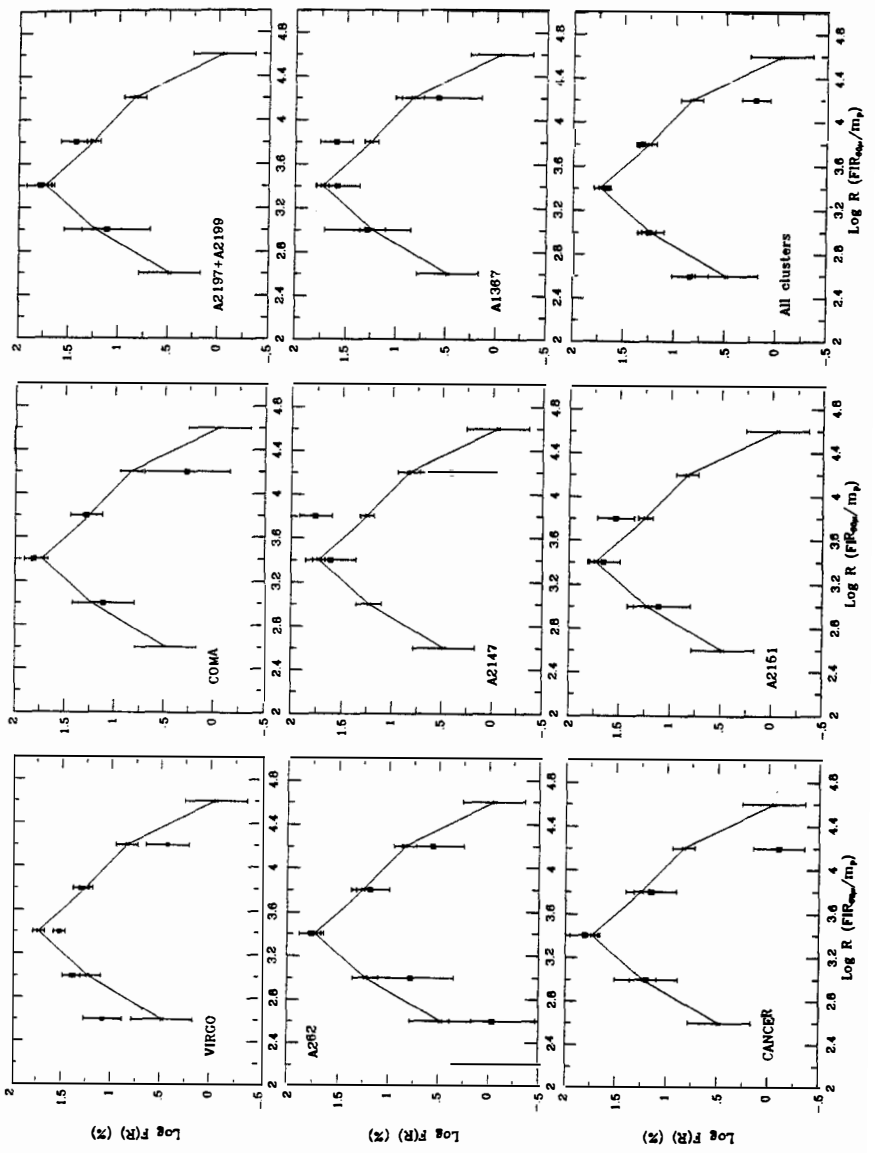

Fig. 11: Fractional, differential distribution of FIR/m_p in 9 clusters (filled squares) and in the reference sample of isolated galaxies (solid line).

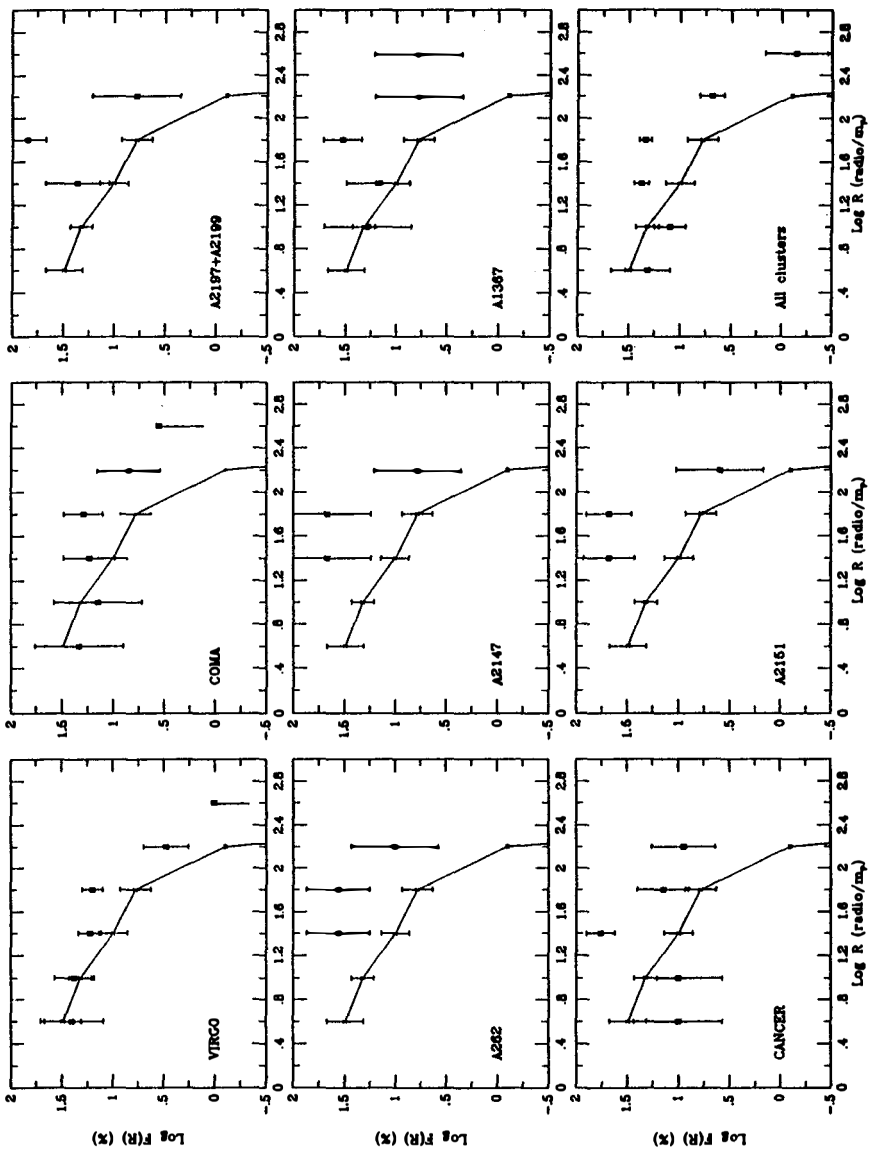

Fig. 12: Same as Fig. 11 for Radio/m_p

the cluster sample. This is not surprising, since it is expected that strong star formation rate is inhibited in clusters of galaxies (gas deficient objects are prevented from producing strong star formation). Alternatively we could argue that the dust content of cluster spirals might be reduced.

Quite unexpectedly, the opposite is found from the radio luminosity function, where an excess of galaxies with strong Radio/optical ratio is found in some clusters with respect to the field (namely in Coma, A262, A2147 and A1367). This implies that either in these clusters the star formation rate is enhanced, or that some other parameter, namely the magnetic field strength, is enhanced in cluster galaxies. This can arise as a consequence of ram-pressure exerted on the fast moving galaxies by the intergalactic medium that permeates clusters of galaxies. If FIR is taken as a direct measure of SFR we should conclude that the average SFR is quenched in clusters (see Fig. 11), therefore that the radio enhancement found in clusters is purely a consequence of magnetic field compression. However we have shown in Section 3 that this assumption is valid only in first approximation, therefore enhanced SFR in clusters cannot be ruled out on this basis. In fact evidence for enhanced star formation rate has been found in the Coma cluster by Bothun and Dressler, (1986), and similar evidences are found in three galaxies in A1367 (Gavazzi et al., this meeting). Therefore we are inclined to conclude that a combination of enhanced star formation rate and magnetic field amplification could produce the observed overabundance of strong Radio/optical ratios in cluster galaxies.

5: CONCLUSIONS

We have analyzed how the SFR and the galaxy environment play an important role in determining the relationship between the luminosity of the old stellar component and those in the FIR and radio continuum in normal disk galaxies. Equation (1) can be once more rewritten as:

$$L_{radio,FIR} \propto L_H^{\alpha(SFR,\rho_{gal})}$$

Where the dependence of α on SFR is almost linear for the radio and slightly milder for FIR and the dependence on the local galaxy density is positive for the radio and marginally negative for the FIR. We have also seen that the dependences on SFR and on ρ_{gal} are not totally independent. However we can say firmly that similar dependence on SFR is present in both the cluster and the reference samples.

Once the database will be completed we will be able to quantify these relatioships on observable quantities: H band magnitudes, H_α E.W., ρ_{gal}. For the time being, we prefer to conclude qualitatively that predictions on FIR and radio properties of disk galaxies can be made with reasonable accuracy once three fundamental parameters are known: an estimate of their old star content (H mag), of their present star formation rate (H_α or U-B) and of their environmental properties (membership to clusters).

ACKNOWLEDGMENTS: I wish to thank Alessandro Boselli and Marco Scodeggio for their invaluable contribution to this work; Bianca Garilli for her precious help in reducing the observations and Tommaso Maccacaro for his criticism on the manuscript. A special thank is due to the telescope operators of the Arecibo, Loiano, KPNO, San Pedro Martir and Tirgo Observatories.

REFERENCES

Bicay, M., and Helou, G., 1990, ApJ., 362, 59
Bothun, G., Dressler, A., 1986, ApJ., 301, 57
Condon, J., Condon, M., Gisler, G., Pushell, J., 1982, ApJ., 252, 102
Dame, T., Koper, E., Israel, F., Thaddeus, P., 1991, Proc. IAU conf. N 146, ed. F. Combes and F. Casoli, p. 23
de Vaucouleurs, G., de Vaucouleurs, A., Corwin, H., Buta, R., Paturel, G., and Fauque, P., 1991, Third Reference Catalogue of Bright Galaxies, Springer Verlag (RC3)
Deveroux, N., and Eales, S., 1989, ApJ., 340, 708
Fitt, A., Howarth, P., Lasenby., A., 1992, MNRAS, 255, 146
Gavazzi, G., 1991, Proc. IAU conf. N 146, ed. F. Combes and F. Casoli, p. 403
Gavazzi, G. and Jaffe, W., 1986, ApJ., 310, 53
Gavazzi, G., Boselli, A., Kennicutt, R., 1991, AJ., 101, 1207
Helou, G., 1986, ApJ., 311, L33
Hummel, E., 1981, A&A, 93, 93
Lequeux, J., 1971, A&A, 15, 42
Kenney, J., 1990, in "The Interstellar Medium in Galaxies" ed. H. Thronson and J. Shull, Kluwer Acad. Pub., p. 151
Kennicutt, R., 1983, A&A, 120, 219
Kennicutt, R., and Kent, S., 1983, AJ., 88, 1094
Kennicutt, R., 1990, in "The Interstellar Medium in Galaxies" ed. H. Thronson and J. Shull, Kluwer Acad. Pub., p. 405
Klein, U., 1982, A&A, 116, 175
Mas-Hesse, J., 1992, A&A, 253, 49
Mas-Hesse, J., and Kunth, D., 1991, A&AS, 88, 399
Nilson, P., 1973, Uppsala General Catalogue of Galaxies, Uppsala Obs. Ann., vol 6 (UGC)
Pellet, A. et al, 1978, A&AS, 31, 823
Trinchieri, G., Fabbiano, G., 1991, ApJ, 382, 82
Unwin, S., 1980, MNRAS, 192, 243
Walterbos, R., Schwering, P., 1987, A&A, 180,27
Walterbos, R., 1986, Phd. thesis, University of Leiden
Young, J., 1990, in "The Interstellar Medium in Galaxies" ed. H. Thronson and J. Shull, Kluwer Acad. Pub., p.67
Zwicky, F., et al, 1963-1968, Catalogue of Galaxies and Clusters of Galaxies. Caltech University Press, Pasadena (CGCG)

ABUNDANCE GRADIENTS IN BARRED SPIRAL GALAXIES

Pierre MARTIN*, Jean-René ROY*, and Julien BELLEY**

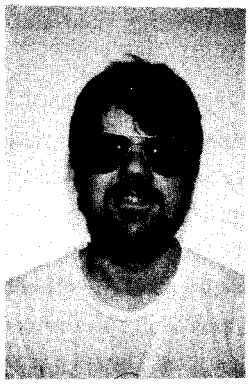
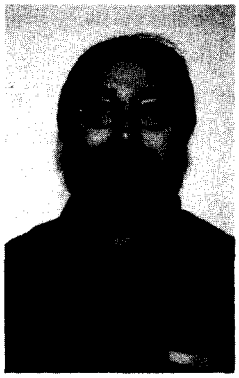
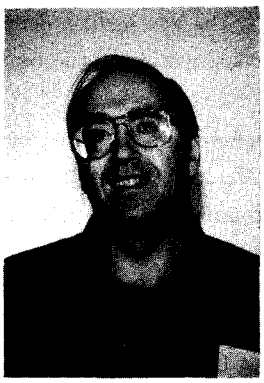

ABSTRACT

Monochromatic imagery in the main nebular lines has been obtained of the barred spiral galaxies NGC 925, NGC 1073, NGC 4303 and NGC 6946. The line ratios [O III]/Hβ and [O III]/[N II] have been used to estimate O/H abundances across the disks of these galaxies. There are well-developed global abundance gradients in galaxies with bars. Evidences for "flatter" inner gradients are found in NGC 1073 and NGC 6946.

* Observatoire du mont Mégantic – Université Laval
** Centre Universitaire St-Louis-Maillet – Université de Moncton

1. INTRODUCTION

The presence of a bar induces strong radial flows of interstellar gas in the disks of galaxies[1]. The various aspects of the hydrodynamics of galaxy disks under the conditions of radial flow have been investigated by several authors[2),3),4),5),6)]. These studies indicate that radial flows should modify the history of star formation and the local element composition in galaxies. Therefore, abundance gradients could hide some of the history of interstellar gas circulation. For example the radial distribution of heavy elements in barred galaxies would differ from that of normal galaxies if large quantities of gas are transported into the inner regions. The "mild abundance gradient" of the southern barred galaxy NGC 1365 has already been noted[7].

A simple approach helps to predict the possible effect of gas inflow[6]. Assuming Σ, the gas surface density, and v_r the azimuthally averaged radial velocity, then mass conservation in the center requires that

$$\Sigma\, v_r\, (2\pi\, r) \;=\dot{M}\; =\; \psi\pi r^2 \;+\dot{M}_{expul},$$

where ψ is the star formation rate in units of mass per unit area per unit time, and $\dot{M}_{expul}$ is the rate of mass loss due to expulsion from the center in a galactic wind, fountain or jet. If we assume that $\dot{M}_{expul}$ is negligible, we can predict the approximate behavior of O/H gradient in barred galaxies. The question becomes the following: **Will there be TOTAL consumption of the inflowing gas by forming NEW stars?**

- **if YES:** metal abundances would build up **ABOVE** the level expected in the absence of radial flow. → `The O/H gradient would appear STEEPER in the inner parts due to a higher mean level of abundances in the region of the bar.`
- **if NO:** The gas *cannot* be consumed as fast as it flows in; incoming low abundance gas (from larger galactocentric distances) will decrease the mean level of metals in the ISM **BELOW** that expected in the absence of radial flow. → `The O/H gradient will be flatter in the inner parts.`

Therefore, the shapes of inner abundance gradients and the mean levels of O/H abundances in the central parts of galaxies should inform us on the importance of radial transport of interstellar gas. Two studies based on a very limited data set have led to the assumption that abundance gradients are flatter in barred galaxies than in normal galaxies[7),8)].

This paper presents the O/H abundance gradients of four barred spiral galaxies derived from large data sets of H II regions.

2. OBSERVATIONS AND DATA REDUCTION

We obtained narrow-band images of the barred galaxies NGC 925, NGC 1073, NGC 4303 and of NGC 6946, which has a molecular bar[9], using a focal reducer on the

Mont Mégantic Observatory 1.6 m telescope. We employed a set of narrow-band ($\Delta\lambda$ = 10 or 20 Å) interference filters to observe the galaxies in the bright nebular lines of Hα, Hβ, [O III] 5007 Å and [N II] 6584 Å. To subtract the contributions of the visual or red stellar continua, two other filters with broader bandpass ($\Delta\lambda$ = 200 Å) centered at 5370 and 7020 Å were used. Image reduction and analysis were performed with the NOAO IRAF software system. Details about our procedures can be found in one of our recent papers[10]. Red continuum and Hα images of the barred galaxies NGC 1073 and NGC 4303 are shown in Figure 1 as examples. Calibrations of the monochromatic images were achieved through comparisons with published spectrophometry of H II regions in NGC 4303 and NGC 6946. For NGC 925 and NGC 1073, we did spectrophotometric measurements of a bright H II region in each galaxy. Integrated fluxes for large samples of H II regions were derived in each galaxy (Table 1). Correction for interstellar reddening was achieved by comparing the Hα/Hβ ratios with the theoretical Balmer decrement for a density of 100 cm^{-3} and a temperature of 8000 K. The reddening law of Savage & Mathis was used[11].

TABLE 1

Parameters of observed barred spiral galaxies

Object	Type	D [Mpc]	R_{eff} [kpc]	i [°]	P.A. [°]	No. H II reg.
NGC 925	SAB(s)d	7.05*	...	55	102	82
NGC 1073	SB(rs)c	11.4*	...	18.5	-15.4	60
NGC 4303	SAB(rs)bc	15.2†	5.3	25	7	79
NGC 6946	SAB(rs)cd	5.9[12]	6.2	30	62	189

$\star$: Using H_0 = 100 km/s/Mpc. $\dagger$: Using H_0 = 75 km/s/Mpc.

3. RESULTS: RADIAL GRADIENTS OF LINE RATIOS AND ABUNDANCES

The azimuthal positions and galactocentric distances of the H II regions of the four galaxies were calculated assuming positions angles of the line of nodes and inclinations as of Table 1.

Figure 2 presents the gradients of the line ratios [O III]/Hβ in NGC 4303 and [N II]/[O III] in NGC 1073 as examples. After verifying that the H II region spectra were consistent with photoionisation by massive stars, we used these line ratios to estimate O/H abundances in the H II regions[13),14]. There is a certain degree of uncertainty

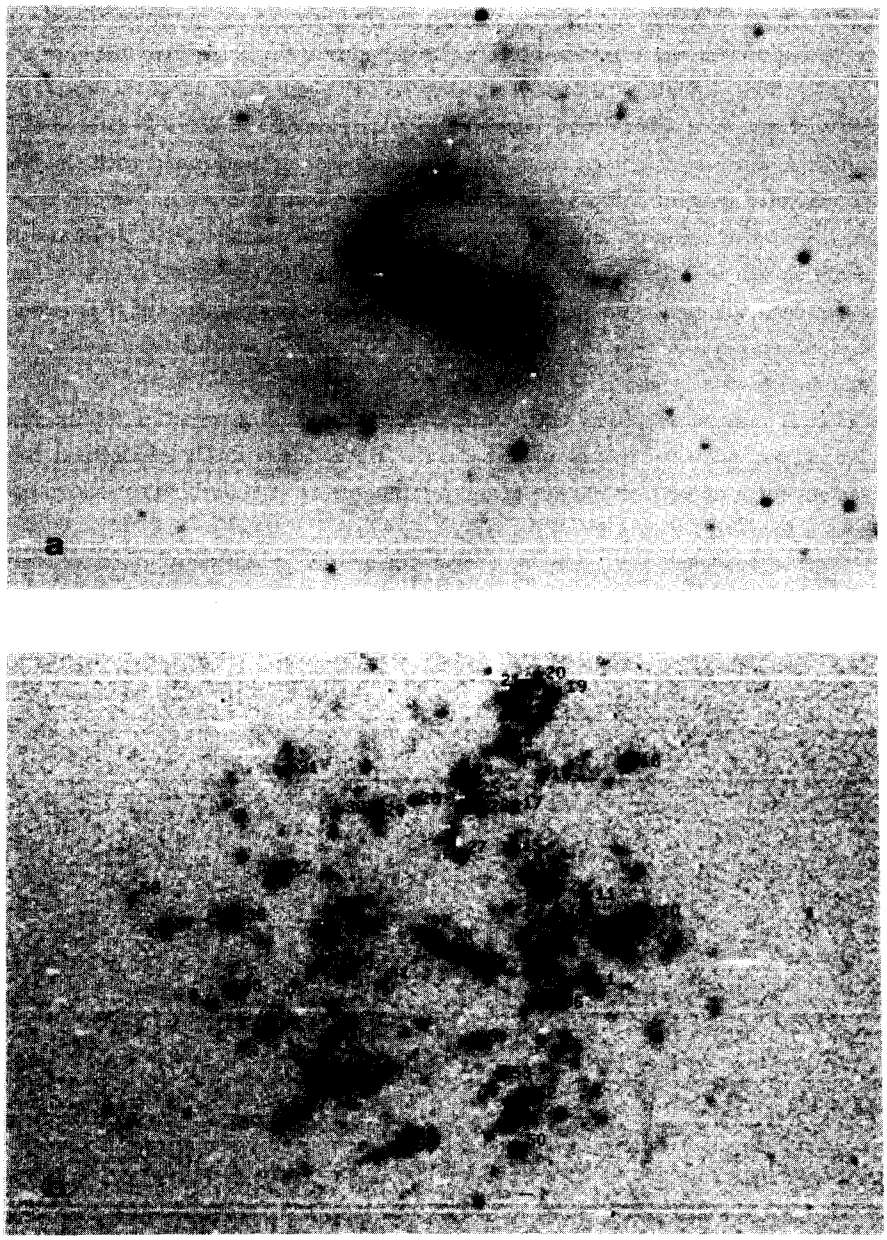

Figure 1. a) Red continuum image (7020 Å $\Delta\lambda$ = 200 Å) of the galaxy NGC 1073. b) Monochromatic Hα image of the galaxy NGC 1073. Numbers correspond to H II regions for which O/H abundances were derived.

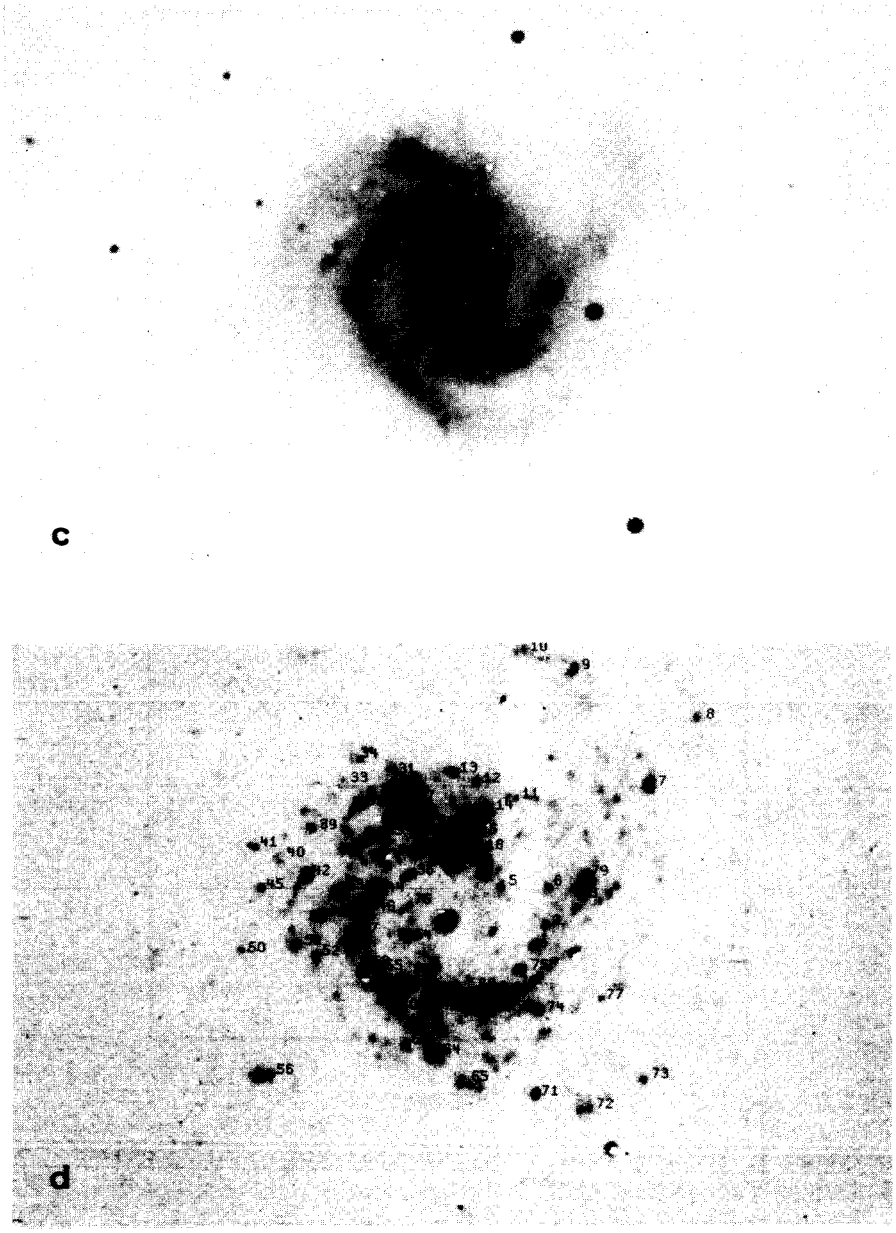

Figure 1. c) Red continuum image of the galaxy NGC 4303. d) Monochromatic Hα image of the galaxy NGC 4303.

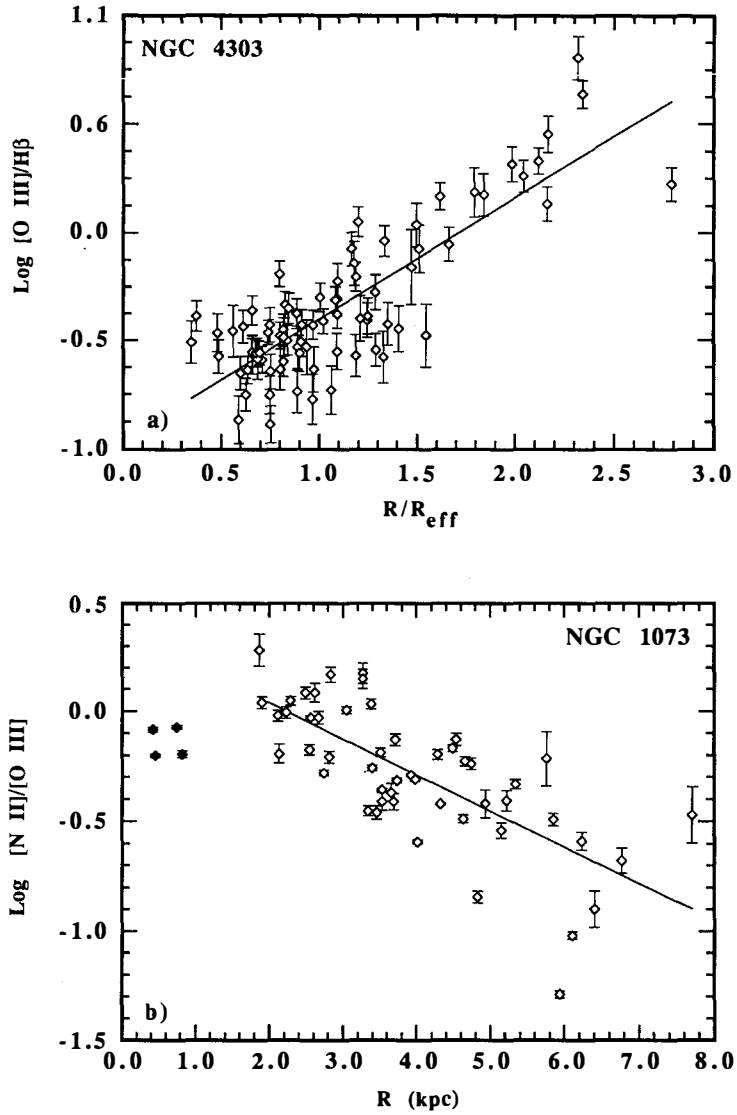

Figure 2. a) The line ratio [O III]/Hβ versus R/R_{eff} in the galaxy NGC 4303. b) The line ratio [N II]/[O III] versus radius in the galaxy NGC 1073. Black symbols correspond to the H II regions in the bar.

in the absolute values of the O/H derived by using such semi-empirical calibrations; nevertheless they give reliable results in term of relative behavior when comparing galaxies between one another. In Figure 3, we show the O/H abundances as a function of radius for the four barred galaxies investigated. In Figure 4, we show the O/H abundance gradient in the *normal* spiral galaxy NGC 628 for comparison. The main findings of our small survey are as follow:

a) The radial distributions of H II regions across the disks of barred galaxies can be quite different. While NGC 925 and NGC 6946 possess a large number of H II regions in their inner parts, NGC 1073 has very few. In NGC 4303, the area within the bar radius is devoid of H II regions except for the very strong nuclear emission. Thus we see a range of conditions where the presence of a bar enhances massive star formation (NGC 925, NGC 1073 and NGC 6946), and others where it apparently quenches it (NGC 4303).

b) The four observed barred galaxies display [O III]/Hβ and [N II]/[O III] gradients which are consistent with well-developed O/H abundance gradients across large fractions of their disks. The exact values of amplitude of the gradients are subject to the distance uncertainties. The presence of the bar has NOT affected the relative distribution of elements in the disks in the regions ***beyond*** the stellar bar. For example the global gradient (based on [O III]/Hβ as an abundance indicator) in NGC 4303 corresponds to ΔLog (O/H)/ΔR = -0.073 $\pm$ 0.006 dex/kpc, which is identical to that found in large normal spirals galaxies like NGC 628, NGC 2997 and the Milky Way. Because of the absence of H II regions in the inner parts, we are unable to tell what abundances are doing in the bar domain of NGC 4303.

c) We observe a somewhat anomalous behavior in the inner parts in two galaxies: NGC 1073 and NGC 6946 are the two barred galaxies where a possible ***flattening*** of the gradient is observed. In these galaxies, the mean level of O/H abundances in the bar domain is consistent with a ***depletion*** of metal abundances. This is indicative of dilution from low-metallicity gas by radial flow along the stellar or molecular bar. The bar drives a radial flow which brings in the inner regions low-metallicity gas from the outer regions at a rate greater than it is consumed by star formation in the bar domain.

4. CONCLUSION

Our survey of several hundreds H II regions in four galaxies with bars shows the following:

– there are well-developed ***global*** abundance gradients in barred galaxies; indeed the slope of the O/H gradients at radii ***beyond*** the bar extremities is identical to that of normal galaxies.

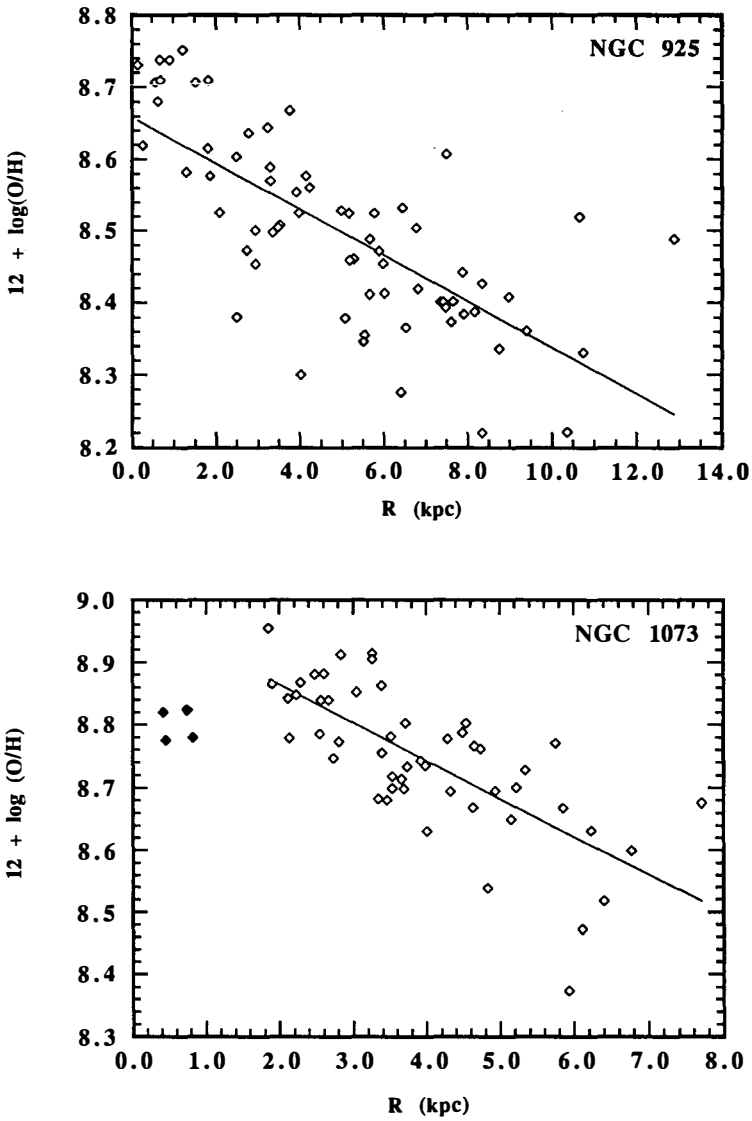

Figure 3. O/H abundances as a function of galactocentric distances derived from the [N II]/[O III] ratio as calibrated by Edmunds & Pagel (1984) in the four barred galaxies.

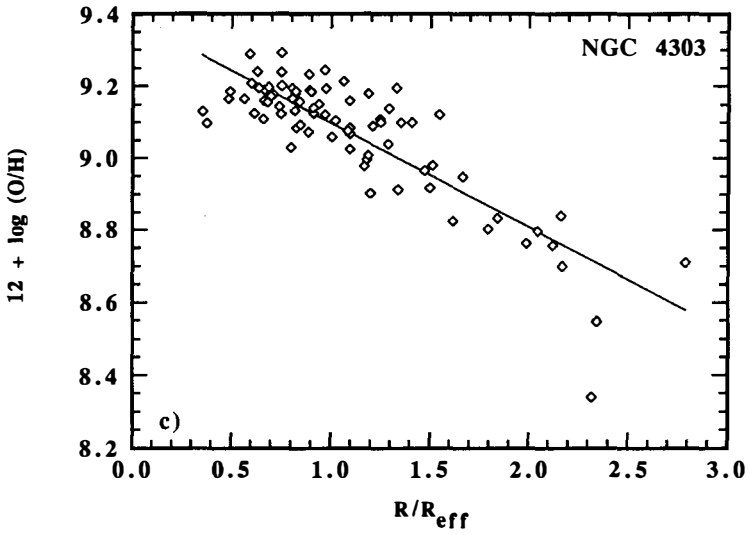

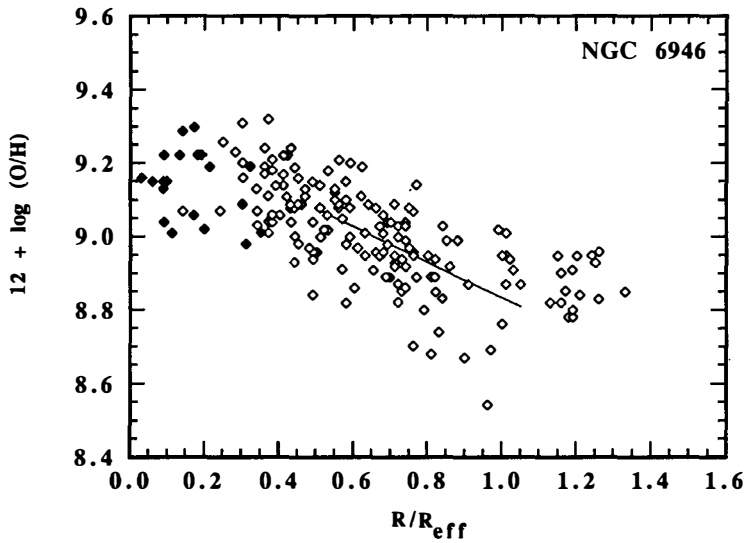

Figure 3. (*continued*)

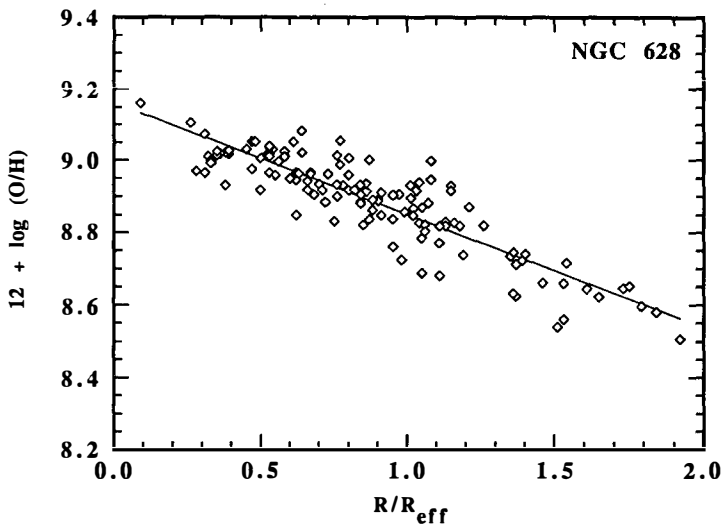

Figure 4. O/H abundances as a function of galactocentric distances derived from the [N II]/[O III] ratio as calibrated by Edmunds & Pagel (1984) in the *normal* spiral galaxy NGC 628.

– evidences for "flatter" inner gradients are found in NGC 6946 and NGC 1073; the levels of O/H derived in the bar regions are also indicative of an apparent depletion of metals compared to what would be expected in the absence of a bar (*e.g.* see Fig. 4).

The presence of bars can modify the history of star formation and the radial distribution of elements in the region where the bar is active. However the effect is not striking, and can be detected only with very large data sets of spectral data on a large number of H II regions across the disks of galaxies.

REFERENCES

1. Huntley, J. M., Sanders, R. H. & Roberts, W. W., 1978, ApJ, 221, 521.
2. Mayor, M. & Vigroux, L. 1981, A&A, 98, 1.
3. Clarke, C. J. 1989, MNRAS, 238, 283.
4. Clarke, C. J. 1991, MNRAS, 249, 704.
5. Edmunds, M. G. 1990, MNRAS, 246, 678.
6. Struck-Marcell, C. 1991, ApJ, 368, 348.
7. Alloin, D., Edmunds, M. G., Linblad, P. O. & Pagel, B. E. J. 1981, A&A, 101, 377.
8. Pagel, B. E. J., Edmunds, M. G., Blackwell, D. E., Chun, M. S. & Smith, G., 1979, MNRAS, 189, 95.
9. Ball, R., Sargent, A. I., Scoville, N. Z. K., Lo, K.-Y. & Scott, S. L. 1985, ApJL, 298, L21.
10. Belley, J. & Roy, J.-R. 1992, ApJS, 78, 61.
11. Savage, B. D. & Mathis, J. S. 1979, ARA&A, 17, 73.
12. McCall, M. L. 1982, Ph. D. Dissertation, University of Texas.
13. Alloin, D., Collin-Souffrin, S., Joly, M. & Vigroux, L. 1979, A&A, 78, 200.
14. Edmunds, M. G. & Pagel, B. E. J. 1984, MNRAS, 211, 507.

THE FAR-INFRARED PROPERTIES OF GALAXIES ALONG THE HUBBLE SEQUENCE

Trinh X. Thuan
Astronomy Department, University of Virginia
P. O. Box 3818, University Station
Charlottesville, VA 22903

and

Marc Sauvage
Service d'Astrophysique, Centre d'Etudes de Saclay
91191 Gif-sur-Yvette, Cedex France

ABSTRACT

We have cross-correlated the magnitude-limited Center for Astrophysics (CfA) galaxy sample (m (Zwicky) $\leq$ 14.5) with the IRAS Faint Source Data Base, resulting in a catalog of 1544 galaxies detected in at least one of the 4 IRAS wavelengths. These galaxies are, as a whole, less infrared-active than those in the IRAS Bright Galaxy Catalog.

The catalog is used to investigate the far-infrared luminosity L(FIR) as a star formation indicator in galaxies. We found that the cirrus component contributes increasingly to L(FIR) along the Hubble sequence, from late-type to early type galaxies. If L(FIR) is to be used as a star formation indicator in galaxies, it needs to be corrected, to first order, for the cirrus component, taking into account the morphological type of the galaxy.

We have also studied the FIR emission of galaxies along the Hubble sequence. We find that, while the FIR emission in spiral and late-type galaxies is mainly controlled by star formation, it is the dust spatial distribution relative to the heating stars which governs the FIR emission in early-type galaxies. The dust in E-SO galaxies must be concentrated in their inner parts ($r \lesssim 1$ Kpc) where the density of heating stars is the highest. The 12μm emission in early-type galaxies is best understood as not coming from photospheres of stars and dust in circumstellar envelopes around mass-losing red giants, but as having the same origin as the 12μm emission in spirals, i.e., PAHs.

1. THE CATALOG

The IRAS all-sky survey has considerably increased our knowledge of the far-infrared properties of galaxies. But most of the attention has been focused on infrared-bright galaxies such as those listed in the IRAS Bright Galaxy Catalog (Soifer et al. 1989). These turn out to be in majority starburst galaxies which are interacting or merging, Seyfert galaxies or quasars. Here, we wish to study the far-infrared (FIR) properties of 'normal' galaxies, distinguished by their optical and not by their FIR apparent luminosities, and which, in terms of absolute space density, dominate the local universe. To this end, we have used the Center for Astrophysics (CfA) galaxy sample which is an optically magnitude-limited sample ($m(Zwicky) \leq 14.5$) and which contains 2445 galaxies. The CfA catalog was cross-correlated with the IRAS Faint Source Data Base, resulting in the detection of 1544 galaxies in at least one of the four IRAS wavelengths, at 12, 25, 60 or 100μm, and giving a 63% detection rate. The details of the construction of the FIR catalog are given in Thuan and Sauvage (1992). In addition to FIR fluxes, the catalog contains complete morphological and magnitude information.

Not surprisingly, the galaxies in our FIR catalog are much less infrared-active than those in the IRAS Bright Galaxy Catalog (BGC). The range of observed FIR luminosities in our catalog extends from $\sim 4 \times 10^6$ $L_\odot$ to $\sim 2.5 \times 10^{12}$ $L_\odot$, with the peak of the distributing occurring at $\sim 6 \times 10^9$ $L_\odot$. In contrast, the range of FIR luminosities in the BGC extends from $\sim 10^8$ to $\sim 2 \times 10^{12}$ $L_\odot$, with the peak of the distribution occurring at a value 5 times higher, at $\sim 3 \times 10^{10}$ $L_\odot$ (Thuan and Sauvage 1992).

2. ON THE USE OF L(FIR) AS A STAR FORMATION INDICATOR

Ever since the release of the IRAS survey, attempts have been made to use the FIR luminosity L_{FIR} of a galaxy to derive its star formation rate

(SFR). But the link between FIR emission and star formation is still controversial. Some authors (e.g. Helou 1986) favor a two-component model where the FIR emission comes from: 1) star-forming regions and 2) quiescent regions not associated with star formation (the cirrus component). Other authors (e.g. Devereux and Young 1991) argue for a 1-component where the FIR emission comes entirely from the star-forming regions.

We use here our catalog in an attempt to resolve the controversy. Since we wish to investigate the validity of L_{FIR} as a star formation indicator, we need to introduce another observational star formation indicator which is independent of L_{FIR}. We choose to use the Hα luminosity. Cross-correlation of our catalog with Kennicutt's (1983) Hα survey resulted in a sample of 48 galaxies (Sample I). There are 135 galaxies in our catalog with Hα + [NII] equivalent widths from Romanishin (1990) and Kennicutt (1992) (Sample II).

If the Hα and FIR luminosities have a common origin, i.e. star-forming regions, we would expect a linear correlation between $L_{H\alpha}$ and L_{FIR} (i.e. n = 1 in the relation $L_{H\alpha} \propto L_{FIR}^{n}$). In both our samples, the slope of the correlation is not unity, but 0.69 $\pm$ 0.07, with a correlation coefficient of 0.89. A plausible reason for the non-linearity is that a significant fraction of L_{FIR} does not come from star-forming regions and that the two-component model is, to first order, correct. In figure 1, taken from Sauvage and Thuan (1992), the mean $L_{FIR}/L_{H\alpha}$ ratio is plotted, with the dispersion about the mean, for the galaxies in both samples I and II, as a function of morphological type. The solid line corresponds to the $L_{FIR}/L_{H\alpha}$ ratio observed for HII regions in the spiral galaxy M33 where the SFR derived L_{FIR} and $L_{H\alpha}$ agree best (Wilson et al. 1991).

Figure 1 shows a systematic increase of the $L_{FIR}/L_{H\alpha}$ ratio towards

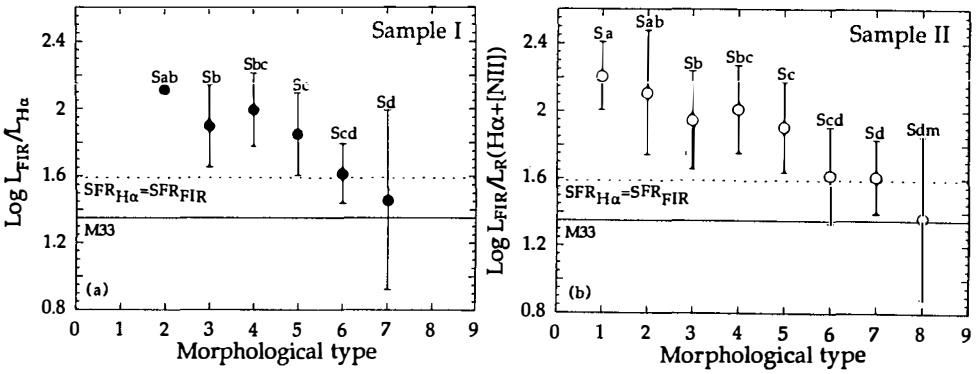

Figure 1. Variation of the $L_{FIR}/L_{H\alpha}$ ratio with galaxian morphological type. For each type, the mean value is plotted with the 1σ dispersion about the mean.

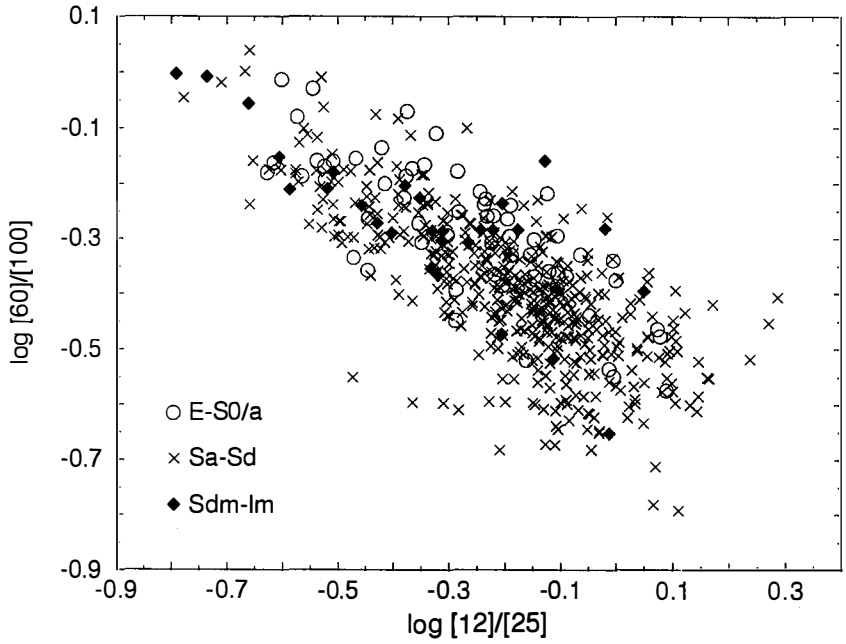

Figure 2. The IRAS color-color diagram for galaxies of different morphological types.

earlier types, from type Sdm to type Sa. We interpret this increase as due to an increasing cirrus component in early-type spiral galaxies: Sdm galaxies have no cirrus contribution to L_{FIR}, Scd galaxies have 46% of L_{FIR} coming from cirrus, while that percentage increases to 86% for Sa galaxies. Observations of nearby galaxies with enough spatial resolution to distinguish between the two components support these findings. Walterbos and Schwering (1987) find that as much as 85% of the FIR emission of M31 (type Sb) comes from cirrus. Rice et al. (1990) attribute 40% of the FIR emission of M33 (type Scd) to cirrus, while Sauvage et al. (1990) find that only 10-20% of the FIR emission of the Magellanic Clouds (type Sdm) come from regions with cirrus colors.

Correcting L_{FIR} of each galaxy in sample I by the morphological type dependent cirrus fraction given in Sauvage and Thuan (1992) does linearize the $L_{H\alpha} \propto L_{FIR}^{n}$ correlation. The new slope is $n = 0.86 \pm 0.05$ with a correlation coefficient of 0.88. While the slope approaches 1, it is still not unity. Clearly, the cirrus contribution is only a first-order correction and the morphological type is <u>not</u> the unique index of mixing between the cirrus and star-forming components. There is at least a second parameter, as evidenced by the large dispersion of the mean value of $L_{FIR}/L_{H\alpha}$ within a morphological type and the fact that the dispersion does not appreciably decrease after the cirrus corrections are applied. This second parameter is probably related to the detailed star formation process in each individual galaxy.

Finally, we note that the variation of $L_{FIR}/L_{H\alpha}$ implies that the high-mass star formation efficiency, defined as the fraction of IR-emitting interstellar medium directly associated with star formation, increases towards later morphological types, the increase being a factor of ~3 from Sa to Scd, and ~5 from Sa to Sdm (Sauvage and Thuan 1992).

3. THE FIR EMISSION IN GALAXIES ALONG THE HUBBLE SEQUENCE

3.1 Late-type galaxies

The IRAS [60]/[100] vs. [12]/[25] color-color diagram[1] is useful for quickly assessing the FIR properties of galaxies because it gives information on the radiation emitted by two different grain populations. The 12 and 25μm emission is thought to come from small grains (< 1.5 nm) composed of macromolecules called Polycyclic Aromatic Hydrocarbons (PAHs) while the origin of the 60 and 100μm emission is believed to be large (10 to 500 nm) silicate and graphite grains. We plot in figure 2 all galaxies in our catalog detected at all 4 IRAS bands, a total of 541 galaxies.

As has been noted previously (e.g. Helou 1986) the galaxies all lie within a relatively narrow band going from the high [12]/[25] and low [60]/[100] end, characteristic of a cirrus-like environment, to the low [12]/[25] and high [60]/[100] end, characteristic a star-forming environment. Thus, the IRAS color-color diagram has been commonly interpreted in terms of a single parameter: the star formation efficiency (SFE); the high [60]/[100] and low [12]/[25] end corresponds to an intense interstellar radiation field (ISRF) and high SFE in starburst galaxies, while the low [60]/[100] and high [12]/[25] corresponds to a weak ISRF, and a low SFE in quiescent galaxies.

Our data, which include also the morphological type of the galaxy, imply that a star formation parameterization alone is not sufficient to account for all the FIR properties of galaxies. To see this, we plot each of the galaxies in figure 2 by one of three symbols: open circles

---

[1] Here [i]/[j] = log [f(i)/f(j)] where i and j are two different IRAS bands

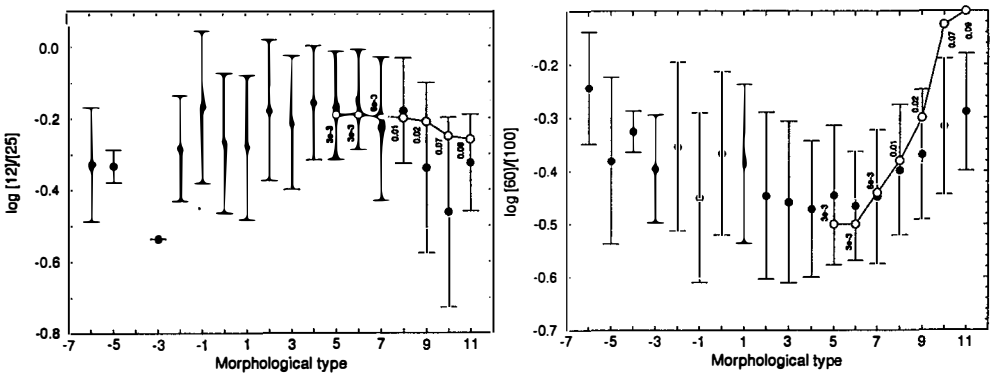

Figure 3. a) The FIR log 12 / 25 color as a function of de Vaucouleurs morphological type: E-SO (T =-5 to T = - 1), Sa (T = 1), Sb (T = 3), Sc (T = 5), Sd (T = 7), Sm (T = 9) .
b) Same for the FIR log 60 / 100 color.

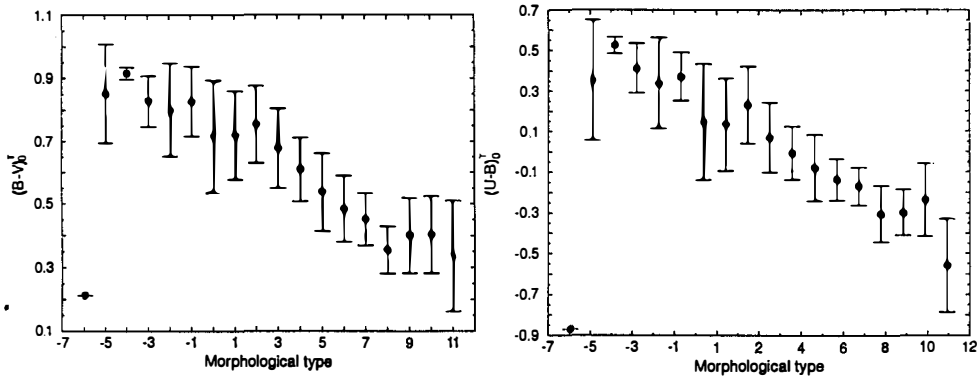

Figure 4. a) The optical $(B-V)_0^T$ color as a function of de Vaucouleurs morphological type.
b) Same for the $(U-B)_0^T$ color.

for E-SO galaxies, crosses for spiral galaxies (type Sa-Sd) and filled diamonds for magellanic irregular and late-type galaxies. The FIR properties of spiral and irregular can be well explained with a variation of the SFE: the former, with a low SFE, populate the low [60]/[100] and high [12]/[25] end, while the latter, with a high SFE, generally occupy the low [12]/[25], high [60]/[100] end.

3.2 Early-type galaxies

But what is unexpected is the location of the early-type E and SO galaxies: they occupy the same region as irregular and magellanic galaxies. Figures 3a and 3b show in detail the similarity of the [12]/[25] and [60]/[100] colors for E-SO and Sdm-Im galaxies.

What is the heating agent of the dust in E-SO galaxies which makes it as hot as that in Sdm-Im galaxies?

3.2.1 Star formation

Figures 4a and 4b show the run of the $(B-V)_T^o$ and $(U-B)_T^o$ colors as a function of morphological type for the galaxies in our catalog. Both show a smooth variation, the colors becoming steadily redder from late-type to early-type galaxies, and reflecting a steady change from young and blue stellar populations to old and red populations. It is clear that the stellar populations of the E-SO galaxies in our sample are not unusual, and it is not star formation which is heating the dust inside them.

3.2.2 AGNs

Can the heating agent be an active galactic nucleus (AGN) which is heating the dust with non-thermal radiation? A good indicator of whether or not the emission of a FIR source is contaminated by that of an AGN is the ratio of the far-infrared flux to radio flux q = log f(FIR)/f(6cm) (Condon et al. 1991). Only 13 E-SO galaxies in our sample were detected in the Condon et al. (1991) 6 cm survey. This detection rate is

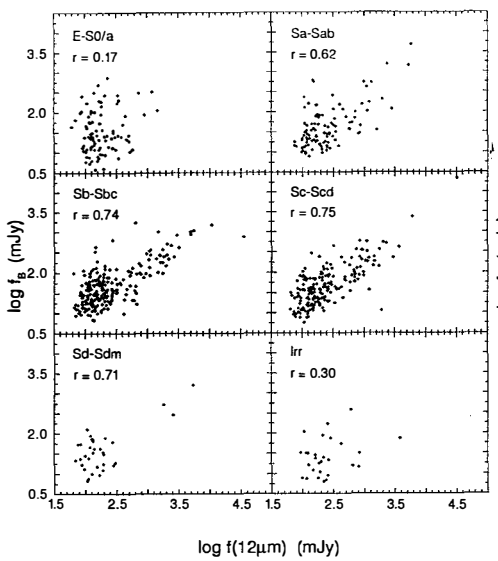

Figure 5. The f(B)-f(12μm) correlation for different morphological types. The correlation coefficient r is given for each type.

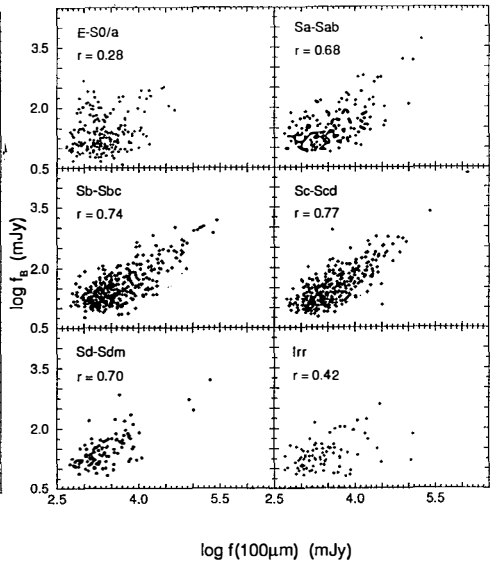

Figure 6. The f(B)-f(100μm) correlation for different morphological types. The correlation coefficient r is given for each type.

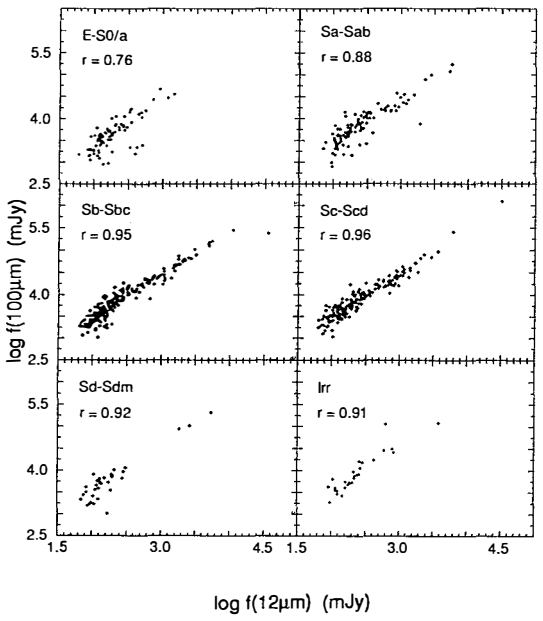

Figure 7. The f(12μm)-f(100μm) correlation for different morphological types. The correlation coefficient r is given for each type.

consistent with q ~ 2.6, which is characteristic of galaxies without 'monsters'. Thus the dust in our E-SO galaxies cannot be heated by AGNs.

3.2.3 Stellar emission

Does the 12μm emission in E-SO galaxies come from photospheres of stars and dust in circumstellar envelopes around mass-losing red giants, as proposed by Jura et al. (1987) and Knapp et al. (1992)? This suggestion is based, for the most part, on a good correlation between the 12μm and blue fluxes, implying a common origin, stars. But that correlation is based on a small data set, the Shapley-Ames catalog with $B_T^o \leq 12$ mag. With our larger data base, the f(B) - f(12μm) correlation is not present for early-type galaxies (figure 5). It is much better for spiral galaxies, becoming worse again for irregular galaxies. This behavior is very similar to that of the f(B) - f(100μm) correlation (figure 6). This implies a very good correlation between the 12μm and 100μm fluxes in galaxies of all types, and figure 7 confirms that expectation. Hence, the most natural hypothesis is that both 12μm and 100μm fluxes come from the interstellar medium, in spiral galaxies as in early-type galaxies. The 12μm emission in E-SO galaxies has probably the same origin as that in spirals, i.e. PAHs.

3.2.4 Spatial distribution of the dust

The FIR colors observed for E-SO galaxies (figures 3a, 3b) imply a dust temperature between ~25 and ~45K. According to the dust heating models of Jura (1982) with different ultraviolet heating spectra (the results are very insensitive to the exact nature of the heating spectrum), these temperatures are found only in the center of early-type galaxies (figure 8). The reason for these high temperatures is the high stellar densities in the center of early-type galaxies as compared to those in spiral disks. Thus to explain the FIR colors of early-type galaxies, we

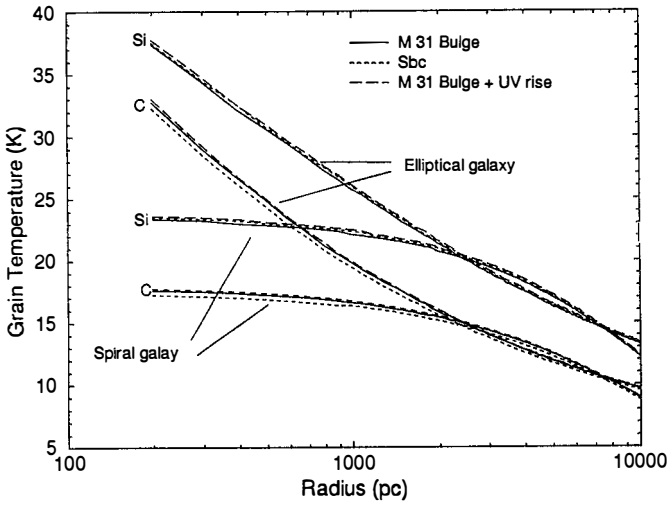

Figure 8. Silicate and graphite grain temperature as a function of the distance from the center of an elliptical galaxy and a spiral galaxy (Jura 1982). Several heating UV spectra have been used (Coleman, Wu and Weedman 1980).

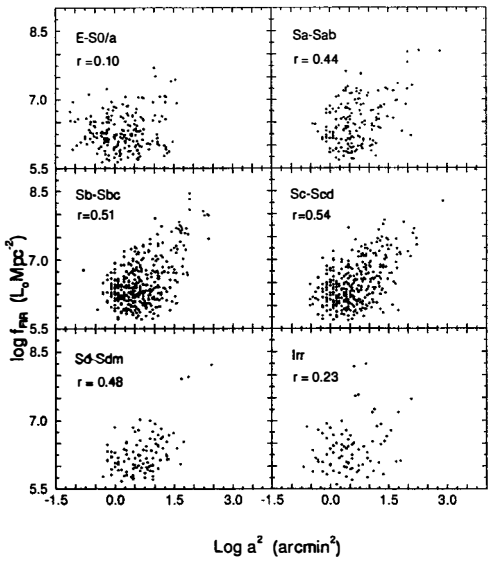

Figure 9. Correlation between the FIR flux and the area of the galaxy for different morphological types. The correlation coefficient r is given for each type.

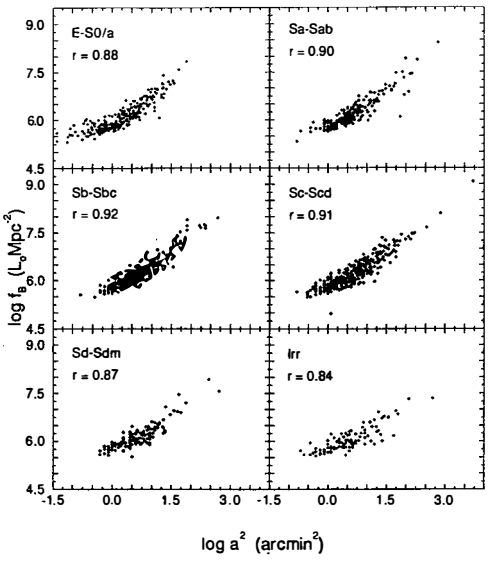

Figure 10. Correlation between the blue flux and the area of the galaxy for different morphological types. The correlation coefficient r is given for each type.

need to postulate that the dust in these galaxies is concentrated in their inner parts ($r \lesssim 1$ Kpc). In these circumstances, f(FIR) should be uncorrelated with the area of the galaxy. Figure 9 shows that this is indeed the case: there is no correlation for E-S0 galaxies, the correlation is the best for Sc-Scd galaxies (de Vaucouleurs type T = 3) where the dust is spread throughout the whole disk, and worsens again for irregular galaxies. As a check, we show in figure 10 the correlation between f(B) and the area of the galaxy. The correlation is very good for all types, as expected.

In summary, the FIR colors (figures 3a and 3b) are governed by the spatial distribution of the dust relative to the heating stars in early-type galaxies, while they are controlled by star-formation in spiral and late-type galaxies.

ACKNOWLEDGEMENTS

TXT thanks the partial financial support of Air Force Office of Scientific Research Grant 89-0467. He is grateful for the warm hospitality of the Service d'Astrophysique at Saclay.

REFERENCES

Coleman, G. C., Wu, C. C. and Weedman, D. W. 1980, Ap. J. Suppl., 43, 393.

Condon, J. J., Frayer, D. T. and Broderick, J. J. 1991, A. J., 101, 362.

Devereux, N. A. and Young, J. S. 1991, Ap. J., 371, 515.

Helou, G. 1986, Ap. J. (Letters), 311, L33.

Jura, M., Kim, D. W., Knapp, G. R. and Guhathakurta, P. 1987, Ap. J. (Letters), 312, L11.

Jura, M. 1982, Ap. J., 254, 70.

Kennicutt, R. C. 1983, Ap. J., 272, 54.

Kennicutt, R. C. 1992, Ap. J., 388, 310.

Knapp, G. R., Gunn, J. E. and Wynn-Williams, C. G. 1992, Ap. J. (in press).

Rice, W., Boulanger, F., Viallefond, F., Soifer, B. T. and Freedman, W. L. 1990, Ap. J., 358, 418.

Romanishin, W. 1990, A. J., 100, 373.

Sauvage, M., Thuan, T. X. and Vigroux, L. 1990, Astr. Ap., 237, 296.

Sauvage, M. and Thuan, T. X. 1992, Ap. J. (Letters), 396, L69.

Soifer, B. T., Boehmer, L., Neugebaueur, G., and Sanders, D. B. 1989, A. J., 98, 766.

Thuan, T. X. and Sauvage, M. 1992, Astr. Ap. Suppl., 92, 749.

Walterbos, R. A. M. and Schwering, P. B. W. 1987, Astr. Ap., 180, 27.

Wilson, C. D., Scoville, N. and Rice, W. 1991, A. J., 101, 1293.

THE ULTRAVIOLET EMISSION OF ELLIPTICAL GALAXIES AND SPIRAL BULGES*

Arthur F. Davidsen
Center for Astrophysical Sciences
The Johns Hopkins University
Baltimore, MD 21218

and

Henry C. Ferguson
Institute of Astronomy
Cambridge University
Cambridge CB3 0HA, England

ABSTRACT

One of the major unsolved problems in ultraviolet astronomy is the origin of the far-UV upturn in the spectral energy distributions of elliptical galaxies and spiral bulges. Observations of NGC 1399 and M31 made by the Hopkins Ultraviolet Telescope on the Astro-1 space shuttle mission shed new light on this problem. Ongoing star formation with a normal IMF is excluded as the principal source of the UV light. Classical post-asymptotic-giant-branch stars also fail to fit the new observations. The dominant source of the UV emission must be cooler and less luminous than the PAGB stars. Recent calculations of evolutionary tracks of Post-Early-AGB stars and AGB-Manqué stars provide promising new candidates for the source of the UV flux. A preliminary comparison of an SED computed from a population of $0.48\,M_{\odot}$, $Y = 0.3$, $Z = 0.02$ (solar metallicity) AGB-Manqué stars with the spectrum of NGC 1399 shows excellent agreement.

1 Introduction

Since the early days of satellite astronomy, observations of nearby galaxies in the vacuum-UV have held an important place in the observing programs of each successive generation of space telescopes, from *OAO-2* (Welch & Code 1972; Code & Welch 1979) to *IUE* (Burstein et al. 1988). Such observations are now becoming increasingly important as deeper and deeper galaxy surveys probe further into the rest-frame UV of high-redshift objects. Our ability to understand the high-redshift data is limited by our knowledge of the types and varieties of spectral energy distributions (SED's) found in nearby galaxies, and of the evolutionary paths that could lead to these SED's (Bruzual 1983; Bohlin et al. 1991). In this regard, one of the major unsolved problems for normal galaxies is the source of the far-UV upturn in the spectral energy distributions of elliptical galaxies and spiral bulges. This paper will focus primarily on that issue and present some recent results from the Hopkins Ultraviolet Telescope (HUT) that may help improve our understanding of these systems.

UV observations from the *OAO-2, ANS*, and *IUE* satellites have shown that elliptical galaxies typically have an upturn in their spectra shortward of 2000 Å, with flux increasing to shorter wavelengths (Welch & Code 1972; Code & Welch 1979; Bertola et al. 1980; Perola & Tarenghi 1980; Bertola, Capaccioli & Oke 1982; O'Connell, Thuan & Puschell 1986; Bertola et al. 1986; Burstein et al. 1988). Galaxies with similar optical spectra can have UV-to-optical flux ratios that vary by nearly an order of magnitude. The major observational clues to the origin of the UV flux are as follows:

1. In galaxies with no optical evidence of star formation or nuclear activity the continuum slope near 1500 Å shows little variation from galaxy to galaxy, and is indicative of stars hotter than ~20000 K.
2. The galaxy surface-brightness profiles are generally similar in the optical and UV (Oke, Bertola & Capaccioli 1981; Welch 1982; Bohlin et al. 1985), although there is recent evidence for a gradient of bluer far-UV minus near-UV colors toward the nuclei (O'Connell 1991; O'Connell et al. 1992).
3. The ratio of the 1500 Å flux to the optical flux varies by an order of magnitude in the galaxies surveyed; it increases with metallicity, and also with galaxy luminosity and velocity dispersion, and may be correlated with the mass-infall rate derived from the X-ray luminosity (Burstein et al. 1988).

4. Galaxies with optical evidence for star formation or nuclear activity fall off the mean trends for quiescent galaxies, and often have different UV continuum shapes (Burstein et al. 1988).

Even the best *IUE* spectra of ellipticals show no clear stellar absorption features in the far-UV, and there is no sign of a turnover in the rising part of the continuum down to the short wavelength cutoff of *IUE.* Nevertheless, the UV upturn is thought to be produced by stars. Suggestions include: 1) young hot stars that are part of a minority star-forming population (Gunn, Stryker & Tinsley 1981; Nørgaard-Nielsen & Kjærgaard 1981); 2) post-asymptotic-giant-branch (PAGB) stars similar to the central stars of planetary nebulae (Bohlin et al. 1985; Mochkovitch 1986; Burstein et al. 1988; Barbaro & Olivi 1989; Brocato et al. 1990); 3) hot horizontal branch stars and their progeny (Nesci & Perola 1985; Arimoto & Yoshii 1987; Greggio & Renzini 1990); and 4) accreting white dwarfs (Greggio & Renzini 1983; Nesci & Perola 1985; Mochkovitch 1986).

Models that require old stellar populations must explain the curious observation that the trend with metallicity seen in ellipticals is more or less the opposite of that seen in globular clusters (see Figure 1). The most metal-poor globulars are as UV-bright as the ellipticals with the strongest UV upturns, but metal-rich globulars are in general very weak in the UV. For some of the more luminous proposed objects (massive PAGB stars and accreting white dwarfs), only one or two per cluster would provide enough flux to produce a strong upturn; thus whether or not the cluster appears UV-bright could depend on whether one of these stars happened to fall in the observing aperture. However, enough globular clusters have been surveyed that it is becoming harder to invoke such stochastic sampling effects as the source of the discrepancy. Furthermore, the UV strengths of globular clusters do seem in accord with elliptical galaxies where they have similar metallicities.

Greggio and Renzini (1990) showed that a fairly minor change in the assumptions for mass loss on the giant branch and the AGB could account for the changing trend, and produce the strong upturns seen in the most metal-rich elliptical galaxies. The crux of their proposal is a plausible but completely *ad hoc* modification of the standard Reimers (1975a,b) mass loss formula to include an extra factor $(1 + Z/Z_{\rm crit})$, thereby producing a direct metallicity dependence. Depending on mass-loss, stars evolving off the red giant branch may or may not evolve onto the horizontal branch, asymptotic-giant branch, or post-asymptotic giant branch. Greggio and Renzini argue that the source of the UV

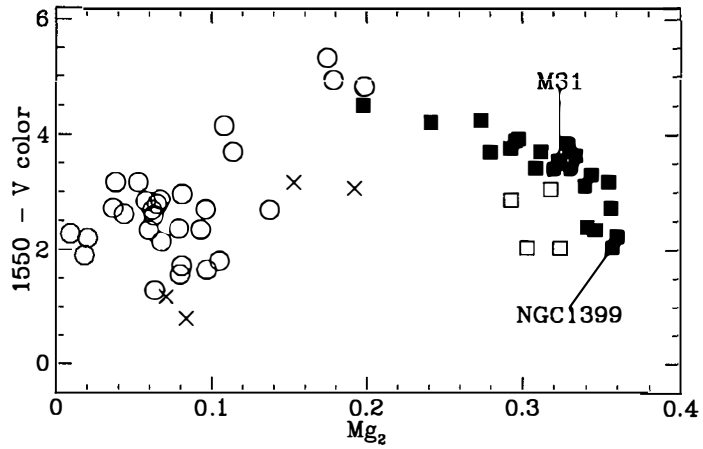

FIGURE 1 — Correlation of 1500 Å$-V$ color vs. Mg_2 index for globular clusters and elliptical galaxies. Data for galaxies have been taken from Burstein et al. (1988) and globular clusters from de Boer (1985). Where direct measurements were unavailable globular cluster Mg_2 indices have been computed from [Fe/H] using the calibration of Huchra and Brodie (1990). Open circles show globular clusters. Solid squares show "quiescent" ellipticals (and the M31 bulge); open squares show galaxies with nuclear activity and and x's show galaxies with optical evidence for recent star formation. The two galaxies observed by HUT and discussed in this paper are marked.

upturn is likely to be stars in one or a combination of several unusual stellar evolutionary phases. The most attractive candidates are Post-Early-AGB (PEAGB) stars, which leave the AGB before reaching the thermally pulsing phase, and AGB-Manqué stars, which evolve directly to high temperatures from the horizontal branch, skipping the AGB phase entirely (Brocato et al. 1990; Greggio & Renzini 1990; Castellani & Tornambè 1991; Horch, Demarque & Pinsonneault 1992). These candidates can produce many more UV photons per star than classical PAGB stars.

A key test of the various hypotheses can be made by looking in detail at the far-UV spectra of nearby ellipticals and spiral bulges. In the sections that follow, we will describe the Hopkins Ultraviolet Telescope (HUT) and some of the observations from its 1990 shuttle flight that shed new light on the origin of the UV upturn.

2 HUT and the Astro-1 Mission

HUT was designed to complement the studies that can be done with *IUE* or HST by pressing beyond the wavelengths covered by these telescopes, down to the Lyman limit and further into the extreme-ultraviolet (Davidsen et al. 1992). HUT performs moderate resolution (3 Å) spectrophotometry in the range 830 Å to 1850 Å in first order,

overlapping the long-lived observatories above 1200 Å, and extending down to 415 Å in second order. Its sensitivity has been maximized over the 900 to 1200 Å region, resulting in a capability to study objects as faint as 16th magnitude.

HUT is a 0.9-m diameter prime focus telescope, with a Rowland circle spectrograph and a photon-counting microchannel-plate detector. At the focal plane there is a choice of several different spectrograph entrance apertures, including 18″ and 30″ diameter round apertures used primarily to observe stellar objects, and 9.4 × 116″ and 18 × 116″ large slits, providing high sensitivity to faint diffuse sources. With its very fast focal ratio (f/2), HUT is more sensitive than the HST in this nebular mode. In fact, the instrument was designed specifically to address the problem of the UV light in elliptical galaxies, among others. The 9.4 × 116″ aperture was used for the galaxy observations discussed here, since it achieves 3 Å resolution on extended objects.

HUT was launched aboard the Astro-1 space shuttle mission for a week of observations during December 1990. In spite of a variety of technical difficulties encountered with the Spacelab instrument pointing system and other components of the payload, HUT performed nearly flawlessly, obtaining about 40 hours of observations on 77 different objects. An absolute calibration of the instrument was performed by observing the DA white dwarf G191-B2B and comparing the result with the predictions of a model atmosphere calculation. The result was checked against pre- and post-flight laboratory calibrations, leading to the conclusion that the absolute fluxes obtained with HUT are accurate to better than 10% (Davidsen et al. 1992; Kimble et al. 1992).

3 HUT Observations of an Elliptical Galaxy and a Spiral Bulge

Our best normal galaxy observations were of M31 and NGC 1399. By necessity, these two galaxies were chosen to yield the highest S/N in the shortest amount of time; however they are probably as representative as any sample of two galaxies can be of normal ellipticals and spiral bulges. NGC 1399 is the "quiescent" galaxy with the bluest 1550 Å $-V$ color in the Burstein et al. (1988) survey. It is a normal luminous elliptical in many respects although it does sit at the center of the Fornax Cluster, is a low-luminosity radio source, and has a massive X-ray halo (none of which are particularly unusual for a galaxy of its luminosity). M31 has a less pronounced UV upturn, but it follows the elliptical-galaxy correlations of UV color with metallicity and velocity dispersion very well.

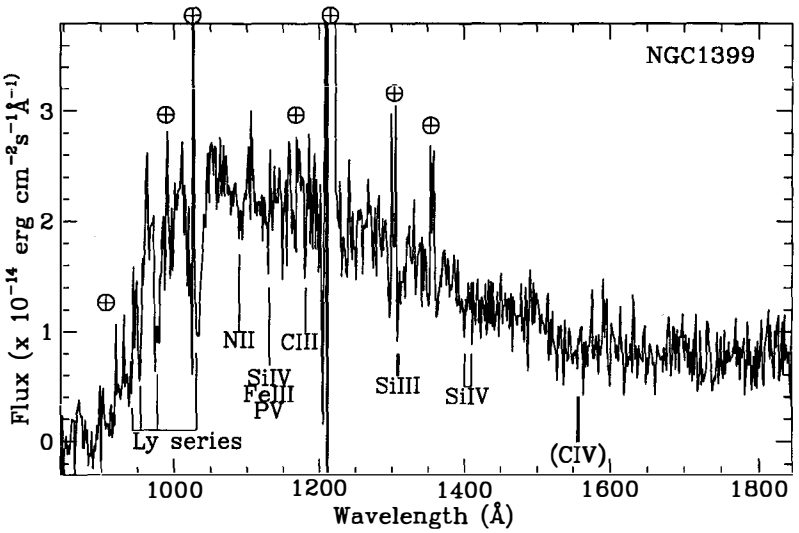

FIGURE 2 — Flux-calibrated HUT spectrum of NGC 1399, binned over 1.5 Å, with airglow subtracted. The wavelengths of the marked absorption features are consistent with the redshift of NGC 1399. The broad absorption features between 1000 and 1150 Å are undoubtedly blends of many features, as *Copernicus* spectra of hot stars show several lines per Angstrom in this wavelength range (Snow & Jenkins 1977). Residual airglow features are indicated with the ⊕ symbol.

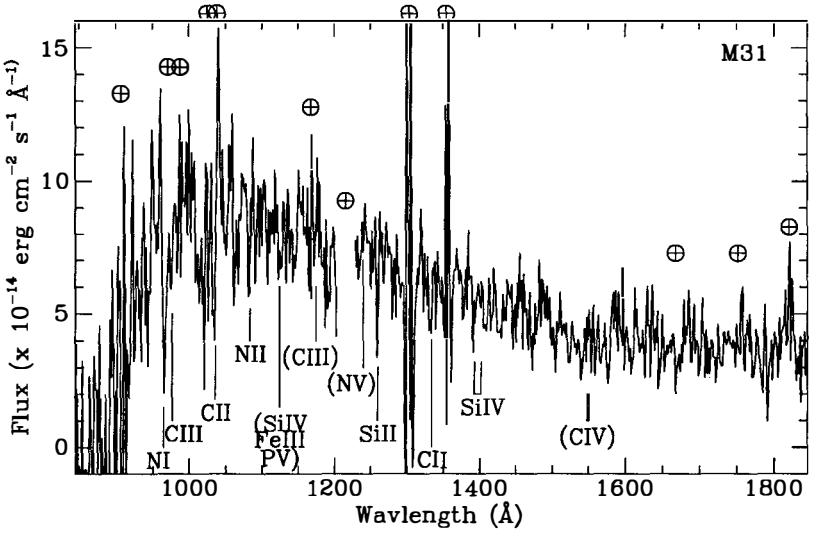

FIGURE 3 — Flux-calibrated, airglow-subtracted HUT spectrum of the M31 bulge, binned to 1.5Å, corrected for extinction assuming $E(B-V) = 0.11$. We have marked positions of the strongest expected absorption features from the stellar population or interstellar medium. Features that are not detected at greater than 3σ are marked in parentheses.

The flux-calibrated, airglow-subtracted, extinction-corrected spectra obtained by HUT are shown in Figures 2 and 3. Aside from residual lines from strong airglow features, there are no significant emission features in either spectrum. In NGC 1399, the Lyman series is clearly seen in absorption; other features are more difficult to detect. The Lyman series in M31 is unfortunately masked by the terrestrial airglow lines, but there are several other features that are probably real (N I λ965, Si II λ1260, and C II λ1335), but whose origin may be interstellar.

The most distinctive feature in the *IUE* spectra of normal O stars is strong C IV absorption at $\lambda\lambda 1548, 1551$. In supergiants, this blend can have an equivalent width of up to 20 Å, and usually exhibits a strong P-Cygni profile. In main-sequence O stars with normal atmospheric carbon abundance, the equivalent width ranges from $\sim$ 12 Å for O4V stars to $\sim$ 3 Å for O9V stars (Walborn, Nichols-Bohlin & Panek 1985). Equivalent widths even at the low end of this range would be detectable in the HUT spectrum. Thus, the lack of a strong C IV absorption feature in NGC 1399 immediately constrains the contribution from young massive stars, confirming the earlier *IUE* result from the sum of three UV-bright galaxies (Burstein et al. 1988), and putting it on a more quantitative footing. Models where the entire UV flux is due to continuing star formation with a Salpeter IMF extending up to more than 25 $M_\odot$ are virtually ruled out from the C IV feature alone (Figure 4A). Comparison of the full SED to star-forming models (Figure 4B) confirms this result (Ferguson et al. 1991). Star-formation models can be made to fit better by modifying the IMF, but the resultant best fit (Figure 4C), with $M_{\rm upper} = 20\ M_\odot$ and an IMF slope $x = -0.1$, seems highly implausible, since it is simultaneously weighted toward massive stars, but cuts off sharply at a rather low upper mass limit. Models where the UV comes from an aging starburst (that happened $\sim 2 \times 10^7$ years ago) may also still be possible, but make the trends of UV upturn with other galaxy properties difficult to understand.

It is immediately obvious from HUT spectra alone that the strong UV upturn in NGC 1399 cannot be due to a stellar population like that in the bluest globular clusters. In Figure 5, NGC 1399 is compared to the integrated spectrum of M79, the bluest globular cluster in the sample of de Boer (1985), also obtained by HUT on the Astro-1 Mission. The extinction toward M79 is low, and the difference in SED's is due to the fact that the metal-poor horizontal branch stars in M79 do not reach the high temperature of the dominant population in NGC 1399.

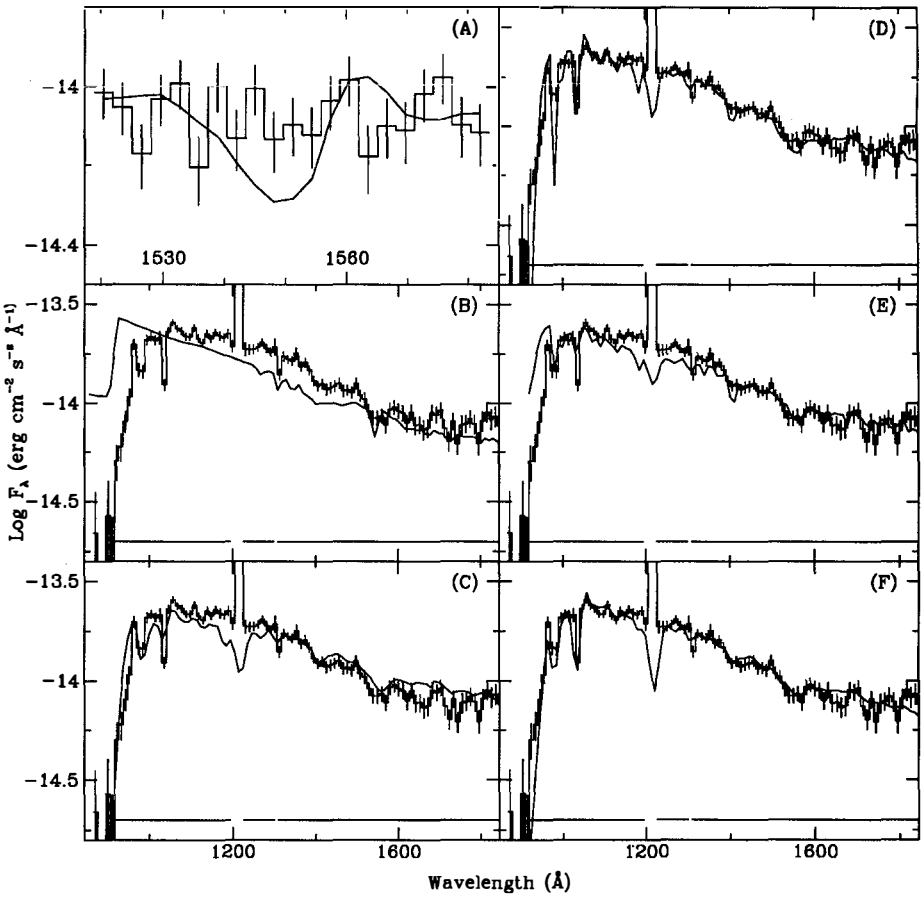

FIGURE 4 — Comparison of NGC 1399 SED to models. In all the panels, the histogram shows the flux-calibrated, airglow-subtracted HUT spectrum of NGC 1399, averaged over 3 Å bins in Panel A and over 10 Å bins in all the other panels. The broken line near the bottom in Panels B through F shows the wavelength ranges used for fitting. Panel (A) shows the region near CIV compared to a synthetic spectrum, constructed from a library of *IUE* stellar observations (Heck et al. 1984), of a population forming stars at a constant rate over 10^8 yr with a Salpeter IMF from 0.85 to 119 $M_\odot$. In panel (B) the data are compared to the Rocca-Volmerange & Guiderdoni (1987) hot-E model at an age of 13 Gyr. This model forms stars at an exponentially declining rate with timescale $\tau = 2.7$ Gyr with an IMF slope $x = 1.7$ and an upper mass limit of 80 $M_\odot$. Panel (C) shows the best-fit constant-star formation model, which has an IMF slope $x = -0.1$ and an upper mass limit $M_{\rm upper} = 20\ M_\odot$. Panel (D) shows the best-fitting solar-metallicity Kurucz (1991) model atmosphere. The model parameters are $T_{\rm eff} = 24000$ K, and $\log(g) = 4.0$. Panel (E) shows a synthetic spectrum of a single mass (0.546 $M_\odot$) population of PAGB stars. Panel (F) shows the synthetic spectrum of a population of AGB-Manqué stars constructed from the 0.48 $M_\odot$, $Y = 0.30$, $Z = 0.02$ model of Castellani and Tornambè (1991). This provides the best fit to the NGC 1399 spectrum we have been able to obtain so far.

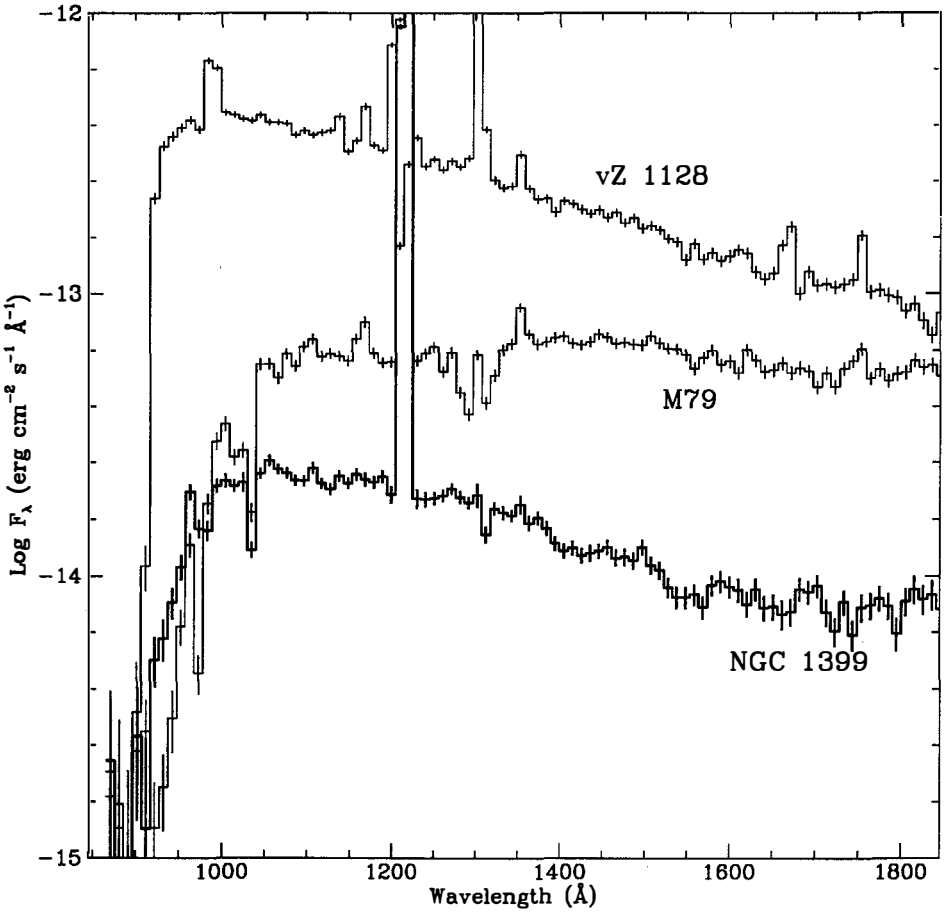

FIGURE 5 — Comparison of three spectral energy distributions observed with HUT. The heavy line is the SED of NGC 1399, corrected for airglow (although Lyman alpha contamination remains obvious). The other SED's are those of M79, a globular cluster with a strong UV component, and vZ 1128, a PAGB star in the globular cluster M3. Apparent emission features in these spectra are all due to airglow lines, which have not yet been subtracted. All the spectra have been binned over 10 Å. The M79 SED is too cool to match that of NGC1399, while that of vZ1128 is too hot (i.e., there is too much flux at the Lyman limit).

Also shown for comparison in Figure 5 is the HUT spectrum of the PAGB star vZ 1128 in the globular cluster M3 (Buzzoni et al. 1992; Dixon et al. 1992). The SED of this star provides a good match to that of NGC 1399 at long wavelengths, but has too much flux near the Lyman limit. A fit of a Kurucz model atmosphere to this star gives $T_{\rm eff} = 33,000$ K and $\log g = 4.0$.

The NGC 1399 SED compares reasonably well to a single-temperature $T_{\rm eff} = 24000$ Kurucz model (Figure 4D), suggesting that the light is dominated by stars of roughly this temperature. There are several reasons to interpret this result with caution: 1) the extinction curve is not well known in this wavelength range, 2) the metallicity of the Kurucz atmospheres probably does not match that of the UV emitting population, 3) the Kurucz models ignore non-LTE effects that are important in hot-star atmospheres, and 4) the HUT calibration is ultimately tied to a white-dwarf model atmosphere, which is clearly subject to some uncertainty near the Lyman limit. Nevertheless, after experimenting within the plausible range of these uncertainties, we think this "characteristic" temperature is fairly secure, barring major problems with the model atmospheres.

While this temperature is much hotter than globular cluster horizontal branches, it is cooler than expected if the UV population is low-mass PAGB stars evolving along the standard (Schönberner 1983) evolutionary tracks. Figure 4E shows a comparison of a synthetic spectrum of $0.546\,M_{\odot}$ PAGB stars to NGC 1399. If the model atmospheres are right, the PAGB stars are on average too hot to account for the bulk of the UV emission from NGC 1399.

After correcting for extinction, the M31 SED is similar to that of NGC 1399 longward of 1200 Å, but differs significantly near the Lyman limit (Ferguson, Davidsen & Kriss 1991; Ferguson & Davidsen 1992). This difference is in excess of anything that might be expected from uncertainties in extinction (at least if it follows something like a Seaton (1979) law) or calibration. Evidently, M31 contains a larger contribution from hotter stars, and may thus allow a significant low-mass PAGB star component. The preliminary FOC results (King 1992) shown by Crane (this volume) are interesting in this regard. A preliminary estimate is that the point sources in the FOC image, if they are $0.565\,M_{\odot}$ PAGB stars, could account for no more than $\sim$ 20% of the flux in our M31 spectrum. Perhaps this is the extra hot component that is not observed in NGC 1399? In any case, the bulk of what we are seeing with HUT must be from the diffuse component in the FOC image, and must therefore be due to stars of lower luminosity.

The implication of these NGC 1399 and M31 results is that the dominant source of the UV emission must be cooler and less luminous than classical low-mass PAGB stars. The low luminosities are in agreement with the suggestion (Brocato et al. 1990; Greggio & Renzini 1990) that most of the light comes from PEAGB or AGB-Manqué stars. Recent models of these stars will now make it possible to compute the expected SED's to see if the temperatures are acceptable. We have made a first step in this direction using one of the evolutionary tracks from Castellani and Tornambè (1991). Figure 4F shows a synthetic spectrum from a population of 0.48 $M_{\odot}$, $Y = 0.3$, $Z = 0.02$ (solar metallicity) AGB-Manqué stars. It provides a better match to the spectrum than anything else we have tried. We are currently exploring the full range of PEAGB and AGB-Manqué models (Ferguson & Davidsen 1992).

Burstein et al. (1988) concluded their important study of this long-standing problem with the hopeful statement:

> *With a combined attack using new observations, new telescopes, and new theory, the origin of the far-UV flux in early type galaxies may soon be a solved problem.*

The observational and theoretical results described briefly in this paper, and much more extensively in the articles cited, go a long way toward confirming their expectations.

ACKNOWLEDGEMENTS

We are grateful for the support of numerous colleagues who helped make HUT and the Astro-1 mission a success. We thank Van Dixon for help in preparing some of the figures for this paper. HUT is supported by NASA grant NAS5-27000 to the Johns Hopkins University.

REFERENCES

Arimoto, N. & Yoshii, Y. 1987, A&A, 173, 23

Barbaro, G. & Olivi, F. M. 1989, ApJ, 337, 125

Bertola, F., Capaccioli, M., Holm, A. V., & Oke, J. B. 1980, ApJ, 237, L65

Bertola, F., Capaccioli, M., & Oke, J. B. 1982, ApJ, 254, 494

Bertola, F., Gregg, M. D., Gunn, J. E., & Oemler, A. Jr. 1986, ApJ, 303, 624

Bohlin, R. C, Cornett, R., Hill, J. K., Hill, R. S., Landsman, W. B., O'Connell, R. W., Neff, S. G., Smith, A. M., & Stecher, T. P. 1991, ApJ, 368, 12

Bohlin, R. C., Cornett, R. H., Hill, J. K., Hill, R. S., O'Connell, R. W., & Stecher, T. P. 1985, ApJ, 298, L37

Brocato, E., Matteucci, F., Mazzitelli, I., & Tornambè, A. 1990, ApJ, 349, 458

Bruzual, G. 1983, ApJ, 273, 105

Burstein, D., Bertola, F., Buson, L. M., Faber, S. M., & Lauer, T. R. 1988, ApJ, 328, 440

Buzzoni, A., Cacciari, C., Fusi Pecci, F., R., Buonanno, & Corsi, C. E. 1992, A&A, 254, 110

Castellini, M. & Tornambè, A. 1991, ApJ, 381, 393

Code, A. D. & Welch, G. A. 1979, ApJ, 228, 95

Crane, P. 1992, in The Physics of Nearby Galaxies: Nature or Nurture?, ed. C. Balkowski & T. X. Thuan (Paris: Editions Frontieres), in press

Davidsen, A. F., Long, K. S., Durrance, S. T., Blair, W. P., Bowers, C.W., Conard, S. J., Feldman, P. D., Ferguson, H. C., Fountain, G. H., Kimble, R. A., Kriss, G. A., Moos, H. W., & Potocki, K. A. 1992, ApJ, 392, in press

de Boer, K. S. 1985, A&A, 142, 321

Dixon, W. V. D., Davidsen, A. F., Ferguson, H. C., Blair, W. P., Bowers, C. W., Durrance, S. T., Feldman, P. D., Henry, R. C., Kimble, R. A., Kriss, G. A., Kruk, J. W., Long, K. S., Moos, H. W., & Vancura, O. 1992, in preparation

Ferguson, H. C. & Davidsen, A. F. 1992, in preparation

Ferguson, H. C., Davidsen, A. F., & Kriss, G. 1991, in Stellar Populations in Galaxies, ed. A. Renzini & B. Barbuy (Paris: IAU), 891

Ferguson, H. C., Davidsen, A. F., Kriss, J. A., Blair, W. P., Bowers, C. W., Dixon, W. V., Durrance, S. T., Feldman, P. D., Henry, R. C., Kimble, R. A., Kruk, J. W., Long, K. S., Moos, H. W., & Vancura, O. 1991, ApJ, 382, L69

Greggio, L. & Renzini, A. 1983, A&A, 118, 217

Greggio, L. & Renzini, A. 1990, ApJ, 364, 35

Gunn, J. E., Stryker, L. L., & Tinsley, B. M. 1981, ApJ, 249, 48

Heck, A., Egret, D., Jaschek, M., & Jaschek, C. 1984, A&AS, 57, 213

Horch, E., Demarque, P., & Pinsonneault, M. 1992, ApJ, 388, L53

Huchra, J. P. & Brodie, J. P. 1990, ApJ, 362, 503

Kimble, R. A., Davidsen, A. F., Blair, W. P., Bowers, C. W., Dixon, W. V. D., Durrance, S. T., Feldman, P. D., Ferguson, H. C., Kriss, G. A., Kruk, J. W., Long, K. S., Moos, H. W., & Vancura, O. 1992, ApJ, in press

King, I. 1992, Personal communication

Kurucz, R. L. 1991, CfA preprint no. 3181

Mochkovitch, R. 1986, A&A, 157, 311

Nesci, R. & Perola, G. C. 1985, A&A, 145, 296

Nørgaard-Nielsen, H. U. & Kjærgaard, P. 1981, A&A, 93, 290

O'Connell, R. W. 1991, in Stellar Populations in Galaxies, ed. A. Renzini & B. Barbuy (Paris: IAU), 891

O'Connell, R. W., Bohlin, R. C., Collins, N. R., Cornett, R. H., Hill, J. K., Hill, R. S., Landsman, W. B., Roberts, M. S., Smith, A. M., & Stecher, T. P. 1992, in press

O'Connell, R. W., Thuan, T. X., & Puschell, J. J. 1986, ApJ, 303, L37

Oke, J. B., Bertola, F., & Capaccioli, M. 1981, ApJ, 243, 453

Perola, G. C. & Tarenghi, M. 1980, ApJ, 240, 447

Reimers, D. 1975a, Mem. Soc. Roy. Sci. Liège, 6, 369

Reimers, D. 1975b, in Problems in Stellar Atmospheres and Envelopes (Berlin: Springer), 229

Rocca-Volmerange, B. & Guiderdoni, B. 1987, A&A, 175, 15

Schönberner, D. 1983, ApJ, 272, 708

Seaton, M. J. 1979, MNRAS, 187, 75P

Snow, T. P. Jr. & Jenkins, E. B. 1977, ApJS, 33, 269

Walborn, N. R., Nichols-Bohlin, J., & Panek, R. J. 1985, NASA Ref. Pub. 1115

Welch, G. A. 1982, ApJ, 259, 77

Welch, G. A. & Code, A. D. 1972, in Scientific Results from the Orbiting Astronomical Observatory, ed. A. D. Code. NASA SP-310, 541

THE Hα AND UV 2000 Å "STRATIGRAPHY" OF THE SPIRAL ARMS AND THE RELATION WITH THE DENSITY-WAVES

G. COURTES
Laboratoire d'Astronomie Spatiale CNRS
Observatoire de Marseille

Abstract :

The spiral structure images obtained from the ionized hydrogen (Hα) (ground based telescopes 120cm OHP and 600cm Caucase) and from the stellar UV continuum of the hot evolved stars (stratospheric 40cm balloon borne telescopes) provide a new method to discriminate from their relative offset the present and the past star formations as well as their relation in time and position with the density waves.
Some examples from NGC 4258, M51 and M31 are given and could initiate a more general fundamental study in view of a better understanding of the star formation mechanisms.
This talk summarizes the preliminar results of several published and submitted papers, from the Marseilles and Geneva groups.

THE "STRATIGRAPHY" OF THE SPIRAL ARMS

The first observations of galaxies made in different colours were an evidence of that we call "stratigraphy" by analogy with another time dependant effect very well known in geology. Zwicky seems to have been the first to investigate from photographic plates obtained through U.B.V. filters the parallel distribution of the different main components of

a spiral arm (Zwicky, 1957). Wray (1988) was extending composite colour photographs in his coloured Atlas of galaxies.

However, these observations, using wide bandwidths, were giving the very broad spiral arms of the evolved stars of many different ages and types. One notes for instance the very smoothed spiral arms of M33 in the red continuum in comparison with the sharp light distribution of Hα of the HII regions (Courtès and Cruvellier, 1961).

A more quantitative approach of Baum (1964) was obtained from a nebular spectrophotometer crossing the spiral structures (Fig. 1). Later, these observations have been renewed in two steps :

1°) The Hα survey of the nearest galaxies thanks to large telescope focal reducers, equipped of very narrow interference filters (Courtès, 1952, Courtès, 1964) have revealed the sharp distribution of the HII regions emission at the front of the arms (Courtès, 1977) ; the others sharp components being the massive star associations, the CO emission and the dust absorbing lanes (coincident or not coincident, but parallel, 300 to 1000 pc with the HII regions of the ionization front (Vogel et al., 1988), (Lord and Kenny, 1991).

2°) The theory of the density waves, Lin and Shu (1964), Roberts (1969) and its observational counterpart with the attempt to evaluate position and time of evolution from individual stellar spectrophotometry and the time-dependant geometrical expansion ($v = -10$ km.s^{-1}) of the OB associations (Courtès and Dubout-Crillon, 1971 ; Dubout-Crillon, 1977).

In our first study on M33 (Courtès and Dubout-Crillon, 1971) we had at our disposal the precise rotational velocity fields of the gas from the Fabry-Perot interferometric observations and the velocity gradient related to density waves (Carranza et al, 1967) giving the possibility to determine any past position of the site of star formation, as soon as a time evaluation would be given. We measured the stellar photometry of the stars in order to evaluate their evolution from the time zero of their formation. Except Tully (1974) and the recent works of Visser (1980) and indirectly of Lord and Kenney (1988) with the Hα-CO offsets, no others attempts to evaluate the density waves velocities or any signature of the density wave effects had been made.

SELECTION OF A STAR POPULATION OF A SPECIFIC LIFE TIME

The UV 2000 Å images have the main advantage to delimit from a relatively well known (Lequeux, 1980) life time of 10^8 years the range and the mean position of the rotation angles of the stellar arms (Donas and Deharveng, 1990 ; Buat, 1989) due to the hot evolved stars of 2 to 5 MΘ observed through the 150 Å bandwidth peaked at 2000 Å with

practically no contribution of the late stars down to F8. The relatively short life time of those stellar structures leading to a small but significant offset, permits us to preserve a clear identification (fossile) of each segment of the spiral arms. The stellar population selected constitutes a good time marker.

It was noted also that the sky background limited by the combination of mirror coatings and the O_2 Shumann-Runge molecular bands of the upper atmosphere is very faint and favourises the detection of the low brightness outer arms, sometimes much better than the conventional HII regions in Hα.

DISCRIMINATION BETWEEN THE Hα AND UV ARMS

Obviously, it is necessary to have a pitch angle large enough in order to detect a clear offset between the Hα, supposed close, to the density wave pattern, and the UV structures defined by the photometric maximum of the UV spiral arms ; the worst case being the galaxies in which the grand design is almost circular. In the three example given in this talk, NGC 4258, M51 and M31, the offset seems related to the sectors of the spiral arms having a sufficient pitch angle or at least some deviations. Radial motions (Roberts, 1969) could be significant but do not seem to play a comparable role.

NGC 4258

The Sbc Hubble type galaxy NGC 4258 was recently studied in detail both in Hα and at 2000 Å (Courtès et al., 1992 ; see this paper for the observation and reduction techniques) ; its deprojection (Fig. 2) gives almost perfectly circular arms with a central barred structure complicated by the "anomalous gas arms" out of our subject. The comparison with the UV structure exhibits an almost perfect obvious, coïncidence with the exception of the N inner arm, Figure 3 shows the offset of this Hα and UV spiral structure. One will see the discussion in (Courtès et al., 1992) the main conclusion being that, if the offset appears only in the large pitch angle area, it is certainly due to the shift increasing with time caused by the different rotation velocities of the density wave and the material. The authors give two possible interpretations of the offset : i) when the two components are situated in the same plane (Fig. 3b Proj.1), the plane of rotation well defined by the general rotation velocities field, ii) when, under the effect of expansion of the UV hot evolved stars, in 10^8 years, one supposes that most of those stars are above the galactic plane of $\leq$ 0.5 kpc (Fig. 3b Proj.2) probably very absorbing (evidence of dust lanes, high Hα/Hß intensity ratios). According to these two approaches, the shift is of the order of 1 kpc $\pm$ 0.5

corresponding to a rotation velocity of the density wave slower by about 20 km.s^{-1} than the rotation velocity of the ionized gas.

M 51

This Sc galaxy was recently studied both in UV and Hα by Bersier (1991) in his thesis. Some new Hα observations with the 6m telescope will be used for the next paper. One finds that the same kind of offsets are restricted to relatively strong pitch angles. The deprojection gives in Figure 4 the main places (labeled 1, 2, 3, 4 by Bersier) in which these offsets appear, with the exception of 5 (circular concentric arm).

In the E inner arm with 1950 α_1 = 13h 27m 52s, δ_1 = 47° 26' 45" and α_2 = 13h 27m 55s, δ_2 = 47° 27' 30" and the NW spiral arm between α = 13h 27' 38", δ = 47° 27' and α = 13h 27' 42", δ = 47° 28', where the pitch angle is again strong (about 25°) as well as in the NE inner spiral arm. The drift is of the order of 10" - 20" corresponding to 0.5 - 1.0 kpc at the distance 9.6 Mpc for M51 (Sandage and Tammann, 1975). Recent investigations of the drift of the CO structures (Vogel et al., 1988 ; Rand and Kulkarni, 1990) contribute to confirm the role of the density waves in the star formation process in spiral arms of galaxies. Some peculiarities (offsets of CO spiral structures from the dust lane) seem to depend on the different interactions of CO with the density waves of various strengths (Lord and Kenney, 1991). The interpretation of the CO offsets and their comparison with our results will be discussed in a future paper. A first evidence is that the zero offset of the CO arm from the dust lane in the NW arm coïncides with a 20" offset of the UV stellar arms from the Hα front.

M 31

The Andromeda nebula is, because of its proximity, much easier to observe ; it was the first galaxy observed by the 13 cm diameter SCAP 2000 (Courtès et al., 1981) balloon borne telescope and after, by the 40cm telescope (FOCA-1000) (Milliard, 1984) with a much better resolution of about 12". Some recent 6m telescope Hα observations in connection with the FOCA-1000 fields have been secured and are ready for publication ; they confirm, in a first view, the Pellet et al. (1978) Hα Atlas of M31, but with a better continuity of the HII regions chains and an almost perfect coïncidence with the HI "holes" discovered by Brinks and Bajaja (1986).

In M31, the shift between HII region chains and the UV stellar component appears along the S4 Baade spiral arm, one sees on the deprojection of Simien et al. (1978) (Fig. 5)

that the pitch angle varies from 20° between X = - 40' Y = - 1' and X = - 43' Y = 10.5' up to the sudden change in pitch angle of 40° at X = - 50' Y = 6.5' vanishing at X = - 42' Y = - 3'. The deprojected drift is of the order of 2' (about 0.5 kpc against 0.7 - 1.5 kpc in NGC 4258). Then, the drift is smaller in M31 and confirms the direct location dependence between the UV evolved stars and the present star formation, while exhibiting a clear offset with the HII regions front at the inner limit of the UV isophots (Fig. 6).

At least for these galaxies NGC 4258, M31 and M51, one finds the same small drift confirming the direct geometrical evolution during the time between the star formation front and the UV evolved stellar spiral structures.

CONCLUSION

In a first analysis, one considers as an obvious evidence the coincidence of the Hα linked to the massive hot star spiral structures (present site of star formation) with the hot stellar arms revealed by the UV 2000 Å images.

In fact, a deeper examination of the UV and Hα imagery shows that some accidental arm deviations or the spiral sectors having a "pitch angle" large enough, permit to discriminate the evolution in time of the stellar UV evolved structures with an almost complete elimination of the later spectral type stars from their origin at the Hα front. The tangential rotation velocity seems predominant and the main cause of the offset (constant correlation with the pitch angle locations).

It is certainly one of the best, and perhaps the unique, simple method to disentangle the past star formation from the present one. This remark seems to be generalized on some large apparent diameter galaxies (NGC 4258, M51 and M31). Extensions of this procedure to other galaxies thanks to the Marseilles-Geneva UV observations in combination with their ground-based Hα couterpart would give strong confirmation of the dominant role, in the star formation processes, of the triggering mechanism of the density waves.

We saw that the rotation velocity of the density waves was measured, or theoretically evaluated in very rare cases. Moreover, determination of the masses of the stars in the UV arms and their related lifetime suffer from other observational and theoretical incertainties. In spite of these fundamental difficulties, when one of these two parameters is relatively well known, the second can be derived.

Generalized observations of the nearest galaxies will certainly clarify the role of density waves in star formation thanks to the homogeneity of the optical gas and stellar information of less complex interpretation than CO distribution, as well as the simplicity of the method.

BIBLIOGRAPHY

Baum, W.A., 1966
IAU Symp. n° 24 Ac. Press. London, New-York, 288
Bersier, D., 1991
Travail de Diplôme de l'Université de Genève
Brinks, E. and Bajaja, E., 1986
Astron. Astrophys. 169, 14-42
Buat, V., 1989
Astron. Astrophys. ,220, 49
Carranza, G., Courtès, G., Georgelin, Y., Monnet, G., Pourcelot, A., 1967
Ann. Astrophys. 31, 63
Courtès, G., Golay, M., Viton, M., Bentz W., Deharveng, J.M., Laget, M., Donas, J., Sivan, J.P. and Milliard, B., 1981
Adv. Space Researches, Vol.I, 81
Courtès, G., 1988
Comptes-Rendus Acad. Sc., t.234, 506
Courtès, G. and Cruvellier, P., 1961
Comptes-Rendus Ac. Sc. Paris CRAS t.253, 218-220
Courtès, G., 1964
Astron. J., vol. 69 n° 5, 325
Courtès, G. and Dubout-Crillon, R., 1971
Astron. Astrophys. 11, 468
Courtès, G., 1977
Topics in Interstellar Matter, IAU (Invited Paper), H. Van Woerden, Ed. Reidel Publ. Company, 209-242
Courtès, G., Petit, H., Hua, C.T., Martin, P., Blecha, A., Huguenin, D. and Golay, M., 1992
Astron. Astrophys. (submitted)
Donas, J. and Deharveng, J.M., 1990
Astron. Astrophys. 140, 325
Dubout-Crillon, R., 1977
Astron. Astrophys. 56, 293
Lequeux, J., 1980
Star formation, 10th Advanced Course of the Swiss Society of Astronomy and Astrophysics, Saas-Fee, Geneva Observatory
Lin, C.C. and Shu, F.H., 1964
Astrophys. J.140, 646-655
Lord, S.D. and Kenney, J.D.P., 1991
Astrophys. Journal 381, 130-136
Milliard, B., 1984
Thèse de l'Université de Provence

Pellet, A., Astier, N., Viale, A., Courtès, G., Maucherat, A., Monnet, G., Simien, F., 1978
Astron. Astrophys. Suppl. Vol.31, 439-461
Rand, R.J. and Kulkarni, S.R., 1990
Astrophys. J. (Letters), 349, L43
Roberts, W.W., 1969
Astrophys. J. 158, 123-143
Sandage, A. and Tammann, G., 1975
Astrophys. J., 196, 313.
Simien, F., Athanassoula, E., Pellet, A., Monnet, G., Maucherat, A., Courtès, G., 1978
Astron. Astrophys. Vol. 67 n° 1, 73-79
Vogel, S.N., Kulkarni, S.R. and Scoville, N.Z., 1988
Nature, Vol. 334, 402
Wray, J., 1988
The coloured Atlas of galaxies, Cambridge, Univ. Press
Zwicky, F., 1955
PASP, 67, 232.

(Contribution presented by Ph. AMRAM)

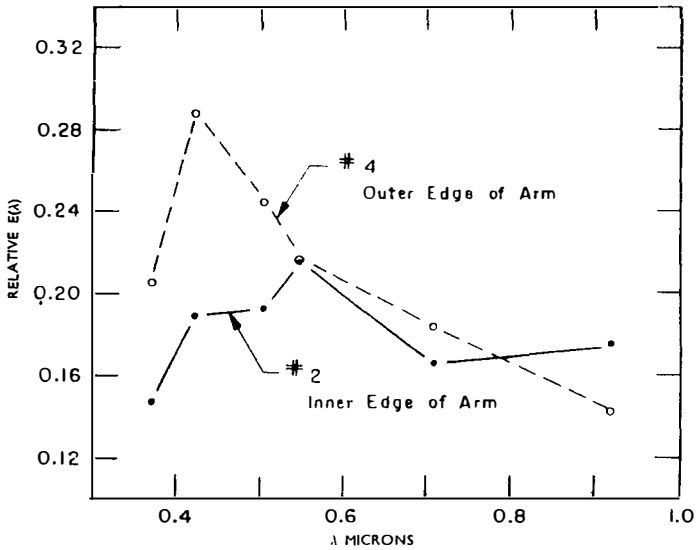

FIG. 1 *Approximate spectral-energy distributions of the inner and outer edges of a spiral arm on the south-east side of Messier 74. The strength of 0·42μ, relative to 0·37μ and other wavelengths, is evidence for a greater representation of A-type stars at the outer edge of the arm than at the inner edge.*

(From Baum, 1964)

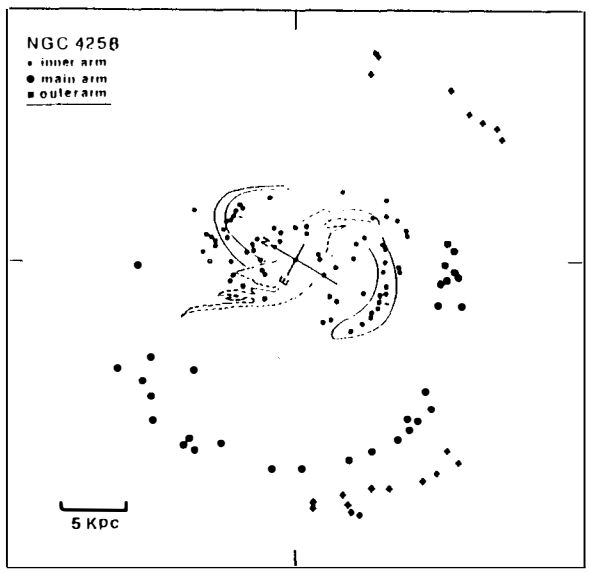

Fig. 2. The Hα spiral structures in the galaxy NGC 4258. One notes the almost circular Hα structures: i) south inner arm with ω = 7.5 kpc; ii) south-east outer arm with ω = 18 kpc. The anomalous arms are represented by dashed lines. See text.

From Courtès, Petit, Hua, Martin, Blécha, Huguenin and Golay
(submitted A & A, 1992).

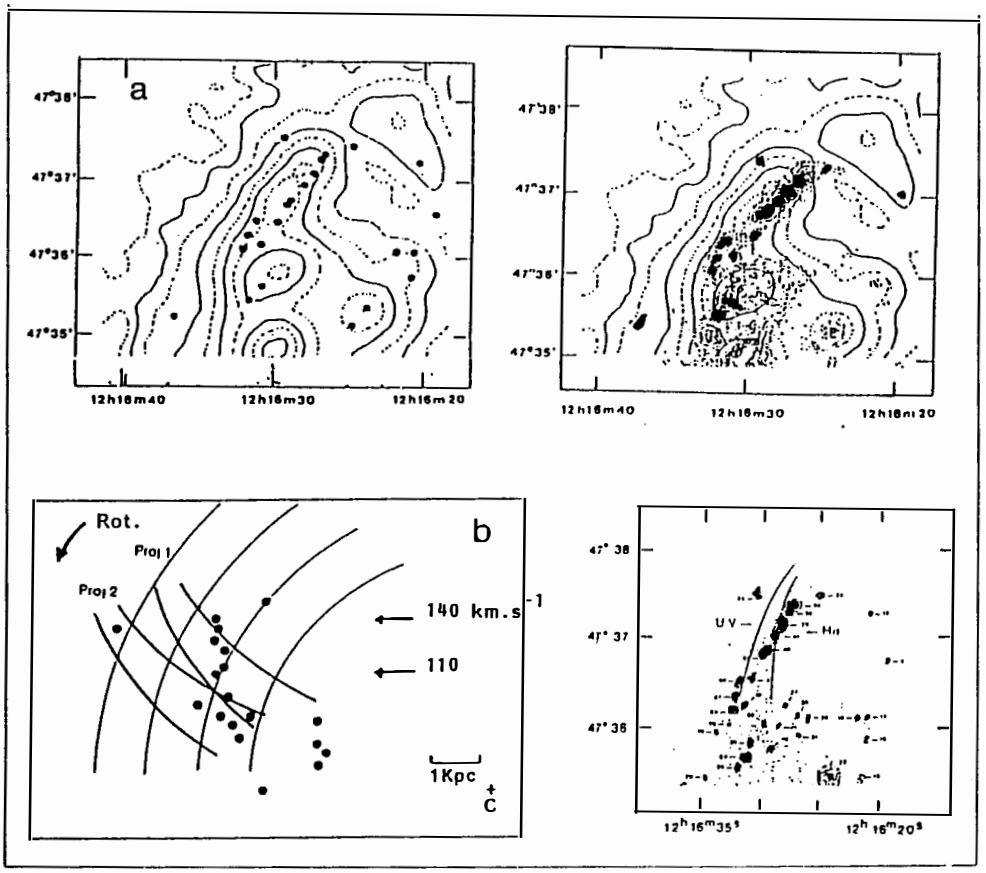

Fig.3. (a): UV(2000Å) isophotal contours and Hα isophotes of HII regions observed with the CCD (top). (b): Observed drift of the UV spiral arm (evolved hot stars) with respect to the HII region rich and recent star formation spiral front.

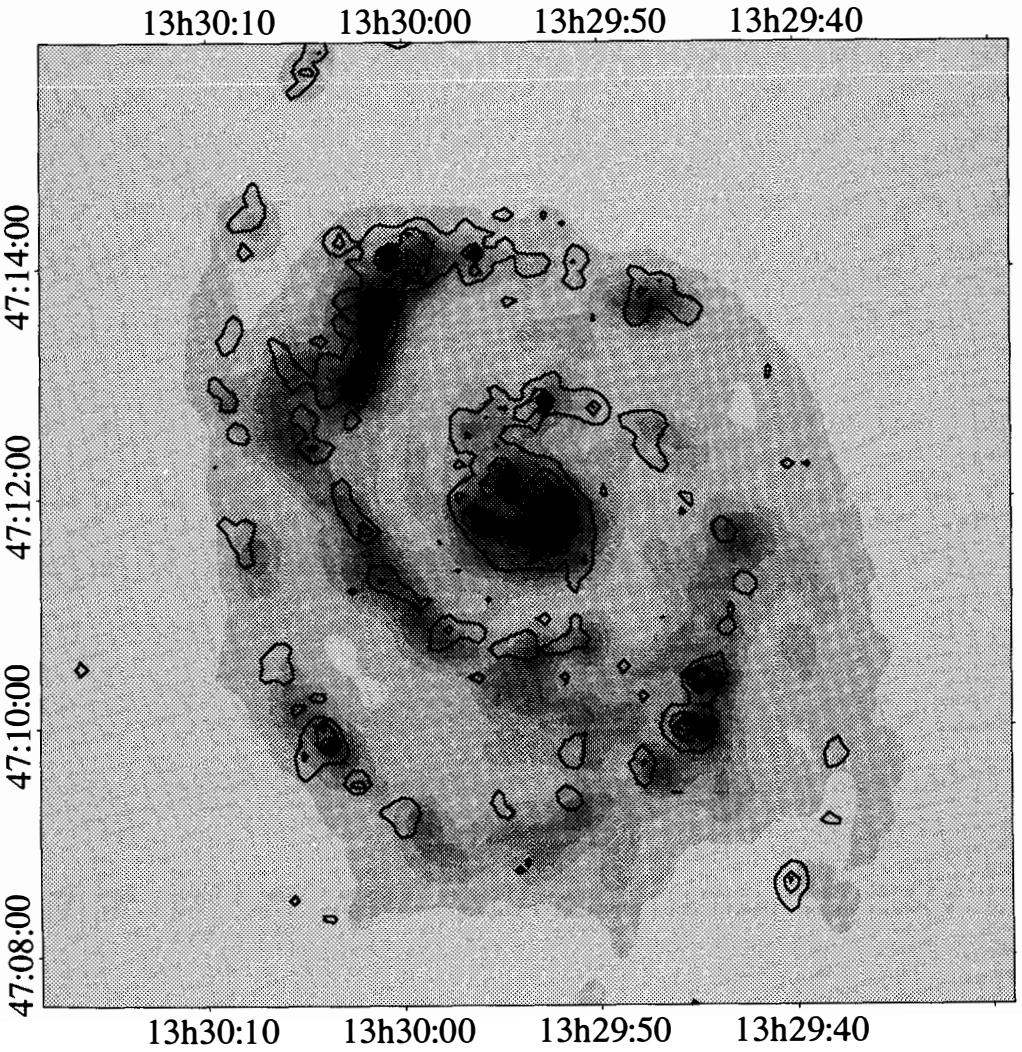

Fig. 4. M51, offsets Hα - UV 10" dowstream of Hα
Hα : contours
UV : Grey (Bersier, 1991)

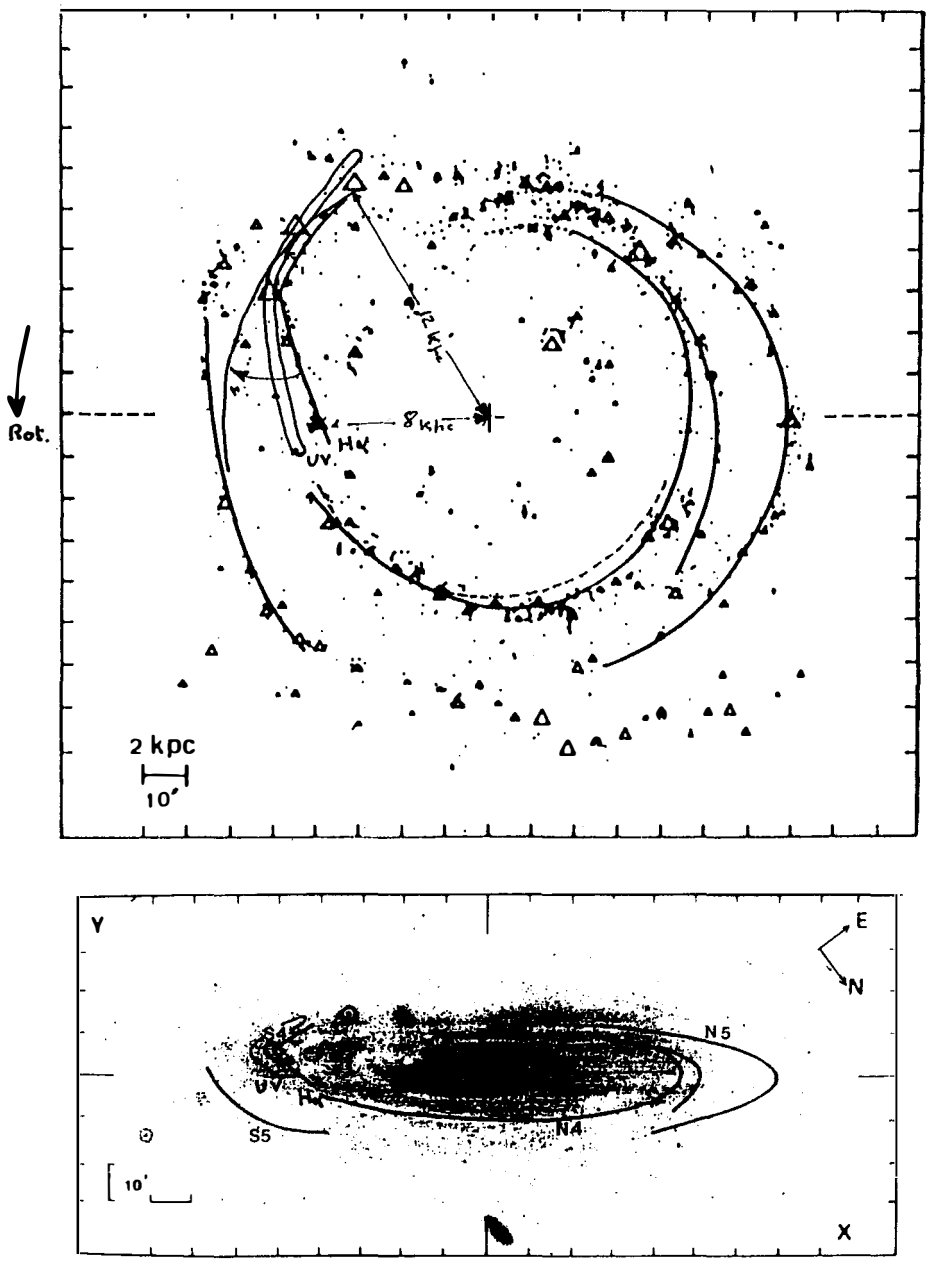

Fig. 5. Hα and UV offset on large pitch angle S4 arm superimposed on deprojection (from Simien et al., 1978).

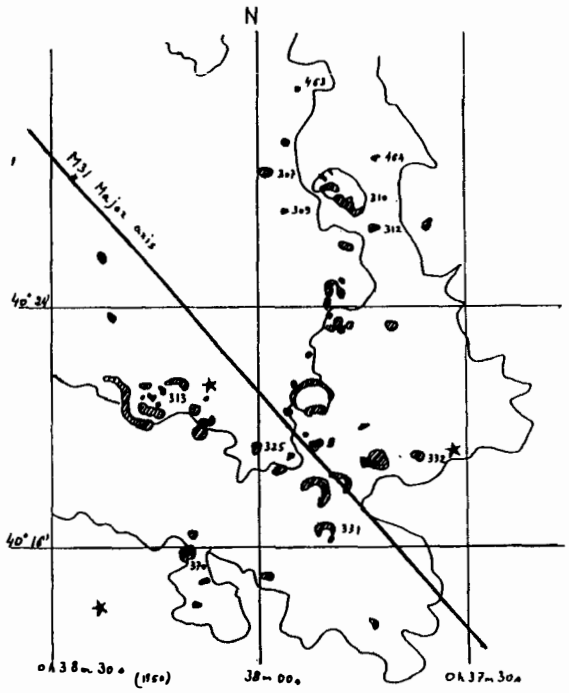

Fig. 6. The HII regions of the M31, S4, NW Baade. Spiral arm in the inner limit of the UV 2000 Å isophots.
. Hα : from 6m telescope, observations by Petit and Dodonov
. UV : from balloon borne 40 cm LAS Geneva telescope (Milliard, 1984).

II- PROPERTIES ALONG THE HUBBLE SEQUENCE

3) STELLAR POPULATIONS

STELLAR POPULATIONS IN SPHEROIDS

Presented by R. Michael Rich
Department of Astronomy, Columbia University
538 West 120th Street, New York, NY 10027
U.S.A.

ABSTRACT

Of the stellar populations in the Hubble sequence, the least is known about the stars comprising bulges and spheroids. Recent work on the bulges of M31 and Milky Way finds that: 1) The stars range from 1/10 to nearly 10 times the solar metal abundance; they likely are enhanced in alpha-capture elements, like Galactic halo stars. There is no G-dwarf problem in spheroids. 2) The first giant branch is dominated by M (oxygen) giants. 3) The populations have AGB stars brighter than $M_{bol} = -5$, OH/IR stars, and Mira variables with periods in excess of 400 days. It is possible that these stellar populations formed after, rather than before, the globular cluster/metal poor stellar halo systems. 4) The oldest stars account for less than 10% of the total luminous mass in these systems.

1. INTRODUCTION

Twenty years after Hubble resolved Cepheids in the spiral arms of Andromeda, Baade[1] resolved the red giants in the bulge of the nearest great spiral. Baade's subsequent discovery of RR Lyraes in the Milky Way bulge established the stellar populations paradigm, conceptually linking these spheroidal populations with globular clusters understood to be far older than the stars in the spiral arms. So powerful was this insight that to the present day textbooks describe bulges as being old and metal poor like the globular clusters. Within the last decade, we have discovered that spheroidal populations are complex, with a wide abundance range and unique histories of chemical evolution.

Stellar populations in spiral arms are easily resolved, and thanks to our location in the disk and the proximity of the Magellanic Clouds, we can confidently state that we understand these populations. A whole conference might be inadequate to address our deep modern understanding, which includes the relationship of gas and dust to populations, the IMF, and galaxy morphology.

Large reflector photographs in the *Hubble Atlas of Galaxies*[2] have exerted a powerful influence on our impression of populations in the Hubble sequence. In particular, there is striking continuity between the disks and irregular galaxies (marked by ongoing star formation and intermediate age stars) and bulge/bar structures that outwardly bear resemblance to ellipticals.

Considering that the vast majority of galaxies are not in dense clusters and are hence related to the disks, it is these galaxies we must understand if we seek to characterize the luminosity and spectral evolution of galaxies as a whole. And these galaxies likely have quite complex histories of star formation, bearing greater resemblance to the Magellanic Clouds than to an idealized single burst picture. In the populations of the present epoch Hubble sequence we may find the imprint of the luminosity, chemical, and spectral evolution of galaxies.

It is tempting to apply intuition and suggest that the bulges were formed at the same time as the ellipticals and globulars. This is clearly a subject where these classic pictures have been worth a thousand words or even a thousand spectra. Because these populations pose perhaps the greatest challenge, I will devote the majority of this review to their characteristics, in §2 immediately following this introduction. As a stellar population is defined by age, chemical composition, spatial distribution, and kinematics, §3 addresses the spatial/kinematic characteristics of the spheroids. §4 explores the history of chemical evolution in these systems, perhaps providing answers to the problems posed in §2. I conclude with a lesson from geology that may bear on our picture of galaxy evolution.

1.1 An Illustration from the Milky Way

To a factor of two, we may reasonably adopt the following masses (solar units) for Milky Way luminous populations[3]. Stellar Spheroid: 10^9; Central bulge: 10^{10}; Disk: 5×10^{10}. If (as §2.1 suggests) the Galactic bulge is between 10 and 15 Gyr old, then only 5% of the luminous mass of the Milky Way is extremely old. This figure would be similar to that for the Large Magellanic Cloud. There is a few Gyr gap between the formation of the stellar spheroid and the bulk of the luminous populations. If other field galaxies have similar histories, it should then come as no surprise that we fail to see large numbers of luminous primeval galaxies at high redshift. In fact, we may be in a position to observe the progeny of the Butcher-Oemler galaxy populations.

The gap in age between the old metal poor halo and the oldest disk stars (cf NGC 188) continues to be a problem. Now, we must add to this well determined age gaps in the LMC clusters and field, and in the Carina dwarf spheroidal galaxy. A repaired HST might be able to determine if M31 also has a similar age gap in its populations. It appears reasonable to propose an alternative hypothesis[4] to the picture of rapid collapse/enrichment/spinup. In this alternative scenario, $\approx 5\%$ of the Galaxy's luminous mass forms early, with the remainder of the Galaxy forming after a few Gyr hiatus, in a separate event. This picture would predict that field galaxies might form initially at high redshift, but attain maximum luminosity at redshifts between 0.5 and 2.

2. SERMONS IN SPHEROIDS

2.1 Galactic Bulges

The nearest examples of populations that begin to resemble the giant ellipticals are found in the Milky Way bulge and in M31. Figure 1 shows the integrated spectrum of the Milky Way bulge at two locations a few hundred pc from the nucleus. Although containing the same metal lines (as Whitford[5] points out) the bulge has weaker metal lines, particularly at the HK break. A recent 1 μm image obtained by the *COBE* satellite reveals the bulge as a distinct component with a flattened peanut morphology.

The Galactic bulge, and particularly that of M31, are good prototypes for distant ellipticals. Their populations may not be quite as metal rich, but there is strong evidence to support similar stellar populations and properties, particularly in considering the properties of the extreme evolved giants. Significantly, M31 lies on the 2.2/12 μm flux ratio relation for ellipticals[6]. This means that the luminous

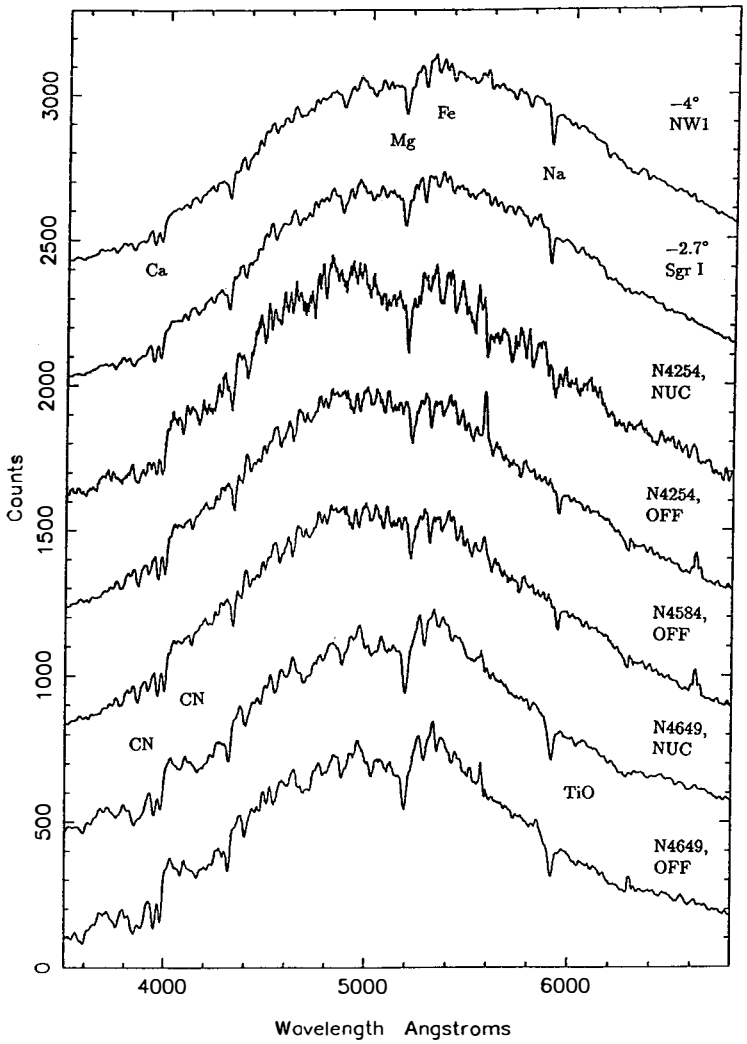

Fig. 1. Integrated spectra of two bulge positions, in Baade's Window and Sgr I (see also Figure 5b) are compared to galaxy spectra. Notice that Mg, Fe and Na are present in the bulge as well as in the galaxies. The weak Ca HK break in the bulge relative to the galaxies is likely due to a foreground sequence of blue stars.

mass losing stars in M31 and ellipticals have similar properties. We may conclude then that the bulges of the Milky Way and M31 are good prototypes for distant elliptical galaxy populations.

Abundances of bulge stars range from -1 to $+0.8$ dex[7] and bulge giants appear to be enhanced $\approx +0.4$ dex in alpha-capture and r-process elements[8].

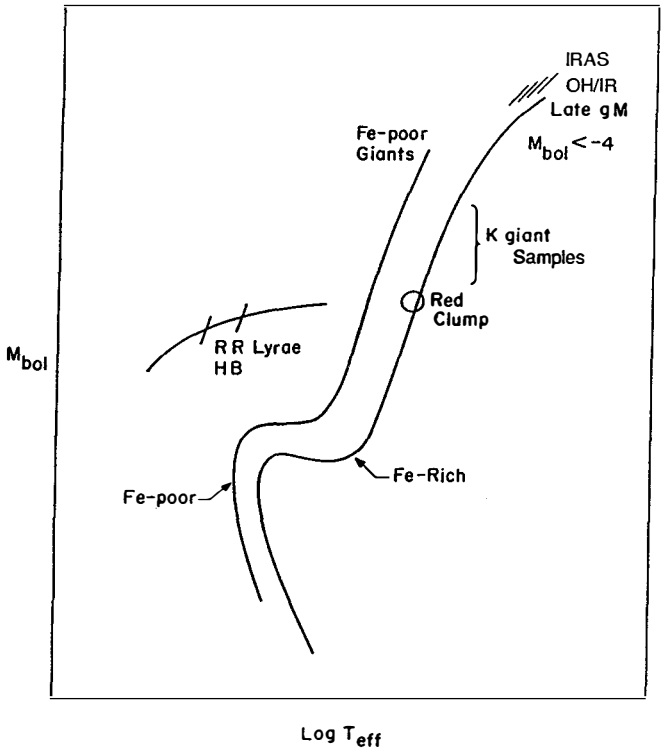

Fig. 2. The 1 dex spread in metal abundance in the bulge giants gives rise to a wide range of evolved progeny from RR Lyrae stars to extreme AGB stars brighter than $M_{bol} = -5$ (see also Figures 3, 5 and 6). Strong lined galaxies likely have numerous OH/IR and Mira stars of periods exceeding 1000 days, likely even more extreme if the populations are slightly young.

These elements are made in massive star SNe as opposed to white dwarf SNe and their enhancements indicate a rapid formation timescale for the bulge.

The large range in abundance gives rise to a wide variety of evolved stellar progeny (Figure 2). We know that that Baade's RR Lyraes evolve from the metal poor tail of the stellar distribution, while the late M giants, IRAS sources, and OH/IR stars are evolved from a metal rich population that may be a few Gyr younger than the globular clusters. Bulge/spheroidal populations have populations that are prominent at other wavelengths; a UV-bright population has long been know to be present in ellipticals and some bulges. King *et al.* report resolution of the M31 bulge into UV-bright sources that appear to be $10^4 L_\odot$ post-AGB stars. However, these account for only $\approx$ 20% of the flux at 1500Å; other stars[9] must account for the rest of the flux.

M giants dominate the first giant branch and AGB[10),11),12)]. Initially, Frogel

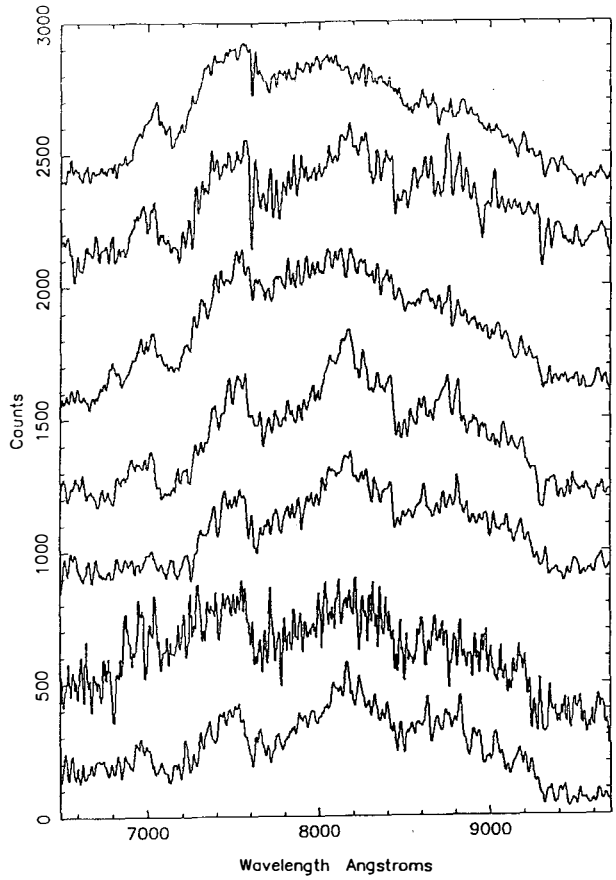

Fig. 3. Spectra of individual M giants in the bulge of M31, 500 pc from the nucleus[51]. A wide range of spectral types is clearly seen, with TiO bands at 7200 and 7600Å, VO at 8400Å, and photospheric H_2O bands at 9200Å. As Blanco first showed, metal rich galaxy populations are dominated by M giants (see also Figure 5b).

& Whitford[11] found a sharp dropoff in the luminosity function at $M_{bol} = -4.2$. They concluded that that this lack of luminous stars was due to the bulge being an old metal rich population, like the globular clusters. An examination of the resolved stellar population of M31's bulge in the infrared reveals a very different picture. Imaging of the M31 bulge in the K band[13] reveals a giant branch extended to $M_{bol} = -5$. Davies *et al.* counter that this may in fact be disk contamination, but a larger study[13] confirms that these luminous stars belong to the M31 bulge. Spectra of these M giants are illustrated in Figure 3, in which one clearly sees stellar TiO and water bands. Following Figure 4 shows a 2 μm mosaic[13] of a field of the M31 bulge 200 pc from the nucleus. Many of the brightest stars in this image would not be detected in the optical I band, at 8000Å. The color-magnitude diagram of these M31 M giants (Figure 5) has many more luminous stars than are

Fig. 4. Image at 1.2 microns of the M31 bulge, 2 arcmin=250 pc from the nucleus. Individual stars resolved here are brighter than $M_{bol} = -5$. Image obtained with the Palomar infrared system, mosaic made by J. Graham[14].

found in a field of the Milky Way bulge 500 pc from the nucleus; the bolometric luminosity function in Figure 6 corresponds to the CMD in Figure 5; more extreme fields in M31 have a giant branch that appears to extend to $M_{bol} = -6$.

In the bulge of M31, we find the counterparts of the luminous Miras that have been found in the bulge and studied so intensively by the South African

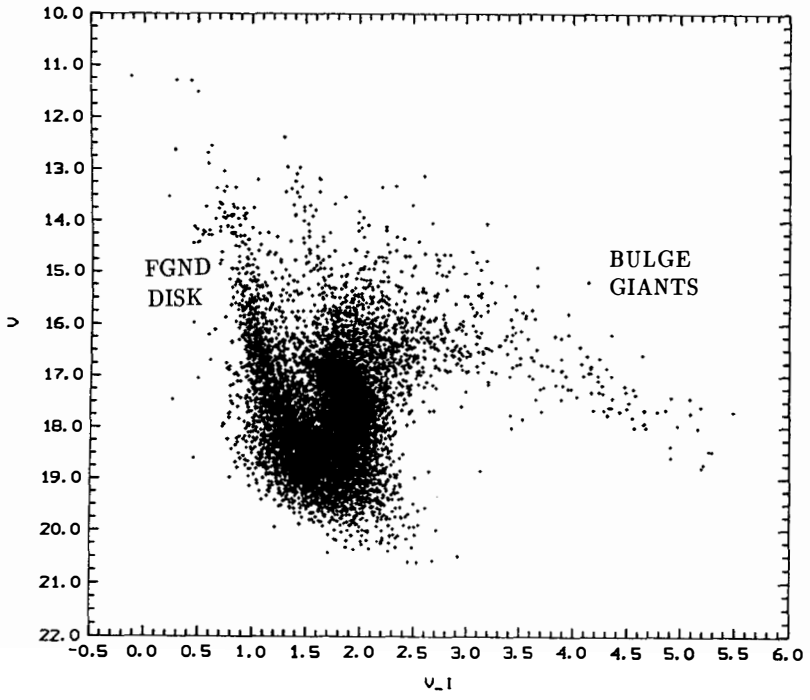
FGND
DISK
BULGE
GIANTS
V
V_I
10.0
11.0
12.0
13.0
14.0
15.0
16.0
17.0
18.0
19.0
20.0
21.0
22.0
-0.5 0.0 0.5 1.0 1.5 2.0 2.5 3.0 3.5 4.0 4.5 5.0 5.5 6.0

Fig. 5a.

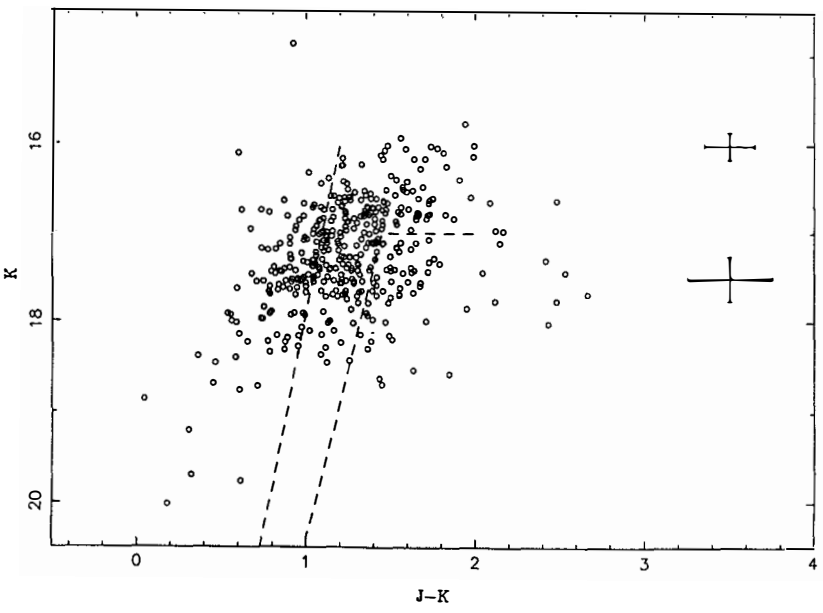
K
J-K
16
18
20
0
1
2
3
4

Fig. 5b.

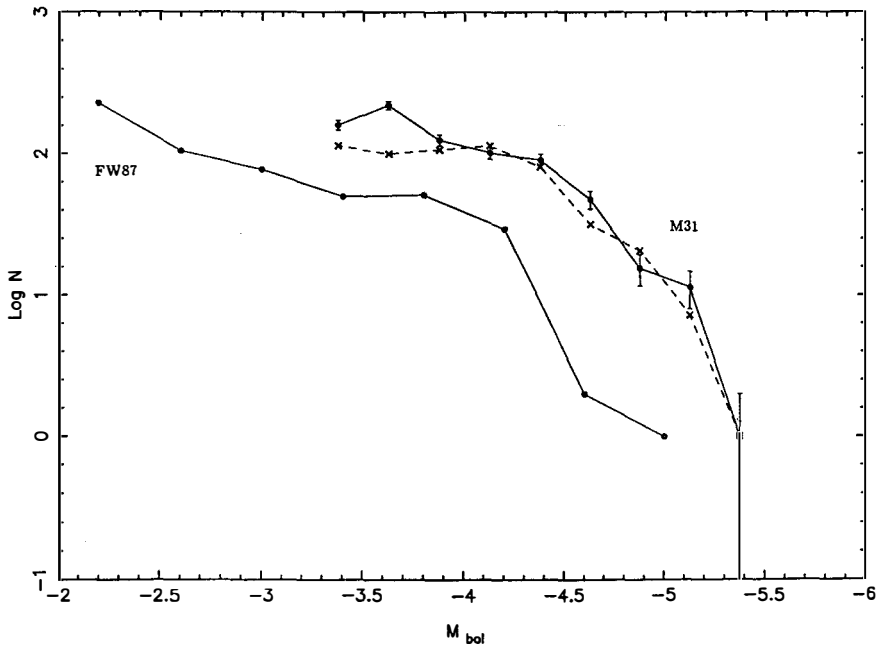

Fig. 5c.

Fig. 5. Three views of stars like those in Figure 4, the resolved stars of galactic bulges. (a) V, V-I color-magnitude diagram by S. Ortolani of Sgr I, 300 pc from the Galactic nucleus. A clear giant branch is visible; the tip is fainter at I due to TiO blanketing in the V band. Virtually all of the giants above the horizontal branch are M stars. Blue sequence is due to foreground disk dwarfs. (b) IR color-magnitude diagram of a similar population in M31. The lines indicate the location occupied by Galactic bulge giants. The late M giants (faint in V) are now bright in J and K bands. Bolometric magnitudes may be determined leading to (c) The luminosity function of stars in (b) from[13]. For comparison, the original Frogel-Whitford Galactic bulge luminosity function is shown (for R_o = 7kpc). If the R_0 = 8kpc, one brightens the FW luminosity function by 0.25 mag; however, we have used a modulus to M31 of 24.2; this may actually be as high as 24.4.

Astronomical Observatory[15] and references therein). These stars, some of which have 800 day periods and are brighter than $M_{bol} = -5$, must surely be a significant component of galaxy populations.

It is difficult to imagine how such luminous stars can have globular cluster ages. Recall that[16] show that the LPV's in globular clusters can be as luminous as $M_{bol} = -4.5$. Perhaps the factor of 4-6 metallicity difference between the bulge and the globular clusters might explain the luminous M31 stars. However, the number of stars found is consistent with the 1.3 Myr/mag of AGB lifetime, not the $\approx 10^5$yr lifetime of the Mira phase: an order of magnitude too many stars are observed to be explained as Miras. Further, the most luminous M31 bulge stars

can be counted, and their numbers compared to the integrated luminosity of the field in which they are discovered. Applying the Fuel Consumption Theorem[17] gives a lifetime of $\approx 5 \times 10^5$ yr for these stars, consistent with that of Miras in metal rich galactic globular clusters, such as 47 Tuc. So if such luminous stars were present in known metal rich populations, we should have found them. In the inner most M31 bulge field, 300 pc from the nucleus, one finds $\approx$ 1500 giants brighter than $M_{bol} = -5.0$, corresponding to a lifetime of 1 Myr/mag. The counts show that these very luminous giants have normal (pre Mira) AGB lifetimes; they are one magnitude brighter than any possible counterpart in a galactic globular cluster.

In the study of M31, we observe both inner disk and bulge fields in the IR. Bulge fields tend to have a sharper cutoff in magnitude than the disk fields, as if reflecting that a single burst of star formation was responsible for their formation. The disk fields actually have flatter slopes in the bright ends of their luminosity functions, as if star formation continued sporadically.

2.2 Young Bulges

While earlier spirals have obvious bulge structures, the later galaxies such as M33 lack bulges but often have stellar nuclei. The clear visiblity of balmer lines in their spectra leaves little doubt as to the presence of a young stellar population. While the presence of an age range in galactic bulges is disputed, the spectra of Sc nuclei are unambiguously young. Is there a transition in populations between the red strong lined bulges and the Sc nuclei?

There are striking examples of blue bulges among field galaxies. NGC 5102 has the classic S0 morphology with no obvious trace of a recent interaction. Yet Figure 6 shows clearly that Balmer lines persist over the entire inner 30 arcsec (= 1000pc) of this bulge. Starbursts remain this visible for only a short time, less than one Gyr. But their trace may remain, perhaps in the form of an extended giant branch with even a few carbon stars. It will be interesting to see whether detailed spectroscopy and luminosity fluctuation study of more distant galaxies turns up unusual variation in galaxy populations.

2.2.1 AGN/Starburst Connections

Stars, gas, and a central engine must properly be considered as a complete system, rather than as separate from the phenomonon of an active galactic nucleus.

It is of interest that excessively strong Ca triplet absorption are found in the nuclei of active galaxies[18]. A population dominated by 10^8 yr old supergiants

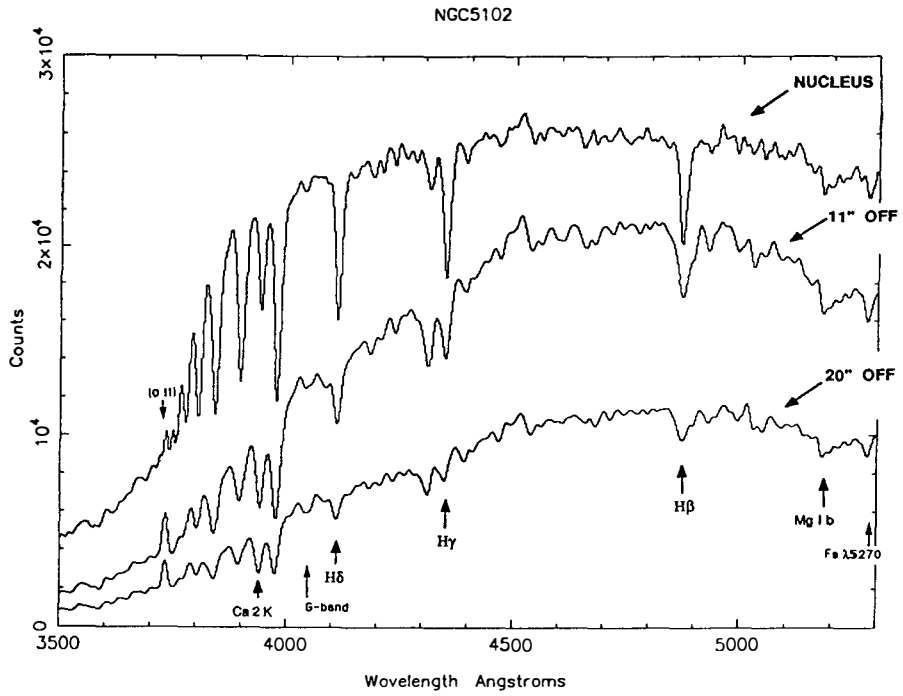

Fig. 6. Balmer lines persist over the entire bulge of NGC 5102[52]. Notice that the metal lines become slightly more prominent off the nucleus. Real spheroids probably have a complex mix of metallicity and age.

might explain such features, and their widespread presence would show that ongoing star formation is characteristic of many AGN. Triaxial systems support orbit families that are capable of transporting gas to the nucleus[19] where it may feed the central engine or form stars. Given the likely widespread triaxiality of bulges and the presence of gas in their disks, a star formation link is plausible.

2.3 Dwarfs vs. Giants: A Controversy Revisited

The strong lines of Na and MgH observed in galactic nuclei, combined with the discovery of the missing mass problem, led to the hypothesis that galaxies have dwarf enriched populations. Subsequently, infrared studies (particularly[20]) seem to rule out dwarfs, due to the large CO line strength. However, if luminous giants dominate the population, in the IR (Fig. 5), their exceptionally strong CO bands could dominate the integrated light. This may explain why[21] find that NGC 4472 has strong Na infrared doublet lines (a dwarf indicator) despite the galaxy having a high CO index. It is possible, then, that populations of AGB stars such as occur

in the M31 nucleus may make it very difficult to understand galaxy populations, particularly if the AGB varies between galaxies.

3. KINEMATICS AND STRUCTURE

Volumes have been written on the kinematics and structure of spheroids. I will pose some questions relevent to the stellar populations.

1. Do many bulges have central mass concentrations, and are these absent in barred systems? It is proposed that our galactic bulge is a separate central component, and that such steep concentrations of baryonic matter stabilize disks and bulges against bar modes. [22] find evidence for such concentrations in some Sc galaxies as well.

2. Is the density distribution of spheroids generally $r^{1/4}$ or exponential? The answer would appear to be obvious, but[23] find that the Galactic bulge follows an exponential of 400 pc scale length perpendicular to the disk. It is possible that many bulges, and perhaps most bars, have a component of disk structure to them. These structures may be more closely related to disks than to spheroids in their history.

3. Are edge-on bars peanut shaped? Several recent studies suggest that bars may undergo substantial thickening in the vertical direction[24),25),26]. Several mechanisms are suggested: scattering of stars by vertical resonances, instabilities, and vertical bending modes. Of note, these mechanisms operate on timescales of order 10 crossing times, very much shorter than a relaxation time. An example of such an effect is the secular increase in velocity dispersion observed for disk stars in the solar neighborhood.

4. What is the importance of secular dynamical evolution? As a student, we all learned that it requires a relaxation time for stellar systems to undergo substantial evolution. Yet the numerical simulations for bar thickening suggest that substantial dynamical evolution occurs in 10 dynamical times. The secular increase in the velocity dispersion of disk stars is another example that has not been fully explained. Obviously, these processes are important in nature, and we do not have a deep physical understanding of why systems can undergo gross dynamical evolution in much less than the relaxation time.

As we will discuss, stellar populations are related to chemistry and dynamics. It is widely believed that spheroidal populations are all of approximately the same age as the globular clusters. We have seen some contradictory evidence in the luminosities of the brightest stars. If bulges and some spheroids form after the halo/globular clusters, there should be supporting evidence in the observed stellar kinematics.

4. COLOR GRADIENTS AND CHEMICAL EVOLUTION

4.1 One Zone and Related Models

The presence of an abundance spread in bulge giants is strong support for the simple one zone model of chemical evolution. The range in the bulge is observed to run from -1 to $+0.8$ dex[27),28)] A wide range in abundance conflicts with models where metals are built up by inflow of enriched material. Wide abundance ranges are seen in the halo of M31[29)] and in M32 by Freedman[30)]. In every galaxy that has been examined, down to the dwarf spheroidals, we find a range in abundance; this is true even at low metallicities. If one imagines a vigorous starburst, outflow of enriched gas is likely to occur when the energy input due to SNe exceeds the binding energy of the galaxy[31)] This is the case of the Simple Model with outflow, and it has been investigated by [32),33)] and (numerically) by [34)]. For both steady and catastrophic outflow, the abundance distribution retains its large spread, which is not the case for an enriched infall model. [35)] find that local escape velocity correlates well with color in ellipticals. If wind outflow controls the local metallicity, then the simple model+outflow is satisfied, and the population will have a wide abundance range. It is reasonable to conclude that wide abundance ranges are a general property shared by the populations of bars, bulges, and halos. It is possible that some highly dissipative structures (such as the faint disks seen in ellipticals or the disk near the nucleus of NGC4594) have chemical evolution histories dominated by infall of enriched material. In this case, the metallicity distribution is essentially a spike at the yield[36)].

The precise abundance distribution has tremendous effect on the content of the stellar population. If a wide range of abundance is present, then at least part of the population will be similar to globular cluster stars,

4.2 Gradients in Bulges and Spheroids

There has been a puzzling result in the literature for a number of years[37)] that bulges appear to have steeper color gradients than ellipticals. Modern CCD photometry and careful correction for dust absorption removes this discrepancy[38)], suggesting that while bulges have dissipative characteristics such as rotation support, their abundance gradients generally resemble those of ellipticals.

Color gradients gained heightened interest after suggestion that color correlates with local escape velocity[39)]. It is important to check if this extends to the lower luminosity bulge-like ellipticals. The implication is that wind outflow controls the mean abundance (i.e. effective yield) and that dissipative processes do

not transport metals. Were this process generally true, one would be surprised to find correlations between abundances and kinematics. As mentioned earlier, one would further expect to find wide abundance ranges right to the very nucleus of galaxies. Indeed, one does not observe galactic nuclei that have the spectra of M giants.

4.3 The Effects of Chemical Evolution on the Observed Population

The spheroids in galaxies will generally have approximately solar metal abundance. For those over a few Gyr old, the first giant branch and AGB will be dominated by M giants and there will also likely be OH/IR stars. There is evidence for luminous mass losing giants, and stellar mass loss has been directly observed[40]. Oxygen rather than carbon stars will dominate the giants; sufficient carbon cannot be dredged up at high metallicities to tip the C/O ratio above unity. Blanco's studies also show that the M/C star ratio varies as a function of metallicity, ranging from $\approx 10^3$ in the SMC to 10^{-3} in the Galactic bulge. In the disk of the Milky Way, carbon stars are predominant in the disk population that is beyond the solar circle[41].

Abundance spreads in spheroids (such as M32) and the possible dependence of local color on escape velocity are quite consistent with the simple model of chemical evolution and outflow. Correlations between abundances and kinematics in spheroids would be best explained by a dissipative formation scenario. It is therefore disturbing that while [42] finds that the simple model of chemical evolution fits the Galactic bulge, the same work also finds some correlations between abundances and kinematics of bulge stars. [43] extend this relationship to proper motions; more metal rich stars have smaller radial and vertical velocity dispersions.

Further complications in the population can arise due to varying element ratios and formation timescales. It has been suggested[44] that elliptical galaxies may have [Mg/Fe] enhanced. In the galactic bulge, [45] find element ratios characteristic of massive star SN element enhancements: Eu and the $\alpha-$ capture elements are enhanced by +0.5 dex. A straightforward interpretation of this result leads to the conclusion that the bulge probably built its metals (and therefore completed its formation) in $< 5 \times 10^8$yr. It is hard to understand how this permits enough time to establish correlations between abundances and kinematics in the bulge. If this timescale is correct, then there should be very little age spread in the bulge population.

My personal prejudice is that there is likely a gap in age between the globular cluster/halo population and the luminous spheroidal populations. The evidence for this gap is the 10 Gyr turnoff age in the Milky Way bulge, the luminous giants

in the M31 bulge, and the intermediate age Bar West population in the LMC. In these 3 cases where detailed study is possible, the oldest stars constitute $\approx$ 5% of the luminous mass.

4.4 Challenges in Stellar Populations

If the Hubble Space Telescope can be repaired, it should be possible to investigate stellar populations in detail in the local group. This in turn should provide a calibration of the luminosity fluctuation method. In principle, one could push the latter technique beyond the Coma cluster. The following questions stand as challenges for these observations:

1. Do most spheroidal populations have bright stars like those found in M31 and M32? In both the Milky Way and M31, there is evidence that the luminosity function brightens toward the nucleus. There is no clear reason at this time to prefer either age or metallicity as the explanation.

2. Are abundance spreads typical of spheroidal populations? It would be useful to explore the color range of giant branches as close to the nuclei of the local group galaxies as possible. If there has been dissipative transport of metals, theory predicts that the abundance distribution should narrow. If winds have removed metals, the abundance distribution should remain wide (in principle) even in the nucleus.

3. What are the properties of the brightest red variables? In the Galactic bulge, recent investigations find red variables with 800 day periods[45]. The presence of even longer period variables would be an almost certain sign of intermediate age.

4. What are the evolutionary lifetimes for the most luminous stars? The Fuel Consumption Theorem[46] is a powerful tool in predicting and analyzing the stellar content of populations. Briefly, the equation relates the number of stars n_j in an evolutionary phase j to the total *bolometric* luminosity of the population L_T and the lifetime of the evolutionary phase t_j. It reads:

$$n_j = L_T B(T) t_j. \tag{1}$$

B(T) is the stellar deathrate, $\approx 2 \times 10^{11}$ stars $L_\odot^{-1}\mathrm{yr}^{-1}$ for populations of order 10 Gyr old. We can, for example, calculate that for an OH/IR star lifetime of 10^4 yr, the Galactic bulge (with 10^{10} $L_\odot$) has $\approx$ 2000 OH/IR stars; Miras have 2×10^5 yr lifetimes and are therefore likely to be 20 times as numerous. Greggio & Renzini[47] work through a number of interesting examples as they explore the UV stellar content of galaxies.

5. What causes the UV rising flux in galaxies? Recent observations by HST[48] give part of the answer; in the bulge of M31 there are $\approx$ 140 UV bright stars of

$\approx 10^4 L_\odot$; these are likely post-AGB stars. However, it appears they do not account for all of the UV flux. [49] suggests that metal rich galaxies also get an important contribution from the evolved progeny of hot horizontal branch stars (the AGB-manqué stars;[50]). The UV population is of interest because it gives the deathrate directly, and also maps out previously unkown phases of stellar evolution. Finally, of cosmological importance, the emergence of these UV-bright stars requires low horizontal branch masses, and may provide a kind of absolute clock.

Clearly, these represent only a handful of the potential questions that one may ask of these spheroidal populations. The most interesting questions are, of course, the ones we have not thought of.

5. A LESSON FROM GEOLOGY

This has been a conference about the evolution of galaxies in their environment. Since the unequivocal demonstration of the Big Bang cosmology, we have naturally viewed galaxy evolution as an event dominated by this cosmology. Until recently, it was believed that hubble type was imprinted on galaxies at birth, which took place shortly after the Big Bang. There is an interesting analogy here with the catastrophist geological theories, in which all observed geology was viewed as being due to (for example) Noah's Flood or some enormous volcanic eruption.

Hutton emphasized that the agents of geologic change are observable: over long time periods, the cumulative effects of erosion and slow mountain building could also account for the observed landscape. In the 1980's, Schweizer argued that we could observe mergers of disks making elliptical galaxies *at the present epoch.* This was almost a heresy at the time, but we now accept that a sizable fraction of ellipticals (particularly in the field) are made by mergers. We can also observe other active processes of galaxy evolution, such as stripping by hot cluster gas and cooling flows. In modern geological theory, the pendulum has swung nearly completely toward Hutton's so-called uniformitarian viewpoint. It is sobering to think that field galaxies especially have literally $\approx$ 10Gyr to undergo substantial evolution, and that the initial conditions of the post Big Bang universe may not necessarily have been preserved. The undersanding that bulges may be built from the secular evolution of bars also fits in to this evolutionary picture, and additional examples are undoubtedly just around the corner. Clearly, galaxy evolution reflects something of the Big Bang and something of these evolutionary effects observable at the present epoch. In any case, the stellar populations of galaxies preserve a fossil record of their past, potentially yielding the most precise insight into the processes of galaxy evolution.

REFERENCES

1) Baade, W. 1944, *Ap.J.*, **141**, 45.
2) Sandage, A. 1961, *The Hubble Atlas of Galaxies,* (Carnegie Inst., Washington, D.C.).
3) Bahcall, J. 1986, *Ann. Rev. Astr. Ap.*, **24**, 577.
4) Eggen, O.J., Lynden Bell, D., & Sandage, A.R., *Ap.J.*, **136**, 748.
5) Whitford, A.E. 1978, *Ap.J.*, **226**, 777.
6) Knapp, G., Wynn-Williams, G. & Gunn J. 1992, *Ap.J.* (in press).
7) Rich, R.M. 1988, *A.J.*, **95**, 828.
8) McWilliams, A. & Rich, R.M. 1992 (in preparation).
9) Greggio, L. & Renzini, A. 1990, *Ap.J.*, **364**, 35.
10) Blanco, V. 1988, *A.J.*, **95**, 1400.
11) Frogel, J.A. & Whitford, A.E. 1987, *Ap.J.*, **320**, 199.
12) Frogel, J.A. *et al.*, 1990, *Ap.J.*, **357**, 143.
13) Rich, R.M. & Mould, J.R. 1991, *A.J.*, **101**, 1286.
14) Rich, R.M., Mould, J.R., & Graham, J. 1992 (in preparation).
15) Whitelock *et al.* 1991, *M.N.R.A.S.*, **248**, 276.
16) Frogel, J.A. & Elias, J.H. 1988, *Ap.J.*, **324**, 823.
17) Renzini, A. & Fusi-Pecci, F. 1988, *Ann. Rev. Astr. Ap.*, **26**, 199.
18) Díaz, A. Terlevich, E., Terlevich, R. 1989, *M.N.R.A.S.*, **239**, 325.
20) Binney, J. *et al.* 1991, *M.N.R.A.S.*, **252**, 210.
21) Boroson, T.A. 1991, *A.J.*, **101**, 111.
22) Rubin, V. & Graham, J.A. 1987, *Ap.J. (Letters)*, **316**, L67.
23) Kent, S.M. *et al.*, *Ap.J.*, **378**, 496.
24) Combes, F. *et al.* 1990, *Astr. Ap.*, **253**, 82.
25) Raha, N. *et al.* 1991, *Nature*, **352**, 411.
26) Pfenniger, D. & Norman, C. 1990, *Ap.J.*, **313**, 391.
27) Rich, R.M. 1988, *A.J.*, **95**, 828.
28) Geisler, D. & Friel E.D. 1992, *A.J.*, **104**, 128.
29) Mould, J. & Kristian, J. 1986, *Ap.J.*, **305**, 591.
30) Freedman, W.L. 1989, *A.J.*, **98**, 1285.
31) Larson, R. 1974, *M.N.R.A.S.*, **166**, 585.
32) Pagel, B.E.G. & Patchett, B.E. 1975, *M.N.R.A.S.*, **172**, 13.
33) Searle, L. & Zinn, R. 1978, *Ap.J.*, **225**, 357.
34) Arimoto, N., & Yoshii, Y. 1987, *Astr. Ap.*, **173**, 23.
35) Franx, M. & Illingworth, G. 1990 *Ap.J. (Letters)*, **359**, L41.
36) Mould, J.R. 1984, *P.A.S.P.*, **96**, 773.

37) Wirth, A. 1981, *A.J.*, **86**, 981.
38) Balcells, M. 1992, in *IAU Symposium 153*, Galactic Bulges.
39) Franx, M. & Illingworth, G. 1990 *Ap.J. (Letters)*, **359**, L41.
40) Knapp, G., Wynn-Williams, G. & Gunn J. 1992, *Ap.J.* (in press).
41) Blanco, V.M. 1965 in Vol. 5, *Stars & Stellar Systems*, A. Blanco and M. Schmidt, eds. p. 241 (Univ. of Chicago Press, Chicago).
42) Rich, R.M. 1990, *Ap.J.*, **362**, 604.
43) Spaenhauer, A., Jones, B., & Whitford, A.E. 1991, *A.J.*, **103**, 297.
44) Worthey, G.*et al.* 1992, *Ap.J.* (in press).
45) Whitelock *et al.* 1991, *M.N.R.A.S.*, **248**, 276.
46) Renzini, A. & Buzzoni, A. 1986 in *Spectral Evolution of Galaxies,* eds. C. Chiosi & A. Renzini (Dordrecht: Reidel), p. 195.
47) Greggio, L. & Renzini, A. 1990, **Ap.J.**, **364**, 35.
48) King, I.R. *et al.* 1992, *Ap.J. (Letters)*, **397**, L35.
49) Ferguson, H., and Davidson, A. (This volume).
50) Greggio, L. & Renzini, A. 1990, *Ap.J.*, **364**, 35.
51) Rich, R.M. *et al.* 1989, *Ap.J. (Letters)*, **341**, L51

STAR FORMATION IN S0 GALAXIES

Jo Ann Eder
N.A.I.C., Arecibo Observatory
P. O. Box 995
Arecibo, PR 00613
U.S.A.

ABSTRACT

The large range in gas content found for S0 galaxies is difficult to explain. While very low upper limits ($< 10^7$ $M_\odot$) can be placed on the mass of atomic hydrogen of some systems, as many as a fourth of the galaxies classified as S0 in the UGC may have gas surface densities as high as those found for Sa or Sb galaxies. This paper compares the star formation properties of gas-rich S0 and Sa galaxies with gas-poor S0's, in order to determine the importance of a gas surface density threshold for star formation, both globally and locally. All of the gas-rich S0's studied manifest low surface brightness structure, either in blue light or in H_α-N II emission line regions, or in both. Comparable images of the gas-poor S0's show no structure except dust lanes, while the intermediate S0's, with marginal gas contents, have diffuse disk line emission associated with very faint blue arms. The local gas surface densities, indicated by maps of the atomic gas for two gas-rich S0's, UGC 2367 and UGC 5419, are consistent with the requirement of a threshold gas density for the appearance of star formation.

1. The S0 Galaxy as a Transition Classification

Hubble originally proposed the S0 classification as a transition between spiral and elliptical galaxies before he actually identified specific galaxies as S0's. Since the prominence of arm structures, as outlined by bright star formation regions, increased along the spiral sequence from Sa to Sd, Hubble reasoned that galaxies must exist with smooth, featureless disks, which lacked arms or obvious star formation regions.

In other morphological classification systems, S0 galaxies are also identified as disk galaxies devoid of any indication of star formation which could be discerned from photographic plate images (Buta, this volume). However, S0 galaxies occupy a large volume of parameter space when other parameters, such as disk-to-bulge ratio (D/B), gas content, and rotational velocity, are considered. These may be the very properties which drive a galaxy's evolution and determine its morphological classification. (Larson, this volume) The distribution of D/B for S0 galaxies is similar to that for Sa - Sb galaxies (Kent 1985, Eder 1990). The rotational velocities of S0 galaxies, like those of Sa's, tend to be higher for a given luminosity than those of later types (Rubin *et al.* 1985, Giovanelli *et al.* 1986). The S0 hybrid neutral hydrogen surface density (σ_{HI}, derived using the *optical* diameter) has a large range, from values typical of Sa and Sb galaxies to upper limits well below that detected within spiral galaxies of similar size. In a recent 21 cm survey of massive early-type disk galaxies, half of the S0 galaxies were detected and half of these detections had values of σ_{HI} as large as that found for Sa galaxies. (Eder, Giovanelli, and Haynes 1991, hereafter EGH).

If the star formation rate depends on gas density (Schmidt 1959, Kennicutt 1989, Larson, this volume), it is surprising that galaxies of similar σ_{HI} have such different levels of star formation such that some would be classified as spirals and others as S0's. Buta cautions that low surface brightness features, such as arms or rings, can be missed on underexposed plates. Could these gas-rich S0 galaxies be either misclassified spirals, or examples of the anemic spirals with low surface brightness structure of van den Bergh's parallel sequence classification system? (van den Bergh 1976)

The remainder of this paper will examine these possibilities and will discuss the relation between σ_{HI} and star formation, both globally and locally. CCD images in B, R, and continuum-subtracted H_α - N II will be compared for four samples: Sa galaxies, gas-rich S0's, gas-poor S0's and marginal S0's, with values of σ_{HI} intermediate between the gas-rich and the gas-poor samples. Also, VLA maps of the atomic gas in two gas-rich S0's will be examined to determine the local H I surface densities near regions of H_α emission.

2. Are Gas-Rich S0's Misclassified?

The galaxies to be imaged were chosen from a 21 cm survey of massive, early-type disk galaxies (EGH), and from a survey of isolated galaxies (Haynes and Giovanelli 1984, hereafter HG), both performed with the Arecibo radio telescope. The galaxies were assigned to the four samples according to their morphological classifications in the UGC (Uppsala General Catalogue of Galaxies, Nilson 1973) and to the value of their hybrid H I surface densities, σ_{HI} , calculated with the integrated H I flux, corrected for pointing errors and source extent, and with diameters measured from the POSS plates, as reported in EGH and HG. The values of σ_{HI} for the four samples are given in Table 1.

The optical images were obtained during two observing sessions: one in March, 1989, at the CTIO 0.9 m telescope and the other in November, 1990, at the KPNO 0.9 m telescope. The CCD cameras were equiped with a TI chip with a scale of 0.49 arcsec per pixel at CTIO, and a TEC chip with a scale of 0.79 arcsec per pixel at KPNO. The images were bias-subtracted and flatfielded utilizing the standard procedures within IRAF. The galaxies were imaged with two 80 A wide filters, one which included the redshifted H_α and N II lines and the other chosen to measure the continuum near the H_α - N II lines. After sky-subtraction and corrections for extinction and slight differences in the filter response functions, the continuum image was subtracted from the H_α - N II image.

A comparison of the R, B, and continuum-subtracted H_α images provides clues to an explanation for the large range in S0 gas densities. Based only on the R images, the galaxies classified as Sa show definite arm structure while those classified as S0 have apparently smooth disks. However, the B images of the gas-rich S0's reveal faint, low surface

Table 1. $H\alpha$ Morphology of Sa and S0 Galaxies

Sample σ_{HI} in $M_\odot pc^{-2}$	UGC	Type UGC, RC2	$H\alpha$ Morphology
Sa:	6695	Sa	central, arms
$\sigma_{HI} > 3$	6746	Sa, SA(r)0/a	central, ring
	9006	S...	arms
	9696	Sa	central, arms
	9960	Sa	central, no arms
Gas Rich S0's:	491	S0, Sa(r)0	ring (skewed)
$\sigma_{HI} > 3$	550	S...	floculent knots
	2367	S0	central, arms
	2774	S0	central, ring
	3201	SB0/SBa, (r)SB(s)0/a	central, open arms, knots
	5419	S0	central, ring, arms
	6322	S0, SA0+ or 0/a	none
	7198	SB0	central, short arms
	8343	S...	central, faint disk
	12760	S0?	inner ring
	12840	SB0, (R)SAB(s)0	central, pseudo-ring, arms
Marginal S0's:	818	SB0	faint ring (skewed)
$\sigma_{HI} = 1.5\text{-}3$	2357	S0, SA0	very little - diffuse disk
	4345	S0a	very little
	5159	Sa?	central, diffuse ring
	5239	S0	faint arms, diffuse disk
	5966	S0a	central
Gas Poor S0's:	4312	S0/Sa	central
$\sigma_{HI} < 1.5$	4875	S0a	central

brightness structure, sometimes including the blue knots associated with active star formation regions. The H_α images indicate star formation activity, concentrated in tight arcs or rings, along many of these low surface brightness features. Details of the H_α morphology for the program galaxies are given in Table 1 along with the classifications from the UGC and the RC3 (deVaucouleurs.*et al.* 1991). Qualitatively, the gas-rich S0's have as much star formation activity as is seen in the Sa galaxies, although it is frequently concentrated in very sharply defined regions. The S0's with marginal gas content show only faint, diffuse H_α emission, if any. The gas-poor S0's have only central emission.

All four samples contain galaxies with central emission. Long-slit spectra of UGC 4312, UGC 5966, UGC 6695, and UGC 6746 show that most of the central emission is due to the N II λ 6584 line. This is likely to be the case for the other galaxies with central emission, as well. Most of the nuclear emission detected in early-type disk galaxies has N[II] λ 6584/H_α ratios greater than one.and therefore emanates from low-ionization regions of gas. (Keel 1983 and Phillips *et al.* 1986)

The H_α images of the Sa galaxy UGC 9960 and the S0 UGC 6322 are puzzling. Faint, smooth arms are clearly present on the blue images but not on the H_α images. These two galaxies could be examples of transition objects, caught between the last epoch of star formation and the fading of the blue stars it produced. If a threshhold gas density is necessary for star formation (Kennicutt 1989), the gas within the Sa's and gas-rich S0's may be close to this threshold value globally. In local regions, where the gas density is enhanced, the σ_{HI} may rise above the threshold value so that star formation can occur.

Besides the expected density enhancement due to spiral waves, several low-order resonances may be responsible for much of the H_α morphology observed in our samples. The nuclear ring of H_α emission seen in UGC 12760 may be a manifestation of star formation triggered by an abrupt perturbation of stable orbits at the Inner Lindblad Resonance, as discussed for NGC 4321 by Arsenault *et al.* (1988). Knots of star formation are clearly present as distinct beads at both ends of the bar in UGC 3201. Kenney and Lord (1991) observed large CO complexes associated with the bright H II regions located at the bar-spiral arm transition zone in M83 and found the kinematics of the gas to be consistent

with a gas density enhancement due to orbit crowding at the intersections of the bar and the spiral arms. The prevalence of H_α rings and pseudo-rings in the gas-rich samples could be associated with the Outer Lindblad Resonance (Schwarz 1981 and Buta and Crocker 1991).

3. Threshhold Gas Surface Density

In order to determine the connection between the gas content and the star formation in these anemic galaxies, we have mapped the neutral hydrogen for two of the gas-rich S0 galaxies, UGC 2367 and UGC 5419 (Eder & Haynes 1993). The observations were made in December, 1990, with the VLA in the C array with a velocity resolution of 21 km s^{-1} and a beam width at FWHM of 18" x 18" for UGC 2367, and of 10 km s^{-1} and 24" x 20" for UGC 5419. Cleaned, continuum-subtracted maps of the total H I surface density and the velocity field for each galaxy were made using programs in AIPS.

The channel maps are typical for rotating gas disks. All of the blue light of the galaxies falls within regions in which the atomic gas surface density, corrected for inclination, is greater than 1 $M_\odot pc^{-2}$. For UGC 5419, there are patches of H I within the star formation regions with surface densities of 2.4 $M_\odot pc^{-2}$. The map of the total H I content of UGC 2367 is shown in Figure 1. The blue extent of the optical image is given by the outer dashed-line ellipse and the extent of the H_α emission is indicated by the inner ellipse. The gaseous disk extends well beyond the optical image, but the surface densities in the outer regions are less than 1 $M_\odot pc^{-2}$. The location of the arcs of H_α emission are shown by the letters a, b, c, d, and e.

A rotation curve was derived for UGC 2367 since it is highly inclined ($\varepsilon = 0.72$). The critical gas surface density necessary for the instability of a gaseous disk was calculated using the formula of Kennicutt (1989) for a gas disk with a flat rotation curve, with a constant velocity dispersion of 6 km s^{-1} , and with a stability parameter of 0.67, as estimated for Sc galaxies. The total gas surface density for the regions of star formation was estimated from the H I maps, assuming a mean ratio of molecular to neutral hydrogen gas of 1.4, as found for S0's by Lees *et al.* (1991). In Table 2, the values of the critical gas density are compared

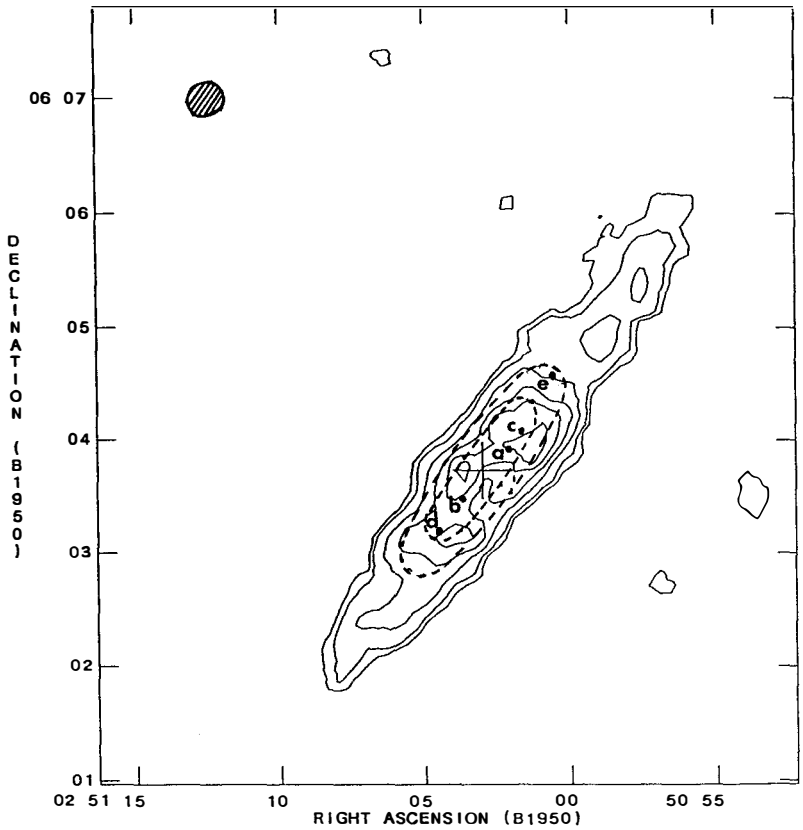

Figure 1. Contour plot of the zeroth moment map for UGC 2367 which shows the atomic gas distribution. The extent of the star formation is indicated by the inner dashed ellipse and that of the optical image (r_{25}) by the outer dashed ellipse. The contours indicate gas surface densities of 0.5, 1, 2, 3, 4, and 5 $M_\odot pc^{-2}$. The locations of the sharp arcs of star formation from the H_α image are shown by the letters a, b, c, d, and e. The beam is shown by the hatched area in the upper left.

Table 2. Gas Densities in Regions of Star Formation for UGC 2367

	r kpc	σ_{thresh} $M_\odot pc^{-2}$	σ_{gas} $M_\odot pc^{-2}$
a	5.4	7.3	11.8
b	5.4	7.3	9.6
c	9.0	7.0	11.8
d	14.4	6.0	9.4
e	22.0	4.7	4.8

with the estimated gas density within the regions of star formation. Within all of the designated star formation regions, the estimated gas density is greater than the critical density.

4. Conclusions

The gas content of S0 galaxies exhibits a large range of values, from amounts comparable to that found in early-type spirals to very low upper limits. Gas-rich S0 galaxies, chosen to have hybrid atomic gas surface densities, σ_{HI}, as large as those commonly found in Sa galaxies ($> 3\ M_{\odot}pc^{-2}$), could all be classified as anemic spirals, with low surface brightness arms and/or distinct regions of star formation. A sample of S0's with marginal gas contents showed less structure and only patchy or diffuse emission on H_{α} images. Gas-poor S0's had only central line emission. Our H_{α} images of S0 galaxies show that star formation occurs when $\sigma_{HI} > 1.5\ M_{\odot}pc^{-2}$ globally, or when local enhancements of the gas density raise the value above a critical value for instability. The hybrid σ_{HI} is thus an important parameter to distinguish between anemic or misclassified spirals and "true" S0's with smooth, featureless disks and no recent star formation.

It is a pleasure to thank Martha Haynes, my collaborator on the VLA observations, and Daniel Puche of NRAO for their help with the intricacies of the VLA and AIPS.

References

Arsenault, R., Boulesteix, J., Georgelin, Y. & Roy, J. -R. 1988, A&A, **200**, 29
Buta, R. & Crocker, D. A. 1991, AJ, **102**, 1715
de Vaucouleurs, G. et al. 1991, *Third Reference Catalogue of Bright Galaxies* (Springer, Berlin (RC3)
Eder, J. 1990, Ph. D. thesis, Yale University
Eder, J., Giovanelli, R. & Haynes, M. P. 1991, AJ, **102**, 572 (EGH)
Eder, J. & Haynes, M. P. 1993, in preparation.
Giovanelli, R., Haynes, M. P., Rubin, V. C., & Ford, W. K. 1986, ApJ, **301**, L7
Haynes, M. P. & Giovanelli, R. 1984, AJ, **89**, 758 (HG)
Keel, W. C. 1983, ApJS, **52**, 227
Kenney, J. D. P. & Lord, S. D. 1991, ApJ, **381**, 118
Kennicutt, R. C. 1989, ApJ, **344**, 685
Kent, S. M. 1985, ApJS, **59**, 115
Lees, J. F., Knapp, G. R., Rupen, M. P. & Phillips, T. G. 1991, ApJ, **379**, 177
Nilson, P. 1973, *Uppsala General Catalogue of Galaxies*, Uppsala Astron. Obs. Ann., **6**

Phillips, M.M., Jenkins, C.R., Dopita, M.A., Sadler, E.M. & Binette, L. 1986, AJ, **91**, 1062
Rubin, V. C., Burstein, D., Ford, W. K., & Thonnard, N. 1985, ApJ, **289**, 81
Schmidt, M. 1959, ApJ, **129**, 243
Schwarz, M. P. 1981 ApJ, **247**, 77
van den Bergh, S. 1976, ApJ, **206**, 883

PREDICTION OF SPECTRA FOR INDIVIDUAL GALAXIES

P. Jablonka
Observatoire de Paris, Section de Meudon
DAEC, URA 173
France

Abstract:
The combined use of the two classical and previously independant methods, the population synthesis using star cluster spectral integrated properties and the evolutionnary synthesis, has permitted, for the first time, the successfull prediction of spectra of individual spiral galaxies.

Until now the spectral study of spiral galaxies was restricted to global variations of properties from one Hubble type to another, and their simplicity kept them unreliable for precise individual analysis of external galaxies .

A new model for stellar population of spiral galaxies has been built recently, taking fully into account the two components, the bulge and the disc , in the evolution of the total galaxy (Arimoto and Jablonka, 1991; hereafter AJ).

It successfully reproduced the chemical and photometric properties of spiral galaxies. Spectroscopy is an even more constraining domain for the AJ model.
In 1988, Bica (hereafter B88), had raised an important and still unresolved question:
B88 had gathered the observed spiral galaxies into several groups corresponding to spectral features and continuum slope similarities. Surprisingly those groups were extremely heterogeneous in term of Hubble types (see B88 table2). However, a spectral similarity between two galaxies of different Hubble types is a priori unexpected, with regards to their different parameters of star formation.

I present here the result, for two spiral galaxies NGC3368 and NGC6744 (respectively of Sbc and Sab types), of the confrontation between the predicted spectra resulting from the AJ model, and the observed data of B88. The size, distance, dynamical parameters and Lb/Ld ratio of the galaxies, necessary parameters for the application of AJ model, were found in Simien and De Vaucouleurs (1986) and Kent (1985).

The model uses the following asumptions :
bulge and discs are formed with different time scales . Their stars are formed from infalling gas of primordial composition, but on different times scales as well. The star formation of the bulge is stopped by a supernovae-driven wind following the same scenario as for elliptical galaxies (Arimoto and Yoshii, 1987). The gas expelled, enriched by the nucleosynthesis in the bulge, is mixed with the gas accreting on the disc. Discs stars are then formed from pre-enriched gas.

AJ demonstrated that the bulge -to -disc luminosity ratio, LB/LD, together with its dispersion at fixed Hubble type, is the fondamental parameter for understanding the chemical and photometric properties of spiral galaxies.

AJ model allows to calculate, for each galaxy, the contribution to the total galaxy light of each generation of stars with given age and metallicity . This corresponds to the prediction of the history of star formation traditionnally deduced by the population synthesis method. B88 had shown that using a base of star cluster spectral integrated properties (Bica and Alloin, 1986) one can analyse a galactic population without any asumption on the parameters and scenario of star formation.

The present work joins the two kinds of analysis of stellar population, the evolutionnary synthesis and the population synthesis, and inverses the latter from analysis to prediction. Indeed, in B88, by measuring the equivalent widths of the galaxy spectrum, one could deduce the generations of stars (star clusters) of given age and metallicity contributing to the light. Here one predicts the generations of stars, and we can calculate the equivalent width of lines , and display the spectrum of the galaxy.

Assuming a de Vaucouleurs law for the surface brightness distribution of the bulge and an exponential law for the disc, we can calculate the local Lb/Ld(r) ratio as a function of the aperture size of the observations. As a consequence the conditions of observations in B88 have been fully taken into account in the predictions.
Fig1. displays the observed and the predicted ones spectra for the two galaxies NGC3368 and NGC6744. Except a small uncorrected reddening effect for NGC6744, the synthetized and the observed spectra are indistinguishable.

In B88, NGC3368 and NGC6744 were found to belong to the same representative group S3. Fig2. displays the predicted spectra together with the averaged spectrum of the group S3 in B88. They are indeed identical.

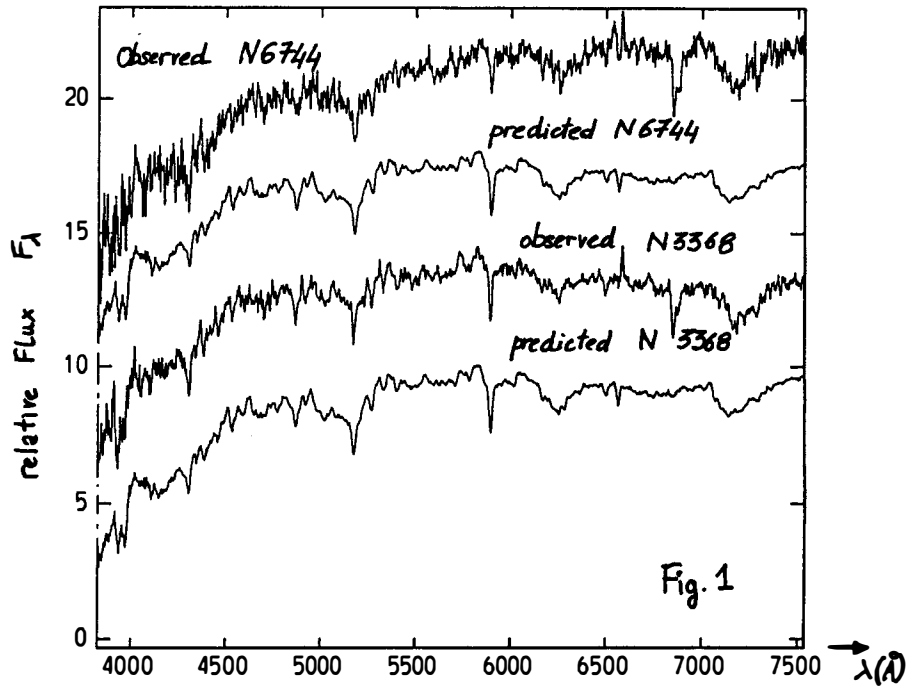
Observed N6744
predicted N6744
observed N3368
predicted N 3368
relative Flux F_λ
20
15
10
5
0
4000
4500
5000
5500
6000
6500
7000
7500
λ(Å)

Fig. 1

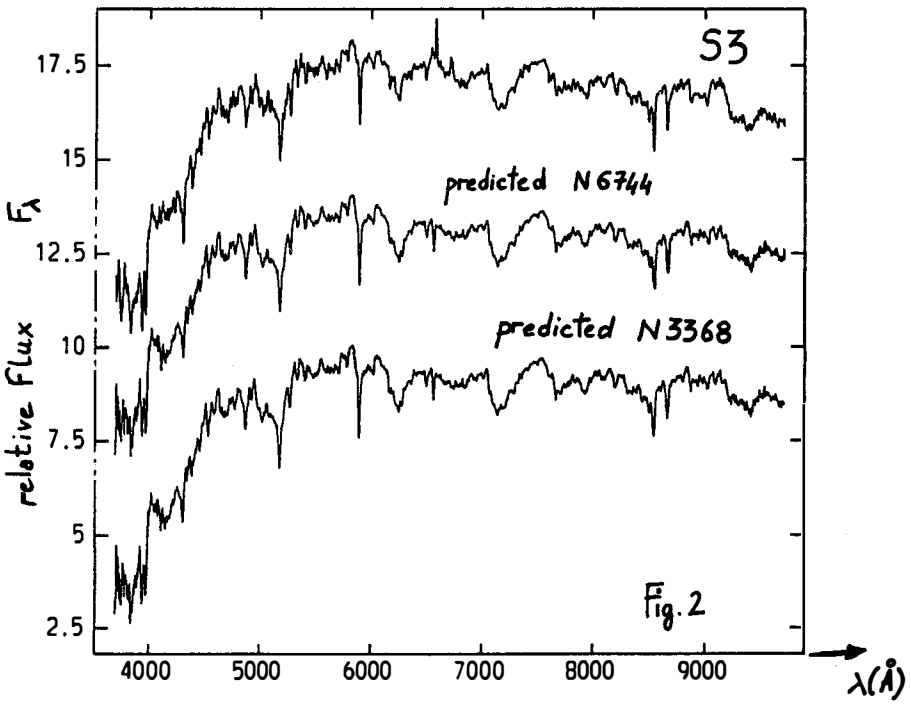
S3
predicted N6744
predicted N3368
relative Flux F_λ
17.5
15
12.5
10
7.5
5
2.5
4000
5000
6000
7000
8000
9000
λ(Å)

Fig. 2

It follows that , here again, the local Lb/Ld(r) ratio plays a fundamental role . This parameter gets the same value - about 2- for the two studied galaxies. As in B88 the aperture of the observations is very small compared to the size of the galaxies , the light analysed is principally coming out from the bulge.

However there is a dilution (the spectra are bluer than a spectrum of a bulge alone) due to the discs . The fraction of disc light being similar for the two galaxies, the resulting spectra , in B88 aperture, are hence identical.

Conclusion

We have been able to reproduce spectra of individual spiral galaxies . For the first time, the evolution of the two components bulge and disc are fully taken into acount, as well as the non-solar metallicity , in particulat metal rich, stellar populations in the display of the spectra and the calculations of equivalent widths of lines and continuum points.

References:

Alloin D., Bica. E., 1986, A&A, **162**, 21
Arimoto N., Jablonka P., A&A, **249**, 374
Bica E., 1988, A&A, **195**, 75
Kent S.M, 1985, ApJS, **59**, 115
Simien F., de Vaucouleurs G.,1986, ApJ, 302, 564

FAINT OBJECT CAMERA OBSERVATIONS OF GALAXY CORES

Philippe Crane
European Southern Observatory
Garching, Germany

and

Massimo Stiavelli
Scuola Normale Superiore
Pisa, Italy

ABSTRACT

This paper presents a summary of Hubble Space Telescope Faint Object Camera observations of the nuclear regions of 10 relatively nearby galaxies. Six galaxies were observed in a uniform manner with both the F342W(U) and the F502M(B) filters. M31, M32, and M87 were observed in the far UV, and M81 was observed with two narrow band blue filters. The main results are summarized, and some details of selected objects are discussed.

1. Introduction

Since the first conception of the Space Telescope, it was clear that one of the important programs would be to observe the nuclei of the relatively nearby galaxies. Indeed, one of the most important results from the stratoscope project[1], which was a precursor to the Space Telescope, is on the nucleus of M31. Thus observations of a number of nearby galaxies was one of the highest priorities with the Faint Object Camera.

The problems of studying the nature of the cores of galaxies have a long history. One of the main conclusions of this history is that the ground based results have been severely influenced by the effects of seeing[2,3]. Thus, even in the cases where the original ground based results seemed to have resolved the light distribution, better data, taken in better seeing conditions, have yielded even smaller core radii and denser cores. The HST observations extend this trend by increasing the resolution by about an order of magnitude.

The Faint Object Camera is ideally suited for studying the nuclear regions of galaxies since it provides the highest spatial resolution available with the HST, and it is particularly sensitive in the ultraviolet. This latter property is useful for studying departures from the normal stellar content of galactic nuclei that might be expected when looking at higher spatial resolution in the nuclear regions.

The main emphasis of the results presented here is a discussion of the light profiles of the galaxies observed. These results are only the very beginning of the detailed analysis which will eventually be carried out using these data. This paper presents a summary of a more extensive paper which will be published elsewhere[4]. Certain aspects of the M87 data have been described by Boksenberg[5]. A paper on the blue objects seen in the nucleus of M31 is also in press[6].

2. Observations and Analysis

The data reported here were all obtained with the Faint Object Camera and many important details of the instrument can be found in the Faint Object Camera Handbook[7]. Table 1 summarizes the data which have been used. The F342W and F502M filters approximate the U and B filters although not very well. The F486N is an Hβ filter, and the F501N is an OIII λ5007 filter. The other filters, F120M, F140W, and F175W, are ultraviolet filters with central wavelengths at approximately the wavelength in nanometers of the filter number. In a few cases, it was necessary to include a neutral density filter in order to insure that the counting rate did not exceed the linear range of the FOC. The

Table 1: Summary of Observations

Object	Mode	Exposure time (sec)	max. count rate (cps)
M31 (NGC 221)	zoomed,F/48,F175W	5161	0.03
M32 (NGC 224)	zoomed,F/48,F175W	5280	0.04
	F/96,F480LP,F4ND	1500	0.12
M81 (NGC 3031)	F/96,F486N	2392	0.50
	F/96,F550M	1196	0.47
M87 (NGC 4486)	F/96,F120M	2400	0.02
	F/96,F140W	4610	0.02
	F/96,F501N	4786	0.12
NGC 3862	F/96,F342W	903	1.32
	F/96,F502M	596	0.28
NGC 4406	F/96,F342W	1196	0.10
	F/96,F502M,F1ND	596	0.05
NGC 4552	F/96,F342W	1196	0.12
	F/96,F502M	896	0.17
NGC 4594 (M104)	F/96,F342W	1196	0.36
	F/96,F502M	896	0.35
NGC 4621	F/96,F342W	1196	0.33
	F/96,F502M	896	0.45
NGC 6251	F/96,F342W	1196	0.60
	F/96,F502M	596	0.27

f/96 mode provides a field of view of $11'' \times 11''$ with a pixel size of 0.0224 arcsec. The f/48 zoom mode used to observe M31 and M32 provides a field of view of $44'' \times 44''$ with pixels of 0.043×0.086 arcsec.

The initial processing of the data was done with the standard pipeline routines. This procedure basically did a geometric correction to the data, and removed some of the flat field artifacts.

2.1. Ellipse fitting

The data have been analyzed by fitting ellipses to the images. Two different procedures have been employed in order to look for possible artifacts associated with the techniques. None were found. The results provided the radial light profile of the objects. These are the basic data which we have used. It is important to note that in many cases, the ellipse fitting routines produced more points along the radial profile than are actually statistically independent. This occurs because the procedure uses radial steps which are often not whole pixels.

We note that we have not deconvolved these images, but have preferred to follow the procedure outlined in the next section. This was done because the deconvolution of extended sources is considerably less well defined than than for point sources.

2.2. MODELING

In order to understand the implications of these data, we have chosen two rather general light profiles which we have convolved with the appropriate point spread function to generate model galaxy profiles to compare with the data. The models that we have adopted are: *i)* Hubble laws modified to account for a central cusp due to central mass concentrations (Σ_{CC}), *ii)* Hubble laws modified to account for an inner residual power law behavior (Σ_{PL}). In addition to the models *i)* and *ii)* it was sometimes necessary to add a central point source. The modified Hubble laws which we consider have a projected density distributions of the form:

$$\Sigma_{CC} = \frac{(1 + r_1/r)^{1/2}}{(1 + (r/a)^2)^n} \tag{1}$$

$$\Sigma_{PL} = \begin{cases} \frac{1}{(1+(r/a)^2)^n} & \text{if } r > r_{match} \\ \left(\frac{1}{(1+(r_{match}/a)^2)^n}\right)\left(\frac{r_n+r_{match}}{r_n+r}\right)^{\alpha} & \text{if } r < r_{match} \end{cases} \tag{2}$$

where a is the core radius, $2n$ is the slope of the outer Hubble profile, r_1 is a scale length for the central spike, α is the slope of the inner power law, $r_n << a$ is a "nuclear" core radius which we initially set to 0 and did not vary unless the observed profiles seem to flatten at very small radii. The radius r_{match} is chosen in such a way as to make the matching between the outer Hubble profile and the inner power law continuous with continuous derivative. As a consequence, we get

$$r_{match} = a\left[\frac{\sqrt{(2n-\alpha)\alpha - n^2(r_n/a)^2} - nr_n/a}{2n-\alpha}\right] \tag{3}$$

Our results presented below are derived by varying the parameter for the model which seemed best suited to the particular galaxy being considered. However, we did not do a formal least squares analysis of the data, so we cannot make a quantitative judgment of the degree to which one or the other model or even some third model actually describes the results. Nevertheless, we believe that the models given are a reasonably good description of the data although perhaps not unique. We note that for the most part the physical parameters which we derive such as luminosity densities are not crucially dependent on the details of the particular model.

Table 2: Summary of Results

Object	a	n	r_n	α	r_1	point source
M31	3.0	0.35	0.070	0.8	-	no
M32	0.3	0.65	0.050	1.0	-	no
M87	8.0	0.90	0.000	0.26	-	yes
NGC 4621	1.2	0.75	0.0	0.9	-	no
M81	1.7	0.60	-	-	0.7	yes
NGC 3862	1.5	1.00	-	-	0.3	yes
NGC 4406	1.4	0.60	-	-	0.07	no
NGC 4552	0.8	0.60	-	-	0.15	no
NGC 4594	2.0	0.70	-	-	0.40	yes
NGC 6251	1.6	1.00	-	-	0.32	yes

One interesting result is that none of our galaxies are well represented by a deVaucouleurs law $r^{\frac{1}{4}}$ all the way into the center. The outside regions, as is well known, are well described by the deVaucouleurs law.

3. Results for Individual Galaxies

This section presents some results for selected individual galaxies and discusses some of the results to be published in the papers mentioned in the introduction. Unfortunately, the body of work presented at the conference cannot be presented in its entirety in this paper. The interested reader is referred to the paper of Crane *et al.*[4].

The results of our model fitting show that the profiles of the observed galaxies fall in three classes: *i)* a featureless ever-increasing profile (M31, M32, NGC 4621), found also by the HST/SV observations of NGC 7457 [8], *ii)* non-isothermal profiles with a central unresolved point source (M87, M81, NGC 3862, NGC 4594, NGC 6251), which are all qualitatively similar to the profile of M87 derived by Young *et al.*[9], and *iii)* non-isothermal profiles without a point source (NGC 4406 and NGC 4552). We note the lack of truly isothermal profiles in our data set. Somewhat surprisingly, even NGC 4406, which appears in the list of isothermal objects of Kormendy[10], possesses a non-isothermal core. Table 2 summarizes the parameters for the models used to describe each galaxy.

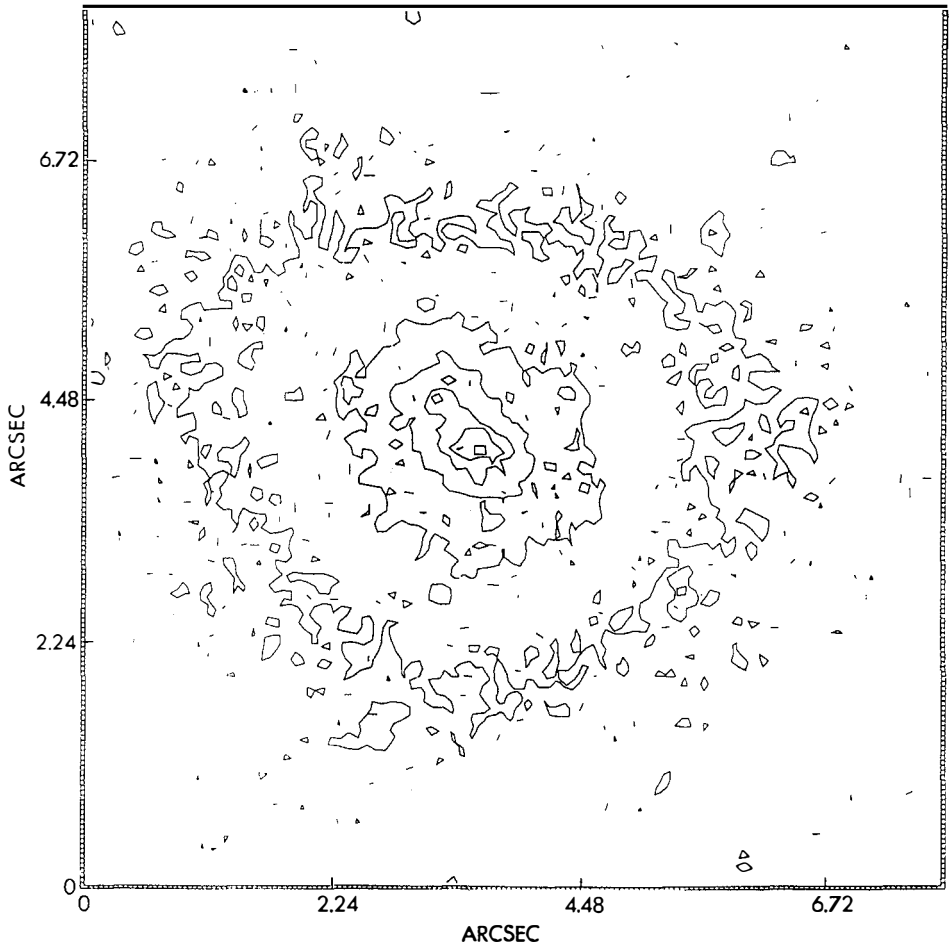

Figure 1: Isophotal plot of the central regions of M31 from the FOC F/48 zoomed images taken with the F175W filter. Note the offset of the brightest point from the center of the next isophote.

3.1. M31

Figure 1 shows the isophotes in the central region of M31. There is a clear increase in the ellipticity towards the center, but the brightest point in this image at 1750Å is offset from the center of the next isophote by about 0.4 pc. This result confirms the results of Nieto *et al.*[11] whose images are almost as good as the FOC images in the zoomed F/48

format.

The F175W images of M31 have revealed a population of hot blue stars which are distributed like the light in the core. These are extremely blue objects since they do not show up in the ground based images of M31 taken by Nieto *et al.*[11]. These are interpreted as PAGB stars, and this interpretation is strengthened by a reasonable correspondence between these objects and planetary nebula identified by Ciardullo *et al.*[12] . The number of these sources is consistent with the expected death rate of stars in the core of M31. The reader is referred to the paper of King *et al.*[6] for further details.

3.2. NGC 3862

NGC3862 (or 3C264) is the sixth brightest galaxy in the cluster Abell 1367. It is a head tail radio source[13] and contains a X-ray source which is unresolved with the Einstein high resolution camera[14]. The FOC observations revealed a prominent jet as shown in Figure 2. Comparison of the UV and B exposures taken with FOC reveal a spectral indices of 0.6 and 1.4 for the nucleus and jet respectively. These are similar to what is found for other synchrotron jets. Thus it is very likely that this is the fifth known synchrotron jet. The discovery of this jet is a clear demonstration of the power of the HST observatory. The jet is very small and its contrast to the star light from the galaxy is greatest in the UV where the FOC is particularly sensitive. Further details of this discovery will be found in the paper by Crane *et al.*[15].

3.3. NGC4621

NGC 4621 is a Virgo elliptical (E4/E5) galaxy, showing substructure in its kinematical profile[16] which could be indicative of the presence of a two-component bulge-plus-disk system. We note that the nuclear core of this galaxy is no broader than the stellar PSFs. The disk is also detected by isophote analysis[16] in the radial range 3–20 arcsec. Our isophotal analysis shows a significant diskiness even inside 3 arcsec, down to 0.06 arcsec, accompanied by a non-significant change in flattening and absence of twisting.

No color gradient is detected inside 1 arcsec. The central luminosity density derived for this object is $\geq 2 \times 10^6 L_{\odot B}$ pc^{-3}. We have assumed a core radius smaller than 0.04 arcsec, since a bigger core radius would be detected in our data. A central luminosity density as high as $4 \times 10^6 L_{\odot B}$ pc^{-3} or more would still be compatible with our data.

These values of the central density are too high to be compatible with even the most extreme dissipation-less galaxy-formation scenarios[17] and call for a dissipative formation mechanism. However, the absence of core color gradients seems to constrain severely even

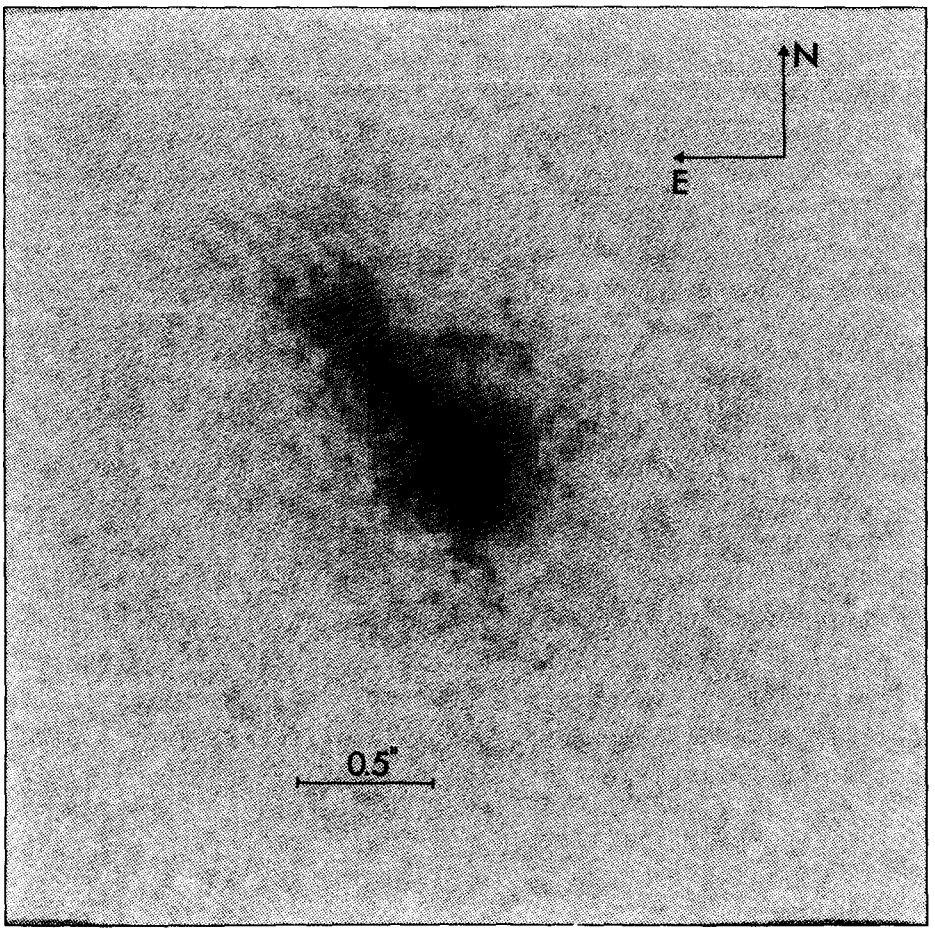

Figure 2: FOC image of NGC3862 with the F342W filter. North is up, and East is to the left. The jet is about 0.65 arcsec long to the point of bifurcation. The bright spots and bending of the jet are very reminiscent of the jets in M87 and 3C66B which this jet is very likely similar to.

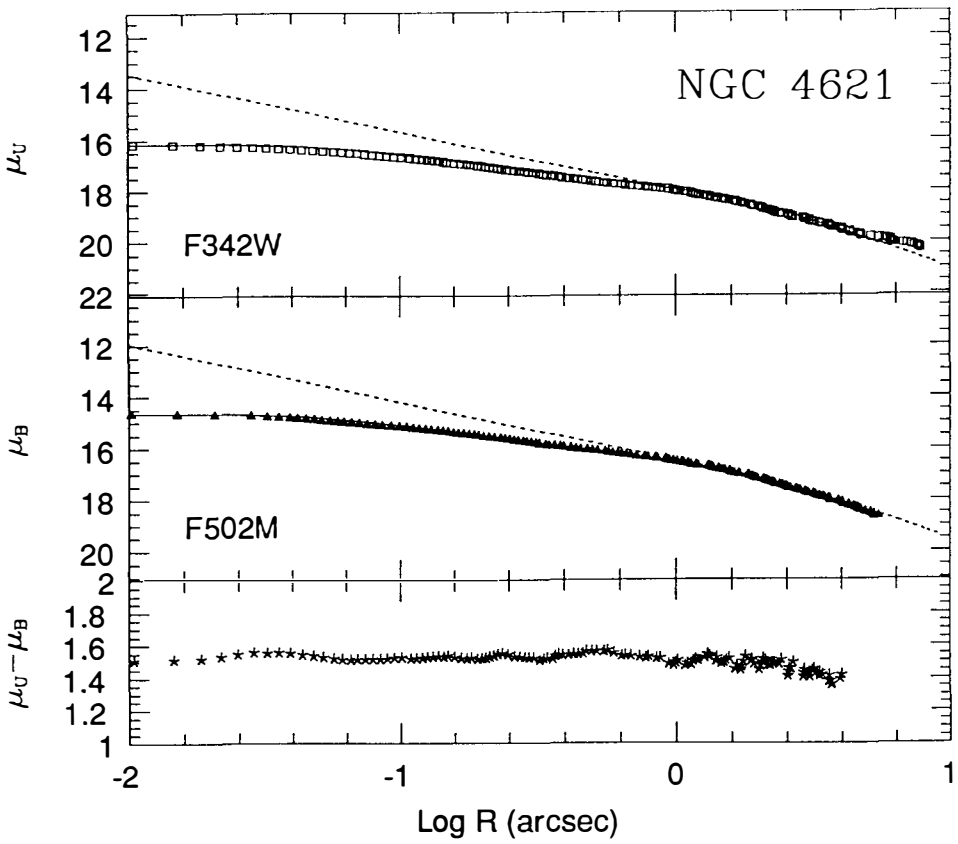

Figure 3: Plot of the surface brightness of NGC 4621 as a function of the radius. The upper panel shows the data (triangles) derived from the ellipse fitting as explained in the text. The dotted line is for one of the models with the parameters given in Table 2. The solid line represents the convolution of the model with an appropriate point spread function. The middle panel shows the same results for the F502M filter. The lower panel shows the color derived from the data in the two other panels.

dissipative formation scenarios, which tend to produce strong color gradients[18]. Figure 3 shows a plot of the surface brightness versus radius.

3.4. NGC 4594

The Sombrero galaxy has long been suspected of harboring a very high mass concentration in the nucleus[19]. The FOC image of the nucleus shown in Figure 4 shows several remarkable features, and confirms the presence of a large mass concentration. Our analysis

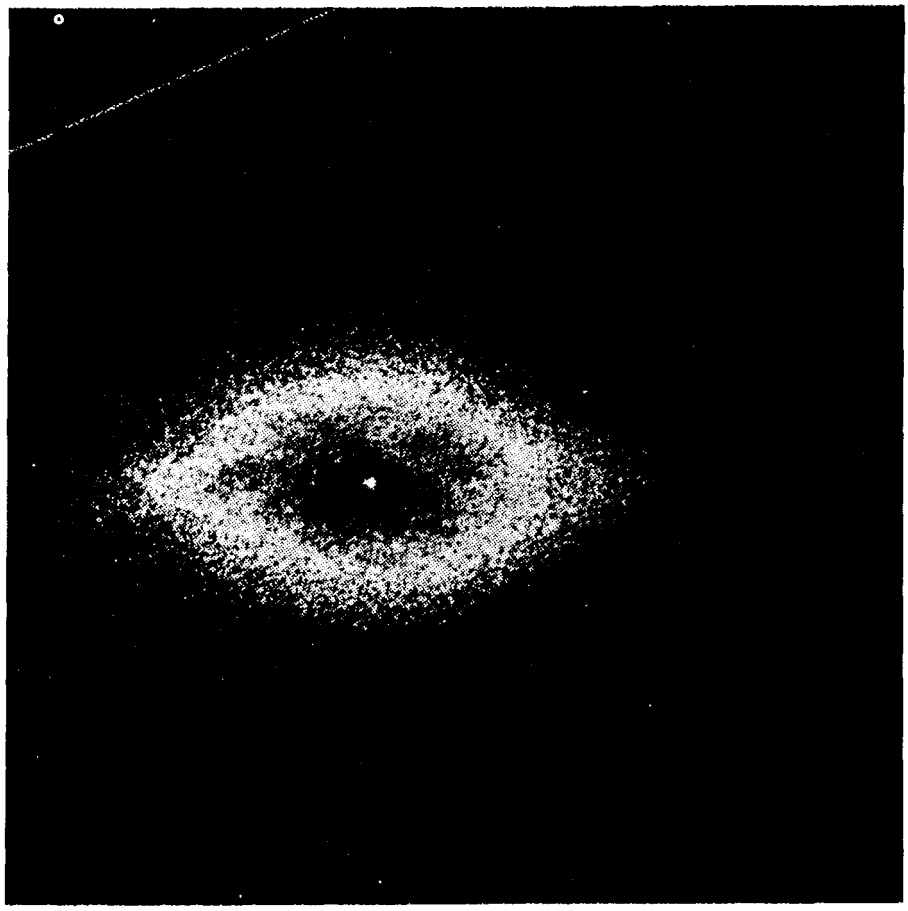

Figure 4: FOC image of the Sombrero galaxy (NGC 4594) with the F342W filter. The presence of a point source in the nucleus is clearly revealed. The light distribution reveals a dust lane in the center, but also shows that the disk extends well into the nuclear region.

indicates the presence of a massive core with a mass of about $10^9 M_\odot$.

4. Summary and Conclusions

One of the strongest conclusions of this work is that the nuclear regions of all the galaxies that we have observed contain large luminosity concentrations in excess of $10^5 L_\odot pc^{-3}$. Conventional wisdom would interpret several of these as indicative of massive black holes

(M32, M87), and this is very likely correct. We note that the central mass concentrations are more or less a fixed fraction of the core mass for all objects. This may provide a clue to the details of the formation of these massive cores.

Although this small survey is by no means complete, we expect that the results presented here will turn out to be quite representative of the core properties of galactic nuclei and bulges. In particular, we recall that, as mentioned above, three qualitatively different core light profiles have been identified: *i)* a featureless ever-increasing profile, *ii)* non-isothermal profiles with a central unresolved source, and *iii)* non-isothermal profiles without a point source.

We note the most of these objects show very small color gradients in the cores. For the objects with points sources in the core, this is rather difficult to confirm, but for the others it seems quite sure.

Several of the objects we have observed are prime candidates for further investigation with the HST after it has been repaired. In particular, the definitive observations to determine whether or not these galaxies harbor black holes will be the measurement of the stellar velocity dispersion as close to the putative black hole as possible. Only HST can provide these data.

If the centers of some of these galaxies do indeed contain massive black holes, it is quite surprising that they do not manifest themselves more definitively!

Acknowledgements

The work presented here has been done in collaboration with the members of the Faint Object Camera Investigative Definition Team: R. Albrecht, C. Barbieri, J.C. Blades, A. Boksenberg, M.J. Disney, J.M. Deharveng, P. Jacobsen, T.R. Kamperman, I.R. King, F.D. Macchetto, C.D. Mackay, F. Paresce, and G. Weigelt. The active support of D. Baxter, P. Greenfield, R. Jedrzejewski, A. Note, and W.B. Sparks is gratefully acknowldeged.

References

1. Light, E.S., Danielson, R.E., and Schwarzschild, M., 1974, Ap.J., **194**, 257.
2. Schweizer. F., 1979, Ap.J., **233**, 23; (erratum: 1980, Ap.J., **236**, 1056).
3. Møller, P., Zeilinger, W., and Stiavelli, M., 1992, MNRAS (submitted).
4. Crane, P., Stiavelli, M., *et al.*, 1992, A.J. (submitted).
5. Boksenberg, A., *et al.*, 1992, Astron. & Astroph. (in press).
6. King, I.R., *et al.*, 1992, Ap.J. (Letters) (submitted).

7. Paresce, F., 1992, *Faint Object Camera Instrument Handbook*, Space Telescope Science Institute.
8. Lauer, T.R., *et al.*, 1991, Ap.J. (Letters), **369**, L41.
9. Young, P.J., *et al.*, 1978, Ap.J., **221**, 721.
10. Kormendy, J., 1985, Ap.J. (Letters), **292**, L9.
11. Nieto J.-L., *et al.*, 1986, Astron. & Astrophys., **165**, 189.
12. Ciardullo, R., Jacoby, G.H., Ford, H.C., and Neill, J.D., 1989, Ap.J., **339**, 53.
13. Gavazzi, G., Perola, G.C., and Jaffe, W., 1981, Astron. & Astrophys., **103**, 32.
14. Elvis, M., Schreier, E.J., Tonry, J., Davis, M., and Huchra, J.P., 1981, Ap.J., **246**, 20.
15. Crane P., Peletier, R., *et al.*, 1992, Ap.J. (Letters), (in preparation).
16. Bender, R., 1990, Astron. & Astrophys., **229**, 441.
17. Londrillo, P., Messina, A., and Stiavelli, M., 1991, MNRAS, **250**, 54.
18. Larson, R.B., 1974, MNRAS, **166**. 585.
19. Kormendy, J., 1988, Ap.J., **335**, 40.

II- PROPERTIES ALONG THE HUBBLE SEQUENCE

4) DARK MATTER

DARK MATTER IN GALAXIES

K.C. Freeman
Mount Stromlo and Siding Spring Observatories
The Australian National University

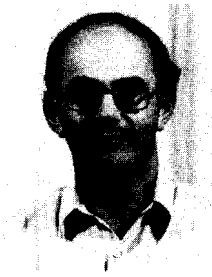

ABSTRACT

We review the observational evidence for dark matter in galaxies. From observations of the kinematics of gas in spiral galaxies and dwarf irregulars, there is not much doubt now that most of these galaxies have dark halos which are at least a few times more massive than their luminous components. Elliptical and dwarf spheroidal galaxies also appear to have massive dark halos, but for these galaxies the evidence is less direct.

1. SPIRAL GALAXIES

1.1. Structure of the dark halos

Spiral galaxies commonly have flat rotation curves, which cannot be produced by a mass distribution that follows the surface brightness distribution. The upper panel of Figure 1 shows the surface brightness distribution for the spiral galaxy NGC 3198 [1]; the lower panel shows the contributions to the rotation curve from the gas and the stellar disk (assuming that the mass to light ratio M/L of the disk is constant with radius). In Figure 1, the adopted M/L ratio for the disk is the maximum allowed by the observed rotation curve. The rotation curve for the disk fits the data well enough in the inner regions (out to about 3 scalelengths as determined from the exponential surface brightness distribution), but beyond 5 kpc the expected rotation curve from this maximum disk plus the gas lies far below the observed rotation curve.

This situation is typical of most spirals with measured rotation curves extending well beyond 3 scalelengths. The usual interpretation is that these galaxies have a massive dark halo which makes up the shortfall in the rotation curve. The flat shape of the rotation curves in the outer regions of spirals suggests that the radial density distribution of this dark halo goes like $\rho(r) \sim r^{-2}$ at large radius. A simple model that is often used has

$$\rho(r) = \rho_\circ/[1 + (r/a)^2] \qquad (1)$$

Figure 1 shows the contribution of such a halo, scaled so that the total expected rotation curve from the disk, gas and dark halo fits the data. This maximum disk model minimises the contribution from the dark halo; models with less massive disks and more massive halos often fit just as well [2]. Even with the maximum disk model, the mass of the dark halo of NGC 3198 is about five times the mass of the luminous disk plus gas within the outermost point on the observed rotation curve.

The simple halo given by equation (1) has two scales: the core radius a and the central density $\rho_\circ$. The estimated values of these two scales from the rotation curve analysis depend on the adopted value for the disk's M/L ratio. The maximum disk models give the largest core radii and the smallest $\rho_\circ$. The typical values of $\rho_\circ$ from maximum disk solutions are in the range $\rho_\circ = 0.001$ to $0.01\ M_\odot$ for giant spirals and 0.01 to $0.1\ M_\odot$ for the smaller spirals and irregulars. The core radii for the large spirals derived from maximum disk solutions are typically 10 to 20 kpc, but could be much smaller if the maximum disk analysis is not the correct procedure [2].

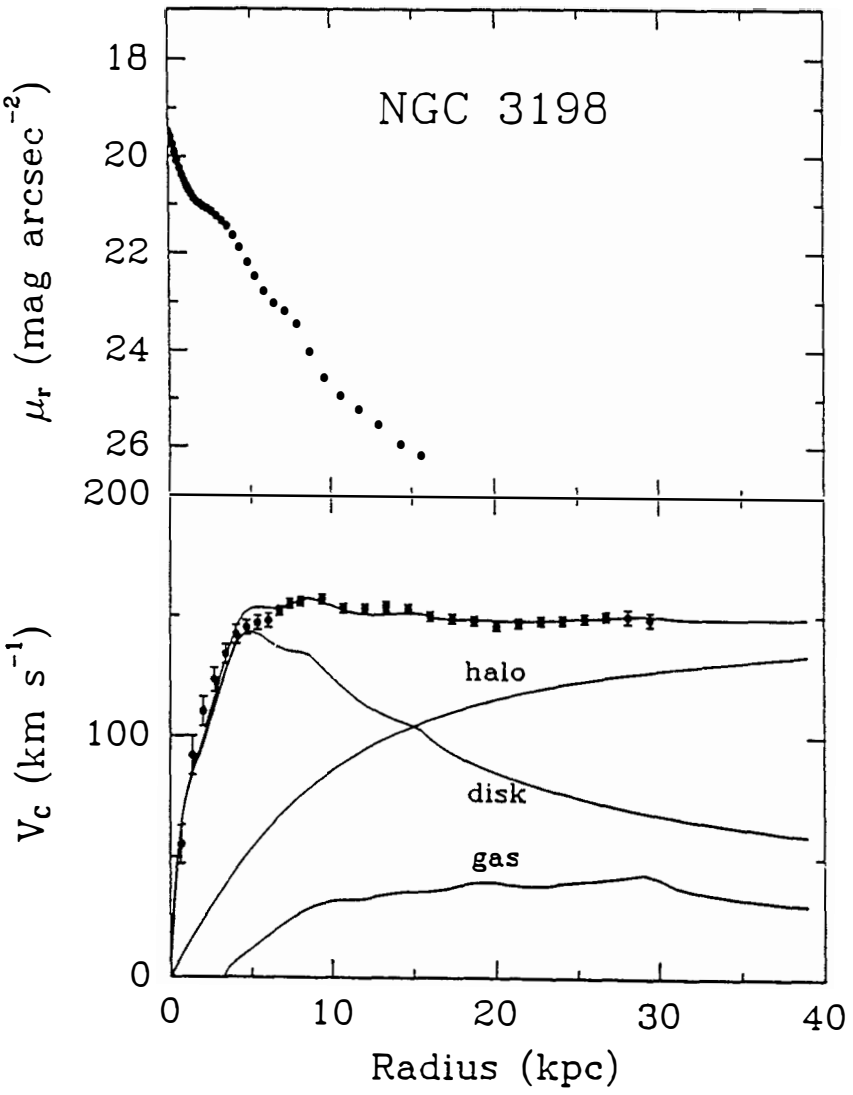

Figure 1:–Upper panel: Surface brightness distribution for NGC 3198 [1]. Lower panel: The filled symbols show the rotation curve for NGC 3198. The labelled curves show the contribution of the gas, disk and halo to the circular velocity. The total circular velocity from these three components is shown as the upper curve.

The core radius, central density and shape of the dark halos are interesting because they relate to simulations of galaxy formation . For example, Warren *et al.* [3] made simulations of a 400 Mpc^3 piece of the universe, using 10^6 particles and various perturbation spectra. In these simulations, the halos grow by dissipationless merging of smaller collapsed structures via dynamical friction and tidal stripping. They find that (i) halos tend to be more prolate than oblate, and (ii) the core radii are typically about 1 kpc for large halos with circular velocities of 250 km s^{-1}. This is much smaller than the halo core radii inferred from maximum disk analysis of rotation curves of large spirals. These results suggest that either the maximum disk solutions are not appropriate or some mechanism is needed to enlarge the cores of large spirals. This core growth may occur naturally as gas settles to a disk during the hierarchial merging: Katz and Gunn [4] showed that the settling gas can transfer more than 50% of its original angular momentum to the dark halo.

The shape of the dark halos are not yet well constrained by observation. The flaring of the gas layer observed in edge-on spirals gives some information about the shape of the potential in the outer parts of these systems. A recent study by Maloney [5] concludes that dark matter distributions as flat as the disk can probably be excluded. In polar ring galaxies, it is possible to estimate the shape of the dark matter distribution from the kinematics of gas and stars in the two perpendicular planes of the stellar disk and the polar ring. Recent results for the system NGC 4650A [6,7] are consistent with a fairly flat (E6) dark halo.

1.2. Maximum Disks

We return now to the question of the maximum disk analysis of rotation curves. This question has been widely discussed (see the review by Sancisi and van Albada [8]), because it is important to know whether this is the right way to proceed. Our knowledge of the structure of dark halos depends on the assumptions about the M/L ratio for the stellar disk. It also affects our view of the dynamics of the inner disk: does the disk dominate the radial potential gradient in the inner two or three scalelengths, or is it dominated even in the inner regions by the dark halo.

Analysis of the rotation curve of our Galaxy does not give a clear answer to the maximum disk question. The rotation curve in the inner regions is not well determined, and the relative contributions to the potential field from the disk and the bulge are difficult to assess. Different studies indicate that the surface density of a maximum disk near the sun would lie somewhere in the range 70 to 130 $M_\odot$ pc^{-2}, depending on the adopted mass of the galactic bulge [9,10]. Recent estimates of

the local surface density, from the kinematics and distribution of stars towards the galactic poles [11,12], are in the range 50 to 80 $M_\odot$ pc^{-2}.

Swing amplifier theory for spiral structure can give some useful limits on the density of the disk, by requiring that the disk should not be so dense as to allow $m = 1$ modes. Athanassoula *et al.* [13] made maximum disk fits to a large sample of rotation curves, with the extra constraint of "no $m = 1$ amplification". They found that their fits (i) are consistent with almost all of their galaxies, (ii) are compatible with the $m > 2$ spirals seen in the outer parts of some of their galaxies, and (iii) give M/L ratios for the disks that are mostly within 20% of the unmodified maximum disk values.

Another useful guide to the M/L ratio of the disk comes from optical rotation curves in the inner few scalelengths of the disk. Some galaxies show wiggles in their optical rotation curves; these wiggles correspond to structure in the surface brightness profiles. If the maximum disk models are correct, then it should be possible to reproduce the wiggles by computing the rotation curve expected from the surface brightness distribution, assuming that the M/L ratio in the disk is constant. Kalnajs [14] was the first to show that this works; his computed rotation curves followed the detailed structure in the observed rotation curves.

Buchhorn and Mathewson [15] have recently analysed optical rotation curves of 552 spirals. The expected rotation curves were computed from their I-band CCD surface photometry, which minimises the effects of internal absorption and regions of young population in the disks. Their galaxies show a wide variety of rotation curve morphology, extending from flat rotation curves to almost solid body rotation. For most of their sample ($> 97\%$), the calculated rotation curves are an excellent fit to the data. Figure 2 shows the good fits for two galaxies with prominent wiggles in their rotation curves. The good fits in these systems are particularly significant for the maximum disk question, because there are two velocity scales (the overall scale of the rotation curve and the scale of the wiggles) to fit with only one parameter (the M/L_I ratio). The success of their fits for this large sample, including some systems with wiggly rotation curves, suggests that either

- the disk dominates the radial potential gradient in the inner few scalelengths of most disk galaxies, or
- the detailed density distribution of the dark halo mimics the surface density structure in the disk (but the fine structure in the halo must be more prominent than in the disk because the gravitational effects of the halo structure are diluted by its probable spheroidal shape).

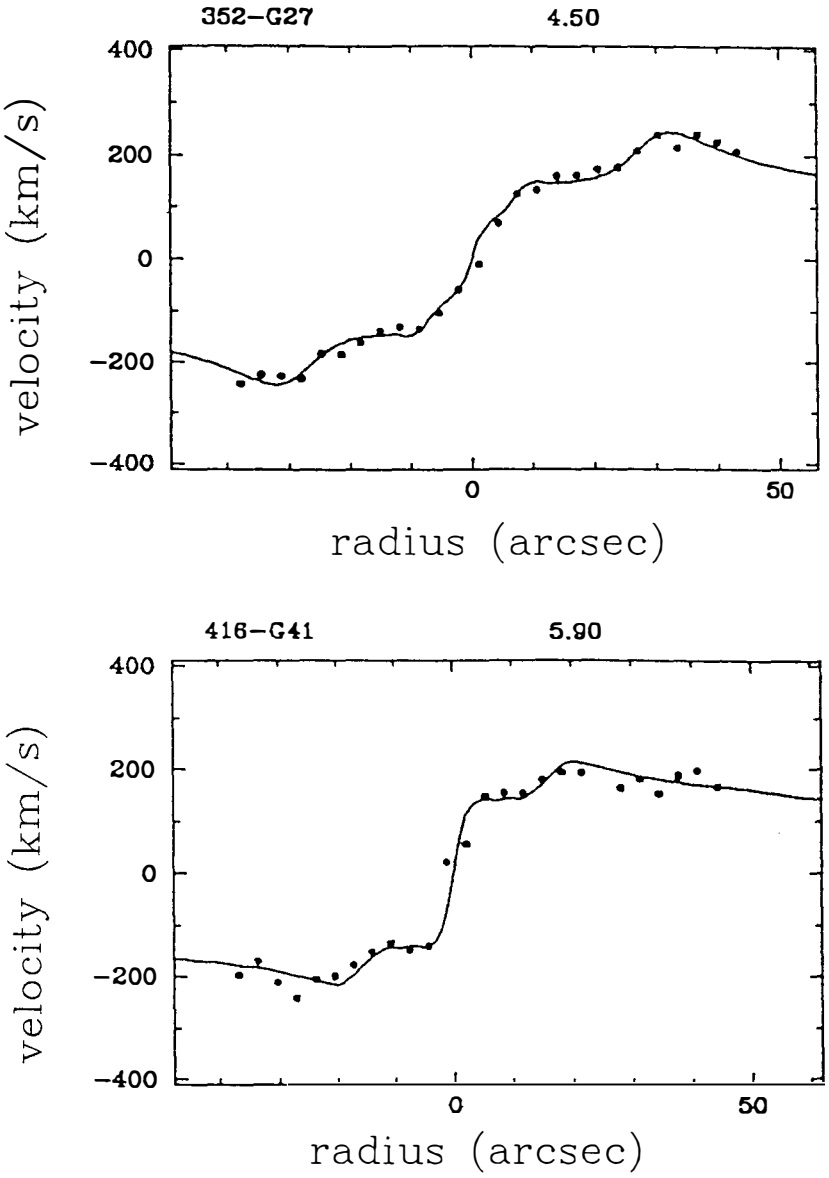

Figure 2:–Two examples of galaxies with wiggly rotation curves from Buchhorn and Mathewson [15]. See text for explanation. Galaxy identification and disk M/L ratio are shown above each panel.

Their sample includes galaxies with rotational velocities from about 40 to 350 km s^{-1}, but they find no trend of the disk's M/L_I ratio with rotational velocity. This indicates that, for most galaxies, the contribution that the halo makes to the inner rotation curve remains small as we go from the largest to the smallest spirals. However, there are a few galaxies (about 3%) for which the calculated rotation curves do not fit the data: usually the observed rotation curves show less shear than the curves expected from the surface photometry. For these few galaxies, it seems likely that the dark halo *is* making a significant contribution to the gravitational field in the inner regions of the disk.

1.3. The Dark Halo of our Galaxy

For our Galaxy, three methods are used to estimate the enclosed mass $M(R)$ within some radius R: (i) the rotation curve, (ii) the random velocities of distant halo stars and satellite galaxies, and (iii) timing arguments. From the inner rotation curve and the adopted structure of the disk and bulge, the total mass of the luminous component (disk and bulge) is at most about $9 \times 10^{10}\ M_\odot$ [9,10].

The rotation curve of the Galaxy is known to be flat out to $R \approx 17$ kpc, and the enclosed mass $M(17\ \text{kpc}) = 2 \times 10^{11}\ M_\odot$ [16]. For the distant halo stars and satellites, the distribution of rv^2 provides a mass estimator [17], where r is the distance of the object and v its radial velocity. From the halo stars, $M(70\ \text{kpc}) = (8 \pm 3) \times 10^{11}\ M_\odot$ [18]. The satellites give $M(150\ \text{kpc}) = (12 \pm 3) \times 10^{11}\ M_\odot$ [19]. The timing arguments use the present separation and relative velocity of M31 and the Galaxy [20] to estimate the total mass of the M31/Galaxy system, assuming that their initial separation was small and adopting some age for the universe. M31 is about 710 kpc from the Galaxy and has a galactocentric radial velocity of −118 km s^{-1}. If the age of the universe is 18 Gyr, then the mass of the Galaxy is $(13 \pm 2) \times 10^{11}\ M_\odot$. A similar argument using the dwarf galaxy Leo I at a distance of about 230 kpc gives $(12 \pm 2) \times 10^{11}\ M_\odot$. These estimates assume radial orbits, so are lower limits.

In summary, the data at large R consistently indicate that the Galactic mass distribution follows

$$M(R) \approx 10^{10} \times R(\text{kpc})\ M_\odot \tag{2}$$

with a total mass of about $10^{12}\ M_\odot$. This is consistent with a flat rotation curve extending out to about 100 kpc from the galactic center. The mass of the dark halo of our Galaxy is then about ten times the mass of the luminous matter.

We should mention here the three microlensing experiments that are in progress now in Chile and Australia. These are aimed at detecting dark matter objects in

the galactic halo. For example, the MACHO experiment (a collaboration between the Lawrence Livermore National Laboratory, the Center for Particle Astrophysics at the University of California, Berkeley, and Mount Stromlo and Siding Spring Observatories) uses a large CCD camera and the dedicated 50-inch telescope at Mt Stromlo to monitor about 10^7 stars in the LMC and SMC (and a similar number in the galactic bulge) for brightness fluctuations due to microlensing by intervening dark matter objects. The experiment is sensitive to dark matter objects in the mass range $2.10^{-8} \lesssim M \lesssim 200\ M_\odot$. At the lower mass limit, the Einstein ring of the lensing object is comparable in diameter to the radius of a distant main sequence star. At the upper limit, the typical timescale of a microlensing event is similar to the likely duration of the experiment.

1.4. Conclusion for Spirals

There seems little doubt now that spirals have extended dark halos with masses of order 3 to 10 times the mass of their luminous components. The rotation curve studies described above support the maximum disk concept in most spirals; for the Milky Way the situation is still unclear. Before leaving the spirals, we should mention three particular problems.

1) The conspiracy: for galaxies with flat rotation curves, the maximum disk solutions mean that the rotation curve contributions from the disk and the dark halo have similar amplitudes, as in Figure 1 for NGC 3198. The reason for this is not yet properly understood. Recently Casertano and van Gorkom [21] and Carignan and Puche [22] studied some disk galaxies for which the rotation curves decline with increasing radius. These are usually fairly compact spirals in which the peak of the rotational velocity contribution from the disk is larger than the maximum rotational velocity for the halo, so in these systems there is no conspiracy. A dark halo is still essential to produce the observed rotation curve in their outer parts.
2) If the maximum disk concept is correct, then the disk dominates the radial potential gradient over the inner two to three scalelengths where the optical rotation curves can be measured. The optical rotation curves typically end (*i.e.* the HII region emission ends) close to the radius at which the disk's contribution to the rotation curve begins to decline and the halo begins to contribute significantly to the radial potential gradient. This observation requires some explanation. We note that, at this radius in most galaxies, the dark halo does not yet dominate

the potential gradient in the radial direction and certainly not in the vertical direction.

3) The dark halo is seen most clearly in galaxies for which the HI distribution extends out to many disk scalelengths. Several authors, most recently Carignan [23] have pointed out that the ratio $\sigma_{HI}/\sigma_{dark}$ of the directly observed surface density of HI to the inferred surface density of the dark halo is roughly constant with radius in these galaxies. Is this an important clue to the nature of dark matter, or is it simply a selection effect ?

2. THE DWARF IRREGULAR GALAXIES

HI synthesis observations of dwarf irregular galaxies give virial mass estimates from the HI profile width, assuming that the HI is in equilibrium. These estimates [24] show that the low luminosity dwarfs ($M_B > -12$) have M/L ratios $\gtrsim 12$ and are likely to have significant dark matter fractions. The brighter dwarfs ($-14.5 < M_B < -12$) have lower M/L ratios, around 3. These lower M/L values tell us little about the dark matter content, because the HI in these systems is often no more extended than the light distribution; the low M/L values just mean that the inner regions of these brighter dwarfs are not dark matter dominated. Two of the well studied dwarf irregulars are particularly interesting.

The first is DDO 154 [25]. This dIrr galaxy has $M_B = -13.8$ and is immersed in an extended HI envelope. Its rotation curve extends out to 15 disk scalelengths and shows that the dark halo dominates the gravitational field at almost all radii; this system is an extreme example of no conspiracy (see §1.4).

The second is GR8 [26]. In this very small system ($M_B = -10.6$), the gas is supported by random motions. Its rotation is small and disorderly (recall that the rotational velocity $\propto$ luminosity$^{1/4}$). However it is still possible to make a fairly straightforward estimate of the enclosed mass $M(R)$. The HI synthesis observations show that the HI velocity dispersion is constant with radius, at about 10 km s^{-1}, and the HI surface density distribution is very close to gaussian: $\mu_{HI} \propto \exp(-R^2/2h^2)$, where h is the scalelength. Assuming that the HI density distribution is spherical, then the volume density distribution of the HI is also gaussian and the equation of hydrostatic equilibrium takes the simple form $GM(R)/R^2 = c^2R/h^2$, where c is the random velocity of the HI. Out to the edge of the observable HI, the gas mass is 2.10^6 $M_\odot$, the stellar mass is 3.10^6 $M_\odot$, the total mass is 4.10^7 $M_\odot$, and the M/L ratio is 15. The hydrostatic equilibrium equation for this gaussian HI distribution with its isothermal turbulent velocity shows that the enclosed mass $M(R) \propto R^3$; *i.e.*

the HI component of GR8 lies in the approximately uniform density core of its dark halo. This is independent evidence for a core in a dark halo. The density in this core is about 0.07 $M_\odot$ pc^{-3}, which is much higher than the typical value for spirals ($\lesssim$ 0.01 $M_\odot$ pc^{-3}) and for DDO 154 (0.016 $M_\odot$ pc^{-3})

3. THE DWARF SPHEROIDAL GALAXIES

These systems have very little gas, very low surface brightness (typically 0.1 of the night sky) and masses of about 10^6 to 10^7 $M_\odot$. For the dwarf spheroidal companions of the Galaxy, the M/L ratios are estimated by using star counts to measure the surface brightness distribution $I(R)$ and radial velocities of individual stars to measure the velocity dispersion $\sigma(R)$. If the mass follows the light, and the system is spherical, isotropic and has a homogeneous core, then the central M/L ratio is given by $M/L = 9\eta\sigma^2_{obs}(0)/2\pi G I(0) R_c$, where $\sigma_{obs}(0)$ is the observed central velocity dispersion, R_c is the half-peak-brightness radius, $I(0)$ is the central surface brightness and $\eta \approx 1$ (see ref. 24). Several of these dwarf spheroidal systems have now been studied. Two of them (Carina and Sculptor) have $M/L \approx 5$ which provides no clear result on their dark matter content. For three others (Fornax, Draco and Ursa Minor) there is strong evidence now that dark matter contributes significantly to the potential gradient in the inner regions.

Fornax [27] has an absolute magnitude $M_V = -12.6$. There is some uncertainty in its $I(R)$ distribution from different sources, and also in its velocity dispersion (depending on whether marginal members are included). The velocity dispersion is in the range 10 to 14 km s^{-1} and the central M/L ratio is between 9 and 15. The central density is 0.07 ± 0.03 $M_\odot$ pc^{-3}.

Draco and Ursa Minor [28] are very small systems, with $M_V \approx -8.5$. Their velocity dispersions are 9 ± 2 and 11 ± 2 km s^{-1} respectively. If their mass follows the light, then their central densities have very high values, about 1.0 $M_\odot$ pc^{-3}, and their M/L ratios are between 60 and 80. These values are lower by about a factor 2 if the dark matter is much more extended than the light.

4. DARK MATTER IN ELLIPTICALS

Elliptical galaxies usually have no HI at large radii (there are some exceptions: see below), so other dynamical tracers are used. These include the integrated starlight, the hot X-ray emitting gas, globular clusters and planetary nebulae, and we give a brief discussion of these different tracers.

4.1. Integrated Light

The radial equilibrium of elliptical galaxies is primarily between gravity and the pressure gradient associated with the velocity dispersion. In most ellipticals, rotation is less important. The momentum equation

$$\frac{\partial \Phi}{\partial R} = \frac{V_\varphi}{R} - \sigma_R^2 \left\{ \frac{\partial \log \rho \sigma_R^2}{\partial R} + \frac{1}{R}(1 - \frac{\sigma_\varphi^2}{\sigma_R^2}) \right\} \tag{3}$$

can be used to estimate the total enclosed mass within radius R from measurements of the line of sight components of the velocity dispersion σ and the mean rotation V_φ. However the observations do not yet reach into the outer regions ($r \gtrsim 2r_e$, where r_e is the half-light radius) where dark matter would dominate the potential. There is also uncertainty about the isotropy of σ, although recent work suggests that the velocity dispersion in the outer parts of giant ellipticals is close to isotropic [29].

4.2. Hot X-ray Gas

The extended X-ray emission from many giant ellipticals indicates the presence of hot gas ($\sim 10^7$ K). Assuming spherical symmetry, the equation of hydrostatic equilibrium

$$\frac{GM(r)}{r} = -\frac{kT(r)}{\mu m_p} \left\{ \frac{d \log \rho}{d \log r} + \frac{d \log T}{d \log r} \right\} \tag{4}$$

gives an estimate of the enclosed mass $M(R)$, where T and ρ are the gas temperature and density. The temperature distributions in the X-ray emitting gas are not yet well determined. Using arguments about convective stability of the hot gas, Fabian *et al.* [30] showed that for 14 E/SO galaxies the M/L ratios within the X-ray emitting region are greater than about 70, compared to typical values of about 5 in the inner regions.

4.3. Centaurus A

Planetary nebulae [31] and globular clusters [32] in Cen A give independent estimates of the enclosed mass M(r) out to about 20 kpc or $4r_e$. The planetary nebulae belong to the diffuse stellar population. The kinematics of a sample of about 500 planetary nebulae show that the velocity dispersion σ decreases with increasing radius and the rotation velocity V_{rot} increases: V_{rot}/σ increases from about 0.25 at $r = r_e$ to about 1.4 at $r = 4r_e$. In contrast, the globular clusters show no systemic rotation, and in this sense are similar to the halo clusters in our Galaxy. In the inner

regions of Cen A ($r < 5$ kpc), the velocity dispersions of planetary nebulae and globular clusters are similar: 141 ± 23 km s^{-1} and 130 ± 20 km s^{-1} respectively.

To estimate the enclosed mass $M(r)$ from the planetary nebulae and globular cluster data, using the momentum equation, some further assumptions are made: (i) isotropy of σ, (ii) spherical potential, and (iii) spherical density distribution $\rho(r)$ derived from the light distribution. These assumptions are obviously a bit rough. However the estimates of $M(r)$ from the globular clusters and the planetary nebulae agree very well, despite the different dynamics of these two populations. The M/L_B ratio increases from 3 at the edge of the dust lane to 15 at a radius of 20 kpc, with $M(20 \text{ kpc}) \approx 3.10^{11}\ M_\odot$.

4.4. Globular Clusters around M87 and NGC 1399

From the kinematics of the globular clusters around the giant elliptical M87, Mould *et al.* [33] showed that the M/L_V ratio in M87 increases from 6.5 at $r = 72''$ to 31 at $r = 8'$. Grillmair *et al.* [34] measured velocities for 57 globular clusters around the giant elliptical NGC 1399 in the Fornax cluster and found again that the M/L ratio increased outwards to at least $M/L = 80$. However, in this case it is not certain whether the M/L value really pertains to the galaxy alone or partly also to the Fornax cluster of galaxies. The dynamical relationship of the globular cluster system around NGC 1399 to the Fornax cluster itself is not clear: the Fornax cluster has a relatively small velocity dispersion and the velocity dispersion of the globular clusters is similar to that of the Fornax cluster itself.

4.5. Ellipticals with Outer HI Rings

The galaxy IC 2006 is a good example of an elliptical with an outer HI ring [35]. This system has an absolute magnitude $M_B = -19.7$. From its stellar velocity dispersion, the central $M/L_B = 5 \pm 1$. From the kinematics of the outer HI ring, the M/L_B ratio within $6.5r_e$ is 16^{+4}_{-2}. Several examples of related objects all show moderate increases of M/L by 2 to 4 times within 1 to 2 Holmberg radii.

4.6. Summary for Ellipticals

All of the tracers which extend out to large enough radii in elliptical galaxies (X-ray emission, planetary nebulae in Cen A, globular clusters around Cen A, M87 and

NGC 1399, and the HI ring data for IC 2006) indicate that the M/L ratio increases from about 5 in the inner regions to values in excess of 15 in the outer regions.

5. CONCLUSION

Dark matter in galaxies is apparently ubiquitous. The ratio of dark to luminous matter out to the most distant tracer is in the range 3 to 10 for the ellipticals and large spirals, and up to about 80 for some dwarf irregulars and dwarf spirals.

REFERENCES

1) Begeman, K.G. 1989. Astron.Astrophys., 223, 47.
2) Van Albada, T.S., Bahcall, J.N., Begeman, K., Sancisi, R. 1985 Astrophys.J., 295, 305.
3) Warren, M., Quinn, P., Salmon, J., Zurek, W. 1992. Astrophys.J., in press.
4) Katz, N., Gunn, J. 1991. Astrophys.J., 377, 365.
5) Maloney, P. 1991. Contribution to Space Telescope Workshop on Dark Matter.
6) Whitmore, B.C., McElroy, D.B., Schweitzer, F. 1987. Astrophys.J., 314, 439.
7) Sackett, P.D., Sparke, L.S. 1990. Astrophys.J., 361, 408.
8) van Albada, T.S., Sancisi, R. 1986. Phil. Trans. R. Soc. Lond. A, 320, 447.
9) van der Kruit, P.C. 1987. in The Galaxy, ed G. Gilmore, R. Carswell, (Dordrecht: Reidel), p 27.
10) Sellwood, J.A., Sanders, R.H. 1988. Mon.Not.R.Astron.Soc., 233, 611.
11) Kuijken, K., Gilmore, G. 1989. Mon.Not.R.Astron.Soc., 239, 605.
12) Bahcall, J.N., Flynn, C., Gould, A. 1992. Astrophys.J., 389, 234.
13) Athanassoula, E., Bosma, A., Papaioannou, S. 1987. Astron.Astrophys., 179, 23.
14) Kalnajs, A. 1983. in Internal Kinematics and Dynamics of Galaxies, ed E. Athanassoula (Dordrecht: Reidel), p 87.
15) Buchhorn, M., Mathewson, D.S. 1992. In preparation.
16) Fich, M., Blitz, L., Stark, A. 1989. Astrophys.J., 342, 272.
17) Little, B., Tremaine, S. 1987. Astrophys.J., 320, 493.
18) Norris, J.E., Hawkins, M. 1991. Astrophys.J., 380, 104.
19) Zaritsky, D., Olszewski, E., Schommer, R., Peterson, R., Aaronson, M. 1989. Astrophys.J., 345, 759.
20) Kahn, F., Woltjer, L. 1959. Astrophys.J., 130, 105.
21) Casertano, S., van Gorkom, J. 1991. Astron.J., 101, 1231.
22) Carignan, C., Puche, D. 1990. Astron.J., 100, 394.

23) Carignan, C. 1991. Contribution to Space Telescope Workshop on Dark Matter.
24) Freeman, K.C. 1986. in Nearly Normal Galaxies, ed S. Faber (New York: Springer), p 317.
25) Carignan, C., Freeman, K.C. 1988. Astrophys.J., 332, L33.
26) Carignan, C., Beaulieu, S., Freeman, K.C. 1990. Astron.J., 99, 178.
27) Mateo, M., Olszewski, E., Welch, D., Fischer, P., Kunkel, W. 1991. Astron.J., 102, 914.
28) Pryor, C., Kormendy, J. 1990. Astron.J., 100, 127.
29) Winsall, M.L., Freeman, K.C. 1992. Astron.Astrophys., in press.
30) Fabian, A.C., Thomas, P.A., Fall, S.M., White, R.E. 1986. Mon.Not.R.Astron.Soc., 221, 1049.
31) Hui, X. *et al.* 1992. In preparation.
32) Harris, H.C., Harris, G.L., Hesser, J.E. 1988. in Globular Cluster Systems in Galaxies, ed J.E. Grindlay and A.G.D. Philip (Dordrecht: Kluwer), p 205.
33) Mould, J.R., Oke, J.B., de Zeeuw, P.T., Nemec, J.M. 1990. Astron.J., 99, 1823.
34) Grillmair, C. *et al.* 1992. In preparation.
35) Schweizer, F., van Gorkom, J., Seitzer, P. 1989. Astrophys.J., 338, 770.

DIRECT DETECTION OF DARK MATTER WITH NaI CRYSTALS

BEIJING - ROMA - SACLAY (BRS) COLLABORATION

C. BACCI [2], P. BELLI [3], R. BERNABEI [3], DAI CHANGJIANG[1], DING LINKAI [1], E. GAILLARD [4], G. GERBIER [4], KUANG HAOHUAI [1], A. INCICCHITTI [2], J. MALLET [4], R. MARCOVALDI [2], L. MOSCA [4], D. PROSPERI [2], C. TAO [*] [1], XIE YIGANG [1]

(*) on leave from LPC Collège de France, Paris

(1) Beijing, China (IHEP); (2) Roma I (La Sapienza); (3) Roma II (Tor Vergata);

(4) CEN-Saclay (DAPNIA / SPP)

Presented by Luigi Mosca

CEN - SACLAY (DAPNIA / SPP) Laboratory

ABSTRACT

As nobody knows the proportion of baryonic / non-baryonic Dark Matter in our Galaxy, both hypotheses are experimentally investigated. After a quick survey of the subject a development presently under way to detect Dark Matter particles with NaI crystals is presented.

This study is performed in parallel in three underground laboratories (Gran Sasso, Fréjus and Mentogou) where the set-ups are efficiently protected from cosmic radiations. Some data are presented on measurements of radioactive contaminants as well as preliminary results from the analysis of low energy event rates. The presently achieved sensitivity to axial coupling WIMP's is comparable to that obtained by Germanium experiments. Systematic investigations are under way to still decrease the radioactive background in all elements of the installation.

I. INTRODUCTION

At large scales in the Universe the Dark Matter ($\Omega \approx 1$) is expected to be essentially of non-baryonic type, while at Galactic scale ($\Omega \approx 0.1$) nobody at present knows the fraction of baryonic / non-baryonic type of Dark Matter. The situation in this respect can be shematically summarized as follows :

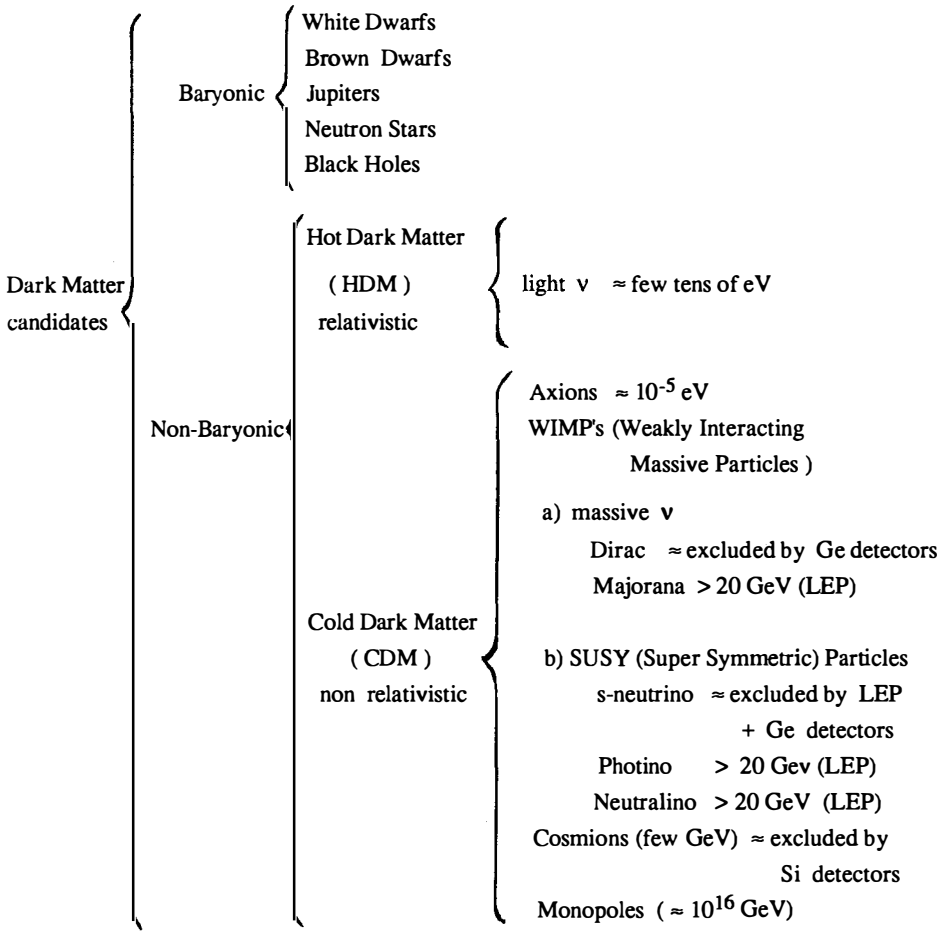

This is the reason why both types of Dark Matter are experimentally investigated : the baryonic hypothesis by looking at the stars of the Large Magellanic Cloud whose luminosity should be modulated (microlensing) by the dark objects possibly forming the halo of our Galaxy, and the WIMPs particles by detecting the nuclear recoils produced by their elastic scattering on ordinary matter.

The first approach is realized by two "MACHO" (Massive Compact Halo Objects) detection experiments presently under way : one is performed by a french collaboration which is collecting data (photographic emulsions and CCD plates) at the ESO observatory of La Silla (CHILI) and another similar experiment performed by a Berkeley, Livermore and Mount Stromlo collaboration which is preparing exposures at the Mount Stromlo observatory (AUSTRALIA) : see K. Freeman's introductory talk at this Conference.

The content of the short presentation of the french MACHO experiment that I made at the beginning of my talk can be found in Ref. 1. The test period of this experiment is completed, most of the data are obtained, measurements and analysis are starting and the first significant results should be available by the end of this year.

Concerning the WIMPs investigation, essentially three types of detectors are under development to measure the recoil energy of scattered nuclei : their advantages and drawbacks are tentatively summarized in the following Table :

DETECTOR	ADVANTAGES	DRAWBACKS
SEMICONDUCTORS	- radioactively "clean " crystals (Ge, Si, ...) - high resolution ($\sigma / E \approx 10^{-3}$ at 1 MeV)	- small masses (expensive!) - only one measured quantity (ionization) - microphony problems in the low energy region
CRYSTAL- -SCINTILLATORS	- easy to reach large masses - PSD possible - easy to handle - no microphony problems - low cost / mass rate	- problem of cleaning the crystal (e.g. ^{40}K contamin.) - only fair resolution - only one measured quantity (scintillation)
BOLOMETERS	- possibility of measuring simultaneously 2 quantities (e. g. heat and ionisation) - high resolution ($\sigma / E < 10^{-2}$) - low energy threshold ($\approx$ 1 keV)	- very sophisticated technology - expensive - microphony problems

The WIMPs-nucleus interaction can occur either via coherent or via axial coupling. Only nuclei with non zero spin, essentially odd-even nuclei, allow the detection of spin-dependent interacting candidates. The coherently coupled WIMPs can give rates as large as ≈ 100 events / day /kg.[2] The axial coupling gives generally much lower rates, down to few events / day / 100 kg. [2]

The existing results on Dark Matter have been obtained with semiconductor detectors : Silicon with 1.2 keV of energy threshold and Germanium with 3 keV energy threshold.[3,4] The lowest published event rate is obtained by the Germanium experiments and is ≈ 3 events / kg / keV / day at threshold energy.[4] Due to the fact that the naturally most abundant isotopes of Germanium and Silicon are even-even nuclei, the results obtained so far by these semiconductor detectors mainly concern the spin independent (coherent) coupling candidates : exclusion of massive Dirac neutrinos and cosmions (solar neutrino solving WIMPs).[3,4]

So far no axially coupled candidates have been completely excluded.

II. THE NaI EXPERIMENT

The NaI (Tl) is an interesting material for Dark Matter detection for several reasons : a) the ^{23}Na has spin 3/2 and the ^{127}I has spin 5/2, so they are sensitive to axial coupling interactions b) the threshold can be as low as a few keV because of the high light output (3 to 4 photoelectrons /KeV) c) it is easy to handle (no cooling needed) d) the ratio: cost/mass is interestingly low and e) an analysis of the pulse shapes allows to discriminate α-particles from β and γs in the few MeV energy region. A partial discrimination between a nucleus recoil and an electron or gammma interaction in the few tens of keV region is also possible (to be better studied and optimized).[5]

The crucial signature for a Dark Matter signal is the annual modulation of the counting rate due to the earth revolution around the sun : about 10% difference is expected between the extreme values in June and December. To detect this modulation effect large statistics are needed. The required mass of the detector is inversely proportional to the expected rate R, namely (if the signal is much larger than the background) : $M \approx 50$ kg / R (in events / kg / day) for a 5 σ evidence with one year of data taking. This large amount is certainly out of reach for other types of detectors (semiconductors, gaseous detectors, and bolometers) in the near future, while it could be realistic for NaI detectors.

III. STATUS OF THE EXPERIMENTAL STUDY

First of all our setups have been installed in underground laboratories (Gran Sasso, Fréjus and Mentogou) to protect them as much as possible from cosmic ray radiation. Then, as for any other approach of non baryonic Dark Matter detection, the main challenge is to fight against the

radioactive background both external and internal to the detector. The external background i mainly reduced by appropriate shieldings (≈ 15 cm of Pb plus, inside it, ≈ 5 cm of Cu), by a selection of low activity PMTs and by N_2 flushing in a pressurized container for Radon removal. The internal background is essentially reduced by an accurate selection of low activity NaI (and TlI) powders, especially concerning the ^{238}U and ^{232}Th chains and ^{40}K impurities. Of course all other components of the setup : reflector, housing and quartz windows of the NaI crystal, light guides, glues, screws, and so on must also be selected with coherent criteria.

Two methods are used to measure the internal background :

a) the use of a transient digitizer allows a Pulse Shape Discrimination (PSD)(*) between α-particle signals and $\beta + \gamma$ contributions to the energy spectrum and by this way to identify the internal radioactive contamination of the NaI(Tl) cristal coming from Uranium and Thorium chains. This is illustrated in Fig. 1 (Fréjus data obtained with a Bicron crystal of 10.7 kg) where a scatter plot of the average decay time $< t >$ versus the electron-equivalent energy shows the α events clearly separated from the $\beta + \gamma$ events. (**) From this plot we can deduce, with reasonable assumptions, that the ^{238}U / ^{232}Th contamination in this NaI crystal represents ≈ 0.1 ppb .

b) the use of a skewed light guide allows to shield the NaI crystal from the radioactive elements of the associated PMT and to isolate the signal coming from the ^{40}K internal to the crystal itself. The result in this case (Bicron crystal of 10.7 kg) is a value of ≈ 1 ppm of natural Potassium (^{39}K) contamination in the crystal. (If improved from the point of view of the light transmission, the skewed light guide solution would allow also to obtain a better low energy spectrum).

IV. PRELIMINARY RESULTS

The best data obtained up to now at low energies (Fig.2) is the result of a 60 days run with a QUARTZ & SILICE / HARSHAW NaI(Tl) crystal of 760 g in the Gran Sasso Laboratory (LNGS).

From the data on Fig.2 we derive the cross section versus WIMP's mass contour limit at 90% CL ("exclusion plot" on Fig.3). This is obtained by comparing the experimental data to a

---

(*) this facility allows two other types of rejection : *i*) against spurious PMT's electronic noise and *ii*) against electron pulses, from $\gamma+\beta$ background, in the low energy region of interest (≈ 4 to 20 keV) in a statistical way.

(**) the validity of this method has been checked by directly detecting the α particles (of ≈ 5.5 MeV) from an ^{241}Am source implemented in a small size NaI crystal, at the same time as the γs from a ^{137}Cs (662 keV) and ^{60}Co (1.17 and 1.3 MeV) sources.

simulated WIMPs spectrum under the following assumptions : *i*) a local galactic halo density equal to 0.4 GeV/cm^3, *ii*) an orbital solar system velocity of ≈ 220 km/sec, *iii*) a WIMPs maxwellian velocity distribution with a V_{rms} = 270 km/sec and an escape cutoff velocity of 600 km/sec, *iv*) as the data have been taken during May and June, the annual modulation coefficient is equal to ≈ 0.92, *v*) for the quenching factor(*) of ^{23}Na recoils we take the measured value of 0.25 [5] while for the quenching factor of ^{127}I recoils we take the calculated value of 0.07 [6]. We have chosen, as "reference target" for the curves presented in Fig.3 the ^{23}Na nucleus. Thus the ^{127}I component of the NaI cross section has been scaled by appropriate kinematical and dynamical factors. [7] The corresponding limit obtained from the best published Germanium data[4] is shown for comparison. To allow this comparison to be meaningful the ^{73}Ge cross section has been treated in a way similar to that previously applied to the ^{127}I. (Note also that only the ^{73}Ge component (7.7 %) of natural Germanium is sensitive to the axial coupling). We stress that this comparison is necessarily model dependent : especially on the type of coupling axial or coherent.

The prediction for the photino cross section, as a function of the neutralino mass, lies about four order of magnitudes below the sensitivity of present day experiments. If the neutralino is the Lightest Susy Particle (LSP) and has a significant coherent coupling component (Higgs mainly exchanged) the corresponding cross section could be about two orders of magnitude higher.

V. CONCLUSION

We presented some preliminary results already comparable in sensitivity for axial coupling to the best published ^{73}Ge data. We have the possibility of performing a good Dark Matter particles detection experiment, complementary to the other approaches under way (semiconductor and bolometers), provided the background level both outside and inside the detector is still significantly decreased. In fact a decrease of one order of magnitude with respect to the presently available data seems within reach : in that case a set up consisting of about ten NaI modules with a mass of 5 to 10 kg each could be installed in the Gran Sasso Laboratory. Each module would be coupled via appropriate light guides to a pair of PMTs in coincidence to minimize the PMT noise and to optimize the light collection. If some kind of WIMPs with a cross section significantly larger than that of photino (for example: neutralino with a coherent coupling component) does exist , a detector of reasonable mass could allow the detection of these WIMP's annual modulation flux. A letter containing most of the results presented here is in preparation.

Finally, let us desperately search for Dark Matter !

(*) scintillation efficiency relative to that of electrons of the same kinetic energy.

REFERENCES :

1) "Search for MACHO's in the Halo of our Galaxy : Status Report (French Collaboration)" Talk given by M. Spiro at the TAUP 91 Conference at Toledo, Spain, 9 - 13 September 1991 and Saclay preprint : DPhPE 91-18, December 1991, by L. Moscoso and M. Spiro.

2) see for example:
   a) M.W. Goodman and E. Witten, Phys. Rev. D31 (1985), 3059.
   b) W.H. Press and D.N. Spergel, Ap. J. 296 (1985), 679.
   c) R.L. Gilliland et al., Ap. J. 306 (1986),703.
   d) P.F. Smith and J.D. Lewin : " Dark matter detection", Physics Report Vol 185 N°5 March 1990.
   e) John Ellis : " Experimental constraints on dark matter ", Nobel Symposium on Early Cosmology , Graftavallen, Sweden , June 1990. Preprint CERN-TH 5822/90.
   f) M.Spiro : " Detection of dark matter ", 25th Int. Conf. on High Energy Physics, Singapore, August 1990. Saclay preprint 90-10.

3) D.O. Caldwell et al.Phys. Rev. Lett. 65 (1990) 1305.

4) D.O. Caldwell et al.Phys. Rev. Lett. 61 (1988) 510 and D.Reusser et al. Phys. Lett. B 255 (1991) 143.

5) a) G.Gerbier : " WIMPs search : the Saclay program." XXVth Rencontre de Moriond (Jan 1990) on New and Exotic Phenomena (page 469 of the proceedings) and
   b) P. Belli : " Scintillators for Dark matter detection." XXVIth Rencontre de Moriond (Jan 1991) on Tests of Fundamental Laws in Physics. Editions Frontières.

6) H. Eijiri, priv. comm. 1991.

7) a) J. Ellis and R.A. Flores, Nucl. Phys. B307 (1988) 883.
   b) J. Ellis and R.A. Flores, Phys. Lett. B263 (1991) 259.

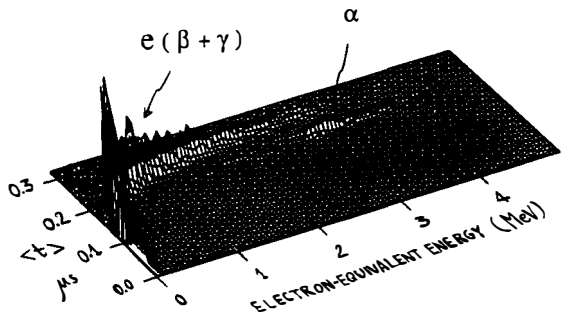

Fig. 1 Average decay time of NaI pulses as a function of their electron-equivalent energy. (Fréjus data obtained with a Bicron crystal of = 10.7 kg).

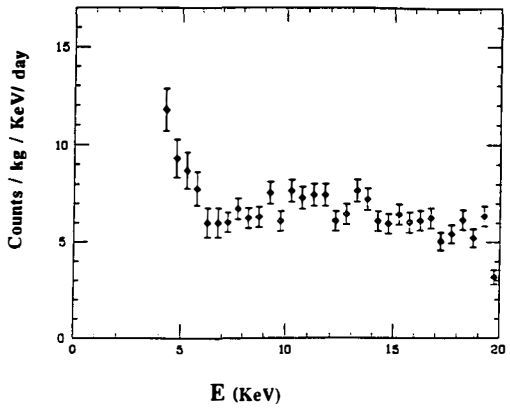

Fig. 2 Low energy spectrum obtained with a Quartz & Silice /Harshaw crystal of 760 g at the Gran Sasso National Laboratory after pulse shape analysis (live time of 46.1 kg x day).

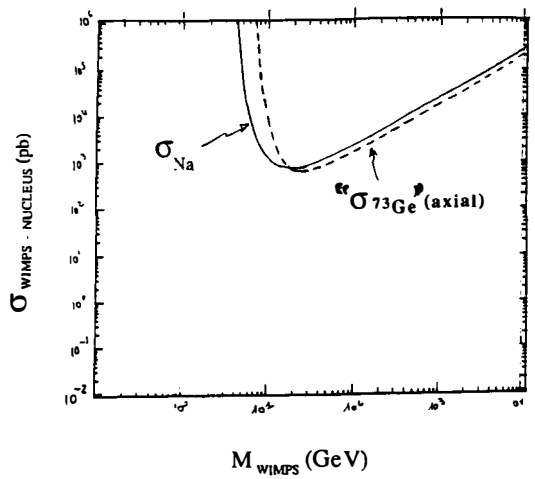

Fig. 3 "Exclusion plot" obtained from the data of Fig. 2. The Na curve represents the cross section versus WIMPs mass contour limit at 90% CL. The ^{73}Ge curve, also a limit at 90% CL, is obtained from the best published data[4] in the axial coupling hypothesis (assuming the ^{23}Na as a "reference target") and is shown for comparison. The procedure adopted for the relative normalisation of the cross sections on different nuclei, is mentioned in the text (section IV).

III - EXTENSION OF THE HUBBLE SEQUENCE

NATURE VS. NURTURE IN DWARF AND LOW-SURFACE-BRIGHTNESS GALAXIES

Trinh X. Thuan
Astronomy Department, University of Virginia
P. O. Box 3818, University Station
Charlottesville, VA 22903

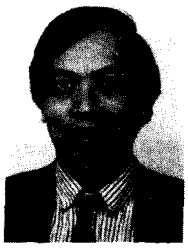

ABSTRACT

A review is given for the physical properties of the different dwarf types: early-type dwarfs, late-type dwarfs and blue compact dwarfs. Environmental effects and possible evolutionary connections between these types are discussed. The properties of non-dwarf low-surface-brightness galaxies and the question of their space density are also reviewed.

1. INTRODUCTION

It is now commonly accepted that galaxian properties are the combined results of genetic processes occurring at birth, and environmental processes which modify them subsequently. While the role of nature versus nurture has been mainly focussed on bright normal galaxies, environmental influences have also been discussed for dwarf galaxies. These studies have, in large part, been stimulated by the availability of extensive dwarf catalogues such as those by Reaves (1983) and especially by Sandage and his collaborators in their massive study of dwarf galaxies in the Virgo cluster (e.g. Binggeli, Sandage, and Tamman 1985). Three main types of dwarf galaxies have been recognized: early-type dwarfs, late-type dwarfs, and blue compact dwarfs. We review the dwarf types in Section 2. We discuss environmental effects and possible evolutionary connections between these types in Section 3. Both early and late-type dwarfs show a correlation of surface brightness with luminosity: low-luminosity dwarfs have a low-surface-brightness. This last property, when used to pick out dwarf systems in photographic surveys, has also uncovered a population of low-surface-brightness (LSB) galaxies which are so luminous and distant that they cannot be dwarfs. Section 4 discusses the properties of these LSB galaxies and addresses the question of their space density. Are we only seeing the tip of the iceberg and are we missing with conventional photographic techniques whole populations of dwarf and LSB galaxies?

2. DWARF TYPES

A thorough discussion of dwarf classification illustrated by an atlas of dwarfs in the Virgo cluster is given by Sandage and Binggeli (1984).

2.1 Early-type dwarfs

We first discuss the dwarf ellipticals (dEs). These are characterized by a low surface brightness along with a smooth intensity

distribution, with or without a central star-like nucleus. Binggeli and Cameron (1991) found, in an extensive surface photometry study of 200 faint early-type Virgo dwarfs, the following results: 1) dE profiles, in the outer parts, can be fitted equally well by an exponential law, characteristic of a disk structure, or by a tidally truncated King model, characteristic of a spheroidal structure. Surface brightness and size decrease systematically as luminosity decreases. 2) In the inner parts, ($r \lesssim 3$ kpc) and only for dEs brighter than $M_{B_T} \sim -16$, there is usually an extended excess luminosity above the fit. This excess luminosity is not due to a star-like nucleus nor a bulge, and increases with increasing galaxy luminosity. The magnitude $M_{B_T} \sim -16$ appears also to signal a discontinuity in the exponential fit properties. For galaxies with $M_{B_T} < -16$, the exponential scale length decreases with decreasing luminosity while the central surface brightness is nearly constant, while for faint dwarfs with $M_{B_T} > -16$, it is the scale length which is nearly constant while the central surface brightness is decreasing. 3) For $0.1 \lesssim r \lesssim 1$ kpc, there is a strong dichotomy between normal ellipticals (Es) and dEs: in the central surface brightness-total magnitude diagram, the dEs form a linear sequence of decreasing surface brightness with decreasing luminosity, while normal Es form an orthogonal sequence of increasing surface brightness with decreasing luminosity, with the two sequences being separated by ~4 mag arcsec^{-2} in surface brightness, and no intermediate types between E and dE (cf. also Kormendy 1987).

Sandage and Binggeli (1984) introduced the new class of dwarf SO (dSO), with a strong warning: 'if indeed it exists'. Whether dSOs are truly physically distinct from dEs is still not year clear. Galaxies classified as dSO do appear to show unusual King parameters, a high flattening, the presence of a lens, a bar-like asymmetry or a central

irregularity, which may suggest a disk structure, although the azimuthally averaged surface brightness profiles of dSOs are indistinguishable from bright dE profiles.

Kinematic studies hold the promise of distinguishing between bright dEs and dSOs. Bender (quoted in Binggeli and Cameron 1991) obtained kinematic data for one dSO (NGC 4431) and two dEs in the Virgo cluster. Only the dSO shows rotation, suggesting the presence of a disk, while the bright dEs show an anisotropic velocity distribution and are not supported by rotation (Bender and Nieto 1990). It would also be interesting to know whether dSOs contain neutral hydrogen, in contrast to most dEs which contain none (Hoffman et al. 1987).

Estimates of the masses of very faint nearby dEs (also known as dwarf spheroidals) from internal stellar velocity dispersions show no compelling evidence for dark matter for systems with $M_V \lesssim -9$. Fainter systems, such as Ursa Minor and Draco, both with $M_V \sim -8.5$, have M/L_V respectively of 60 and 80, and do appear to contain a large amount of dark matter (Aaronson 1987, Kormendy 1987, Freeman 1987).

In a study of Virgo dEs, Thuan (1985) found that the near-infrared colors of dEs are intermediate between that of bright E and SO galaxies and galactic globular clusters. If the (J-K) color is used as a metallicity indicator, then Virgo dEs have $Z_\odot/3 \lesssim Z \lesssim Z_\odot$. Optical-infrared colors combined with galactic evolution models imply that the last burst of star formation in the Virgo dEs occurred less than $\sim 8 \times 10^9$ ago. Vigroux et al. (1984) found a Virgo dE where there is ongoing star formation, like in NGC 205, one of the dE companion of M31.

2.2 Late-type dwarfs

Hubble lumped together all late-type dwarfs in the class of 'irregular' galaxies, although Holmberg (1958) later recognized the

irregular class to contain both bona-fide late-type dwarf systems (IrrI) and amorphous non-dwarf systems such as M82 (IrrII). To take into account the very late systems, de Vaucouleurs (1959) subdivided the Hubble Sc class into Sc and Sd and added the Sd, Sdm and Im classes. The luminosity class V was introduced by van den Bergh (1960) to include low-surface-brightness dwarf systems with little or no central concentration of light on red images. We shall designate here all late-type dwarf systems under the generic name of dwarf irregulars (dIs). The disk structure is less evident in dIs than in spirals. On average, dIs are fat rather than flat objects. Thuan and Seitzer (1979b) found that a flat intrinsic distribution of axial ratios from 0.25 to 1, with a mean axial ratio of 0.63, fits best their data. Binney and de Vaucouleurs (1981) and Staveley-Smith et al. (1992) found similar results. The dIs contain large amounts of HI, of the order of $\sim 10^8 M_\odot$ (Thuan and Seitzer 1979a,b; Schneider et al. 1990, 1992). Their single-dish 21cm profiles are often single-peaked in contrast to the steep-sided double horn profiles observed for spiral galaxies. Their mean velocity width at 20% of peak intensity Δv_{20} can be as low as 40 km s^{-1} for the lowest luminosity systems. These have low rotational velocities and important random gas motions. An example of such an extreme dwarf is M81 dwA with $M_B = -11.0$ and a rotation curve which rises only to 7 km s^{-1} in the first 300 pc and then drops to $\sim$ 1 km s^{-1} at the outer edge. The rotation, in this case, is smaller than the velocity dispersion of 7 km s^{-1} (Westpfahl and Puche 1992). Optically, dIs are characterized by a smooth low-surface-brightness component on which are superimposed blue clumps of star formation. There is one known exception. The dI LGS3 (Thuan and Martin 1979) is resolved not in blue but red stars: it has no blue supergiants and apparently no star formation has occurred more recently than 10^8 years

ago (Christian and Tully 1983).

The ratio of neutral hydrogen mass to luminosity appears to increase towards lower luminosity systems: M_H/L_B is ~0.6 for a dI with $M_B \sim -16$ and increases to ~1.6 for a system with $M_B \sim -12.5$. Staveley-Smith et al. (1992) find $M_H/L_B \propto L_B^{-0.3}$.

For the brighter dIs ($-16 \lesssim M_B \lesssim -14.5$), there is rotation curve data which extend far enough (beyond 3 disk scale lengths) to show, in some systems, evidence for dark matter. DIs in the magnitude range $-14.5 \lesssim M_B \lesssim -12$ do not possess HI data extending much beyond their optical size, so that their generally low M/L_B (2 to 10) do not rule out a substantial amount of dark matter beyond the optical galaxy. Systems fainter than -12 do appear to show high M/L_B (10 to 30), but these M/L_B may be overestimated if the HI gas in these low-luminosity systems possess substantial non-virial motions induced by galactic winds (Meurer et al. 1992) or supernova-driven expansion (Westpfahl and Puche 1992). For example, the double-peaked spectra in the HI shells of M81 dwA can be interpreted as produced by supernova-driven expansion motions. These motions thicken the galaxy, accounting perhaps for the dI axial ratio distribution discussed before. Expanding models require very little dark matter. For M81 dwA, at most 50% of the mass is dark (Westpfahl and Puche 1992). Using the (J-K) color as a metallicity indicator, dIs have a metallicity range between 1/30 and 1/3 that of the Sun (Thuan 1985).

Finally, we note that dIs do not exhibit spiral structure. There are no dwarf spirals: galaxies with masses less than $\sim 5 \times 10^9$ $M_\odot$ apparently cannot sustain a density wave (Sandage and Binggeli 1984).

2.3 Blue compact dwarfs

I have recently reviewed the observations and models of blue compact dwarf (BCD) galaxies (Thuan 1991), so I shall only discuss here

BCD properties which are relevant to the nature vs. nurture question. The colors and gas content of BCDs imply that they are undergoing intense bursts of massive star formation lasting less than ~10^7 years, with a time interval between bursts of several billion years. In the optical, the large majority of BCDs show a smooth underlying low-surface-brightness stellar component on which are superposed compact high-surface-brightness star-forming regions (Loose and Thuan 1985). The most common (~70%) BCD type shows a complex structure with several centers of star formation and irregular isophotes in the central regions (the iE type in the morphological classification of Loose and Thuan 1985). These isophotes become increasingly more regular (elliptical or circular) further away from the star-forming regions. The next most common BCD type is the nE type with a distinct nucleus and regular isophotes in the central region. Surface photometry of a few BCDs (Loose and Thuan 1986, Kunth et al. 1988) reveals that the light profile of the low-surface-brightness underlying component is similar to those of dEs. The colors become redder as radius increases, reflecting a change towards older stellar populations. The amount of neutral hydrogen in BCDs is ~$10^8 M_\odot$, the same as in dIs (Thuan and Martin 1981). The HI velocity widths of the two dwarf types are also similar (Δv_{20} ~ 100 km s^{-1}). HI interferometric maps yield M/L_B = 2 for the BCD IZw36 (M_B = - 13.9) (Viallefond and Thuan, 1983), and M/L_B = 4 for the BCD IZw18 (M_B = - 14.3) (Lequeux and Viallefond 1980). These low ratios do not suggest a substantial amount of dark matter in BCDs.

Finally, BCDs span the same range of near-infrared colors as dIs, implying similar old stellar populations (Thuan 1985). Their metallicity ranges from $Z_\odot/30$ to $Z_\odot/3$, with a peak of the distribution at ~$Z_\odot/10$ (Kunth and Sargent 1986).

3. EVOLUTIONARY CONNECTIONS

We now use the above observational results to discuss possible evolutionary scenarios which may link dEs, dIs and BCDs.

3.1 dEs and dIs

It has long been thought that gas-rich dIs (or BCDs) can become gas-poor dEs by expelling their gas (e.g. Faber and Lin 1983). Several mechanisms have been proposed for the gas removal:

3.1.1 Supernova-driven expansion

The gas is driven out of the dI by supernova explosions which create large expanding cavities surrounded by dense HI shells. Evidence for such a scenario comes from HI interferometric maps. The dI Holmberg II shows a large number of HI shells and bubbles (Puche et al. 1992) while the low luminosity dI M81 dwA has already most of its gas pushed beyond the optical limits of the galaxy: it exhibits a single large HI shell whose inner radius coincides with the optical radius of the galaxy, and has little or no gas left in the center (Westpfahl and Puche 1992). Other observational support for this scenario comes from Hα pictures of HoII which show the presence of HII regions on the borders of the largest bubbles, and Fabry-Perot Hα interferometric observations of a few BCDs which show Hα loops and filaments in the vicinity of the most prominent HII region (Thuan et al. 1987). An interesting consequence of this scenario is the possible existence of HI shells around dEs (Puche and Westpfahl 1992).

3.1.2 Galactic winds

This mechanism is a variant of the first one and is also driven by supernovae. But instead of a shell structure, the observations show a bipolar flow morphology. The best-studied example is NGC 1705, a nucleated BCD, by Meurer et al. (1992). In Hα, this galaxy shows a bipolar flow roughly aligned with the continuum minor axis. A comparison

of the Hα and HI velocity profiles suggests that the neutral gas is pulled along in this flow, some of it escaping from the galaxy's gravitational potential. Depending on the amount of mass loss, this can lead to a complete destruction of the galaxy, an evolution into a nucleated dE, or retention of some gas for future star formation. The case of NGC 1705 is not unique: one of the most metal-deficient BCD known, IZw18 ($Z \sim Z_{\odot}/30$), also shows a bipolar Hα morphology (Dufour and Hester 1990).

3.1.3 Ram-pressure stripping

In this scenario, the dI galaxy plows through a hot X-ray emitting gas which exerts ram-pressure to remove the neutral gas from the galaxy. One of the best places to study ram-pressure stripping is in the Virgo cluster known to contain a large amount of X-ray emitting gas in its central regions, and where there is strong observational evidence that such a gas-removal process is at work for bright galaxies. Several cases of ram-pressure stripping of dIs have been found in the Virgo cluster. One such example is IC 3475, a dwarf galaxy near the core of the Virgo cluster, which belongs to the class of huge (the diameter is ~10 Kpc), very low surface brightness dIs discussed by Sandage and Binggeli (1984). Vigroux et al. (1986) found that IC 3475, which contains intermediate-age ($1\text{-}7 \times 10^9$ yr) star clusters, is completely devoid of gas. The very large size of the galaxy (~ 1.8 times larger than a normal dI) appears to rule out evolution of IC 3475 to a dE. Another example is UGC 7636, located in the X-ray halo of the brightest elliptical galaxy in the Virgo, NGC 4472. Sancisi et al. (1987) found HI gas between UGC 7636 and NGC 4472, but none in the dI. Patterson and Thuan (1992a) showed that not only has UGC 7636 lost its gas through ram-pressure stripping by the hot X-ray gas, it has also been tidally perturbed by NGC 4472, as evidenced by the presence of a

red optical tidal tail and counter-tail in the dwarf, with the same colors as the stars in the dwarf's outer regions, as well as a disturbed morphology in the dwarf's inner parts.

3.1.4 Mixed evidence

Admitting that gas can be removed from dIs by the above mechanisms, are the observational properties of stripped dIs consistent with those of dEs? The following evidence does argue for an evolutionary connection: 1) dIs and dEs have similar surface brightness profiles (e.g. Faber and Lin 1983, Binggeli and Cameron 1991); 2) both dwarf types show the same decrease of surface brightness with decreasing luminosity (Binggeli 1985); 3) a morphology-density relation holds for dwarfs just as for bright galaxies (Binggeli et al. 1990). The frequency of dEs in the Virgo cluster increases drastically with increasing local density, over a factor of 1000 in spatial density, while the frequency of dIs is decreasing concurrently, suggesting a mutation of dIs into dEs. 4) If fading is taken into account, the photometric properties of faint dEs ($M_B > -15$) are consistent with those of stripped dIs (Binggeli 1985).

But there exists also counter-evidence for an evolutionary link between dIs and dEs: 1) Most dIs (in the Virgo cluster) have significantly larger isophotal diameters at a given average surface brightness than dEs. Moreover the central surface brightness of dIs is already 0.3 mag fainter than in dEs. Thus dIs are too big and too faint to be the progenitors of dEs. On the other hand, faded BCDs can produce objects with photometric properties and shapes similar to dEs (Bothun et al. 1986). 2) The metallicity distributions of Virgo dEs and dIs, using near-infrared colors as a metallicity indicator, are substantially different: dEs are much more metal-rich ($Z_\odot/3 \lesssim Z \lesssim Z_\odot$) than dIs ($Z_\odot/30 \lesssim Z \lesssim Z_\odot/3$) (Thuan 1985; Bothun et al. 1986). 3) Low-luminosity dEs, such

as Ursa Minor and Draco, have $M/L_B \sim 150$-200, while low-luminosity dIs, such as M81 dwA, have $M/L_B \lesssim 10$-30 (non-virial motions would decrease M/L_B), so that excessive fading ($\gtrsim 3$ mag) of dIs is required to reconcile the M/L_B ratios; 4) the ellipticity distributions of complete samples of dEs and dIs differ, although the problem may disappear with better data (Binggeli and Cameron 1991); 5) A large ($\gtrsim 40\%$) fraction of dEs are nucleated while dIs are not. A scheme to form dE nuclei has been proposed by Sandage and Hoffman (1991) who have found a galaxy, NGC 4286, with a mixed morphology between the dI and dE types. They suggest that the galaxy has evolved from a dI into a dE/dSO by losing most of its gas through a supergalactic wind generated by a superluminous star cluster. The remnant of this cluster then sinks to the center by dynamical friction to form the dE nucleus. Whether this mechanism can account for the large number of nucleated dEs is unclear.

In summary, the evidence is mixed and does not point to a clear conclusion. There is no doubt that some dIs are being stripped of their gas. The basic idea, by Dekel and Silk (1986), that some of the observed properties of dwarf galaxies require a model in which substantial gas loss occurs as the result of supernova-driven winds in galaxies with weak gravitational potentials, is probably right. Whether all dEs can be explained as stripped dIs is not clear.

3.2 dIs and BCDs

DIs are thought to be BCDs in their quiescent phase, when the intense bursts of star formation have died out. There is ample evidence to support that view: 1) The HI properties of dIs and BCDs are indistinguishable (Thuan 1985; Staveley-Smith et al. 1992); 2) Their near-infrared colors are similar, implying the same older stellar populations and the same metallicity range $Z_\odot/30 \lesssim Z \lesssim Z_\odot/3$ (Thuan 1985). 3) The

photometric structure of the low-surface-brightness underlying component in the two dwarf types is similar (Loose and Thuan 1985; Patterson and Thuan 1992b); 4) To reconcile the M/L_B ratio of dIs (~5) and of BCDs (~3), a brightening in bursting BCDs of a factor of ~2 is required, which is not unreasonable. There are two observational programs which can be carried out to test the above hypothesis more stringently: 1) determine the space densities n of dIs and BCDs. We have $n(BCD)/n(dI) = n\tau(BCD)/T$, where τ is the duration of the bursts in BCDs, n is the average number of bursts, and T the Hubble time. With $\tau(BCD) \sim 10^7$ years, $n \sim 5$ and $T \sim 10^{10}$ years, we should observe $n(BCD)/n(dI) \sim 5 \times 10^{-3}$. 2) Map the large-scale space distribution of the two dwarf types. This has already been done for dIs. Thuan et al. (1991) found that, in general, dIs follow closely the structures delineated by bright galaxies and do not fill in the voids seen in the bright galaxy distribution. Contrary to dIs, there is a suggestion that some BCDs are found in voids (Moody et al. 1987; Pustilnik et al. 1991). If this result holds up with more data, it may invalidate the idea that BCDs are dIs which are bursting.

4. LOW-SURFACE-BRIGHTNESS GALAXIES

4.1 A non-dwarf galaxy population

Dwarf galaxies are selected from photographic surveys using the criteria of 'low surface brightness' and 'little or no central concentration of light on red images'. But these selection criteria do not isolate dwarf galaxies alone. Witness the University of Virginia (UVa) sample of 1845 galaxies classified as dwarf, irregular, magellanic irregulars or with a luminosity class IV-V or V, assembled by Thuan and Seitzer (1979a,b) and Schneider et al. (1990, 1992) from the Nilson (1973) catalog for a 21-cm dwarf redshift survey. The HI detection rate is ~84%, giving a total sample of 1557 galaxies with 21-cm redshifts. Based on

their redshifts, many of the detected galaxies prove actually to be much more distant and more luminous than their morphological classifications initially suggested. They are low-surface-brightness (LSB) galaxies. The two galaxy populations can be seen in figure 1 which shows the velocity distribution of the galaxies in the UVa dwarf and LSB sample in the Arecibo telescope declination range ($-2° \leq \delta \leq 38°$): the dwarf half with diameters smaller than the median (13.3 h^{-1} Kpc where h = Ho/(100 km s^{-1} Mpc^{-1})) is shown shaded, while the LSB half is unshaded. On the average, LSB galaxies are larger, more distant and more luminous than dwarf galaxies (Schneider et al. 1990).

4.2 Physical properties

The most comprehensive study of LSB galaxies to date is that of McGaugh (1992). He finds that: 1) the light profiles of LSB galaxies are well fit by an exponential, characteristic of a disk structure, with no preferred value of scale length or central surface brightness. The median scale length is 2.5 Kpc and the blue median central surface brightness is 23.4 mag $arcsec^{-2}$, well below the Freeman (1970) value of 21.65 mag $arcsec^{-2}$ for spiral disks. 2) LSB disks are very blue, with median colors B-V = 0.44, U-B = - 0.12 and V-I = 0.95, with a large spread in colors. This rules out the possibility that LSB galaxies are the result of faded high-surface-brightness (HSB) disks, since fading would make stellar populations redder not bluer. The blueness is most plausibly explained by young stellar populations with few red giants. 3) LSB galaxies are generally metal poor, with $Z_\odot/25 \lesssim Z \lesssim Z_\odot/3$. Figure 2 shows the histogram of oxygen abundances (hatched) in the LSB sample of McGaugh (1992), as compared to that of BCDs (open). LSB galaxies nearly cover the whole range of BCD metallicities, although there is no known LSB galaxy as metal-deficient as the most-metal deficient BCDs known ($Z \sim Z_\odot/30$), IZw18

(Kunth and Sargent 1986) and SBS 0335-052 (Izotov et al. 1990). Thus, LSB galaxies are chemically unevolved systems with little massive star formation in the past. A floor to the nitrogen, neon and sulfur abundances in LSB galaxies, appears to suggest that part of these elements came from infall of pre-enriched intergalactic medium. 4) The conclusion that LSB galaxies are less evolved than their bright counterparts is also supported by their high $M(HI)/L_B$: the median value for McGaugh (1992)'s sample is ~0.9, as compared to ~0.4 for HSB galaxies. Interferometric HI maps show them to have larger HI disks than HSB galaxies ($M(HI) \sim 10^9 M_\odot$), and very low HI surface densities, mostly lower than the threshold density for star formation (Kennicutt 1989), which explains their relative quiescence. These low HI surface densities imply also that LSB galaxies probably arise from low initial protogalactic density fluctuations.

In summary, LSB galaxies are <u>not</u> faded HSB galaxies. They have too blue colors and too low HI surface densities and metallicities.

4.3 <u>An iceberg-universe?</u>

The fact that LSB have mostly HI surface densities below the threshold density for star formation does raise the possibility that there is a whole population of protogalactic HI clouds, so diffuse that they will never form stars to emerge as LSB galaxies, or even if they do, they would be below the sky's surface brightness and remain undetected. In that case, the HSB galaxies would constitute only the tip of the iceberg of the galaxy population. HI blind searches of the sky, either with interferometers (Weinberg et al. 1991) or single-dish telescopes (Schneider and Spitzak 1992), do detect uncataloged objects, but on subsequent examination of the Palomar Sky Survey prints, the HI detections are nearly <u>always</u> ($\gtrsim$70%) associated with visible starlight. Thus, these

data do not support the view that a substantial population of dwarf and LSB galaxies may have been missed entirely by optical surveys. For the UGC sample, Thuan and Seitzer (1979b) found that LSB galaxies constitute only ~2% of all galaxies at B = -19 and only 0.2% at B = -20 (Figure 3).

ACKNOWLEDGEMENTS

I am grateful to S. McGaugh, S. Schneider, P. Knezek, J. Spitzak and R. Patterson for communicating to me their results in advance of publication. I especially thank S. McGaugh for graciously sending me a copy of his Ph.D. thesis and allowing me to quote results from it. I acknowledge the partial financial support of Air Force Office of Scientific Research grant 89-0467.

REFERENCES

Aaronson, M. 1987, in Nearly Normal Galaxies, ed. S. M. Faber, (New York: Springer-Verlag) p. 57.
Bender, R. and Nieto, J. L. 1990, Astr. Ap., 239, 97.
Binggeli, B. 1985, in Star-Forming Dwarf Galaxies and Related Objects, eds. D. Kunth, T. X. Thuan, J. T .T. Van (Paris: Editions Frontieres), p. 53.
Binggeli, B., and Cameron, L. M. 1991, Astr. Ap., 252, 27.
Binggeli, B., Sandage, A. and Tammann, G. A. 1985, A. J., 90, 1681.
Binggeli, B., Tarenghi, M. and Sandage, A. 1990, Astr. Ap., 228, 42.
Binney, J. and de Vaucouleurs, G. 1981, M.N.R.A.S., 194, 679.
Bothun, G. D., Mould, J. R., Caldwell, N. and MacGillivray, H. T. 1986, A. J., 92, 1007.
Christian, C. A. and Tully, R. B. 1983, A. J., 88, 934.
Dekel, A. and Silk, J. 1986, Ap. J., 303, 39.
de Vaucouleurs, G. 1959, Handbuch der Physik (Berlin: Springer-Verlag), Vol. 53, p. 275.
Dufour, R. J. and Hester, J. J. 1990, Ap. J., 350, 149.
Faber, S. M. and Lin, D. N. C. 1983, Ap. J. (Letters), 266, L17.
Freeman, K. C. 1970, Ap. J., 160, 811.
Freeman, K. C. 1987, in Nearly Normal Galaxies, ed. S. M. Faber, (New York: Springer-Verlag) p. 317.
Hoffman, G. L., Helou, G., Salpeter, E. E., Glosson, J. and Sandage, A. 1987, Ap. J. Suppl., 63, 247.
Holmberg, E. 1958, Medd. Lund. Obs. Ser. 2, No. 136.
Izotov, Y. I., Lipovetsky, V. A., Guseva, N. G., Kniazev, A. Y., and Stepanian, J. A. 1990, Nature, 343, 238.
Kennicutt, R. C. 1989, Ap. J., 344, 685.
Kormendy, J. 1987, in Nearly Normal Galaxies, ed. S. M. Faber, (New York: Springer-Verlag) p. 163.

Kunth, D. and Sargent, W. L. W. 1986, Ap. J., 300, 496.
Kunth, D., Maurogordato, S. and Vigroux, L. 1988, Astr. Ap., 204, 10.
Lequeux, J. and Viallefond, F. 1980, Astr. Ap., 91, 269.
Loose, H. H. and Thuan, T. X. 1985, in Star-Forming Dwarf Galaxies and Related Objects, eds. D. Kunth, T. X. Thuan and J. T. T. Van (Paris: Editions Frontieres), p. 73.
Loose, H. H. and Thuan, T. X. 1986, Ap. J., 309, 59.
McGaugh, S. S. 1992, Ph.D. thesis, University of Michigan.
Meurer, G. R., Freeman, K. C., Dopita, M. A. and Cacciari, C. 1992, A. J., 103, 60.
Moody, J. W., Kirshner, R. P., MacAlpine, G. M. and Gregory, S. A. 1987, Ap. J. (Letters), 314, L33.
Nilson, P. 1973, Uppsala General Catalogue of Galaxies, Uppsala Astr. Obs. Ann., Vol. 6.
Patterson, R. J. and Thuan, T. X., 1992a, Ap. J. (Letters). December 1.
Patterson, R. J. and Thuan, T. X., 1992b, in preparation.
Puche, D. and Westpfahl, D. 1992, Ap. J. (submitted).
Puche, D., Westpfahl, D., Brinks, E. and Roy, J. R. 1992, A. J., 103, 1841.
Pustilnik, S. A., Ugryumov, A. V., and Lipovetsky, V. A. 1991, in Galaxy Environments and the Large Scale Structure of the Universe, eds. G. Giuricin, F. Mardirossian and M. Mezetti.
Reaves, G. 1983, Ap. J. Suppl., 53, 375.
Sancisi, R., Thonnard, N. and Ekers, R. D. 1987, Ap. J. (Letters), 315, L39.
Sandage, A. and Binggeli, B. 1984, A. J., 89, 919.
Sandage, S. and Hoffman, G. L. 1991, Ap. J. (Letters), 379, L45.
Schneider, S. E. and Spitzak, J. 1992, in preparation.
Schneider, S. E., Thuan, T. X., Magri, C. and Wadiak, E. J. 1990, Ap. J. Suppl., 72, 245.
Schneider, S. E., Thuan, T. X., Mangum, J. G. and Miller, J. 1992, Ap. J. Suppl., 81, 5.
Staveley-Smith, L., Davies, R. D. and Kinman, T. D. 1992, M.N.R.A.S., 258, 334.
Thuan, T. X. 1985, Ap. J., 299, 881.
Thuan, T. X. 1991, in Massive Stars in Starbursts, eds. C. Leitherer, N. Walborn, T. Heckman, and C. Norman (Cambridge: Cambridge University Press).
Thuan, T. X. and Martin, G. E. 1979, Ap. J. (Letters), 232, L11.
Thuan, T. X. and Martin, G. E. 1981, Ap. J., 247, 823.
Thuan, T. X. and Seitzer, P. O. 1979a, Ap. J., 231, 327.
Thuan, T. X. and Seitzer, P. O. 1979b, Ap. J., 231, 680.
Thuan, T. X., Williams, T. B. and Malumuth, E. 1987, in Starbursts and Galaxy Evolution, eds. T. X. Thuan, T. Montmerle and J. T. T. Van (Paris: Editions Frontieres), p. 151.
Thuan, T. X., Alimi, J. M., Gott, J. R. and Schneider, S. E. 1991, Ap. J., 370, 25.
van den Bergh, S. 1960, Ap. J., 131, 215.
Viallefond, F. and Thuan, T. X. 1983, Ap. J., 369, 444.
Vigroux, L., Souviron, J. and Vader, J. P. 1984, Astr. Ap., 139, L9.
Vigroux, L., Thuan, T. X., Vader, J. P., and Lachieze-Rey, M. 1986, A. J., 91, 70.
Westpfahl, D. J. and Puche, D. 1992, A. J. (submitted).
Weinberg, D. H., Szomoru, A., Guhathakurta, P., and van Gorkom, J. H. 1991, Ap. J. (Letters), 372, L13.

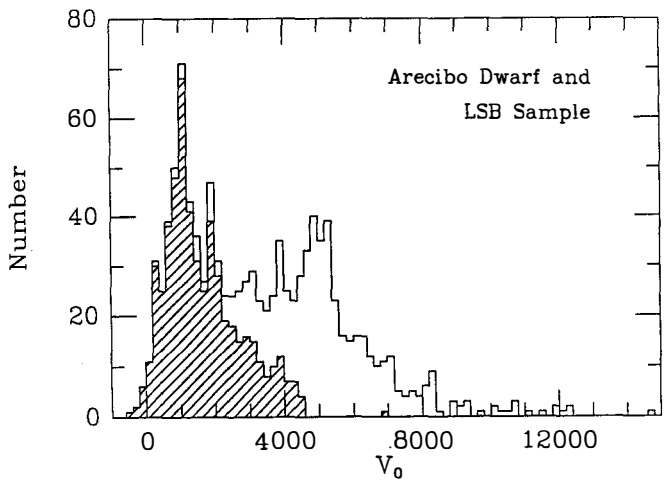

Figure 1. Histogram of the velocity distribution of the UVa dwarf and LSB sample detected at Arecibo. The half of the sample with diameters smaller than the median (13.1 h^{-1} Kpc) is shown shaded, and the remainder unshaded. (Schneider et al. 1990)

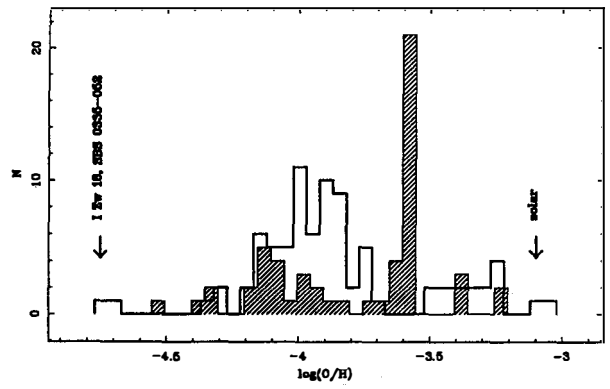

Figure 2. Histogram of oxygen abundances for LSB galaxies (hatched) and for BCDs (open). The strong peak at log(O/H) = - 3.6 is partly an artifact of the method used to derive the oxygen abundance (McGaugh 1992).

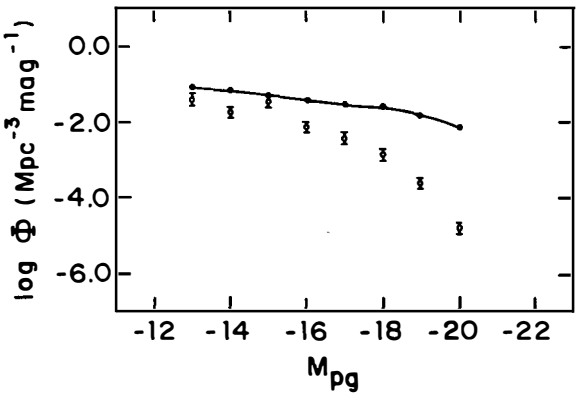

Figure 3. Space density of bright galaxies (solid line) and LSB galaxies (open circles). A Hubble constant of 75 km s^{-1} Mpc^{-1} is used (Thuan and Seitzer 1979b).

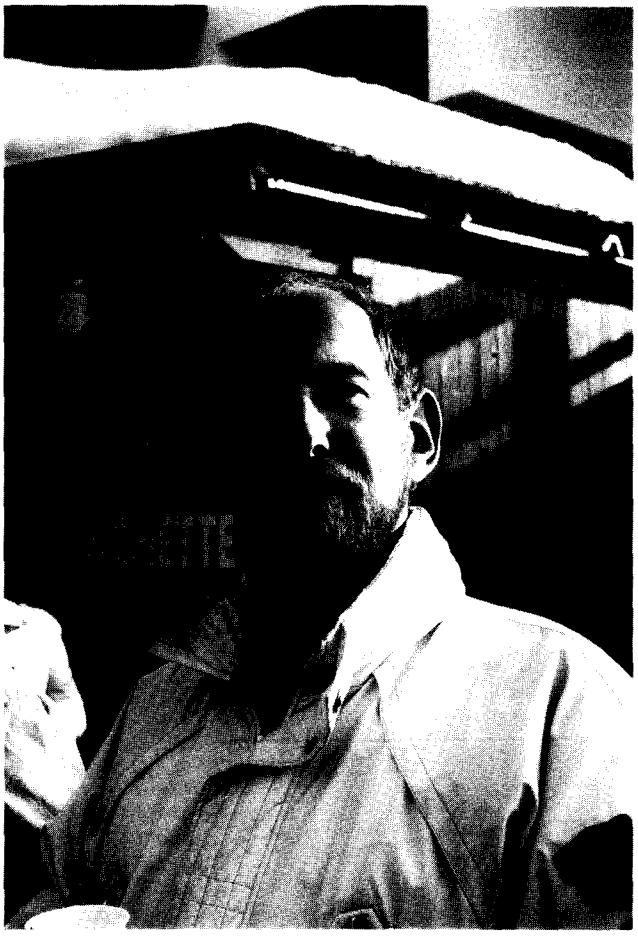

THE UNUSUAL RADIO SPECTRA OF BLUE COMPACT DWARF GALAXIES

Hans-Jörg Deeg
Institute for Astrophysics
University of New Mexico
Albuquerque, NM 87131, USA
and
National Radio Astronomy Observatory
PO. Box O, Socorro, NM 87801

ABSTRACT

A sample of seven radio bright Blue Compact Dwarf Galaxies from the survey by Klein, Weiland and Brinks (1991) was observed with the NRAO-VLA* in B-array at frequencies of 325 MHz and 1.489 GHz. The sample exhibits a diversity of radio spectra, strongly shaped by a variety of energy loss, emission and absorption mechanisms. Four of the seven galaxies have radio spectra which show a significant flattening towards lower frequencies. The spectra of two galaxies can be understood as the combination of thermal and non-thermal power law spectra. II Zw 40's spectrum does not fit well in any category and seems to be dominated by thermal emission. Several models which could cause the flattening at low frequencies are discussed, covering absorption as well as relativistic electron loss mechanisms. The most important ones are: (1.) free-free absorption of long wavelength radio emission by thermal electrons, and (2.) synchroton loss spectra resulting from a one-time electron injection or from electron injection which began approximately 10^7 yrs ago. Synchroton spectra shaped by a galactic wind can be discounted except in one case. The applicability of these mechanisms is discussed. We find that HII regions with thermal electron densities of ~ 25 cm^{-3} and emission measures of a few 10^5 pc cm^{-6} are needed to establish a case for free-free absorption. Hα images for two galaxies show HII regions with sizes sufficient to uphold free-free absorption. If the spectra are interpreted as time dependent synchroton loss spectra, they show signs of an electron distribution generated by SNR's a few 10^6 yrs ago. Observations needed to discriminate between models (1.) and (2.) are discussed.

* The National Radio Astronomy Observatory is operated by Associated Universities, Inc., under cooperative agreement with the National Science Foundation

1. INTRODUCTION

Blue Compact Dwarf Galaxies (BCDGs) were originally described as "isolated extragalactic HII regions"[1] because of their similarity to giant HII regions in the arms of spiral galaxies. Their main optical features are small angular size, high surface brightness, narrow emission lines and blue colors from the presence of young stars produced in a starburst. They also display large gas rich HI envelopes, low metal abundances, and up to 10 times higher radio/optical luminosity than spiral galaxies. A widely used 'Masterlist' of BCDGs was compiled by Thuan & Martin (1981)[2]. A very useful and diverse, albeit today somewhat outdated collection of papers on BCDGs are the proceedings of an earlier workshop[3]. The low metallicity and the limited reservoir of gas in BCDGs imply that the currently observed abundances of short lived blue stars must have originated in a starburst that has been either relatively recent (less than a few 10^7 years ago) or is still ongoing. Thuan [4] (1983) set an upper limit for the age of the starbursts from multi color photometry to less than 5 x 10^7 years. Krüger et. al[5] (1992) derive similar estimates for the age of a starburst and a duration of the starburst of the order of a few times 10^6 years from population synthesis models. The most complete work on the radio continuum spectra of BCDGs so far has been performed by Klein, Weiland and Brinks (KWB)[6]. They surveyed a sample of about 25 BCDGs and found their radio continuum spectra to be generally flatter than those of normal galaxies. The radio spectra of any galaxy may consist of one or both of the radio emission processes:

Thermal emission or free-free emission is collisional bremsstrahlung emitted from *thermal* electrons in an ionized gas. The ionized gas coincides usually with optically observable HII regions with temperatures of about 10^4K. The thermal emission S_{th} can be approximated for radio frequencies of $\nu \approx 10^9$ Hz by the power law: $S_{th} \sim (\nu/\nu_o)^{-0.1}$. The other emission mechanism is nonthermal or synchroton emission, which is bremsstrahlung emitted from gyrorotating *relativistic* resp. cosmic ray (CR) electrons in a magnetic field. CR electrons are most likely produced in the aftermath of a supernovae and are a possible age indicator for the presence of short lived O stars in a star burst. If the the energy spectrum of the relativistic electrons is given by $N(E)dE \sim E^{-\gamma}dE$, then the synchroton radiation emissivity is given by the power law: $S_{nth} \sim (\nu/\nu_o)^{-\alpha}$, with α =

$(\gamma - 1)/2$. A schematic of the decomposition of a radio spectrum with observed flux density S_{obs} into thermal and nonthermal components is shown in Fig. 1. KWB performed radio spectrum decompositions for several BCDGs. In the frequency range which KWB analyzed, the radio spectra of the BCDGs do not display any unusual properties besides relatively strong thermal emission and a steep synchroton component. The strength of the synchroton emission can be used to estimated the strengths of the magnetic fields in these galaxies using the energy equipartition between the CR energy density (which can be estimated from the synchroton emission of the relativistic electrons) and energy density of the magnetic field.

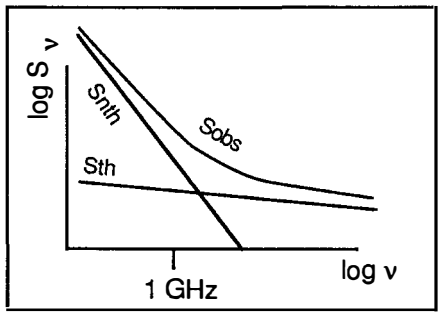

Fig. 1 Decomposition of a radio spectrum into its thermal and nonthermal components.

Table 1: Galaxies observed at 325 MHz

	Haro 15	II Zw 40	II Zw 70	Mkn 297	Mkn 314	Mkn 527	III Zw 102
α [1950]	00 46 04	05 53 05	14 48 54	16 03 01	23 00 31	23 10 41	23 18 00
δ [1950]	-12 59.45	+03 23.1	+35 47.0	+20 40.7	+16 20.0	+06 02.9	+16 57.0
m_b	13.48	12.9	14.86	13.03	13.95	14.50	12.01
Distance[Mpc]	95.4	10.1	17.1	63.0	31.1	50.3	25.0
M_b	-21.42	-17.12	-16.30	-20.97	-18.51	-19.01	-19.98
B[μG]	15	32	11	33	19	30	27

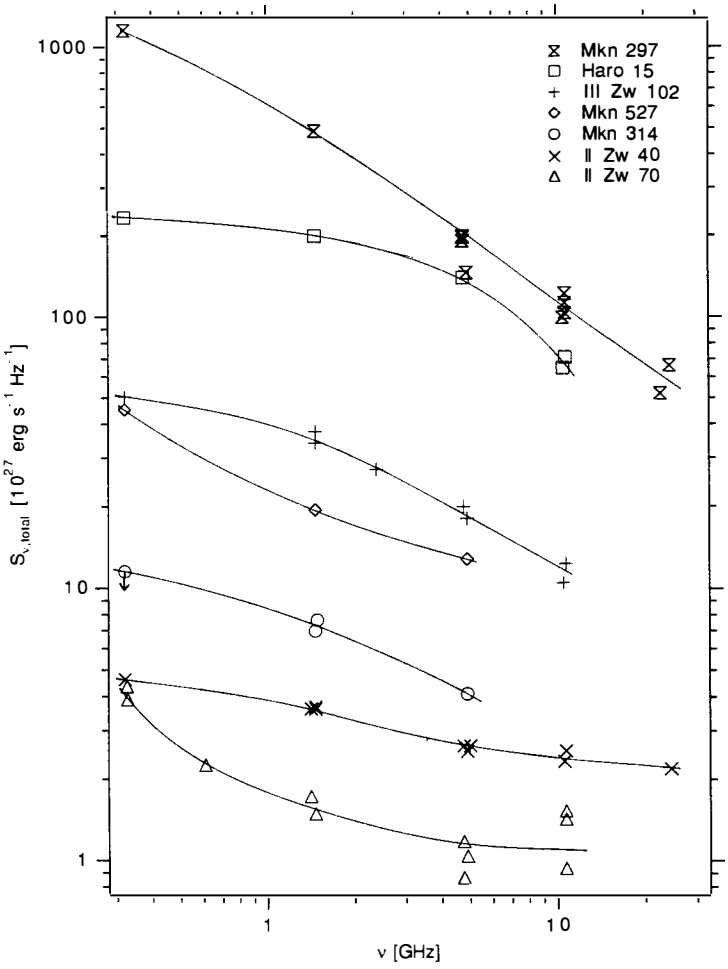

Fig. 2 Absolute radio fluxes of the BCDGs observed.

THE RADIO OBSERVATIONS AND THEIR INTERPRETATION

We extended the frequency range of the radio spectra available towards lower frequencies by observing a sample of seven radio bright BCDGs at the VLA in B-array at 325 MHz and 1.5 GHz. Only one BCDG, II Zw 70, had ever been observed before at a comparably low frequency[7]. Some basic properties of the galaxies are listed in Table 1. The distances are derived using H_o = 75 kms^{-1} Mpc^{-1}. The magnetic field strengths of the BCDGs obtained by equipartition are relatively high. The selection of radio bright galaxies from the

sample of KWB is biased towards larger galaxies than typically considered in samples of BCDGs. If the 325 MHz values are taken into account, the radio spectra fit in only two cases (Mkn 527, II Zw 70) in the thermal-nonthermal separation scheme contrary to expectations. In four out of the seven galaxies (Mkn 297, Mkn 314, Haro 15, II Zw 102), we find an unusual flattening of the spectra at lower frequencies. Slowly varying changes in the spectral index across the frequency range have been observed in normal spiral galaxies[8], but spectra with such an extreme low frequency turn-over had not been found before for entire galaxies. The radio spectrum of the remaining galaxy, II Zw 40, is extremely flat over its entire range and is probably entirely dominated by thermal emission. An overview of the radio-spectra, corrected by distance to absolute radio luminosities, is given in Fig. 2. Fig. 3 shows 1.5 GHz radio continuum maps (contour lines) overlaid on optical B-band (grey scale) images for two BCDGs. To explain the low frequency flattening we investigated a large range of mechanisms. One mechanism, which has been used by Hummel (1991)[9] and Pohl at al. (1991)[10] to explain the flattening in normal spiral galaxies, is the effect of a galactic wind on the integrated radio spectra. This mechanism could be fitted to our data for only case, Mkn 297. The spectral turnovers in the other BCDGs are too abrupt to be consistent with galactic wind models. Two other mechanisms appear more appealing: free-free absorption and time dependent synchroton losses.

Free-free absorption of electromagnetic radiation in a thermal gas is the reversal of the emission mechanism introduced above. The optical depth at a frequency ν is given by:

$$\tau_\nu = 8.3 \cdot 10^{-2}\ T_e^{-1.35} \left(\frac{EM}{pc\ cm^{-6}}\right) \left(\frac{\nu}{GHz}\right)^{-2.1}$$

where the emission measure EM is a product of thermal electron density n_e and column length l: $EM = \int n_e^2\, dl$. Free-free absorption occurs only in the regions which also have strong thermal emission. For significant absorption of 300 MHz radio waves in a hot ($T \approx 10^4$ K) medium to occur, emission measures of a few 10^5 pc cm^{-6} are needed. For a given optical depth through free-free absorption, a lower limit for the thermal emission can be calculated. Fig. 4 shows the spectrum of III Zw 102 with a fit of free-free absorption combined with thermal emission.

Synchroton losses: All relativistic electrons which emit synchroton radiation in a magnetic field lose energy. The energy dependency of these *synchroton losses* is given by $\dot{E}_{sync} = k\, E^2$.

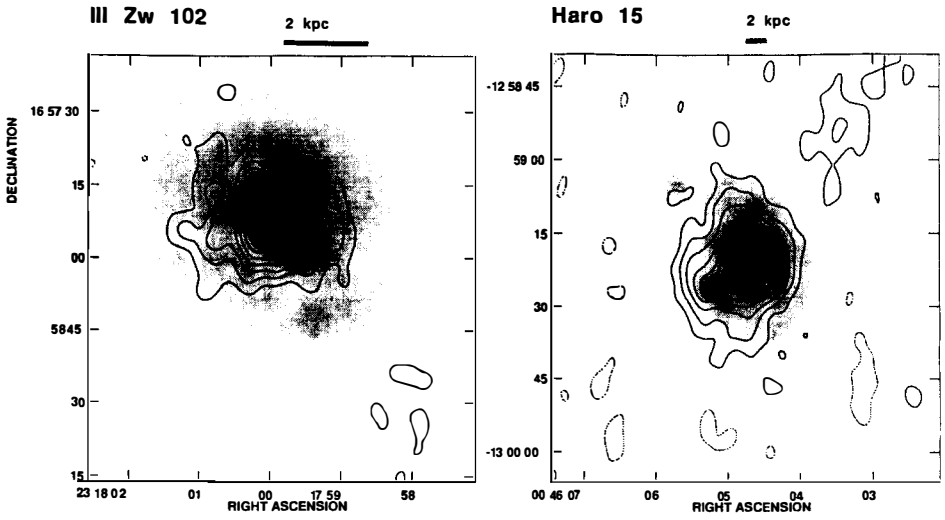

Fig. 3. 20 cm continuum maps (contour lines) and B-band images (grey scale) for two BCDGs

Synchroton losses will steepen an electron spectrum $N(E)dE \sim E^{-\gamma}dE$ by a power of 1 to $N(E)dE \sim E^{-(\gamma+1)}\,dE$, which corresponds to a steepening of the spectrum of the emitted electromagnetic radiation by a power of 1/2. If relativistic electrons got injected into the ISM over a relatively short time only - as would be expected from a starburst with a duration of less than a few 10^7 years- no steady state situation can develop. If electron injection *ceases* , the high energy electrons get depleted much faster, and a very steep radio spectrum at high frequencies will result. A different situation is an electron injection which *began* so long ago, that only the number densities of the highest energy relativistic electrons are affected by synchroton losses whereas lower energy electrons still reflect the injection spectrum. In that case, the synchroton radiation will have a sharp spectral break of 1/2 at the frequency $\tilde{\nu}_T = 1.116 \times 10^{24}\, B^3\, t'^{-2}$, where B is the magnetic field strength, and t' the time since injection began. A fit is included in Fig. 4.

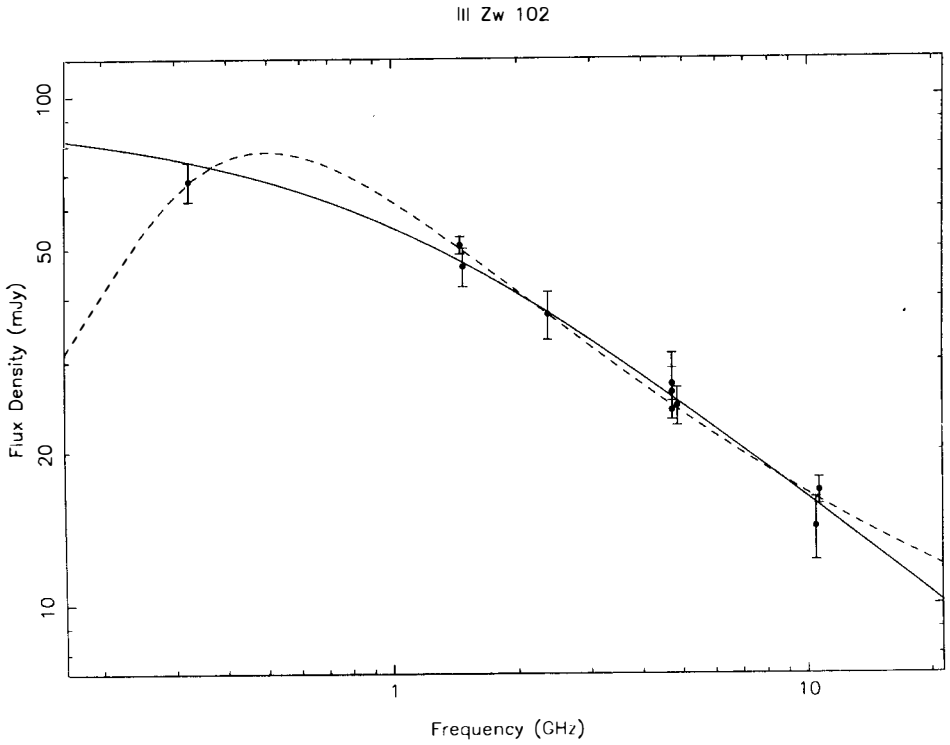

Fig. 4: Plot of the flux density of III Zw 102 versus frequency. Dashed line: fit of free-free absorption and thermal emission. Solid line: fit from synchroton losses of CR electrons whose injection began a time t' ago.

DISCUSSION AND CONCLUSION

Our sample of galaxies exhibits radio spectra which are strongly shaped by differing mixes of emission and absorption processes and energy loss mechanisms. Currently, we have two competing models explaining the spectral shape of BCDGs. Both are inherently coupled to the special situation present in these galaxies. Free-free absorption requires that a large fraction of the radio-emitting area of a galaxy is covered with an ionized gas which is relatively dense (25 cm^{-3}) and with emission measures of the order of 10^5 pc cm^{-6}. For free-free absorption to work, BCDGs - also known as extragalactic HII regions - need relatively large HII masses in of the order of 10^7 $M_\odot$. For two galaxies - unfortunately none of them with a pronounced spectral flattening (Mkn 297 and II Zw 40) we have obtained Hα images. The Hα resp. HII regions in these galaxies have sizes of

about 200 pc - which would make free-free absorption plausible as long as the synchroton emission (which gets absorbed) is emitted in about the same regions. A rough estimate can be made by using the Alfvén speed as the CR electron's propagation speed and an age - and lifetime - of a CR electron of about 10^7 years. This leads to a smearing of the synchroton emission of about 100 pc from their origin -presumably supernovae remnants within HII regions. The other possibility, synchroton losses on a time dependent electron injection spectrum, requires a starburst to have either begun in the last few 10^6 years, or to have ended a few 10^6 years ago. Detailed color photometry could lead to more precise estimates of the ages of the star bursts, as well as Hα photometry, which can be used to estimate the thermal emission, emission measures of the HII regions, and the numbers of O stars. In conjunction with these measurements, the radio continuum spectra are a very powerful way to extract physical quantities from these remarkable galaxies as well as to date and verify their star formation history. A thorough discussion of the radio spectra will be given in a forthcoming paper.

References

[1]Sargent , W.L.W., Searle, L.,:1970, ApJ, **162,** L155

[2]Thuan, T.X., Martin , G.E.: 1981, ApJ, **247**, 823

[3]Workshop on Star-Forming Dwarf Galaxies and related objects 1986, eds. D. Kunth, T.X Thuan, J. Tran Thanh Van, Editions Frontieres, Paris.

[4]Thuan, T.X.: 1983, ApJ, **268,** 667

[5]Krüger, H., Fritze-v. Alvensleben, U., Loose, H.-H., Fricke, K.J.:1991, A&A,**242,** 343

[6]Klein, U., Weiland, H., Brinks, E. (KWB): 1991, A&A, **246**, 323

[7]Skillman, F.D., Klein, U.: 1988, A&A, **199**, 61

[8]Israel, F.P., Mahoney, M.J.: 1990, ApJ, **352,** 30

[9]Hummel, E.: 1991, A&A, **251, 442**

[10]Pohl, M., Schlickeiser, R., Hummel, E.:1991, A&A, **250**, 301

A STUDY OF EXTREME IRAS GALAXIES

Presented by Wim van Driel
Astronomical Institute "Anton Pannekoek", University of Amsterdam,
Kruislaan 403, NL-1098 SJ Amsterdam, The Netherlands

ABSTRACT

We studied a statistically complete sample of 57 so-called extreme IRAS galaxies, i.e. objects with relatively high L_{FIR}/L_B^0 ratios ($\geq$3), using optical CCD broad-band B, V, R and Hα images and spectra, VLA radio continuum maps and CO(1–0) line spectra. (We also studied near-infared luminosities and 21 cm H I line observations of a similar sample of IRAS galaxies). We find that our sample can be almost completely divided into three distinct classes of objects: dwarfs (20%), barred spirals (35%), and interacting systems (35%). The dwarf galaxies have relatively the lowest star formation rates but the largest star forming regions of size ~2–6 kpc. The barred spirals have intermediate star formation rates and efficiencies, showing star formation occurring mainly near the centre but also in the bars, while the interacting systems have the highest rates and efficiencies and the most compact (ranging from less than one to several kpc diameter) star forming regions which are always found in their nucleus. In about 93% of these galaxies the infared emission is enhanced through intensive star formation. Applying a simple exponentially declining starburst model we estimate burst decay times of order 10^8 yr for a similar sample of IRAS galaxies, for which sample we also find a near-infared Tully-Fisher relation similar to that of normal spirals.

1. SAMPLE DESCRIPTION

We used the IRAS survey database to select a statistically complete sample of so-called extreme IRAS galaxies with high far-infrared/blue luminosity ratios L_{FIR}/L_B^0 in the southern sky, observable from the European Southern Observatory (ESO). The galaxies have L_{FIR}'s ranging from 10^9 to 10^{12} $L_\odot$ [H_0= 75 km s^{-1} Mpc^{-1}]. The galaxies are generally optically faint ($\leq$14 mag) objects not studied before of on average 1′ diameter.

We selected[1),5)] all IRAS sources in two southern fields with (1) flux densties larger than 1 and 2.5 Jy at 60 and 100 μm, respectively, ensuring completeness, (2) flux densities at 60 and 100 μm exceeding those at 12 and 25 μm, selecting galaxies, and (3) L_{FIR}/L_B^0 ratios $\geq$3 initially using estimated optical magnitudes. For one field only (at $10^h < \alpha < 14^h$ and -40° $< \delta <$ -20°) containing 57 galaxies possibly associated with 42 IRAS sources all observations were completed. We later obtained co-added IRAS flux densities, greatly improving the detection rates at 12 and 25 μm.

2. OBSERVATIONS AND THEIR INTERPRETATION

We investigated the properties of the extreme IRAS galaxies through a multi-wavelength study[1)] at optical, radio continuum, CO line and (for a similiar sample) near-infrared and 21 cm H I line wavelengths.

2.1 Optical observations

We obtained[5)] B, V, R, and Hα CCD images and low-resolution long-slit spectra of the project galaxies at ESO. The images show, among other things, that the sample consists predominantly of barred spirals and interacting systems, with in most cases compact Hα emitting regions, as well as dwarf galaxies with relatively larger Hα emitting regions. The dominating (75%) type of spectrum is the H II-type, although a significant fraction are LINER or Seyfert types. So the spectra indicate that for about 92% of the galaxies studied active star formation is the source of the enhanced far-infrared emission. Only one galaxy (NGC 3597) was found to be a classical merger with an $r^{1/4}$ luminosity profile and a double nucleus.

We find[3)] that the Hα luminosities corrected for dust absorption using the Hα/Hβ line ratios and for stellar H II absorption lines are correlated with L_{FIR} with slope unity. Using this correlation and a simple starburst model[4)] we find that in the

starburst relatively more massive stars are formed than in the solar neighbourhood and star formation rates of order 0.3–300 $M_{\odot}yr^{-1}$.

2.2 Radio continuum observations

All optically observed galaxies were mapped[6] at 6 cm wavelength with the VLA at low- (10″) and high (1″) resolution. In about 30% of the galaxies the star forming regions are clearly resolved. From the low-resolution data the total flux densities are derived, while in the high-resolution images on average only about 60% of the total flux density is detected due to a lower sensitivity for extended low-surface brightness emission. The observed high-to-low flux density ratio appears to be correlated with the L_{FIR}/L_B^0 ratio of the galaxies, implying that in galaxies with higher star forming activity this activity occurs in smaller regions. The radio power is found to be well correlated with the L_{FIR}, in fact following the same correlation as samples of both optically and infrared selected galaxies. From a comparison with Hα luminosities corrected for both extinction and stellar absorption lines we estimate that about 20% of the total radio emission has a thermal origin, not much higher than the fraction found in normal spirals. The average radio surface brightness of the resolved sources is comparable to that of galactic nuclei and considerably higher than that of normal galactic disks.

2.3 CO(1–0) line observations

We observed a distance-limited ($V<6000$ km s^{-1}) subsample in the CO(1–0) line with the SEST at ESO. The galaxies are gas-rich and H_2 gas masses of order 0.5-2.5 10^9 $M_{\odot}$ are derived. The estimated gas masses and star formation rates indicate that the present-day star formation activity can be sustained for about 10^8 years in these galaxies. We find L_{FIR}/M_{H_2} ratios, considered to be a measure of the star formation efficiency, of order 6–30 $L_{\odot}/M_{\odot}$. Both M_{H_2} and L_{FIR}/M_{H_2} are comparable to the values found for other IRAS galaxies of comparable luminosity. The star forming efficiency appears to be correlated with the Hα equivalent width and the L_{FIR}/L_B^0 ratio (both indicators of the ratio of the present and average past star formation activity), indicating that a higher star formation activity involves a more efficient conversion of gas into stars. Gas-to-dust gas mass ratios comparable to the Galactic values are found if we use a two-component (18 and 60 K) dust distribution model.

2.4 Near-infrared observations

Since we only have near-infared (J, H, K) magnitudes for a dozen objects from our sample, we used the extensively observed so-called IRAS minisurvey galaxy sample instead, which consists of actively star forming galaxies similar to those in our sample. We find[4] that the near- and far-infrared luminosities of these galaxies are well correlated, which we can successfully reproduce using a population synthesis model simulating an exponentially declining star burst and applying a two-component (cool and warm) dust model. The calculations imply that the near-infrared luminosity is dominated by red (super) giants, evolved from stars of masses $\geq$6 $M_{\odot}$. It is argued that the burst decay time is rather long for these galaxies, of order 10^8 yr, and adopting this timescale star formation rates of order 2–60 $M_{\odot}$ yr^{-1} are estimated for the minisurvey galaxies.

2.5 21 cm H I line observations

We intended to determine the near-infrared Tully-Fisher relation of actively star forming IRAS galaxies, but since our sample of extreme IRAS galaxies sample is not accesible with the sensitive Arecibo radio telescope needed for this project and we do not have near-infrared magnitudes of all our objects (see above), we instead observed the similar IRAS minisurvey galaxy sample (see above) in the 21 cm H I line. Due to the (strongly) enhanced star formation activity in the IRAS galaxies one might expect to see an increase in near-infrared luminosity for a certain total galaxy mass, compared to more quiescent spirals, and hence a difference between the Tully-Fisher relations of normal and extreme IRAS galaxies. No striking difference is found[8] in the raw data, however, but there is a considerable scatter in the correlations as well as various systematic effects, so no firm conclusions can be drawn yet.

3. SUMMARY OF THE RESULTS

The sample of extreme IRAS galaxies studied can be almost completely divided[2] into three distinct subgroups; in order of increasing infrared activity: dwarfs (20%), barred spirals (35%), and interacting systems (35%). Our working definition of dwarfs is all objects with $\log(L_B^0/L_{\odot})\leq 9.6$. The star forming regions in these dwarfs are of order 2–6 kpc in size and they cover up to 50% of the optical disks, while the star formation regions in the barred and interacting systems are generally confided to the nuclear region with typical diameters of a few kpc or (considerably) less. Only one

non-peculiar non-barred spiral is found in our sample implying that star formation in spiral arms is not an efficient way to power the far-infrared luminosity and to raise the L_{FIR}/L_B^0 ratio.

About a quarter of the galaxies in our sample show spectra typical of active galactic nuclei (AGN's). These galaxies are all barred or interacting systems with $\log(L_{FIR}/L_\odot) \geq 10.3$. It is argued that only four of these AGN galaxies are (real) 'classical' Seyferts, while the remaining AGN-type spectra, mainly LINERs, are generated by an intense nuclear starburst, like the H II-type spectra of the majority (75%) of the sample.

The optical (B, V, R) colours of the galaxies are completely dominated by the emission from the older population of stars already existing before the starburst. The observed range in optical colours is due to extinction by dust in the disk. However, the global extinction estimated in this way does not correlate with the extinction found towards the star forming regions determined from the $H\alpha/H\beta$ line ratios.

Acknowledgements

This project was mainly carried out together with Bert van den Broek and Teije de Jong of the University of Amsterdam; the H I line observations were done with Willem Baan of Arecibo Observatory.

References

(1) van den Broek, A.C.: 1990, A Study of Extreme IRAS Galaxies, Ph.D. thesis, University of Amsterdam, The Netherlands
(2) van den Broek, A.C.: 1992a, A & A, in press (paper IV)
(3) van den Broek, A.C.: 1992b, A & A (Letters), in press
(4) van den Broek, A.C., de Jong, T., Brink, K.: 1991, A & A 246, 313
(5) van den Broek, A.C., van Driel, W., de Jong, T., et al.: 1991, A & AS 91, 61 (paper I)
(6) van Driel, W., van den Broek, A.C., de Jong, T.: A & AS 90, 55 (paper II)
(7) van Driel, W., van den Broek, A.C.: 1991, A & A 251, 431 (paper III)
(8) van Driel, W., van den Broek, A.C., Baan, W.A.: 1992, A & A in preparation

MODELS FOR STARBURST REGIONS: HOW WARM ARE WARMERS?

Claus Leitherer[1,2], Ruth Gruenwald[3], and Werner Schmutz[4]

[1] Space Telescope Science Institute, Baltimore, Maryland, USA
[3] Instituto Astronômico e Geofísico da Universidade de São Paulo, Brazil
[4] Institut für Astronomie, ETH-Zentrum, Zürich, Switzerland

ABSTRACT

We present new model calculations for the theoretical stellar and nebular spectrum of a starburst region containing large numbers of Wolf-Rayet (WR) stars. The energy distribution of WR stars is obtained from a grid of extended, expanding non-LTE model atmospheres. These atmospheres are coupled to stellar evolutionary models with mass loss covering a metallicity range of $0.1\ Z_\odot \leq Z \leq 2\ Z_\odot$. The integrated spectrum in the range $0.1\ eV < E < 300\ eV$ resulting from the burst is calculated. We compute the strengths of the most important nebular lines which are formed in the interstellar medium, with particular emphasis on the phase $\sim 3\ Myr$ after the on-set of the burst when large numbers of WR stars appear. This phase has been called *Warmer* phase due to the high surface temperatures previously associated with WR stars. New evolutionary models yield significantly lower temperatures for WR stars. On the other hand, non-LTE effects can strongly enhance the far-UV flux ($E > 24.6\ eV$) of WR stars, even at lower temperatures. The net result is a moderate softening of the the far-UV flux with respect to earlier models. The consequences for the strength of nebular emission lines such as [O III]λ5007 or [N II]λ6584, however, are dramatic. We compare theoretical line strengths to observed values in diagnostic diagrams containing data of H II galaxies, LINER's, and Seyfert2's. It is found that line ratios observed in AGN's are hard to explain in terms of photoionization by WR stars.

[2] Affiliated with the Astrophysics Division, Space Science Department of ESA

OVERVIEW: THE STARBURST HYPOTHESIS FOR ACTIVE GALACTIC NUCLEI

Despite extensive work in recent years, a comprehensive theory for the structure, evolution, and nature of the central source in active galactic nuclei (AGN's) is not yet available. In the 'standard model'[21] a supermassive black hole powers the physical processes observed in the nuclei of AGN's. The total amount of energy produced by AGN's over a Hubble time[22] is roughly equal to the energy associated with the nucleosynthesis of heavy elements in massive stars[3]. This equality could in principle indicate a causal connection between AGN's and starbursts producing massive stars[3]. Evolutionary links between AGN's and starbursts can be expected to exist. On the one hand, compact stellar remnants of a nuclear starburst could power the nucleus by gravitational accretion[36]. It has also been argued that the central engine of an AGN could trigger circumnuclear star formation[4,5].

Although star-formation activity may be a related phenomenon in AGN's, the general consensus is that a central 'monster' is the ultimate mechanism which is responsible to explain the majority of the physical properties in AGN's[8]. This view has been challenged in a series of papers by Terlevich and co-workers[20,31,32,33,35] who argue that at least a subset of AGN's can as well be explained by pure starburst models without the need for a central 'monster'. The distribution of AGN's over Hubble type (and as a consequence over metallicity) suggests that nuclear activity in galaxies is more likely to be observed in metal-rich than in metal-poor systems[35]. Models for the evolution of massive stars with mass loss[18] predict substantial differences between late evolutionary stages at high ($Z \geq Z_{\odot}$) and low ($Z \leq 0.25 Z_{\odot}$) metal content. If Z is high, stars lose large amounts of their surface layers due to Z-dependent, radiatively driven winds in the course of evolution. As a consequence, after a few Myr hot inner stellar regions rich in processed material are exposed. Observationally, these objects are identified with WR stars. In contrast, mass loss in a low-Z environment is not strong enough to transform significant numbers of O stars into WR stars[19]. The phase when large numbers of hot WR stars occur has been called the *Warmer* phase due to copious amounts of high-energy photons supposedly produced by these objects[31]. The *Warmer* hypothesis suggests that (some) AGN's are the manifestation of a violent starburst observed at an epoch when large numbers of WR stars have formed.

The original *Warmer* model has been extensively updated and is now able to make quantitative predictions for the spectral energy distribution from the radio to X rays, for the emission spectrum, the morphology, and the variability of AGN's[29,30]. The models, however, are based on earlier evolutionary computations[16,17] and stellar atmospheres[12,37] to predict parameters of WR stars. Drastically improved models and observational results have become available in recent years. WR stars are surrounded by winds dense enough to entirely shroud the photosphere. Model atmospheres appropriate for such conditions have now been computed[7,9,10,27]. Furthermore, empirical analyses of individual WR stars[26] have led to a significant downward revision of the effective temperatures of WR stars. In view of these improvements we are re-addressing some of the predictions of the *Warmer* model.

NEW EVOLUTIONARY SYNTHESIS MODELS

The emergent flux from WR stars is obtained from a grid of new model atmospheres described in more detail elsewhere[27]. In short, the non-LTE radiative transfer in the expanding atmosphere is solved in spherical geometry. Pure helium models are considered, as appropriate for WR stars. The effect of including metal-line blanketing has been studied

in one representative case[25] and found to be insignificant for the purpose of this study. A complete model is characterized by the effective temperature T_{eff}, radius R (both taken where the outflow velocity is still subsonic), mass-loss rate $\dot{M}$, and terminal wind velocity v_∞. The velocity field in the supersonic regime is parameterized in its usual form, *i.e.* $v(r) = v_\infty \left(1 - \frac{R}{r}\right)^\beta$ with $1 \leq \beta \leq 2$. In Figure 1 we compare the emergent flux of the new models to the results obtained from traditional[12] atmospheres. If the wind density is relatively low, the new models predict significantly higher fluxes in the He I $\lambda 504^-$ and He II $\lambda 228^-$ continua than a Kurucz model with equal T_{eff}. If the wind density exceeds a critical value, He^{++} begins to recombine at some distance from the stellar surface, and no radiation shortward of 228 $\AA$ is emitted. To summarize, the new atmospheres predict fluxes in the He I continuum which are always significantly above those of traditional models with equal T_{eff}, whereas for $\lambda < 228$ $\AA$ the emergent flux critically depends on the wind density.

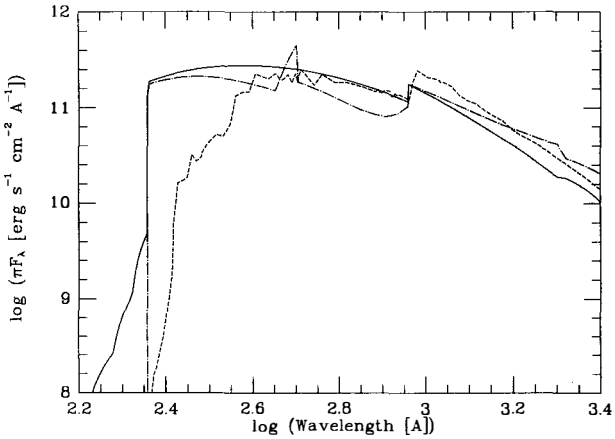

Figure 1. Comparison of the new expanding, non-LTE models for WR stars to a classical static, LTE atmosphere. Dashed line: LTE model[12]; solid: new model with low wind density; dash-dotted: new model with high wind density. $T_{eff} = 45,000$ K in all cases.

Evolutionary models were taken from[18]. These models cover the metallicity range $0.1\ Z_\odot \leq Z \leq 2\ Z_\odot$ and describe the evolution of massive stars from the zero-age main-sequence until the end of central carbon-burning. Convective overshooting from the convective cores and stellar mass loss are included. The influence of metallicity enters directly, *viz.* in the form of modified opacities, and indirectly, *viz.* by metallicity dependent mass-loss rates. WR stars are defined as having $\log T_{eff} > 4.4$ and a surface hydrogen content < 0.4 (by mass). They are the low-mass descendants of O stars.

In their original version, these evolutionary models are not sufficient to compute the synthetic spectrum of WR stars. Wind-blanketing has only been roughly accounted for by increasing the stellar radius due to electron scattering opacity in the wind. We removed the correction for wind-blanketing in the evolutionary models and coupled the wind-free stellar cores to our WR model atmospheres, which give a much more realistic treatment of the wind-blanketing. This has been done only for stars in the WR phase.

We follow the evolution of massive stars from the time they are formed until a certain maximum time, which is larger than the lifetime of the least massive stars of relevance. The mass spectrum is parameterized by a power-law IMF of the type $\phi(M) \propto M^{-\alpha}$. The

normalization is given by the star-formation rate or the total gas mass converted into stars. Details are given in[15].

The ionizing spectrum calculated for each evolutionary time step is input for the photoionization code AANGABA[6,23]. Each model corresponds to a single density. We studied densities in the range $10^2 cm^{-3} \leq n \leq 10^6 cm^{-3}$ and ionization parameter $U = Q_H/(4\pi c r^2 n)$ between $10^{-1.5}$ and $10^{-4.0}$. We assumed that no significant chemical enrichment due to stellar winds occurs over the lifetime of the starburst.

ENERGY DISTRIBUTION OF THE BURST IN THE FAR-UV

We adopted burst parameters very close to the original[2,31] *Warmer* model: an initial, δ-function shaped burst with no subsequent star formation, a total gas mass of $M = 10^6 M_\odot$ converted into stars with masses between 3 $M_\odot$ and 120 $M_\odot$, a Salpeter-type IMF with $\alpha = 2.35$, and metal abundances of 0.1 $Z_\odot$, 0.25 $Z_\odot$, $Z_\odot$, 2 $Z_\odot$.

The computed continuous energy distribution and its evolution with time is shown in Figure 2. The number of hydrogen ionizing photons close to 912$^-$ $\AA$ declines smoothly from $t = 0$ until $t = 10$ Myr when the hottest and most massive stars evolve from the zero-age main-sequence and eventually explode as supernovae. The occurrence of WR stars is easily recognizable from the 'hump' shortward of 24.6 eV. If $Z = Z_\odot$, this phase — which is identical to the *Warmer* phase — lasts from 2.5 Myr to 8 Myr. The duration of this phase is determined by the lifetimes of the O-star progenitors in the mass range $22\ M_\odot \leq M_o \leq 120\ M_\odot$. In contrast, if $Z = 0.1\ Z_\odot$, WR stars form only from stars above 65 $M_\odot$, which explains the short duration of the *Warmer* phase in this case. As already found earlier[31], this suggests that starbursts with hard far-UV spectra are preferentially found in metal-rich galaxies.

How do the new results compare to those found in the original[31] *Warmer* model? The spectrum in Figure 2 between 13.6 eV and 24.6 eV at $t \approx 3$ Myr is close to a power law index of -2, which is not too different from the original model. This agreement seems surprising considering the drastically different evolutionary and atmospheric models used in our and in the original *Warmer* model. The average T_{eff} of WR stars is well below 100,000 K in our models whereas values more than twice as high had been assumed before. On the other hand, the stellar fluxes of WR stars in the He^+ continuum are much higher now (cf. Figure 1) at all temperatures. The net result of these two competing effects is the close agreement between the original and the new *Warmer* model calculations. At energies above 54.4 eV, however, our models predict a significant steepening of the spectrum ($F_\nu \propto \nu^{-5}$) due to the comparatively low temperature. Even non-LTE effects cannot compensate for the lower T_{eff}.

LINE STRENGTHS OF DIAGNOSTIC EMISSION LINES

We concentrate in our discussion of the emission-line spectrum on the phase $t = 3.3$ Myr and $Z = Z_\odot$. This represents the most favorable case for the *Warmer* scenario when the UV spectrum is hardest (cf. Figure 2). Figure 3 gives the results for the line ratios [O III]/Hβ and [N II]/Hα. This type of diagnostic diagram is particularly well-suited to discriminate between classical H II regions and AGN's[1]. AGN's in this figure comprise Seyfert2's and LINER's. Both are clearly separated from the region occupied by H II galaxies. Theoretical

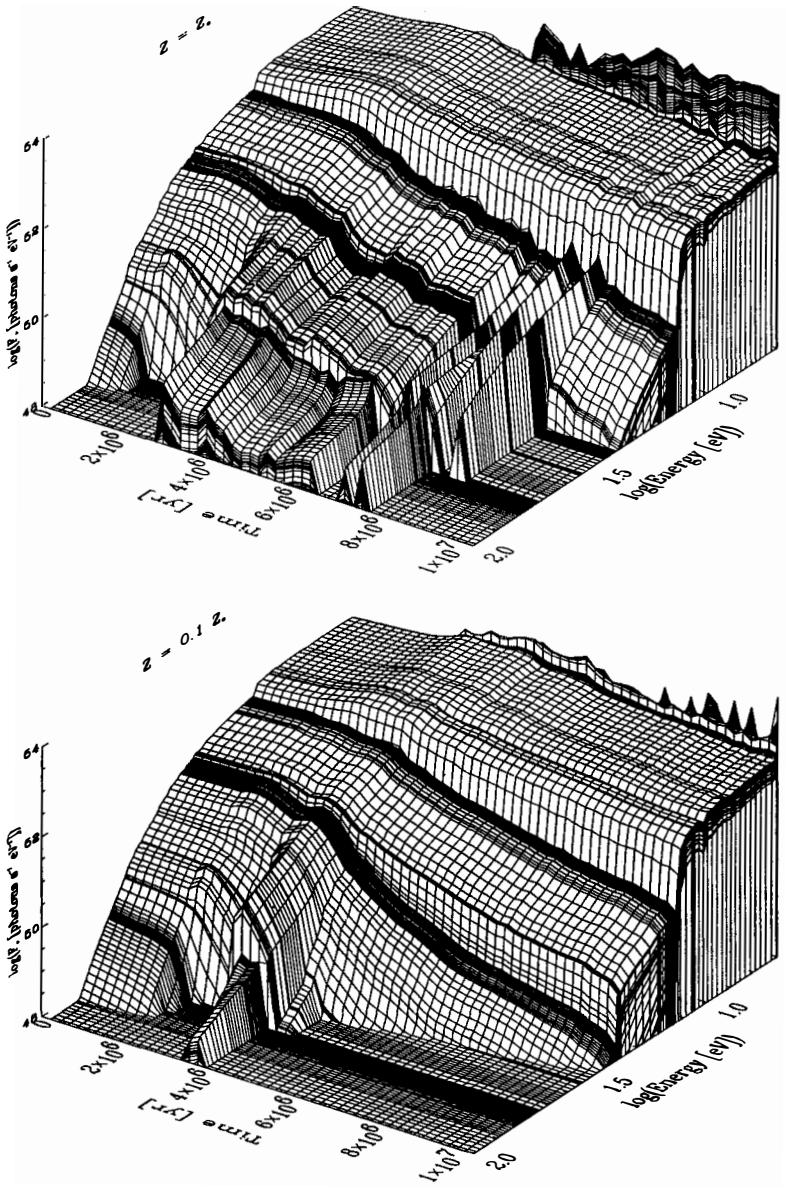

Figure 2. Three-dimensional representation of the computed spectrum. Plotted quantity is F_ν in photons $s^{-1}eV^{-1}$ versus time (from 0 to 10 Myr) and photon energy. Note the H^+, He^+, and He^{++} discontinuities at 13.6 eV, 24.6 eV, and 54.4 eV, respectively. The upper and lower parts are for $Z = Z_\odot$ and $Z = 0.1\ Z_\odot$, respectively. High flux levels above 24.6 eV indicate the presence of WR stars.

line ratios predicted by models with different U are above and to the right of the ratios observed in H II galaxies. Yet they are systematically too small to explain the observed [O III]/Hβ *and* [N II]/Hα ratios.

We also included in Figure 3 the line ratios following from the original *Warmer* model[2], *i.e.* using high T_{eff} and plane-parallel, static LTE atmospheres for WR stars but otherwise the same model parameters. Our new models predict line ratios which are typically lower by about a factor of 2. A quantitative comparison of the original *Warmer* emission-line spectrum with observations by[2] implied that AGN spectra might be understandable in terms of photoionization. Significant nitrogen overabundances had to be invoked to explain the observed [N II] line strengths. In principle large amounts of nitrogen can be released via processed material in massive stellar winds. However, high star-formation efficiencies in excess of 50% are required to process sufficient hydrogen into nitrogen within a few Myr[2]. Theoretical considerations[13] suggest efficiencies of less than 5%. The starburst scenario for AGN's becomes even harder to explain with the lower line ratios of the new models.

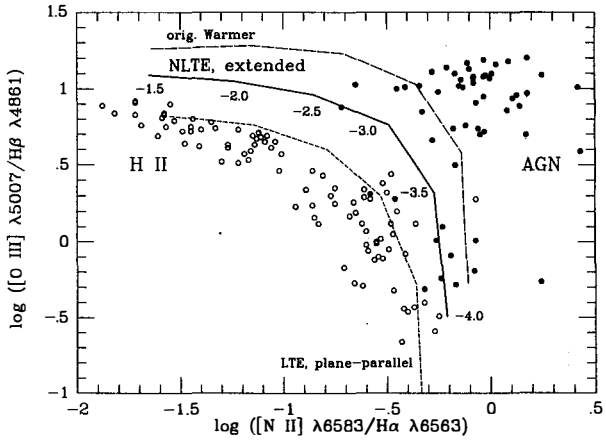

Figure 3. [O III]λ5007/Hβ *vs.* [N II]λ6584/Hα. Observations of Seyfert2's and LINER's (full dots) are from[28], H II galaxies (open dots) are from[34]. The solid line represents the results of our new models for various values of U. For comparison, the long-dashed line gives the corresponding results of the original *Warmer* model[2], and the short-dashed line is based on the latest evolutionary models[18] but with traditional model atmospheres[12]. ($Z = Z_{\odot}, n = 10^4 cm^{-3}$)

The dashed line in Figure 3 indicates the line ratios which result from the latest evolutionary models[18] but with classical, static LTE atmospheres[12] and black bodies for WR below and above $T_{eff} = 50,000\ K$, respectively. The theoretical line ratios coincide with the values of H II galaxies. This is immediately understandable. These models are a good approximation for hot stars with moderate mass loss (like OB stars). Since WR and O stars coincide in their observed positions in the HRD[14], photoionization models for WR stars without extended atmospheres simply produce spectra similar to those of classical H II regions. The offset between the solid and dashed lines is entirely due to the influence of the model atmospheres.

We studied the consequences of varying Z and n on the theoretical line ratios. It is found that the parameters used in Figure 3 are most favorable for the *Warmer* scenario.

The combination of abundance effects on the line strengths and radiative losses on the electron temperature produces [O III] and [N II] strengths which disagree more with the observed values of AGN's if $Z \neq Z_{\odot}$ or $n \neq 10^4 cm^{-3}$.

Other lines studied (*e.g.* He IIλ4686) give the same result as [O III] and [N II]: *Warmer* spectra generally display higher excitation than H II regions photoionized by O stars. However, the agreement with observed values of AGN's is marginal at best.

IMPLICATIONS FOR THE WARMER MODEL

Our results suggest that photoionization by thermal radiation from hot stars in a starburst can probably not account for the UV continuum and the emission-line spectrum observed in AGN's. Choosing the most favorable parameters for the *Warmer* scenario ($Z = Z_{\odot}, n = 10^4 cm^{-3}, t = 3.3\ Myr$) leads to emission-line ratios which are marginally consistent with observations. However, even slight modifications of the 'optimum' parameter set produces line strengths which differ vastly from those typically observed in AGN's.

There are indications that at least in some starbursts the upper cut-off mass of the IMF is as low as $M_{up} \approx 30\ M_{\odot}$ [11,24]. If this value of M_{up} applies to starburst galaxies in general, the *Warmer* scenario can essentially be ruled out since WR stars as the prime source of hard UV photons almost exclusively evolve from stars above 30 $M_{\odot}$.

Although WR stars have $T_{eff} < 100,000\ K$ during most of their lifetime in the models, they reach $T_{eff} \approx 150,000\ K$ for a short period ($10^4 yr$) at the endpoint of their evolution. This phase is far too short to be detectable in the synthetic spectrum. A few objects having such high temperatures may exist in galaxies of the Local Group, and their existence has been taken as proof of the *Warmer* scenario[31]. However, both evolutionary models and empirical stellar statistics suggests that these objects are not numerous enough to produce significant quantities of hard UV photons. It is not even clear that these hot objects are related to evolved, massive single stars. They might as well be a consequence of peculiar binary evolution where stellar surface layers are stripped of by gravitational forces. The frequency of such systems would be rare in any case.

We restricted our study on the spectrum produced by a *Warmer* at $t = 3.3\ Myr$. There may be other aspects which pose potential problems for the starburst hypothesis of AGN's[8]. From our new stellar models alone we conclude that the *Warmer* scenario is more difficult to maintain than it has been on the basis of older evolutionary and atmospheric models.

Acknowledgements R. Gruenwald and W. Schmutz acknowledge support by the Visitor Fund of STScI. Support for this work has also been provided by the Director's Research Fund of STScI.

REFERENCES

1) Baldwin, J. A., Phillips, M. M., & Terlevich, R. 1981, PASP, 93, 5
2) Cid-Fernandes Jr., R., Dottori, H. A., Gruenwald, R. B., & Viegas, S. M. 1992, MNRAS, 255, 165
3) Cowie, L. L. 1988, in The Post-Recombination Universe, ed. N. Kaiser, & A. N. Lasenby (Dordrecht: Kluwer), 1
4) Daly, R. 1990, ApJ, 355, 416

5) DeYoung, D. 1989, ApJL, 342, L59
6) Gruenwald, R. B., & Viegas, S. M. 1992, ApJS, 78, 153
7) Hamann, W.-R., & Schmutz, W. 1987, A&A, 174, 173
8) Heckman, T. M. 1991, in Massive Stars in Starbursts, ed. C. Leitherer, N. R. Walborn, T. M. Heckman, & C. A. Norman (Cambridge: Cambridge University Press), 289
9) Hillier, D. J. 1987a, ApJS, 63, 947
10) ——. 1987b, ApJS, 63, 965
11) Joseph, R. 1991, in Massive Stars in Starbursts, ed. C. Leitherer, N. R. Walborn, T. M. Heckman & C. A. Norman (Cambridge: Cambridge University Press), 259
12) Kurucz, R. L. 1979, ApJS, 40, 1
13) Larson, R. B. 1987, in Starbursts and Galaxy Evolution, ed. T. X. Thuan, T. Montmerle, & J. Tran Thanh Van (Paris: Edition Frontières), 467
14) Leitherer, C. 1991, in IAU Symposium 143, Wolf-Rayet Stars and Interrelations with Other Massive Stars in Galaxies, ed. K. A. van der Hucht, & B. Hidayat (Dordrecht: Kluwer), 465
15) Leitherer, C., Robert, C., and Drissen, L. 1992, ApJ, in press
16) Maeder, A. 1983, A&A, 120, 113
17) ——. 1987, A&A, 173, 247
18) ——. 1990, A&AS, 84, 139
19) ——. 1991, A&A, 242, 93
20) Melnick, J., Moles, M., & Terlevich, R. 1985, A&A, 149, L24
21) Netzer, H. 1989, in IAU Symposium 114, Active Galactic Nuclei, ed. D. E. Osterbrock, & J. S. Miller (Dordrecht: Kluwer), 69
22) Padovani, P., Burg, R., & Edelson, R. A. 1990, ApJ, 353, 438
23) Péquinot, D., Baluteau, J.-P., & Gruenwald, R. B. 1988, A&A,191, 278
24) Rieke, G. H. 1991, in Massive Stars in Starbursts, ed. C. Leitherer, N. R. Walborn, T. M. Heckman, & C. A. Norman (Cambridge: Cambridge University Press), 205
25) Schmutz, W. 1990, in Properties of Hot Luminous Stars, ed. C. D. Garmany (Provo: Brigham Young University), 117
26) Schmutz, W., Hamann, W.-R., & Wessolowski, U. 1989, A&A, 210, 236
27) Schmutz, W., Leitherer, C., & Gruenwald, R. 1992, PASP, submitted
28) Storchi Bergmann, T., & Pastoriza, M. G. 1991, PASP, 102, 1359
29) Terlevich, R. 1989, in Evolutionary Phenomena in Galaxies, ed. J. E. Beckman, & B. E. J. Pagel (Cambridge: Cambridge University Press, 149
30) ——. 1990, in Windows on Galaxies, ed. A. Renzini, G. Fabbiano, & J. S. Gallagher (Dordrecht: Kluwer), 87
31) Terlevich, R., & Melnick, J. 1985, MNRAS, 213, 841
32) ——. 1987, in Starbursts and Galaxy Evolution, ed. T. X. Thuan, T. Montmerle, & J. Tran Thanh Van (Paris: Edition Frontières), 393
33) ——. 1988, Nature, 333, 239.
34) Terlevich, R., Melnick, J., Masegosa, J., Moles, M., & Copetti, M. V. F. 1991, A&AS, 91, 285
35) Terlevich, R., Melnick, J., & Moles, M. 1986, in IAU Symposium 121, Observational Evidence of Activity in Galaxies, ed. E. Ye. Khachikian, K. J. Fricke, & J. Melnick (Dordrecht: Reidel), 499
36) Weedman, D. W. 1983, ApJ, 266, 479
37) Wesemael, F. 1982, ApJS, 45, 171

ACTIVE GALACTIC NUCLEI : NATURE OR NURTURE?

Suzy Collin-Souffrin
DAEC, Observatoire de Paris, Section de Meudon
92195, Meudon, France

ABSTRACT

Active Galactic Nuclei (AGN) are first presented from a phenomenological point of view, emphasizing their different "aspects" and discussing the proposed "Unifying Schemes". The central engine is then discussed in the framework of the "Accretion onto a Massive Black Hole Model". Possible fuelling mechanisms, the connection of AGN with starburst galaxies and their triggering by galaxy interactions, are briefly reviewed. Finally a scenario linking normal galaxies, quasars and local AGN is proposed.

1. INTRODUCTION

I found rather difficult the task of reviewing AGN in the context of this meeting on "Nature or Nurture?", first because it requires to describe these complex and not yet understood objects, and second because their link to normal galaxies is a matter of controversy.

The last three decades spent since the discovery of quasars and more generally of AGN have been mainly devoted to understanding how they work, the nature of the central engine and of its immediate surroundings, assuming they live in superb isolation. The problem of their link with either their host galaxies, or a fortiori with a more general environment, was almost not examined. This was partly due to the fact that observational studies concerning host galaxies failed to show any significant difference with normal galaxies not harboring an active nucleus. There is indeed more than six orders of magnitude from the size of the galaxy to the gravitational sphere of influence of the black hole, and about ten orders of magnitude to that of the black hole. Consequently the lack of influence of the active nucleus did not appear too astonishing, although it was clear for a long time

that the radio structure at very large scales of megaparsecs is tightly connected with that of the compact radio source lying in the nucleus at scales of one parsec. And it is only these last few years that the relation between AGN and their galactic environment begins to be seriously questioned, both from a theoretical and from an observational point of view.

My intention is not to give here a well documented and exhaustive review of the subject, but only to discuss very qualitatively the present "state of the art" concerning AGN, and emphasize several problems. I will also not refer to published papers, except to a few seminal ones, because they would be obviously too many of them. In the next section, I will present AGN from a phenomenological point of view, with the aim of showing that an unifying principle underlies the various classes of AGN. In Section 3 this principle is identified with the accreting black hole, and fuelling mechanisms are discussed, with an emphasis given onto the starburst connection and interactions between galaxies. Finally in the last section cosmological evolution of AGN is briefly sketched, and a suggestion for a consistent picture is tentatively made.

2. A PHENOMENOLOGICAL VIEW OF AGN

2.1. A question of semiotics

Before any discussion, let us define what is an AGN. According to Heckman (1990): "By "activity" I mean luminosities that are significantly larger and/or high energy phenomena that are significantly stronger than could be sustained over a Hubble time by a normal population of stars". This definition includes not only classical AGN (quasars and Seyfert nuclei) whose properties require the presence of a supermassive black hole (although this point is controversed by Terlevich and Melnick, 1985, and subsequent papers), but also starburst galaxies. My definition, admitted by people studying quasars and Seyfert nuclei, is restricted to objects exhibiting **at least one** of the following phenomena, all being very ill-defined, owing to the heaviness of old observational techniques:

1. a "stellar", i.e. smaller than one arc second, very bright nucleus; clearly this definition corresponds to distant-dependent dimension and power; for instance a dimension of a few tens pcs and a luminosity of at least 10^{43} ergs s^{-1} in nearby galaxies, a dimension of a few kpcs and a luminosity of 10^{48} ergs s^{-1} in high redshift quasars;
2. a "non-thermal" continuum spanning a large wavelength range from radio or infrared up to X-rays; this definition is in fact obsolete, since there are increasing pieces of evidence that a large fraction of the infrared, visible, ultraviolet, and perhaps also X-ray continuum, is of thermal origin: a "non stellar" continuum would now be a better definition;
3. broad spectral lines, with Full Width at Half Maximum ranging from a few 10^2 km s^{-1} for the narrowest (called in fact "Narrow Lines") to 10^4 km s^{-1} (the ones called "Broad Lines"), implying high velocity bulk motions;

4. rapid variations of the continuum, especially in the X-ray range, implying a small size;
5. a compact (parsec scale) and powerful radio core.

With such a definition, optically selected starburst galaxies are excluded, but not necessarily ultraluminous far infrared (FIR) galaxies, which sometimes display broad lines in the infrared range.

2.2. The "zoo" of AGN

It is difficult to give a logical description of all classes of active objects: their taxonomy is mainly historical, and was the result of detection techniques and of observational bias linked with the distance. Even trying to classify AGN by order of "decreasing activity" is quite subjective. Moreover it is interesting to note that almost all classes of objects are shared into radio loud and radio quiet objects. One can then distinguish:

1. An ensemble of objects displaying all the above-mentioned characteristics (for the radio louds):
   - type 1 Seyfert nuclei, which are nearby radio quiet objects located in giant spiral galaxies;
   - Radio quiet quasars, whose host galaxies seem to be giant spirals;

and their radio loud counterparts:

   - Broad Line Radio Galaxies (BLRG), which are strong radio sources, and always giant elliptical galaxies;
   - Radio loud quasars, whose host galaxies seem to be giant elliptical.

It is commonly admitted that radio quiet (respt. radio loud) quasars are very luminous Seyfert 1 (respt. BLRG) located at large distances, although the difference may be more subtle (cf. later).

2. An ensemble of objects whose line spectrum is made only of "narrow" lines, and with a weak or absent non-thermal continuum:
   - type 2 Seyfert nuclei, which are nearby radio quiet objects located in giant spiral galaxies
   - and their radio loud counterparts Narrow Line Radio Galaxies (NLRG), which are strong radio sources, and always giant elliptical galaxies; among them one finds low radio luminosity (FRIs) and high radio luminosity (FRIIs) galaxies.
   - FIR ultraluminous galaxies with a luminosity of the order of 10^{45} ergs s^{-1} may well be members of AGN, since they display sometimes broad infrared lines, although they do not have a non resolved stellar nucleus, as all previous objects.

3. Finally an ensemble of highly variable objects characterized by intense radio and X-ray emissions and a strongly variable and highly polarized continuum; among them, BL lac have weak or absent emission lines; the others constitute the class of blazars.

Many of these objects display a non spherical structure: a radio jet with a relativistic bulk motion (in particular in superluminal sources), an extended emission line region (when resolved) with a conical distribution. Theoretically (cf. later), one infers also the presence of an accretion disk. These facts strongly suggest axial symmetry. This leads to the idea that orientation should play a role in the observed properties of AGN, and to the so-called "Unifying Schemes".

2.3. The Unifying Schemes

- First Unifying Scheme

The first Unifying Scheme was proposed to explain BL lac objects and Blazars: these objects are assumed to be AGN seen very close to the direction of the relativistic jet (within an angle smaller than 10°). Their synchrotron emission is thus relativistically boosted, while the other more isotropic emissions (thermal continuum and lines) are not amplified and are weak compared to the non-thermal emission. This assumption has been recently more precisely stated by testing the morphology, the luminosity function and the overall spectrum of these objects. The conclusion is that the non boosted counterpart of BL lac is probably FR1 radiogalaxies, while that of more luminous blazars is FRII radiogalaxies.

- Second Unifying Scheme

Once the importance of the viewing angle is established for BL lac and Blazars, one should ask wether there are other manifestations of the viewing angle. A second unifying scheme was proposed by Antonnucci and Miller (1985) for Seyfert 2 and Seyfert 1, and later extended to radio loud quasars and radiogalaxies. These authors discovered that the spectrum of the archetypal Seyfert 2 galaxy NGC 1068 displays broad lines in polarized light. They proposed that NGC 1068 contains a Seyfert 1 nucleus, whose central emission (non thermal continuum and broad lines) is hidden from our view by an absorbing molecular and dust "torus" with an opening angle of about 45°, and is reverberated in the direction of the observer by a scattering hot medium. They suggest that this scheme may apply to all Seyfert 2 galaxies. Barthel (1989) made then the suggestion that strong radio galaxies could be the counterparts of radio loud quasars, when viewed "edge on", i.e. in the direction of the torus. Since the torus has an opening angle of about 45°, it would mean that about half of the radio loud quasars would have their central engine hidden from our view. Going one step further, Barthel also suggested that superluminous FIR galaxies could be the counterparts of radio quiet quasars (cf. Figure 1).

Many observations have been invoked in favor of this picture: the existence of an extended emission region with a conical structure and/or aligned with the radio axis, often implying a higher level of ionization than computed if the central continuum would be emitted isotropically, the existence of polarized light in extended regions of radiogalaxies, etc....

But the most important proof in my opinion is the lack of influence of the nuclear radiation on the surrounding galaxy. The central UV-X radiation is indeed so strong that logically it should

heat and ionize the gas of the galaxy, and blow it away through strong induced nuclear winds. The best explanation for this lack of influence is that the central radiation is blocked into the nucleus by an absorbing shell or torus over a large opening angle. And indeed the discovery of strong spatially unresolved emission of CO and H_2 in Seyfert 1 and Seyfert 2 galaxies indicate that the nucleus contains an amount of molecular gas often larger than 10^8 M_O, comparable to the whole mass of the nucleus, while on the contrary the ionized fraction of nuclear gas is surprisingly small, only $1M_O$ in the Broad Line emitting region, and 10^4 to 10^6 M_O in the Narrow Line emitting region, whose dimension is of the order of the whole nucleus.

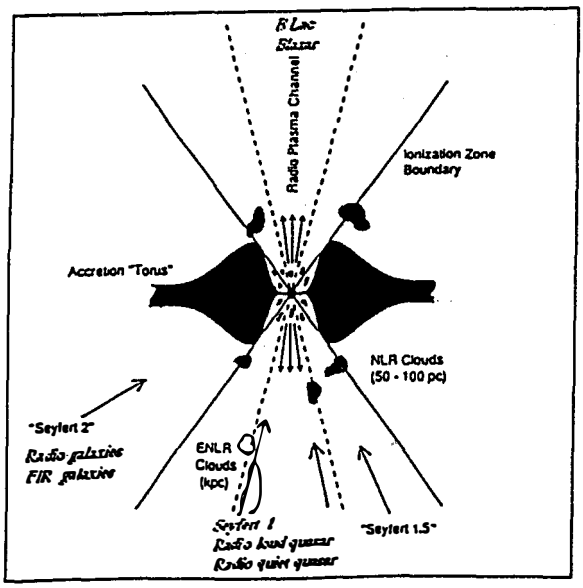

Figure 1: The Unified Schemes, after Pogge (1989).
Some changes (in italics) have been introduced by the author.

This second unifying scheme is however controversial. Several important problems are not solved, for instance the fact that there are **intrinsic** differences between Seyfert 1 and Seyfert 2 which cannot be attributed to the orientation. The last ones have a higher FIR and molecular luminosity, as if they were displaying starburst activity. Another problem is that many Seyfert 2 do not show broad polarized lines, while they have an excess of blue continuum, which can also correspond to an enhanced starburst activity. So the picture which may finally prevail in the future is that Seyfert 2 are indeed Seyfert 1 whose line of sight crosses a molecular torus, but the torus is more massive than in Seyfert 1, owing to an enhanced starburst activity. There are also several problems in the unification between radiogalaxies and radio loud quasars (alignements of the line emission regions for instance), and between ultraluminous FIR galaxies and radio quiet quasars.

Here also one gets the impression that **AGN span a large range of starburst activity.** The following question is now whether the **underlying fundamental principle governing these objects is overlaid by some intrinsic difference in starburst activity, linked with an evolutionary process,** as it would be the case if Seyfert 2 (respt. ultraluminous FIR galaxies) are recently formed Seyfert 1 (respt. radio quiet quasars), in which a large molecular mass connected with nuclear starburst activity is still present.

According to these unifying schemes however the difference between radio loud and radio quiet objects is still not unserstood. Except in radio properties, radio loud and radio quiet quasars do not differ in any respect, but the host galaxies of radio loud quasars seem more likely to be elliptical than spiral galaxies. Elliptical galaxies contain less gas than spiral galaxies. It is therefore possible that the relativistic jet is blocked in a small volume by a denser environment in spiral galaxies, so on one hand self-absorption inhibites the synchrotron emission, and on the other hand the jet cannot fuel the radio lobes. Clearly, to understand the difference between radio loud and radio quiet objects, it is necessary to understand the difference between spiral and elliptical galaxies.

3. HOW ARE AGN ENERGIZED?

3. 1. The theoretical view of AGN

We have seen that all AGN can be considered as objects displaying a broad and powerful non stellar continuum, having a small size and a privileged direction. I shall not discuss why these properties are commonly attributed to **accretion onto a supermassive black hole** (Rees, 1984). Note however that an alternative "pure starburst" model is proposed by Terlevich and Melnick (1985 and more recent papers), but that at the present time it is not able to account for radio loud quasars and blazars.

To facilitate the discussion let us recall the value of some basic parameters.

- the gravitational radius R_G:

$$R_G = \frac{2GM}{c^2} = 3\,10^{13}\,M_8 \text{ cm} \qquad (1)$$

where M_8 is the black hole mass expressed in $10^8\,M_\odot$

- the Eddington Luminosity:

$$L_{Edd} = 1.3\,10^{46}\,M_8 \text{ erg s}^{-1} \qquad (2)$$

- the efficiency for mass-energy conversion, $\eta \sim 0.1$ (0.05 for a non rotating black hole, and 0.4 for a maximally rotating Kerr black hole)

- the accretion rate:

$$\dot{M} \sim 1.8\,\left(\frac{\eta}{0.1}\right)^{-1}\left(\frac{L_{bol}}{10^{46}}\right) M_\odot \text{ yr}^{-1} \qquad (3)$$

where L_{bol} is the bolometric luminosity

- the life time (given by the size of radio sources, the proportion of S1 and S2, etc...) $\geq 10^7$ yrs
- finally the e-folding time of growth of a black hole with an Eddington limited accretion rate $\dot{M}_{crit} = L_{Edd}/\eta\, c^2$:

$$\tau = \left(\frac{\eta}{0.1}\right)^{-1} 4\ 10^7 \text{ yrs} \qquad (4)$$

An accretion rate of at least one $M_o\ yr^{-1}$ on a $10^8\ M_o$ black hole is therefore required to account for the luminosity of a modest quasar. This amount of matter should necessarily be in gaseous form, in order to be able to radiate efficiently before feeding the black hole. The accretion should persist for periods of 10^8 years, which means that a total mass of fuel of $10^8\ M_o$ is involved. Where is then found the gas necessary to fuel the black hole?

First proposed fuelling mechanisms were based on the idea that the black hole should receive its gas from the nucleus itself. Tidal disruption of stars were very early proposed (Hills, 1975). This mechanism has to overcome the problem of replenishing the loss cone, and moreover it works only for modest black hole masses ($< 3\ 10^8$ Mo) and consequently for modest luminosities. For higher black hole masses, main sequence stars are swallowed as a whole without emitting any radiation. This mechanism has been revitalizied recently in the framework of galaxy merging, which can boost the tidal disruption (Roos, 1985). Star collisions were also invoked. To be efficient, this mechanism implies the presence of a preexisting dense star cluster inside the nucleus ($10^9\ M_o\ pc^{-3}$).

Then stellar mass loss from the host galaxy was suggested, but a very high mass loss rate is required, not consistent with a galactic stellar population.

Finally it was put forward that the gas fuelling the nucleus should be of external origin, from infall of intergalactic gas or accretion of gas rich galaxies (Gunn, 1979). The status of the problem has strongly evolved this last decade, with increasing evidence that host galaxies of active nuclei have more often than inactive galaxies a distorted morphology indicating a recent interaction with another galaxy.

But if the reservoir of fuel is distributed on a galactic scale of 10 kpc, it means that the material must contract by 8-10 orders of magnitude to reach the black hole horizon! The problem is thus to get rid of the angular momentum.

Through viscous transport mediated by turbulent viscosity, an accretion disk is a powerful tool for both extracting angular momentum and dissipating energy which is radiated as UV and soft X-ray continuum (Shields, 1978). There are numerous observations supporting the existence of an accretion disk: not only the observation of jets and cones strongly suggests an axial structure, but the intense smooth UV and soft X-ray continuum emitted by AGN is difficult to account otherwise (Collin-Souffrin, 1992). Moreover, recent X-ray observations of AGN prove the existence of a relatively cold medium reverberating a hard X-ray "primary" continuum, and the disk is a very likely structure for this process. However there is now increasing evidence that turbulent viscosity is not

the only mechanism at work in these accretion disks: for instance magnetic stresses transmitted outside the disk by linkage through a magnetized corona or a wind may be an efficient process, and can account for an intense X-ray emission which could be ultimately reprocessed as UV radiation.

Unfortunately the accretion disk is a viable mechanism only on scales smaller than about 10^4 -$10^5 R_G$, typically 0.1 pc in a Seyfert galaxy, because:

1. at larger distances the inflow time scale (the "viscous time") is too long. For instance in a "thin viscous disk", i.e. a disk where the scale height to radius ratio H/R is much smaller than unity (these disks are often advocated for accretion rates smaller than $\dot{M}_{crit}$), the viscous time is equal to:

$$t_{visc} = \frac{R^2}{\alpha\, c_s\, H} \sim 10^{-2}\, \alpha^{-0.5}\, \eta_{-1}^{0.4} \left(\frac{f_{Edd}}{0.1}\right)^{0.4} L_{46}^{1.2} \left(\frac{R}{RG}\right)^{1.9} \text{yr} \qquad (5)$$

where α is the so-called viscous parameter, close to unity, c_s is the sound speed, L_{46} is the luminosity expressed in 10^{46} erg s^{-1}, and f_{Edd} is the Eddington ratio L_{bol}/L_{Edd}. The viscous time is larger than the Hubble time for $R/R_G \sim 10^6$.

2. the disk becomes locally and globally gravitationally unstable, leading to fragmentation and probably to star formation.

At larger distances, the mechanism by which matter is transported is poorly understood. Several suggestions have been made for the different scales into consideration.

At scales where the disk becomes unstable, it was suggested that gravitational instabilities lead to the formation of gaseous clouds, whose collisions provide a high viscosity and maintain the disk in a marginally self-gravitational situation (Lin and Pringle, 1987). It was also proposed that self-gravitating disks, trailing spiral density waves triggered by non axisymmetric gravitational instability, lead to efficient angular momentum transport (Lin, Pringle and Rees, 1988) . These mechanisms were included in a more general picture of the accretion process at large distances (Begelman, Frank and Shlosman, 1989). These authors proposed that the first mechanism is working at intermediate scales (0.1 to 1 pc), and that at larger scales, up to one kpc, the inflow is driven by global non axisymmetric gravitational instabilities, such as bars provided by tidal interactions and mergers (cf. Figure 2).

Finally, for larger scales, 100 pc - 10 kpc, the subject has been given a great deal of progress by Hernquist (1989) who appealed to numerical simulation, using an hybrid N-body / hydrodynamics code. He showed that the tidal field of a companion galaxy during a merger can drive a mass of gas larger than 10^9 $M_\odot$ into the central hundreds parsecs of the largest galaxy, in a time scale of the order of 10^8 years. This should lead to the formation of a nuclear starburst which can further contract to scales of 1-10 pc through one of the previous mechanisms.

If the density of the starburst cluster has reached this high value within a time smaller than its evolution time scale (10^8 years), its interaction with the black hole can well account for the AGN phenomenon. Supernova explosions will lead to the creation of shocks in a highly pressured

medium, whose cooling through inverse Compton process will lead to the formation of large velocity cold clouds responsible for the broad line emission (Perry and Dyson, 1985). On the other

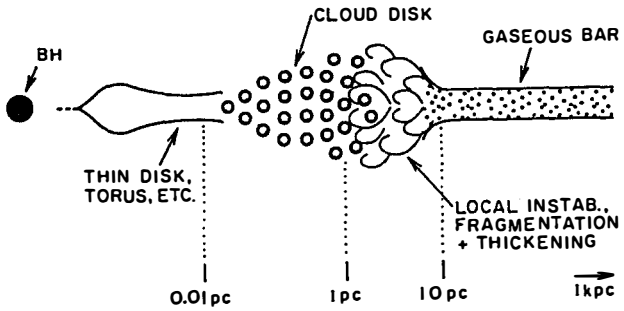

Figure 2: The different mechanisms leading to a radial flow in AGN, after Begelman, Frank and Schlosman (1989)

hand, the evolution of the star cluster towards post main sequence stars gives a large mass loss rate, able to feed the black hole at the required amount during about 10^8 years and also to provide the broad line emitting region (Norman and Scoville, 1988). For very extreme values of the mass of the initial star cluster (10^{10} $M_\odot$), this process can even lead to the growth of the black hole itself.

3.2. Are there observational evidences that AGN are triggered by galaxy interactions?

The reader is invited for this part to read Heckman's reviews (1990, 1991). The subject is also discussed in K. Borne's talk at this meeting.

Although a concensus was reached some years ago on the idea that nuclear activity is observationally connected with galaxy interactions, there is now increasing evidence that the case is not so simple, and that interactions are probably more tightly linked with nuclear starburst activity than with AGN. Let us review briefly observations of the host galaxy and the galaxy environment.

1. Seyfert galaxies.

The fact of whether Seyfert galaxies are or are not interacting galaxies is quite controversial. Nevertheless some important results can be considered as definitively acquired:

- Seyfert 2 galaxies have more often a companion than Seyfert 1 (remember that they have also a higher starburst activity)

- the connection of activity with interaction rises at large redshifts, or alternatively at large luminosities

- a large fraction of AGN host galaxies display a peculiar morphology (amorphous structure, rings, boxes, ovals, bars...), characteristic of a post merging or interacting state.

2. Radiogalaxies

FR1 radio galaxies present an average galaxy density 2-3 times larger than for comparable elliptical radio quiet galaxies.

FR2 radio galaxies, which are generally located at large distances, are associated with an emission nebula, making difficult the study of the parent galaxy morphology. Nevertheless, one finds:

- a very large incidence of distorted structures, with perturbed dynamics
- very blue colors, which can be due either to young stars, or to a scattered AGN continuum, according to the Unifying Scheme
- strong infrared and molecular emission, possibly also due to starburst activity

3. Quasars

Radio loud quasars have characteristics very similar to FR2 radiogalaxies: they have a distorted morphology, an intense molecular and FIR emission, and are associated with extended line emission regions, most probably ionized by the nuclear radiation.The results concerning radio quiet quasars are not so clear.

A last important result is that interacting galaxies have FIR, molecular, and radio emissions comparable to starburst galaxies.

This set of observations, plus the results mentioned at the end of Section 2, tend to prove that, at least for local AGN:

- the more interacting, the more starburst activity
- there is a clear connection between nuclear starburst activity and AGN in at least a fraction of AGN (Seyfert 2 galaxies, possibly ultraluminous FIR galaxies and radiogalaxies)

In summary the following evolutionary scheme is observationally acceptable:

interaction and merger ⇒ nuclear starburst activity ⇒ AGN

From a theoretical point of view it is also satisfactory. However, unless the star cluster reaches a very high density in less than 10^8 years, the AGN phenomenon requires the presence of **a preexisting black hole** with a mass of at least 10^7 $M_\odot$, necessary to power a Seyfert galaxy. In the next section we shall examine this possibility.

4. COSMOLOGICAL EVOLUTION OF AGN

4.1. Luminosity function

Over the past few years, observers have determined how the luminosity function of quasar evolves back to $z \sim 4$. The luminosity function has a shape almost invariant with redshift, and can be parametrized by a two power-law form, with a steep slope at the high luminosity end, and a flatter slope at the faint end. The "break" occurs at a luminosity which increases with the redshift. The similarity of the luminosity functions of distant quasars and local Seyfert strongly suggests a pure luminosity evolution; i.e. the number of AGN is constant, but their integrated luminosity decreases with time by about two orders of magnitude from $z = 2$ to $z = 0$. This strong evolution does not continue beyond $z = 2$. The most astonishing recent result is that the comoving space density of AGN does not seem to decrease between $z = 2$ and $z = 4$, implying a very early epoch of quasar formation.

4.2. Comoving mass density of quasars

If quasars and AGN are fuelled by accretion onto massive black holes, it is possible to determine the total mass accumulated in black holes per covolume unit, using the observed quasar counts (Soltan, 1982):

$$M_{BH} = \frac{1}{\eta c^2} \frac{4\pi}{c} \int dz(1+z) \int dS \; S \; n(S,z) \qquad (6)$$

where S is the observed flux and n(S,z) the observed differential quasar count number.

This method does not depend on any assumption on H_0 and q_0, nor on the rate at which black holes are accreting (their Eddington ratio must not be specified). For $\eta = 0.1$, Soltan found a density of about $5\ 10^{13}\ M_0\ Gpc^{-3}$. This value is increased to $2\ 10^{14}\ M_0\ Gpc^{-3}$ by more recent determinations (Padovani et al, 1990). The mass is dominated by quasars at an average redshift of about 2 and at the break of the luminosity function, $L = 10^{45}$ ergs s^{-1}, i.e. quasars with a mass of a few $10^7\ M_0$. The problem is to find out how this mass is distributed among galaxies in the local Universe and which proportion of time this mass is spending in an "active phase".

A very natural explanation for the similarity of the luminosity functions of local Seyfert galaxies and high redshift quasars would be that each quasar has dimmed down monotonically, giving rise to a less luminous AGN, namely a Seyfert galaxy. In this case Seyfert galaxies should harbor all black holes required to account for the past quasar luminosity. However this explanation does not hold, both because it would imply extremely large masses in the nuclei of local AGN (10^{11} M_0 or more), which are not observed, and because the total mass density of local AGN, which should be equal to the covolume mass density of past quasars, is much smaller, as shown below (Cavaliere and Padovani, 1988, 1989).

4.3. Mass density of black holes in local Seyfert galaxies

The mass of individual black holes can be determined, either by fitting AGN continua in the near UV range with accretion disk emission, or by a dynamical method, amounting to studying the velocities in the broad line region and assuming that it is near gravitational binding. Both methods are very uncertain but they give about the same result: the mass of local AGN, with $L_{bol} \leq 10^{45}$ ergs s^{-1}, is about one order of magnitude smaller than the mass of high luminosity quasars, with $L_{bol} \sim 10^{47}$ ergs s^{-1}. In other words the Eddington ratio L_{bol}/L_{Edd} is smaller in Seyfert than in quasars (it is close to unity for quasars, which corresponds to the average quasar mass given in 4.2.). It is difficult to disentangle the influence of redshift and luminosity in these studies, but at least one does know that the Eddington ratio is a few 10^{-2} in local Seyfert galaxies.

The total mass of black holes in AGN per unit volume in the local Universe can then be computed using these Eddington ratios and scaling them with the luminosity function of Seyfert galaxies. This mass is found smaller than the quasar mass by at least two orders of magnitudes. It means that **99% of the mass of past quasars should be archived in nuclei of inactive galaxies.**

Another way of reasoning is to consider the different possible activity patterns in relation with the local Eddington ratio or L/M value. Since statistically the luminosity decreases with time, while the mass goes on increasing, the longer the activity lasts in each nucleus the smaller will be L/M locally. On this basis Cavaliere and Padovani showed that the local Eddington ratio is compatible only with a short lived activity (cumulated time $\sim 10^8$ years), implying that a large fraction of galaxies with $L \geq L_*$ have been involved in the activity process and should contain a massive black hole.

4.4. Mass of black holes in inactive galaxies

This result is confirmed by recent dynamical studies of nearby galaxies which show the presence of large non-luminous mass concentrations $\sim 10^7 - 10^8$ M_o, in the nuclei of inactive galaxies such as M31 and M32, or even of larger masses $\sim 10^9$ M_o in some elliptical galaxies. The Galactic centre may be an exception. The fact that this mass is in the form of a black hole and not in a star cluster is not confirmed, but there are strong hints for this to be the case. For instance in the central parsec of M31 (Kormendy, 1988):

1. the L/M ratio is larger than 100, which is very uncommon for a star population
2. the time for collapse of such a dense star cluster would be smaller than the life time of the galaxy.

By scaling these central masses with the luminosity function of normal galaxies, Cavaliere et Padovani (1989) derived the mass distribution of black holes hosted by normal galaxies. Adapted from their results, the mass distribution of the central mass is:

$$N(M) = \frac{10^{13}}{M^2} \qquad M_o^{-1}\ Gpc^{-3} \qquad (7)$$

where M is the mass of the hole expressed in solar mass and N(M) the number density of holes per

mass interval also expressed in solar mass.

This leads to the following important results.

- First the integrated mass is ~ 6 10^{13} M_o Gpc^{-3}, and more probably ~ 2 10^{14} M_o Gpc^{-3} to take into account the faint and high ends of the mass distribution. This mass is equal to the total comoving black hole mass at z ~ 2.
- Second the average individual black hole mass is equal to 3 10^7 M_o, which is also in agreement with the average quasar mass at z ~ 2.
- Finally this average mass is also equal to the average mass found from the Eddington ratios in Seyfert nuclei.

4.5. Physical mechanisms governing the formation and evolution of quasars

One can ask whether the **formation** of quasars takes place through the same physical mechanisms as their subsequent **evolution**.

There is actually a problem, in particular for the $z \geq 4$ quasar population discovered recently. The age of Universe at z ~ 5 is less than 10 times the e-folding timescale of a black hole, so black holes would not have sufficient time to grow from stellar mass. In a recent scenario proposed by Rees (1992) in the framework of Cold Dark Matter (CDM), 10^8-10^9 M_o accumulate very rapidly in a free-fall time (10^7 yrs) at high redshifts (z>5) in the central few pcs of deep potential wells of dark matter halos. This matter then falls in an almost spherically symmetric flow inside a seed black hole with a very small efficiency η, due to radiation trapping. This low efficiency corresponds to a very high critical accretion rate (cf. Equation 4), and therefore to a very small e-folding time. A crucial problem in this model is to get rid of the angular momentum of the infalling material in the first phase, for instance by intense star formation which maintains a high viscosity. If the angular momentum is still large, then a highly supercritical accretion rate can also be mediated by a "thick disk", but the dynamical stability of these disks - and consequently their existence - is not proved.

Concerning the evolution of quasars, a requirement for any scenario is also to account for the evolution of the luminosity function at $z \leq 2$. The above mentioned CDM scenario proposed by Rees is a viable mechanism in this context (Haehnelt, 1992). Although smaller halos form first in this hierarchical scenario, their higher density leads to the earlier formation of more massive black holes, and therefore to the decrease of quasar luminosity with time.

It is also possible that the most powerful radiogalaxies and radio loud quasars are fuelled by "cooling flows", i.e. regions of hot X-ray emitting gas found at the centers of clusters of galaxies, with a cooling time shorter than the Hubble time (Fabian et al, 1988 and subsequent papers). In this scenario, the active merger rate of clusters at past epochs, which leads to the disruption of the intracluster gas, could be responsible for switching off these sources. However this mechanism would not apply to radio quiet quasars.

A last possibility, which may be the most promising, is that once the first generation of high redshift quasars is formed and has faded in a short time scale, owing to the exhaustion of fuel, reactivation by the [merger - starburst - AGN] mechanism begins to take place at a rate which is decreasing with time, owing to the decrease of merger rate. We have seen indeed that at low redshift there is a clear connection between galaxy interactions, starbursts and AGN. Although the connection is not so clear in high redshift AGN, owing to observing difficulties, it seems nevertheless present, and in particular the link of AGN with galaxy interactions increases with redshift. This scenario needs however to be quantified and its results compared to the luminosity functions. In particular it would probably imply a mixed density and luminosity evolution of AGN, which, according to our present knowledge, is not excluded.

To summarize this section:

- Seyfert and quasar activity is a short lived phenomenon ($< 10^8$ years)
- a large fraction of galaxies harbor a massive black hole, whose average mass (a few 10^7 M_o) is equal to the z=2 quasar average black hole mass and to the average black hole mass of Seyfert galaxies
- these black holes are built at a redshift > 2 in a very small time scale.
- they can be reactivated by interaction and merging.

5. CONCLUSIONS

The accreting black hole is a very good working model. According to the Unifying Schemes, it can account for many classes of objects. However, it is highly probable, both from theoretical and from observational considerations, that a pure black hole model is not sufficient, and the additional ingredient of a nuclear starburst, triggered by galaxy interaction and merging, should also be taken into account.

These results can be linked to cosmological evolution in the following tentative scenario.

Massive black holes grow at high redshifts ($z \geq 4$) in a large fraction of protogalaxies, according for instance to a "à la Rees" scenario. When they are massive enough, they begin to radiate and constitute a first AGN (quasar) phase culminating at $z \sim 2$-4. This phase stops rapidly (in 10^8 yrs) in a given object, but lasts for a few 10^9 yrs as a whole. These black holes can be reactivated through interactions or mergers which trigger a nuclear starburst activity. When there is a preexisting massive black hole in the starburst nucleus, as is it should be the case for a majority of L_* galaxies, it will evolve into an AGN. This mechanism gives rise to the local (Seyfert) AGN activity. Note that in this scenario, not all galaxy interactions and starburst galaxies lead to an AGN.

ACKNOWLEDGMENTS

I am grateful to J. Frank and M. Joly for reading the manuscript and suggesting improvments.

REFERENCES

- Antonucci, R.R.J., Miller J.S., 1985, ApJ 297, 621
- Barthel, P.D., 1989, ApJ 336, 606
- Begelman M.C., Frank J., Shlosman I., 1989, in the proceedings of the meeting held at Garching, "Theory of Accretion Disks", Eds. Meyer, Duschl, Frank, Meyer-Hofmeister, NATO ASI, p. 373
- Collin-Souffrin S., 1992, in the proceedings of the meeting held in Maryland, "Testing the AGN paradigm", Eds.Holt, Neff, Urry, AIP, p. 119
- Cavaliere, A., Padovani P., 1988, ApJ 333, L33
- Cavaliere, A., Padovani P., 1989, ApJ 340, L5
- Fabian A.C., Crawford C.S., Johnstone R.M., Allington-Smith J.A., Hewett P.C., MNRAS 235, 13p
- Gunn J.E., 1979, in "Active Galactic Nuclei", Eds. Hazard, Mitton, CUP, p.213
- Haenhelt M., 1992, preprint
- Heckman T., 1990, in the proceedings of the IAU Colloquium 124 "Paired and Interacting Galaxies", Eds. Keel, Sulentic
- Heckman T., 1991, in the proceedings of the meeting held in Baltimore, "Massive stars in starbursts"Eds. Leitherer, Walborn, Heckman, Norman, STSI symposium series, p. 289
- Hernquist L., 1989, Nature 340, 687
- Hills J.G., 1975, Nature 254, 295
- Kormendy J., 1988, ApJ 325, 128
- Lin D.N.C., Pringle J.E., 1987, MNRAS 225, 607
- Lin D.N.C., Pringle J.E., Rees M.J., 1988, ApJ328, 103
- Norman C., Scoville N., 1988; ApJ 332, 124
- Padovani, P., Burg R., Edelson R.A., 1990, ApJ 353, 438
- Perry, J.J., Dyson, J.E., 1985, MNRAS 213, 665
- Pogge R.W., 1989, A.J. 98, 124
- Rees M.J., 1984, Ann. Rev. Astr. Ap. 22, 471
- Rees M.J., 1992, to appear in the proceedings of the meeting held in Heidelberg, "Physics of Active Galactic Nuclei", Eds.Camenzind, Wagner, Springer Verlag
- Roos N., 1985, ApJ 294, 486
- Shields, G.A., 1978, Nature 272, 423
- Soltan, A., 1982, MNRAS 200, 115
- Terlevich R., Melnick J., 1985, MNRAS 213, 841

IV - ENVIRONMENTAL EFFECTS : MERGERS

MERGERS

FRANÇOIS SCHWEIZER
Carnegie Institution of Washington
Department of Terrestrial Magnetism
5241 Broad Branch Road, N.W.
Washington, DC 20015, USA

ABSTRACT

There is growing evidence that collisions and mergers can modify and even transform the Hubble types of galaxies. After briefly reviewing estimates of the merger rate, I focus on recent progress in our observational understanding of merger physics: (1) There is now good evidence that violent relaxation redistributes the stars in many Arp and IRAS mergers into the characteristic $r^{1/4}$ distribution; (2) dissipation in mergers leads to enormous central concentrations of molecular gas and oddly rotating cores that may be the precursors of the high-density cores observed in E's and S0's; (3) young globular cluster systems seem to form as part of the massive starbursts triggered by mergers; and (4) starbursts seem to occur not only in the nuclei of colliding galaxies, but also at the interface between the colliding disks, thus yielding young stars that will form part of the outer bulge population in the future merger remnants and will heat the gas throughout the body. I also briefly review evidence in favor of bulge building through mergers and report on a first attempt to date the formation of nearby E + S0 galaxies borne from major mergers. The combined evidence suggests that the Hubble sequence may rank galaxies mainly by the number and vehemence of mergers in their past history.

1. SKIPPING ALONG THE HUBBLE SEQUENCE

The idea that galaxy interactions and mergers might transform the Hubble (1936) types of some galaxies took root more than 50 years ago. In 1940 already, Holmberg realized that the average separation between galaxies is small relative to their dimensions. Speculating that this may lead to frequent and often large tidal disturbances with a resultant loss of kinetic energy sufficient to effect capture, he wrote: "The general result will be a gradual contraction of the relative orbit, which may continue until the two components form practically one object." Although in the end Holmberg favored type transformations within double and multiple systems over outright mergers, he was clearly envisioning interactive evolution along the Hubble sequence toward earlier types. Alladin (1965) demonstrated the extreme stickiness of close galaxy collisions, concluding that "Given long enough, the components of a double galaxy will disrupt each other and give rise to a single loose system." Finally, Toomre & Toomre (= TT, 1972) sharpened such thinking to the by now well-known hypothesis that the remnants of major disk mergers may be ellipticals.

Here I shall review the evidence that, indeed, galaxies involved in major mergers tend to skip along the Hubble sequence, mostly from later types to early types, but occasionally perhaps also in the opposite direction.

Before I begin, however, let me clarify the term "merger." Currently, this term is often applied indiscriminately to galaxies that show only weak signs of tidal interaction or are simply peculiar, with the nature of the peculiarity unclear. Yet, if we ever wish to do serious merger statistics, it is important to distinguish between mild interactions, stronger collisions, and outright mergers. For example, the prototypical interacting galaxy pair M 51 = NGC 5194/95 can hardly be called a merger yet: though the recent encounter must have cost the companion some orbital energy, the best model simulations still feature a parabolic orbit (Hernquist 1990) and it remains unclear whether a merger will occur within the next 10 Gyr.

Similarly, in the imaginary sequence of orbital decay shown in Figure 1 the first pair of galaxies can certainly not be called a merger, though there are some signs of a tidal interaction. On the other hand, in the second pair, The Antennae, the collision is already so strong that an imminent merger can be predicted with confidence (Barnes 1988). The third pair appears to be in an even more advanced stage of merging, while the fourth galaxy, NGC 3921, is clearly a single merger remnant. Thus, I shall restrict the use of the term "merger" to galactic systems that can confidently be expected to merge within the next 1–2 orbital periods or that have actually completed merging.

Since TT, the focus on mergers has shifted at least twice, from initial attempts to answer the question "Can colliding galaxies merge?" through the unraveling of various merger signatures such as tails, ripples (="shells"), and polar rings to the present

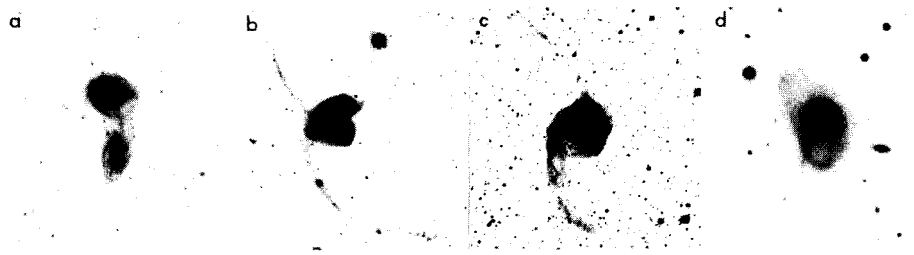

Fig. 1. Four increasingly strong interactions of disk galaxies: (a) Weakly interacting pair NGC 5426/27; (b) strongly interacting pair NGC 4038/39, where a merger is predicted within next orbital period; (c) NGC 3256, pair of colliding and partially merged disks; and (d) NGC 3921, remnant of two merged disks with two tails.

emphasis on dissipational phenomena associated with gas in mergers. This review will concentrate on this most recent topic, and especially on starbursts as episodes of intense galaxy building. Note that all dimensions, fluxes, etc., will be quoted for $H_0 = 50$ km s^{-1} Mpc^{-1}. When compared to $H_0 = 75$, this choice increases linear dimensions by 50% and fluxes, including molecular gas masses derived from fluxes, by a factor of 2.25. It will be important to keep this in mind when I discuss some of the record molecular gas masses recently found in ultraluminous IRAS galaxies (§3.2).

2. MERGER RATE

A reliable estimate of the merger rate would be invaluable in assessing the importance of mergers for the evolution of an average galaxy. Yet, this rate is difficult to determine. Estimating the fraction of galaxies that have been strongly affected by mergers may be a bit easier. Fortunately, there are two good estimates of this fraction that bracket its likely range.

A lower limit is provided by Toomre's (1977) estimate, made from 11 ongoing disk–disk (DD) mergers and their estimated median age of 0.5 Gyr, that ***at least 250 relics*** of such mergers must have accumulated among the 4000^+ galaxies in the NGC during the last 10–15 Gyr, and more likely about 750 relics. Presumably it is no coincidence that the latter number just about corresponds to the number of E + S0 galaxies in the NGC. An upper limit has been set by Schechter & Dressler (1987), who estimate from a study of B/D ratios in a complete sample of galaxies that at $z = 0$ "roughly equal amounts of mass are incorporated in bulges and disks." Under the extreme assumption that gaseous collapses form only disks and all spheroids are due to mergers, this estimate restricts the maximum amount of galactic structure affected by mergers to about 50% by mass.

We conclude that between 5% and 50% of all stars within galaxies owe their present kinematics, and in some cases also their existence, to mergers. Or, stated somewhat

less accurately, between $1/20^{\rm th}$ and 1/2 of all galaxies seem to have been visibly affected by mergers.

3. MERGER PHYSICS: PILING UP STARS AND GAS

From an observer's point of view, merger physics consists of gathering evidence concerning the processes that occur when two galaxies merge their stellar and gaseous contents. The following subsections discuss evidence concerning violent relaxation, gas concentration through dissipation, the formation of kinematic subsystems and globular clusters, and the heating of the gas.

3.1 Violent Relaxation

I remember my intense surprise upon discovering that NGC 7252, with its many loops and two tails, has a mean radial light distribution characterized by an $r^{1/4}$-law: apparently, violent relaxation (Lynden-Bell 1967) has been remarkably efficient at redistributing matter in the fluctuating gravitational field of the two merging disk galaxies (Schweizer 1982). The recent advent of infrared imaging arrays makes now possible the study of merger systems even more chaotic than NGC 7252, since measurements in the K band (2.2 μm) are much less sensitive to dust extinction and young hot stars than in the optical. By now, $r^{1/4}$ light distributions have been observed in many, though not in all, imaged mergers. Wright *et al.* (1990) find infrared $r^{1/4}$ distributions in two out of six mergers: Arp 220 and NGC 2623 (Figure 2). Given the blob-like appearance of Arp 220 (Arp 1966), its $r^{1/4}$ light distribution hardly surprises, but that same light distribution comes as a total surprise for NGC 2623 = Arp 243, where optical images show two fragments with much structure! In another IR imaging survey of eight DD mergers, Stanford & Bushouse (1991) find four with an $r^{1/4}$-law to the limit of the K photometry and an additional three with an $r^{1/4}$-law out to $\sim$3 kpc radius. All these various observations present strong evidence for the efficiency of violent relaxation in mergers and for the *delayed transformation of Hubble types.* Apparently to this date, mergers continue to transform pairs of disk galaxies into either ellipticals or at least major bulges.

3.2 Gas Concentration through Dissipation

It has long been clear that mergers involve a great deal of gaseous dissipation. Already in 1972 and writing under the subtitle *Stoking the Furnace*, TT remarked: "Would not the violent mechanical agitation of a close tidal encounter — let alone an actual merger — already tend to bring *deep* into a galaxy a fairly *sudden* supply of fresh fuel in the form of interstellar material, either from its own outlying disk or by accretion from its partner? And in a previously gas-poor system or nucleus, would not the relatively mundane process of prolific star formation thereupon mimic much of the 'activity' that is observed?"

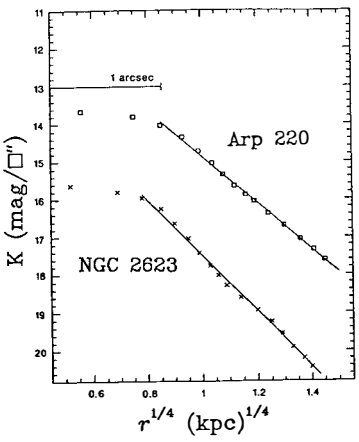

Fig. 2. Surface brightness in K band plotted against $r^{1/4}$ for ongoing mergers Arp 220 and NGC 2623 (from Wright *et al.* 1990).

Thus, I have always been puzzled by some of the fierce opposition to the idea that ellipticals might form through disk mergers. Much of this opposition was based on the notion that dissipationless mergers cannot increase the phase density of disk galaxies to the high values characterizing the centers of many ellipticals. As one well-known astronomer objected vigorously at an MIT meeting in 1981: "You cannot make even one elliptical from 1,000 spirals!" Yet, the evidence for gaseous, dissipative processes in interacting galaxies was unmistakable even then. First, Arp (1969) had already noted signs of global youth in the gigantic H II regions and the underlying A-type absorption spectra of compact companions at the ends of spiral arms of large disk galaxies. Second, observations of merger *remnants* like NGC 3921 and 7252 were showing the aftereffects of major starbursts in the form of composite spectra dominated by strong Balmer absorption lines, now commonly called $E+A$ *spectra* (Schweizer 1978, 1982, 1990; Hamilton & Keel 1987; Oegerle *et al.* 1991). And third, in a landmark paper Larson & Tinsley (1978) had demonstrated convincingly that the large scatter of *UBV* colors of Arp galaxies can be understood if many of these galaxies undergo intense episodic starbursts that convert up to 5% of the visible mass from gas to stars.

The big surprise from millimeter-wave observations following IRAS has been how incredibly concentrated the gas can become and how strong the ensuing starburst. Early on, Young *et al.* (1984) and Sanders *et al.* (1986) found unusually large amounts of molecular gas, $\sim 4 \times 10^9 - 4 \times 10^{10}\ M_\odot$, in such systems, or 2–20 times as much as the H_2 content of the entire Milky Way (see review by Young & Scoville 1991). In the last few years, record upon record has been broken. The current claimed record amount of molecular gas stands at $1.4 \times 10^{11}\ M_\odot$, corresponding to nearly 70 times the H_2 content of the Milky Way (Sanders *et al.* 1991; H_0=50). And in two recent investigations, Sargent & Scoville (1991) and Scoville *et al.* (1991) measured surface mass densities of ~3,000–80,000 $M_\odot$ pc^{-2} of molecular gas in Arp 220 and Arp 299 (see Fig. 3b).

Compared to the *total* surface mass density of the Milky Way near the sun (45–80 $M_\odot$ pc^{-2}) these amounts are $10^2 - 10^3$ times higher! Since most of the high column density occurs in the central few 100 pc, the spatial density there must be very high as well. Indeed, in the above-mentioned two mergers the *mean* central number density of H_2 molecules is claimed to reach $\sim$3,000 cm^{-3}, leading to a nearly incredible $A_V \approx$ 1,000 mag. (Of course, all these record numbers depend on the assumed conversion factor between CO luminosity and H_2 mass. Yet, yesterday Françoise Combes assured us that errors in the adopted conversion coefficients are relatively small.) If these conversion coefficients are correct, then in the case of Arp 299 about 95% of the mass in one nucleus (IC 694) is estimated to be in the form of H_2!

In this highly concentrated molecular gas, vehement starbursts are taking place and are rapidly exhausting the available gas supply on timescales of $10^7 - 10^9$ yr (see Thuan *et al.* 1987). Thus we have reason to believe that a fair fraction of the H_2 mass will turn into stars and will provide just about the central density observed at higher, optical resolution in E's and bulges ($10^2 - 10^5$ $M_\odot$ pc^{-3}, corresponding to 2×10^3 – 2×10^6 H_2 cm^{-3}). More evidence for this view comes from very recent detections of the molecule HCN, which traces H_2 at twenty times higher densities ($\sim 10^4$ cm^{-3}) than CO does: Solomon *et al.* (1992) find densities of up to $\sim$500 $M_\odot$ pc^{-3} in central regions of ultraluminous IRAS galaxies, again well within the range of central mass densities observed in ellipticals.

Thus, the old argument against elliptical formation through mergers of disk galaxies — based on the high phase-space density at the centers of E's and paraphrased by Gunn (1987) as "I do not think you can make rocks by merging clouds" — is now refuted by observations. Indeed, the vehement starbursts and enormous central concentrations of H_2 observed in mergers provide strong evidence that, *at least in the world of galaxies, rocks can be made by merging clouds!*

In addition, evidence is accumulating that the compressed gas in mergers may fuel not only starbursts, but also some central engines. Virtually all ultraluminous IRAS galaxies and several nearby QSO's such as 3C48 ($z = 0.369$, Stockton & Ridgway 1991), 3CR249.1 ($z = 0.312$), and Ton 202 ($z = 0.363$; Stockton & MacKenty 1983) occur in mergers. Thus mergers seem not only to modify the positions of galaxies within the Hubble Sequence, but also to ignite relatively short-lived fireworks that appear to us as those strange beacons called AGN's and Quasars.

3.3 Oddly Rotating Cores

Since mergers tend to concentrate up to several 10^{10} $M_\odot$ of H_2 into the central few kpc and gas tends to settle into disks, merger remnants observed after the fading of the central starburst should show some central disk of comparable mass. It is perhaps no coincidence that the oddly rotating cores discovered in ellipticals (Franx & Illingworth

1988; Bender 1988; Jedrzejewski & Schechter 1988) seem to be disky structures of about the right size and mass. Although first guesses were that these structures might be the remains of gas-rich dwarfs or of spinning, dense companions (Kormendy 1984; Kormendy & Djorgovski 1989; Bender 1990), I proposed in Heidelberg the alternative hypothesis that they might be remnants of the central gas accumulated in DD mergers (Schweizer 1990).

Evidence in favor of the latter hypothesis has mounted in the past three years. First, in NGC 7252 — the 1 Gyr old remnant of two merged, nearly equal-mass disks — the rotation pattern of the central ionized gas matches that of stars in the counterrotating core of IC 1459 remarkably well (see Fig. 3 of Schweizer 1990), and there is a large mass of $\sim 8 \times 10^9$ $M_\odot$ of molecular gas near the center (Dupraz *et al.* 1990). New, interferometric observations of NGC 7252 confirm the central location, mass, and disky distribution of this gas (Wang *et al.* 1992). In addition, these observations now also establish that the H_2 disk corotates with the central H II disk, and that both disks together rotate in the opposite sense of the diffuse H II in the outer body. Since there is evidence for continued star formation in the central gas (Bica 1992), the chain of evidence leading from a DD merger via gas concentration and star formation in a central disk to a counterrotating *stellar* core is now complete.

A second good piece of evidence stems from observations of Mg lines in four E's with oddly rotating cores (Bender & Surma 1992). In these ellipticals, the Mg_2 index stays roughly constant throughout the outer body, but shows a distinct central increase beginning just about at the edge of the kinematic subsystem. This increase clearly supports the notion of extra metal enrichment in a central pool of gas that is being polluted by the byproducts of stellar evolution.

And third, model simulations of DD mergers with gas suggest that in roughly 25% of all possible orientations more than half the gas ends up in a central disk rotating in the opposite sense of the outer gas, just as observed in NGC 7252 (Hernquist & Barnes 1991; Barnes 1992).

I believe these various pieces of evidence support the notion that *ellipticals with oddly rotating cores formed through mergers of roughly equal-mass disk galaxies.* At least one of the two premerger disks must have contained significant amounts of gas, and both disks must have contained more stars than gas. Otherwise, if both components had been mostly gaseous protogalaxies, it would be difficult to understand the relatively sharp boundaries of the present-day disky cores (Nieto *et al.* 1991) in both kinematics and metallicity. If we accept these arguments, then the ~25% detection rate of oddly rotating cores (de Zeeuw & Franx 1991), coupled with the guess that about half of all such cores remain undetected due to unfavorable viewing geometry, suggests that the fraction of E's formed through DD mergers may be $\gtrsim$50%.

TABLE 1. Merger Remnants with Candidate Young Globular Clusters

Galaxy NGC	Type (Source)	$cz_\odot$ (km s^{-1})	Young (Globular) Clusters			
			r (kpc)	$M_B^{(1)}$	Color	Reference
1316	D3–4 (MMS'64)	1793	<10	-13^*	reddish	Schweizer 1980
7252	"Merger" (RSA)	4749	<7	$-15\,^1/_2{}^*$	bluish	Schweizer 1982
3597	S0$^+$ (RC3)	3513	<10	$-14^\dagger$	blue	Lutz 1991
1275	Epec (RSA)	5260	<7	$-15^\ddagger$	blue	Holtzman$^+$ '92

NOTES: *Estim. from photogr. plates; † diam. < 100 pc; ‡ typical GC: -11 to -13.

3.4 Forming Young Globular Clusters

A potentially serious objection raised against a merger origin of ellipticals is that the specific globular cluster frequency S is nearly an order of magnitude higher in E's than in disk galaxies (van den Bergh 1982, 1990a). Yet, this argument is based on the unproven assumption that the number of globular clusters (GC) is preserved during mergers. Various authors have pointed out that new GC's might form along with all the other young stars in merger-induced starbursts, whence S might actually increase and young GC's might be concentrated near the centers of merger remnants (Schweizer 1987; Burstein 1987; Ashman & Zepf 1992).

The latest example of a system of candidate young globular clusters that might have formed during a recent merger is that discovered in NGC 1275 (Holtzman *et al.* 1992). On high-resolution V and R frames obtained with the Hubble Space Telescope, over 40 relatively blue and unresolved knots appear within 7 kpc from the center (H_0=50). The brightest of these knots reach $M_B \approx -15$. Typical knots are -11 to -13, have colors $V - R = +0.4$ to $+0.6$, and are thought to be a few 10^8 yr old. Their nearly uniform colors argue strongly for a coeval origin and, therefore, against continuous production of these objects in a cooling flow. Holtzman *et al.* conclude that most likely these knots are young star clusters that will evolve to look like globular clusters.

Yet, this is not the first time that young GC's formed in mergers have been found. Table 1 lists three merger remnants previously known to possess candidate young GC's and compares them with the NGC 1275 system. Strikingly, all four galaxies feature similarly bright pointlike sources within a radius of less than 10 kpc. Whereas the absolute magnitudes of the brightest candidate GC's in NGC 1316 and 7252 are photographic estimates, those for NGC 3597 (Lutz 1991) are based on CCD photometry. In the latter galaxy, the CCD images also yield an upper limit of 100 pc for the GC diameters.

Therefore, we now have some observational evidence to support the suggestion that

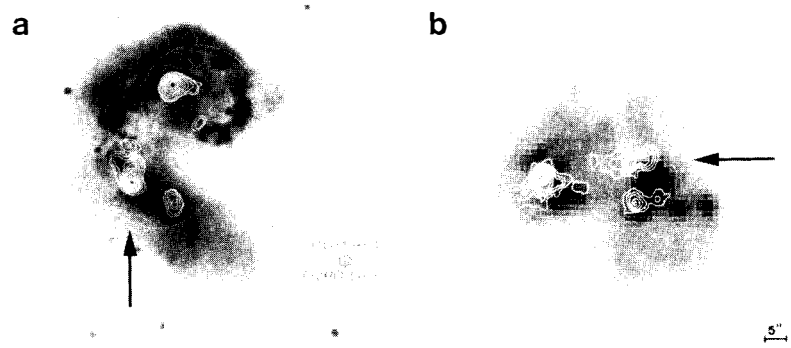

Fig. 3. Molecular gas in presumed shock fronts at disk interfaces in (a) NGC 4038/39 (from Stanford *et al.* 1990) and (b) Arp 299 (= IC 694 + NGC 3690; from Sargent & Scoville 1991). The extranuclear CO at the disk interfaces is marked by arrows.

the specific GC frequency S may increase as disk mergers form ellipticals or build up bulges (§4). As already argued earlier (Schweizer 1987), this picture of merger-induced GC formation explains the presence of radial abundance gradients in GC systems just as naturally as the galactic collapse picture does. Also, given the strong central concentration of merger-induced starbursts, the similarly strong central concentration of GC systems is a natural consequence.

3.5 Heating the Gas

One of the most promising areas of merger research for the next few years centers on the fate of gas. In this brief overview, I shall touch upon four subjects: starbursts in shock fronts at disk interfaces, supernova rates, galactic winds, and the possible involvement of mergers in the formation of X-ray coronae.

Some of the most vehement *shock phenomena* affecting gas in mergers may occur during first contact of the colliding H I disks at their interface. It is well known that the radio continuum emission of The Antennae peaks not at the nuclei, but in the overlap region between the two disks (Burke & Miley 1973; Hummel & van der Hulst 1986); this suggests compression of the magnetic field and/or extra supernova activity at an interface. A similar phenomenon is observed in NGC 5256 (= Mrk 266), where an extended radio-continuum source with no optical counterpart appears between the two nuclei (Mazzarella *et al.* 1988). Thus, I find it fascinating that two recent observations reveal that the molecular gas, too, can be concentrated at collision interfaces, as Figure 3 illustrates. In NGC 4038/39 (Fig. 3a), there are $\sim 2.7 \times 10^9\ M_\odot$ of molecular gas at the above-mentioned interface, several times more than in either of the two nuclei (Stanford *et al.* 1990). This H_2 is distributed in four clumps that coincide with Hα, 10 μm, and radio continuum peaks, suggesting sites of extremely vigorous star formation. In-

terestingly, in this same region soft X-rays indicative of $\sim 10^5$ K gas have been detected (Fabbiano & Trinchieri 1983). A similarly complex interface region seems to also exist in Arp 299 (Fig. 3b), where a clump of nearly 5×10^9 $M_\odot$ of H_2 is observed between the two nuclei, again with multiple signs of extreme star formation (Sargent & Scoville 1991). Once formed, stars in such extranuclear bursts are decoupled from the gas dynamics and are bound to become part of the outer bulge population in the future merger remnant. Such stars may help explain why NGC 7252 shows the characteristic E + A postburst spectrum *throughout its body*, rather than just at its center (Schweizer 1990).

A puzzling aspect of starbursts is how *few supernovae* have actually been observed in them, despite predictions of SN rates of up to 2–3 yr^{-1}. Perusal of Appendix 5 in the RC3 (de Vaucouleurs *et al.* 1991) shows that no supernova has been observed optically in M 82, NGC 3256, NGC 6240, and Arp 220. Only 1 SN each has been observed in NGC 253, NGC 3310, and probably NGC 4038, and 2 SNe in NGC 5253. The likely cause of this paucity of observed SNe is extinction, since (1) the central starbursts are heavily obscured and (2) even in normal spirals extinction favors face-on over edge-on galaxies for SN detection (van den Bergh 1990b). Some SNe or young remnants may have been found at radio wavelengths in M82 (Kronberg *et al.* 1985) and in the ongoing merger NGC 6052 (Yin & Heeschen 1991). There is an urgent need for *supernova surveys with infrared cameras* to check on the predicted high SN rates in mergers. A new, promising technique is the study of the near-IR emission of [Fe II], which traces SN remnants and can be used to infer the SN rate (Greenhouse *et al.* 1991).

Supernovae in mergers are important because they may be the main source for heating the gas and may be responsible for *large-scale galactic winds* of the kind observed in NGC 6240 and Arp 220 (Heckman *et al.* 1987; Chevalier & Clegg 1985). Such winds may lead to both a significant loss of gas and the formation of X-ray coronae. Hibbard *et al.* (1992) find a striking central void in the HI distribution of NGC 7252, making one wonder what happened to the gas in the intermediate region between the central molecular-gas disk ($r \lesssim 4$ kpc) and the inner edge of the H I distribution ($r \gtrsim 15$ kpc). One hypothesis is that gas pervades this apparent cavity, but has been heated to X-ray temperatures. If X-ray observations confirm this hypothesis, then (1) the link between merger remnants and E's with X-ray coronae would be strengthened and (2) the old puzzle of the fate of gas in DD mergers that are to become ellipticals would be solved. The same hypothesis of gas heating in mergers seems to get support from a recent study of gas in early-type galaxies which emphasizes that "the cold gas is a disk phenomenon, while the hot gas is a bulge phenomenon, with little interaction between the two. Therefore, the progression of galaxy type from E to Sa is not only a sequence of decreasing bulge-to-disk ratio, but also of hot-to-cold-gas ratio" (Bregman *et al.* 1992). For a detailed discussion of possible gas heating mechanisms in mergers, see Jog & Solomon (1992).

4. BUILDING BULGES ...

4.1 ...Before Disk Formation

It seems currently fashionable to predict that any merger of two disk galaxies will form an elliptical. Yet, for this to occur, at least two conditions must be fulfilled: (1) The two colliding disks must have comparable masses for a maximum of violent relaxation to occur; and (2) after the merger there must be so little cold gas left in the environs that no major new disk can form. The example of Arp 220 serves as a warning that the latter condition may not always be fulfilled: only about $^2/_3$ of its $\sim 6 \times 10^{10}\ M_\odot$ of molecular gas are located in the highly concentrated central clump, whereas the remaining $^1/_3$, or $\sim 2 \times 10^{10}\ M_\odot$, of H_2 lies in an extended, 10 kpc diameter disk that coincides with the optical dust lane bisecting the main body (Scoville *et al.* 1991). At present, we cannot forecast with certainty how much this disk may get heated and what fraction of it will convert into stars. Yet, given its present extent and cool temperature, this disk of H_2 seems likely to survive the central starburst and form stars at a more leisurely rate, whence Arp 220 may end up being an S0 or perhaps even a Sombrero-like Sa galaxy.

In this hypothetical scenario, a highly destructive merger may temporarily *seem* to form an elliptical, but may eventually lead to the formation of an early-type galaxy with a considerable disk. This scenario corresponds closely to the traditional view that bulges formed first, in accord with the observational fact that in general bulges tend to be redder than their associated disks. Yet, note that even such "old" bulges may have formed with considerable delays long after galaxy formation began.

4.2 ...Episodically and Concurrent with Disk Growth

There is tantalizing evidence that bulges may grow episodically and concurrently with disks, whence we occasionally observe a galaxy with a bulge that appears younger than its disk (see review by Schweizer 1990). Briefly, this evidence includes (1) bulges with "E + A" type spectra such as that of NGC 5102 or those observed in several polar-ring galaxies, (2) ripples in early-type galaxies that suggest merger activity in disks as well (Schweizer & Seitzer 1988), and (3) X-structures that are most easily explained as remnants of accreted companion galaxies (Hernquist & Quinn 1989), such as the deformed bulge and associated X-structure observed in IC 4767 (Whitmore & Bell 1988). This and other evidence, though too scant to make a strong case, nevertheless suggests that disks can and in fact do survive minor, bulge-building mergers as long as the mass of the accreted companion is less than a rather small fraction (perhaps $\sim$10%) of the main galaxy (Quinn & Goodman 1986).

5. A FIRST ATTEMPT AT DATING ANCIENT MERGER EVENTS IN E AND S0 GALAXIES

Despite the growing evidence for past mergers in many E and S0 galaxies, it has been difficult until very recently to rank early-type galaxies by the age of their last major merger event. If indeed such galaxies are remnants of disk mergers, then where are the "young" E's and S0's, the transition objects between recent, ~1–2 Gyr old merger remnants such as NGC 3921 and 7252 and bonafide old (10–15 Gyr) E and S0 galaxies? Or, as King (1977) commented to Toomre (1977) at the Yale Conference: "You showed us 10 merging pairs and then asked us to look for, or at least accept the existence of, 500 remnants from so long ago that they no longer bear the 'made by Toomre' label. I would be much more impressed if you showed us the 20 or 30 systems in the box immediately adjacent in your histogram. What do these merged pairs look like in their next few galactic years?"

With such questions in mind, Patrick Seitzer (Univ. of Michigan) and I undertook a CCD imaging survey of 74 E + S0 galaxies located mostly in the field and in groups in order to catalog all discernible fine structure in them. First results were presented by Seitzer & Schweizer (1990) and the catalog itself is to be published next year. The main result is that fine structure exists in a surprisingly large fraction of the observed galaxies. More than half of the ellipticals and one third of the S0 galaxies feature ripples. And fully 69% of E's and 53% of S0's possess at least one of four types of fine structure thought to be formed by mergers: ripples, boxiness, X-structure, and "jets" (= tails, plumes, etc). Thus, a majority of these early-type galaxies seem to have experienced at least one merger in the not too distant past.

In order to facilitate the search for correlations with other observables indicative of recent merger activity, we formed a fine-structure index $\Sigma = S + \log(1+n) + B + X + J$, where S, B, X, and J are our visual estimates of ripple strength, boxiness, X-structure, and jets, and n is the number of ripples. This index varies between zero for galaxies with no detectable fine structure and 7.6 for NGC 3610, the sample galaxy with the most fine structure. For comparison, the recent merger remnants NGC 3921 and 7252 have $\Sigma = 8.8$ and 10.1, respectively. There is every reason to believe that shortly after a major merger, Σ reaches a maximum and then slowly declines to small values or zero.

As a first application, Schweizer *et al.* (1990) looked for, and found, correlations between Σ and the vertical scatter observed in line-strength vs. luminosity relations of ellipticals. Specifically, the E's with the most fine structure ($\Sigma = 4$–8) have, at any given luminosity, systematically stronger Hβ absorption and weaker CN and Mg features than E's with little or no fine structure. Since Σ is a rough measure of dynamical youth or rejuvenation, these line-strength vs. Σ correlations are most likely due to systematic variations in the mean age, rather than mean metallicity, of the stellar

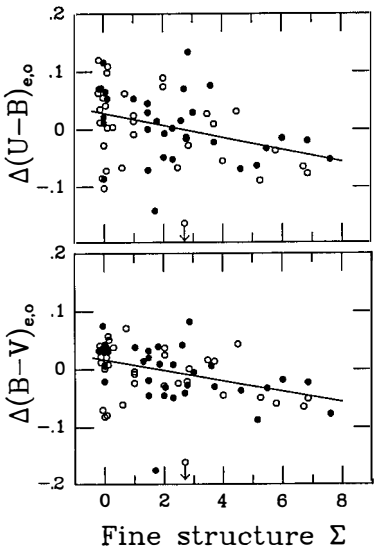

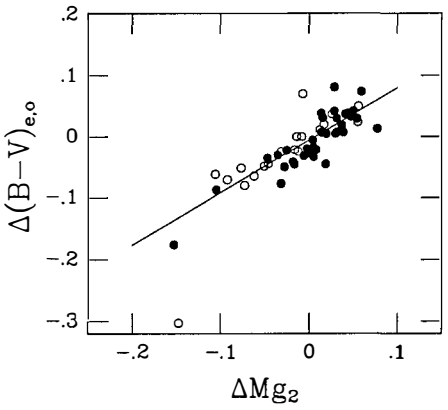

Fig. 4. (*left*) Color residuals $\Delta(U-B)_{e,0}$ and $\Delta(B-V)_{e,0}$ plotted vs. fine-structure index Σ for 35 E (*solid dots*) and 34 S0 (*open circles*) galaxies. Lines mark least-squares fits. Note that galaxies with much fine structure are systematically bluer.

Fig. 5. (*right*) Color residuals $\Delta(B-V)_{e,0}$ plotted vs. residuals ΔMg_2. Vertical scatter in the color–magnitude and line-strength–magnitude relations is strongly correlated.

populations. One needs only a relatively small fraction of intermediate-age (0.5–5 Gyr) stars — presumably part of an aging, merger-induced starburst — to enhance the Hβ absorption and dilute the CN and Mg features of the older populations through the added continuum. We concluded that at least half of the vertical scatter in the line-strength vs. luminosity relations must be caused by mean-age variations.

After this study, we had two remaining worries. The first was that, perhaps, our sample of ellipticals might be biased in some unknown way. Hence, it seemed desirable to increase the sample size. The second worry was that the line-strength indices refer only to small nuclear regions, whereas Σ is a global parameter. Could it be that we were detecting the aftereffects of minor central starbursts that were interesting in their own right, but had little to do with *major* mergers associated with the formation of these E and S0 galaxies?

A new study of correlations between *UBV* colors and Σ has dispelled both worries and has allowed us to make some first estimates of merger ages in E + S0 galaxies (Schweizer & Seitzer 1992). There are four main advantages to using *UBV* colors for such a study. First, *UBV* colors are available for most S0 galaxies of our sample, whence we could nearly double the number of galaxies by adding 34 S0's to the 35 E's with

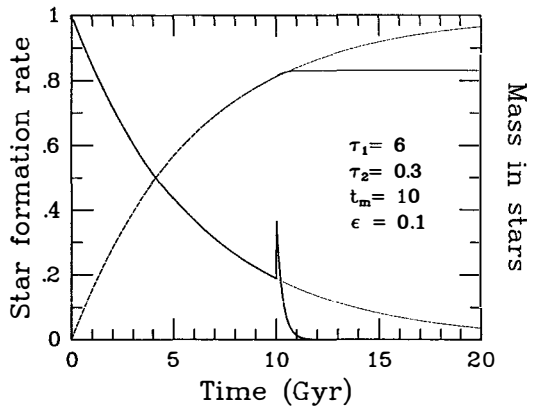

Fig. 6. Star formation rate (*solid line*) and fraction of mass in stars (*dashed*) as functions of time in a model of two galaxies that would have become present-day Sb's, but collided and merged at epoch 10 Gyr (i.e., ~5 Gyr ago).

both *UBV* colors and Σ available for study. Second, high-quality *UBV* colors available from the RC3 (electronic version) refer to the effective or half-light aperture and are therefore much more nearly a global measure of population properties than the nuclear line-strength indices. Third, the broad-band colors measure mostly the continuum and are thus relatively more sensitive to age variations than the line-strength indices are. And fourth, there are excellent models available of the *UBV* color evolution of star clusters, thus making age-dating from *UBV* colors possible.

Figure 4 shows color *residuals* obtained after subtracting linear least-squares solutions from the corresponding color-magnitude relations and plotted versus the fine-structure index. The subtraction of the mean relations removes the systematic color dependency on luminosity, generally attributed to systematic metallicity variations, and isolates the vertical scatter. As the figure shows, both $\Delta(U{-}B)_{e,0}$ and $\Delta(B{-}V)_{e,0}$ correlate with Σ in the sense that galaxies with much fine structure are systematically bluer than those with little or no fine structure. The mean relations for E and S0 galaxies treated separately are the same to within the combined errors, whence we have grouped the two types together. The main results from Figure 4 are: (1) The bluing associated with high Σ supports the earlier conclusion that mean-age differences exist between E + S0's with and without fine structure; and (2) doubling the sample by adding the S0's has strengthened the correlations, thus reducing the likelihood of sample bias.

Figure 5 illustrates another important result: The residuals $\Delta(B{-}V)_{e,0}$ correlate very well ($r = 0.85$) with the line-strength residuals ΔMg_2, showing that the vertical scatter in the color–magnitude and line-strength–magnitude relations is strongly correlated. Thus this scatter is clearly not due to observational errors and must be caused by an intrinsic variable, which we identify as the mean age of the stellar populations. Since $\Delta(B{-}V)_{e,0}$ refers to half the total light, yet ΔMg_2 only to a central few percent of the light, this correlation also supports the notion that the detected age variations are a global phenomenon, and thus are presumably due to some *major* mergers.

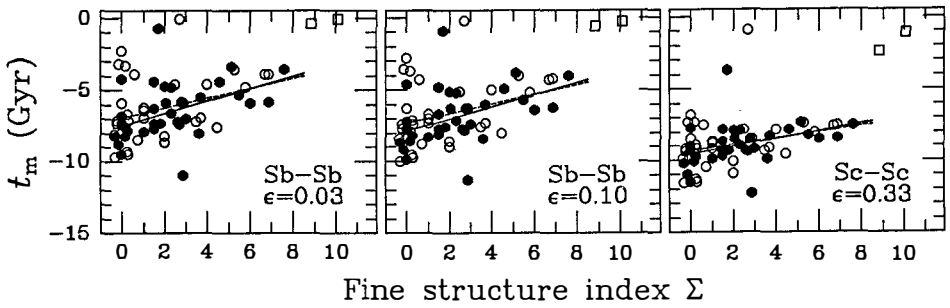

Fig. 7. Heuristic merger ages t_m plotted vs. fine-structure index Σ for three different model assumptions. The merger ages are counted backward from the present (t_m = 0) and expressed as negative numbers in Gyr. The *solid* and *open circles* mark E and S0 galaxies, respectively, while the two *open squares* mark the recent merger remnants NGC 3921 and 7252. Since the median type of colliding galaxies in the field is Sb, the two left panels probably respresent the true distribution of merger ages best.

In order to derive heuristic merger ages from the color variations, we had to make one more assumption. Since older, major starbursts lead to very similar color variations as younger, minor starbursts, we postulated — based on some of the evidence mentioned above and on much other evidence — that most of the detected fine-structure stems from *major* disk–disk mergers. Based on this assumption, we computed two-burst models of evolving stellar populations in mergers. For simplicity, we assumed that two galaxies *of equal Hubble type* evolved toward becoming present-day Sb–Sb or Sc–Sc pairs, but collided and merged some t_m years ago. Both before and after the merger the galaxies evolve with exponentially declining star formation rates, but the time constant is long before the merger (τ_1 = 6 Gyr for Sb and 10 Gyr for Sc galaxies, see Searle *et al.* 1973) and quite short after the merger (τ_2 = 0.1–0.3 Gyr). Figure 6 shows a typical SFR as function of time for a merger that occurs at epoch 10 Gyr and in which only 10% of the remaining gas gets converted into stars.

Using single-burst cluster models by Charlot & Bruzual (1991) to convolve with the various SFR of our two-burst models, we computed extensive grids of color evolution and used the young merger remnants NGC 3921 and 7252 to narrow down the ranges of some of the model parameters. Finally, we determined heuristic merger ages (HMA) from these models and the *UBV* colors of our E + S0 galaxies for different assumptions about the mean Hubble type of the pre-merger disks and the gas-to-star conversion efficiency ϵ during the merger.

Figure 7 shows the resulting HMA's of 65 E + S0 galaxies plotted versus Σ for three different model assumptions: low-efficiency (ϵ = 0.03 and 0.10) Sb–Sb mergers and higher-efficiency (ϵ = 0.33) Sc–Sc mergers. There are three main conclusions from this figure: (1) If indeed E + S0 galaxies form through DD mergers, the process is prolonged

and lasts *at least* 5–10 Gyr or $^1/_3$ to $^2/_3$ the age of the Universe. (2) For efficient ($\epsilon \gtrsim 0.3$) Sc–Sc mergers, most E + S0 formation would have stopped 6–7 Gyr ago, leading to a serious (factor $\gtrsim$ 2–3) disagreement between the color-evolution timescale and the dynamical timescale inferred from some of the fine structure (e.g., estimated ripple lifetimes of 2–3 Gyr). On the other hand, for inefficient ($\epsilon \lesssim 0.1$) Sb–Sb mergers, E + S0 formation lasts essentially until the present and there is near agreement between the two timescales; the latter case probably approximates the true distribution of HMA's best since the median Hubble type of field galaxies of the same luminosity as our sample galaxies is Sb. And (3), surprising as it may be, the relatively small vertical scatter observed around the mean color–magnitude relations of E + S0 galaxies is consistent with the Toomre hypothesis of E formation through major disk mergers and with the delayed formation of E's (and S0's) that this hypothesis implies (for details, see Schweizer & Seitzer 1992).

6. CONCLUSIONS

Much of the evidence reviewed above supports the view that mergers of galaxies continue to the present date and lead to transformations in Hubble type. Due to violent relaxation, the trend is definitely towards more massive spheroids and earlier Hubble types. The most destructive disk–disk mergers form remnants like NGC 3921 and 7252 that evolve into ellipticals. Dissipation leads to molecular-gas concentrations compatible with the high central mass densities observed in bonafide E's, thus eliminating a former objection to the merger picture. Less destructive mergers ($m/M \lesssim 0.3$) may lead to bulge building and S0, Sa, or perhaps even Sb remnants, depending on the amount of gas left for disk rebuilding (e.g., Arp 220). There is now some evidence that young globular clusters are a natural byproduct of the starbursts occurring during such mergers. There is also strong evidence that at least half of the vertical scatter in the line-strength–magnitude and color–magnitude relations of E and S0 galaxies is caused by mean-age differences in their stellar populations, most likely caused by major mergers at different epochs. Color deviations from the mean relations can be used to derive heuristic merger ages for individual early-type galaxies, and there are now at least two dozen candidate young E and S0 galaxies that may have formed through mergers during the past 5–7 Gyr. Overall, the available evidence suggests that *the Hubble sequence may rank galaxies mainly by the number and vehemence of mergers in their past history.*

I thank Chip Arp, Vera Rubin, Anneila Sargent, Adam Stanford, and Gillian Wright for their kind permission to reproduce some figures, and Patrick Seitzer for his permission to present some of our results in advance of publication.

REFERENCES

Alladin, S.M. 1965, ApJ, **141**, 768.
Arp, H. 1966, *Atlas of Peculiar Galaxies* (California Institute of Technology, Pasadena).
Arp, H. 1969, A&A, **3**, 418
Ashman, K.M., & Zepf, S.E. 1992, ApJ, **384**, 50
Barnes, J.E. 1988, ApJ, **331**, 699
Barnes, J.E. 1992, see this volume
Bender, R. 1988, A&A, **202**, L5
Bender, R. 1990, in *Dynamics and Interactions of Galaxies*, ed. R. Wielen (Springer, Heidelberg), p. 232
Bender, R., & Surma, P. 1992, A&A, **258**, 250
Bica, E., 1992, in *The Stellar Populations of Galaxies*, ed. B. Barbuy & A. Renzini (Kluwer, Dordrecht), in press
Bregman, J.N., Hogg, D.E., & Roberts, M.S. 1992, ApJ, **387**, 484
Burke, B.F., & Miley, G.K. 1973, A&A, **28**, 379
Burstein, D. 1987, in *Nearly Normal Galaxies*, ed. S.M. Faber (Springer, New York), p. 47
Charlot, S., & Bruzual, A.G. 1991, ApJ, **367**, 126
Chevalier, R.S., & Clegg, A.W. 1985, *Nature*, **317**, 44
de Vaucouleurs, G., *et al.* 1991, *Third Reference Catalogue of Bright Galaxies* (Springer, Berlin) (RC3)
de Zeeuw, T., & Franx, M. 1991, ARA&A, **29**, 239
Dupraz, C., Casoli, F., Combes, F., & Kazès, I. 1990, A&A, **228**, L5
Fabbiano, G., & Trinchieri, G. 1983, ApJL, **266**, L5
Franx, M., & Illingworth, G.D. 1988, ApJL, **327**, L55
Greenhouse, M.A., *et al.* 1991, ApJ, **383**, 164
Gunn, J.E. 1987, in *Nearly Normal Galaxies*, ed. S.M. Faber (Springer, New York), p. 459
Hamilton, D., & Keel, W.C. 1987, ApJ, **321**, 211
Heckman, T.M., Armus, L., & Miley, G.K. 1987, AJ, **92**, 276
Hernquist, L. 1990, in *Dynamics and Interactions of Galaxies*, ed. R. Wielen (Springer, Heidelberg), p. 108
Hernquist, L., & Barnes, J.E. 1991, Nature, **354**, 210
Hernquist, L., & Quinn, P.J. 1989, ApJ, **342**, 1
Hibbard, J.E., van Gorkom, J.H., & Schweizer, F. 1992, in preparation
Holmberg, E. 1940, ApJ, **92**, 200
Holtzman, J.A., *et al.* 1992, AJ, **103**, 691
Hubble, E. 1936, *The Realm of the Nebulae* (Yale Univ. Press, New Haven), esp. p. 45
Hummel, E., & van der Hulst, J.M. 1986, A&A, **155**, 151
Jedrzejewski, R., & Schechter, P. 1988, ApJL, **330**, L87
Jog, C.J., & Solomon, P.M. 1992, ApJ, **387**, 152
King, I.R. 1977, in *The Evolution of Galaxies and Stellar Populations*, ed. B.M. Tinsley & R.B. Larson (Yale Univ. Obs., New Haven), p. 418
Kormendy, J. 1984, ApJ, **287**, 577
Kormendy, J., & Djorgovski, S. 1989, ARA&A, **27**, 235
Kronberg, P.P., Biermann, P., & Schwab, F.R. 1985, ApJ, **291**, 693
Larson, R.B., & Tinsley, B.M. 1978, ApJ, **219**, 46
Lutz, D. 1991, A&A, **245**, 31
Lynden-Bell, D. 1967, MNRAS, **136**, 101
Mazzarella, J.M., Gaume, R.A., Aller, H.D., & Hughes, P.A. 1988, ApJ, **333**, 168
Nieto, J.-L., Bender, R., Arnaud, J., & Surma, P. 1991, A&A, **224**, L25
Oegerle, W.R., Hill, J.M., & Hoessel, J.G. 1991, ApJL, **381**, L9
Quinn, P.J., & Goodman, J. 1986, ApJ, **309**, 472
Sanders, D.B., *et al.* 1986, ApJL, **305**, L45

Sanders, D.B., Scoville, N.Z., & Soifer, B.T. 1991, ApJ, **370**, 158
Sargent, A., & Scoville, N. 1991, ApJL, **366**, L1
Schechter, P.L., & Dressler, A. 1987, AJ, **94**, 563
Schweizer, F. 1978, in *Structure and Properties of Nearby Galaxies*, ed. E.M. Berkhuijsen & R. Wielebinski (Reidel, Dordrecht), p. 279
Schweizer, F. 1982, ApJ, **252**, 455
Schweizer, F. 1987, in *Nearly Normal Galaxies*, ed. S.M. Faber (Springer, New York), p. 18
Schweizer, F. 1990, in *Dynamics and Interactions of Galaxies*, ed. R. Wielen (Springer, Heidelberg), p. 60
Schweizer, F., & Seitzer, P. 1988, ApJ, **328**, 88
Schweizer, F., & Seitzer, P. 1992, AJ, **104**, in press
Schweizer, F., *et al.* 1990, ApJL, **364**, L33
Scoville, N.Z., Sargent, A.I., Sanders, D.B., & Soifer, B.T. 1991, ApJL, **366**, L5
Searle, L., Sargent, W.L.W., & Bagnuolo, W.G. 1973, ApJ, **179**, 427
Seitzer, P., & Schweizer, F. 1990, in *Dynamics and Interactions of Galaxies*, ed. R. Wielen (Springer, Heidelberg), p. 270
Solomon, P.M., Downes, D., & Radford, S.J.E. 1992, ApJL, **387**, L55
Stanford, S.A., Sargent, A.I., Sanders, D.B., & Scoville, N.Z. 1990, ApJ, **349**, 492
Stanford, S.A., & Bushouse, H.A. 1991, ApJ, **371**, 92
Stockton, A., & MacKenty, J.W. 1983, Nature, **305**, 678
Stockton, A., & Ridgway, S.E. 1991, AJ, **102**, 488
Thuan, T.X., Montmerle, T., & Tran Thanh Van, J. 1987, editors, *Starbursts and Galaxy Evolution*, XXIInd Rencontres de Moriond (Editions Frontières, Gif sur Yvette)
Toomre, A., & Toomre, J. 1972, ApJ, **178**, 623 (TT)
Toomre, A. 1977, in *The Evolution of Galaxies and Stellar Populations*, ed. B.M. Tinsley & R.B. Larson (Yale Univ. Observatory, New Haven), p. 401
van den Bergh, S. 1982, PASP, **94**, 459
van den Bergh, S. 1990a, in *Dynamics and Interactions of Galaxies*, ed. R. Wielen (Springer, Heidelberg), p. 492
van den Bergh, S. 1990b, A&A, **231**, L27
Wang, Z., Schweizer, F., & Scoville, N.Z. 1992, ApJ, in press
Whitmore, B.C., & Bell, M. 1988, ApJ, **324**, 741
Wright, G.S., James, P.A., Joseph, R.D., & McLean, I.S. 1990, Nature, **344**, 417
Yin, Q.F., & Heeschen, D.S. 1991, Nature, **354**, 130
Young, J.S., Kenney, J., Lord, S.D., & Schloerb, F.P. 1984, ApJL, **287**, L65
Young, J.S., & Scoville, N.Z. 1991, ARA&A, **29**, 581

EXPERIMENTAL STUDIES OF MERGERS

Joshua E. Barnes
University of Hawaii

ABSTRACT

Numerical modeling of interacting galaxies has the potential to settle a number of interesting theoretical questions. In this review I focus on results for slow collisions and mergers of equal-mass disk galaxies embedded in massive dark halos. Simulations show that orbital decay in such collisions is governed by the interactions of the extended halos, which absorb orbital angular momentum from the luminous components. Orbital decay leads to the formation of merger remnants with many of the properties of normal elliptical galaxies. However, remnants produced by pure stellar-dynamical mergers of equal-mass disk galaxies have rather diffuse cores and may exhibit more major-axis rotation than typical ellipticals. Simulations including gas dynamics suggest that dissipative effects may resolve these discrepancies.

1. Introduction

Traditionally, astronomers have used observations to motivate and test their ideas. But recently, as computer simulations have become more detailed and comprehensive, experimental methods are augmenting the observations. Perhaps nowhere is this trend better illustrated than in studies of interacting galaxies. Toomre and Toomre's[1] simplified but effective models showed that tidal forces, acting on cold, purely stellar disks, sufficed to explain the peculiar forms seen in many interacting systems. Their results set the stage for two decades of increasingly sophisticated numerical simulations.

This article presents recent numerical experiments on interactions and mergers of disk galaxies. For simplicity, all of the encounters discussed involve parabolic collisions of identical pairs. § 2 describes one particular simulation in detail and explains how the initial conditions are constructed. § 3 illustrates some of the consequences of tidal interactions for disk galaxies. § 4 describes the remnants of equal-mass disk mergers. § 5 offers a brief discussion of the main results.

2. Numerical Experiments

In the purely stellar-dynamical limit, encounters of galaxies are governed by the Collisionless Boltzmann Equation. N-body simulations are essentially Monte-Carlo solutions of this equation[2], and the accuracy of this approach is limited by the density of the Monte-Carlo sampling. Since the self-consistent potential is obtained from the particle distribution, fluctuations of order $N^{-1/2}$ in the latter give rise to a diffusive process in phase-space[3]. Some simple aspects of collisions between spherical systems may be studied with $N < 10^3$ particles, but $N \gg 10^4$ particles are needed to obtain moderately faithful models of disk galaxies. Hierarchical N-body codes[4], which offer asymptotic complexity of $O(N \log N)$ or better and high spatial resolution, are well-suited for simulations of interacting disk systems; the code used for the pure N-body simulations presented here was described by Barnes[5].

It is often interesting to also include the dynamics of the interstellar gas. A first-principles treatment of star formation, interstellar chemistry, and MHD is far beyond the capabilities of present computer programs; thus simulations including gas dynamics must gloss over many physical details. Two distinct approaches have been used in modeling gas dynamics in interacting galaxies. The "sticky particle" technique represents the interstellar medium as a collection of clouds which dissipate energy when they collide[6]. In "smoothed particle hydrodynamics" or SPH, the interstellar material is assumed to obey the standard equations of motion for a continuous gas, represented using particles[7,8]. Both methods give similar results in regimes where radiative cooling is efficient and pressure forces insignificant except in shocks; the gas-dynamical calculations described here were run with the SPH code of Hernquist & Katz[9].

2.1. Pictures of a collision

As an example, consider the pure N-body simulation shown in figure 1. In the first two frames the galaxies approach each other along the indicated parabolic trajectory. Pericenter occurs shortly before the third frame; already at this stage violent tidal forces have strongly perturbed both disks. The next two frames show the continued development of these tidal features. Both disks develop extended, curving tails, but only the direct disk, which lies to the left of center from the third frame on, exhibits a proper bridge. The last three frames show the second passage and merger of the two galaxies.

The further evolution of this merger remnant is shown in figure 2. The plots on the left show the development of the tidal tails. These tails, launched at first passage, are in essentially free expansion and continue to spread out at later times. The frames on the right show close-ups of the remnant. The elongated, nearly prolate form of this remnant is a legacy of the nearly head-on final encounter of the two original galaxies; its figure rotates slowly in the same direction as the two galaxies once orbited each other. The material around the remnant has an irregular distribution in the first frame, but becomes smoothed by phase-mixing at later times.

2.2. Galaxy models

The galaxy models used in these experiments are composite objects, each consisting of a central bulge, an exponential disk, and an extended dark halo[10]. To describe the models and the results, an arbitrary system of units with $G \equiv 1$ are used. In these units, each galaxy has a halo with mass $M_H = 1$ and half-mass radius $R_{H,1/2} \simeq 0.27$, a disk with mass $M_D = 3/16$ and exponential scale length $\alpha^{-1} = 1/12$, and a bulge with mass $M_B = 1/16$ and half-mass radius $R_{B,1/2} \simeq 0.032$. Thus the mass ratios of the three components are 1:3:16, and each galaxy has total mass $M = 1.25$, half-mass radius $R_{1/2} \simeq 0.25$, and binding energy of -1.38. A few runs were also made using galaxy models with halos of twice the standard mass and extent. All these model disks may be crudely scaled to the Milky Way by equating the units of length, mass, and time to 40 kpc, 2.2×10^{11} $M_\odot$, and 250 Myr, respectively.

2.3. Encounter parameters

Initial conditions for the simulations were generated by constructing pairs of galaxy models and launching them on approaching orbits. In every case here the galaxies were placed on parabolic orbits; that is, they were given the velocities they would have acquired falling together from resr at a very great distance. Such relatively slow passages naturally result when pairs of galaxies, bound by gravity since before their formation, come together for the first time along an eccentric orbit, and it is just such

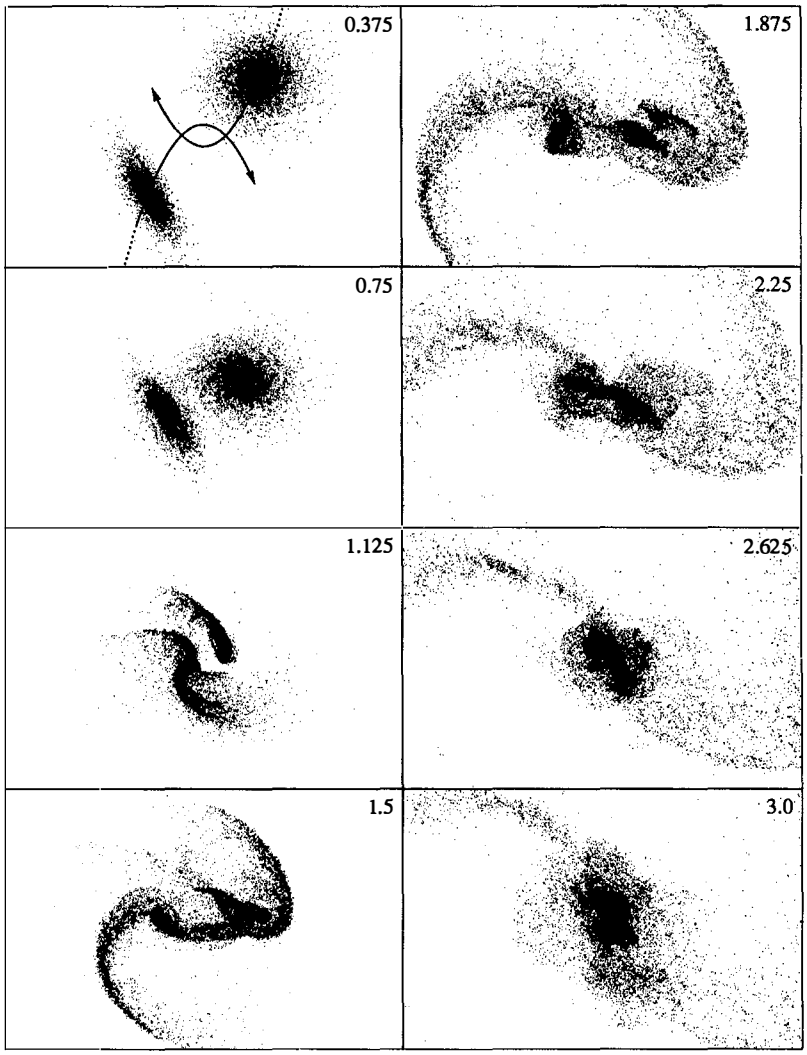

Figure 1. Parabolic collision and merger of two equal-mass disk/halo galaxies. Particles belonging to the halos are not plotted. This is a relatively close encounter, with a pericentric separation of $R_p = 0.2$ length units (see § 2.2). The disk on the right in the first frame lies exactly in the orbital plane ($i = 0°$) while the one on the left is inclined ($i = 71°$, $\omega = 30°$; see § 2.3). The smooth curves show the projected trajectories of two point masses with the same orbital parameters as these extended galaxies. Elapsed times are shown in the upper-right corners. Each frame is 3.6×2.4 length units.

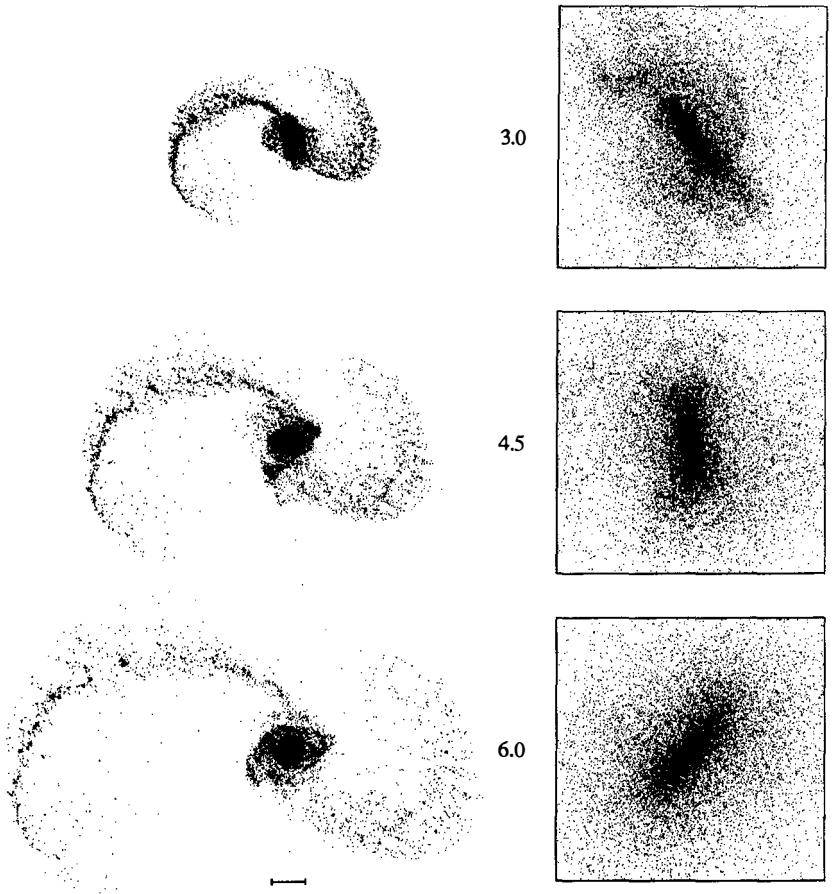

Figure 2. Continuation of the model shown in the previous figure. The plots on the left show the development of the tidal tails, while the enlarged frames on the right show the relaxation of the merger remnant. Elapsed times are indicated. The scale bar at the bottom is 1 unit long, while the frames are 0.8×0.8 units square.

slow encounters which are required to account for the structures of interacting disk systems[1].

The pericentric separation of a pair of galaxies – or equivalently, their orbital angular momentum – depends on the tidal force field generated by the mass distribution at larger scales. Only relatively close encounters yield really striking examples of galactic interaction, at least on the first passage. Orbital decay brings bound pairs of galaxies closer together each time around. However, such repeated encounters are more expensive to simulate, and their evolution depends on the overall distribution of the dark

matter, which is not (yet) well-constrained observationally. Thus the present experiments focus on relatively close encounters, with projected pericentric separations of $R_p = 0.2$ to 0.8 length units.

Two angles are required to specify the orientation of each axisymmetric disk. This article will use the inclination i with respect to the orbital plane, which ranges from $i = 0°$ for a direct passage to $i = 180°$ for a retrograde one, and the pericentric argument ω, which is the angle between the disk's line of nodes and the separation vector at pericenter, measured in the orbital plane from the former to the latter.

3. Tidal Interactions

Simulations by Toomre & Toomre[1] and others showed that tidal forces could extract rather narrow "bridges" and "tails" from disk galaxies. This basic result, obtained using disks of massless test particles, is completely confirmed in more recent self-consistent simulations.

3.1. Response of galactic disks

Figure 3 presents four tidally-perturbed disk galaxies. Three of these galaxies exhibit well-developed tidal tails and bridge-like features of varying definiteness. Only the bridge extracted from the direct disk actually extends to its companion; material flowing along this bridge has produced the shell-like feature seen to the right of the other galaxy. In the $\omega = 30°$ disk the bridge is quite weak, but this plunging, rather close passage has given the tidal tail the form of an expanding, nearly-circular arc. Such an arc is also seen in recent HI maps of M51[11], bolstering the argument that this system is the product of a tidal interaction[1,12].

These calculations reveal tidally-induced features which could not have been reproduced in test-particle models. For example, three of these disks have developed bars in response to tidal perturbations. Models including gas dynamics indicate that such bar-forming is an important factor in concentrating gas within the central regions of interacting galaxies[13,14]. The fourth disk has not developed a bar, but instead exhibits a "grand-design" spiral pattern reminiscent of galaxies like M51 and M81[15].

3.2. Dwarf galaxies in tidal tails

Self-consistent simulations also reveal interesting phenomena in the *tails* of interacting disk galaxies. Although such tails are unbound overall, small overdense regions may collapse gravitationally to form bound objects one might be excused for terming "dwarf galaxies". Such dwarfs have been observed in a number of interacting systems, including NGC 4038/9[16,17], NCG 7252[18], and IRAS 19254–7245[19,20]. They have also been found in numerical simulations, which shed light on their origins and formation[21].

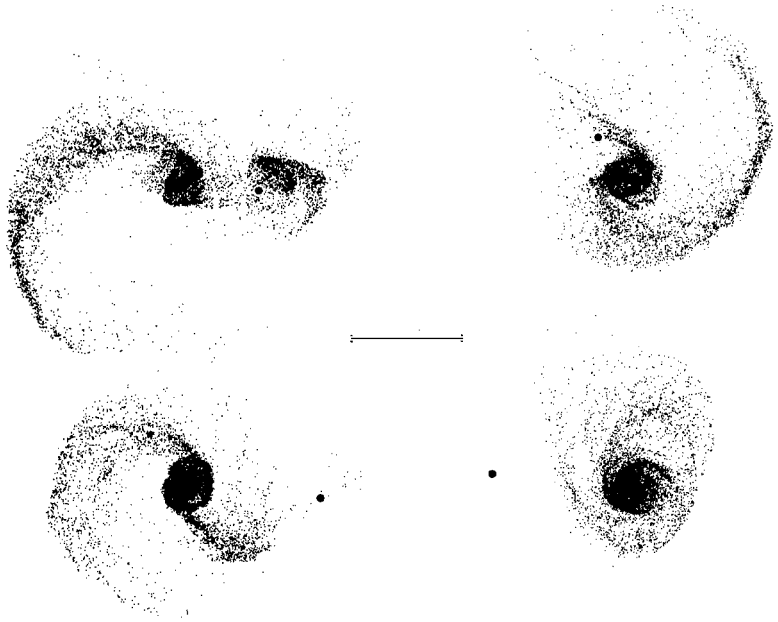

Figure 3. Responses of self-gravitating disks to tidal perturbations, 1 time unit after pericenter. Only disk particles are plotted, with the other galaxy indicated by a filled circle. The upper plots show the results of a close ($R_p = 0.2$) encounter on a direct disk (left: $i = 0°$) and its inclined companion (right: $i = 71°$, $\omega = 30°$). The lower plots are taken from a wider ($R_p = 0.4$) encounter between an inclined, slightly prograde disk (left: $i = 71°$, $\omega = 90°$) and a equally retrograde one (right: $i = 109°$, $\omega = 90°$). The scale bar is 1 unit long.

Figure 4 shows a number of such dwarfs identified in a combined N-body/SPH version of the encounter shown in figure 1. All these objects are gravitationally bound and fit within their present tidal radii. The most massive, which lies along the left-hand tidal tail quite close to the merger remnant itself, is quite gas-rich; others have potential wells too shallow to retain gas at temperatures of $\sim 10^4$ K. These objects incorporate relatively little dark matter from the halos of their parent galaxies, and so should have unusually low mass-to-light ratios when compared to galaxies formed directly by collapse of primordial perturbations.

3.3. Orbital decay

Bridges; tails, spirals, and bars are but outward and visible signs of tidal forces; more significant for the long-term evolution of interacting galaxies are the tidal responses of their dark halos. As White[22] noted, extended dark halos greatly increase the interaction cross-sections of galaxies.

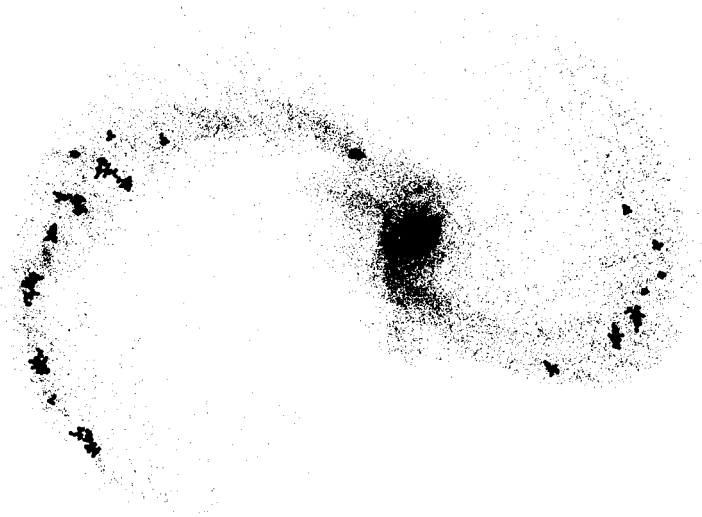

Figure 4. Bound objects in the tidal tails of a merged pair of disk/halo galaxies. Only particles from the disks and bulges of the original galaxies are shown. Particles belonging to bound "dwarf galaxies" are plotted as small filled circles. A total of 23 such objects were identified (some of which overlap in this view).

The physics of encounters between spherical, single-component systems was already well-illustrated in early simulations[22,23]. Particles which orbit within their parent galaxy in the same direction that the galaxies orbit each other receive angular momentum as a result of tidal forces. This angular momentum is taken from the relative orbit of the two galaxies, which therefore decays. In deeply interpenetrating parabolic encounters between equal-mass galaxies this mechanism is quite effective, leading to a merger on the subsequent passage.

Encounters between multi-component systems – such as the disk/halo galaxies in Figure 1 – exhibit more complex behavior. A naive application of Chandrasekhar's[24] dynamical friction formula to the motion of the tightly-bound luminous components of each galaxy through the extended dark halo of the other would predict a long orbital decay timescale, in sharp contrast to the numerical results. It turns out that the extended halos interact directly with ***each other*** much as single-component systems would, while the more compact luminous components subsequently lose their orbital angular momentum by interacting with their ***own*** halos[25]. Thus the direct interaction between the extended halos governs the orbital decay timescale for the entire system, and the compact luminous components can lose orbital angular momentum without being spun up by tidal torques.

4. Merger Remnants

Many peculiar galaxies appear to be the results of recent mergers. In cases such as NGC 7252 it is quite clear from the presence of two long tidal tails that the precursors were disk galaxies of comparable mass[18]. Yet NGC 7252 is clearly not now a disk galaxy – indeed, it appears to share certain features, such its de Vaucouleurs[26] luminosity profile, with elliptical galaxies[27].

4.1. Profiles and core radii

The luminosity profiles of elliptical galaxies were probably set up by *violent relaxation*[28]; that is, by the collisionless evolution of the stellar distribution in a rapidly changing gravitational field. Such a field is in fact temporarily created when galaxies merge. The left-hand side of figure 5 shows circularly-averaged luminosity profiles for a merger remnant (solid curves), and for an initial bulge/disk/halo galaxies (dotted curve). As expected, the remnant is much closer to a de Vaucouleurs profile than the galaxies it was assembled from; note that it also has a higher surface brightness at all radii. The effective radius of this remnant is ~ 0.1 length units.

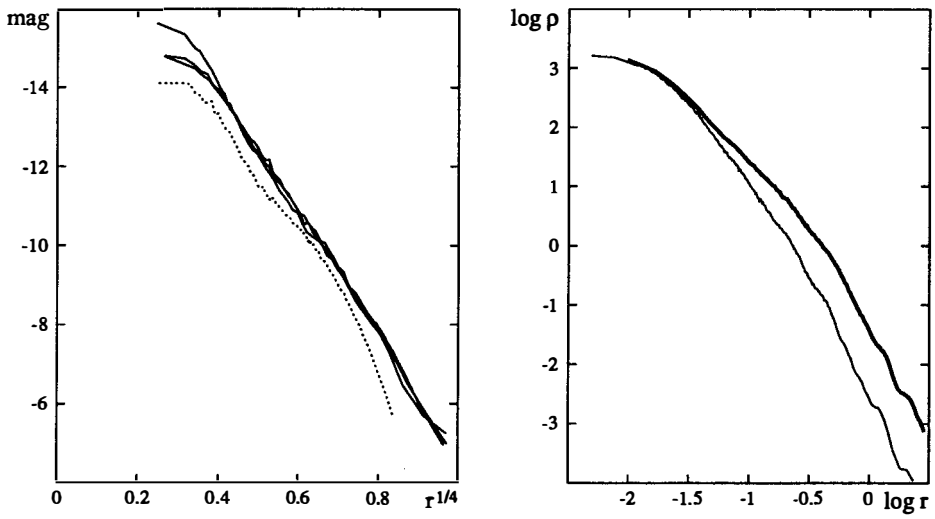

Figure 5. (*Left*) Projected luminosity profiles for a bulge/disk/halo galaxy viewed face-on (dotted curve), and for a typical remnant produced by the merger of two such galaxies, viewed along its three principal axes (solid curves). On this plot, a de Vaucouleurs profile is a straight line. (*Right*) Density profiles for a typical remnant. The heavy curve shows the total mass density, while the lighter curve shows the mass density of the luminous components (particles from bulges and disks).

The right-hand side of figure 5 shows spherically-averaged density profiles for various components of this merger remnant. The total density falls approximately as r^{-2} within the remnant body, and as r^{-4} at larger radii as predicted from the continuity of the distribution function[29,30]. The luminous density falls roughly as r^{-3} within the remnant body, showing that mass and luminosity are still significantly segregated. Evidently, the merging of equal-mass galaxies produces only partial violent relaxation, tending to smooth out features in the density profiles but largely preserving whatever abundance or color gradients may have been present in the original galaxies[31].

Even the most violent relaxation would not obliterate all traces of the original galaxies: pure N-body dynamics can only reduce a system's maximum coarse-grained phase-space density F_{max}, while a de Vaucouleurs profile extending all the way to the center implies $F_{max} = \infty$[32]. Detailed measurements indicate that F_{max} for material from the bulges of the original galaxies is reduced by only $\sim 30\%$ during the course of the merger. Thus the remnant featured in figure 5 has a rather large core radius – approximately 0.02 length units – as a direct consequence of the comparable core radii of the original bulges. Mergers between disk galaxies without central bulges may produce remnants with even larger core radii, since the scrambling of cold, rotationally-supported disks to produce a hot, pressure-supported remnant is accompanied by a factor of ~ 5 or more reduction in the coarse-grained F_{max}[25].

4.2. Orbital structure and kinematics

Remnants formed by purely stellar-dynamical mergers of disk galaxies exhibit a fairly wide range of shapes and kinematics, but all are basically triaxial in shape, and most tumble so slowly that figure rotation may be ignored. In the potential of such a galaxy one typically finds the following orbit families[33]:

1. *Box* orbits fill out a box-shaped region passing through the center.
2. *Z-tube* orbits loop around the minor axis without changing direction.
3. *X-tube* orbits loop around the major axis without changing direction.

Automatic classification of particle orbits according to this general scheme turns out to be very useful in analyzing the structure of simulated merger remnants[25]. Figure 6 presents results for particles from the luminous component of a remnant formed by the merger of two inclined disk galaxies. The plot on the left indicates, as a function of specific binding energy $E \equiv \phi + \frac{1}{2}v^2$, the relative number of luminous particles in each of the three main families listed above. Almost all particles in the most tightly bound quartile ($E \lesssim -8.6$) are on box orbits, helping to support the triaxial form of the system. Box orbits are also common among the less tightly bound particles, but so are X-tube and (to a lesser extent) Z-tube orbits. The plot on the right shows the major-axis component of the specific angular momentum j_X plotted against binding

energy for luminous particles on X-tube orbits. Note that particles from one disk tend to have $j_X > 0$, while those from the other tend to circulate the opposite way; this counter-streaming is a legacy of the anti-parallel spin vectors of the initial disks.

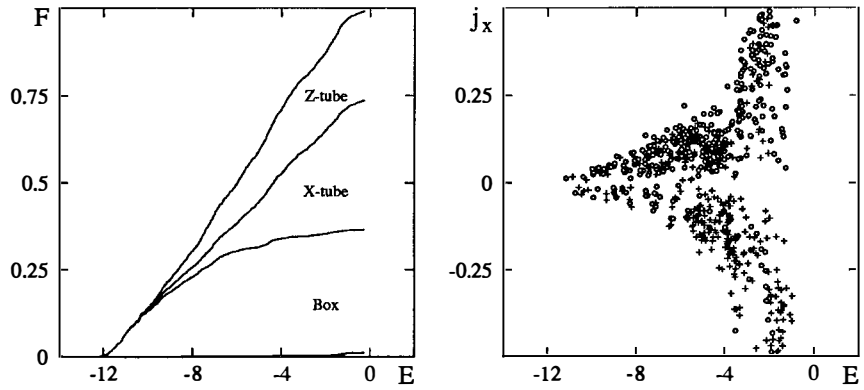

Figure 6. Orbit structure of the luminous component of a remnant produced by a close encounter of two inclined disk galaxy models. (*Left*) Orbit classifications, plotted as cumulative functions of particle binding energy, E. (*Right*) Major-axis component of angular momentum, j_X, plotted against binding energy. Circles are particles from one galaxy, crosses from the other.

Most significant for the present discussion is the asymmetry with respect to the line $j_X = 0$ seen for tightly-bound ($E \lesssim -6$) particles on X-tube orbits in figure 6. Such an asymmetry leads to significant major-axis rotation[34], and this remnant is not unique in exhibiting appreciatable angular momentum about its major axis[25]. However, the available data suggests that most elliptical galaxies, even though not rotationally supported, have fairly well-aligned spin and minor axes[35]. Purely stellar-dynamical mergers of randomly-oriented equal-mass disk galaxies appear to produce too many merger remnants with large spin-minor axis misalignments, a result which may yield important constraints on merger models for the formation of elliptical galaxies.

4.3. Dissipative merging

In all but the most extreme cases, gas comprises $\lesssim 10\%$ of the visible material in spiral galaxies, and an even smaller fraction of the total mass. Thus it seems plausible to suppose that the gas has only a modest influence on the collisionless dynamics of a pair of merging galaxies. But in fact, the gas can have an influence quite out of proportion to its mass if it becomes sufficiently concentrated.

Figure 7 shows the result of a merger between two gas-rich disk galaxies, simulated using a combined N-body/SPH code. The plot on the left shows the stellar distribution, while the enlarged view on the right shows that more than half of all the gas in this

object has been concentrated into a compact central cloud[6,14]. The physical parameters of this cloud are consistent with the central concentrations of molecular gas seen in infrared-luminous starburst galaxies such as NGC 520 and Arp 220[36].

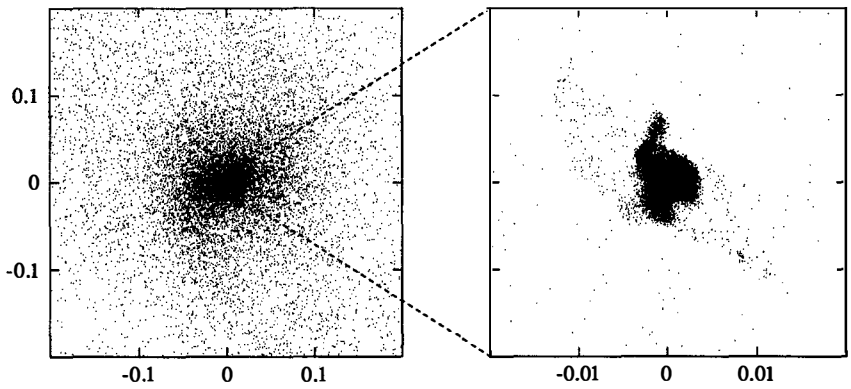

Figure 7. Merger of two gas-rich disk galaxies. (*Left*) Distribution of luminous particles, projected onto the orbital plane. (*Right*) Central distribution of gas, enlarged by a factor of 10.

Numerical experiments indicate that central gas clouds typically form during violent encounters between disk galaxies, a result which helps explain why so many extremely luminous infrared galaxies seem to be merging systems. As Kormendy & Sanders[37] note, such gas clouds attain masses and densities comparable to the central regions of elliptical galaxies, and the stars they form may account for the compact cores and high central metalicities of typical ellipticals. In some respects, this picture of elliptical galaxy formation resembles the classical "dissipative collapse" theory[38], but the circumstances in which these collapses occur are hardly standard!

The most striking difference between the classical and merger-induced collapse pictures is the redistribution of angular momentum during a merger. The gas which reaches the central regions of a remnant must first lose a great deal of angular momentum, and what spin it does retain may not be well-correlated with the rotation of the remnant as a whole. Figure 8 shows the gas distribution in a remnant produced by the merger of two inclined disk galaxies. The gas within a radius of ~ 0.1 length units has settled into a pair of nested disks; as the plot of line-of-sight velocities shows, the inner of these disks counter-rotates with respect to the outer[39]. If the inner gas disk was converted into stars, the result would be a galaxy with a counter-rotating core[40] – much like the counter-rotating cores observed in some elliptical galaxies[41].

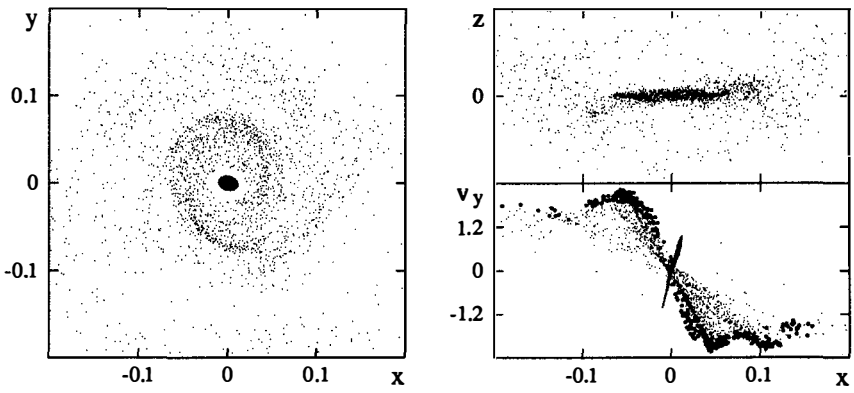

Figure 8. (*Left*) Face-on view of nested gas disks in the remnant of two inclined galaxies. (*Right, top*) Edge-on view of the gas disks. (*Right, bottom*) Line-of-sight velocities for gas particles within $|z| < 0.025$; those also within $|y| < 0.025$ are plotted as filled circles to highlight the rotation curve.

Gas-dynamical effects may also reduce the misalignments between rotation and minor axes reported above. Remnants produced by merger simulations including gas dynamics seem to be more oblate than their purely stellar dynamical analogs. Massive central gas clouds such as the one in figure 7 may deepen the potential well enough to destabilize box orbits[42], thereby removing the orbital family required to support triaxial structure. In addition, the stars formed from gas which has settled into a disk may dominate the velocity measurements even if they do not dominate the mass, causing the rotation axis to appear more accurately aligned with the minor axis than it really is.

5. Discussion

The "merger hypothesis" for the formation of elliptical galaxies is now being tested in detailed numerical simulations. Pure stellar-dynamical models of merging disk galaxies yield remnants matching the overall luminosity profiles, triaxial shapes, and slow rotation of normal elliptical galaxies[10]. However, these models fail to account for the small cores and good alignment between the rotation and minor axes of most Es[25]. Simulations including a modest amount of gas indicate that dissipative effects may resolve these discrepancies. Models of starburst systems are needed to complete the evolutionary link between mergers and elliptical galaxies; such models are currently held up by our incomplete understanding of star formation.

When combined with the observational results reviewed by Schweizer in this volume, the numerical experiments lend strong support to the idea that merging spirals are in fact forming elliptical galaxies – perhaps late, but better late than never! Moreover,

nearby mergers of disk galaxies offer us a glimpse of events at redshifts $z > 1$ which could well have formed the majority of cluster ellipticals. Successful modeling of mergers and starburst systems may be a prerequisite for an attack on the general problem of modeling galaxy formation.

It is a pleasure to thank Lars Hernquist for permission to present results of our work in advance of publication. Numerical calculations were run at the Pittsburgh Supercomputing Center.

REFERENCES

1. Toomre, A. & Toomre, J. *Ap. J.* **179**, 623 (1972).
2. White, S. in *The Origin and Evolution of Galaxies*, ed. B. Jones & J. Jones, p. 227 (Reidel: Dordrecht, 1983).
3. Hernquist, L. & Barnes, J. *Ap. J.* **349**, 562 (1990).
4. Greengard, L. *Comput. Physics* **4**, 142 (1990).
5. Barnes, J. *J. Comput. Phys.* **87**, 161 (1990).
6. Negroponte, J. & White, S. *MNRAS* **205**, 1009 (1983).
7. Lucy, L. *A. J.* **82**, 1013 (1977).
8. Gingold, R. & Monaghan, J. *MNRAS* **181**, 375 (1977).
9. Hernquist, L. & Katz, N. *Ap. J. Sup.* **70**, 419 (1989).
10. Barnes, J. *Ap. J.* **331**, 699 (1988).
11. Rots, A., Bosma, A., van der Hulst, J., Athanassoula, E., Crane, P. in *Dynamics and Interactions of Galaxies*, ed. R. Wielen, p. 112 (Springer-Verlag: Berlin, 1990).
12. Hernquist, L. in *Dynamics and Interactions of Galaxies*, ed. R. Wielen, p. 108 (Springer-Verlag: Berlin, 1990).
13. Noguchi, M. *Astr. Ap.* **203**, 259 (1988).
14. Barnes, J. & Hernquist, L. *Ap. J.* **370**, L65 (1991).
15. Toomre, A. in *The Structure and Evolution of Normal Galaxies*, ed. M. Fall & D. Lynden-Bell, p. 111 (Cambridge University Press: Cambridge, 1981).
16. Zwicky, F. *Ergeb. Exskten Naturwiss.* **29**, 344 (1956).
17. Mirabel, F., Dottori, H., & Lutz, D. *Astr. Ap.* **256**, L19 (1992).
18. Schweizer, F. in *Structure and Properties of Nearby Galaxies*, ed. E. Berkhuijsen & R. Wielebinski, p. 279 (Reidel: Dordrecht, 1978).
19. Mirabel, F., Lutz, D., & Maza, J. *Astr. Ap.* **243**, 367 (1991).
20. Colina, L., Lipari, S. & Macchetto, F. *Ap. J.* **379**, 113 (1991).
21. Barnes, J. & Hernquist, L. *Nature*, submitted (1992).
22. White, S. *MNRAS* **184**, 185 (1978).
23. White, S. *MNRAS* **189**, 831 (1979).

24. Chandrasekhar, S. *Ap. J.* **97**, 255 (1943).
25. Barnes, J. *Ap. J.* **393**, 484 (1992).
26. de Vaucouleurs, G. *Ann. d'Astrophys.* **11**, 247 (1948).
27. Schweizer, **F.** *Ap. J.* **252**, 455 (1982).
28. Lynden-Bell, D. *MNRAS* **136**, 101 (1967).
29. White, S. in *Structure and Dynamics of Elliptical Galaxies*, ed. T. de Zeeuw, p. 339 (Reidel: Dordrecht, 1987).
30. Jaffe, W. in *Structure and Dynamics of Elliptical Galaxies*, ed. T. de Zeeuw, p. 511 (Reidel: Dordrecht, 1987).
31. White, S. *MNRAS* **191**, 1P (1980).
32. May, A. & van Albada, T. *MNRAS* **209**, 15 (1984).
33. Binney, J. & Tremaine, S. *Galactic Dynamics*, (Princetion University Press: Princeton, 1987).
34. Levison, H. *Ap. J.* **320**, L93 (1987).
35. Franx, M., Illingworth, G., & de Zeeuw, T. *Ap. J.* **383**, 12 (1991).
36. Joseph, R. in *Dynamics and Interactions of Galaxies*, ed. R. Wielen, p. 132 (Springer-Verlag: Berlin, 1990).
37. Kormendy, J. & Sanders, D. *Ap. J.* **390**, L53 (1992)
38. Eggen, O., Lynden-Bell, D., & Sandage, A. *Ap. J.* **136**, 748 (1962).
39. Hernquist, L. & Barnes, J. *Nature* **354**, 210 (1991).
40. Schweizer, **F.** in *Dynamics and Interactions of Galaxies*, ed. R. Wielen, p. 60 (Springer-Verlag: Berlin, 1990).
41. Bender, R.. in *Dynamics and Interactions of Galaxies*, ed. R. Wielen, p. 232 (Springer-Verlag: Berlin, 1990).
42. Miralda-Escude, J. & Schwarzschild, M. *Ap. J.* **339**, 752.

SIMULATING GALAXY MERGERS WITH AN EVOLUTIONARY SYNTHESIS MODEL

U. Fritze - v. Alvensleben
Universitätssternwarte, Geismarlandstr. 11
W - 3400 Göttingen, Germany

O. E. Gerhard
Landessternwarte, Königstuhl
W - 6900 Heidelberg, Germany

ABSTRACT

During the merger of two spiral galaxies powerful starbursts can be induced. With a spectrophotometric and chemical galaxy evolution model we study the evolution of the stellar population of the progenitor galaxies through burst and merging, and beyond. The results of a parameter study are briefly described in terms of optical to NIR colours. Using the well-known galaxy NGC 7252 as an example we show how our models can be used to constrain the parameters, and to predict the future appearance of merger remnants. Comparison of the colours of NGC 7252 with our models and dynamical age estimates shows that in this merger the main burst must have started prior to final merging.

1. Introduction

Mergers between two approximately equal-mass spiral galaxies such as witnessed in the case of NGC 7252[1)] are believed to lead to the formation of an elliptical galaxy[2)]. The stellar dynamics of tidal interaction and merging is now fairly well understood[3)]; the fate of the gas in the two spiral disks is less certain. Probably most of the gas is eventually converted into stars, and at least part of the gas goes to the center before star formation[4,5)].

Here we describe recent work[6)] on the spectrophotometric evolution of mergers, starting with galaxies of various Hubble types and ages, and including the interaction - induced starburst. The aim of our investigation is to explore which spiral - spiral mergers may evolve into elliptical galaxies and on what timescale, and also to determine possible signatures of past merger events and how long these might serve to identify merger remnants among ellipticals. In the case of the well - studied merger remnant NGC 7252 we show how one can use the available information from observations and dynamical calculations to begin to constrain the parameters. The models then predict further observable quantities as well as the future evolution.

For the simulations we have used a chemical and spectrophotometric evolutionary synthesis model, which describes well the spectrophotometric properties of nearby galaxies of various Hubble types and the photometric evolution of galaxies for redshifts $z \lesssim 2$ [7)], as well as the detailed chemical evolution of the Milky Way and of gaseous galaxy halos for $z \lesssim 4$ [8,9)]. A major advantage of such a unified chemical and spectrophotometric model is that the number of observable quantities it predicts as compared to the number of input parameters is larger than in previous models. To fully exploit this advantage requires as much spectral and chemical information as possible.

2. Model

Here we outline only briefly some principal aspects of our models and refer the reader to a forth-coming paper[6] for further details. Starting from a gas cloud of given initial mass and primordial composition, stars are formed according to a star formation law specific for each spiral type[10] (see Fig. 1a). The total stellar mass is distributed in some 40 discrete mass bins in the range $0.4 \ldots 85\ M_{\odot}$, assuming a Scalo IMF. We use recent stellar evolutionary tracks, yields, and remnant masses to calculate the evolution in time of the gas content, the abundances of several individual elements, and the population of the HR diagram as a function of time and Hubble type. SNIa,b contributions are taken into account according to Stiavelli & Matteucci[11]. With photometric calibrations for UBVRIJHKL colours as a function of (T_{eff}, LC) for some 600 points along the 44 stellar evolutionary tracks we obtain the colour evolution of our model galaxies. Furthermore, we have built up a library of observed stellar spectra from the UV to the NIR comprising 31 stars from O5 V to M8 III[12,13] and 4 WR stars from P. Conti and collaborators. Thus, from the population of the HR diagram synthetic galaxy spectra can be calculated in an evolutionarily consistent way as a function of time and Hubble type. Gaseous emission lines are included in the way described by Guiderdoni & Rocca - Volmerange[14].

It should be stressed, however, that our model is a simple one zone closed box model, where no dynamical effects are taken into account. Stellar evolutionary tracks, photometric calibrations and stellar spectra are all for solar metallicity, which is, however, not too bad an assumption for late type mergers such as NGC 7252. For simplicity we only consider mergers between progenitor galaxies of equal Hubble type and comparable ages and masses. Thus the most important parameters in this study are the Hubble type and age of the progenitor galaxies, and the strength and

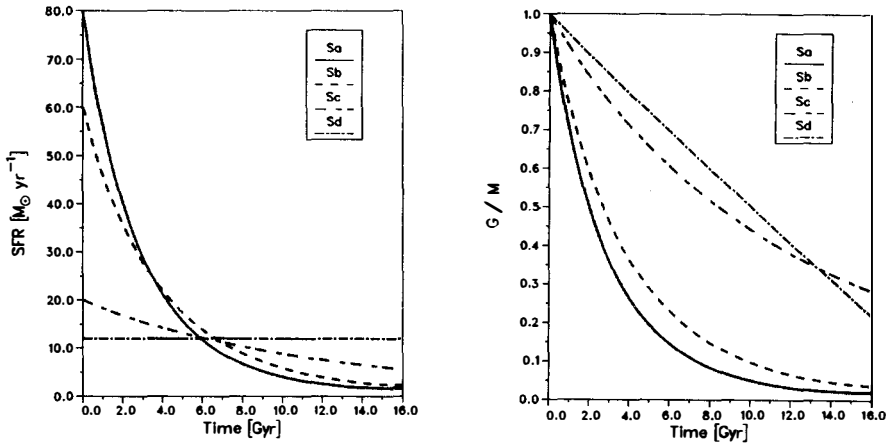

Fig. 1. Time evolution of star formation rates SFR [18] **(a)** and gas content G **(b)** for various undisturbed spiral types.

duration of the merger induced starburst. We define the burst strength b by the increase in stellar mass during the burst, $\Delta S_{\rm burst}$, normalized by the stellar mass present in the galaxy pair at the onset of the burst, $S_{\rm preburst}$, $b \equiv \Delta S_{\rm burst}/S_{\rm preburst}$.

3. Parameter study

Not very much is known about the detailed time dependence of star formation rate (SFR) in the course of merger events. One might expect some SF enhancement in the two disks to start around the time of first pericenter passage, and the maximum SFR to occur somewhere between then and shortly after actual core merging. Whether the global SFR rises continuously or in a series of bursts is not known, and might depend on the geometry of the encounter.

For our parameter study – presented here in terms of 2 colour diagrams – we have assumed a simplified rectangular form for the SFR during the burst. If not stated otherwise, the ages of the progenitor galaxies are as-

sumed to be $t_b \sim 12$ Gyr and the burst duration is $\tau_b \sim 10^8$ yr. Here we briefly describe the influence of the main parameters from our study[6].

Hubble type of the progenitors (Fig. 2a).

For a maximal burst, i.e. one consuming virtually all of the gas available at $t_b = 12$ Gyr for a given star formation law (see Fig. 1b), we find:

- Despite widely different burst strengths in the different Hubble types the blue loops in the (U-B) vs. (B-V) diagram differ only by $\lesssim 0.3$ in (B-V). In (V-I) the differences are distinctly larger as I shows the old population and V reflects the burst strength.
- All paths in the 2 colour diagram join into one passive evolution track some Gyrs after the burst, and even for maximal bursts in old $Sa - Sa$ through $Sc - Sc$ progenitors (but not $Sd - Sd$), the remnants evolve into the colour domain of ellipticals ($\oplus$) at a total age of about 15 Gyr. The colour difference between E/S0 galaxies and our merger remnants in Figs 2 and 3 is accounted for by some low level SFR (1.5 $M_\odot \mathrm{yr}^{-1}$).

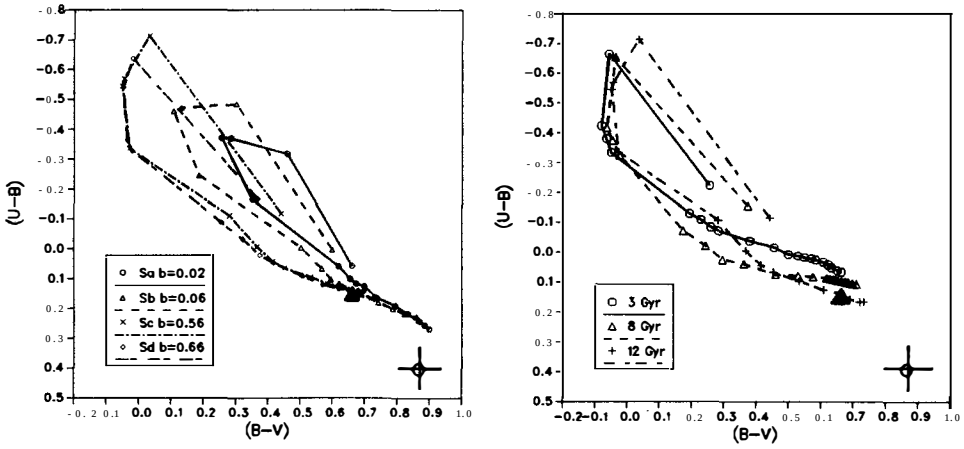

Fig. 2. Colour evolution during and after bursts of maximal strengths in mergers of various Hubble types at $t_b = 12$ Gyr **(a)** and of $Sc - Sc$ mergers at different progenitor ages **(b)**. $\oplus$ E, $S0$ colours from RC2, ▲ NGC 7252.

Age of the progenitor galaxies (Fig. 2b).

- For $Sc - Sc$ pairs with pre-merger ages in the range 3 – 12 Gyr the blue loops for maximal bursts are similar in the optical colours, but less so in (V-I).
- Only the remnants of **late** $Sc - Sc$ mergers ($t_b \gtrsim 12$ Gyr) can develop elliptical galaxy colours at around 15 Gyr.
- In the case of $Sa - Sa$ mergers somewhat younger progenitors ($t_b \gtrsim 8$ Gyr) can evolve into ellipticals because of the higher mean age of the preburst stars.

Burst strength (Fig. 3a).

For $Sc - Sc$ mergers at $t_b = 12$ Gyr we find that

- strong bursts with $0.35 \leq b \leq 0.60$ lead to very similar blue loops in (U-B) vs. (B-V) as well as in (V-I) vs. (U-V),
- for weaker bursts $0.12 \leq b \leq 0.35$ the loops slightly reflect the burst strength differences,
- about 10^8 yr after the end of the burst all tracks join smoothly,
- even small bursts can leave remnants which develop elliptical like colours if only the SFR after the burst is small enough ($\ll 1\ M_\odot \mathrm{yr}^{-1}$). However, these small bursts leave over considerable gas masses.
- Only strong bursts ($b \gtrsim 0.24$) result in a conspicuous A - type spectrum as is observed e.g. in NGC 7252.

Burst duration (Fig. 3b).

Models for $Sc - Sc$ mergers at $t_b = 12$ Gyr with fixed burst strength $b = 0.5$ and various burst durations $2.5 \cdot 10^7 \leq \tau_b \leq 10^9$ yr show

- an accumulation of massive blue stars saturating at $\tau_b \gtrsim 10^8$ yr,
- very similar elliptical like end colours for $2.5 \cdot 10^7 \leq \tau_b \leq 5 \cdot 10^8$ yr.
- At fixed burst strength M/L_B is, of course, strongly dependent on τ_b.
- About 1 Gyr after the end of the burst M/L_B reaches again its original value of $\simeq 4$.

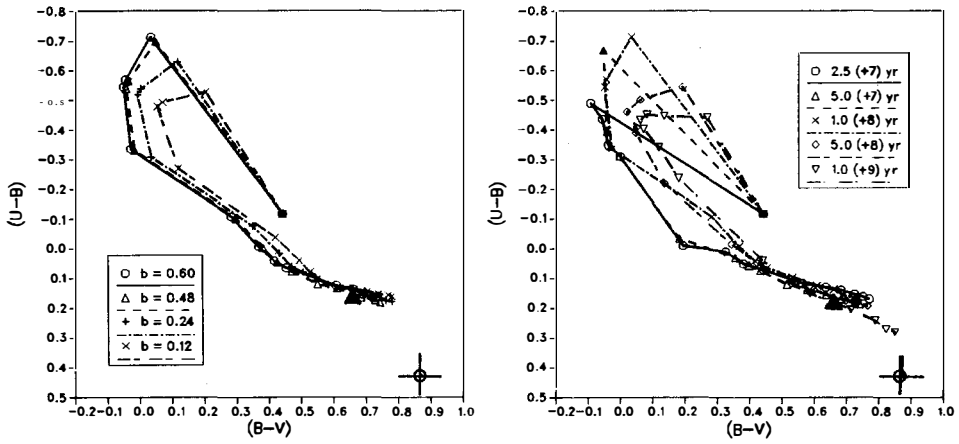

Fig. 3. Colour evolution in a 12 Gyr old $Sc - Sc$ pair for bursts of various strengths **(a)** and for a burst of fixed strength $b = 0.5$ and various durations τ_b **(b)**.

4. An example: NGC 7252

NGC 7252 (= Arp 226) is a well-known merger remnant observed by Schweizer in 1982[1]. It shows two extended tails and a wealth of ripples and loops. Yet the azimutally averaged inner light distribution already follows an $r^{1/4}$ – law. The tails and the presence of two kinematic subsystems point to a merger of two disk galaxies of comparable mass. The colours are observed to be (U-B) = 0.17, (B-V) = 0.66, (V-R) = 0.74, and are constant over a large radial range. $M_V \simeq -22.8$ ($H_0 = 75$). Dupraz et al[15] measured a molecular gas mass of $3.6 \cdot 10^9$ $M_\odot$ and a mass of neutral hydrogen of $3.4 \cdot 10^9$ $M_\odot$, and thus deduce a present gas content of about 4 % of the total mass. NGC 7252 shows an A7 type Balmer absorption line spectrum, in the nuclear region a small H_β emission feature might hint to a nonnegligible amount of ongoing SF[16]. Extinction is low, $E_{B-V} \leq 0.1$ [17], and late type disk progenitors ($\sim Sc$) seem to be more plausible than Sa. Comparing with dynamical models

Borne & Richstone[18] found that, while the morphological structure may be obtained from a variety of merging geometries, the velocity profiles seem to strongly constrain the orbital parameters.

Comparison with UBVR 2 colour diagrams for our models shows that the observed NGC 7252 colours are in fact matched by old ($\gtrsim 12$ Gyr) $Sc - Sc$ or $Sd - Sd$ mergers at some time after the burst. No information, however, can be deduced about the strength and duration of the burst because all the curves are close together in the interesting regime. So we decided to take 12 Gyr old $Sc - Sc$ spirals and explored a large variety of burst strengths, durations and forms in an attempt to fit the short observed spectrum (3600 - 4900 $\AA$) from Schweizer[16]. The best fit we could obtain is for a SF scenario A or B (Fig. 4a) at a time 1.3 - 2 Gyr after the beginning of the burst (Fig. 4b).

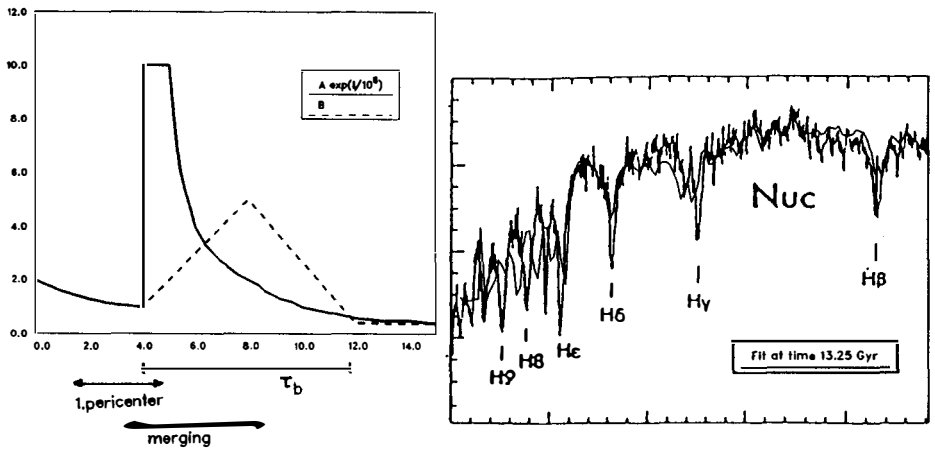

Fig. 4. Star formation scenarios during merger events **(a)** and best fit to the observed spectrum of NGC 7252[13] **(b)**.

Time evolution of our best fit model over the entire wavelength range (1150–10680 $\AA$) covered by our synthesized spectra is presented in Fig. 5. Once SF will have ceased another 1 or 2 Gyr from now, the spectrum will be that of a "typical" elliptical galaxy.

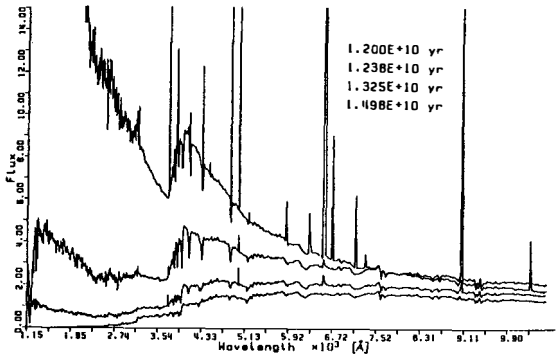

Fig. 5. Time evolution of the synthesized spectrum of NGC 7252.

The UBVRIJHKL colours our model gives for the present state of NGC 7252 are (U-B) $\simeq$ 0.18, (B-V) $\simeq$ 0.64, and (V-R) $\simeq$ 0.75, in good agreement with the observed values, and (R-I) $\simeq$ 0.58, (I-J) $\simeq$ 0.29, (H-K) $\simeq$ 0.12, (J-H) $\simeq$ 0.57 and (K-L) $\simeq$ 0.17 to be tested by future observations. "Typical" elliptical galaxy colours will be reached within $\sim$ 1 Gyr from now for UBV bands and within 2 – 4 Gyr for JHKL. The dominant luminosity contributions at present are seen in our models to arise from stars in the range 1 – 1.25 $M_{\odot}$ in all passbands (U,...,L). In U the relative luminosity contributions of dwarfs and giants are 83 % and 17 % respectively, whereas in L the ratio is nearly reversed, 25 % compared to 75 %, respectively. These ratios will, of course, change as the remnant evolves. At present the A star feature is made up to $\sim$ 70 % by the A7 V stars in our stellar library and to $\sim$ 30 % by the F4 V and F5 IV stars.

Our attempts to fit the observed part of the spectrum clearly indicated that a long burst duration $\tau_b \sim 3 - 5 \cdot 10^8$ yr is required and this result seems to be in agreement with van Driel's findings (this conference). The

burst strength for this best fit model has been set to the high value of $b \sim 0.5$, since we wanted to reproduce the actually observed gas content of ~ 4 %. This is because estimates based on our models showed that in no case a large scale galactic wind is expected in NGC 7252 (such as, e.g., in the "Superantennae" with its much higher SFR). These estimates refer to the balance between kinetic energy input from type I and II SNe and the binding energy of the gas according to Arimoto & Yoshii[19] and Matteucci & Tornambè[20], assuming a static spherical potential for the remnant. While a fit to the short part of the spectrum would be possible with burst strengths as low as $b \sim 0.1$, none of these models seemed to match the observed colours from (U-B) to (V-R) at the same time.

Our 'best fit time' for NGC 7252 is 1.3 – 2 Gyr after the beginning of the burst/enhanced SF, while Borne & Richstone's (BR) [18] dynamical simulations suggest an age of 1.1 – 1.3 Gyr ($H_0 = 75$) since apocenter (corresponding to $\sim 7 \cdot 10^8$ yr since first pericenter passage). Thus the main burst/enhanced SF in NGC 7252 should have begun significantly **before** the final merger. This is not implausible if one keeps in mind that with BR's orbital parameters the halos should already have merged completely at the time of apocenter.

Our models also predict chemical abundances/abundance ratios and, without going into detail, we briefly mention here that in our best fit model [C/O] e.g. decreases from a value of -0.09 at the onset of the burst to a minimum of -0.23 and then increases again to a present value of +0.02. It subsequently remains constant at this value, which is higher by about 0.07 than the [C/O] from our undisturbed E galaxy model SFR for the same Scalo IMF.

References

1 Schweizer, F. 1982, *Astrophys. J.* **252**, 455
2 Toomre, A. 1977, in "Evolution of Galaxies and Stellar Populations", eds. B. M. Tinsley & R. B. Larson (Yale Univ. Obs., New Haven), p. 401
3 Barnes, J. 1990, in "Dynamics and Interactions of Galaxies", ed. R. Wielen (Springer, Heidelberg), p. 186
4 Hernquist, L., Barnes, J. 1991, Nature **354**, 210
5 Joseph, R. D. 1990, in "Dynamics and Interactions of Galaxies", ed. R. Wielen (Springer, Heidelberg), p. 132
6 Fritze - v. Alvensleben, U., Gerhard, O. E. 1992, in preparation
7 Fritze - v. Alvensleben, U. 1989, PhD Thesis, Universität Göttingen
8 Fritze - v. Alvensleben, U., Krüger, H., Fricke, K. J., Loose, H.-H. 1989, *Astron. Astrophys.* **224**, L1
9 Fritze - v. Alvensleben, U., Krüger, H., Fricke, K. J. 1991, *Astron. Astrophys.* **246**, L59
10 Sandage, A. 1986 *Astron. Astrophys.* **161**, 89
11 Stiavelli, M., Matteucci, F. 1991, *Astrophys. J.* **377**, L79
12 Wu et al. (eds.) 1983, IUE Ultraviolet Spectral Atlas, *NASA* No. **22**
13 Gunn, J.E., Stryker, L.L. 1983, *Astrophys. J. Suppl.* **52**, 121
14 Guiderdoni, B., Rocca – Volmerange, B. 1987, *Astron. Astrophys.***186**, 1
15 Dupraz, C., Casoli, F., Combes, F., Kazès, I. 1990, *Astron. Astrophys.***228**, L5
16 Schweizer, F. 1990 in "Dynamics and Interactions of Galaxies", ed. R. Wielen (Springer, Heidelberg), p. 60
17 Prugniel, P., Bica, E. 1991, private communication
18 Borne, K. D., Richstone, D. O. 1991, *Astrophys. J.* **369**, 111
19 Arimoto, N., Yoshii, Y. 1987, *Astron. Astrophys.* **173**, 23
20 Matteucci, F., Tornambè, A. 1987, *Astron. Astrophys.* **185**, 51

Are Cluster Ellipticals Formed by Mergers?

GARY A. MAMON
DAEC, Observatoire de Paris-Meudon, 92195 Meudon, FRANCE

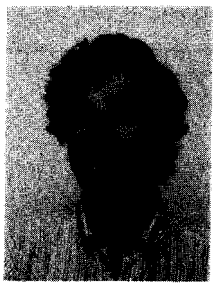

Abstract

The rates of evolution of cluster galaxy morphologies are integrated within a collision model where merger remnants have elliptical morphologies. Cluster and galaxy properties are set by cosmological spherical infall in an $\Omega = 1$ Universe, and once galaxies fall into the cluster, they are severely tidally stripped by the cluster potential. Mergers become efficient as galaxies rebound out of the cluster core. The local merger rate is shown to be constant in time. The precise shape of the morphology-density relation for ellipticals versus disks (spirals and S0s) is naturally explained by a simple toy model with equal mass galaxies falling into the cluster, including the sharp increase in elliptical fraction recently found by Whitmore & Gilmore within the central 100 kpc of clusters. The normalization of the relation is fit for galaxies satisfying on average $M/L = 50\,h$. Hence, mergers may well be responsible for elliptical morphologies in clusters.

1. Introduction

Are galaxy morphologies determined from evolutionary processes or from the conditions of their formation? Although simulations of merging galaxies yield elliptical-like

remnants[1],[2], questions have been raised as to whether *most* ellipticals could be formed by mergers[3],[4],[5] one objection being that the large velocity dispersion in clusters ought to prohibit merging[3]. Here, a merger model is presented to test whether or not galaxy mergers can produce the observed morphology-density[6] and morphology-radius[7],[8] relations in clusters of galaxies if initially nearly all the galaxies are non-elliptical. The mix of morphologies is evolved in time, assuming mergers yield ellipticals, in the context of galaxies falling into a cluster and being tidally stripped by the cluster potential as they pass through its center.

2. Cosmological Infall

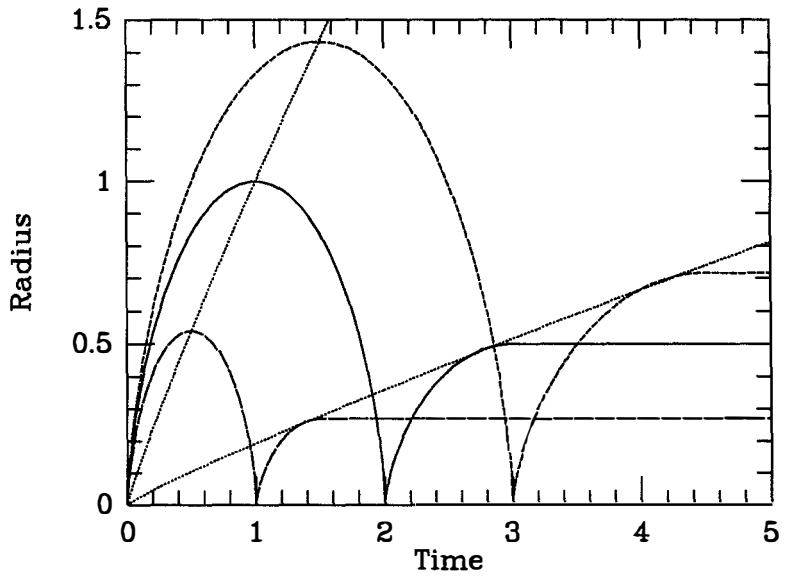

Figure 1. Time evolution of the radii of three shells (*solid*, and *dashed curves*). The locus of turnaround radii (eq. [1]) is given by the *upper dotted curve*, while that of the "mixing" radii is given by the *lower dotted curve*.

Figure 1 shows the time evolution of the radius of a shell of matter infalling into a cluster. The figure indicates that at a given time the regions beyond the turnaround radius of the cluster are expanding with the Universe, the outer regions of the cluster situated between the turnaround radius and the mixing radius, both shown in Figure 1, are infalling, while the inner regions of the cluster, within the mixing radius are the sites of shell crossing.

Top hat spherical infall[9] leads to the following scaling relations (for $\Omega = 1$):

$$M_{\rm ta} \sim t^{2/3} , \qquad R_{\rm ta} \sim t^{8/9} , \qquad \bar{\rho}(R_{\rm ta}) \sim t^{-2} . \tag{1}$$

As shells spend most of their time at a fixed fraction of their initial turnaround radius, one obtains a "pile-up" model of successive shells, where one can relate the properties of shells at different radii from the laws in equation (1) above[10]:

$$M(R) \sim R^{3/4} , \qquad \rho(R) \sim R^{-9/4} , \qquad v_{\rm cl}(R) \sim R^{-1/8} . \tag{2}$$

Finally, a consequence of the pile-up model is that all properties are fixed in time:

$$M(R,t) = M(R) , \qquad \rho(R,t) = \rho(R) , \qquad v_{\rm cl}(R,t) = v_{\rm cl}(R) . \tag{3}$$

The mean merger rate is low before the shell enters the cluster, because the local density of galaxies is low. Once it falls in, the merger rate remains low because the shell moves rapidly in the cluster. Only when the shell bounces back to its apocenter, its velocity relative to the cluster galaxies will be small, and only then will the merger rate be important. This occurs a little before three times the turnaround time $T_{\rm ta}$, and to be conservative, mergers are assumed to start precisely at $3\,T_{\rm ta}$.

3. Cluster Tides

As galaxies fall into the cluster their outer halos will be stripped from the tides emanating from the cluster potential itself. The tidal acceleration felt by a star in an infalling galaxy can be written

$$\mathbf{a_{tid}} = \frac{GM(S)}{S^3}\mathbf{S} - \frac{GM(R)}{R^3}\mathbf{R} , \tag{4}$$

where R and S are the distances of the galaxy center and the star to the cluster center, respectively. Each star then feels an impulse $\Delta\mathbf{v_{tid}} = \int_{-\infty}^{\infty} \mathbf{a_{tid}} dt$, and integrating equation (4), for the case of a scale-free density distribution $\rho \sim R^{-\alpha}$ and assuming an impulse approximation of constant velocity of the galaxy $\mathbf{V}$ yields

$$\Delta\mathbf{v_{tid}} = {\rm Cst} \times \frac{GM(R_p)r}{R_p^2 V} = {\rm Cst} \times f(\epsilon) \left(\frac{GM(R_p)}{R_p^3}\right)^{1/2} r , \tag{5}$$

where R_p is the pericentric distance, r is the distance of the star to the center of the galaxy ϵ is a measure of the ellipticity of the galaxy's orbit and $V(R_p)/V_{\rm circ} = 1/f(\epsilon)$.

Now identify the tidal radius with the radius of the last bound shell after the passage of the galaxy through the cluster center[11],[12]. Thus, $\Delta E(r_t) + E(r_t) = 0$, and with $E \sim Gm(r)/r$ and $\Delta E \simeq (\Delta v)^2/2$, equation (5) yields:

$$\bar{\rho}_{\rm gal}(r_t) = {\rm Cst} \times \bar{\rho}_{\rm cl}(R_p) . \tag{6}$$

From cosmological infall $\rho \sim r^{-9/4}$ for both galaxy and cluster (eq. [2]), equation (6) leads to $r_t \sim R_p$. If galaxies fall right through the cluster center then $R_p = 0$. However, galaxies acquire angular momentum through galaxy collisions and will thus miss the cluster center. Because the evolution of clusters is self-similar in the $\Omega = 1$ cosmology, it is natural to assume that $R_p \sim R_{\rm ta}$, *i.e.*, orbit elongations do not depend on when the galaxy falls into the cluster. Hence

$$r_t \sim R_{\rm ta} \ . \tag{7}$$

4. Merger Rate

The merger rate can be written $k(t) = \int_0^\infty s(v,t) v f(v,t) dv$, where $s(v,t)$ is the merger cross-section at time t, while $f(v,t)dv$ is the probability that the relative velocity of two merging galaxies is between v and $v + dv$ at time t. The merger criterion is a simplified version of that of Roos & Norman[13] giving a cross-section depending on a critical impact parameter that falls linearly with velocity:

$$s = \pi p^2 \ , \tag{8a}$$

$$p = \begin{cases} \alpha_p r_h \left(1 - \frac{v}{\alpha_v v_g}\right) & v < \alpha_v v_g \ , \\ 0 & v \geq \alpha_v v_g \ , \end{cases} \tag{8b}$$

where r_h and v_g are the average half-mass radius and the one-dimensional internal velocity dispersion of the two colliding galaxies, respectively, while α_p and α_v are dimensionless numbers. If the cluster is virialized, then $f(v)$ should describe a Maxwellian velocity distribution of dispersion $2^{1/2} v_{\rm cl}$, where $v_{\rm cl}$ is the one-dimensional velocity dispersion of the cluster. After some algebra, the merger rate turns out to be

$$k = 2\pi^{1/2} \alpha_p^2 \alpha_v r_h^2 v_g K(v_{\rm cl}/v_g) \ , \tag{9}$$

where K is a dimensionless merger rate that is maximum for $v_{\rm cl} \simeq 1.4 v_g$ and falls off as $(v_{\rm cl}/v_g)^{-3}$ for $v_{\rm cl} \gg v_g$ to values roughly 25 times lower for ratios typical of clusters. With $\alpha_p = 4$[14] and $\alpha_v = 3.1\sqrt{3}$[13] one gets the merger rate

$$k \simeq 8 \frac{G^2 m^2}{v_{\rm cl}^3} \ . \tag{10}$$

5. Simple Model

Consider the chemistry between disks (D) and ellipticals (E):

$$\mathrm{D} + \mathrm{D} \rightarrow \mathrm{E}$$

evolving with rate k. The elliptical fraction follows $df_E/dt = nk(1-f_E)^2$, which integrates to

$$\frac{f_E - f_i}{(1-f_E)(1-f_i)} = \int_{t_i}^{t_0} nk dt \ ,$$

where f_i is the initial elliptical fraction when a shell enters the cluster.

Consider now a shell at given radius R. In the cosmological pile-up model (eq. [3]) the local properties of the cluster are fixed. This implies that *the local merger rate is constant in time*. Then

$$\int_{t_i}^{t_0} nk dt = nk(t_0 - t_i) \simeq nkt_0 \tag{11}$$

Now from equation (7), tides limit the galaxies to $r_t \sim R_{\rm ta} \sim R$, hence $m \sim R^{3/4}$ (eq. [2]) and $v_g \sim v_{\rm cl}$. Hence $v_{\rm cl} \gg v_g$ at all times, and from equations (2) and (10), $k \sim R^{15/8}$. Now, $n \sim \rho(R)/m \sim R^{-3}$ (using eq. [2]), hence $nk \sim n^{3/8}$. Therefore, the merger model predicts

$$\frac{f_E - f_i}{1-f_E} \sim n^{3/8} \ . \tag{12}$$

Note that, generally, if $\rho \sim R^{-\alpha}$, the same analysis predicts a slope of $\alpha/6$.

6. Comparison with Observations

6.1 Shape and normalization

As shown in Figure 2, the observed morphology-density relation[6], derived from cluster data[15] yields an excellent fit to the power-law of slope 3/8 for the left-hand-side of equation (12) (with a best fit field elliptical fraction of 7.3%), giving $\chi^2 = 4.69$ for 6 degrees of freedom, while the best fit slope is 0.45 (with $f_i = 8.7\%$) giving $\chi^2 = 4.42$ for 5 degrees of freedom.

The model also predicts the morphology-radius relation $(f_E - f_i)/(1-f_E) \sim R^{-\alpha/2}$, which for the standard case of spherical infall ($\alpha = 9/4$) yields

$$\frac{f_E - f_i}{1-f_E} \sim R^{-9/8} \ . \tag{13}$$

Whereas a recent reanalysis[7],[8] of the cluster data[15] shows a sharp increase of the elliptical fraction within 100 kpc from the cluster cores, this increase is consistent[16] with the $-9/8$ slope in equation (13). Hence, *this simple merger model predicts the shape of the observed morphology-density relation probably even in the inner cores of clusters.*

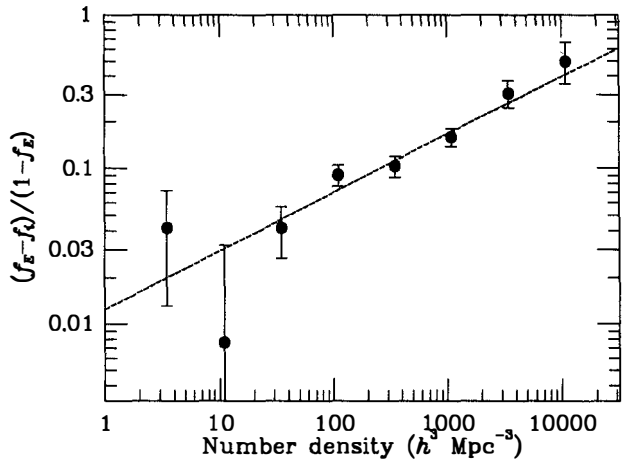

Figure 2. Morphology-density relation, with a best fit field elliptical fraction of 7.3%. *Points:* Observational data[15] transformed to space number densities[6]. *Lines:* Power-law predictions from equation (12).

The normalization to the fit of the observed morphology-density relation[6] is $f_E - f_i = 1.25 \times 10^{-2}[n/(h^3\,\mathrm{Mpc}^{-3})]^{3/8}$, which matches equations (10) and (11) if $8G^2nm^2t_0/v_{\rm cl}^3 = 0.43[n/(10^4h^3\,\mathrm{Mpc}^{-3})]^{3/8}$. For galaxies in the cluster cores (adopting $v_{\rm cl} = 1000\,\mathrm{km\,s}^{-1}$) this yields $m \simeq 2.1\,h^{-1}\,10^{11}[n/(10^4h^3\,\mathrm{Mpc}^{-3})]^{-5/16}\mathrm{M}_\odot$, which corresponds to $m/l_* \simeq 20\,h$ for $n = 10^4h^3\,\mathrm{Mpc}^{-3}$. Because the observed morphology-density relation is normalized to luminosities brighter than $0.174\,L_*^{6]}$, for which the harmonic mean luminosity is $\bar{l} = 0.38\,L_*$, giving a mean galaxy mass-to-light ratio $m/l \simeq 50\,h$, which is a reasonable value for galaxy halos. Note that once the halos of galaxies merge, the luminous components merge soon thereafter[2].

6.2 Groups versus clusters

Table 1 below shows how mergers should compare in rich clusters, loose groups, and compact groups.

Table 1

Environment	$n(h^3\,\mathrm{Mpc}^{-3})$	k (relative units)	nk (relative units)
Rich clusters	$10^3 - 10^4$	1/25	4
Loose groups	$10 - 100$	1	1
Compact groups	$10^3 - 10^4$	1	100

As the elliptical fraction is roughly given by the product nk, one sees from Table 1 that in loose groups ellipticals should be less frequent than in rich clusters. On the other hand, the fraction of ellipticals in compact groups[17] should be much higher

than in rich clusters and in fact nearly all the galaxies in compact groups should be merger remnants. Now this is clearly not so, as compact groups have much fewer ellipticals than rich clusters of comparable density[18], which seems best explained by the hypothesis that compact groups are merely chance alignments of galaxies within larger loose groups[18],[19]. The hypothesis of a universal morphology-density relation for groups and clusters[6] is not validated by this merger model and for the densities where both loose groups and rich clusters are present the loose group elliptical fraction should be much larger. The continuity found earlier[6] may be caused by the Virgo and Coma clusters contaminating the densest bin in their loose group sample[20].

6.3 Differences between rich clusters and between compact groups

Analysis of X-ray data from EXOSAT[21],[22] reveal interesting constraints on cluster properties: The spiral in clusters fraction *decreases* with cluster gas temperature as $f_S \sim T^{-1.2}$, whereas rich clusters tend to be hot as measured by $n(< 250\,h^{-1}\mathrm{kpc}) \sim \mathrm{T}^{0.9}$, where the term on the left is the number of galaxies within 250 kpc from the cluster center. From equation (10), one predicts $f_E \sim nm^2/T^{3/2}$. If the numerator were independent of cluster temperature, than one would expect *fewer* ellipticals in hot clusters, contrary to what is seen[22]. The metric galaxy number density n helps towards the opposite trend but is not sufficient. The mean galaxy mass is then the crucial variable, and one has

$$f_E \begin{cases} \sim T^{1.4} & \text{if } m \sim L_1 \ , \\ \sim T^{-0.6} & \text{if } m \text{ independent of } L_1 \ . \end{cases}$$

where L_1 is the luminosity of the brightest cluster member, and making use of the relation[21] $L_1 \sim T$. Hence the merger model cannot work unless the mean mass in galaxies scales as the luminosity of the brightest cluster member.

Note that in compact groups a similar trend exists[23]: $f_S \searrow$ with $v_{\mathrm{cl}} \nearrow$. The merger model here predicts that $f_E \sim n r_h^2 v_g$ with a negligible dependence on the group velocity dispersion v_{cl} (because the dimensionless merger rate K is near maximum for groups). Now, there is some question on how real the morphology-velocity dispersion relation is in compact groups. Indeed, compact group properties are strongly dependent on redshift[24], and the most distant groups tend to be elliptical rich, luminous, large, and with high velocity dispersions. These trends may be interpreted as being caused by the contamination of the distant compact groups in Hickson's catalog by the bright-ends of clusters[19],[25]. So if the morphology-velocity dispersion relation in compact groups is caused by a few distant compact groups being the bright-ends of clusters, than the merger model is OK, but if, on the other hand, the morphology-velocity dispersion relation is real, the merger model would not be adequate.

In summary, *despite their high velocity dispersions, clusters of galaxies should witness enough mergers to explain the high fraction of ellipticals seen in them.* These mergers occur from the low-end tail of the distribution of collision velocities in clusters. Nevertheless, the trend of increasing elliptical fraction with increasing cluster velocity dispersion may signify that processes other than mergers may contribute significantly to elliptical morphologies.

References

1] Barnes, J., 1988, *Ap. J.*, **331**, 699.

2] Barnes, J., 1993, in these proceedings.

3] Ostriker, J.P., 1980, *Comm. Ap.*, **8**, 177.

4] Tremaine, S.D., 1981, *in "The Structure and Evolution of Normal Galaxies"*, ed. S.M. Fall & D. Lynden-Bell (Cambridge: Cambridge University Press), p. 67.

5] van den Bergh, S., 1982, *P.A.S.P.*, **94**, 459.

6] Postman, M. & Geller, M.J., 1984, *Ap. J.*, **281**, 95.

7] Whitmore, B.C. & Gilmore, D., 1991, *Ap. J.*, **367**, 64.

8] Whitmore, B.C., 1993, in these proceedings.

9] Gunn, J.E. & Gott, J.R., 1972, *Ap. J.*, **176**, 1.

10] Gott, J.R., 1975, *Ap. J.*, **201**, 296.

11] White, S.D.M., 1983, *in Saas Fee Lectures, "Morphology and Dynamics of Galaxies"*, ed. L. Martinet & M. Mayor (Sauverny: Geneva Obs.), p. 289.

12] Mamon, G.A., 1987, *Ap. J.*, **321**, 622.

13] Roos, N. & Norman, C.A., 1979, *Astr. Ap.*, **95**, 349.

14] Aarseth, S. & Fall, S.M., 1980, *Ap. J.*, **236**, 43.

15] Dressler, A., 1980, *Ap. J.*, **236**, 351.

16] Mamon, G.A., 1993, in preparation.

17] Hickson, P., 1982, *Ap. J.*, **255**, 382.

18] Mamon, G.A., 1986, *Ap. J.*, **307**, 426.

19] Mamon, G.A., 1993, in these proceedings.

20] Whitmore, B.C., 1992, private communication.

21] Edge, A.C. & Stewart, G.C., 1991, *M.N.R.A.S.*, **252**, 414.

22] Edge, A.C. & Stewart, G.C., 1991, *M.N.R.A.S.*, **252**, 428.

23] Hickson, P., Kindl, E. & Huchra, J.P., 1988, *Ap. J.*, **331**, 64.

24] Mamon, G.A., 1990, *in IAU Colloquium 124 "Paired and Interacting Galaxies"*, ed. J.W. Sulentic & W.C. Keel (Washington: NASA), p. 619.

25] Mamon, G.A., 1993, *in 2nd DAEC meeting on "Distribution of Matter in the Universe"*, ed. G. Mamon & D. Gerbal (Paris: Obs. de Paris), p. 51.

ACTIVITY IN INTERACTING GALAXIES

Kirk D. Borne[1], Luis Colina[2], and James H. Scott[1]

[1] Space Telescope Science Institute[3], Baltimore, Maryland, USA
[2] Universidad Autónoma de Madrid, Spain

ABSTRACT

There is a large and growing body of evidence now available to support the idea that there is a connection between the observed activity in galaxies (whether nuclear or otherwise) and the apparent involvement of these active galaxies in tidal interactions with other galaxies. To investigate this phenomenon, we are studying the morphologies and environments of particular samples of active galaxies, and we are developing detailed models of specific pairs of interacting galaxies showing evidence of activity. In particular, we present here some preliminary results from our investigations of the claimed interaction–activity connection, both for a sample of starbursting IRAS galaxies and for a sample of colliding radio galaxies endowed with a bent radio jet morphology. We find that the IRAS sample galaxies are found in environments consistent with a tidal–triggering origin for their massive starburst event. For the radio jet sample we find that the timing of the jet activity is also consistent with a tidal–triggering hypothesis. Our results therefore lend further support to the idea that the various forms of galactic activity observed in these samples of "interactive" galaxies are in fact collision–induced.

[3]Operated by the Association of Universities for Research in Astronomy, Inc., for NASA

1. INTRODUCTION

Activity in galaxies has been the subject of increasingly intense study for nearly half of a century ever since the discovery of unusual emission lines in the nuclear spectra of some galaxies by Seyfert (1943), the optical identification of many powerful radio sources with extragalactic objects (*e.g.*, Baade & Minkowski 1954*a*,*b*), and the discovery of quasars (Schmidt 1963). The idea that interactions between galaxies may be related to the observed activity was suggested by Baade & Minkowski (1954*b*), with a similar suggestion by Arp (1966). While much work was done on active galaxies during the nearly thirty years following Seyfert's announcement, a plausible physical model for this ***interaction–activity connection*** was first elaborated upon (using graphic metaphorical language) in the bold hypotheses of Toomre & Toomre (1972) and Gunn (1977) that interactions could actually "stoke the furnace", or "feed the monster", in active galactic nuclei (AGN).

Further evidence for tidally–induced activity in galaxies came to light when Larson & Tinsley (1978) noted that the colors of a subsample of Arp's (1966) peculiar galaxies were consistent with recent star formation activity when compared against an undisturbed control sample; Sharp & Jones (1980) and Lonsdale, Persson, & Matthews (1984) later confirmed these findings.

In spite of these various suggestions, for a long time, research focussed more on the "personal" activity within AGN and not so much on their "social" interactions with their neighbors. Mergers and collisions among galaxies were at best an interesting side issue in the field of AGN research — at least, until recently (see reviews by Hernquist 1989, Stockton 1990, and Heckman 1990).

The study of interacting and merging galaxies has become very active in the last few years, due in large part to the discoveries by IRAS that the most IR–luminous galaxies are nearly all products of galaxy collisions and that these may be the missing link in the chain of evolution from quasars to normal quiescent galaxies (Sanders *et al.* 1988*a*,*b*). These highly luminous galaxies have a higher space density than quasars, emit >90% of their power in the IR, are rich in the raw materials of star formation (*i.e.*, molecular gas), and to a large extent owe their peculiar morphologies to interactions and/or mergers with other galaxies. The physical processes at work here are hypothesized to be the same as those at work in quasars — tidally disturbed galactic gas loses angular momentum in the tidal encounter and falls to the center of the galaxy, where it undergoes violent dissipation (and probably star formation), ultimately collapsing into the galaxy's nucleus, where it either falls into the lurking "monster" or else it contributes to the formation of the dense central star cluster that will itself ultimately form the massive central black hole (*i.e.*, the AGN engine; see Norman & Scoville 1988 and also the reviews by Heckman 1991*a*,*b*).

The evidence for tidal phenomena in a plethora of different active systems is now overwhelming: in quasars (*e.g.*, Yee & Green 1984; Stockton & MacKenty 1987; Hutchings 1987; Hutchings & Neff 1988,1990*a*), in AGN (*e.g.*, Dahari 1984; MacKenty 1989; Hutchings & Neff 1990*b*; Mazzarella, Bothun, & Boroson 1991), in radio–jet galaxies (*e.g.*, Colina & Pérez–Fournon 1990*a*,*b*), in powerful radio galaxies (*e.g.*, Heckman *et al.* 1986; Smith & Heckman 1989), in actively star–forming galaxies (= Starbursts; *e.g.*, Joseph & Wright 1985; Keel *et al.* 1985; Bushouse 1986; Kennicutt *et al.* 1987; Kennicutt 1990), in IRAS galaxies (*e.g.*, Sanders *et al.* 1988*a*,*b*; Lawrence *et al.* 1989; Carico *et al.* 1990;

Hutchings & Neff 1991), and in galaxies with strong central concentrations of molecular gas (*e.g.*, Sargent & Scoville 1991; Scoville *et al.* 1991). The particular importance of IR–luminous galaxies in the grand scheme of cosmology and galaxy evolution has been underscored by the luminosity function studies of Soifer *et al.* (1986), which have indicated that most galaxies have gone through a high–IR luminosity stage. It is therefore of tremendous importance to understand the relationship between this period in galaxies' lives and the occurrence of interactions and mergers.

A tantalizing discovery in recent years has been the so–called "alignment affect" in distant radio galaxies, wherein their radio, optical, and IR morphologies appear to be aligned over many decades in wavelength (Chambers, Miley, & van Breugel 1987; van Breugel & McCarthy 1990; Chambers & Miley 1990). Whether this is evidence for jet–induced star formation or for something else, it appears now that the early stages of galaxy formation and star formation within galaxies may be significantly affected, if not controlled, by galactic activity. While this effect has not been linked with tidal activity, it nevertheless demonstrates once again the tremendous importance of studying the causes and physical development of nuclear and starburst activity in galaxies as a means of increasing our understanding of the origin and evolution of the basic building blocks of the universe.

We describe in this paper some of our results in investigating the interaction–activity connection. We present an overview of our project in §2, including some technical remarks and a discussion of the numerical simulation techniques that we are applying to the theoretical aspects of the problem; we describe in §3 some observational results on the environments of the ultraluminous IRAS galaxies; and in §4 we present the results of a theoretical study of bent radio jets seen in pairs of colliding galaxies, with emphasis on one specific source, 3C 278.

2. STUDYING THE INTERACTION–ACTIVITY CONNECTION

It is clear from the weight of evidence now in hand that there is an important connection between galaxy interactions and galactic activity. Given the vast literature on the demographics of this interaction–activity connection, from so many research groups, there is very little doubt any more that somehow the two sets of phenomena are related. However, in spite of this wealth of observational supporting evidence, the precise relationship between interaction and activity is difficult to characterize as several studies have indicated that the majority of active galaxies do in fact show morphological signs of interaction, while other studies have shown that only a minority of all interacting systems are actually endowed with corresponding signs of activity (Smith & Hintzen 1991). This one–sided relationship was noted very early by Baade & Minkowski (1954*b*), and by many others since then (*e.g.*, Bushouse 1986). Thus, while morphological distortions may be good indicators of potential sites of galactic activity, every interaction does not appear to produce the same type or degree of activity. The physics and "sociology" of this unbalanced dichotomy are the subjects of our investigation (see §2.a). We note in particular that while several groups have begun theoretical studies of the problem of inducing galaxy activity via tidal interactions (*e.g.*, Hernquist 1989; Olson & Kwan 1990*a*,*b*; Barnes & Hernquist 1991), there has been no direct test of these methods against detailed observations. This is the gap that we are attempting to fill with the on–going work described here.

Detailed studies of interacting galaxies have traditionally concentrated on single objects, and these have yielded tremendous physical understanding and insight into these particular systems. The most significant new work that is needed to assess the importance of interaction dynamics in the production of various forms of galaxy activity is a similarly detailed one–on–one investigation of collision–activity models for individual active galaxies among a sample of interacting systems. Working with these models, we hope to accomplish the following: (1) either to find or to exclude an appropriate and possibly unique collision scenario for each *specific* active system (as in the work of Borne & Richstone 1991, and references therein); (2) to test the relevance of interactions to the observed activity in terms of mass transfer, gas shocking, nuclear gas accumulation, bursts of star formation, burst/activity timescales, potential for chemical enrichment, etc. (*e.g.*, Borne & Colina 1992); (3) to delimit and to parameterize the range of collision models that lead to potentially active systems; (4) to classify a wider variety of observed systems in the context of the derived collision model parameter space within which activity is found to accompany interactions; and (5) to predict the expected properties, frequencies, and interrelations of active and interacting galaxies as a function of both increasing redshift and galaxy environment.

In order to attack the various issues that are itemized above, sophisticated numerical simulation algorithms are required, as described below (§§2.a–2.c). Models containing purely stellar dynamical effects must be supplanted by similar models containing, in addition, simple hydrodynamic terms, which ultimately are to be replaced by models in which the gas phase is tracked on a galactic scale, including realistic effects: shocks, cloud collisions, angular momentum loss, "star formation", galactic winds, and nuclear gas accumulation. Each of these algorithmic steps has an important role and each can contribute to our understanding of "interactive" galaxies. But, it is at the last step in this development where substantial new ground will be broken and where our ability to test the interaction–activity connection will reach its fullest potential. We describe in the following sections some of the essential features and applications of these different methods.

(a) Stellar Dynamical Simulations

It has been shown that it is possible to model the optical morphological and kinematic properties of many merging and interacting galaxies (*e.g.*, Borne 1988*b*, 1990*a*, and references therein) with straightforward stellar dynamical simulation techniques. In these cases the final collision solutions can be used to derive various physical and orbital parameters of the constituent galaxies (Borne 1990*b*). *Galaxy masses, shapes, spins, and orientations, and orbital sizes, shapes, timescales, and orientations can all be constrained to various levels of precision*, depending on the quality and quantity of available data, with particular dependence on the kinematic data (Borne 1988*a*, 1990*a*,*b*). Merger remnants like NGC 7252 with a very complicated morphology and very complex kinematics can be reproduced in such simulations, even without including gas dynamical effects (Borne & Richstone 1991), and similarly for other complex collision remnants (*e.g.*, smoke–ring galaxies; Pence, Oegerle, & Borne 1990, and references therein).

Another result from these purely stellar dynamical simulations relates to the aforementioned dichotomy between activity and interactions, wherein most active systems

show evidence for interactions, but few interacting systems show evidence for activity. We have studied tidal phenomena in a large number of simulations of colliding galaxies. We find that the very large tidal disturbances that are often induced in galaxy encounters can even be produced in collisions where the galaxies are on strongly hyperbolic trajectories (*i.e.*, with high relative velocities, as would be found in moderately rich clusters of galaxies). This requires the encounter to have a reasonably small impact parameter, which in fact is also the prerequisite for inducing tidal effects in the cores of the constituent galaxies. Furthermore, we find that these disturbances (even in low–speed encounters) tend to be very long–lived, particularly at large galactic radii. Therefore, if the activity in galaxies is induced by tidal interactions and if that activity is relatively short–lived (on dynamical timescales), then we would expect the following results: (a) most active systems would show evidence for tidal interactions, and (b) very few colliding galaxies would show evidence for activity. These conclusions are in fact consistent with the statistical results of many different studies of the environments of active galaxies (see review by Heckman 1990).

On the whole, simple *stellar dynamical* collision models can do a modestly reasonable job at reproducing the *optical* observations of many interacting and merging galaxies. However, if one also attempts to model the *radio* observations, then additional input physics is required (§2.b), and if one tries to go further by attempting to model the full complement of *radio, infrared, and optical* observations of tidally–disturbed active galaxies, then nothing less than a full stars+gas simulation will suffice (§2.c).

(b) Ballistic Radio Jet Simulations

Over the past two years we have developed a new numerical simulation algorithm for modeling the propagation and morphology of ballistic radio jets in colliding galaxies (see §4 and Borne & Colina 1992). This algorithm has already been used quite successfully to fit the specific two–sided jet morphology seen in the radio source associated with 3C 278 (see §4). In our models the evolution of the radio jets is determined by their response to the time–dependent mechanical forces (*i.e.*, gravity and ram pressure) that act on the constituent jet blobs. Studies that combine the results of galaxy–collision models (§2.a) with the results of ballistic–jet models will help us to derive various properties of the sample of low–power radio galaxies involved in collisions. In particular, we hope to elucidate those systemic properties that are related to the galaxies' interaction dynamics, nuclear activity, and interstellar media. Specifically, these studies will permit us to check in a quantitative way the onset of nuclear activity in galaxies being subjected to the tidal shocks that are produced in strong galaxy collisions, such as the shocks now seen in NGC 4782 (3C 278), thereby directly testing the interaction–activity connection in this particular sample of "interactive" galaxies.

(c) Hybrid (Stars+Gas) Simulations

While much has been accomplished with the techniques described above, a new step must be taken in the simulations in order to attack the theoretical problems related to the gas that is inherently the intermediary of the interaction–activity connection. It

will therefore be necessary to add gas dynamical processes to the collision models, to complement the stellar dynamics and the simple jet kinematics that are already incorporated therein. Only with these additions will the goal of modeling the dominant radio and IR properties of these active systems be approachable with some reasonable degree of physical plausibility.

Many workers are making substantial and heartening progress in this most difficult area of numerical simulation research (*e.g.*, Noguchi & Ishibashi 1986; Hernquist 1989; Olson & Kwan 1990*a*,*b*; Barnes & Hernquist 1991; Mihos, Richstone, & Bothun 1991). These numerical models must be put to the "acid test" — *are we or are we not using the correct input physics for these objects, and can we actually model their full complement of observations?* Put another way: are these *numerical* models also *physical* models?

We ultimately hope to apply the hybrid stars+gas code to our continuing research program — the detailed matching of *specific* collision models to the observations of *specific* interacting galaxy pairs for which there is evidence for nuclear and/or starburst activity. This will substantiate directly, like nothing else, the validity both of these modeling techniques and of our understanding of the interaction–activity connection.

3. ULTRALUMINOUS IRAS GALAXIES

As a pilot observational study of the interaction–activity connection, we have chosen to investigate the morphological and environmental properties of the most intensely active and tidally disturbed sample of "nearby" galaxies, the ultraluminous IRAS galaxies. We report here only on the results of our study of their environments.

We have examined the digitized all–sky scans that were used to produce the STScI Guide Star Catalog in order to determine the projected density of non–stellar objects around the galaxies comprising the IRAS Ultraluminous IR Galaxy Sample and the Warm Ultraluminous Galaxy Sample (Sanders *et al.* 1988*a*,*b*). It has been suggested that each of the 19 galaxies identified in the combined sample is undergoing a major starburst event. From the distorted appearances of most of the galaxies, the starburst may have been triggered by a recent interaction (*i.e.*, a collision or merger) with another galaxy. The spatial frequency of galaxies in the neighborhoods of these IR–bright galaxies can therefore provide some indication of the likelihood and frequency of such collisions.

We have measured the number of non–stellar objects in fields 30–arcmin square centered on each of the galaxies in these samples, and in two similarly–sized adjacent fields (one each to the immediate west and east of the primary field). We find that *there is no significant difference in the local projected galaxy density around the 19 starbursting ultraluminous IR galaxies from that in the adjacent fields* (Fig. 1). We also find that *these galaxies inhabit a wide range of environments, from low– to high–density* (Fig. 2): range of projected densities $\approx 20 - 260$ non–stellar objects per square degree, down to our limiting instrumental magnitude.

If the galaxy density around these strongly starbursting galaxies had been higher than that of the adjacent fields, then the interaction hypothesis for the origin of the starbursts would *apparently* have been supported. However, if that were true, then it would be hard to understand how these galaxies could have avoided until the present epoch a

rapid gas–exhausting starburst event of the type that they are now experiencing. Conversely, if the galaxy density around these starburst galaxies had been significantly lower than in the adjacent fields, then galaxy–galaxy collisions would have been rare indeed, making it very difficult to explain their apparently tidally disturbed morphologies. But, if their local galaxy densities were like that of the surrounding field galaxy population, then each of these galaxies could have maintained a dense ISM until late times, at which point a single random collision would produce both its very disturbed morphology and the currently observed "once–in–a–lifetime" major starburst event, thereby permitting the galaxy to be included in the present Ultraluminous IR Galaxy Samples.

Given the insignificant difference in the projected galaxy densities around these disturbed ultraluminous IR galaxies compared to that in adjacent fields, and given the wide range of local galaxy densities in the neighborhoods of these galaxies, we conclude that ***galaxy interactions may indeed be responsible for these starburst events and that such events are occurring at the present epoch in a random, environment–independent manner.***

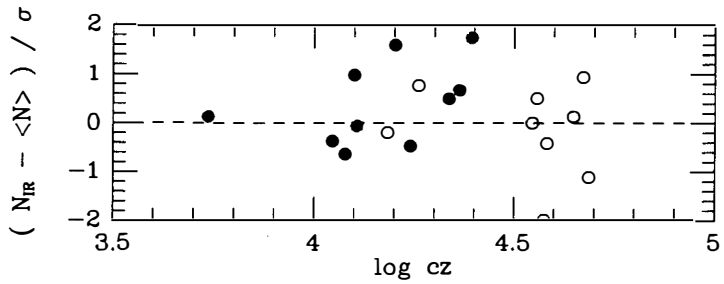

Figure 1 — Excess galaxy counts around each of the ultraluminous IR galaxies, as a function of the redshift of the IRAS galaxy. The ordinate is the difference between the number of galaxies in the IRAS galaxy field N_{IR} and the average number of galaxies in two adjacent control fields $< N >$, divided by $\sigma \equiv (N_{IR})^{1/2}$. Filled symbols represent the Ultraluminous IR Galaxies; open symbols represent the Warm Ultraluminous IR Galaxies.

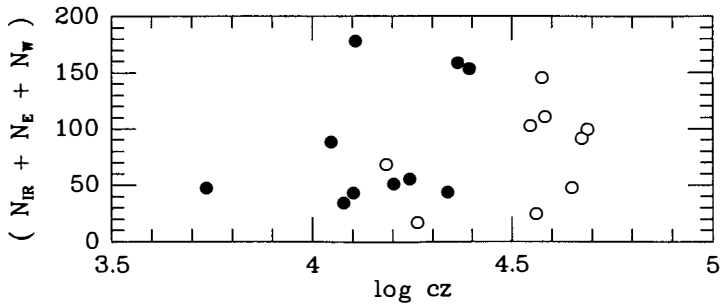

Figure 2 — Total galaxy counts around each ultraluminous IR galaxy and its two adjacent control fields, as a function of the redshift of the IRAS galaxy. Filled symbols represent the Ultraluminous IR Galaxies; open symbols represent the Warm Ultraluminous IR Galaxies.

4. RADIO JETS IN COLLIDING GALAXIES

A second project that we are pursuing related to the interaction–activity connection is a study of radio jet galaxies involved in collisions with other galaxies. In a recent CCD optical study of galaxies selected on the basis that they all contain well defined radio jets, it was found that almost half of the sample consists of pairs of elliptical galaxies (Colina & Pérez–Fournon 1990*a*,*b*). Many of these low–luminosity radio galaxies with companions (*e.g.*, 3C 31, 3C 278, 3C 449, and NGC 1044) show a well defined distorted radio jet structure at the VLA scale with an *S*– or *C*–shaped morphology.

We have developed a general numerical simulation algorithm for ballistic radio jets with the intention of applying this model to the study of the bent jets seen in colliding pairs of galaxies and with the hope of testing the well documented interaction–activity connection (Borne & Colina 1992). In our model the morphological evolution of the jets is determined by their response to the simple mechanical forces (*i.e.*, gravity and ram pressure) imposed on them from both the host and the companion galaxies. Radiative losses, jet precession, magnetic effects, relativistic terms, and hydrodynamic instabilities have all been ignored.

Starting with a previously derived collision model for the interacting pair of elliptical galaxies NGC 4782/4783, we have used our algorithm to simulate the specific two–sided jet morphology seen in the radio source 3C 278, associated with NGC 4782. *This is the first time that such jet simulations have been produced for a galaxy pair whose relative orbit was determined independently from the jet modeling.* The masses of the galaxies and their relative orbit (including its 3–dimensional de–projection) were all derived from stellar dynamical numerical simulations by Borne, Balcells, & Hoessel (1988). Their best–fit collision model (as used here in the radio jet simulations) was constrained by a combination of optical morphological and kinematic data for this strongly disturbed pair of galaxies.

Our jet models constrain the initial jet parameters (*i.e.*, ejection speed, direction, and starting time), the properties of the hot (x–ray emitting) gaseous medium into which the jets are ejected, and the relative importance of gravitational deflection versus ram pressure bending in influencing the jet morphology. For 3C 278, *we find that the effects of ram pressure dominate the structural evolution of the jets.* In our best–fit model the jet ejection speed is of order 10^4 km s^{-1}, the jets are ejected within $\sim 5°$ of the line–of–sight, the hot ISM in the non–jet galaxy (NGC 4783) has a much larger effect on the jet deflection than does that of the host galaxy (NGC 4782), and the jet activity began just over 70 million years ago, roughly 50 million years before the pericenter passage of the two galaxies ($H_0 = 60$ km s^{-1} Mpc^{-1}). *If there is a causal connection between the collision and the radio source generation, as indicated here, then it must become important early in the interaction.* This is not unreasonable since the derived collision model for the NGC 4782+4783 pair indicates that they have suffered a very strong tidal encounter, approaching one another on a deeply penetrating trajectory that had the cores of the galaxies separated by a little less than one galaxy diameter at the time that our model jet activity began. Therefore, *the onset of nuclear activity in 3C 278 appears to be related to the kinematically observed tidal shock* (*i.e.*, very large central stellar velocity dispersion, 392 km s^{-1} [Tonry & Davis 1981]) *and the very high central surface brightness* (Burbidge *et al.* 1964) *that have been induced in the core of NGC 4782 as a result of its deeply penetrating collision with NGC 4783.*

The general morphological features of the jets seen in 3C 278 (*e.g.*, position angles, lengths, curvature, and deflection angles) are well matched by our simulations, indicating that our model for the mechanical forces acting on the jets can indeed reproduce most of the basic details of the jet morphology. Alternative jet–bending models have been investigated (*i.e.*, collisions with cold gas clouds, and flow against an external, intergalactic gaseous medium), but these produce jets that are not consistent with the observations. Our simulations therefore provide opportunities both to model a combination of detailed optical, radio, and x–ray data for a wide variety of interacting radio–jet galaxies and to investigate the causal connection between the interaction and activity seen in these systems, *a connection that appears to be confirmed in our study of 3C 278.*

5. SUMMARY

The study of interacting galaxies has become very diversified and very productive in recent years. One of the clear results of these manifold studies is the apparent causal connection between some interactions and various forms of activity within the participating galaxies. Considering the preponderance of active galaxies in high–redshift samples of galaxies (selected on the basis of high IR or radio flux), deeper analysis and investigation of this interaction–activity connection holds promise for tremendous insight into the formation and evolution of galaxy–scale structures in the universe.

It is our intention to study those systems that are near enough for their morphology to be discerned and for which there exists clear evidence of both activity and an ongoing interaction. The ultimate success in interpreting these objects, including the numerical modeling of their interaction dynamics (in the stars and the gas), will be assessed for the various cases, demonstrating whether we are using the right physical model for the observed phenomena. The result will be a validation check on the apparent relationship between interaction and activity in galaxies and this in turn will shed light on the likely physical origins of that relationship, thus providing a measure of the overall cosmological significance of interactions and activity in galaxies. This will ultimately help to answer the fundamental questions that have been inspired by the wealthy accumulations of radio and IR observations of galaxies: Is activity in galaxies actually triggered by tidal interactions? And: what is the validity and relevance of the interaction–activity connection for the origin, structure, and evolution of galaxies in the universe?

REFERENCES

Arp, H. C. 1966, ApJS, 14, 1.

Baade, W., & Minkowski, R. 1954*a*, ApJ, 119, 206.

_____. 1954*b*, ApJ, 119, 215.

Barnes, J. E., & Hernquist, L. E. 1991, ApJ, 370, L65.

Borne, K. D. 1988*a*, ApJ, 330, 38.

_____. 1988*b*, ApJ, 330, 61.

_____. 1990*a*, in Dynamics and Interactions of Galaxies, ed. R. Wielen (Berlin: Springer), p. 196.

_____. 1990*b*, in Paired and Interacting Galaxies, IAU Colloquium #124, eds. J. W. Sulentic, W. C. Keel, & C. M. Telesco (NASA), p. 537.

Borne, K. D., Balcells, M., & Hoessel, J. G. 1988, ApJ, 333, 567.

Borne, K. D., & Colina, L. 1992, ApJ, submitted.

Borne, K. D., & Richstone, D. O. 1991, ApJ, 369, 111.

Burbidge, E. M., Burbidge, G. R., & Crampin, D. J. 1964, ApJ, 140, 1462.

Bushouse, H. 1986, AJ, 91, 255.

Carico, D. P., Graham, J. R., Matthews, K., Wilson, T. D., Soifer, B. T., Neugebauer, G., & Sanders, D. B. 1990, ApJ, 349, L39.

Chambers, K. C., & Miley, G. K. 1990, in Evolution of the Universe of Galaxies, ed. R. G. Kron (San Francisco: ASP), p. 373.

Chambers, K. C., Miley, G. K., & van Breugel, W. 1987, Nature, 329, 604.

Colina, L., & Pérez–Fournon, I. 1990*a*, ApJS, 72, 41.

_____. 1990*b*, ApJ, 349, 45.

Dahari, O. 1984, AJ, 89, 966.

Gunn, J. E. 1977, in Active Galactic Nuclei, eds. C. Hazard & S. Mitton (Cambridge: Cambridge University Press), p. 213.

Heckman, T. M. 1990, in Paired and Interacting Galaxies, IAU Colloquium #124, eds. J. W. Sulentic, W. C. Keel, & C. M. Telesco (NASA), p. 359.

_____. 1991*a*, in Massive Stars in Starburst Galaxies, eds. C. Leitherer, N. Walborn, T. Heckman, & C. Norman (Cambridge: Cambridge University Press), p. 289.

_____. 1991*b*, in Testing the AGN Paradigm, proceedings of a University of Maryland Symposium, in press.

Heckman, T. M., Smith, E. P., Baum, S. A., van Breugel, W. J. M., Miley, G. K., Illingworth, G. D., Bothun, G. D., & Balick, B. 1986, ApJ, 311, 526.

Hernquist, L. 1989, Nature, 340, 687.

Hutchings, J.B. 1987, ApJ, 320, 122.

Hutchings, J. B., & Neff S. G. 1988, AJ, 96, 1575.

_____. 1990*a*, AJ, 99, 1715.

_____. 1990*b*, in Paired and Interacting Galaxies, IAU Colloquium #124, eds. J. W. Sulentic, W. C. Keel, & C. M. Telesco (NASA), p. 383.

_____. 1991, AJ, 101, 434.

Joseph, R., & Wright, G. 1985, MNRAS, 214, 87.

Keel, W. C., Kennicutt, R. C., Hummel, E., & van der Hulst, J. M. 1985, AJ, 90, 708.

Kennicutt 1990, in Paired and Interacting Galaxies, IAU Colloquium #124, eds. J. W. Sulentic, W. C. Keel, & C. M. Telesco (NASA), p. 269.

Kennicutt, R. C., Keel, W. C., van der Hulst, J. M., Hummel, E., & Roettiger, K. A. 1987, AJ, 93, 1011.

Larson, R. B., & Tinsley, B. M. 1978, ApJ, 219, 46.

Lawrence, A., Rowan–Robinson, M., Leech, K., Jones, D. H. P., & Wall, J. V. 1989, MNRAS, 240, 329.

Lonsdale, C. J., Persson, S. E., & Matthews, K. 1984, ApJ, 287, 95.

MacKenty, J. 1989, ApJ, 343, 125.

Mazzarella, J. M., Bothun, G. D., & Boroson, T. A. 1991, AJ, 101, 2034.

Mihos, J. C., Richstone, D. O., & Bothun G. D. 1991, ApJ, 377, 72.

Noguchi, M., & Ishibashi, S. 1986, MNRAS, 219, 305.

Norman, C., & Scoville, N. 1988, ApJ, 332, 124.

Olson, K. M., & Kwan, J. 1990*a*, ApJ, 349, 480.

_____. 1990*b*, ApJ, 361, 426.

Pence, W. D., Oegerle, W., & Borne, K. D. 1990, AJ, 100, 1766.

Sanders, D. B., Soifer, B. T., Elias, J. H., Madore, B. F., Matthews, K., Neugebauer, G., & Scoville, N. Z. 1988*a*, ApJ, 325, 74.

Sanders, D. B., Soifer, B. T., Elias, J. H., Neugebauer, G., & Matthews, K. 1988*b*, ApJ, 328, L35.

Sargent, A., & Scoville, N. 1991, ApJ, 366, L1.

Schmidt, M. 1963, Nature, 197, 1040.

Scoville, N., Sargent, A. I., Sanders, D. B., & Soifer, B. T. 1991, ApJ, 366, L5.

Seyfert, C. K. 1943, ApJ, 97, 28.

Sharp, N., & Jones, B. 1980, Nature, 283, 275.

Smith, E. P., & Heckman, T. M. 1990, in Dynamics and Interactions of Galaxies, ed. R. Wielen (Berlin: Springer), p. 450.

Smith, E. P, & Hintzen, P. 1991, AJ, 101, 410.

Soifer, B. T., Sanders, D. B., Neugebauer, G., Danielson, G. E., Lonsdale, C. J., Madore, B. F., & Persson, S. E. 1986, ApJ, 303, L41.

Stockton, A. 1990, in Dynamics and Interactions of Galaxies, ed. R. Wielen (Berlin: Springer), p. 440.

Stockton, A., & MacKenty, J. 1987, ApJ, 316, 584.

Tonry, J., & Davis, M. 1981, ApJ, 246, 666.

Toomre, A., & Toomre, J. 1972, ApJ, 178, 623.

van Breugel, W. J. M., & McCarthy, P. J. 1990, in Evolution of the Universe of Galaxies, ed. R. G. Kron (San Francisco: ASP), p. 359.

Yee, H., & Green R. 1984, ApJ, 280, 79.

V - ENVIRONMENTAL EFFECTS IN GROUPS AND CLUSTERS

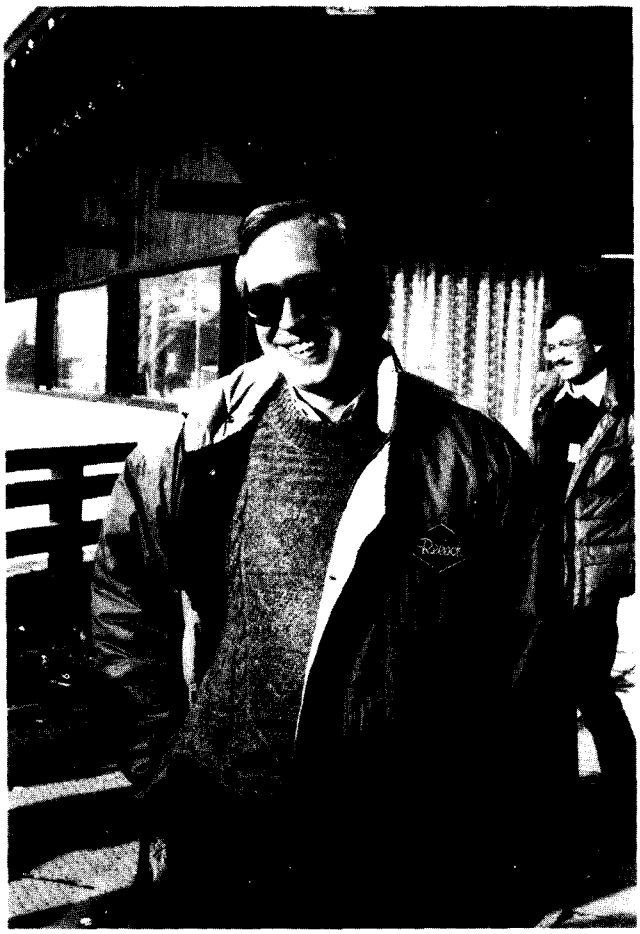

THE EFFECT OF THE GROUP ENVIRONMENT ON GALAXIES

Bradley C. Whitmore
Space Telescope Science Institute
3700 San Martin Drive
Baltimore, MD 21218

ABSTRACT

Groups, especially compact groups, represent an ideal place to study interactions and mergers in the present universe, since they have high spatial densities and low velocity dispersions. While there are several indications that interactions between galaxies in groups are frequent, there are fewer indications that actual mergers are occuring, at least mergers that result in the formation of elliptical galaxies. This may be explained by recent results which indicate that compact groups may last longer than originally believed, probably on the order of 5 Gyr.

1. INTRODUCTION

The motivation for studying galaxies in groups, especially compact groups, is clear to anyone who has seen an image of Seyfert's Sextet (Seyfert 1948; Figure 1 below), Stephan's Quintet (Stephan 1877 !; = HCG 92 = ARP 319; see Arp 1966), or Shakhbazyan 1 (Shakhbazyan 1957, Robinson and Wampler 1973, Kirshner and Malumuth 1980). If interactions and mergers between galaxies are important anywhere in the universe they should be important in compact groups, both because of the high spatial density of galaxies (*i.e.,* 10 - 10^6 times the density in the field; higher than in the cores of clusters in many cases), and the low group velocity dispersions (*i.e.,* roughly 200 km s^{-1}: Hickson, Kindl, and Huchra 1988; hereafter HKH). The group velocity dispersions are roughly the same as the orbital velocities of the stars in the galaxies; a situation that maximizes the chances of severe interactions and mergers.

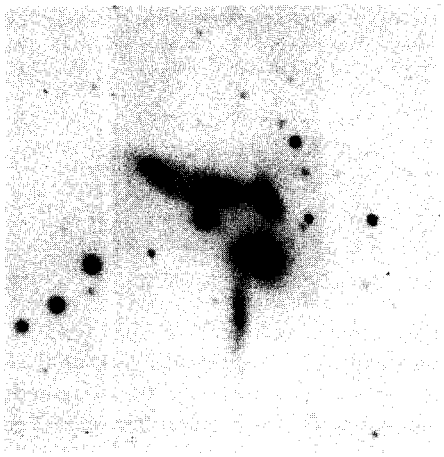

Figure 1: HCG 79 (Seyfert's Sextet: photograph from Rubin, Hunter, and Ford 1991); one of the densest of the 100 Hickson (1982) compact groups.

Theoretical expectations, especially those based on computer simulations, have also played a major role in spurring interest in groups of galaxies. Early simulations indicated that compact groups should only last about 1/100 - 1/10 of a Hubble time (*e.g.,* Carnevali, Cavaliere, and Santangelo 1981, Ishizawa *et al.* 1983; see Mamon 1989 for an extensive reference list). Such short lifetimes would imply that a large fraction

of the objects in the universe should be the remnants of compact groups. Essentially all simulations find that the remnant of a compact group should be an elliptical galaxy. While recent, more realistic simulations (*e.g.,* Barnes 1985, 1989, Navarro, Mosconi, and Lambas 1987, Governato, Bhatia, and Chincarini 1991) find considerably longer lifetimes (*i.e.,* 1/10 - 1/3 of a Hubble time), it is still true that compact groups should be an excellent place to study interactions and mergers.

Defining a group is a difficult task. Many early group catalogs were based on subjective criteria or surface brightness enhancements (see Hickson 1989 for a review). Most current work on this subject is based on objective methods such as friends-of-friends algorithims (Huchra and Geller 1982, Geller and Postman 1983, Postman and Geller 1984, and Maia and da Costa 1990), or hierarchical clustering algorithms (Materne 1978, Tully 1987). However, even these objective methods can result in subtle (and in some cases not so subtle !) selection effects that can result in spurious correlations.

Much of the work concerning groups of galaxies has focussed on the identification of groups and the determination of the global properties of group (*e.g.,* the mass-to-light ratio). These issues continue to be important because of their relevance to questions concerning large-scale structure and the nature of dark matter. The current review will focus on how the group environment affects the structure and dynamics of the galaxies within the groups, rather than on the properties of the groups themselves. The emphasis will be on compact groups, both because these systems have been more thoroughly studied, and because we expect stronger evolution in these more concentrated groups. There will also be an emphasis on recent results since the review by Hickson (1989) covered many of the earlier studies. Other relevant reviews are White (1982, 1990; dynamical effects in groups and clusters), Mamon (1989, 1992; simulations in groups and the estimation of the number of chance alignments), Dressler (1984), Whitmore (1990), and Balkowski (1992; all three on the effect of the cluster environment on galaxies).

2. EFFECT ON THE MORPHOLOGY OF GALAXIES

2.1 General Appearance and Isophotal Shapes

A cursory look at a few compact groups shows a large fraction of peculiar-looking galaxies, roughly 30 % according to Hickson (1989). These include galaxies with tails, filamentary structures, asymmetric isophotes, and warps. While a careful comparison with the field population has not been made, it is clear that the frequency of distorted galaxies is higher in the compact groups. Zepf (1991) has estimated the frequency of a certain type of peculiarity, tidal tails, at roughly 7 %. This is considerably larger than the fraction in the field, which Toomre (1977) estimates at about 0.3 %.

A more quantitative approach is to determine the deviations from perfect ellipses for the ellipticals, using techniques pioneered by Carter (1978). Table 1 shows a comparison of galaxies measured by Zepf (1991) with observations of ellipticals in other environments. There are fewer ellipticals with symmetric isophotes and more with irregular isophotes in compact groups. The number of disky ellipticals is about normal. The number of boxy ellipticals is significantly lower than in the field, which is quite surprising given the evidence that boxy galaxies may be caused by mergers (Binney and Petrou 1985, Whitmore and Bell 1988, Bender 1990). Bettoni and Fasano (1991) also find that the percentage of boxy ellipticals is lower than in the field. The lack of boxy ellipticals may indicate that it takes longer for the box to settle than the lifetime of the group, or it may simply indicate that mergers don't preferentially make boxy isophotes.

Table 1 - Distribution of Isophotal Shapes for Elliptical Galaxies

Study	No.	Symmetric	Irregular	Boxy	Disky
Bender *et al.* (1989) (field + cluster)	47	30 % (14)	17 % (8)	17 % (8)	36 % (17)
Peletier *et al.* (1990) (field + cluster)	39	33 % (13)	21 % (8)	26 % (10)	21 % (8)
Zepf (1992) (compact groups)	32	9 % (3)	50 % (16)	6 % (2)	34 % (11)

2.2 Morphological Fractions

If mergers are common in groups, and mergers make elliptical galaxies, we might expect groups to have a higher percentage of ellipticals than found in the field. While this appears to be true, the enhancement is small. HKH find that 22 % of the galaxies in compact groups are ellipticals. The value for the field, loose groups, or the outer regions of clusters is about 10 % (*e.g.,* Dressler 1980, Postman and Geller 1984). Rood and Williams (1989) have compared the morphological fractions within compact groups with the fractions in the neighborhoods around the groups. They find a significant elliptical enhancement for the total sample ($\Delta = 8 \pm 3$ %) and for the dense groups ($\Delta = 12 \pm 5$ %) , but not for the sparse groups ($\Delta = 4 \pm 4$ %). In a similar study, Sulentic (1987) only finds an enhancement for those groups with superior plate material.

Zepf and Whitmore (1991) point out that while the elliptical enhancement seems quite small given the expectation that mergers are frequent in compact groups, it is actually difficult to make models where the enhancement is this high. If the lifetimes of compact groups are relatively short, objects that have recently merged will not have enough time to settle into a normal-looking elliptical galaxy before the group collapses.

In addition, some of the original ellipticals will undergo mergers which will temporarily remove them from the elliptical fraction. These results indicate that the elliptical fraction by itself may not be a good tool for constraining the amount of merging in clusters. Perhaps we should be looking for correlations with the number of distorted galaxies.

2.3 Morphology-Density Relation (and other correlations with morphology)

Another test of whether mergers are forming ellipticals in groups would be to determine whether the elliptical fraction is a function of the local density, since the higher density groups would be expected to have more merging activity. Following Dressler's (1980) discovery of a relationship between the morphological fractions and the projected local density of galaxies in clusters, several authors attempted to determine whether a similar relation holds for groups. Early attempts (Bhavsar 1981, deSouza *et al.* 1982) suffered from the lack of redshift information, the inclusion of cluster galaxies, and using either visual estimates or surface brightness enhancements as the criteria for selecting the groups (*e.g.*, in the Bhavsar 1981 study nearly all the high-density "groups" are close binaries; see Postman and Geller 1984 for further comments).

Postman and Geller (1984) studied loose groups identified from the CfA redshift survey (Huchra *et al.* 1983) using a friends-of-friends algorithm. The primary result was that at lower space densities than found in clusters (*i.e.*, less than about 5 galaxies Mpc^{-3}) the morphological fractions in the groups joined smoothly with the fractions found in the outskirts of the clusters. The morphological gradients were flat in this region (*i.e.*, no morphology-density relation). However, a second conclusion from this paper, that the same morphology-density relation holds for groups and clusters, may have been premature. Many of the "groups" defined using friends-of-friends algorithms contain cluster galaxies. For example, the groups defined in a similar manner by Geller and Huchra (1983) include # 94 (170 members; the Ursa Major cluster), # 106 (248 members; the Virgo cluster), and # 113 (30 members; the Coma cluster). The apparent correlation between the morphological fractions and local density in the intermediate density region may therefore be caused by the inclusion of cluster galaxies. Whitmore (1992) is currently reevaluating this result by removing the groups with 10 or more members from the sample.

Hickson and Rood (1988) and HKH found that in compact groups, where more mergers would be expected than in the groups studied by Postman and Geller (1984), the spiral fractions did not correlate very well with the local density. Instead, they found a much stronger correlation between morphology and the velocity dispersion of the group, and argued that this indicated that morphology was determined by initial conditions

rather than the environment.

Whitmore (1990) found that several properties of the Hickson compact groups correlate with distance, raising the possibility of introducing spurious correlations. This distance dependence is not too surprising since the Hickson groups span a wide range in redshift from V = 1,410 km s^{-1} to 21,660 km s^{-1}. Some of the nearest groups may actually be irregular galaxies with large HII regions masquerading as separate galaxies (*e.g.*, HCG 18 - Williams and VanGorkom 1988), while distant groups may tend to be in clusters (*e.g.*, HCG 58 - Williams 1985). We have therefore reexamined the HKH data by performing a least-squares fit between the spiral fraction and the redshift, and correlating the residuals in the spiral fraction with the other quantities, hence removing the redshift dependence in the sample. Table 2 shows the results. Note that when using the uncorrected data, the correlations with distance (fits # 1-3) are as strong or stronger than the the correlations between the physical properties (fits # 4-6). When the distance dependence is removed, the correlation between spiral fraction and velocity dispersion is still present (fit # 9), but it is slightly weaker (99.4 % probability of being correlated). The morphology-density relation is still very weak (fit # 8).

Table 2 - Correlations in the HKH Sample of Compact Groups

#	parameters	N	r	significance	probability
	(uncorrected data)				
1	f_s vs. z	95	-0.42	4.5 σ	99.99 %
2	log σ_v vs. z	78	+0.36	3.4 σ	99.87 %
3	log ρ vs. z	95	+0.04	0.2 σ	30.0 %
4	log σ_v vs. log ρ	78	-0.10	0.9 σ	61.3 %
5	f_s vs. log ρ	95	-0.19	1.3 σ	93.5 %
6	f_s vs. log σ_v	78	-0.42	4.0 σ	99.99 %
	(distance dependence removed from F_s)				
7	Δf_s vs. z	95	0.00	0.0 σ	0.00 %
8	Δf_s vs. log ρ	95	-0.14	1.3 σ	82.4 %
9	Δf_s vs. log σ_v	78	-0.31	2.8 σ	99.4 %

Table 2 (continued)

#	parameters	N	r	significance	probability
	(distance dependence removed from D_1)				
10	ΔD_1 vs. log ρ	95	-0.37	3.9 σ	99.98 %
11	ΔD_1(ell. + S0) vs. log ρ	43	-0.23	1.6 σ	86.2 %
12	ΔD_1(spirals) vs. log ρ	52	-0.50	4.1 σ	99.98 %
13	ΔD_1(Sa + Sb) vs. log ρ	26	-0.58	3.5 σ	99.8 %
14	ΔD_1(Sc ... I) vs. log ρ	26	-0.50	2.9 σ	99.0 %

Notes to table 2:
1). r = linear-correlation coefficient; probability = probability that parameters are correlated; f_s = fraction of spiral galaxies in the group; z = redshift of group; log σ_v = log of the group velocity dispersion; log ρ = log of the space number density; Δf_s = residual in f_s from relation $f_s = -8.5665 \times z + 0.7606$, ΔD_1 = residual in diameter of first-ranked galaxy in group from relation $D_1 = 3.718 \times z + 1.2184$.
2). HCG 54 has been removed from all fits, since its velocity dispersion, density, luminosity, and D_1 are radically different than other groups.

We conclude that while the distance dependence accentuate the underlying physical correlations, the correlation between spiral fraction and group velocity dispersion does appear to be real, and to be better than the morphology-density relation.

Maia and Da Costa (1990) have examined the properties of a set of groups defined from the Southern Sky Redshift Survey. These are primarily loose groups defined using a friends-of-friends algorithm similar to Huchra and Geller (1983). Maia and Da Costa also find a strong distance dependence in their sample. They therefore examined a subsample of groups within V = 4000 km s^{-1}, where distance dependence was negligible. For this sample they find a fairly strong morphology-density relation (probability = 99.6 %) but a very weak morphology-velocity dispersion relation (probability = 62 %). However, their sample also includes cluster galaxies (*e.g.*, # 52 is the Fornax cluster with 55 galaxies; # 72 has 61 galaxies). It is therefore possible that much of the morphology-density relation they observe is due to cluster galaxies rather than galaxies in loose groups.

2.4 Morphological Concordance

KHK find that in 20 of the 58 quartets the galaxies all have the same morphological types. They calculate the chance of this occurring from a random distribution is

10^{-5}. White (1990) points out that the distribution is not random, and the probability calculation must take into account the morphology-velocity dispersion relation (or more generally, a morphology-"anything" relation). However, it is unclear whether this effect will fully explain the morphological concordance in compact groups, since the correlations with morphology are relatively weak (Table 2).

2.5 First-ranked Galaxies

Another approach is to study the properties of the first-ranked galaxies, since mergers should tend to build increasingly brighter galaxies. Several studies (Hickson 1982, Geller and Postman 1983, Mardirossian *et al.* 1983, HKH, and Maia and Da Costa 1990) have found that the first-ranked galaxies are not brighter than field galaxies, are not preferentially ellipticals, and are not more centrally located than other galaxies in the same groups. These surprising results led several authors to conclude that while there is ample evidence for interactions between galaxies, there is little direct evidence from the properties of the first-ranked galaxies for mergers.

2.6 Discussion

Another possible explanation for the lack of a strong morphology-density relation, or any differences in the properties of the first-ranked galaxies, would be if mergers don't generally make elliptical galaxies. For example, the large amount of gas that remains in NGC 7252, a prototypical disk-disk merger, suggests that the remnant may become an Sa galaxy rather than an elliptical. Barnes (1992) finds that roughly half the gas in a simulations of a disk-disk merger remains in the outer regions, and unless it is blown out by rapid star formation, may reform a disk. Recent observations of spirals in the Virgo cluster (Rubin 1992) show that about 25 % have dynamically distinct inner disk components, presumably from a merger event. S0 galaxies are also known to have dynamically distinct components (*e.g.,* Bettoni, Fasano, and Galletta 1990, Whitmore *et al.* 1990). A particularly interesting case is NGC 4550, an S0 galaxy which Rubin (1992) finds has two stellar disks rotating in opposite directions. While n-body simulations indicate that equal mass mergers probably result in the formation of elliptical galaxies, it seems quite likely that the far more numerous mergers between unequal mass galaxies may not significantly change the morphological type of the galaxy.

3. EFFECT ON THE SIZE AND LUMINOSITY

Hickson, Richstone, and Turner (1977) found that the size of the largest galaxy in a group correlates with the intergalactic separation (*i.e.,* galaxies are smaller in denser groups), and suggest that tidal stripping might be the cause. However, the reliability of

this result is questionable since it was determined from visual estimates off the Palomar Sky Survey for only 18 groups chosen in a non-systematic manner.

Whitmore (1990) examined the data from Hickson, Kindl, and Auman (1989) and reports a weak dependence between the size of the largest galaxy, D_1, and the local density, log ρ. We have reexamined this question to determine whether the distance dependence of the sample affects the result. Fits # 10 through # 14 from Table 2 show the results. The removal of the distance dependence actually improved the correlations from those reported in Whitmore (1990). The correlation for the spirals is especially strong, and holds for both the sample of Sa + Sb galaxies as well as the sample of Sc and later galaxies. Although further checks need to be made (*e.g.,* determine the effect of overlapping isophotes in the denser groups), the data suggest that tidal stripping may be operating in the denser groups. Maia and DaCosta (1990) find a similar correlation between the size of the largest galaxy and the intergalactic separation in their southern group survey, but conclude that it is partially caused by distance dependent selection effects.

Rubin, Hunter, and Ford (1991) and Zepf and Whitmore (1991) show that the integrated group luminosity lies in the range of giant ellipticals, especially after taking into account the dimming that would occur following the cessation of active star formation. These results are consistent with the hypothesis that the remnant of a collapsed compact group can be a normal field elliptical.

de Oliveira and Hickson (1991) find that the luminosity function of galaxies in compact groups are different than in the field, loose groups, or clusters, with a lack of low-luminosity galaxies and an enhancement of bright galaxies in the groups. This might be interpreted as evidence for mergers which tend to form brighter galaxies. However, they find no difference in the luminosity functions of spiral-poor groups as compared to spiral-rich groups.

4. EFFECT ON STAR FORMATION AND RELATED ACTIVITY

4.1 H_α Emission

Weak evidence for an enhancement of H_α emission in high-density compact groups, as compared to low-density groups or isolated field galaxies, is reported by Maia and da Costa (1990). However, they caution us that selection effects may be affecting this result (*i.e.,* the samples have different mixes of morphological types and luminosities).

Rubin, Hunter, and Ford (1991) find that 10 of the 12 ellipticals they studied have

H_α emission in the nucleus, and about half of these have extended gas disks beyond the nucleus. While this seems like quite a high fraction, a field sample observed under similar conditions is needed to quantify the significance of this result.

4.2 Blue Ellipticals in Compact Groups

Two spiral galaxies which merge to form an elliptical galaxy should retain their bluish color for a few Gyr after the encounter. Zepf, Whitmore, and Levinson (1991) find a higher percentage of blue ellipticals in compact groups (5.5 % ; defined as a difference of more than 0.10 in B-V, compared with normal ellipticals with the same luminosity) than are found in other environments (2.4 %; Burstein *et al.* 1987). However, based on a simple model which combines dynamical evolution with stellar evolution, Zepf and Whitmore (1991) find that the number of blue ellipticals should be about 15 %, assuming "standard" values for various parameters such as the merger rate and the original fraction of elliptical galaxies in compact groups. In order to explain the relatively low percentage of blue ellipticals, along with constraints set by the total numbers of ellipticals in groups, the number of ongoing mergers, and the number of both blue and normal galaxies in the field, they find that the typical compact group must: 1) have a lifetime of about 6 Gyr, and, 2) have collapsed from a region that was already richer in elliptical galaxies than in loose groups. Another possibility is that ellipticals are only produced by nearly equal-mass mergers, in which case the data could still be compatible with somewhat shorter group lifetimes.

4.3 Infra-red emission

Ultraluminous IRAS sources are almost invariably associated with interacting and merging galaxies, so we might expect many galaxies in compact groups to be IRAS sources. Hickson *et al.* (1989) find an enhancement in far-infrared emission for galaxies in compact groups compared to isolated field galaxies, although the effect is not very dramatic. However, Sulentic and Rabaca (1989) argue that the far-infrared luminosity function is nearly indistinquishable from the field. Zepf (1992) shows that the far-infrared color, which is a more robust indicator of enhanced star formation activity, is warmer for compact group galaxies than comparable samples of galaxies in other environments.

4.4 Radio Observations

Williams and Rood (1987) find that galaxies in compact groups are HI deficient, with roughly half the HI content of their counterparts in more isolated environments. This suggests that either ram-pressure stripping from a hot intergroup medium is occuring; galaxy-galaxy collisions have stripped the gas; or star formation has been more effective.

Menon and Hickson (1985) and Menon (1990) find that: 1) the percentage of continuum radio sources in compact groups is higher than in the field, 2) in 9 out of the 10 ellipticals where continuum emission has been detected, the radio source is the brightest galaxy in the group, 3) for the spirals that have been detected the radio source is just as likely to be the first, second, or third brightest galaxy in the cluster. The emission is only located in the central regions of the ellipticals while it is extended in the spirals. These results indicate that accretion events are probably occuring in compact groups, but the reason for the differences between spirals and ellipticals is still unclear.

5. EFFECT ON THE DISTRIBUTION OF MASS

5.1 Intragroup Medium

The presence of an intragroup medium in some compact groups provides one of the best pieces of evidence that compact groups are physically bound systems. The initial attempt to detect this material was made by Rose (1979), who searched two groups for the presence of diffuse intragroup light, with negative results. This needs to be redone using CCD detectors and a larger sample. Searches for diffuse neutral hydrogen have been made using the VLA by Williams and van Gorkom (1988, 1992) and Williams, McMahon, and van Gorkon (1991). In some cases they find that the gas is closely associated with the individual galaxies, albeit, often with a non-symmetric appearance (*e.g.*, HCG 44). In other cases the gas appears to be distributed, at least partially, in a common envelope (*e.g.*, HCG 31). Searches for a hot intragroup medium are difficult due to the low X-ray luminosities of groups (*e.g.*, Hickson *et al.* 1989). However, Bahcall, Harris, and Rood (1984) report that the x-ray emission in HCG 16 is associated with the individual galaxies while the x-ray emission is extended in HCG 92 (Stephan's Quintet). Observations of looser groups (Biermann and Kronberg 1983, Bahcall, Harris, and Rood 1984) provide further evidence for an intragroup medium in certain cases. New results from ROSAT are eagerly awaited.

5.2 Emission-line Rotation Curves in Spirals

Rubin, Hunter, and Ford (1991) have obtained long-slit spectroscopy for 33 spiral galaxies in 21 compact groups. They find that roughly 1/3 have normal rotation curves typical of galaxies in the field; 1/3 have abnormal rotation curves (*e.g.*, rising on one side but falling on the other side); and 1/3 have rotation curves which are too peculiar to classify, including a few which are sinusoidal (*i.e.*, go through zero three times !). This provides perhaps the clearest evidence yet that interactions are prevalent in compact groups, and can do a great deal of damage to a galaxy. Figure 2 shows the rotation curves for four galaxies in HCG 16.

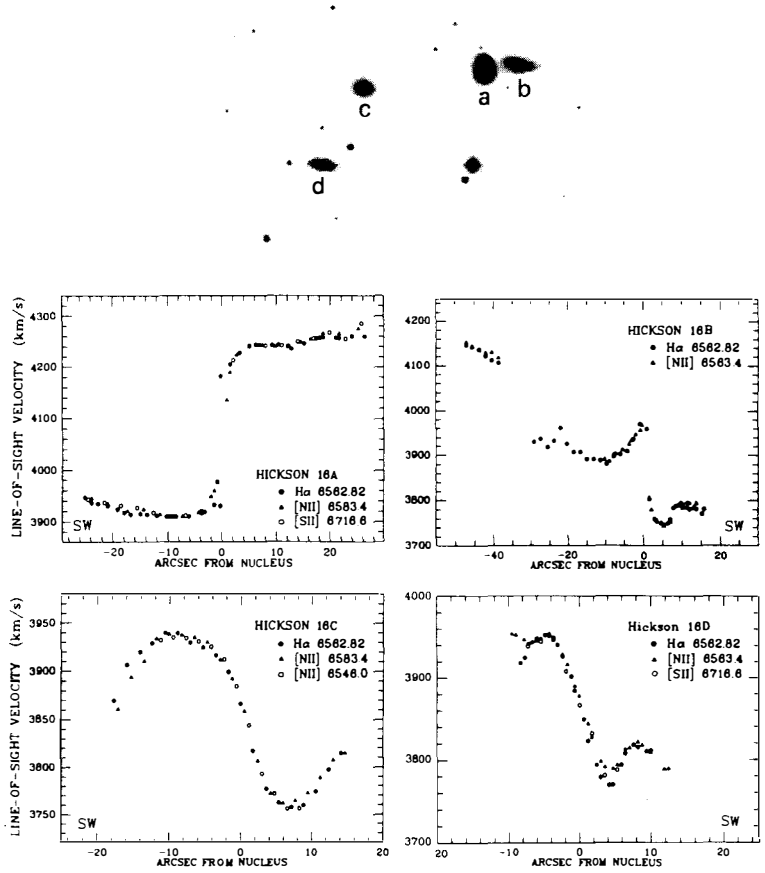

Figure 2: Image and emission-line rotation curves for galaxies in HCG 16. (from Rubin, Ford, and Hunter 1991)

5.3 The Fundamental Plane for Ellipticals

Zepf and Whitmore (1992) have measured stellar velocity dispersions for 20 elliptical galaxies in compact groups in order to determine whether the galaxies fall along the same "fundamental plane" found by Dressler *et al.* (1987) for ellipticals in other environments. They find tentative evidence that the ellipticals in compact groups are different, in the sense that velocity dispersions are lower for galaxies with the same values of effective radius and mean surface brightness. The results must be considered tentative because of

the small number of galaxies which have been measured, but the fact that the galaxies with the largest residuals from the normal fundamental plane are also the galaxies with bluer (B-V) colors, and disky isophotes, suggests that the difference is real.

6. CONCLUSIONS

The observational results reported in this review only partially support the theoretical expectations discussed in §1. While there is extensive evidence for frequent interactions and accretion events in compact groups (*e.g.*, abnormal rotation curves) there is less compelling evidence for mergers (*e.g.*, first-ranked galaxies are similar to other galaxies), at least if mergers generally result in the formation of an elliptical galaxy. This leads several authors to conclude that the current interactions are relatively minor irritants; that the primary influence on a galaxy occurs mostly at the time of galaxy formation. However, given the frequent interactions, mergers must be happening at some level. Some possibilities for why they are less apparent than expected are offered below.

1. The fraction of compact groups which are actually bound systems may be lower than generally believed (Mamon 1992). While the existence of some of the correlations (*e.g.*, the morphology vs. velocity dispersion relation) and the intragroup medium (§4.4) both indicate that most of the compact groups are real, it is still quite possible that a fair percentage of the galaxies in compact groups may be chance alignments. Hickson (1990) estimates that 13 % of the galaxies are superposed members of loose groups and another 17% are superposed field galaxies with discordant redshifts. This would tend to dilute the evidence for mergers.

2. The time scale for conversion from a merger to a normal-looking elliptical may be longer than the lifetime of the group. Perhaps we should be looking for an enhancement in the number of peculiar-looking galaxies rather than ellipticals.

3. Mergers may only result in the formation of an elliptical galaxy when two relatively equal mass galaxies are involved (§2.6). The evolution of the Hubble sequence from spirals toward ellipticals would therefore be quite slow.

4. The lifetime of compact groups may be longer than generally believed (*i.e*, roughly 5 Gyr instead of 1 Gyr), and the merger rate correspondingly lower. Both observational results (*e.g.*, the low fraction of blue ellipticals) and some of the recent computer simulations support this conclusion.

Some of the questions we might see answered in the next few years are: What is the fraction of distorted galaxies in groups? Are these the remnants of mergers rather than

the elliptical galaxies? Is tidal stripping making the galaxies in the dense groups smaller? How prevalent is an intragroup medium in visible light, neutral hydrogen, and x-ray emission? Is the fundamental plane for elliptical galaxies in compact groups different than for ellipticals in other environments? New observational results from HST and ROSAT will probably help answer a few of these questions while introducing some new questions of their own. The increased sensitivity of ROSAT should provide a definitive answer about the presence of a hot intragroup medium. HST will provide a clearer window into the past, when interactions and mergers were almost certainly more frequent. While these spacecraft provide a welcomed addition to our observational arsenal, the detailed study of galaxies in nearby groups from ground-based observatories will continue to provide one of our best means of studying mergers and interactions in the current epoch, and hence, providing insight into the more prevalent interactions in the past.

I would like to thank Herb Rood, Barbara Williams, and Steve Zepf for useful discussions, and for providing comments on the manuscript. A special thanks is owed to Steve Zepf, who sparked my interest in this subject and collaborated with me on several of the results reported in this review.

REFERENCES

Bahcall, N. A., Harris, D. E., and Rood, H. J. 1984, *Ap. J.*, **284**, L29.

Balkowski, C. 1992, this conference.

Barnes, J. 1985, *M.N.R.A.S.*, **215**, 517.

Barnes, J. 1989, *Nature*, **338**, 123.

Barnes, J. E. 1992, this conference.

Bender, R. 1990, *The Dynamics and Interactions of Galaxies*, ed. R. Wielen, (New York: Springer-Verlag).

Bender, R., Surma, P., Dobereiner, S., Mollenhof, C., Madejsky, R. 1989, *Astron. Ap.*, **217**, 35.

Bettoni, D. and Fasano, G. 1991, *Galaxy Environments and the Large Scale Structure of the Universe*, ed. G. Giuricin, F. Mardirossian, and M. Messetti, (Trieste: SISA).

Bettoni, D., Fasano, G., and Galletta, G. 1990, *Dynamics and Interactions of Galaxies*, ed. R. Wielen, (New York: Springer-Verlag).

Bhavsar, S. P. 1981, *Ap. J.*, **246**, L5.

Biermann, P., Kronberg, P. P. 1983, *Ap. J.*, **268**, L69.

Binney, J. J., and Petrou, M. 1985, *M.N.R.A.S.*, **214**, 449.

Burstein, D., Davies, R. L., Dressler, A., Faber, S. M., Stone, R. P. S., Lynden-Bell, D.,

Terlevich, R. J., and Wegner, G. 1987, *Ap. J. Supp.*, **64**, 601.
Carnevali, P., Cavaliere, A., and Santangelo, P. 1981, *Ap. J.*, **249**, 449.
Carter, D. 1978, *M.N.R.A.S.*, **182**, 172.
de Oliveira, C. M., and Hickson, P. 1991, *Ap. J.*, **380**, 30.
de Souza, R. E., Capelato, H. V., Arakaki, L., and Logullo, C. 1982, *Ap. J.*, **263**, 557.
Dressler, A. 1980, *Ap. J.*, **236**, 351.
Dressler, A. 1984, *A. R.A.A*, **22**, 185.
Dressler, A., Lynden-Bell, D., Burstein, D., Davies, R. L., Faber, S. M., Terlevich, R. J., and Wegner, G. 1987, *Ap. J.*, **313**, 42.
Geller, M. J. and Postman, M. 1983, *Ap. J.*, **274**, 31.
Governato, F., Bhatia, R., Chincarini, G. 1991, *Ap. J.*, **371**, L15.
Hickson, P. 1982, *Ap. J.*, **255**, 382.
Hickson, P. 1989, *Paired and Interacting Galaxies: IAU # 124*, ed. J. W. Sulentic, W. C. Keel, and C. M. Telesco, (Washington: NASA).
Hickson, P. 1989, private communication (as quoted in White 1990).
Hickson, P., Kindl, E., and Auman, J. R.. 1989, *Ap. J. Suppl.*, **70**, 687.
Hickson, P., Kindl, E., and Huchra, J. P. 1988, *Ap. J.*, **331**, 64. (HKH)
Hickson, P., Menon, T. K., Palumbo, G. G. C., and Persic, M. 1989, *Ap. J.*, **341**, 679.
Hickson, P., Richstone, D. O., and Turner, E. L. 1977, **213**, 323.
Hickson, P., and Rood, H. J 1988, *Ap. J.*, **331**, L69.
Huchra, J. P., Davis, M., Latham, D., and Tonry, J. 1983, *Ap. J. Suppl.*, **52**, 89.
Huchra, J., and Geller, M. 1982, *Ap. J.*, **257**, 423.
Ishizawa, T., Matsumoto, R., Tajima, T., Kageyama, H., and Sakai, H. 1 983, *P.A.S.J.*, **35**, 61.
Kirshner, R. P., and Malumuth, E. M. 1980, *Ap. J.*, **236**, 366.
Maia, M. A. G., and da Costa, L. N. 1990, *Ap. J.*, **352**, 457.
Mamon, G. 1989, *Paired and Interacting Galaxies: IAU # 124*, ed. J. W. Sulentic, W. C. Keel, and C. M. Telesco, (Washington: NASA).
Mamon, G. A. 1992, this conference.
Mardirossian, F., Giuricin, G., and Mezzetti, M. 1983, *Astron. Ap.*, **126**, 86.
Materne, J. 1978, *Astron. Ap.*, **63**, 401.
Menon, T. K., and Hickson, P. 1985, *Ap. J.*, **296**, 60.
Menon, T. K. 1990, *Dynamics and Interactions of Galaxies*, ed. R. Wielen (New York: Springer-Verlag).
Navarro, J. F., Mosconi, M. B., and Lambas, D. G. 1987, *M.N.R.A.S.*, **228**, 501.
Peletier, R. F., Davies, R. L., Illingworth, G. D., Davis, L. E., Caws on, M. C. 1990, *A. J.*, **100**, 1091.
Postman, M., and Geller, M. J. 1984, *Ap. J.*, **281**, 95.
Robinson. L. B., and Wampler, E. J. 1973, *Ap. J. Lett.*, **170**, L135.

Rood, H. J., and Williams, B. A. 1989, *Ap. J.*, **339**, 772.
Rose, J. A. 1979, *Ap. J.*, **231**, 10.
Rubin, V. C. 1992, private communication.
Rubin, V. C., Hunter, D., and Ford, W. K., Jr., 1991, *Ap. J. Suppl.*, **76**, 153.
Schweizer, F., 1992, this conference.
Seyfert, C. K. 1948, *A. J.*, **53**, 203.
Shakhbazyan, R. K. 1957, *Astron. Tsirk*, **177**, 11.
Stephan, M. E. 1877, *M.N.R.A.S.*, **37**, 334.
Sulentic, J. W. 1987, *Ap. J.*, **322**, 605.
Sulentic, J. W. and Rabaca, C. 1989, *Paired and Interacting Galaxies: IAU # 124*, ed. J. W. Sulentic, W. C. Keel, and C. M. Telesco, (Washington: NASA).
Toomre, A. 1977 *The Evolution of Galaxies and Stellar Populations* , ed. B. Tinsley, R. Larson (New Haven: Yale University Observatory), 401.
Tully, R. B. 1987, *Ap. J.*, **321**, 280.
White, S. D. M. 1982, *Morphology and Dynamics of Galaxies*, ed. L. Martinet, M. Mayor, (Geneva: Geneva Obs.).
White, S. D. M. 1990, *Dynamics and Interactions of Galaxies*, ed. R. Wielen (New York: Springer-Verlag).
Whitmore, B. C., and Bell, M. 1988, *Ap. J.*, **324**, 741.
Whitmore, B. C. 1990, *Clusters of Galaxies: STScI Symposium Series # 4*, ed. Oegerle, W. R., Fitchett, M. J., and Danly, L., (Cambridge: Cambridge University Press).
Whitmore, B. C. 1992, in preparation.
Whitmore, B. C., and Gilmore, D. M. 1990, *Ap. J.*, **367**, 64.
Whitmore, B. C., Gilmore, D. M. , and Jones, C. 1992, submitted.
Whitmore, B. C., Lucas, R. A., McElroy, D. B., Steiman-Cameron, T. Y., Sackett, P. D., and Olling, R. P. 1990, *A. J.*, **100**, 1489.
Williams, B. A. 1985, *Ap. J.*, **290**, 462.
Williams, B. A., McMahon, P. M., and van Gorkom, J. H. 1991, *A. J.*, **101**, 1957.
Williams, B. A., and Rood, H. J. 1987, *Ap. J. Suppl.*, **63**, 265.
Williams, B. A., and van Gorkom, J. H. 1988, *A. J.*, **95**, 352.
Williams, B. A., and van Gorkom, J. H. 1992, private communcations.
Zepf, S., Whitmore, B. C., and Levison, H. 1991, *Ap. J.*, **383**, 524.
Zepf, S., and Whitmore, B. C. 1991, *Ap. J.*, **383**, 542.
Zepf, S., and Whitmore, B. C. 1992, in preparation
Zepf, S. 1991, Thesis: Johns Hopkins University.
Zepf, S. 1992, *Ap. J.*, submitted.

Are Compact Groups Dense Quartets?

GARY A. MAMON
DAEC, Observatoire de Meudon, 92195 Meudon, FRANCE

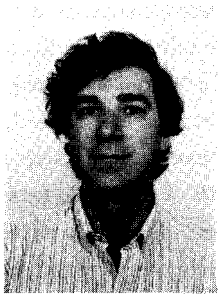

Abstract

Various theories are reviewed to explain the nature of Hickson's compact groups. Results of recent N-body work, involving large simulated databases of loose groups of galaxies, are presented. These indicate that within loose groups, of the subsystems that form and that meet Hickson's compact group selection criteria when viewed in projection, 90% are one-dimensional *chance alignments*, while the remaining 10% are three dimensional configurations, of which very roughly half are bound. Moreover, the 1D chance alignments are binary-rich, and averaging over the different types of "Hickson-like" configurations that are seen in projection, one finds that roughly half of these show more than two galaxies in interaction, thus explaining the high level of interaction seen in compact groups.

1. Introduction

The compact groups catalogued by Hickson[1] (hereafter, HCGs) correspond to the isolated systems of highest apparent density in the Universe, with densities comparable to or greater than those of the cores of rich clusters of galaxies. As such, these systems

should be the ideal place to look for galaxy interactions. And indeed, signs of dynamical interaction have been found in many galaxies belonging to these systems. First, roughly 30% of HCGs have more than two galaxies displaying morphological signs of interaction[2]. Second, only one-third of the rotation curves of the spiral galaxies in nearby HCGs can be considered normal[3]. Third, HI synthesis observations of now 5 HCGs point in some cases to HI emission extending around the full group[4].

On the basis of these interactions, many workers[2],[3],[5],[6] have concluded that HCGs are bound dense systems, probably formed recently. Alternatively, it has been argued that HCGs may not be physical systems of at least 4 galaxies, but would be caused by chance alignments of galaxies along the line-of-sight within loose groups[7] and clusters[8]. While there has been considerable debate between the proponents of these two hypotheses, it would be fair to state all the other possibilities for explaining HCGs. First, HCGs may indeed be bound and dense, but forming at early epochs from the densest primordial density fluctuations. Indeed, the fact that one study points to a simulated dense group that survives (until it loses it's HCG appearance when viewed in projection) for roughly one-fifth of a Hubble time[9] could indicate that a small but non-negligible fraction of dense groups could survive until the present epoch. Second, HCGs could represent *unbound* subsystems within loose groups, which only survive for roughly their crossing time[10]. Third, HCGs could simply be loose groups at the epoch of cosmological collapse. Fourth, there must be some HCGs that are caused by chance alignments *in the field*. Fifth, some HCGs may simply be HII regions within a single galaxy[11],[12]. Sixth, and finally, there is some indication that the most distant HCGs may be the bright-ends of rich clusters[13]. Below, various arguments are presented for or against these different hypotheses.

2. Old Points of Debate

In spite of the strong interactions seen in HCGs, there are many arguments working against the bound dense group hypothesis. First and foremost, it is difficult to see how such bound dense groups will form in the numbers observed today (roughly 1% of the number of loose groups in a comparable portion of the Universe[13]). As mentioned in §1, HCGs could be the lucky survivors of primordial dense groups, but previous *statistical* N-body simulations of dense groups show that of nearly 1000 simulated dense groups, none survive for a Hubble time[14]. Because groups as dense as HCGs appear to be will condense out of their initial Hubble expansion in a short time, there is perhaps 10 times more time to form loose groups than to form primordial dense groups. One would have to invoke that primordial dense groups formed at a rate 10 to 100 times higher than loose groups today, which seems unlikely. The fact that in one

study[9], the only N-body simulation performed gave a dense group that lived rather long (0.2 Hubble times) is more the result of well-chosen initial conditions than of luck, as the authors had placed their two most massive galaxies on a circular orbit, thus maximizing the survival time against the merging of the pair.

Alternatively, a bound dense group would have to form by two-body processes, by which sufficient exchange of energy between the galaxies in a loose group may cause a bound dense subgroup to form inside. Unfortunately, no signs of such subsystems were seen in the statistical sets of dynamically simulated loose groups[14], although the database of simulated groups was still not large enough to conclude. This issue is addressed in §3 below.

If HCGs are bound and dense, there should be enough mergers to show a statistically significant increase in the mean difference of first to second rank galaxy magnitudes[15]. Not only is this seen to occur in simulated dense groups, half-way between their virialized initial conditions and the time when they lose their HCG identity[14] but the time average of the value of $\langle m_1 - m_2 \rangle$ between the initial conditions and the time they lose their HCG identity is statistically significantly large. In contrast, the HCGs show a normal $\langle m_1 - m_2 \rangle$[7], which thus seems to rule out that HCGs are primordial bound dense groups.

Moreover, two tests favor the chance alignment idea over the bound dense group one. First, HCGs do not obey the group/cluster morphology-density relation[16], but follow instead a parallel relation, which, at a given density, makes them too spiral-rich[7] (hence elliptical-poor). In contrast, because mergers should be operating in dense groups, and that these have the ideal low velocity dispersions in comparison with rich clusters, one would expect the HCGs to have a larger elliptical fraction than rich clusters[17]. Alternatively, if their spiral fraction is indicative of their density, then HCGs would be 200 times less dense in 3D then what they appear in 2D[7]. The chance alignment idea predicts a similar ratio and also predicts that the HCG relation is roughly parallel to the group/cluster one, because if HCGs are chance alignments, their morphological mix should mimic that of their parent system, while scaling arguments show that the denser parent systems will lead to more compact chance alignments[7].

Second, if HCGs are chance alignments within loose groups, then the ratio of HCG to loose group M/Ls should be equal to

$$\frac{R_{\rm HCG}/R_{\rm LG}}{N_{\rm HCG}/N_{\rm LG}} \simeq \left(\frac{200^{-1/3}}{4/8}\right) \simeq 1/3 \ , \qquad (1)$$

where R and N refer to projected radius and number of galaxies, respectively, and where the system velocity dispersions and mean galaxy luminosities are assumed to be

the same between chance alignment and parent loose group. Now the mean M/L of HCGs is roughly $40 - 50\,h$[2], whereas for loose groups one gets $125\,h$[18] and $190\,h$[19], and the ratio of these two M/Ls is in fine agreement with equation (1).

Finally, there has been some debate on the expected frequency of chance alignments within loose groups. Whereas dynamical simulations yielded values of a few percent[14], static Monte-Carlo simulations[5] produced only $\sim$ a few 10^{-5} for typical loose groups. An analytical study[8] explained this discrepancy as caused by the strong dependence of the frequency of chance alignments to the size of the parent system ($\sim R^{-4.5}$) coupled with the relatively small loose group sizes used in the dynamical simulations. As a consequence, the *median* frequency used in the Monte-Carlo study is an order of magnitude smaller than the more relevant *mean*[8]. Finally, the underlying model in the Monte-Carlo and analytical studies is a Poisson distribution of galaxies in the projected loose group, whereas in reality, the gravitational attraction of galaxies causes loose groups to be relatively rich in binaries. Now in the Monte-Carlo study it has been shown that adding one binary per group increases the frequency of chance alignments by 1.5 orders of magnitude[5], whereas, loose groups tend to have on average 1.5 binaries, defined in the same way[8], and one thus reaches (or surpasses!) the frequencies of 0.5% (see above) necessary to explain half of the HCGs as chance alignments[13].

3. New Dynamical Simulations

3.1 Methods

A series of new simulations of loose groups, based upon a the code of a previous study[14] have been run to establish accurately the frequency of formation of bound dense subgroups within loose groups, and the frequency of binaries within chance alignments appearing in loose groups. The statistics on compact configurations is improved in three ways: 1) The simulations are run for 2.5 Hubble times instead of one. 2) The simulations are viewed (in projection along three orthogonal axes) 80 times per Hubble time, instead of 8. 3) For each set of parameters, 100 simulations are run (with different initial positions and velocities), instead of 20 to 50. Thus altogether, the statistics are typically 100 times better than previously.

The standard runs involve loose groups of initially 8 galaxies, sampled from a Schechter[20] luminosity function of index -1 with a faint cut-off at $0.01\,L_*$ with the mean galaxy luminosity forced at $4.2\,h^{-2} \times 10^9\,L_\odot$ to within 1%, starting with random positions inside a sphere of radius $650\,h^{-1}$ kpc and random velocities satisfying on average the virial theorem. As in the previous study[14], the dark matter is placed either mainly within galaxy halos, or in a common envelope. In both cases the group

mass-to-light ratio is $120\,h$ to conform with NBG groups[18], while the galaxies have mass-to-light ratios of $20\,h$ without halos and $92\,h$ with halos.

3.2 Chance alignments versus dense subgroups

The results of the new simulations are shown in Tables 1 and 2. The first important point from Table 1 is that 1D chance alignments are typically 10 times more frequent than 3D subgroups. If the dark matter is in individual halos, the dense subgroups are mostly bound, but if the dark matter is in a common envelope then because the galaxies react mainly to the potential of the full group, the dense subgroups are usually unbound, as predicted in one of the alternative hypotheses[10]. The frequency of chance alignments increases with increasing number of galaxies and decreasing parent group size as predicted in the analytical study on chance alignments[8]. Its global value is a few percent for standard (POSS E-band surface magnitude $\mu \leq 26$) HCGs, but reduced to typically 10^{-3} for very compact ($\mu < 24$) HCGs.

Table 1: Compact Configurations within Simulated Loose Groups

Model	Dark Matter	P(CA)	3×3D/1D	bound 3D/all 3D
Standard	Halos	1.1%	7.8%	81%
$R = 500\,h^{-1}$ kpc	Halos	2.0%	12.4%	90%
$N = 12$	Halos	3.3%	4.3%	86%
$(M/L)_{\rm gp} = 200\,h$	Halos	1.4%	14.5%	98%
Standard	Envelope	4.8%	13.9%	33%
$R = 500\,h^{-1}$ kpc	Envelope	6.5%	19.0%	22%
$N = 12$	Envelope	10.3%	8.0%	26%
$(M/L)_{\rm gp} = 200\,h$	Envelope	5.7%	12.3%	43%

NOTES: P(CA) is the frequency of chance alignments. The next column gives the fraction of chance alignments that are 3 dimensional. The final column lists the fraction of 3D subgroups that are bound.

3.3 Binaries within Chance Alignments

Table 2: Chance Alignments along the Viewing Axis

Dark Matter	1+1+1+1	2B+1+1	2B+2B	2U+1+1	2U+2U	3B+1	3U+1
Halos	28%	50%	9%	<1%	<1%	11%	1%
Envelope	26%	12%	1%	39%	8%	4%	10%

NOTES: B and U stand for bound and unbound, respectively.

Table 2 above shows that binaries occur often within 1D chance alignments. The fraction of chance alignments with one single binary is 50%, two binaries: 10%, a triplet: 10 to 15%, with only a little more than one-quarter of all chance alignments without binaries (1+1+1+1). These figures depend very little on the location of the dark matter within the parent loose groups. However, if the dark matter lies in galaxy halos, most of these binaries and triplets are bound, and conversely if the dark matter is in a common envelope most of the binaries and triplets are unbound.

If bound binaries and triplets produce slow and hence strong dynamical interactions, while unbound binaries and triplets produce fast and weak interactions, then one can estimate that among chance alignments within "Halo" loose groups, 70% have at least one strongly interacting pair, while among chance alignments within "Common Envelope" loose groups, 17% have at least one strongly interacting subsystem, and 57% at least one weakly interacting subsystem. Also, the total number of strongly and weakly interacting galaxies is respectively 2.0 and 0.1 for chance alignments within Halo loose groups, and 0.5 and 1.7 respectively for chance alignments within Common Envelope loose groups. In summary, these simulations confirm that chance alignments are binary-rich, as suggested earlier[21], while the strength of these interactions is a measure of how distributed is the dark matter within the parent loose group. Finally, the numbers given above agree roughly with the 63% of abnormal and peculiar rotation curves found for HCG spirals[3], especially when one folds in the $\sim$ 10% of HCGs that would be dense (Table 1), hence interacting, and strongly so, if the loose group dark matter is in galaxy halos.

4. Alternative Hypotheses

Among the alternative hypotheses listed in §1, some can be ruled out quite easily to explain the majority of HCGs, although they may well explain a few of these groups. Spectroscopic measurements have been performed on all the galaxies in HCGs and, although these have still not been published, the latest published subset suggests that perhaps 15% of the HCGs would no longer be quartets if one removed the galaxies with grossly discordant redshifts[12],[22]. So far, only two HCGs seem to have been misclassified single galaxies whose different component may correspond to HII regions and of these one (Hickson 18) is at best a triplet from the spectroscopical data[11]. If HCGs were loose groups at cosmological collapse, then their mass-to-light ratios ought to be double those of virialized loose groups, since their kinetic energy will be roughly equal to the absolute value of its potential energy instead of half of that in virial equilibrium. Instead, the mass-to-light ratios of HCGs are roughly one-third of the corresponding loose group M/Ls (§2), although it remains to be verified what fraction

of these loose groups are indeed virialized. Finally, many properties of HCGs are very distant dependent[12],[21],[23]. The most distant HCGs tend to be elliptical rich, luminous, large, and with higher velocity dispersions. All these trends are features associated with rich clusters of galaxies. It is therefore possible that a non-negligible number of the distant HCGs represent the bright-ends of such clusters[13], and one can show[13] that this would explain the trends observed in the environments of HCGs[24],[25].

5. Summary

The compact groups in Hickson's catalog[1] arise from a variety of origins. Table 3 below gives an estimated rundown of the different hypotheses.

Table 3: The Origin of Hickson Compact Groups

Nature	Number
Primordial Bound Dense Groups	5
Recently Formed Bound Dense Groups	7
Unbound Dense Subgroups of Loose Groups	5
Chance Alignments in the Field (incl. Triplets)	15
Chance Alignments within Loose Groups	35
Chance Alignments within Clusters	15
Collapsing Loose Groups	10
Bright-Ends of Clusters	6
HII Regions	2

Notice the total of 100 HCGs. These values have been obtained as follows: From the recent N-body simulations there should be 8 times more chance alignments in groups or clusters than bound or unbound systems forming within loose groups. As the distribution of dark matter in loose groups is still unknown, the average between the two probabilities for bound 3D systems is taken, giving 57% of bound systems among the 3D subgroups in the standard runs (see Table 1). Then altogether, the difficulty in forming dense groups and the statistical arguments on group M/L, $\langle m_1 - m_2 \rangle$, and morphology-density relation seem to impose that the majority of HCGs are not real. The values in Table 3 then follow, assuming a rather optimistic value of 5 primordial dense groups, and a wild guess for the number of collapsing groups (which cannot be too large or else so would be M/L) and with the observational constraints on alternative hypotheses mentioned in §4.

References

1] Hickson, P., 1982, *Ap. J.*, **255**, 382.

2] Hickson, P., 1990, *in IAU Colloquium 124, "Paired and Interacting Galaxies"*, ed. J.W. Sulentic & W.C. Keel (Washington: NASA), p. 77.

3] Rubin, V.C., Hunter, D. & Ford, W.K. Jr., 1991, *Ap. J. (Suppl. Ser.)*, **76**, 153.

4] Williams, B.A., McMahon, P.M.& van Gorkom, J.H., 1991, *A. J.*, **101**, 1957.

5] Hickson, P. & Rood, H.J., 1988, *Ap. J. (Letters)*, **331**, L69.

6] Palumbo, G.G.C., 1993, *in 2nd DAEC meeting on "Distribution of Matter in the Universe"*, ed. G. Mamon & D. Gerbal (Paris: Obs. de Paris), p. 46.

7] Mamon, G.A., 1986, *Ap. J.*, **307**, 426.

8] Walke, D.G. & Mamon, G.A., 1989, *Astr. Ap.*, **295**, 291.

9] Governato, F., Bhatia, R. & Chincarini, G., 1991, *Ap. J. (Letters)*, **391**, L15.

10] Rose, J.A., 1979, *Ap. J.*, **231**, 10.

11] Williams, B.A. & van Gorkom, J.H., 1988, *A. J.*, **95**, 352.

12] Tikhonov, N.A., 1990, *in IAU Colloquium 124, "Paired and Interacting Galaxies"*, ed. J.W. Sulentic & W.C. Keel (Washington: NASA), p. 105.

13] Mamon, G.A., 1993, *in 2nd DAEC meeting on "Distribution of Matter in the Universe"*, ed. G. Mamon & D. Gerbal (Paris: Obs. de Paris), p. 51.

14] Mamon, G.A., 1987, *Ap. J.*, **321**, 622.

15] Tremaine, S.D. & Richstone, D.O., 1977, *Ap. J.*, **212**, 311.

16] Postman, M. & Geller, M.J., 1984, *Ap. J.*, **281**, 95.

17] Mamon, G.A., 1993, in these proceedings.

18] Tully, R.B., 1987, *Ap. J.*, **321**, 280.

19] Ramella, M., Geller, M.J. & Huchra, J.P., 1989, *Ap. J.*, **344**, 57.

20] Schechter, P.L., 1976, *Ap. J.*, **203**, 297.

21] Mamon, G.A., 1990, *in IAU Colloquium 124, "Paired and Interacting Galaxies"*, ed. J.W. Sulentic & W.C. Keel (Washington: NASA), p. 619.

22] Hickson, P., Kindl, E. & Huchra, J.P., 1988, *Ap. J.*, **331**, 64.

23] Whitmore, B.C., 1990, *in STScI Sypm Ser. 4, "Clusters of Galaxies"*, ed. W.R. Oegerle, M.J. Fitchett & L. Danly (Cambridge: Cambridge University Press), p. 139.

24] Rood, H.J. & Williams, B.A., 1989, *Ap. J.*, **339**, 772.

25] Palumbo, G.G.C., Tornatore, V., Baiesi-Pillastrini, G., Hickson, P. & Mendes de Oliveira, C., 1992, in preparation.

THEORETICAL STUDIES OF ENVIRONMENTAL EFFECTS ON GALAXIES

August E. Evrard

Physics Department, University of Michigan
Ann Arbor, MI 48109-1120 USA

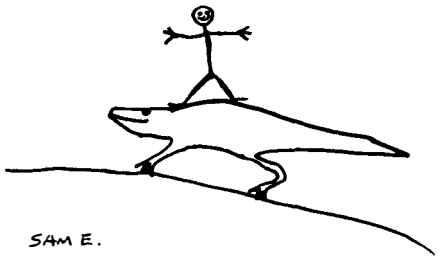

ABSTRACT

A wide array of environmental processes, both stellar and gas dynamical, can affect the formation and evolution of galaxies. Many issues, such as merging, accretion and ram pressure stripping, have been recognized for years. However, a global view incorporating the range of known processes in a self-consistent manner is beyond our grasp. The major obstacle is the fact that we must first understand galaxy formation in a cosmological setting before we can address questions of environment in a quantitative fashion. This paper will review some of the physical processes generally thought of as environmental, with emphasis on uncertain links to theories of galaxy and large-scale structure formation.

1. INTRODUCTION

Galaxies, like people, reside in a variety of environments. A small fraction, around 10%, live in the fast-paced "urban" setting of rich clusters. The environment there can be quite hostile. The space density of galaxies is a factor of ~ 100 above the global mean when averaged over the whole cluster and a factor of $\gtrsim 10^4$ above the mean within the central "core" a few hundred kpc in radius (see Sarazin 1986 for a review of cluster properties). The probability of running into a friend or enemy is enhanced by these factors and thus galaxy encounters are much more frequent in clusters than in general. The outcome of an encounter depends on the orbital and internal characteristics of the colliding galaxies. In addition, cluster galaxies are forced to swim in a bath of hot ($T \sim 10^8$ K), dilute ($n \lesssim 10^{-3}$ cm^{-3}) plasma, the intracluster medium or ICM. A galaxy wandering innocently through the ICM risks losing a large fraction of its warm gas content through ram pressure stripping, as proposed by Gunn and Gott (1972), or by thermal or viscous transport (Cowie and Songaila 1977; Nulsen 1982).

The majority of galaxies reside in the more sedate, suburban setting outside of rich clusters often referred to as the "field". In this environment, disk galaxies like our own Milky Way may develop within comfortable cocoons of dark matter over a Hubble time without suffering any dramatic gravitational interactions with large neighbors (such as Andromeda in our case). Still, it is likely that mergers played an important role at some time in its formation history (see Larson 1993) although the cold nature of disks does not seem to allow much recent merging (Toth and Ostriker 1992). The local environment at early times imparts tidal torque on the protogalactic cloud that subsequently spins up as it collapses to form a centrifugally supported disk (Fall and Efstathiou 1980). It may also be the case that the local metagalactic UV background plays an important dynamical role in the early stages of galaxy formation (Dekel and Rees 1987; Efstathiou 1992). In this case, galaxy properties may be modulated by the local density of active (in a nuclear sense) or starbursting galaxies.

It is important to remember, of course, that there is a continuum of possibilities for galactic environment ranging from isolated individuals to binaries to small groups, then poor clusters and, finally, rich clusters. However, just as a demographer may divide a country's population into urban *vs.* suburban or city dwellers *vs.* country folk to highlight differences in birthweight, median income, or favorite breakfast cereal; so, too, have astronomers historically drawn a mental dividing line separating galaxies in rich clusters from their cousins in the field. In reviewing the subject of environmental effects, one is generally compelled to adopt such a mind set, and I will prove no exception.

The physical processes controlled by environment can be broadly classed into two categories — stellar dynamical and gas dynamical. The distinction arises naturally because galaxies are composed of gas, stars, and dark matter; and these components, in general, respond differently to a given environmental stimulus. The stellar and dark matter constituents are described as collisionless fluids coupled gravitationally. Their

dynamical evolution in the non-linear regime has been extensively investigated with N-body experiments (White 1976; Van Albada 1978; McGlynn 1980; Barnes 1984; Evrard 1986; Davis *et al.* 1985; Carlberg and Couchman 1989; Gelb 1991). Even with tremendous advances in hardware technology and software algorithms, it is certainly not the case that all questions for collisionless systems have been answered. For example, the issue of "previrialization" (Davis and Peebles 1977) in hierarchical clustering remains somewhat controversial (Peebles 1990; Evrard and Crone 1992). It is fair, however, to say that our understanding of gas dynamical issues is crude in comparison to stellar dynamical issues. This is a direct result of the complexity introduced by extra gas dynamical processes on top of gravity. Shocks will form at caustic surfaces, energy can be gained from or lost to a radiation field, and coupling to magnetic fields can affect the transport of energy and momentum in the gas. Furthermore, the cooling rate of a plasma depends on its chemical composition; thus, detailed treatment of the thermal state of the gas requires knowledge of the local star formation history.

On a final semantical note, the purpose of this meeting was to debate the issue of "Nature" *vs.* "Nurture" in determining galaxy morphology. For a particular galaxy of mass M_{gal}, the most reasonable division is to ascribe to "Nature" those processes operating on mass scales $M < M_{gal}$ and to "Nurture" processes arising from scales $M > M_{gal}$. By definition, environmental processes fall into the latter category. Galaxies, of course, cover a range of masses, so the immediate consequence of the above division is that the "Nurturing environment" is a *relative* term. A similar problem arises when considering the "formation" *vs.* "evolution" of galaxies (Peebles 1989). Because of the fuzziness of terminology, I prefer to avoid such categorization. Instead, I will concentrate on specific, relatively well posed issues and include only speculation on how future developments may be able to tie these diverse elements together into a unified description of galaxy formation and evolution.

2. PHYSICAL PROCESSES

The formation of galaxies almost certainly involved gravitational amplification of small initial fluctuations generated at some very early epoch (*cf.* Peebles 1980). The detection of fluctuations in the temperature of the microwave background by the COBE DMR experiment (Smoot *et al.* 1992) is the best direct evidence for such an assumption. Reconciling the small amplitude of the fluctuations ($\Delta T/T \sim 10^{-5}$) with the observed degree of local inhomogeneity is best done in the context of a universe dominated by some type of dark, weakly interacting matter which is probably cold (*e.g.*, axions, photinos, WIMPS) rather than hot (*e.g.*, a light neutrino) (Bennett *et al.* 1992). Galaxy formation is then a "bottom-up" process in which small, protogalactic units form first and then merge to assemble a galaxy size object. Dissipation via radiative cooling plays a key role by providing a mechanism for baryons to condense within their parent halos, become self-gravitating and form stars. Cooling becomes relatively less efficient at higher masses and temperatures — a natural maximum mass scale for galaxies of about $10^{12}M_{\odot}$ can be deduced solely from cooling timescale arguments (Rees and

Ostriker 1977; Silk 1977; White and Rees 1978). In rich clusters, the leftover primordial gas mixes with enriched ejecta from galaxies to become the X-ray emitting intracluster medium.

Details of the full dynamical problem outlined above remain sketchy. Analytical approaches to the dynamics are limited by the fact that there is no preferred spatial symmetry to exploit, the problem of clustering from an initial (probably Gaussian) random field is inherently three dimensional. End runs around the dynamics — for example, assuming galaxies form at peaks in the smoothed density field — involve assumptions for which there are typically sketchy physical justifications. However, there is a considerable body of work focusing on processes that occur after galaxy formation is essentially complete; that is, after the bulk of the primordial gas in the potential well has been turned into stars. In the following sub-sections, I will review work that concentrates on post-formation issues and return briefly to galaxy formation in the subsequent section.

2.1 Stellar Dynamics

One can categorize the effects of galaxy encounters by the degree of damage done to its potential. A reasonable ordering based on increasing strength is :

$$\text{tidal interactions} \Longrightarrow \text{accretion} \Longrightarrow \text{mergers} \Longrightarrow \text{cannibalism.}$$

The independent variables controlling the outcome are the masses and internal phase space distributions of the original galaxies and their orbital structure expressed via an impact parameter p and relative velocity v. The presence or absence of a dark matter halo is an important extra condition. Numerical work in the early to mid-eighties concentrated on purely stellar systems (Roos and Norman 1979; Dekel, Lecar and Shaham 1980; Van Albada 1982; White 1983; McGlynn 1984; Aguilar and White 1985). Improvements in algorithms and computers has allowed serious modelling of multi-component galaxies in recent years (Barnes 1993).

In cluster environments, galaxies encountering one another at high relative velocities will briefly shake up each others' potentials without causing serious permanent damage. Some stars will become unbound from the galaxy and be lost to create a diffuse background light in the cluster such as that recently detected in A2029 (Uson *et al.* 1991). Tidal stripping of weakly bound stars during high velocity encounters was investigated using an impulsive approximation by Spitzer (1958). Numerical examination of the mass loss problem dates back to the mid-sixties (Contopoulos and Bozis 1964). Full N-body simulations involving just a few hundred particles per galaxy was state of the art only a decade ago (Roos and Norman 1979; Dekel, Lecar and Shaham 1980; Gerhard 1981). Mass loss rates below 10% cannot be reliably measured in experiments with such small numbers of particles.

Aguilar and White (1985) performed an extensive parameter space study for spherical galaxies interacting with a point mass perturber. They produced useful fitting formulae for the fractional energy and mass loss as a function of impact parameter and a

strength parameter β based on the relative velocity. Comparison of N-body simulation results with the impulse approximation solution indicated that the impulse approximation worked surprisingly well, even in the regime of strong encounters. Shortcomings of this work are that it ignored dark matter halos for the galaxies and the perturber was "dead" in the sense that there was no internal response of the perturber to the target galaxy. The latter matters little for truly impulsive encounters but becomes important as the strength of the interaction increases and merging becomes the more likely outcome. It has not clear how strongly this approximation affects their conclusion regarding the validity of the impulse approximation for strong encounters.

Several authors (Gallagher and Ostriker 1972; Richstone 1976; Merritt 1983, 1984; Aguilar, Hut and Ostriker 1988) addressed the impact of tidal stripping on the evolution of cluster galaxies, with a particular emphasis on formation of cD envelopes. Merritt (1984) examined the role of tidal stripping from the mean cluster tidal field. Recent reviews of the subject by Whitmore (1990) and Richstone (1990) indicate that the observed structure of cD envelopes (*e.g.*, Schombert 1987; 1988) is in favor of tidal stripping of cluster galaxies as the likely formation mechanism. As Aguilar and White (1985) point out, proper treatment of cluster evolution requires that the stochastic nature of the encounters be taken into account. One strong collision can do much more damage than the cumulative effect of many weak encounters.

Another tidal mechanism of importance to galaxy formation is the spin-up of protogalactic clouds during the linear era of perturbation growth (Peebles 1980). Work by Mestel (1963), Crampin and Hoyle (1964) and Freeman (1970) demonstrated a link between the observed angular momentum distribution of present day galactic disks with slowly rotating initial clouds under the assumption of dissipative collapse conserving specific angular momentum. This work was put in the context of a dark matter dominated universe by Fall and Efstathiou (1980). The spin imparted to perturbations, as measured by the dimensionless parameter $\lambda = J|E|^{1/2}/GM^{5/2}$ for an object with net angular momentum J, mass M and binding energy E, is typically small $\lambda \sim 0.06$, but there is a reasonably large scatter. Initially, it was hoped that the spin parameter might correlate well with environment in such a way as to produce low λ objects, the assumed progenitors of elliptical galaxies, preferentially in high density regions. N-body studies by Barnes and Efstathiou (1987) and Zurek, Quinn and Salmon (1988) dashed that hope by demonstrating no significant dependence of λ on local density. It appears that significant dissipation played a role in the formation of both spheroid and disk galaxies. The key element differenciating morphology is most likely the star formation history of the protogalactic objects that merged to create the final galaxy (Larson 1993).

For low impact parameters and low relative velocities, merging becomes the likely result of an encounter (*e.g.*, Roos and Norman 1979). The term *accretion* is appropriate for situations in which the smaller object (the satellite) is insignificant in mass compared to its partner, say a mass ratio $\lesssim 10\%$. Satellite orbital decay and accretion is the likely explanation for observed fine-scale structure in elliptical galaxies such as shells

and kinematically distinct cores (Schwiezer 1993). In hierarchical cosmologies such as the cold, dark matter model, collapsed objects grow in mass through mergers and accretion of objects spanning a spectrum of masses. Carlberg (1990) extended the analytic approach developed by Press and Schechter (1974) to calculate the probability of mergers as a function of look-back time and satellite mass. His work and the N-body work of Frenk *et al.* (1988) indicate that roughly half of all present-day galactic halos have experienced a merger with an object 10% as massive in the past 5 billion years. The probability of accreting smaller objects is even higher since the mass spectrum is a power law with steep negative slope $n(M)dM \propto M^{-1.8}dM$.

White and Frenk (1991) and Lacey *et al.* (1992) emphasized this feature as an advantage in providing an explanation for the excess counts seen in faint blue fields (Guthakurta *et al.* 1990) and the APM survey (Loveday *et al.* 1992). On the other hand, Toth and Ostriker (1992) have used this feature as an argument against the cold, dark matter model. They examined the heating of galactic disks by satellite accretion, extending earlier work of Quinn and Goodman (1986) and Hernquist and Quinn (1987). They argue that no more than 4% of the present mass inside the solar radius could have been accreted in the past 5 billion years or else its scale height and Toomre Q-parameter would be in conflict with observations. The statement is certainly model dependent, but their assumptions regarding orbital parameters and satellite composition were not unreasonable. It is unknown at present how to reconcile this result with the increasing evidence cited above both for recent mergers and for the relatively rapid evolution in galaxy counts.

The existence of cD galaxies with luminosities well in excess of $10L_*$ in the centers of rich clusters can be explained as arising from a sort of galactic feeding frenzy as proposed by Ostriker and Tremaine (1975). In a variation of the "feeding the monster" theme, galaxies are thought to spiral slowly into the center of the cluster via the process of dynamical friction (Chandrsekhar 1943) where they merge into a continually growing central galaxy. Tremaine (1990) has recently reviewed this process and concludes that simple models involving galaxies sinking in a fixed cluster potential over a Hubble time fall short by a factor of ~ 2 in reproducing the observed excess cD luminosities. He emphasizes Merritt's conclusion that merging in sub-clusters before the collapse of the main cluster may be more effective in adding bulk to the central object because the lower velocity dispersion in subclusters makes merging a more likely outcome of an encounter. Recent numerical simulation discussed below lend support to this point of view.

2.2 Gas Dynamics

Gas dynamical environmental effects have received less attention than stellar dynamical issues. The exception is the problem of ram pressure stripping of interstellar gas in cluster galaxies. Other possible effects of environment have been raised in the context of biased galaxy formation (Kaiser 1984; Dekel and Rees 1987; Babul and Rees

1992; Efstathiou 1992). In general, these effects are motivated by a desire to reproduce some observed aspect of large-scale galaxy clustering. Plausible physical mechanisms for modulating galaxy formation on large scales have not been explored in sufficient quantitative detail. Suppression of dwarf galaxy formation via internal supernova-driven winds (Larson 1974; Yoshii and Arimoto 1985; Dekel and Silk 1986) is an inherently local mechanism and therefore cannot be considered an environmental effect. Below, I will focus on gas dynamical interactions between the interstellar medium in galaxies and the intracluster medium.

In a seminal paper, Gunn and Gott (1972) examined the question of whether ram pressure stripping of cluster spiral galaxies was a viable mechanism for making S0's. In the frame of a galaxy moving with velocity v through an intracluster plasma with density ρ_{ICM}, the interstellar gas will absorb momentum per unit area at a rate $\rho_{ICM}\ v^2$. This is the ram pressure the ICM exerts on the interstellar medium. Consider the galaxy plowing face-on into the cluster. Then the interstellar gas will be lost from the galaxy if the restoring force per unit area of the disk is insufficient to fight against the ram pressure. Sarazin (1986) rewrites their stripping condition for a uniform disk of mass M_{disk} and radius r_{disk} with interstellar mass M_{ISM} in succinct fashion

$$\left(\frac{n_{ICM}}{10^{-3}\ \mathrm{cm}^{-3}}\right)\left(\frac{v}{10^3\ \mathrm{km\ s}^{-1}}\right)^2 \gtrsim 3\left(\frac{M_{disk}}{10^{11}\mathrm{M}_\odot}\right)^2\left(\frac{r_{disk}}{10\ \mathrm{kpc}}\right)^{-4}\left(\frac{M_{ISM}}{0.1\ M_{disk}}\right). \quad (1)$$

The above condition is likely to be satisfied by a typical spiral galaxy with modest gas fraction embedded in a rich cluster. Observational evidence that stripping takes place in cluster environments comes from the reduced HI content of cluster spirals (see Balkowski 1993). However, Valluri and Jog (1991) argue that the observed trend of HI deficiency with spiral size does not follow that expected from ram pressure stripping. They argue for tidal interactions in subclusters as the mechanism responsible for limiting the size of HI disks in clusters.

A number of hydrodynamic simulations of stripping from spherical galaxies have been performed, Sarazin's (1986) review contains a complete listing of the literature. Among the most frequently cited recent work are papers by Takeda, Nulsen and Fabian (1984) and Gaetz, Salpeter and Shaviv (1987). Takeda *et al.* focused on the effect of variations in ram pressure for galaxies on plunging cluster orbits. They included mass loss from evolved stars replenishing the interstellar medium in between excursions into the cluster center. They generalized the sudden stripping condition of Gunn and Gott to spherical galaxies. Their two-dimensional hydrodynamic study emphasized the importance of sudden stripping for galaxies on radial orbits. A "blob" of gas was expelled from the galaxy sufficiently massive and, they estimate, long lived to lend credence to model of Fabian *et al.* (1980) for the X-ray emission from M86 in Virgo (*cf.* White *et al.* 1991).

Takeda *et al.* also developed a continuous stripping criterion for galaxies moving subsonically through a cluster that differs from that of Gunn and Gott by being based

on energy rather than momentum transfer. Assuming a galaxy with mass loss rate $\alpha = \rho_* / \tau$ with $\tau \sim 10^{12}$ yr and gravitational potential ϕ, their condition for stripping is

$$\rho_{ICM}\ v^3 \gtrsim \int_{-\infty}^{\infty} dz\, \alpha\, \phi \tag{2}$$

which can be written in terms of the galaxy's surface density Σ and velocity dispersion σ

$$\rho_{ICM}\ v^3 \gtrsim 16\ \Sigma\ \sigma^2\ \tau. \tag{3}$$

Their Figure 4 summarizes the above condition and provides the expected linear extent of gas retained by the galaxy as a function of cluster environment. For example, an early-type galaxy with $\sigma = 300$ km s^{-1} moving at 1000 km s^{-1} through ICM of number density 10^{-3} cm^{-3} would be stripped down to a surface density of $10^4 M_\odot$ pc^{-2} or a radius of 1 kpc.

Gaetz *et al.* (1987) incorporated stellar mass loss and gas cooling into their two-dimensional modeling of a spherical galaxy in a steady wind (*i.e.*, on a circular orbit in the cluster). The degree of stripping was found to be dependent on the parameter $\xi \propto \rho_{ICM}\ v^{2.4}\ \dot{M}_{rep}$, with $\dot{M}_{rep}$ the rate of mass replenishment. This parameter has dimension intermediate between the sudden (momentum driven) and continuous (energy driven) stripping criteria. They presented fitting formula for the fraction of interstellar mass lost from the galaxy as a function of ξ. They also discussed the morphology of the flow and its dependence on model parameters, but did not address observable consequences in detail.

Other transport processes such as laminar viscous stripping, thermal conduction and turbulent stripping were addressed by Nulsen (1982). If even weak magnetic fields are present, the flow around a galaxy will be turbulent and the first two processes will be highly suppressed. Turbulent stripping may explain the the fine details seen in HRI X-ray images of some cluster cores such as A2029 (Sarazin 1993). Nulsen (1982) estimates that these transport processes can result in stripping rates in excess of those based solely on ram pressure. The numerical work to date has modelled only pure ram pressure ablation. Modelling turbulent flows with tangled magnetic fields in three dimensions remains a daunting numerical task (see Figure 1).

The enhanced fraction of post-starburst (E+A) galaxies in rich clusters at moderate redshifts has been interpreted in terms of a model in which galaxy-ICM interactions induce a starburst in infalling gas rich galaxies (*cf.* Gunn 1989). It is thought that sudden stripping may remove the warm phase the interstellar medium but leave behind dense, molecular gas which is incited to copious star formation by overpressure or some other mechanism. Support for this model comes from the time evolution and kinematic properties of a suitably defined active population of galaxies derived from three-dimensional numerical simulations of cluster formation (Evrard 1991). However, galaxy-galaxy interactions have also been invoked as the source of the enhanced E+A activity (Lavery and Henry 1986).

Figure 1: Conceptual rendering by Sam Evrard (age 6) of the difficulties one encounters in attempting to solve three-dimensional MHD problems.

3. TOWARD A GLOBAL VIEW

Getting back to the analogy with demographics, a true understanding of differences in attitudes between city dwellers and country folk requires a knowledge of the historical development of their cultural differences. In the same way, our understanding of galaxy populations in different environments will be complete only when we have a quantitative picture of galaxy formation in a cosmological context. This Holy Grail of cosmology remains elusive.

Two avenues of attack are currently being pursued. The first involves invoking *ad hoc* rules for deciding where galaxies of a certain morphological type will form in a given cosmology. With this approach, one can examine statistical features of the galaxy population while ignoring the fine details (like all the physics of galaxy formation). The second approach is to simulate the formation of galaxies with as much of the physics as is technically feasible. In principle, this is the preferred path. However, the wide dynamic range of all the physical scales involved combined with our uncertainty of the physics of large-scale star formation means that, in practice, one is forced to simulate part of the problem and make justifications for the physics one has left out.

3.1 Statistical Treatments

The emergence in the mid-1980's of the so-called "standard" cold dark matter model has provided cosmologists with their first well-defined (*i.e.*, calculable) theory of galaxy and large-scale structure formation (see Frenk 1991 for a review). Recent observations

indicating more power on large scales than the standard version of the theory have led to proposed modifications, such as a non-zero cosmological constant, rather than complete abandonment. The recent COBE DMR measurement of large-scale anisotropy in the microwave background (Smoot *et al.* 1992) is marginally consistent with standard CDM (Efstathiou *et al.* 1992) but agrees better with models having more power on large scales. Microwave anisotropy experiments probing smaller angles will provide information on the amplitude of fluctuations on scales of galaxies and clusters of galaxies. It is not unreasonable to suspect that the form of the fluctuation spectrum on galactic scales will be preserved even after patches are applied to add power on large scales.

The key feature of CDM on galactic scales is that the effective spectral index n_{eff}, defined as the logarithmic slope of the power spectrum $n_{eff} = \mathrm{d}\ln P(k)/\mathrm{d}\ln k$ (*cf.* Peebles 1980) has a value $n_{eff} \simeq -2$. Faber (1982) noted that, for objects collapsed from such a spectrum, one expects relations between the mass M and characteristic velocity v similar to the observed Tully-Fisher and Faber-Jackson relations $M \sim v^4$. This point was expanded by Blumenthal *et al.* (1984), who argued that the observed narrow scatter in the relations could only be reproduced if galaxies formed from peaks in the linear density distribution and morphology was linked to thresholds in peak height. Kaiser (1984), Davis *et al.* (1985) and Bardeen *et al.* (1986) demonstrated the advantages of associating galaxies with peaks, paving the way for general acceptance (and frequent abuse) of the terms "biasing" and "biased galaxy formation".

In the midst of this peak activity, Evrard (1989) attempted to test these ideas quantitatively using a model based on the Press-Schechter formulism. Linking morphology to initial peak height produced several attractive features : (i) mass functions for bright (*i.e.*, non-dwarf) galaxies of all morphological types should overlap and span roughly two decades in mass; (ii) the shape of the mass functions are independent of environment but the mix of types is modulated by power on larger scales in such a way as to enhance early type galaxies in rich clusters and suppress their formation in voids. Both of these features are in agreement with observations (Sandage *et al.* 1985; Ferguson 1993). Evrard *et al.* (1990) examined the morphology-density relation in more detail. An ensemble of N-body simulations was used to allow straightforward analysis in the regime of non-linear clustering. Dressler's (1980) morphology-density relation for ellipticals was reproduced extremely well by a model in which bright galaxies form from fluctuations above twice the *rms* level (a 2σ threshold) and the elliptical population arises from the fraction above 3σ. A possible physical basis for such a model comes from dimensional arguments. For an $n = -2$ spectrum, objects on a fixed σ threshold will have constant surface density and constant pressure (Evrard 1989). If copious star formation on galactic scales requires reaching a critical threshold in either of these physical parameters, the model would acquire physical motivation. Kennicutt's (1990) work on star formation in nearby spirals indicates that gas surface density plays a critical role, but he interprets the data in terms of a local instability and does not present a case for a global threshold.

Lacey and Silk (1991) and Lacey *et al.* (1992) used a statistical model based on the idea that star formation in galaxies is triggered by tidal interactions in groups. The latter study combined the spectrophotometric models of Guiderdoni and Rocca-Volmerange (1987) with star formation histories derived from their peak-based model. This allowed them to make predictions for a wide range of observables such as present-day galaxy colors, galaxy counts in both the blue and red, luminosity functions for particular bands at various epochs, etc.. Their success in reproducing many of these observations is somewhat diluted when one considers the large number of tunable parameters in their model. Also, it is not clear how the existence of the Milky Way and M31 is explained in the context of a model in which bright galaxies form via tidal interactions in collapsed groups. Still, their approach is powerful in the sense that it admits many independent observational constraints.

3.2 Numerical Simulations

The recent coupling of three dimensional hydrodynamics codes with N-body algorithms (Evrard 1988; Hernquist and Katz 1989; Cen 1992) has provided the technology needed to model realistically the the formation of galaxies in a cosmological context. Katz and Gunn (1991) and Katz (1992) examined the formation of a single galaxy from an initially lumpy, rotating cloud of dark matter and baryons. Their work emphasized the point made by Larson (1975) and later Zurek *et al.* (1988) that the star formation rate is a critical parameter in determining the final morphology of a collapsed object. Rapid conversion of gas to stars in sub-galactic units leads to collisionless mergers resulting in a spheroidal galaxy. Alternatively, inefficient star formation in sub-units leads to merging of primarily gaseous systems resulting in disks after rearrangement of angular momentum by oblique shocks and viscous transport.

Navarro and Benz (1991) performed SPH simulations of galaxy formation in a cosmological setting using ~ 5000 particles to represent the baryons in a comoving 5 Mpc radius sphere, along with an equal number to represent dark matter. They focused on the angular momentum content of the baryonic cores of galactic scale halos. The surprising result of their work was their claim that the low specific angular momentum content of the baryonic material meant that disks could not form naturally via dissipative settling and that some extra agent, such as feedback from early star formation may be required.

However, this result is not supported by a recent SPH simulation (Evrard *et al.* 1992) employing $524,288$ particles in 16 Mpc comoving cube. This simulation was intended to model the early formation of a cluster in the CDM model. The coupled evolution of the dark matter and baryonic components was followed from an initial redshift $z = 9$ to a final $z = 1$. The imposition of a cluster in the center of the periodic volume raised the mean density above critical which precluded evolution to $z = 0$. The mass per baryonic particle was $1.1 \times 10^8 M_\odot$, implying roughly 1000 particles per L_* galaxy. The baryon thermal energy is subject to change due to adiabatic (PdV) work,

shock heating and radiative cooling. Star formation is not included. The baryons and dark matter are coupled gravitationally, the minimum scale resolved is ~ 10 kpc, roughly the optical size of a bright galaxy. A slice through the final state of the simulation is displayed in Figure 2.

In collapsed regions, a two-phase structure develops in the baryons consisting of cold, high density gas in rough pressure equilibrium with enveloping hot, tenuous halos at roughly the virial temperature of the dark matter halo. We identify a population of galaxies using a group finding algorithm designed to pick out concentrations of baryons above a fixed physical density of ~ 0.5 cm^{-3}. A minimum cutoff of 30 particles per galaxy, $3 \times 10^9 M_\odot$ in baryons, is imposed. The mass fraction of baryons in the galaxy population increases with time from roughly 5% at $z = 5.3$ to 18% at $z = 1.0$. During this time, the number of objects above the mass cutoff grows from 40 to 208.

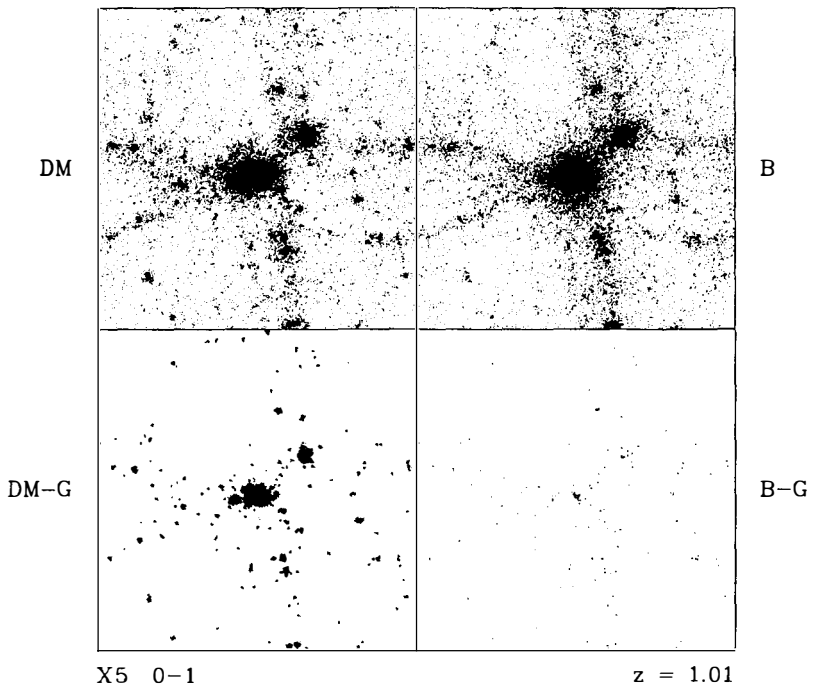

Figure 2 : Projections of a $16 \times 16 \times 3.2$ comoving slice ($H_o = 50$ km s^{-1} Mpc^{-1}) at redshift $z = 1$ from a simulation modelling galaxy formation in a CDM universe. Only one in roughly ten particles are displayed for clarity. The dark matter is in the upper left panel, baryons in upper right. The lower left panel displays dark matter particles grouped at an overdensity of ~ 200 while the lower right shows the population of galaxies defined as groups of baryonic particles at very high ($\sim 10^5$) density contrast. The central cluster which forms at the intersection of sheets and filaments contains 27 galaxies.

A cluster containing 27 galaxies with total mass $6 \times 10^{13} M_{\odot}$ (defined within a sphere of physical radius $r = 530$ kpc within which the mean density is 170 times the background value) has formed by the end of the run. A viable interpretation is that this object represents the core of what would ultimately become a rich Abell cluster. We find the galaxies represent a cooler, more centrally concentrated population with respect to the dark matter. The ratio of the velocity dispersions of galaxies and dark matter is $\sigma_{gal}/\sigma_{DM} = 0.77$ and the ratio of half-mass radii is $r_{gal}/r_{DM} = 0.73$. These numbers vary by $\sim 20\%$ during the dynamical evolution of the cluster. Projected mass estimates are systematically low by factors of $2 - 3$. This, coupled with an enhanced efficiency of galaxy formation in clusters, leads to an estimate of the density parameter $\Omega_o = 0.28$ based on the cluster "mass-to-light" ratio.

As is evident in Figure 2, the galaxies in the cluster represent a small fraction of the total. Most are formed along filaments and end up relatively isolated or in small groups. A large fraction of this population possesses rotationally supported baryonic disks. Figure 3 shows projected images of a prime example and Figure 4 shows its velocity field. The velocity field is very quiet, the major feature is a flat rotation curve of 200 km s^{-1} amplitude outside the resolution limit. Examination of the growth history of this disk shows that the only significant merger in its recent history involved a small

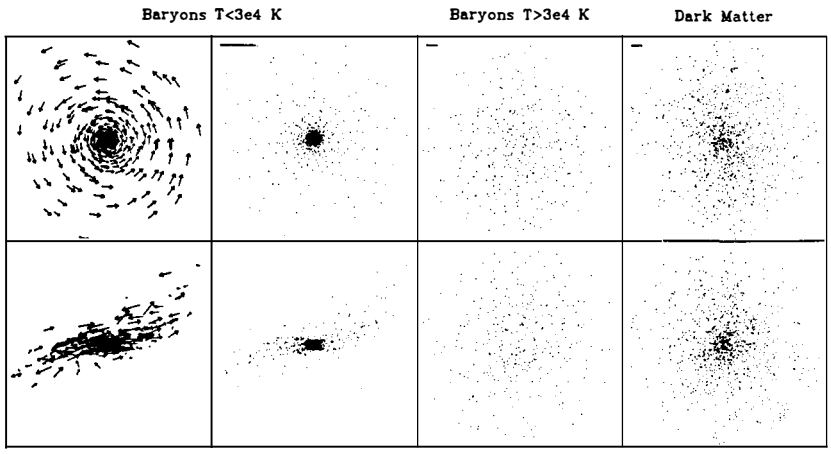

Figure 3 : Face on (top row) and edge on (bottom row) views of the mass within 100 kpc of the center of the twelfth largest galaxy found at the end of the simulation. The small bar denotes the 10 kpc resolution limit. The leftmost panels show baryons in the cold phase. The velocity field in the disk is regular and an outer warp is apparent. Of the total baryonic mass of $1.2 \times 10^{11} M_{\odot}$ within 100 kpc, 65% is in the cold disk and 35% is in a hot halo with $T = 3 \times 10^6$ K shown in the right center panels. The dark matter halo is very nearly spherical and isothermal. The ratio of dark to baryonic mass is unity at 10 kpc, rising to 7.8 at 100 kpc.

satellite with mass $\lesssim 10\%$ of its own. Such quiet dynamical histories appear for the majority of galaxies identified in the simulation.

The frequency of merging is enhanced for galaxies in the cluster relative to those in the field. We define a perturbed population as those galaxies which have experienced a merger with an object of mass $>10\%$ of its own within a 2 Gy interval prior to the end of the simulation. Using the top 34 galaxies which are resolved by 300 or more particles, we find 4 out of 9, or 45%, of the cluster galaxies satisfy the perturbed criterion while only 7 out of 25, or 28%, of galaxies outside the cluster qualify. Although one would like better statistics, the result is clearly in the right direction for explaining the observed morphology-density relation (Larson 1993).

The most emphatic result of the enhanced merger activity is a large, cD-like object with baryonic mass $6 \times 10^{11} M_{\odot}$ which forms at the cluster center. Half of its mass is acquired in the first 2 Gy of the evolution, well before the bulk of the final cluster is in place, by a flurry of merging involving primarily three L_* sized objects. During the final 2.5 Gy, it grows in mass by "cannibalizing" nine much smaller objects. This formation history points to the importance of *both* early merging and cannibalism in building cD galaxies.

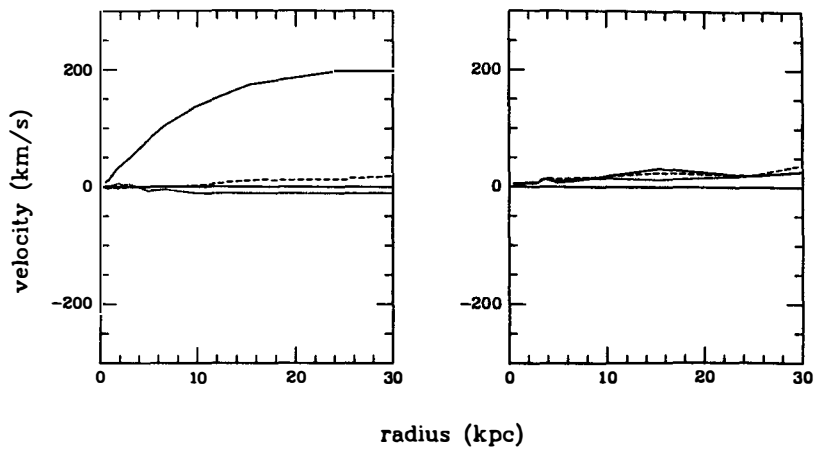

Figure 4 : The left panel shows the mean tangential (solid), radial (dotted) and perpendicular (dashed) velocities as a function of radius for the object shown in Figure 3. Right panel shows the dispersion about the mean values.

4. SUMMARY

Environmental processes operating on present-day galaxies have been explored theoretically in some detail over the past few decades. Stellar dynamical processes such as mass loss from tidal encounters and the outcome of mergers are fairly well understood,

although more work needs to be done in the area of multicomponent systems. Work on gas dynamical processes is limited by our inability to model the complex, multi-phase structure of interstellar and intergalactic gas as well as our uncertainty in the roles played by magnetic fields, turbulence and feedback from star-forming or nuclear active galaxies. Our eventual aim must be to understand environmental effects in the context of galaxies forming within a given cosmological theory. Although advances in numerical simulation methods allow this problem to be investigated in unprecedented detail, there is still much physics that is either modelled crudely or omitted entirely. The "Nature *vs.* Nurture" puzzle is taking shape, but is far from finished.

I am grateful to my collaborators Frank Summers and Marc Davis for allowing me to include results of our project. This work was supported by NASA grant NAGW-2367 and the NSF via Cray Y-MP CPU time at the San Diego Supercomputer center.

REFERENCES

Aguilar, L.A., Hut, P. and Ostriker, J.P. 1988, *Ap. J.*, **335**, 720.
Aguilar, L.A. and White, S.D.M. 1985, *Ap. J.*, **295**, 374.
Babul, A. and Rees, M.J. 1992, *M.N.R.A.S.*, **255**, 346.
Balkowski, C. 1993, this volume.
Bardeen, J.M., Bond, J.R., Kaiser, N. and Szalay, A.S. 1986, Ap. J., **304**, 15.
Barnes, J. 1984, *M.N.R.A.S*, **208**, 885.
Barnes, J. 1993, this volume.
Barnes, J.E. and Efstathiou, G. 1987, *Ap. J.*, **319**, 575.
Bennett, C.L. *et al.* 1992, preprint.
Blumenthal, G.R., Faber, S.M., Primack, J.R., and Rees, M.J. 1984, *Nature* , **311**, 517.
Carlberg, R.G. 1990, *Ap. J. Letters*, **359**, L1.
Carlberg, R.G. and Couchman, H.M.P. 1989, *Ap. J.*, **340**, 47.
Cen, R.Y. 1992, *Ap. J. Suppl.*, **78**, 341.
Chandrasekhar, S. 1943, *Ap. J.*, **97**, 255.
Contopoulos, G. and Bozis, G. 1964, *Ap. J.*, **139**, 1239.
Cowie, L.L. and Songaila, A. 1977, *Nature*, **266**, 501.
Crampin, D.J. and Hoyle, F. 1964, *Ap. J.*, **140**, 99.
Davis, M. and Peebles, P.J.E. 1977, *Ap. J. Suppl.*, **34**, 425.
Davis, M., Efstathiou, G., Frenk, C.S. and White, S.D.M. 1985, Ap. J., **292**, 371.
Dekel, A., Lecar, M. and Shaham, J. 1980, *Ap. J.*, **241**, 946.
Dekel, A. and Silk, J. 1986, *Ap. J.*, **303**, 39.
Dekel, A. and Rees, M.J. 1987, *Nature*, **326**, 455.
Dressler, A. 1980, *Ap. J.*, **236**, 351.
Efstathiou, G. 1992, *M.N.R.A.S.*, **256**, 43p.

Efstathiou, G., Bond, J.R. and White, S.D.M. 1992, submitted to *M.N.R.A.S.* .

Evrard, A.E. 1986, *Ap. J.*, **310**, 1.

Evrard, A.E. 1988, *M.N.R.A.S.*, **235**, 911.

Evrard, A.E. 1989, *Ap. J.*, **341**, 26.

Evrard, A.E. 1991, *M.N.R.A.S.*, **248**, 8p.

Evrard, A.E. and Crone, M.M. 1992, *Ap. J. Letters*, in press.

Evrard, A.E., Silk, J. and Szalay, A. 1990, *Ap. J.*, **365**, 13.

Evrard, A.E., Summers, F.J. and Davis, M. 1992, submitted to *Ap. J.*.

Fabian, A.C., Schwarz, J. and Forman, W. 1980, *M.N.R.A.S.*, **192**, 135.

Faber, S.M. 1982, in *Astrophysical Cosmology*, ed. H.A. Bruck, G.V. Coyne and M.S. Longair, (Vatican:Pontificia Academia Scientiarium), p. 191.

Fall, S.M. and Efstathiou, G. 1980, *M.N.R.A.S.*, **193**, 189.

Ferguson, H. 1993, this volume.

Freeman, K.C. 1970, *Ap. J.*, **160**, 811.

Frenk, C.S. 1991, *Physica Scripta*, **T36**, 70.

Frenk, C. S., White, S. D. M., Davis, M., and Efstathiou, G. 1988, *Ap. J.*, **327**, 507.

Gaetz, T.J., Salpeter, E.E. and Shaviv, G. 1987, *Ap. J.*, **316**, 530.

Gallagher, J.S. and Ostriker, J.P. 1972, *A.J.*, **77**, 288.

Gelb, J. 1991, *Ph.D. thesis*, MIT.

Gerhard, O.E. 1981, *M.N.R.A.S.*, **197**, 179.

Guiderdoni, B. and Rocca-Volmerange, B. 1987, *Astr. Ap.*, **186**, 1.

Gunn, J.E. 1989, in *The Epoch of Galaxy Formation* , eds. C.S. Frenk *et al.* (Dordrecht:Kluwer), p. 109.

Gunn, J.E. and Gott, J.R. 1972, *Ap. J.*, **209**, 1.

Guthakurta, P., Tyson, J.A. and Majewski, S.P. 1990, *Ap. J. Letters*, **357**, L9.

Hernquist, L. and Quinn, P.J. 1987, *Ap. J.*, **312**, 1.

Hernquist, L. and Katz, N. 1989, *Ap. J. Suppl.*, **70**, 419.

Kaiser, N. 1984, *Ap. J. Letters*, **284**, L9.

Katz, N. 1992, *Ap. J.*, **391**, 502.

Katz, N. and Gunn, J.E. 1991, *Ap. J.*, **368**, 325.

Kennicutt, R.C. 1990, in *The Interstellar Medium in Galaxies*, eds. H.A. Thronson, Jr. and J. M. Shull (Kluwer:Dordrecht), p. 405.

Lacey, C.G. and Silk, J. 1991, *Ap. J.*, **381**, 14.

Lacey, C., Guiderdoni, B., Rocca-Volmerange, B. and Silk, J. 1992, submitted to *Ap. J.*.

Larson, R.B. 1974, *M.N.R.A.S.*, **169**, 229.

Larson, R.B. 1975, *M.N.R.A.S.*, **173**, 671.

Larson, R.B. 1993, this volume.

Lavery, R.J. and Henry, J.P. 1986, *Ap. J. Letters*, **304**, L5.

Loveday, J., Peterson, B.A., Efstathiou, G. and Maddox, S.J. 1992, *Ap. J.*, **390**, 338.

McGlynn, T.A. 1984, *Ap. J.*, **281**, 13.

Merritt, D. 1983, *Ap. J.*, **264**, 24.

Merritt, D. 1984, *Ap. J.*, **276**, 26.

Mestel, L. 1963, *M.N.R.A.S.*, **126**, 553.

Navarro, J.F. and Benz, W. 1991, *Ap. J.*, **380**, 320.

Nulsen, P.E. 1982, *M.N.R.A.S.*, **198**, 1007.

Ostriker, J.P. and Tremaine, S. 1975, *Ap. J. Letters*, **202**, L113.

Peebles, P.J.E. 1980, *The Large-Scale Structure of the Universe*, (Princeton : Princeton University Press).

Peebles, P.J.E. 1989, in *The Epoch of Galaxy Formation* , eds. C.S. Frenk *et al.* (Dordrecht:Kluwer), p. 1.

Peebles, P.J.E. 1990, *Ap. J.*, **365**. 27.

Press, W.H. and Schechter, P. 1974, *Ap. J.*, **187**, 425.

Quinn, P.J. and Goodman, J. 1986, *Ap. J.*, **309**, 472.

Rees, M. J. and Ostriker, J. P. 1977, *Ap. J.*, **179**, 541.

Richstone, D.O. 1976, *Ap. J.*, **204**, 642.

Richstone, D.O. 1990, in *Clusters of Galaxies*, eds. W.R. Oegerle, M.J. Fitchett and L. Danly, (Cambridge: Cambridge Univ. Press), p. 231.

Roos, N. and Norman, C.A. 1979, *Astr. Ap.*, **74**, 75.

Sandage, A.R., Bingelli, B. and Tammann, G.A. 1985, *A.J.*, **90**, 1759.

Sarazin, C.L. 1986, *Rev. Mod. Phys.*, **58**, 1.

Sarazin, C.L. 1993, this volume.

Schombert, J.M. 1987, *Ap. J. Suppl.*, **64**, 643.

Schombert, J.M. 1988, *Ap. J.*, **328**, 475.

Schweizer, F. 1993, this volume.

Silk, J.I. 1977, *Ap. J.*, **211**, 638.

Smoot, G.F. *et al.* 1992, preprint.

Spitzer, L. 1958, *Ap. J.*, **127**, 17.

Takeda, H., Nulsen, P. and Fabian, A. 1984, *M.N.R.A.S.*, **208**, 461.

Toth, G. and Ostriker, J.P. 1992, *Ap. J.*, **389**, 5.

Tremaine, S. 1990, in *Dynamics and Interactions of Galaxies* , eds. R. Wielen *et al.* , (New York : Springer Verlag), p. 121.

Uson, J.M., Boughn, S.P. and Kuhn, J.R. 1991, *Ap. J.*, **369**, 46.

Valluri, M. and Jog, C.J. 1991, *Ap. J.*, **374**, 103.

Van Albada, T.S. 1982, *M.N.R.A.S.*, **201**, 939.

White, D.A., Fabian, A.C., Forman, W., Jones, C. and Stern, C. 1991, *Ap. J.*, **375**, 35.

White, S.D.M. 1976, *M.N.R.A.S.*, **177**, 717.

White, S.D.M. 1983, *M.N.R.A.S.*, **274**, 53.

White, S.D.M. and Frenk, C.S. 1991, *Ap. J.*, **379**, 52.

White, S.D.M. and Rees, M.J. 1978, *M.N.R.A.S.*, **183**, 341.

Whitmore, B.C. 1990, in *Clusters of Galaxies*, eds. W.R. Oegerle, M.J. Fitchett and L. Danly, (Cambridge: Cambridge Univ. Press), p. 139.

Yoshii, Y. and Arimoto, N. 1987, *Astron. Astrophys.*, **188**, 13.

Zurek, W., Quinn, P. and Salmon, J. 1988, *Ap. J.*, **330**, 519.

OBSERVATIONAL EVIDENCE OF ENVIRONMENTAL EFFECTS IN CLUSTERS

Chantal Balkowski
Observatoire de Paris
Département d'Astrophysique Extragalactique
et de Cosmologie
Unité associée au CNRS (URA 173) et à l'Université Paris 7
5 Place Janssen 92195 Meudon Cedex France

ABSTRACT

Various observations show that the cluster environment can affect the properties of galaxies. This review concentrates on the environmental effects on the HI content of galaxies and their dynamics.

The example of the Virgo cluster will be discussed in details together with new results obtained on rotation curves of galaxies in some clusters. If it is obvious that the environment affects the HI content of galaxies, it is shown that the effects on the rotation curves have still to be proved.

1. INTRODUCTION

Several reviews have been already written on the subject (Haynes 1990; Whitmore 1990) showing evidences that the environment affects the optical and radio properties of galaxies in clusters.

The idea that galaxies in clusters are different from galaxies in the field appeared as early as 1931 when Hubble and Humason noticed that galaxies in clusters had different morphological types, finding early type galaxies preferentially inside clusters. It took about 50 years before that effect was quantified (Dressler 1980). Since then the number of observing and theoretical works has increased and the fundamental question is wether the influence on the morphology of a galaxy is due to the initial conditions at the time of its formation or to the influence of its environment during its life time. This difficulty is well addressed by Evrard (1992): if the formation of galaxies is still unclear, it will be difficult to tell what is the influence of the environment during and after its formation.

Nevertheless, in this review we will give evidences of differences between galaxies in clusters and in the field, showing some examples of parameters which could have been influenced, we will mostly concentrate on some of the observationnal evidences in the Virgo cluster and present the controversy on wether or not there is an effect of the environment on rotation curves of galaxies in clusters.

2. SUMMARY OF THE BASIC OBSERVATIONAL EVIDENCES

In this chapter, we will review some evidences that basic parameters of galaxies such as the morphological type, the diameter, the luminosity, the star formation rate and the HI content, are affected by the environment.

2.1 The morphological type segregation

Using a sample of about 6000 galaxies in 55 clusters, for which he measured positions, morphological types, magnitudes and ellipticities, Dressler (1980) established the well-known correlation between morphological type and local projected density showing that the fraction of elliptical and S0 galaxies increases as a function of local galaxy density while the fraction of spirals decreases.

Since then other works have been done showing that the fundamental correlation could be rather with the clustercentric radius than with the local density (Sanroma and Salvador-Solé 1990, Whitmore and Gilmore 1991, Whitmore 1992).

2.2 Influence on the diameter and the luminosity

Peterson et al. (1979) found that the disk galaxies in the Virgo cluster are about 30% smaller than the disk galaxies in the Hercules cluster and attributed this effect to environmental differences. However, Girardi et al. (1991) conclude that there is no effect on the luminosity-diameter relation for disk galaxies in different density regions. Bagget and Anderson (1992) using a detailed observation study of the spiral galaxies in three different clusters have shown that there is no apparent correlation between the galaxy parameters and the projected distance from cluster center. The most pronounced correlation they found was with the projected galaxy density: both the isophotal radius and the slope of the disk brightness profiles are affected, and the color profile may be also affected. They attributed these influences to environmental processes such ram-pressure stripping of the galaxy gas by the intracluster medium and tidal stripping of the stellar material by the prolonged exposure to the gravitational field of subclusters.

2.3 Star formation

Using H alpha emission line photometry, Kennicutt (1983) found that the Virgo cluster exhibits a systematic deficiency of star formation in its spirals, but a similar behaviour is not detected in Cancer, Coma and A1367 (Kennicutt et al. 1984). Although there are some examples of star formation enhancement for individual galaxies in A1367 and an evidence of a higher star formation rate in the Coma supercluster (Gavazzi et al. 1992). From ultraviolet observations at 2000 A of A1367, Donas et al. (1990) find that the star formation seems to be more efficient for galaxies in the central part of the cluster than for galaxies in the outer part or for field galaxies. From far UV observations of the Virgo cluster at 1500 A, Kodaira et al. (1990) find that the star formation activity is depleted in the Virgo spirals galaxies and that there is an indication of star formation in elliptical galaxies.

It is clear from that list of results that the question of the enhancement of star formation in clusters is still controversial, one of the reason could be that there are too many parameters involved and the only way to clear the problem is to analyse a larger data base including all the involved parameters.

2.4 Butcher-Oemler effect

Butcher and Oemler (1978,1984) have shown the presence of an unexpectedly fraction of blue galaxies in distant clusters ($z>0.2$). A similar effect has been looked for in nearby clusters.

Bothun and Dressler (1986) have shown that 7 gas-poor blue spiral galaxies in the central region of the Coma cluster have Balmer absorption lines and emission line strengths that are excessive compared with normal field galaxies. These are signs of ongoing star formation, these galaxies, according to Bothun and Dressler (1986) have fallen in the cluster center for the first time and are interacting with the hot intracluster gas.

Vigroux et al. (1989) have shown that this effect is also present in the Pegasus cluster. Five of the ten studied galaxies show evidence of recent star formation. This large fraction of early type galaxies is well in excess of that found in nearby "field" galaxies and in the Virgo

cluster. Moreover, like in distant cluster these galaxies tend to be preferentially located outside of the central region of the cluster.

2.5 Neutral hydrogen and CO content

The most obvious effect is probably the one concerning the HI content of galaxies in clusters. The very first attempt to prove that effect was the one done by Davies and Lewis (1973). This result was followed by a long controversy on the idea that the HI content of galaxies in clusters could be affected by their environment . The very first quantitative analysis was made possible as soon as a large sample of field galaxies observed in HI was available to make the comparison. Chamaraux et al. (1980) established clearly the HI deficiency of the spiral galaxies of the Virgo cluster by a factor of 2. This result in the Virgo cluster was confirmed soon after by Giovanelli and Haynes (1983). A study of the HI deficiency in 9 clusters has shown that the HI deficiency is in fact correlated with the luminosity of the X ray emitting gas in these clusters, the ones having X ray emission present an HI deficiency whether the others do not (Giovanelli and Haynes 1985).

The effect is even more drastic in early type galaxies, in the Virgo cluster for example they are 10 times more deficient than the field galaxies of the same morphological type (Chamaraux et al. 1986). Related to this is the possibility to explain the large number of early type galaxies in clusters. These galaxies could be in fact the remnant of spiral galaxies which have been severely stripped (Salvador-Solé 1992).

The processes responsible for the HI deficiency are reviewed by Evrard (1992), the most popular one is the ram-pressure stripping: galaxies moving in the hot intracluster gas lose their HI gas (Gunn and Gott 1972). This will be clearly illustrated in the chapter of this review devoted to the VLA observations of the Virgo cluster.

The only problem in this scheme is the existence of relatively HI rich dwarf galaxies in the Virgo cluster. Hoffman et al. (1987) have shown that, if the dwarf galaxies show some evidence of ram-pressure stripping, they do not as a group seem to be stripped more heavily

than spirals. This result is quite surprising because the contrary was expected in such small systems.

Contrary to the HI content of cluster galaxies, the CO content is not affected, this has been shown in the Virgo cluster (Kenney and Young 1988) as well in the Coma cluster (Casoli et al. 1991). It can be easely understood because the distribution of CO is more concentrated toward the galaxy center than that of HI, the high surface density of CO and its location deep in the gravitational well of the galaxy are responsible for its survival against ram-pressure stripping. See also Combes (1992) who presents evidence that interacting and merging galaxies have a higher molecular mass than normal isolated galaxies.

2.6 Multiwavelength analysis

As said hereabove, the best way to approach the influence of the environment on galaxies properties is probably a multiwavelength approach. This is being done by Gavazzi (1991,1992) who has done multifrequency observations of 874 spiral galaxies including radio continuum, HI, far infrared, near infrared, UBV CCD photometry and H alpha observations. The data indicate that galaxies in clusters have their FIR(60μ)/optical luminosity functions not distinguishable from those of isolated galaxies. The most obvious interpretation of this result is that the global star formation process in spiral galaxies is not significantly altered by the cluster environment. The data indicate also that spiral galaxies in clusters have their radio emission (per unit visible light) enhanced by a factor of 5 with respect to isolated galaxies. Enhanced radio continuum activity might be induced in objects experiencing the hostile environment from a time sufficient to produce some HI ablation, but short compared with the evolution time scale, i.e. objects that have entered the cluster only recently. Gavazzi (1992) concludes that a combination of enhanced star formation rate and magnetic field could produce the observed overabundance of strong radio/optical ratios in clusters.

It is clear that if multiwavelength analysis is necessary, the obtained results obtained so far are sometimes contradictory: we would for example have expected a FIR/optical luminosity

enhancement in cluster galaxies because in some individual cases there are signs of enhanced star formation. The statistical approach on a large number of objects is certainly the best to disentangle all the phenomenons involved. The next approach to be done is certainly a multivariate analysis to extract the most fundamental parameters of the distribution.

3.VLA OBSERVATIONS OF THE VIRGO CLUSTER

If single dish observations have shown that the Virgo spirals are deficient and that this deficiency is correlated with the distance to the cluster center it is important to see where the neutral hydrogen is missing. Being the closest, the Virgo cluster is the first to have been observed with an array of radiotelescopes. The only existing surveys of a large number of spiral galaxies in clusters have been performed at Westerbork (Warmels 1986) and at the VLA (Cayatte et al. 1990). The most important results obtained at the VLA are visible on Figure 1 which shows all the individual maps obtained for each observed galaxy (except one, NGC4303 located too far south to be drawn on that synthetic map). The first striking effect which catches the eye is the small HI size of the very central galaxies where the density of the intracluster gas is higher and therefore where the ram-pressure stripping is more efficient.

This effect is also clearly seen on Figure 2 which shows the dependence of the HI size normalized to the optical one versus the distance to the cluster center (taken as Messier 87).

In order to understand more deeply the processes responsible for the HI deficiency in the Virgo cluster Cayatte et al. (1992) have analysed the HI surface density profiles in each galaxy. They have evidenced 4 different groups of galaxies according to the ratio of the HI diameter to the optical one (D_H/D_0). The different groups are illustrated in Figure 3. The first group includes all the galaxies with $D_H/D_0 \geq 1.3$. The HI density is fairly constant out to a radius normalized to $D_0/2$ and presents an exponential decreases in the outer part. The galaxies appear quite normal over most of the disk. These galaxies (NGC4178, 4192, 4254, 4303, 4654) are located in the outer part of the cluster (see Fig.1). The given interpretation is that these galaxies

are in a very early stage of stripping. In this early stage only the outer parts of the galaxies are depleted.

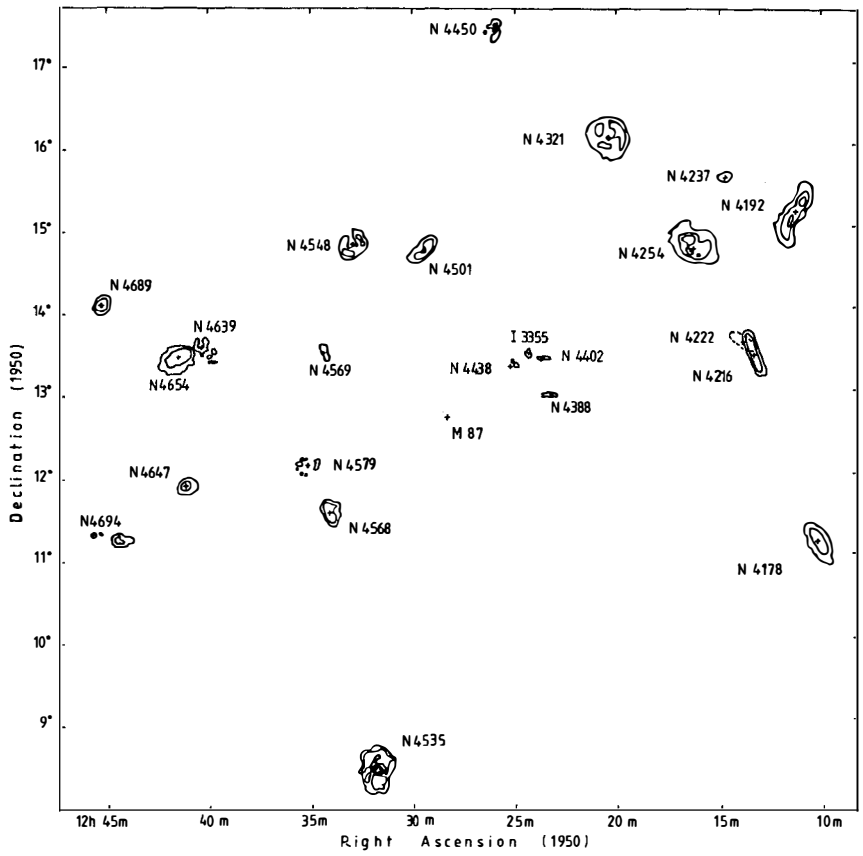

Fig.1: Integrated neutral hydrogen maps of the brightest spirals in the Virgo cluster. Each map has been drawn at the galaxy position indicated by a cross and magnified by a factor of 5 compared with the scale in right ascension and declination. The first contour in each map corresponds to a column density of 10^{20} atoms cm^{-2}; (from Cayatte et al. 1990).

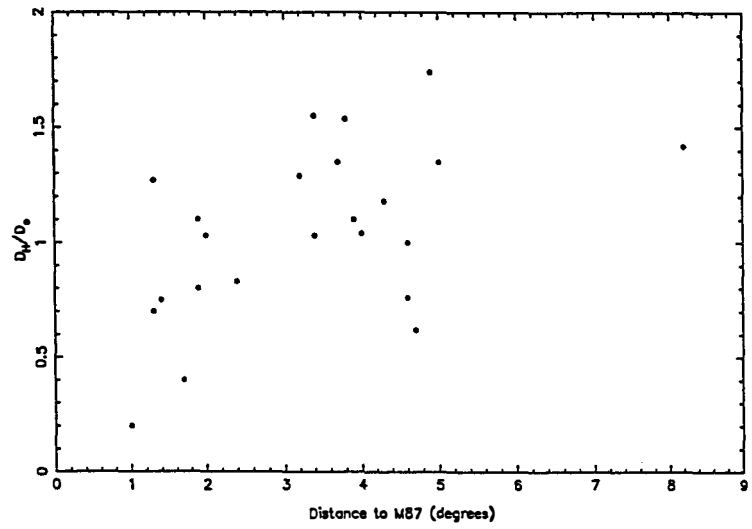

Fig.2: Ratio of the isophotal HI diameter to the optical one versus the projected distance to the Virgo cluster center; (from Cayatte et al. 1992).

The second group incudes galaxies with $0.75 < D_H/D_0 < 1.3$. They show a tendency for a lower central density. These galaxies (NGC4216, 4321, 4501, 4535, 4647, 4689) are located in the outer part of the cluster (see Fig.1).

The third group includes galaxies with strongly truncated disks $D_H/D_0 \leqslant 0.75$. The HI profile shows a strong decline. These galaxies are deep in the cluster core (NGC4388, 4402, 4569). They undergo a violent stripping with a possible enhancement of their central density due to compression.

The fourth group includes anemic galaxies with $0.6 < D_H/D_0 < 0.85$. They are located in the cluster core (NGC4450, 4548, 4579). The HI density is generally lower than in the other groups. Their peculiar HI profile is due to the distribution of the gas in a small ring with a strong central hole. This annular HI distribution might be due to gas replenishment by stellar mass lost after complete stripping.

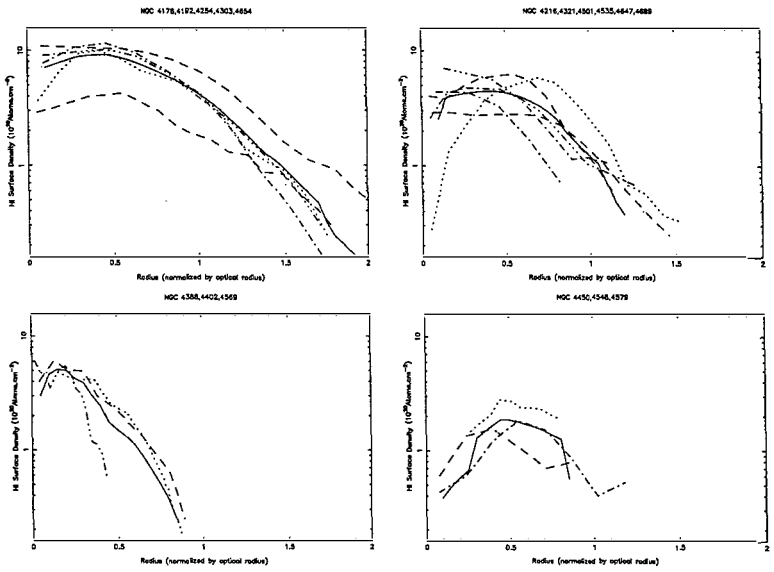

Fig.3: Radial surface density in the four groups. The radius is normalized by the optical corrected radius at the 25th magnitude arcsec^{-2} isophote. The solid line is the averaged surface density distribution for each group; (from Cayatte et al. 1992).

In order to compare spiral galaxies in clusters and in the field, Cayatte et al. (1992) have also analysed a sample of 84 field galaxies to obtain the typical HI density profiles along the morphological sequence. They have reviewed and quantified all the possible processes which could be responsible for the obtained density profiles. Their main conclusion is that the ram-pressure is the most important phenomenon without solving the problem of the HI rich dwarf galaxies. Two of them were observed during their survey (IC3355 and NGC4694 companion) and the most probable interpretation is that these objects are in fact HI clouds eject from galaxies inside which star formation occured later on. Such a conclusion on NGC4694 dwarf

was also given by van Driel and van Woerden (1989). Such a dwarf embedded in an HI cloud (near Zw 160-106) also exists in the Coma cluster (Sullivan 1989, Amram et al. 1992a).

A tentative mapping of the spiral galaxies of the Coma cluster has been done (Sullivan 1989), an ongoing survey of the Hydra cluster is being done by McMahon et al. (1992). The first results show that the 3 central spiral galaxies are not affected by their environment leading to the conclusion that these objects belong in fact to a group seen in projection on the cluster.

4. ROTATION CURVES OF GALAXIES IN CLUSTERS

If it is clear that the HI content of galaxies is influenced by the environment, it is yet not clear if it is the same for their dynamics.

Chincarini and de Souza (1985) found that the rotation curves of the Virgo cluster did not differ from those of field galaxies. This result was confirmed by Guhathakurta et al. (1988) on a larger sample from our VLA observations. Rubin et al. (1988) and Whitmore et al. (1988) suggested that the gradient of rotation curves is correlated with the distance of the galaxies from the cluster center, decreasing curves being found preferentially in the central regions of clusters. If correct, this result would be of great importance because it would mean that either the massive halos (suppose to be responsible for the flat rotation curves) have been stripped or even never formed. Amram et al. (1992a,b) do not confirm Whitmore et al. (1988) results.

We have observed 35 galaxies in different clusters at the 3.6m CFH telescope equipped with a scanning Fabry-Pérot and reobserved some of the galaxies observed by Rubin et al. (1988) in order to compare the slit spectroscopy observations with the Fabry-Pérot ones. The main difference between the two technics is that a slit gives only access to the velocity along the major axis wether a Fabry-Pérot gives a 2 dimension velocity field from which the rotation curve is deduced. Figure 4 gives an exemple of UGC 4329, a galaxy in common to the 2 samples. The large squares are data from Rubin et al. (1988), the other symbols are explained in the figure caption. It is clear from that example that the gradients we have obtained for that

galaxy do not agree and that we reach regions along the major axis further than with slit spectroscopy.

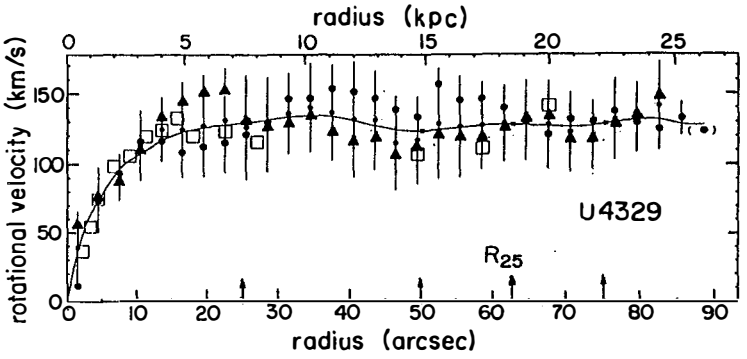

Fig.4: Rotation curve of UGC4329 in the Cancer cluster. The isophotal radius R_{25} is indicated, as well as 0.4, 0.8 and 1.2 R_{25}. The large filled circles represent the weighted mean values of rotation velocities in successive annuli in the plane of the galaxy on the receding side; the triangles represent the approaching side and the small filled circles are the overall means, through which a spline function has been fit. The error bars on each mean value represent + or - 1 sigma in the distribution of measured pixels making up that mean; the error in the mean is typically lower by a factor of 3 to 7. The large open boxes are the data point obtained by Rubin et al. (1988); (from Amram et al. 1992b).

Another advantage of the Fabry-Pérot technics is that from our data we can also determine the inclination and the position angle of the galaxy with a good precision wether these quantities need to be known in advance when using slit spectroscopy. All these important differences and others are discussed in details in Amram et al. (1992a). They could be the source of our desagreement. Our second data paper (Amram et al. 1992c) confirm the results found with the first data set.

Figure 5 gives the plot of the outer gradient (OG= $(V_{0.8}-V_{0.4})/V_{max}$) where $V_{0.8}$ and $V_{0.4}$ are the velocities at 0.4 and 0.8 times the radius at the 25^{th} magnitude and V_{max} is the maximum velocity of the rotation curve, versus the distance to the cluster center. The full line is the regression we obtained using the black dots, the other ones (crosses and plus) have been rejected because they had a peculiarity (a nearby companion, a warp, too high inclination...). The dotted line is the one obtained by Whitmore et al. (1988) with a different sample containing more galaxies toward the center of the clusters but for some of these we obtained very different values of the gradient.

The controversy is still going on, if we find a slight tendency for a correlation it is not as strong as the one found by Whitmore et al. (1988), it is clear that the present situation could evolved when a larger sample of rotation curves of galaxies in clusters will be available.

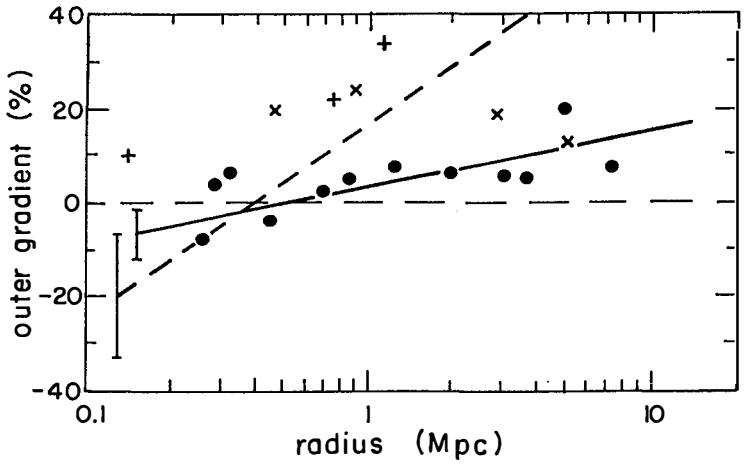

Fig.5: Outer gradient OG for each galaxy versus its projected radius from its cluster center. Three sample are distinguished, the black dots are for the galaxies without any peculiarity, the crosses are for galaxies with an inclination greater than 65°, the plus are for galaxies with close companions, evidence for non-circular motion or rotation data requiring extrapolation; (from Amram et al. 1992b).

5. CONCLUSION

Some observationnal evidences of the influence of the environment on the properties of cluster galaxies have been given from the morphological type segregation to the dynamics of galaxies through the star formation and radio properties.

The most evident fact with almost no counter examples is the HI deficiency of galaxies in clusters. The VLA survey has allowed to map the 25 brightest galaxies showing that the central objects have their HI disk truncated and much smaller than the optical ones. Four groups of galaxies have been identified according to the shape of their HI surface density, showing galaxies at different stages of interaction with the X-ray gas, from the non affected ones just entering into the cluster to the Anemics ones probably seen long after they crossed the cluster core.

Thirty five rotation curves of galaxies located in 7 different clusters have been obtained from 2D velocity fields, the gradients of the rotation curves do not show any correlation with the distance to the cluster center therefore the dynamics of galaxies in clusters does not seem to be affected by the environment , a result in contradiction with earlier ones and which will have to be confirmed whith a larger sample.

REFERENCES

Amram, P., Le Coarer, E., Marcelin, M., Balkowski, C., Sullivan, W.T. III and Cayatte, V. 1992a, Astron. Astrophys. Suppl. Ser. 94, 175

Amram, P., Marcelin, M., Balkowski, C., Cayatte, V. and Sullivan W.T. III 1992c, Astron. Astrophys. to be submitted

Amram, P., Sullivan, W.T. III, Balkowski, C., Marcelin, M. and Cayatte, V. 1992b, submitted to Astrophys. J. Letters

Bagget, W.E. and Anderson, K.S.J. 1992, Astron. J. 103, 436

Bothun, G.D. and Dressler, A. 1986, Astrophys. J. 301, 57

Butcher, H. and Oemler, A. 1978, Astrophys. J. 219, 18

Butcher, H. and Oemler, A. 1984, Astrophys. J. 285, 426

Casoli, F., Boissé, P., Combes, F. and Dupraz, C. 1991, Astron. Astrophys. 249, 359

Cayatte, V., van Gorkom, J.H., Balkowski, C. and Kotanyi, C. 1990, Astron. J. 100, 604

Cayatte, V., Kotanyi, C., Balkowski, C. and van Gorkom, J.H. 1992, submitted to Astron. J.

Chamaraux, P., Balkowski, C. and Fontanelli, P. 1986, Astron. Astrophys. 165, 15

Chamaraux, P., Balkowski, C. and Gérard, E. 1980, Astron. Astrophys. 83, 38

Chincarini, G. and de Souza, R. 1985, Astron. Astrophys. 153, 218

Combes, F. 1992, this volume

Davies, R.D. and Lewis, B.M. 1973, Monthly Notices Roy. Astron. Soc. 165, 231

Distefano, A., Rampazzo, R., Chincarini, G. and de Souza, R. 1990, Astron. Astrophys. Suppl. Ser. 86, 7

Donas, J., Buat, V. Milliard, B., and Laget, B. 1990, Astron. Astrophys. 235, 60

Dressler, A. 1980, Astrophys. J. 236, 351

Evrard, A.E. 1992, this volume

Gavazzi, G. 1991, in Proceeding of the IAU conference 146 on "Dynamics of Galaxies and their Molecular Cloud Distributions", editors F. Combes and F. Casoli, p.23

Gavazzi, G. 1992, this volume

Gavazzi, G., Boselli, A., Scodeggio, M., Kennicutt, R., Carrasco, L., Cruz-Gonzales, I. and Jaffe, W. 1992, this volume

Giovanelli, R. and Haynes, M.P. 1983, Astron. J. 88, 881

Giovanelli, R., and Haynes, M.P. 1985, Astrophys. J. 292, 404

Girardi, M., Biviano, A., Giuricin, G., Mardirossian, F. and Mezetti, M. 1991, Astrophys. J. 366, 393

Guhathakurta, P., van Gorkom, J.H., Kotanyi, C.G. and Balkowski, C. 1988, Astron. J. 96, 851

Gunn, J. and Gott, J. 1972, Astrophys. J. 176, 1

Haynes, M.P. 1990, Clusters of galaxies : STScI Symposium series ≠4, ed. Oegerle, W.R., Fitchett, M.J. and Danly, L., Cambridge University Press

Hoffman, G.L., Helou, G., Salpeter, E.E., Glosson, J. and Sandage, A. 1987, Astrophys. J. Supp. Ser. 63, 247

Hubble, E. and Humason, M. 1931, Astrophys. J. 74, 43

Kenney, J.D. and Young, J.S. 1988, Astrophys. J. Supp. Ser. 66, 261

Kennicutt, R.C. 1983, Astrophys. J. 272, 54

Kennicutt, R.C., Bothum, G.D. and Schommer, R.A. 1984, Astron. J. 89, 1279 (Kluwer, Dordrecht), p 227

Kodaira, K., Watanabe, T., Onaka, T. and Tanaka, W. 1990, Astrophys. J. 363, 422

Mc Mahon, P.M., Richter, O.-G., van Gorkom, G.H. and Fergusson, H.C. 1992, Astron. J. 103, 399

Peterson, B.M., Strom, S.E. and Strom, K.M. 1979, Astron. J. 84, 735

Rubin, V.C. Whitmore, B.C. and Ford, W.K. 1988, Astrophys. J. 333, 522

Salvador-Solé, E. 1992, this volume

Sanromà, M. and Salvador-Solé, E. 1990, Astrophys. J., 360, 13

Sullivan, W.T. III 1989, Proceedings of the World of Galaxies, ed. H.G. Jr. Corwin and L. Bottinelli, (Springer Verlag), p. 404

van Driel, W. and van Woerden, H. 1989, Astron. Astrophys. 225, 317

Vigroux, L., Boulade, O. and Rose, J.A. 1989, Astron. J. 98, 2044

Warmels, R.H. 1986, Thesis University of Groningen

Whitmore, B.C. 1990, Clusters of galaxies : STScI Symposium series ≠4, ed. Oegerle, W.R., Fitchett, M.J. and Danly, L., Cambridge University Press

Whitmore, B.C. and Gilmore, D.M. 1991, Astrophys. J. 367, 64

Whitmore, B.C. Forbes, D.A. and Rubin, V.C. 1988, Astrophys. J. 333, 542

Whitmore, B.C. 1992, this volume

ENHANCED ACTIVITY IN THREE GALAXIES IN THE CLUSTER A1367

G. Gavazzi[1], A. Boselli[1,2], M. Scodeggio[1,3] R. Kennicutt[4], L. Carrasco[5], I. Cruz-Gonzales[5], W. Jaffe[6]

1: Osservatorio di Brera, Milano, Italy
2: Observatoire de Meudon, France
3: Cornell University, Ithaca, NewYork
4: Steward Observatory, Tucson, Arizona
5: Universidad Autonoma de Mexico, Mexico city
6: Sterrewacht, Leiden, Holland

ABSTRACT: radio continuum, 21 cm line and optical observations of three irregular galaxies at the north-west periphery of the cluster A1367 are presented. The asymmetry found in their brightness distributions suggests that they are undergoing ram-pressure sweeping in the dense cluster environment. It is proposed that this mechanism enhances the star formation rate in these galaxies and produces magnetic field amplification.

The origin of the observed morphology segregation in clusters of galaxies is among the most intriguing, yet unsolved questions concerning the origin and the evolution of galaxies. Theories of biased galaxy formation in the CDM cosmological scenario (Davis et al, 1985) give a possible, though not exhaustive explanation of this phenomenon. Other mechanisms, such as merging, tidal disruption or ram-pressure sweeping by strong intergalactic winds provide us with alternative explanations, as this meeting has emphasized (see contributions by Schweizer, Whitmore and Balkowski).

In the present paper we show a case which we consider perhaps the best studied candidate for ram-pressure induced galaxy evolution in a cluster environment. It refers to three galaxies in the N-W periphery of the cluster A1367 (z=0.02) in the Coma Supercluster "wall" which we have reasons to suspect are falling onto the "hostile" cluster environment for the first time.

Since the discovery of unusually bright and extended radio sources associated with three irregular, quite inconspicuous galaxies CGCG 97-073, 97-079 and 97-087 in early Westerbork maps (Gavazzi, 1978), an increasing observational effort was devoted to their study at various wavelengths. The galaxies are faint objects in the visible (m_p=15.6; 15.7; 14.3 mag respectively) but have among the highest radio/optical excess as compared with similar galaxies in the survey presented earlier at this meeting. Their location in the cluster is rather peripheral (about 30 arcmin away from the X-ray cluster centroid), just outside the X- ray emitting region as mapped in the IPC observation of the cluster (Bechtold et al, 1983) (notice however that the apparent absence of X-ray emission in correspondence of 97073 and 79 is an artifact due to the IPC window supporting structure).

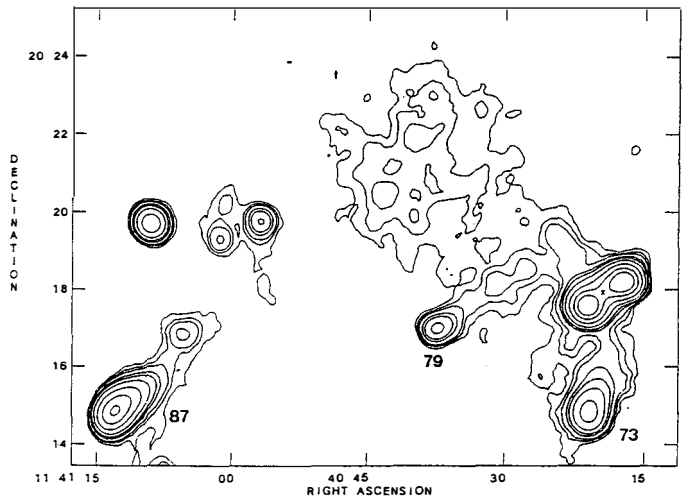

Fig.1: 1.4 Ghz map of the region in A1367 obtained with the VLA in C+D array configuration. The three galaxies under study are labelled 73, 79 and 87. The bright double radio source found at the interception between the tails is associated with a 21 mag quasar at z=1.06. The cluster center is located at S-E of the mapped region.

Repeated observations in the radio continuum (1.4 GHz) with the VLA in C and C+D array configuration (beam FWHM=20" and 40" respectively) (Gavazzi and Jaffe, 1985, 1987) revealed that the three objects show evidences of very asymmetric radio structures with a sharp brightness gradient on the side facing the cluster center and a smooth, low brightness trail on the opposite direction. The total length of the trails is up to 50 kpc (see Fig. 1). This characteristic, often found associated with Elliptical galaxies in clusters (Head-tail radio galaxies) is exceptional in spiral/irregular galaxies, and by itself indicates the presence of an external pressure acting on these galaxies.

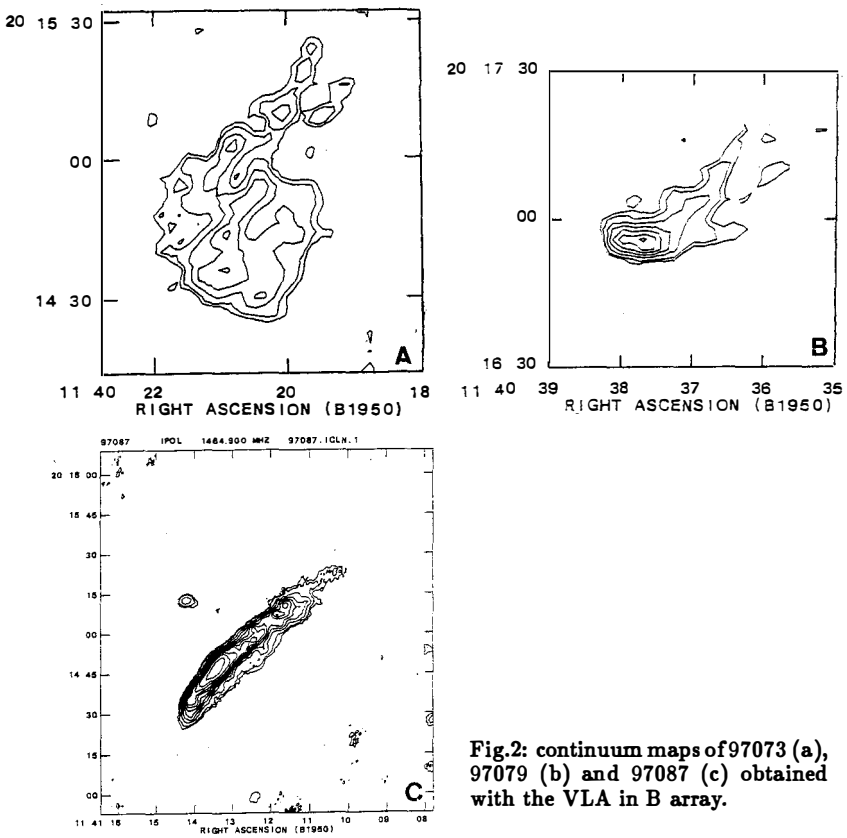

Fig.2: continuum maps of 97073 (a), 97079 (b) and 97087 (c) obtained with the VLA in B array.

Recently the galaxies were observed with the VLA in the B array configuration with a resolution comparable with that of optical observations. Preliminary maps are shown in Fig. 2. Also at this resolution 97073 and 79 show clearly an asymmetric brightness distribution with a low brightness feature trailing in the N-W direction (more about the comparison of these maps with the optical frames below). Follow-up 21 cm line observations done at Arecibo (Gavazzi, 1989) and at the VLA (Dickey and Gavazzi, 1991) revealed that in the three objects the distribution of the neutral gas is also asymmetric, with most of the HI content being found in the galaxy side coincident with the radio trail and with strong HI deficiency on the "head". The transient character of the observed HI asymmetry (which should be smeared out by differential

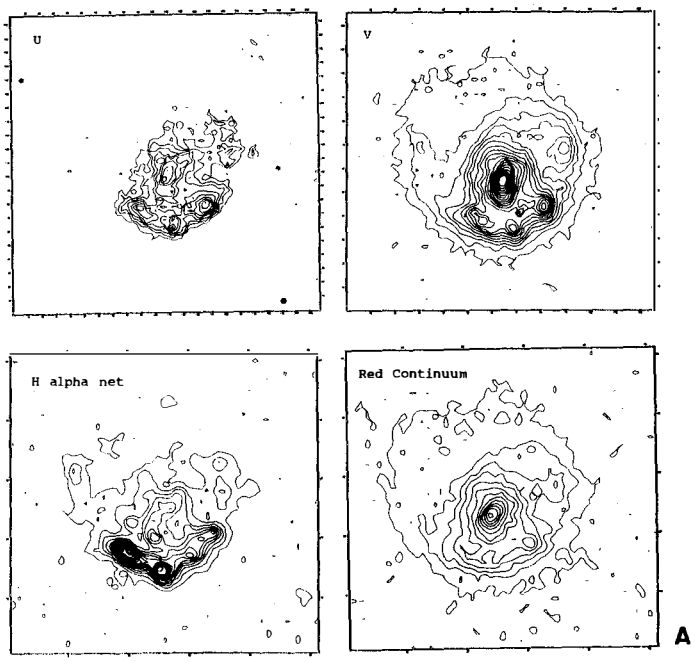
U
V
H alpha net
Red Continuum
A

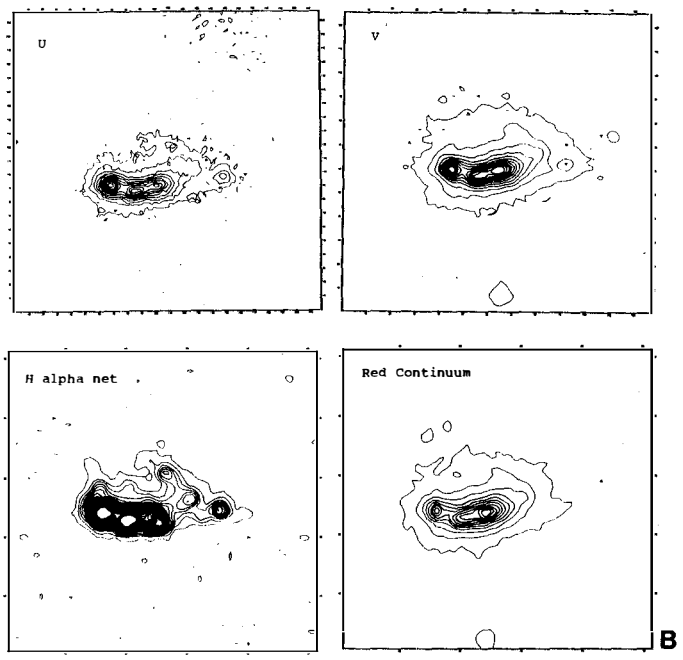
U
V
H alpha net
Red Continuum
B

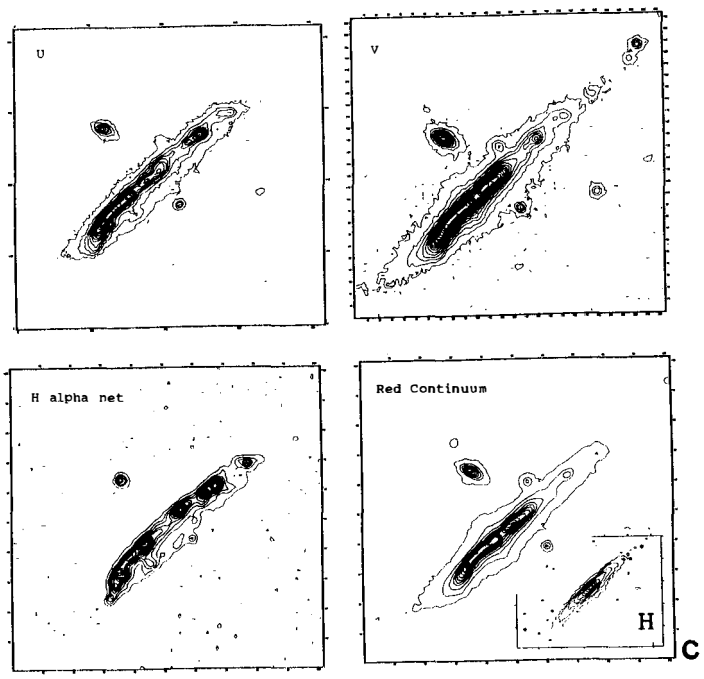

Fig. 3: V, U bands, H_α net and continuum near H_α frames of galaxies 97073 (a); 97079 (b) and 97087 (c). The inset shows an IR H band frame of 97087. The figures are on the same scale as Fig.2. (North is up, East to the left)

rotation in few 10^8 years), led Gavazzi (1989) to argue that gas ablation is actually presently taking place.

Early observations in the visible (broad-band V, B and H_α surface photometry) were obtained at KPNO by Gavazzi et al, 1984. Deeper frames in the V, U bands obtained at the 1.5m Loiano telescope (Italy) and at the 2.1m San Pedro Martir telescope (Mexico) and H_α+[NII] frames obtained with the 2.3m telescope of the Steward Observatory (Arizona) are displayed in Fig. 3. These observations reveal that in the three galaxies a prominent peripheral chain of giant HII regions (L=10^{40-41} erg s^{-1}) is formed at the galaxy side where the steep radio gradient is observed. The red narrow band continuum near H_α is also given in Fig. 3 to indicate that the distribution of the old stellar population is more centrally peaked than that of blue stars and generally tends to anticorrelate with the luminosity of the HII regions. An IR H band frame of the central region of 97087 is also shown to emphasize this last property. This frame was obtained during some test time of a new IR array at the San Pedro Martir Observatory. The frame shows a single peak symmetric feature, which on the basis of the its red excess can be identified with the galaxy nucleus. Notice that no sign of the absorption feature visible near the nucleus at other wavelengths is present in the IR frame.

The spatial coincidence between the regions of intense star formation (Fig. 3) and the peaks of the non-thermal radio emission (Fig. 2) is striking. This coincidence leads to the firm identification of the cosmic ray electron sources with regions of massive star formation (e.g. supernova explosions).

Altogether the multiwavelength material in our hands perhaps gives the best evidence for galaxies presently undergoing ram-pressure in the cluster environment. Not only there is strong evidence that the studied objects moving at high velocity ($V \sim 1000$ Km s^{-1}) in the dense intergalactic medium ($\rho \sim 10^{-3} cm^{-3}$ from X-rays estimates) are suffering from HI depletion, but also that the magnetic field structure is accordingly disturbed, producing enhanced synchrotron emission on the "head" and large scale line stretching on the "tail". Moreover the signature of a shock, possibly formed on the interface between the galaxy and the IGM is revealed by the elongated appearance of the regions of abnormal star formation.

We wish to stress that the evidence we collected seems to indicate that in the early phases of infall of galaxies on clusters the dynamical processes might trigger, instead of inhibiting, processes of violent star formation, contrary to the general wisdom on this subject. The time scale of this phase, however, is short compared with the cluster crossing time due to rapid gas consumption and ablation, and the future fate of these cluster "intruders" is certainly that of a progressive evolution toward more anemic and earlier morphological types.

REFERENCES

Bechtold, J., et al, 1983, Ap.J. 265, 26
Davis, M., Efstathiou, G, Frenk, C., and White, S., 1985, Ap.J., 292, 371
Dickey, J., and Gavazzi, G., 1991, Ap.J., 373, 347
Gavazzi, G., 1978, A.A.,69, 355
Gavazzi, G., 1989, Ap.J., 346, 59
Gavazzi, G., Tarenghi, M., Jaffe, W., Butcher, H., and Boksenberg, A., 1984, A.A., 137, 235
Gavazzi, G., Jaffe, W., 1985, Ap.J., 294, L89
Gavazzi, G., Jaffe, W., 1987, A.A., 186, L1

MORPHOLOGICAL SEGREGATION AMONG DISK-GALAXIES IN CLUSTERS

Eduard Salvador-Solé and José María Solanes
Departament d'Astronomia i Meteorologia, U.B. i
Laboratori d'Astrofísica, Societat Catalana de Física, I.E.C.
Avda. Diagonal 647, E-08028 Barcelona, Spain.

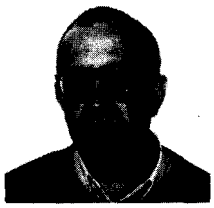

ABSTRACT
We discuss the current status of the nature vs. nurture problem concerning disk-galaxies. Revisiting the main objections against the possible evolutionary origin of an important fraction of S0's from S's in rich galaxy clusters allows us to conclude that this is fully plausible. In particular, we find that ram-pressure stripping (in its simplest momentum-exchange version) is able to produce a morphological segregation among disk-galaxies with the same local and global properties as observed.

1. INTRODUCTION

The well-known morphological segregation of galaxies indicates that morphology is greatly influenced by galactic environment. But when did this happen, at galaxy formation or after it? As far as the environment found by a galaxy during its lifetime is determined, at least statistically, at its formation, this question is somewhat ill-posed. However, the following one can still be addressed: do galaxies *change* their morphological appearance according to their changing environment? Scenarios giving a negative answer can be referred to as "innate", while those which admit that morphology can change as "evolutionary". Of course, the true solution probably depends on particular types and environments. In this contribution we focus on the possible origin of disk-galaxies in rich clusters under the constraints imposed by their observed morphological segregation.

2. NATURE VS NURTURE

Taking into account the basic morphological characteristics of disk-galaxies[1] it has been proposed for a long time that S0's, or a significant fraction of them, can be the result of S's having being depleted of their gas by the action of some external mechanism. Many external mechanisms have been proposed to account for this gas loss: direct collisions between galaxies[2], tidal stripping[3], ram-pressure stripping by the intergalactic medium[3,4], thermal evaporation[5], and bursts of star formation induced

by interactions[6,7]. Among all these mechanisms ram-pressure stripping, in its original simple momentum-exchange form or in any of the most recent accurate versions[9] is likely the most efficient in high density regions such as rich galaxy clusters. This mechanism is believed to be the main responsible for the observed deficiency in HI of disk-galaxies in nearby clusters[10] and possibly also for the existence of anemic spirals[11]. Although it is not yet proved that stripped S's necessarily become S0's, this is plausible. For this reason, this mechanism has also been invoked as the possible cause for the observed correlations between total S fraction in clusters and their X-ray total luminosity[12] and, indirectly, between total S fraction and cluster richness[13,14]. Finally, it could naturally explain the higher fraction of S-like galaxies in high redshift clusters compared with that of nearby ones[15,16].

The evolution from S's into S0's faces, however, important observational problems. First, the above mechanisms cannot explain the rather important fraction of S0's (about 25 %) found in low density regions. Second, none of these mechanisms alter bulges, so they cannot explain the difference between the bulges of S's and S0's (with respect to total luminosity[17,1] or central surface brightness[18,19]). These two objections refer to the overall properties of S's and S0's irrespective of their location. Thus, although some innate differentiation seems mandatory, the possibility remains that a significant fraction of S0's inside rich clusters may arise from S's felt into them. (The lack of *any* known S0's with very small bulge could be due to misclassifications[20] and/or sampling biasses similar to that explained below). Yet, there are two more objections which are specifically against such an evolution inside rich clusters. These concern[16]: i) the

spatial segregation found among disk-galaxies with different bulge luminosity, and ii) the apparent universality of the morphological segregation among bright galaxies. As far as ram-pressure stripping (or any other evolutionary mechanism proposed) does not alter bulges it cannot explain any spatial segregation of bulge luminosities. Conversely, if this is innate there are good reasons to believe that the morphological segregation is too. Besides, the effects of ram-pressure stripping depend on the intracluster medium density. Yet the observed morphological segregation is roughly the same in high concentration (or high X-ray luminosity) clusters as in low concentration ones.

For all these reasons most theoretical efforts have been made for the last decade in trying to explain the origin of S's and S0's in the frame of pure innate scenarios. Following a statistical description[21,22,23] galaxies which have formed from high amplitude peaks in the primordial density fluctuations field (convolved down to galactic scales) must be more clustered (*i.e.*, they must be more frequent in high density regions) than those arising from low amplitude peaks. A number of possible processes have been proposed in order to justify a biassed galaxy formation scenario[24] like this. One interesting possibility is the so-called birth deffect scenario[16] according to which the formation of disks might be aborted by interactions among galaxies emerging from high amplitude peaks, which would lead to a larger fraction of early type galaxies in high density regions, and conversely. Moreover, the biassed galaxy formation scheme can also easily yield a natural correlation between morphology and bulge properties[25].

3. MORPHOLOGICAL SEGREGATION IN CLUSTERS REVISITED

The preceding are but qualitative arguments in favor of a pure innate scenario. Theory is not yet able to make accurate quantitative predictions on the morphological properties of emerging galaxies. However, it begins to be possible to make them on the morphological segregation that results. Recent N-body simulations[26] of the standard biassed galaxy formation scenario in a CDM, $\Omega = 1$, cosmogony have shown that the quantitative trends of the observed morphological segregation among bright galaxies in rich clusters can only be partially recovered. The correct segregation is found between E's and disk-galaxies, but not between S's and S0's, which is found much less marked than observed. (The standard biassed galaxy formation scenario is now called seriously into question by the observed characteristics of the recently detected anisotropy of the CBR.) This suggest that, after all, some evolution from S's into S0's might have taken place in clusters. In fact, revision of the above two main objections against this possibility shows that these are actually not.

First, the repported segregation in bulge luminosity is simply due to an incompleteness bias in the sample of galaxies used to infer it. When the analysis is repeated from the same original sample though limited in bulge magnitude instead of total magnitude, no appreciable segregation is found[27]. Since the general correlation between bulge luminosity and morphological type is a well-established observational fact, and clusters show anyhow a clear morphological segregation, the new result strongly points at the fact that the latter has been (at least partly) reproduced from a largely mixed

population of disk-galaxies. Virialization of clusters can easily yield this important mixture.

Second, the apparent universality of the observed morphological segregation is due to the fact that it refers to 2D instead of 3D. Projection tends to erease any small "deviation"; actually, one can detect slight signs of a dependence of the local type-density relation on cluster richness (correlated with X-ray luminosity)[28]. But even if this effect was not real one should be careful to infer any consequence of the observed relation without previously inverting it. When this is done under the only simple assumption that clusters are, in the average, well-described by means of a universal (except for the normalization factor) radial density profile with an asymptotical power-law behavior it is found that the 3D local type-density relation (which in each given cluster follows a similar trend as in 2D) does depend, indeed, on cluster richness[29]. Of course, such an inversion is correct as far as the observed type-density relation is equivalent to a type-radius relation. If morphological segregation arises, as usually thought, from the local density associated to possible clumps inside clusters rather than from the overall radial density profile, our results would be wrong. Recent accurate analysis by different authors and by means of different techniques[30,31] show, however, that the well-known morphological segregation inside clusters is really equivalent to a type-radius relation. (It is interesting to note that the dependence of the normalization factor of cluster radial density profile on cluster richness yields a 2D type-radius relation which is apparently even more universal than the type-density one[32].)

4. RAM-PRESSURE-INDUCED MORPHOLOGICAL SEGREGATION

These results prove worthwhile trying to derive the type-density relation among disk-galaxies in clusters arising from evolutionary mechanisms such as ram-pressure stripping and compare it with observation. Although the full accurate effects of ram-pressure by ICM are not yet well-known, a first interesting approach consists on modelling the simple original momentum-exchange version[4]. This requires previously modelling galaxy clusters, in particular their potential well, the local (anisotropic) velocity tensor of galaxies, and the ICM density profile. All these properties have been calculated in terms of one unique parameter, the cluster richness, by means of a self-consistent cluster model which takes into account all known properties of nearby clusters[33]. The results are that, except for poor clusters, one is able to recover, for very reasonable values of the only two free parameters of the model, the initial uniform S fraction and the disk-restoring force, the observed local type-density (or type-radius) relation for disk-galaxies as well as its observed dependence on cluster richness. So the conclusion of this simple model is that observation *is not* inconsistent with the idea that a large fraction (of about 50 %) of S0's in rich clusters comes from stripped S's.

REFERENCES

1. Buta, R. 1992, this meeting
2. Spitzer, L., & Baade, W. 1951, ApJ, 113, 413
3. Toomre, A. 1972, ApJ, 178,623

4. Gunn, J.E., & Gott, J.R. 1972, ApJ, 176, 1
5. Nulsen, P.E.J. 1982, MNRAS, 198, 1007
6. Cowie, L.L., & Songaila, A. 1977, Nature, 226, 501
7. Icke, V. 1985, AA, 144, 115
8. Bothun, G.D., & Dressler, A. 1986, ApJ, 301, 57
9. Evrard, A.E. 1992, this meeting
10. Balkouski, C. 1992, this meeting
11. van den Bergh, S. 1976, ApJ, 206, 883
12. Bahcall, N. 1977, ApJ, 218, L93
13. Oemler, A. 1974, ApJ, 194, 1
14. Sarazin, C.L. 1986, Rev. Mod. Phys., 58, 1
15. Butcher, H., & Oemler, A. 1978, ApJ, 219, 18
16. Mellier, Y. et al. 1988, AA, 199, 13
17. Dressler, A. 1980, ApJ, 236, 351
18. Sandage, A. 1983, in Internal Kinematics and Dynamics of Galaxies, ed. E. Athanassoula (Dordrecht: Reidel), 367
19. Kent, S.M. 1985, ApJS, 59, 115
20. Edder, J.A. 1992, this meeting
21. Kaiser, N. 1984, ApJ, 284, L1
22. Politzer, D.H., & Wise, M.B. 1984, ApJ, 285, L1
23. Bardeen, J.M. et al. 1986, ApJ, 304, 15
24. Dekel, A., & Rees, M.J. 1987, Nature, 326, 455
25. Evrard, A.E., Silk, J., & Szalay, A.S. 1990, ApJ, 365, 13
26. Salvador-Solé, E. 1992, in The Distribution of Dark Matter in the Universe, ed. D. Gerbal & G. Mamon (Paris: Ed. Obs. de Paris), in press
27. Salvador-Solé, E., Sanromà, M., & Rdz. Jordana, J.J. 1989, ApJ, 337, 636
28. Giovanelli, R., & Haynes, M.P. 1985, ApJ, 292, 404
29. Sanromà, M., & Salvador-Solé, E. 1990, ApJ, 360, 13
30. Withmore, B.C., & Gilmore, D.M. 1991, ApJ, 367, 64
31. Withmore, B.C. 1992, this meeting
32. Solanes, J.M., & Salvador-Solé, E. 1992, ApJ, to be published in the August 10th issue

WHAT DETERMINES THE MORPHOLOGICAL FRACTIONS IN CLUSTERS OF GALAXIES ?

Bradley C. Whitmore
Space Telescope Science Institute
3700 San Martin Drive
Baltimore, MD 21218

ABSTRACT

A reexamination of Dressler's sample of nearly 6000 galaxies in 55 clusters shows that the morphology-clustercentric distance relation is more fundamental than the morphology-density relation. Only one parameter, R/R_c^{opt} (where R_c^{opt} is a characteristic optical radius of the cluster) is needed to predict the morphological fractions in all types of clusters. The elliptical fraction in the outer regions of clusters is relatively constant at about 15 %. Only within about 0.5 Mpc of the cluster center does the elliptical fraction begin to rise dramatically, reaching values of roughly 70 % near the center. The S0 fraction rises moderately as the center is approached, and then falls sharply within 0.2 Mpc of the cluster center. The spiral fraction is nearly zero near the center. These facts lead us to suggest that the spiral and S0 protogalaxies have been destroyed near the cluster centers, and that the material from the failed galaxies forms the hot intracluster medium.

1. INTRODUCTION

The morphology-density relation discovered by Dressler (1980) should provide a basic clue for understanding the origin of the Hubble sequence. For example, if the fundamental correlation is with the *local* density, this would indicate that interactions with nearby galaxies are primarily responsible for determining the morphological type of a galaxy. If the fundamental correlation is with some *global* property of the cluster (*e.g.*, clustercentric position, velocity dispersion, central concentration), this would indicate that the formation of the cluster plays an important role in determining the morphological fractions.

Melnick and Sargent (1977) demonstrated the existence of morphological gradients as a function of radius from the centers of seven clusters. Dressler (1980) readdressed this question by comparing the relationship between morphology and local projected galaxy density (defined over the area needed to encompass the nearest 10 galaxies) to the relationship between morphology and projected clustercentric radius for six irregular clusters. He concluded that "the gradients are much more striking when the density is employed as the independent parameter, which indicates that the local density enhancements represent real physical associations, and that populations are largely a function of local rather than global conditions". This result has focused much of the recent work on the existence of substructure in clusters, rather than the origin of the Hubble types. While substructure has clearly been found in many clusters (see Fitchett 1988 for a review), it is often quite weak, and it would be surprising (at least to this author) if such small enhancements were responsible for such a dramatic difference in the nature of galaxies.

2. IS THE FUNDAMENTAL RELATION WITH LOCAL DENSITY OR WITH CLUSTERCENTRIC RADIUS ?

Recently, two groups have independently reexamined this question, and have concluded that the morphology-density relation is not the fundamental relation. Sanromà and Salvador-Solé (1990) used Dressler's data on 55 clusters to generate artificial clusters with the same global properties, but with the substructure removed. This was done by randomly scrambling the galaxies in each cluster along annuli at the same distance from the cluster center. Any existing substructure was therefore broken up. The normal morphology-density relation was then constructed from the 55 artificial clusters, and compared with the morphology-density relation for the real clusters. They found that the two relations were essentially identical, indicating that substructure cannot be determining the morphological fractions in clusters.

Whitmore and Gilmore (1991; hereafter WG) repeated Dressler's (1980) comparison of the morphology-density relation and the morphology-radius relation for the same six irregular clusters. Contrary to the earlier result, they found that the morphology-radius relation resulted in correlations that were as good, or slightly better than the morphology-density relation. The analysis in WG differed in two important ways from Dressler. First, the inner bin that extended to 1 Mpc in Dressler (1980; Figure 5) was divided into three bins. Second, the position of the galaxy with the highest value of the local density was used as the cluster center, rather than the cluster centroid. Figure 1 shows the results. WG found that most of the variation in the morphological fractions occurs within 0.5 Mpc of the cluster centers, a result that was diluted by the use of the 1 Mpc binning. Similar results were found when all 55 clusters were used. The elliptical fraction was nearly constant at about 15 % in the outer regions of clusters. Only within the inner 0.5 Mpc did the elliptical fraction rise dramatically, with a peak value of about 60 % at the centers of clusters which have D galaxies. WG also found tentative evidence that the fraction of S0 galaxies falls sharply within 0.2 Mpc of the cluster centers.

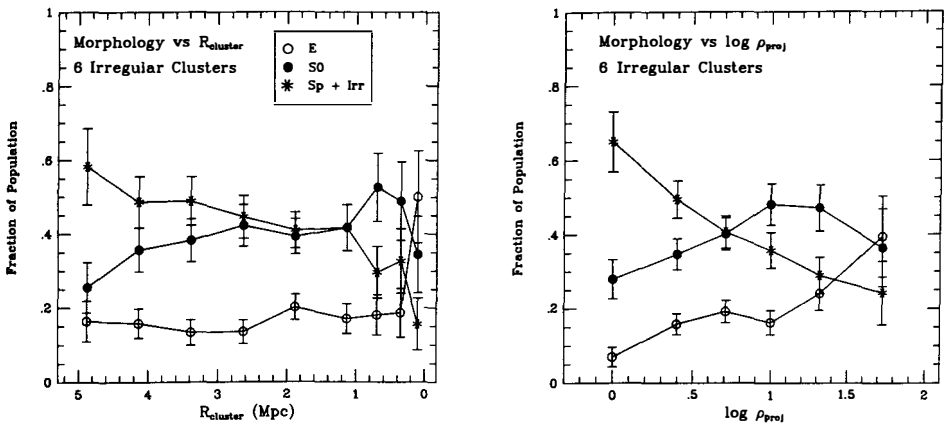

Figure 1: A comparison of the morphology-clustercentric radius relation with the morphology-local density relation for the six irregular clusters used by Dressler (1980; Fig. 5). The morphology-radius relation shows that most of this variation occurs very near the cluster center. (from WG)

Determining which is the more fundamental correlation is complicated by the fact that the local density correlates relatively well with clustercentric radius. However, two tests have been made which allow us to decouple the dependencies. In the first test (see Whitmore 1991 and Whitmore, Gilmore, and Jones; hereafter WGJ), regions with the same local density but different clustercentric radii are compared. If local density

is the fundamental parameter these regions should all have the same elliptical fractions. However, the fraction of elliptical galaxies near the cluster centers is about 15 % higher than the fraction for the outer regions, as predicted by the morphology-radius relation.

For the second test, galaxies at the same clustercentric position but different local density are compared. Figure 2 shows the morphology-density relation for galaxies within 0.25 R/R_c^{opt} of the cluster centers, where R_c^{opt} is a characteristic cluster radius defined as the radius at which the cumulative number density falls below 20 galaxies Mpc^{-2}. This plot provides striking evidence that the morphology-radius relation is the more fundamental correlation, since the morphological fractions are nearly constant even though the local density is changing by more than an order of magnitude. The success of the morphology-density relation is primarily due to the fact that local density is roughly correlated with clustercentric position.

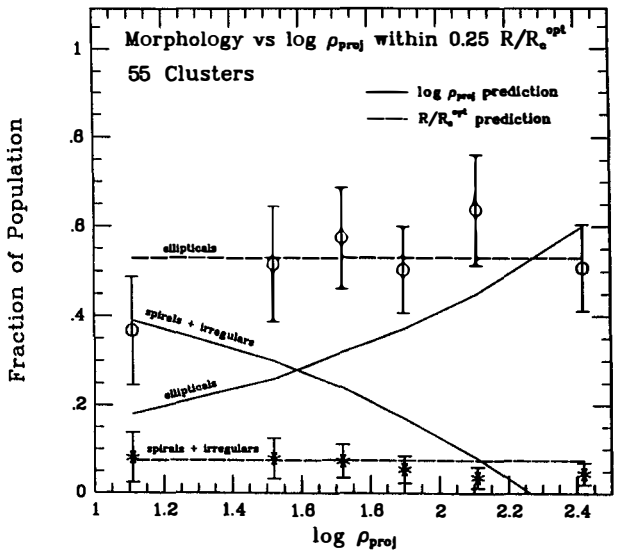

Figure 2: The morphology-density relation for the galaxies within 0.25 R/R_c^{opt} of the cluster centers. The solid lines are the predictions for the morphology-density relation; the dashed lines are the predictions for the morphology-radius relation. The data clearly favor the morphology-radius relation.

WGJ make several corrections designed to "tune up" the morphology-radius relation. These include corrections for foreground/background galaxies, normalization to a constant magnitude cutoff, use of x-ray positions for the cluster centers, removal of double clusters, and normalization of the cluster radius using R_c^{opt}.

Figure 3 shows the resulting morphology-radius relation when all the corrections are made except the normalization by R_c^{opt}. The elliptical fraction has risen from 44 % (Figure 2 of WG) to 59 % for galaxies within 0.12 Mpc of the cluster center. The drop in the S0 fraction near the center is also more convincing than in WG. The percentage

of spirals in the inner bin is now only 6 %. These results strengthen our conclusion that the morphology-radius relation is the more fundamental correlation.

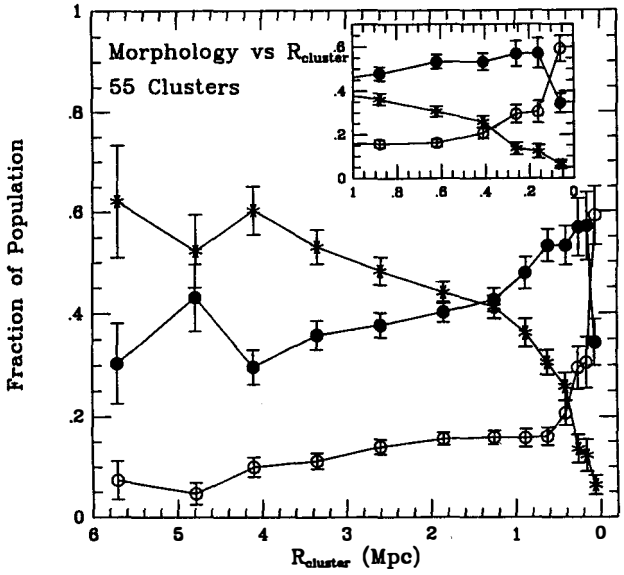

Figure 3: The morphology-clustercentric radius relation for all 55 clusters. (from WGJ)

Figure 4 shows the morphology-radius relation normalized by R_c^{opt}. The sample of 55 clusters has been divided into four subsamples according to the number of galaxies within 0.5 Mpc of the center, $N_{0.5}$. We find that within the statistical scatter, the same normalized morphology-radius relation fits the data for all four subsamples. The elliptical fraction is very high in the centers of all clusters, even very poor clusters. However, it should be kept in mind that the *number* of ellipticals involved is much smaller for the low $N_{0.5}$ clusters, since R_c^{opt} is smaller in these clusters. *It appears that only one parameter is necessary to determine the morphological fractions in clusters, the value of* R/R_c^{opt}. The same results are found if the sample is broken into different subsamples according to cluster velocity dispersion, x-ray luminosity, or cluster concentration.

3. A SIMPLE MODEL FOR THE ORIGIN OF MORPHOLOGICAL FRACTIONS

Several results discussed in this paper point an accusatory finger toward the cluster center as the primary cause of morphological segregation in clusters, and suggest that some mechanism which is unique to the center of the cluster favors the existence of ellipticals rather than disk galaxies. This argues for a hybrid model, where initial conditions are responsible for the morphological mix in the outer regions of the cluster, and in the field, but some evolutionary effect modifies these fractions near the centers of clusters.

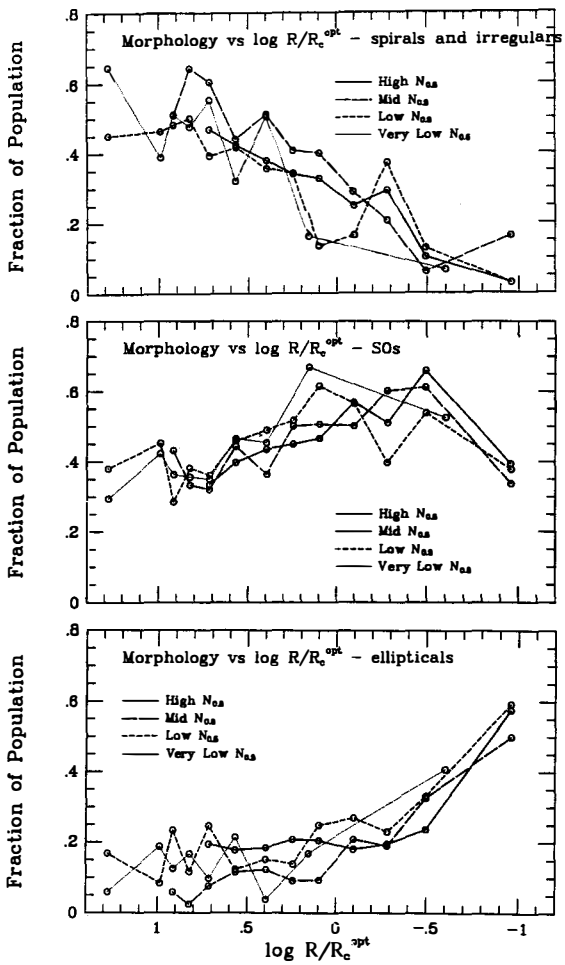

Figure 4:
The normalized morphology-clustercentric radius relation for subsamples with different values of the central number density, $N_{0.5}$. We find the same relation for all clusters.

There are two ways to increase the fraction of elliptical galaxies in the centers of clusters. We can either make more elliptical galaxies or we can make fewer spiral and S0 galaxies. The fact that spiral galaxies predominate in most regions of the universe, but are essentially absent at the very centers of rich clusters, suggests the latter possibility is the correct choice. The centers of clusters represent a very hostile environment for the slow formation of a disk (*i.e.*, strong tidal shear from the mean field of the cluster, high density of rapidly moving galaxies, presence of X-ray gas, cannibalism by the D galaxy). *This leads us to conclude that destructive processes are responsible for controlling the morphological fractions in cluster centers rather than formation processes.*

If the destruction of spiral and S0 galaxies is required to increase the elliptical

fraction near the center, the obvious question is where does the material from the failed galaxies end up. The lack of a bright intracluster medium in visible light requires most of the material to still be in a gaseous state when the galaxies were destroyed (*i.e.*, most galaxies were still protogalactic gas clouds). A reasonable assumption would therefore be that the material ends up forming the hot intracluster medium.

The model is based on three assumptions: 1) The intrinsic fraction of elliptical galaxies is 10 % (*i.e.*, the value in the outer regions of clusters, in loose groups, and in the field). 2) The order of formation is ellipticals, followed by the cluster collapse, the formation of S0s, and finally, the formation of spiral and irregular galaxies. 3) Any galaxy near the cluster center which is still in the form of a protogalactic gas cloud when the cluster collapses is destroyed, and the material is added to the intracluster medium. This simple model is able to provide a qualitative explanation for a wide range of the observations, a few of which are listed below (see WGJ for more details).

1. The morphological gradients in Figure 3 (*i.e.*, high elliptical fractions and low spiral fractions near the cluster centers).

2. The gas-to-stars ratio is larger in rich clusters than in poor clusters (Arnaud, *et al.* 1992; *i.e.*, a higher percentage of protogalactic gas clouds are destroyed in richer clusters).

3. The morphological gradient for Sa galaxies is nearly flat, with a dip within 0.3 Mpc of the center, while the gradient for Sc galaxies is falling, with a dip within 0.5 Mpc of the center (WGJ; *i.e.*, more proto-Sc galaxies were destroyed since they form more slowly).

4. The elliptical fraction in compact groups is only slightly higher than in the neighborhoods around the groups (Rood and Williams 1989; *i.e.*, compact groups do not have the large gravitational potentials of clusters, and probably formed later than clusters, hence their protogalaxies were able to form galaxies).

4. A QUANTITATIVE CHECK ON THE MODEL: THE MASS OF THE X-RAY GAS

Perhaps the most basic prediction from the model is that the mass of the x-ray gas should be equal to the amount of gas from the failed spiral and S0 protogalaxies. Figure 5 shows the result of such a calculation (see WGJ for details). We find that the predicted gas mass is only about 40 % less than the observed x-ray gas mass. Even the slope of the relation is roughly correct. The dotted line shows the prediction if an intrinsic value of 5 % is used for the elliptical fraction.

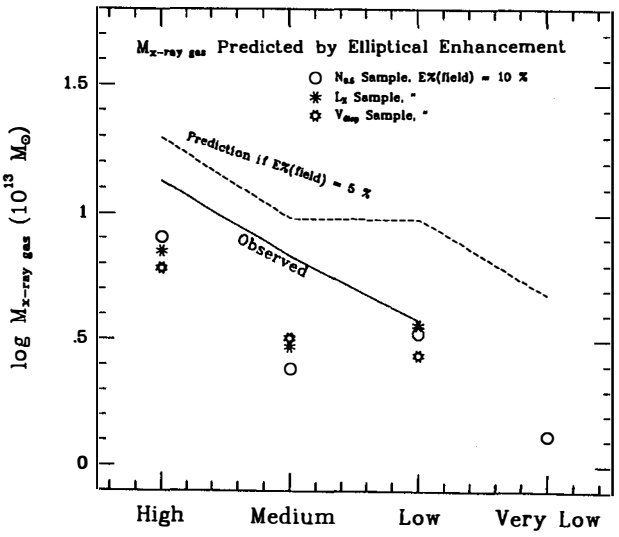

Figure 5: The mass of the x-ray gas as predicted by the enhancement of the elliptical fraction. The data points show the values for the various subsamples of $N_{0.5}$, V_{disp}, and L_X. The solid line shows the observed values of $M_{x-ray\ gas}$. The dashed line shows the average of the predicted values from the elliptical enhancment if a value of 5 % is used for the intrinsic elliptical percentage. (from WGJ)

Taken at face value, the fact that the predicted values are slightly lower than the observed values of $M_{X-ray\ gas}$ might lead us to conclude that the intrinsic elliptical fraction was about 7.5 %. However, it is just as likely that the simplistic nature of the model is responsible for the gap. For example, we have assumed that all the material in the intracluster medium is produced by failed spiral and S0 galaxies. It is quite likely that some of the gas was primordial, and was never associated with a protogalaxy.

The exact physical mechanism responsible for the destruction of protogalaxies need not be specified for the model. However, tidal disruption by the mean field of the cluster is an attractive option since tidal forces vary as R^{-3}. Since the mass of the cluster increases roughly as R, the tidal shear would decreases as R^{-2}, possibly explaining the sharpness of the rise in the elliptical fraction. WGJ explore this possibility in more detail. Several other authors have suggested similar scenarios (Larson, Tinsley, and Caldwell 1980, Binney 1980, Gunn 1982, Postman and Geller 1984, Merritt 1984).

5. DISCUSSION

The issue of which is more fundamental, the morphology-density relation or the morphology-radius relation, is not just a semantic question. The goal is to identify the relevant physical mechanisms responsible for determining the morphological fractions in clusters. The fact that the morphology-radius relation appears to be the more fundamental correlation suggests that global mechanisms, rather than local mechanisms, are responsible for controlling the morphological fractions in clusters.

One of the surprising results of this study was finding that the morphological fractions only depend on one parameter, the normalized radius, R/R_c^{opt}. A high percentage of ellipticals is found in the very center of nearly all clusters, even if they are very diffuse, have low velocity dispersions, or low x-ray luminosities. Spirals are almost completely absent in the centers of all clusters. These results would seem to indicate that clusters are quite similar, at least the central regions of clusters. Perhaps it indicates that the cores of nearly all clusters have gone through a collapse phase.

Our original hope in this project was to learn something about how galaxies form. As it turns out, we have probably learned more about how protogalaxies are destroyed.

I would like to thank Alan Dressler for providing his computer files for the 55 clusters he studied; Diane Gilmore and Christine Jones who collaborated on various aspects of this project; and James Binney, and Craig Sarazin for useful discussions.

REFERENCES

Arnaud, M., Rothenflug, R., Boulade, O., Vigroux, L., and Vangioni-Flam, E. 1992, *Astron. Ap.*, **254**, 49.

Binney, J. 1980, *X-Ray Astronomy*, ed. R. Giacconi and G. Setti, (Boston: Reidel).

Dressler, A. 1980, *Ap. J.*, **236**, 351.

Fitchett, M. 1988, *The Minnesota Lectures on Clusters of Galaxies and Large-Scale Structure*, ed. J. M. Dickey, (San Francisco: Astron. Soc. Pac.).

Gunn, J. E. 1982 *Astrophysical Cosmology*, ed. H. A. Bruck, G. V. Coyne, and M. S. Longair (Rome: Pontifica Academica Scientifica Scripta Varia), 233.

Larson, R. B., Tinsley, B. M., and Caldwell, C. N. 1980, *Ap. J.*, **237**, 692.

Melnick, J., and Sargent, W. L. W. 1977, *Ap. J.*, **215**, 401.

Merritt, D. 1984, *Ap. J.*, **276**, 26.

Postman, M., and Geller, M. J. 1984, *Ap. J.*, **281**, 95.

Rood, H. J., and Williams, B. A. 1989, *Ap. J.*, **339**, 772.

Sanromà M., and Salvador-Solé E. 1990, *Ap. J.*, **360**, 16.

Whitmore, B. C. 1991, *Galaxy Environments and the Large Scale Structure of the Universe*, ed. G. Giuricin, F. Mardirossian, and M. Mezzetti, (Trieste: SISA).

Whitmore, B. C., and Gilmore, D. 1991, *Ap. J.*, **367**, 64. (WG)

Whitmore, B. C., Gilmore, D., and Jones, C. 1992, in preparation. (WGJ)

THE ORIENTATION OF GALAXIES IN CLUSTERS

Włodzimierz Godłowski

Jagiellonian University Observatory

ul.Orla 171 30-244 Kraków

Poland

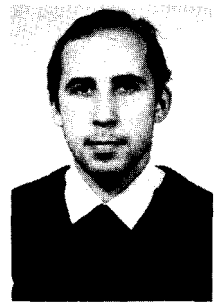

Summary:

The method of investigating the orientation of galaxy rotation axes in the Local Supercluster originally introduced by Jaaniste and Saar (1977), which takes into account both galaxy position angle and inclination, has been applied to a sample of 2227 galaxies based on UGC and ESO catalogues. We complete also the second independent sample of galaxies taken from Tully Nearby Galaxy Catalog. These sample reach 2367 galaxies. We used new advanced statistical method. We analyze the orientation of galaxies in the whole Local Supercluster and in the reach groups of galaxies taking from NGC catalogue. We found that the distribution of galaxy planes in the whole LSC is anisotropic. Galaxy planes rather tend to be perpendicular to the LSC plane. The projection of galaxy rotation axes on the LSC plane rather tend to point toward the Virgo Cluster center. The distributions the spirals galaxies are different then non-spirals. In the most reach group we observed anisotropy too but the direction deviation from isotropy is rather in the various groups. For the Virgo cluster itself the result is the same as for the whole LSC. Our result support pancake scenario but "hedgehog model" is possible too.

1. Introduction

The investigation of the distribution of galaxy orientation in the Local Supercluster has a long history. Most previous papers showed that distribution is not uniform. These papers mostly based on the analysis of galaxy position angle ρ. Nearly all from this results could be interpreted as parallelism of galaxy planes to the supergalactic plane. When we analyzed distribution of galaxy position angels ρ we my take into account only "edge-on" galaxies, for which this parameter may be determined. Jaaniste and Saar (1977;JS) found that galaxy rotation axes tend to be distributed parallel to the LSC plane. They analyzed not only the distribution of galaxy position angles ρ, but also took into account their inclination i to the observer's line-of sight, so they my included to our analysis galaxies seen "face-on" or nearly "face-on".

The JS is full of inconsistencies as was showed by the preliminary analysis of it. Some of them have already been mentioned in our previous work. Moreover, JS used only angle δ_D, giving the orientation of galaxy planes with respect to the LSC plane. We used also the second important parameter, angle η, which is the angle between the projection of rotation axis on the supergalactic plane and the direction toward Virgo Cluster center. Of course we should remember that for particular galaxies we have 4 solution given angular momentum of galaxies. Consideration of orientation axes only, we may decreases this to the two solutions.

2. Observational data.

We used two independent sample of galaxies. First sample based on UGC and ESO catalogues of galaxies and second taken from Tully "Nearby Galaxy Catalogue" (1988).

In the first sample we take from catalogues "Upsala General Catalogue of Galaxies" (Nilson 1973) and "Upsala Survey of ESO" (Lauberts 1982) all galaxies with know from literature radial velocities (correct for solar motion) below 2600 km/s. For that galaxies we take from these catalogues position on the celestial sphere in equatorial coordinates: α and δ, its magnitude, the diameters a and b of the major and minor axes and the position angle ρ_*. The inclination angle, i.e. the angle between the normal to the galaxy plane and the observer's line-of-sight was computed from the formula: $\cos^2 i=(q^2-q_0^2)/(1-q_0^2)$, which is valid for oblate spheroids (Holmberg 1946). The true axial ratios q_0 are taken from H^2V (Heidman et al. 1971). For peculiar galaxies it was assumed that $q_0=0.2$. Value q is converted to standard, photometric axial ratios which removes the Holmberg

effect.

In the second sample we take into account galaxies from Tully NGC catalogue. This catalogue given all necessary data only with exception of position angle. So we was forced take position angles ρ of galaxies from other sources. Data from this catalogue is very well because according Tully they are free of Holmberg effect. Moreover author given the most probably distance of galaxy from us ant what is very important group affiliation. So we may tested orientation of galaxies not only in the whole Supercluster but also in the particulars clusters.

The sample was divided into three groups according to morphological type; groups containing spirals and lenticular galaxies are denoted as "spirals", the remaining ones are denoted as "non-spirals". Both groups together are denoted as "all". Investigating the distribution of galaxy in the LSC it is convenient to express the galaxy position and theirs position angle in the supergalactic coordinate system, instead of the equatorial system. The supergalactic coordinate system is defined (Flin, Godłowski 1986):

a:the coordinates of the supergalactic pole in the equatorial system are: $\alpha=285^{0}.5$, $\delta=+16^{0}$

b:the basic great circle "meridian" of the supergalactic system passes through the Virgo Cluster center with coordinates (Sandage and Tammann 1976): $\alpha=186^{0}.25$, $\delta=+13.1$. In this system we obtain /where $p=\rho-\pi/2$/ :

$\sin\delta_D=-\cos i*\sin B\overset{+}{-}\sin i*\cos p*\cos B$

$\sin\eta=(\cos\delta_D)^{-1}*(-\cos i*\cos B*\sin L+\sin i*(\overset{-}{+}\cos p*\sin B*\sin L\overset{+}{-}\sin p*\cos L)$

3.Angular distribution isotropy tests.

We should check if the distributions of the angles δ_D and η are isotropic. I applied three different statistical tests, following Hawley and Pebbles (1975) and Kindl (1986) but more advanced then in original papers. These are: χ^2 test, the Fourier test and the auto correlation test. In all tests the range of the angle θ (where $\theta=\delta_D+\Pi/2$ or η) was divided into n bins (n=36 - it mean 35 degree of freedom in the χ^2 test).

Let N denotes the total number galaxies (solution) in the sample, N_K the number of galaxies in k-th bin N_0 the mean number of galaxies per bin and N_{0K} expected number of galaxies in k-oh bin. In the χ^2-test the measure of deviation of the observed distribution from the theoretical, isotropic distribution is given by the statistics: $\chi^2=\sum_1^n(N_K-N*p_K)^2/N*p_K$ where p_K is the probability that a chosen galaxy falls into k-th bin.

The Fourier test checks how the departure from isotropy slowly varies

with the angle θ. The model is:

$N(\theta_K)=N_0*(1+\Delta_{11}*\cos2\theta_K+\Delta_{21}*\sin2\theta_K+\Delta_{12}*\cos4\theta_K+\Delta_{22}*\sin4\theta_K)$

In original H-P papers the authors check distribution of the position angles. On that situation all probability p_K are equal. When we analyzed distribution δ_D angle probability p_K are not equal. Moreover H-P take into account only first Fourier mode. So our formulas are much more complicate then in H-P papers. If we take into account only first fourier mode then obtain formulas:

$\Delta_{1J}=\sum_1^n(N_K-N_{0K})*\cos2J\theta_K/\sum_1^n N_{10K}*\cos^2 2J\theta_K$ where $\sum_1^n N_{10K}*\cos^2 2J\theta_K\approx\frac{n}{2}*N_0$ and

$\Delta_{2J}=\sum_1^n(N_K-N_{0K})*\sin2J\theta_K/\sum_1^n N_{10K}*\sin^2 2J\theta_K$ where $\sum_1^n N_{10K}*\sin^2 2J\theta_K\approx\frac{n}{2}*N_0$.

The probability that the amplitude $\Delta_J=(\Delta_{1J}^2+\Delta_{2J}^2)^{1/2}$ is greater than a certain chosen values given by formula $P(>\Delta_J)=\exp(-\frac{n}{4}*N_0\Delta_J^2)$. The standard deviation of the amplitude is $\sigma(\Delta)=(2/n*N_0)^{1/2}$. We may found the direction of departure from isotropy or from Δ_{11} or from coefficient F considering the model $N(\theta_K)=N_0(1+F*\cos2\theta_K)$, (where the F-coefficient is obtained from the fit). If $F<0$, $\Delta_{11}<0$ then an excess of galaxies with rotation axes parallel to the supergalactic plane is observed, whereas for $F>0$, $\Delta_{11}>0$ the rotation axes tend to be perpendicular to the plane. The standard deviation of the F-coefficient is: $\sigma_F=(\sum_1^n(F_K-F)^2/n(n-1))^{1/2}$

Tab.I Orientation of Galaxies in the LSC (UGC ESO catalogue)

		N	χ^2	C	$P(\Delta_1)$	$P(\Delta)$	Δ_{11}	$\sigma(\Delta_{11})$	W_A	$\sigma(W_A)$
δ_D	ALL	4454	48.2	8.70	.030	.048	-.053	.022	0.063	.022
	S	3130	29.6	-0.27	.828	.608	-.006	.026	0.017	.026
	N-S	1324	54.7	22.11	.000	.001	-.164	.040	0.170	.040
η	ALL	4454	51.5	15.60	.001	.003	0.078	.021	-.038	.015
	S	3130	33.5	7.42	.290	.339	0.039	.025	-.010	.018
	N-S	1324	51.8	8.73	.000	.000	0.172	.039	-.104	.027

Tab.II Orientation of galaxies in the LSC (NGC Tully catalogue)

		N	χ^2	C	$P(\Delta_1)$	$P(\Delta)$	Δ_{11}	$\sigma(\Delta_{11})$	W_A	$\sigma(W_A)$
δ_D	ALL	4734	60.3	7.30	.080	.159	-.045	.021	0.039	.021
	S	3270	40.3	-5.98	.973	.852	0.005	.026	-.010	.025
	N-S	1464	71.5	22.60	.000	.001	-.156	.038	0.147	.038
η	ALL	4734	59.7	6.94	.000	.000	0.095	.021	-.059	.015
	S	3270	42.7	-9.49	.032	.107	0.029	.025	-.010	.017
	N-S	1464	87.3	50.85	.000	.000	0.241	.037	-.168	.026

If we take into account next Fourier mode the formulas are:

$\Delta_{11}=(C*K-U*L)/(A*C-U^2)$, $\Delta_{21}=(D*L-W*M)/(B*D-W^2)$,

$\Delta_{12}=(-U*K+A*L)/(A*C-U^2)$, $\Delta_{22}=(-W*L+B*M)/(B*D-W^2)$

where

$$A=\sum_1^n N_{0k}*\cos^2 2\theta_k,\quad B=\sum_1^n N_{0k}*\sin^2 2\theta_k,\quad C=\sum_1^n N_{0k}*\cos^2 4\theta_k,\quad D=\sum_1^n N_{0k}*\sin^2 4\theta_k,$$

$$U=\sum_1^n N_{0k}*\cos 2\theta*\cos 4\theta_k,\quad W=\sum_1^n N_{0k}*\sin 2\theta*\sin 4\theta_k,\quad K=\sum_1^n (N_k-N_{0k})*\cos 2\theta_k,$$

$$L=\sum_1^n (N_k-N_{0k})*\sin 2\theta_k,\quad \L=\sum_1^n (N_k-N_{0k})*\cos 4\theta_k,\quad \text{and}\quad M=\sum_1^n (N_k-N_{0k})*\sin 4\theta_k$$

Covariance matrix $C=G^{-1}$ is:

$$C=G^{-1}=\begin{pmatrix} C/(A*C-U^2) & 0 & -U/(A*C-U^2) & 0 \\ 0 & D/(B*D-W^2) & 0 & -W/(B*D-W^2) \\ -U/(A*C-U^2) & 0 & A/(A*C-U^2) & 0 \\ 0 & -W/(B*D-W^2) & 0 & B/(B*D-W^2) \end{pmatrix}$$

It mean for example that:

$$\Delta_{11}=\frac{((\sum_1^n N_k-N_{0k})*\cos 2\theta_k)*(\sum_1^n N_{0k}*\cos^2 4\theta_k)}{(\sum_1^n N_{0k}*\cos^2 2\theta_k)*(\sum_1^n N_{0k}*\cos^2 4\theta_k)-(\sum_1^n N_{0k}*\cos 2\theta*\cos 4\theta_k)^2}-$$

$$-\frac{((\sum_1^n N_k-N_{0k})*\cos 4\theta_k)*(\sum_1^n N_{0k}*\cos 2\theta_k*\cos 4\theta_k)}{(\sum_1^n N_{0k}*\cos^2 2\theta_k)*(\sum_1^n N_{0k}*\cos^2 4\theta_k)-(\sum_1^n N_{0k}*\cos 2\theta*\cos 4\theta_k)^2}$$

$$\sigma^2(\Delta_{11})=((\sum_1^n N_{0k}*\cos^2 2\theta_k)*(\sum_1^n N_{0k}*\cos^2 4\theta_k)-(\sum_1^n N_{0k}*\cos 2\theta*\cos 4\theta_k)^2)^{-1}*\sum_1^n N_{0k}*\cos^2 4\theta_k$$

Moreover we need formulas for probability that analyzed distribution are the same than theoretical one. Let I denote:

$$I=\begin{pmatrix}\Delta_{11}\\ \Delta_{21}\\ \Delta_{12}\\ \Delta_{22}\end{pmatrix}$$

then formulas for probability is:

$$P(\Delta)=(1+J/2)^2*\exp(-J/2)\qquad \text{where } J=\sum_1^4\sum_1^4 G_{ij}*I_i*I_j$$

The auto correlation test measures the correlations between the number of galaxies in adjoining angle bins. The correlation function is:

$$C=\sum_1^n (N_K-N_{0K})*(N_{K+1}-N_{0K+1})/(N_{0K}*N_{0K+1})^{1/2}$$

In cease isotropic distribution we expect C=0. The standard deviation is: $\sigma(C)=n^{1/2}$. The W-coefficient is: $W_B^*=(N_{\|}-N_{\perp})/N$ where $N_{\|}$ and $N_{\perp}$ denote the number of galaxies with rotation axes parallel and perpendicular to the supergalactic plane. $W_B=W_B^*-\bar{W}_B$ where $\bar{W}_B=2p_{\|}-1$. The coefficient W_A is: $W_A=(\Sigma_{\|}N_i/p_i n-\Sigma_{\perp}N_i/p_i n)/N$, while variance are: $\sigma^2(W_B)=(4p_{\|}(1-p_{\|}))/N)$ and $\sigma^2(W_A)=\sum_1^n((1-p_k)/p_k+1)/(n^2*N)$.

4. The orientation of rotation axis of galaxies in the LSC

Results for the whole Supercluster are presented in the Table I and II. The anisotropy is observed for all and non-spirals galaxies. For "spirals" galaxies situation is not so clear. The shapes of all distributions are of

Tab. III Orientation of galaxies in the clusters δ_D (NGC)

		N	χ^2	C	$P(\Delta_1)$	$P(\Delta)$	Δ_{11}	$\sigma(\Delta_{11})$	W_A	$\sigma(W_A)$
δ_D	11	626	68.8	8.46	.037	.031	-.150	.058	0.091	.057
		454	32.2	2.37	.581	.516	0.033	.069	-.061	.067
		172	125.0	38.54	.000	.000	-.634	.112	0.493	.110
	12	332	42.8	1.58	.593	.642	-.082	.080	0.122	.079
		246	35.6	-1.49	.899	.510	-.036	.093	0.102	.092
		86	54.2	-11.72	.357	.638	-.213	.158	0.178	.155
	13	128	59.0	7.11	.705	.930	-.074	.129	0.094	.127
		76	64.5	4.90	.978	.766	-.009	.168	-.114	.165
		52	42.2	11.07	.548	.327	-.170	.203	0.400	.199
	14	426	40.5	7.32	.126	.359	-.106	.071	0.085	.070
		202	33.4	-0.32	.799	.496	-.020	.103	-.046	.101
		224	37.9	2.12	.074	.179	-.184	.098	0.204	.096
	15	130	40.9	4.30	.870	.844	0.067	.128	-.055	.126
		94	34.2	4.12	.120	.343	0.192	.151	-.151	.148
		36	47.3	12.34	.011	.103	-.261	.244	0.196	.240
	21	248	49.0	12.60	.000	.003	-.171	.093	0.157	.091
		180	45.4	11.74	.001	.003	-.217	.109	0.178	.107
		68	33.3	-3.88	.142	.490	-.047	.177	0.102	.174
	22	126	29.2	-5.76	.748	.652	-.063	.130	0.061	.128
		80	43.9	-11.94	.338	.497	0.043	.164	-.066	.161
		46	25.1	-7.79	.338	.470	-.247	.216	0.282	.212
	23	100	44.1	-14.33	.340	.675	0.215	.146	-.229	.144
		74	59.1	-11.78	.074	.198	0.367	.170	-.408	.167
		26	28.4	1.91	.350	.651	-.219	.287	0.279	.282
	31	210	59.3	1.66	.004	.021	0.239	.101	-.255	.099
		158	52.4	-0.63	.070	.199	0.232	.116	-.230	.114
		52	38.8	6.95	.012	.035	0.262	.203	-.329	.199
	41	192	31.7	5.70	.405	.186	0.072	.106	0.037	.104
		126	25.8	-1.80	.612	.365	0.094	.130	0.046	.128
		66	50.5	-2.88	.014	.090	0.029	.180	0.022	.177
	42	230	47.8	-1.31	.113	.137	-.067	.097	0.074	.095
		164	56.3	-7.22	.538	.120	-.071	.114	0.099	.112
		66	43.8	13.93	.081	.016	-.057	.180	0.013	.177
	51	228	48.5	5.18	.001	.010	0.011	.097	0.121	.095
		160	36.6	-4.14	.362	.251	-.032	.116	0.115	.114
		68	61.1	6.93	.000	.001	0.111	.177	0.135	.174
	52	172	37.4	2.81	.077	.155	-.083	.112	0.089	.110
		128	26.5	-3.07	.305	.512	-.035	.129	0.110	.127
		44	44.8	3.62	.157	.335	-.222	.221	0.031	.217
	53	260	49.2	-3.49	.597	.037	0.058	.091	-.030	.089
		182	45.6	-7.89	.327	.131	-.043	.108	0.087	.107
		78	67.2	8.69	.000	.001	0.295	.166	-.302	.163
	61	258	40.4	5.82	.002	.020	-.261	.091	0.242	.089
		198	38.2	-2.42	.259	.464	-.152	.104	0.194	.102
		60	37.6	17.93	.000	.000	-.620	.189	0.403	.186
	64	102	34.2	1.36	.084	.428	-.050	.145	0.088	.142
		66	33.7	2.35	.533	.637	-.133	.180	0.169	.177
		36	40.8	-2.59	.035	.075	0.101	.244	-.060	.240

the same character. In the case of δ_D the signs of the F-coefficient and Δ_{11} are negative (W are positive). It mean that galaxy rotation axes are parallel to the supergalactic plane. In the case of η the sign of F and Δ_{11}

are positive it mean that projection of rotation axes on the supergalactic plane tend to point toward center of the Virgo Cluster.

In the tab.III and IV we have result for various groups going from NGC

Tab.IV Orientation of galaxies in the clusters η (NGC)

		N	χ^2	C	$P(\Delta_1)$	$P(\Delta)$	Δ_{11}	$\sigma(\Delta_{11})$	W_A	$\sigma(W_A)$
η	11	626	74.8	27.92	.000	.000	0.327	.057	-.192	.040
		454	55.6	16.22	.002	.008	0.218	.066	-.101	.047
		172	77.9	30.19	.000	.000	0.616	.108	-.430	.076
	12	332	33.9	8.37	.011	.021	-.076	.078	0.054	.055
		246	28.5	4.54	.278	.132	-.032	.090	0.041	.064
		86	44.6	11.53	.006	.025	-.202	.152	0.093	.108
	13	128	41.3	0.81	.124	.175	0.247	.125	-.203	.088
		76	32.9	1.68	.544	.845	0.179	.162	-.184	.115
		52	40.8	-1.46	.153	.073	0.346	.196	-.231	.139
	14	426	39.1	7.77	.210	.046	0.028	.069	0.000	.048
		202	35.7	0.63	.157	.071	-.177	.100	0.119	.070
		224	52.4	15.63	.001	.002	0.213	.094	-.107	.067
	15	130	40.6	7.08	.532	.169	0.049	.124	0.000	.088
		94	43.9	2.89	.707	.218	-.017	.146	0.021	.103
		36	28.0	7.00	.510	.143	0.224	.236	-.056	.167
	21	248	32.5	-7.18	.453	.733	0.087	.090	-.040	.064
		180	38.4	-9.60	.930	.951	0.021	.105	0.022	.075
		68	31.5	4.00	.038	.117	0.262	.171	-.206	.121
	22	126	30.6	-8.29	.634	.877	0.102	.126	-.063	.089
		80	34.3	-2.15	.725	.856	0.077	.158	0.000	.112
		46	29.1	-4.52	.784	.916	0.145	.209	-.174	.147
	23	100	36.1	7.64	.127	.058	-.143	.141	0.120	.100
		74	29.1	4.81	.369	.253	-.143	.164	0.108	.116
		26	48.8	-2.46	.251	.252	-.143	.277	0.154	.196
	31	210	34.8	6.17	.006	.011	0.188	.098	-.086	.069
		158	43.9	5.37	.132	.019	0.096	.113	-.025	.080
		52	38.0	6.85	.009	.014	0.467	.196	-.269	.139
	41	192	49.1	2.06	.037	.011	0.207	.102	-.135	.072
		126	40.9	-0.29	.588	.246	0.056	.126	-.032	.089
		66	63.8	13.09	.006	.014	0.497	.174	-.333	.123
	42	230	52.7	-7.11	.259	.241	0.018	.093	0.000	.066
		164	38.0	-7.27	.907	.942	-.048	.110	0.012	.078
		66	56.2	4.91	.007	.008	0.183	.174	-.030	.123
	51	228	47.1	-3.00	.199	.265	0.166	.094	-.114	.066
		160	37.5	0.20	.829	.839	0.025	.112	-.013	.079
		68	36.8	-1.82	.014	.047	0.498	.171	-.353	.121
	52	172	46.1	9.05	.000	.002	0.223	.108	-.186	.076
		128	49.8	-4.81	.005	.018	0.177	.125	-.156	.088
		44	41.1	-6.36	.039	.077	0.356	.213	-.273	.151
	53	260	38.2	2.11	.923	.744	0.027	.088	-.031	.062
		182	42.3	-2.40	.875	.383	0.012	.105	-.022	.074
		78	31.8	-1.38	.433	.566	0.062	.160	-.051	.113
	61	258	27.5	-4.88	.475	.353	0.090	.088	-.070	.062
		198	39.1	-1.09	.213	.180	0.082	.101	-.101	.071
		60	45.6	0.00	.281	.044	0.117	.183	0.033	.129
	64	102	79.4	8.47	.053	.133	0.320	.140	-.275	.099
		66	64.9	2.18	.683	.768	0.149	.174	-.212	.123
		36	66.0	-8.00	.007	.035	0.634	.236	-.389	.167

Tully catalogue. The anisotropy is rather observed but direction of departure is rather for various groups. The most important are: Virgo Cluster (11) where anisotropy is the same then in the whole supercluster, Ursa Major (12) where we observed anisotropy only on the η angle but Δ_{11} and F coefficient are negative (on the whole LSC are positive - because of position on this cluster in the LSC it is going to the "hedgehog model"), and Coma (14) where we don't observe the anisotropy.

5.Conclusions

Our sample is uncontaminated by background objects. The distribution of galaxy planes tend to be perpendicular to the LSC plane. The projection of rotation axes on the supergalactic plane tend to point toward center of the Virgo Cluster. This effects are greatest for "non-spirals" then for "spirals galaxies". Result for UGC/ESO and NGC (Tully) sample of galaxies are very similar. It should be remembered that detected perpendicularity of galaxy planes to the LSC plane can also be caused by the perpendicularity of galaxy planes to the vector to the LSC center "hedgehog model". The separate galaxy cluster belonging to the LSC was analyzed too. The anisotropy is observed but direction of the departure from isotropy are different in various groups.

The dependence of orientation on the morphological type is a curious phenomenon. Partially it is probably because we lose from analyses low face-on spirals. Because of shape of LSC most of them are galaxies with low absolute value δ_D and values η near 0 or Π, so observed anisotropy for that galaxies should be lowest. Within the framework of the tree main scenarios for origin of galaxies (primeval turbulence, hierarchical clustering and pancake model) our result (perpendicularity of galaxy planes to the LSC plane) excludes primeval turbulence and supports the pancake scenario. However it cannot be excluded that complicated structure of the LSC is due to a hybrid model or and to evolutionary effects.

References

Flin,P.,Godłowski,W., 1984 in Cluster and Groups of Galaxies (eds F.Mardirossian et.al.) p.65, D.Reidel, Dordrecht
Flin,P.,Godłowski,W.,1986 The orientation of galaxies in the Local Supercluster Mon. Not. Roy. Astr. Soc V222.p.525
Flin,P.,Godłowski,W.,1989 The Distribution of galaxy planes in the Local Supercluster Pisma w Astron. Zurnał. 15. 10 p.867
Flin,P.,Godłowski,W.,1990 On the Orientation of galaxies in the selected regions of the Local Supercluster Pisma w Astron. Zurnał. 16. 6 p.490
Godłowski,W.1990 in Particle Astrophysics - The Early Universe and Cosmic Structures eds J.M Alim et.all, p.499 Edytion Frontiers

THE GALAXY LUMINOSITY FUNCTION IN DIFFERENT ENVIRONMENTS

Henry C. Ferguson
University of Cambridge
Institute of Astronomy
The Observatories, Madingley Road
Cambridge CB3 0HA

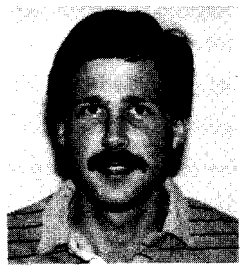

ABSTRACT

Knowledge of the galaxy luminosity function (LF) is a key ingredient in many theories of galaxy formation and evolution. Significant advances have been made over the last several years in characterizing the faint end of the luminosity function and its variation with environment. We compare recent measurements of the cluster and field LF with particular emphasis on whether selection effects can explain the difference in the faint-end slope at magnitudes $M_B \sim -16$. Although the isophotal limits of the field surveys are fairly bright, we conclude that the difference in slope ($\phi(L) \propto L^{-1.25}$ in clusters compared to L^{-1} in the field) is probably not due to a bias toward high-surface-brightness galaxies in the field surveys. Nevertheless, for the few samples complete to $M_B \sim -13$, the faint end slope appears to be steep, ~ -1.3 in both clusters and the field. Thus the shallow slope of the field LF measured to $M_B = -16$ may bear little relation to the true asymptotic behavior of the LF. We suggest that the observed LF variation is due to an environmental variation in the proportion of dwarf ellipticals relative to giants. This variation is *not* density dependent in the way that the spiral/elliptical fraction is, because the dE fraction appears constant with radius within individual clusters.

1 Introduction

The luminosity function (LF), that is, the number of galaxies per unit luminosity as a function of luminosity in a given volume of space, is central to many different areas of extragalactic astronomy. Knowledge of the LF is essential for constraining the baryon density of the universe, understanding observations of galaxy evolution with look-back time, interpreting QSO absorption lines, and testing theories of galaxy formation. More generally, we would like to know the distribution of fundamental galaxy parameters (mass, luminosity, diameter, surface brightness, etc.) and whether these distributions vary with environment. All these galaxy parameters are interrelated, and it is not yet obvious which are the most fundamental, so in confining my review to the luminosity function I am in danger of missing the point. Even more so, since I will concentrate almost exclusively on the LF determined from optical, mostly B-band observations, and will completely gloss over the important work that is being carried out, for example, at infrared wavelengths (Lawrence *et al.* 1986; Isobe & Feigelson 1992). Binggeli *et al.* (1988) committed a similar sin in their otherwise comprehensive review of the LF and its variation with environment. Rather than summarize what Binggeli *et al.* have written, in this talk I will concentrate primarily on work done since 1988, and in particular on the faint end of the LF.

There are several motivations for examining the faint LF in more detail. First, since the concept of "biased galaxy formation" became fashionable, quite a lot of effort has been devoted to studying the luminosity dependence of galaxy clustering. This is often done using the two-point correlation function (e.g. Eder *et al.* 1989; Salzer *et al.* 1990), but another way to pose the question is to ask whether the relative numbers of luminous and low-luminosity galaxies are the same in both high- and low-density environments. In fact, evidence that the relative numbers vary precedes most of the correlation-function studies, but the interpretation was not (and still is not) obvious, since most of the data show a ***higher*** proportion of faint galaxies in high-density environments, the opposite of what simple biasing models predict. In §3 and §4, I will review some recent work in this area.

A second reason for interest in the faint LF is the current explosion of deep surveys for studying galaxy evolution (Tyson 1988; Cowie 1989; Lilly, Cowie & Gardner 1991; Broadhurst, Ellis & Shanks 1988; Cowie, Songaila & Hu 1992). These surveys have revealed a huge apparent population of relatively low-luminosity (sub-L^*) galaxies at

moderate redshifts, and raise the immediate question – what happened to all these galaxies in the last five billion years? Or is there something wrong with the local LF that just makes it *seem* like all these galaxies have disappeared?

A final reason to be interested in the details of faint end of the luminosity function is that it provides leverage for constraining theories of galaxy formation and evolution. The LF reflects both the initial conditions (e.g. the power spectrum of density fluctuations in the gravitational instability scenario) and the complicated physics of collapse, cooling, star formation, and feedback that govern how the mass is converted into light. Galaxies at the faint end of the LF should be less affected by merging, but convert a different fraction of their mass into stars than more luminous galaxies, and are probably more susceptible to environmental interactions such as ram pressure stripping. In the next section I will briefly review some of the physical processes that influence the luminosity function and in §5 I will look at the evidence for environmental effects.

2 Theory – Should we expect a universal LF, and what should it be?

The luminosity function as parametrized by observers shows a single "characteristic" luminosity (L^*) and a "characteristic" faint-end slope (α). The most popular expression used to fit the data is that proposed by Schechter (1976) : $\phi(L)dL \propto (L/L^*)^\alpha \exp(-L/L^*)dL$. However, it is widely acknowledged that this is little more than a convenient fitting function. Indeed, many of the existing data sets are equally well fit by a banana, which has the advantage of not inspiring false hopes that there is any physical significance in the comparison of the model to the data.

There are numerous reasons for supposing that the Schechter function is only a first approximation that must soon fail to meet the test of the current deluge of data. First, as Thompson and Gregory (1980) and Binggeli *et al.* (1988) have emphasized, the composite LF that is usually fit is the sum over separate LF's for the individual Hubble types. The strong dependence of the relative proportions of different galaxy types on local density (Hubble & Humason 1931; Dressler 1980) should show up as a variation in the composite LF between clusters and the field. It would thus be a remarkable coincidence if the Schechter function ultimately provided a good fit to both cluster and field data, since the individual spiral and elliptical LF's would have to change in such a way as to cancel the difference in their relative numbers. A second reason to question the universality of the

Schechter function is that the luminosities of different Hubble types evolve at different rates. Five Gyr ago late-type spirals would likely have been slightly fainter than they are now, while giant ellipticals would have been $\sim$ 1.5 mag brighter in B (e.g. Arimoto & Yoshii 1986; 1987), so the composite LF would be quite different from what it is today. If a Schechter function really describes the present-day LF, then it could not have described the LF 5 Gyr ago. But I see no reason to suppose that we are living in a preferred era when the Schechter function is the true description of the galaxy LF. Rather, I suspect that differences will emerge as the LF is computed from larger data sets with better photometric accuracy. These differences should be taken seriously, as they may provide some insight into the physics of how mass in the early perturbations was converted into luminous material.

There is also a purely practical caution against taking the Schechter-function fits too seriously. The parameters α and L^* are highly correlated (Schechter 1976; Lugger 1986); photometric errors, uncertainties in background subtraction, and completeness corrections, even if dominant at the faint limits of the surveys can significantly affect L^*, while the effects of small-number statistics at the bright end can modify α. A specific example is the problem of how to treat the brightest cluster member in fitting the LF. Lugger (1986) showed that excluding this one galaxy can change the faint-end slope by $\Delta\alpha = 0.2$. This is already comparable to the apparent difference in α between clusters and the field (-1.25 compared to -1.0, respectively), and raises the interesting possibility that the discrepancy could be due to changes in the LF at the very *bright* end.

Having said all this, it must be noted that the Schechter function is a very useful first approximation that fits most of the available data to within the uncertainties. Exceptions have been found for individual clusters (Dressler 1978), and the fits are in general better if the brightest cluster members are excluded (Schechter 1976; Lugger 1986), but no clear correlation between cluster properties and LF has been identified. Recent surveys of the field LF, summed over all galaxy types (Sandage, Tammann & Yahil 1979; Efstathiou, Ellis & Peterson 1988; Loveday *et al.* 1992) are also fully consistent with Schechter's parametrization. Thus α and L^* must have some very close connection with galaxy formation, and it is incumbent on theory to explain both the general form of the LF and the observed values of these parameters.

Unfortunately, theories for galaxy formation are still quite far from being able to reproduce the observed LF without invoking along the way several fairly *ad hoc* assumptions

about the physics of galaxy evolution. The number of halos that collapse and virialize as a function of mass can be predicted analytically once the power spectrum is chosen (Press & Schechter 1974; White & Rees 1978; Bond *et al.* 1990). While the problem is complicated by uncertainties of how to treat smaller clumps collapsing within larger ones, N-body simulations produce reasonable agreement with the analytic theory (Frenk *et al.* 1988; Efstathiou *et al.* 1989). The mass scale of the halos that actually condense into galaxies is thought to be governed by cooling (Hoyle 1953; Rees & Ostriker 1977; Silk 1977; White & Rees 1978). Halos that can cool on a dynamical timescale are able to collapse and form stars, while on larger scales the halos simply go on merging to form groups and clusters. An oft-touted success of the gravitational instability theory is the close correspondence between estimates for the largest systems that can radiatively cool on a dynamical time scale ($\sim 10^{12} M_\odot$) and the inferred masses of the most luminous galaxies (e.g. Blumenthal *et al.* 1984). Comparison to observations is hampered by uncertainties in M/L, so really the only confirmation of the theory is that there is an exponential cutoff at roughly the expected luminosity in the observed LF. On the theoretical side, the details of where exactly that cutoff occurs and whether it really should be an exponential are sensitive to assumptions for the subsequent merging of galaxies that have already collapsed and cooled.

The slope of the low-mass tail of the halo distribution is governed by the power spectrum. For the standard assumption $|\delta_k|^2 \propto k^n$, the Press-Schechter formalism gives a power-law slope of $(n-9)/6$ (Gott & Turner 1977; White & Rees 1978). For typical values in the range $1 > n > -3$, this is much steeper than the observed value of α in the Schechter function. This is not surprising because the efficiency of forming luminous material probably depends on the mass of the halo. The reigning paradigm is that feedback from supernovae regulates the star-formation efficiency, causing galaxies with lower binding energy to form fewer stars per unit mass (Larson 1974; White & Rees 1978; Dekel & Silk 1986; White & Frenk 1991). The details of how this feedback operates depend on the IMF and how it varies with different initial conditions, the efficiency with which supernova energy is deposited into the gas, and whether any other effects such as photoionization by the UV background (Babul & Rees 1991) are of comparable importance. Different authors invoke different plausible but fairly arbitrary assumptions, and the form of the resultant LF largely reflects these assumptions rather than the initial power spectrum. For example, White and Rees (1978) assumed that the fraction f of gas turned into stars

scales with the mass and radius of the halo as $f \propto M/r$, and derived a power-law slope at the faint end of the LF of $\alpha = (n-13)/(7-n)$, which has a rather different behavior with n than the halo mass function, but nevertheless is too steep for reasonable values of n. More recent studies encounter the same problem (White & Frenk 1991; Cole 1991).

Thus standard theories for the growth of structure from gravitational instabilities have very few concrete predictions for the luminosity function. There is some hope that the situation will improve at the bright end as N-body simulations incorporating gas dynamics (e.g. Evrard, this volume) begin to treat the merging and cooling of galaxy halos simultaneously. It may also be possible to make some progress for luminous galaxies by trying to predict the LF for individual Hubble types (e.g. late-type spirals) where there are tighter constraints on M/L, the amount of merging, and the rate of star formation over time (Martínez-González & Sanz 1988; White & Frenk 1991). At the faint end, explorations of the parameter space of the different physical mechanisms that control dwarf galaxy structure (Athanassola, this volume) should help to narrow down the choices for the processes that limit cooling and star formation in low-mass galaxy halos.

An almost unavoidable consequence of the general theoretical framework outlined above is that we should *expect* to see environmental variations in the LF. Statistical biasing of the density peaks predicts more giant galaxies per dwarf in high density regions (Kaiser 1985; Dekel & Silk 1986; Schaeffer & Silk 1988). The merger rate is sensitive to the surrounding local density field and to the details of how structures collapse, so the shape of the truncation at the bright end should be quite sensitive to environment (Hausman & Ostriker 1978). The ability of galaxies to cool and form stars may depend on the input of energy from nearby star-forming galaxies and AGN, on the pressure of the surrounding intergalactic medium (Babul & Rees 1991), and on the buildup of angular momentum through tidal torques (Hoyle 1949; Harrison 1971). All of these possibilities suggest that we should be surprised if we *don't* see significant differences between the LF of clusters and the field.

3 The global luminosity function in clusters and the field

Studies of the field-galaxy LF in the last decade have fairly consistently found a faint-end slope $\alpha \sim -1.0$, flatter than what was previously thought to be the "universal" slope of $\alpha = -1.25$ (Schechter 1976; Felten 1977). Detailed studies of clusters, however,

arrive at a value closer to $\alpha = -1.25$ (Sandage, Binggeli & Tammann 1985; Lugger 1986; Ferguson & Sandage 1991), and it is thus important to see if we can understand this difference. An obvious possibility is that the field galaxy LF's, which are usually constructed from catalogues of bright galaxies, are biased toward high-surface-brightness galaxies, while cluster surveys, which typically go much fainter in apparent magnitude, are not. Disney and collaborators (Disney 1976) have repeatedly emphasized that galaxy catalogues are never really magnitude limited, but are instead limited by diameter and surface brightness (μ_B). Low-surface-brightness dwarf galaxies start to dominate the cluster LF at $M_B \sim -17$. In many cases central surface-brightnesses are fainter than $24\,\mathrm{mag\,arcsec^{-2}}$, so there is a possibility that field LF's that are based on catalogues with rather bright isophotal limits such as $\mu_B \sim 24.5\,\mathrm{mag\,arcsec^{-2}}$ (Loveday *et al.* 1992; hereafter LPEM) will miss galaxies at the faint end. Whether or not this is a problem depends on the extent to which surface brightness and luminosity are correlated. If there is no correlation, low-luminosity galaxies will be preferentially missed because they will more often fall below the diameter limits of the surveys. However, studies of nearby clusters suggest that, at least along the elliptical and dE sequence, there is a fairly tight $\mu_B - M_B$ relation (Binggeli, Sandage & Tarenghi 1984; Ferguson & Sandage 1988). That this is a real correlation and not a consequence of morphological selection procedures is most clearly illustrated by the different spatial distributions of faint high- and low-SB galaxies in the Fornax Cluster (Ferguson 1989; but see Irwin *et al.* 1990). If we assume the Fornax Cluster $\mu_B - M_B$ relation and some intrinsic scatter, we can estimate how many dE's should be missing from the LPEM field LF. Fig. 1 illustrates the procedure. The actual limits of the LPEM survey are mixed up in the details of star/galaxy separation, however we have approximated these by selecting rather conservative isophotal diameter limits, i.e. requiring that the isophotal diameter be well above the effective FWHM of stellar images. Fig. 1 shows that the assumption that the survey is magnitude limited is not very good. For galaxies with exponential profiles, the survey is essentially limited by effective surface-brightness; however few galaxies would be missed in the Fornax cluster down to $M_B = -15$. Assuming that the photometry done after galaxy selection yields reasonably precise total magnitudes, the LF for this one cluster should be reasonably free from SB selection effects down to the apparent magnitude limit ($B_J = 17$) of the LPEM survey. To see whether SB selection limits affect the LF from a sample distributed uniformly in volume, we can take the Fornax $\mu_B - M_B$ relation, assume an intrinsic scatter of $\sigma = 1$ mag in SB at a given M and a measurement error of $\sigma(M) = 0.3$ mag,

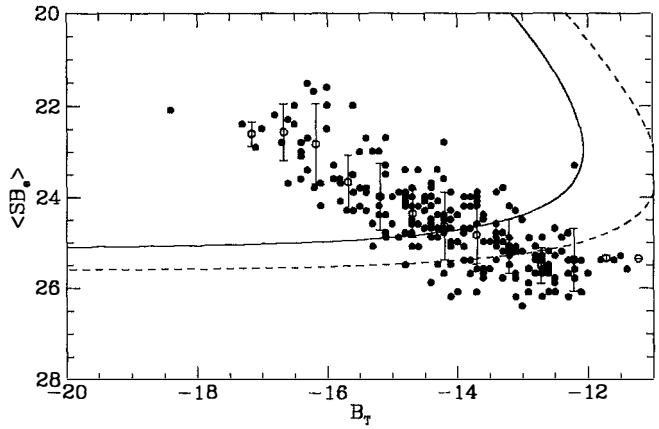

FIG. 1 — Surface-brightness limits of the Loveday *et al.* (1992) survey. The data shows the effective surface brightness–apparent magnitude correlation for dE galaxies in the Fornax Cluster. For galaxies with exponential surface-brightness profiles, the curves show the limits of a survey that selects galaxies by isophotal diameter. The solid curve corresponds to a minimum diameter of 4″ above an isophote of $B_J = 24.0$; the dashed curve is for 3″ above an isophote of $B_J = 24.5$. The true LPEM survey limits after star/galaxy separation probably lie between these extremes.

choose galaxies randomly from a Schechter function with $\alpha = -1.25$ and distribute them randomly in volume, impose the strict limits $15 < B_T < 17$ and the implicit SB limit for dE's, and compute the LF from the simulated data set. The result (Fig. 2) is that down to $M_B = -15$, the Loveday *et al.* (1992) sample should be reasonably unbiased by its high isophotal magnitude limit (about five galaxies out of 1440 would be missed). The difference between this field-sample LF and that of the Virgo and Fornax Clusters is therefore probably not due to surface-brightness selection.

4 Variations in the Dwarf/Giant ratio

What, then, is causing the difference in α between clusters and the field? The dominant population in clusters is dE galaxies, and there is mounting evidence that their proportion relative to giants changes with environment. Ferguson and Sandage (1991; FS91) showed that there are significant differences between clusters and loose groups in the dwarf-to-giant ratio. In the Virgo Cluster, for example, 54% of all galaxies brighter than $M_B = -13.5$ are dE or dS0 galaxies, while this fraction is only 33% in a combined sample of the Leo and Dorado groups. While the variations between groups are evident when high- and low-luminosity galaxies are counted irrespective of morphology,

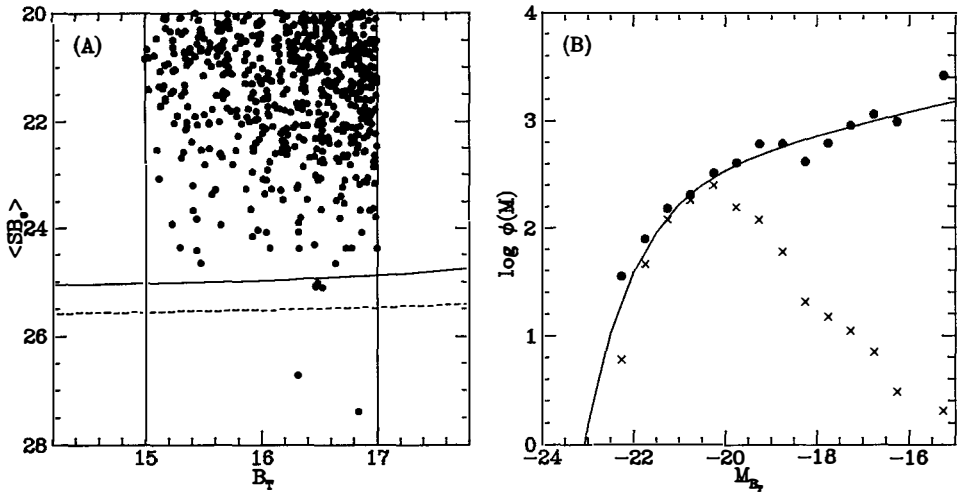

FIG. 2 — (A) Simulated field galaxy data set. A Schechter function with $M_B^* = -21.2$, $\alpha = -1.25$ is used to generate a random sample of galaxies out to a distance of 300 Mpc. All galaxies are assumed to follow the Fornax Cluster $\mu_B - M_B$ relation, but with an intrinsic scatter of 1.0 mag arcsec^{-2} (larger than seen in Fornax), and a photometric error of $\sigma = 0.3$ in measured B. The vertical lines show the LPEM apparent magnitude limits, while the nearly horizontal curves show roughly where the effective-surface-brightness cutoff occurs for galaxies with exponential profile. Galaxies that fall below the curves would probably not be detected above the LPEM limiting isophote. (B) Shows the reconstructed field galaxy luminosity function from this simulated data set. The x's show the "observed" data, while the dots show the LF after correcting for the volume sampled at different apparent magnitudes. The solid curve shows the input model LF.

the differences are most significant when the comparison is restricted to early-type (E and S0) giants and (dE, dE,N, and dS0) dwarfs. This dwarf/giant ratio is positively correlated with richness (Fig. 3), or possibly the group velocity dispersion. There seems to be no strong correlation with local density (other than the rather subtle effect discussed in the next section) either within clusters, or between groups of different central densities. The variation in dwarf/giant ratio is thus a completely different phenomenon from the morphology-density relation. Vader and Sandage (1991) have recently shown that the trend for clusters and groups extends to very loose groups. Their results are also plotted in (Fig. 3), corrected for the different definitions of "richness" in the two papers. (The offset between the two samples is probably due to Vader and Sandage's defining richness N_g as the number of galaxies in each group in the CfA catalog, while their survey for dwarfs in general covers a smaller portion of each group.) The origin of trend shown in Fig. 3 is not currently understood, although suggestions have been made that dynamical friction plays a role in depleting the dwarf population in the field (Vader & Sandage 1991; Ferguson 1992) or that cluster dwarfs can form more stars than field dwarfs due to

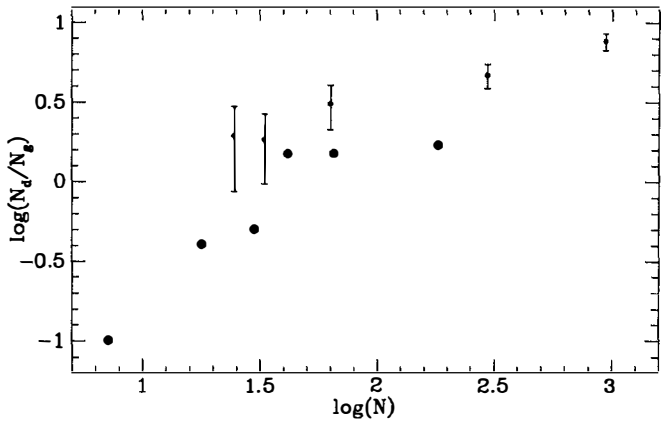

FIG. 3 — Variation of the dwarf/giant ratio for early type galaxies (E, S0, dE, dE,N , and dS0) with richness. The points with error bars show the group and cluster data (Ferguson & Sandage 1991) down to $M_B = -13$. The points without error bars are from Vader and Sandage (1991), scaled to the same limiting magnitude assuming a Virgo-Cluster LF. The abscissa shows the log of the total number of galaxies in the group down to $M_B = -13$, taken as an indicator of richness.

pressure in the IGM (Babul & Rees 1991).

It is interesting, and possibly significant, that when the group luminosity functions of FS91 are fit to the typical limit of field surveys ($M_B = -16$) they show a systematic trend toward steeper slopes with increasing richness (Fig. 4). Since most of the galaxies in field surveys are in loose groups, this may account for the apparent change in α between clusters and the field. It is still more interesting to note that all the group LFs in the FS91 survey rise steeply when considered down to fainter magnitude limits. In the five groups that are fairly complete to $M_B = -13$ the mean α was -1.35. Thus the apparent flattening of the LF in field surveys may just be a local feature near $M_B = -16$, rather than a true power-law behavior of the low-luminosity tail of the LF.

There is some hope that studies of companion galaxies (Phillips & Shanks 1987; Vader 1992) can set limits on the very faint end of the field galaxy LF, since galaxies can be selected to much fainter magnitude limits. For the time being, we can get a rough estimate from galaxies catalogued in the local group and the M81 group (Binggeli 1990; Karachentseva, Karachentseva & Börngen 1985). Taking the ratio of the number of galaxies between $-13 > M_B > -15$ to the number between $-15 > M_B > -17$, we find $\alpha = -1.9$ for the M81 group, -1.2 for the local group and -1.6 for the combined sample. While this is closer to the steep slopes expected from CDM (White & Frenk 1991), some

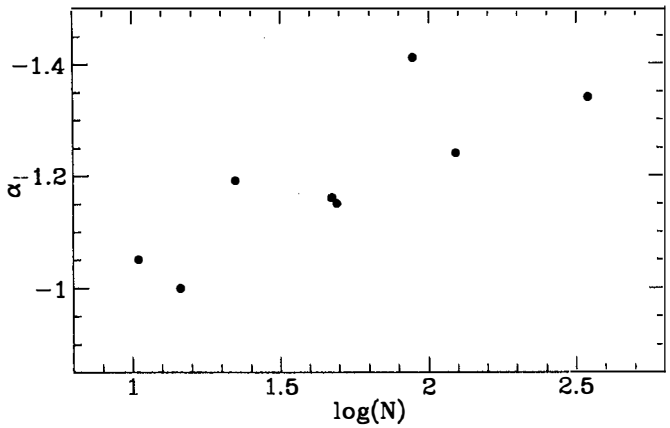

FIG. 4 — **Results of fitting a Schechter function down to $M_B = -16$ for the groups in the FS91 sample. The best-fit value of α is plotted against the group richness.**

steepening of the faint-end slope among satellite galaxies is expected because dynamical friction preferentially causes high-mass companions to spiral into their primaries (Ostriker & Turner 1979).

5 Local variations in the dwarf content of clusters

The mechanisms that control galaxy collapse and cooling probably also influence the Hubble type, so it is natural to seek a luminosity-function–density relation analogous to the morphology–density relation. Binggeli *et al.* (1988) have reviewed the few attempts that have been made in this direction for bright galaxies. In this section I will review the evidence for variations at the faint end of the LF within clusters. Such variations might be expected to arise from (1) mass segregation during violent relaxation (West & Richstone 1988), (2) late-time infall of low-luminosity galaxies expected in some models of biased galaxy formation, or (3) interaction with the cluster IGM either triggering or suppressing star formation.

To look for luminosity-function variations, the FS91 sample was broken into four bins of local projected density (with 0-50, 50-100, 100-200 and more than 200 galaxies Mpc^{-2} as determined from the ten nearest neighbors) and the LF computed for each bin (Ferguson 1990). For the LF summed over all Hubble types, the differences in α and M^* in the different density bins were found to be insignificant. Evidently, there is little luminosity segregation in these groups, a result that can be seen quite easily by comparing

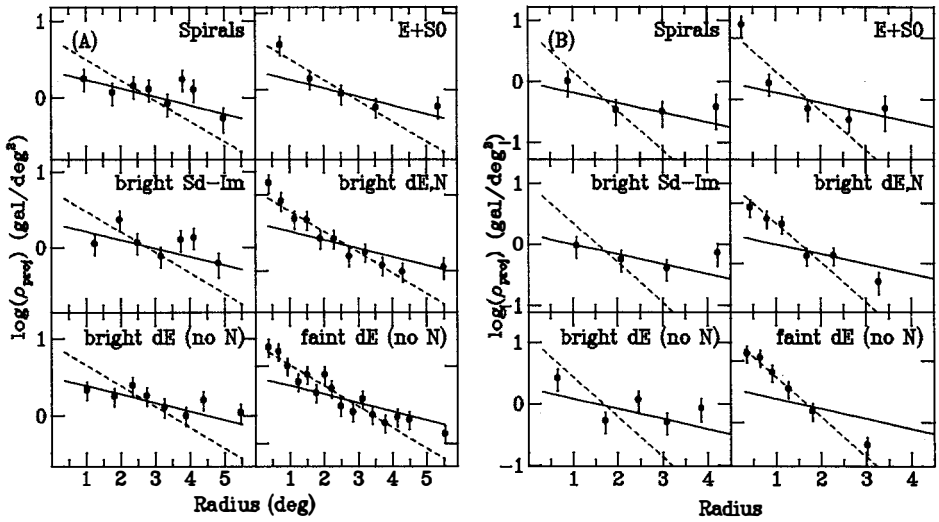

FIG. 5 — (A) The projected density of galaxies as a function of radius in the Virgo Cluster. The solid line shows the best-fit exponential to the bright nonnucleated dE distribution; the dotted line shows the best fit to the faint nonnucleated dE distribution. Both fits are normalized to the number of galaxies in each sample. The bright samples contain likely cluster members down to $M_B = -14.2$. The faint dE sample contains galaxies fainter than $M_B = -13.3$. (B) The projected density distributions in Fornax.

the spatial distributions of bright E's and the faintest dE's in Fig. 5.

Within a given Hubble type, only the nonnucleated dE's show a significant LF variation with local density. The reason for this is shown in Fig. 5. Bright nonnucleated dE's show essentially the same spatial distribution as spirals and irregulars, while dE,N's and fainter dE's (which may just have nuclei that are too faint to see) follow the E+S0 spatial distribution. The cause of this spatial segregation is unknown. Ferguson and Sandage (1989) suggest that it may be due to stripping of Im's on radial orbits, and cite the similar flattening distributions of the Im's and the nonnucleated dE's as supporting evidence. Alternatively, nuclei may form preferentially in galaxies that pass through the centers of clusters (Silk, Wyse & Shields 1987; Babul & Rees 1991). Whatever the reasons, the resultant change in the LF is fairly subtle and is washed out in comparing the combined LF's over all types.

6 Conclusions

In the standard bottom-up scenario where clusters form by the accretion of smaller groups, and where infall onto clusters continues to the present epoch, it is difficult to account for the both variation of the dwarf/giant ratio from rich to poor groups and the relative constancy of the LF within the rich groups. If the Virgo Cluster grew out of the mergers of Leo- and Dorado-like groups, why are there so many more dwarfs per giant in Virgo? If groups with a low dwarf/giant ratio are raining in on Virgo at the present epoch, they will presumably be on predominantly radial orbits with a wider spatial distribution than the virialized core of the cluster. Why, then, don't we see spatial variations in the dwarf/giant ratio within Virgo?

Constraints on the faint end of the LF in different environments are clearly important for understanding the mechanisms that control galaxy and cluster formation. The considerations of §4 suggest that the difference in α between clusters and the field at $M_B = -16$ is real (i.e. not due to selection), but α measured to this limit may bear little relation to the asymptotic behavior of the LF two or three magnitudes fainter. The few deep samples that exist suggest $\alpha \sim -1.3$ at $M_B \sim -13$ in both clusters and the field. While existing field surveys are relatively unaffected by surface-brightness bias to their present limits, in pushing them fainter it will be important to change the selection criteria to favor low-SB galaxies. This will be especially important in searching for the local faded counterparts to the bursting intermediate-redshift galaxies (Cowie, Songaila & Hu 1992). Of course, we must take care to include high-SB galaxies as well. Salzer (1989) estimates that emission-line galaxies constitute $\sim 7\%$ of the local galaxy population. Most of these are compact star-forming dwarfs, like the blue compact dwarfs (BCD's) discussed by Thuan and Deeg in this volume. Since the star-forming phase is presumably short, there may be a large population of faded BCD remnants lurking among the dE's and Im's, or hiding as faint compact galaxies. In any case, further study of the faint tail of the luminosity function should help narrow down the wide array of choices for the physical processes that govern galaxy evolution.

REFERENCES

Arimoto, N. & Yoshii, Y. 1986, A&A, 164, 260
Arimoto, N. & Yoshii, Y. 1987, A&A, 173, 23
Babul, A. & Rees, M. 1991, Preprint
Binggeli, B. 1990, private communication
Binggeli, B., Sandage, A., & Tammann, G. A. 1988, Ann.Rev., 26, 509

Binggeli, B., Sandage, A., & Tarenghi, M. 1984, AJ, 89, 64
Blumenthal, G. R., Faber, S. M., Primack, J. R., & Rees, M. J. 1984, Nature, 311, 527
Bond, J. R., Cole, S., Efstathiou, G., & Kaiser, N. 1990, ApJ, 379, 440
Broadhurst, T. J., Ellis, R. S., & Shanks, T. S. 1988, NMRAS, 235, 827
Cole, S. 1991, ApJ, 367, 45
Cowie, L. L. 1989, in The Epoch of Galaxy Formation, ed. C. S. Frenk (Dordrecht: Kluwer), 31
Cowie, L. L., Songaila, A., & Hu, E. M. 1992, Nature, 354, 460
Dekel, A. & Silk, J. 1986, ApJ, 303, 39
Disney, M. 1976, Nature, 263, 573
Dressler, A. 1978, ApJ, 223, 765
Dressler, A. 1980, ApJ, 236, 351
Eder, J., Schombert, J. M., Dekel, A., & Oemler, A. 1989, ApJ, 340, 29
Efstathiou, G., Ellis, R. S., & Peterson, B. A. 1988, MNRAS, 232, 431
Efstathiou, G., Frenk, C. S., White, S. D. M., & Davis, M. 1989, MNRAS, 235, 715
Felten, J. E. 1977, AJ, 82, 861
Ferguson, H. C. 1989, AJ, 98, 367
Ferguson, H. C. 1990, Johns Hopkins Univ. Thesis
Ferguson, H. C. 1992, MNRAS, 255, 389
Ferguson, H. C. & Sandage, A. 1988, AJ, 96, 1520
Ferguson, H. C. & Sandage, A. 1989, ApJ, 346, L53
Ferguson, H. C. & Sandage, A. 1991, AJ, 101, 765
Frenk, C. S., White, S. D. M., Efstathiou, G., & Davis, M. 1988, ApJ, 327, 507
Gott, J. R. & Turner, E. L. 1977, ApJ, 216, 357
Harrison, E. R. 1971, MNRAS, 154, 167
Hausman, M. A. & Ostriker, J. P. 1978, ApJ, 224, 320
Hoyle, F. 1949, in Problems of Cosmical Aerodynamics (Dayton: Central Air Documents Office), 195
Hoyle, F. 1953, ApJ, 118, 513
Hubble, E. & Humason, M. L. 1931, ApJ, 74, 43
Irwin, M., Davies, J., Disney, M., & Phillips, S. 1990, MNRAS, 245, 289
Isobe, T. & Feigelson, E. D. 1992, ApJS, 79, 197
Kaiser, N. 1985, ApJ, 284, L9
Karachentseva, V. E., Karachentseva, I. D., & Börngen, F. 1985, A&AS, 60, 213
Larson, R. B. 1974, MNRAS, 169, 229
Lawrence, A., Walker, D., Rowan-Robinson, M., Leech, K. J., & Penston, M. V. 1986, MNRAS, 219, 687
Lilly, S. J., Cowie, L. L., & Gardner, J. P. 1991, ApJ, 369, 79
Loveday, J., Peterson, B. A., Efstathiou, G., & Maddox, S. 1992, ApJ, 390, 338
Lugger, P. M. 1986, ApJ, 303, 535
Martínez-González, E. & Sanz, J. L. 1988, ApJ, 332, 89
Ostriker, J. P. & Turner, E. L. 1979, ApJ, 234, 785
Phillips, S. & Shanks, T. 1987, MNRAS, 227, 115
Press, W. H. & Schechter, P. L. 1974, ApJ, 187, 425
Rees, M. J. & Ostriker, J. P. 1977, MNRAS, 179, 541
Salzer, J. 1989, ApJ, 347, 152
Salzer, J. J., Hanson, M. M., & Gavazzi, G. 1990, ApJ, 353, 39
Sandage, A., Binggeli, B., & Tammann, G. A. 1985, AJ, 90, 1759
Sandage, A., Tammann, G. A., & Yahil, A. 1979, ApJ, 232, 352
Schaeffer, R. & Silk, J. 1988, A&A, 203, 273
Schechter, P. 1976, ApJ, 203, 297
Silk, J. 1977, ApJ, 211, 638
Silk, J., Wyse, R. F. G., & Shields, G. A. 1987, ApJ, 322, L59
Thompson, L. A. & Gregory, S. A. 1980, ApJ, 242, 1
Tyson, J. A. 1988, AJ, 96, 1
Vader, J. P. 1992, private communication
Vader, J. P. & Sandage, A. 1991, ApJ, 379, L1
West, M. J. & Richstone, D. O. 1988, ApJ, 335, 532

White, S. D. M. & Frenk, C. S. 1991, ApJ, 379, 52
White, S. D. M. & Rees, M. J. 1978, MNRAS, 183, 341

VI - FUTURE INSTRUMENTS

IR OBSERVATIONS OF NORMAL GALAXIES FROM SPACE OBSERVATORIES

Laurent Vigroux
Service d'Astrophysique
CEN Saclay, F91191 Gif sur Yvette Cedex

ABSTRACT

The importance of space for infrared observations have been demonstrated by the spectacular scientific succes of the IRAS and COBE missions. In this review, we will first emphasis the gain provided by space observatories compared to ground based observations. Then a short review of scientific capabilities of past, present and future observatories is presented. For normal galaxies, we describe the main results obtained from the IRAS data, and we discuss how future ISO observations can help in solving some of the pending problems.

1. Introduction

The development of space technologies after the sixties has opened new windows in astronomy. The first and spectacular result was the discovery of the high energy sky, in X and gamma rays. The progress in infrared and submillimeter waves was slower. The presence of atmospheric windows, spread all over this wavelength range, while not perfect, weakens the need for space observations, at the opposite of high energy where the opacity of the atmosphere imposes space observation. The complexity of infrared instrumentation, the need for cryogenic detector housing, which were beyond the technical space technologies until the beginning of the eighties, explains also why the first developements of infrared astronomy were made from ground based high altitude observatories like the Mauna Kea, with some pioneering observations in balloon or in plane.

In the infrared, space offers two main advantages. There are of course no more atmospheric transmission windows. A space infrared observatory provides a full access to the whole wavelength range. The second is a reduction of infrared background. On earth, the background is due to atmospheric emission, thermal plus emission bands, and to the thermal radiation of the telescope itself. In space, the background is due to zodiacal light, from 5 to 20 microns, and interplanetary dust emission above 20 microns. These are orders of magnitude below the background experienced by ground based instruments. At 10 microns, the background at the entrance of the ISO instrument will be 10^7 lower than the background observed on Mauna Kea with a 4 m. telescope. At 10 microns, in space, the background is even lower that the background experienced on ground in the K band.

To take full advantage of this small background, the thermal self emission of the telescope also must be reduced, and the telescope and the instruments have to be cooled down. The telescope and the focal plane instrument of IRAS, the first infrared satellite, was cooled by superfluid helium contained in a large toroidal tank surrounding all the optical subsystem. ISO, the next european infrared satellite keeps the same concept. The optimisation of a satellite is a good balance between total weight, which sizes the He tank, diameter of the telescope and duration of the mission. IRAS and ISO were designed for about 2 year mission with telescopes of 60 cm diameter. A larger telescope, but still a moderate 80 cm diameter, is planned for the US mission SIRTF. No larger telescope can fit within a helium cooled satellite. It means that these projects have a poor angular resolution. At 100 microns, the diffraction will limit the resolution of ISO to 1 arcmin, far below the resolution achieved on ground based observatories. New generation 8 meters, with adaptive optic can be diffraction limited from 2 to 10 microns, with resolution better than 0.1 arcsec. Ground based and space observatories are complementary, good resolution and background limited sensitivity on ground, poor resolution and high sensitivity for extended emission for space, airborne observatories beeing in the mid between.

The first part of this paper is devoted to a short presentation of past, present and future space infrared observatories. In the second part it makes a review of our current understanding of far infrared properties of normal galaxies, and of the pending problems; for each problem, we explain what will be be the strategy of the ISO observations to improve our knowledge.

2 Space Observatories

2.1 IRAS

The scientific results of IRAS have been such a revolution in astronomy, that it is not necessary to make a detailed presentation. I will summarize only some performances to enlighten the gain to be expected with the new generation, ISO in particular. IRAS was a survey satellite with some pointed observations after the mission. The most successful instrument, was the camera that had four photometric bands at 12, 25, 60 and 100 μm. The resolution was poor. The nominal resolution is 3 arcmin at 100 μm. It can be improved by deconvolution algorithms to about 1 arcmin, the so called High Resolution maps. The sensitivity was limited by the transit time of a source on each detector. For a point source, it is ≈ 1 Jansky, and for extended sources, it is ≈10 μJy arcsec^{-2}.

With its poor resolution, IRAS could resolve star forming regions only in the local group. Detailed observations of galaxies have been possible in the local group, with an emphasis on the Magellanic Clouds and M33, and on some nearby large galaxies, like M51 or M101. On the other hand, IRAS has achieved a complete survey of galaxies brighter than 1 Jy. The most spectacular result of this survey was the discovery of starburst galaxies, that emit most of their energy in the far infrared, but the IRAS database of infrared colors of normal galaxies is also an invaluable tool to understand galaxy evolution. We will discuss this later in this paper.

2.2 COBE

The main goal of COBE was not, of course, the study of galaxies. Its coarse resolution, 5°, prevents it from obtaining images of individual galaxies, except one, our own Galaxy. The maps of the Galaxy provided by COBE are useful complement of the IRAS map, at wavelength longer than 100 μm, for example in the emission line of NII at 205 μm.

2.3 Kuiper Airborne Observatory

This airborne based 92 cm telescope is used for far infrared and submillimeter observation. It provides a resolution of 55 arcsec at 150 μm. For normal galaxies,

the most useful instrument is a far infrared camera which has been used to map galaxies from 60 to 200 μm. besides continuum observations, spectral line filters can also be used, such as the C_{II} line at 157 μm which, as the main cooling emission line, is very useful to understand the thermal balance of the interstellar medium. While less sensitive than a He cooled satellite, the lower cost of the observations and the possibility to upgrade the instruments, make the KAO still very attractive.

Airborne observatory developements will continue, since the US and Germany have a joint project SOFIA, which is in very good shape. It is a 2.5 m telescope set up in a Boeing 747.

2.4 Infared Space Observatory

This european satellite is planned for a launch near the end of 1994, or early in 1995. It is a 60 cm LHe cooled telescope, diffraction limited at 5 μm. The 2500 liters of liquid Helium should ensure scientific observations for 18 months. Gain in sensitivity will be from 2 to 3 orders of magnitude, compared to IRAS. This is due to a new generation of infrared detectors, and of the ISO capability for long pointed observations. The spatial resolution will be 6 arcsec at 15 μm and 40 arcsec at 100 μm. Thanks to this resolution, distant galaxies will be resolved and detailed maps of the infrared emission will be obtained for galaxies up to 20 Mpc. Table 1 compares the size of the resolution element in some nearby galaxies.

	distance	spatial resolution IRAS (3 arcmin.)	ISO (6 arcsec. at 10 μm)
LMC	52 kpc	45 pc	1.5 pc
SMC	61 kpc	53 pc	1.8 pc
M31	730 kpc	0.65 kpc	21. pc
M33	800 kpc	0.70 kpc	23. pc
M82	3.6 Mpc	3.1 kpc	105 pc
M51	10.8 Mpc	9.3 kpc	310 pc
Virgo cluster	18. Mpc	15. kpc	500 pc

Even at the distance of the Virgo cluster, a giant star forming regions, with typical size of 400 pc, can be separated from a diffuse emission. ISO maps of the Virgo cluster galaxies will be even better than the IRAS map of M33.

The total focal plane of 20 arcmin is split in 4 by a pyramidal mirror which feeds 4 instruments, a camera, a photometer and 2 spectrographs. Only one instrument can be operated at a time, but the camera can be used in parallel mode to make serendipity observations in the field adjacent to the prime instrument during long observations.

The camera, ISOCAM, is a double camera, with a short wavelength channel from 2.5 to 5 μm, and a long wavelength channel from 4 to 18 μm. The detectors have 32 x 32 pixels. Each channel has a filter wheel, which holds 10 filters, broad band filters or centered on spectral features, and circular variable filters with resolution 40. The magnification can be adapted by selecting one of the 4 available lenses which provide sampling of 1.5, 3, 6 and 12 arcsec/px. Three polarizers can be set in the optical path for polarization measurements. An internal calibration device can be used for rough photometric calibration or flat fielding. The sensitivity will be ≈ 1 mJy with a signal to noise ratio of 10 for 100 s integration, and can be improved by longer exposures, up to 2 hours.

The photometer, ISOPHOT, includes besides the normal mode of multi aperture photometry, a spectrophotometric instrument, with a spectral resolution of 100 from 2.5 to 18 μm, polarimetric capability and some imaging possibilities at wavelength longer than 50 μm. An internal calibration device can be used as a photometric reference. Compared to IRAS, ISOPHOT offers a better sensitivity, a control of the aperture and the possibility to observe up to 200 μm. This last aspect should have a very strong scientific impact since it will allow to measure the amount of very cold dust, $T < 30$ K that were not detectable by IRAS. A filter similar to the 12 μm filter of IRAS, common to ISOPHOT and ISOCAM, will be used to cross calibrate ISOCAM, ISOPHOT and IRAS.

The 2 spectrographs cover a domain from 3.5 to 200 μm, with a separation at 45 μm. Both have a normal grating mode which provide a spectral resolution of 1000 for the Short Wavelength Spectrometer, and 200 for the Long Wavelength Spectrometer, and a Fabry Perrot mode with resolutions of 15 000 and 10 000 respectively. Spectra of point sources of ≈ 1 Jy can be obtained in 1 hour for the whole wavelength range. They can also map galaxies in proeminent emission lines, such as NeII at 18 μm or CII at 157 μm, using the raster pointing capabilities of ISO. To give an example, the sensitivity of the LWS in the CII line is 10 times better than the best available camera on the KAO, but with a lower spatial resolution, 2 arcmin, compared to 1.0 for the KAO.

ISO is a general user observatory. 2/3 of the observing time is open for guest observers from ESA member states, with a quota reserved for US and Japanese observers as a return for their support in a second ground station. The first call for proposal is expected between 18 and 12 months before launch, late in 1993.

2.5 Future space observatories

The funding situation in US and in ESA is not so well established that a reasonable planning can be given for the future missions. We can only list the existing projects.

SIRTF is a US satellite, analog to ISO but with a larger telescope (90 cm). The payload looks like the ISO payload, with better performances due to the larger format of the detectors. Although SIRTF has been put in first priority by the Bacahll report on astronomy, cut in the NASA funding has put it in a very bad situation, and there is still no start authorization.

FIRST is a submillimeter observatory. It is one of the four corner stones of ESA. In this sense, it is approved, but the planning is still unknown. It may be either the third or the fourth mission, with a choice in 1993. If third, it should be launched around 2003. In the original design, the emphasis was on a very large antenna, with spectro-imagers from 200 μm to 1 mm. New developments, from technical and scientific points of view, call for a smaller 4.5 meter antenna with observing capabilities from 50 μm to 1 mm. If this new payload is accepted, FIRST would be the direct extension of ISO. It would offer the same spatial resolution at 100 μm than ISO at 10 μm. NASA has also similar projects in the far infrared and submillimeter domains, like SMMM, but their funding status is still very uncertain. A joint mission ESA - NASA might even be possible for such a submillimeter observatory, due to the very high cost of the spacecraft and of the payload.

Again in the spacecraft domain, a new concept is slowly growing. Instead of cooling the optic with liquid helium as in IRAS or ISO, it is possible to design a telescope protected by a conductive thermal screen cooled by passive radiators, as in the EDISON project. The former technic provides very low temperature, below 3 K, but at the expense of a short lifetime limited by the He consumption, while the latter authorizes only higher temperature, 40 K or more, but can be operated on a much longer period, up to 10 year. The other advantage of the passive cooling is that it can accommodate larger telescope, up to 3 m diameter in the EDISON project. Comparison of performances shows that the EDISON approach is a very good solution in the range 20 to 50 μm; at shorter wavelengths, a LHe cooled telescope is always better, while at longer wavelengths, the size of the telescope becomes more important due to the increasing confusion. Mixed missions, cooled by LHe at the beginning, and by passive radiators when all the helium is exhausted, might be worked out. It was already the COBE concept.

3 Dust properties and infrared emissions of galaxies

3.1 Dust models

In the far infrared, we are sensing the emission from interstellar dust. From 5 to 200 μm, the observations allow to probe different grains and different temperatures. The exact dust grain distribution is still a matter of debate, as are their compositions. Grains of silicate, iron oxides, dirty ice, and various forms of amorphous carbon coexist in space, but in unknown proportions. The main result of IRAS was a clear demonstration that infrared properties of galaxies cannot be reproduced by a single grain population. A mass distribution of grains is required to explain the shape of typical galaxy spectrum between 25 and 100 μm, since it cannot be reproduced by a single black body emission. At shorter wavelengths, the spectrum exhibits broad emission bands that are attributed to species of intermediate size between macromolecules and small grains. They are too small to be heated as real grains. When hit by a UV photon, they jump on excited states and release the energy by emitting light in large bands. The lines correspond to transitions of the carbon - carbon and carbon - hydrogen bonds, but several composite materials, amorphous carbon, coal, or poly-aromatic molecules (PAH) can reproduce the observed spectra. For the sake of simplicity, we shall keep PAH as a generic name for these particles. They are very important to understand the IRAS observations, since one of the most prominent lines, at 11.3 μm, lies in the middle of the 12 μm filter band pass. This emission line is so strong, that it dominates the flux received through the IRAS 12 μm filter.

Additional constraints on the nature of dust can be obtained from UV absorption, which depends on grain size and composition. UV absorption can be measured in the Galaxy or in front of the Magellanic Clouds. A consistent dust model has been presented by Desert et al (1991). Even if it might be still an approximation, it can explain a large part of the infrared properties of the galaxies. In the following sections, we will use it as a guideline. The next table summarizes the ingredients of the model.

From IRAS data, it is possible to draw a color color diagram, with far infrared colors, 60 μm to 100 μm ratio, versus the near infrared color, 12 μm to 25 μm (fig. 1). The vertical axis corresponds to an increase of large grain temperature, while the horizontal axis to a sequence of increasing PAH emission at a given dust temperature. The variation of the infrared colors with the distance from the central star in the California Nebula (Boulanger et al, 1988), (see fig. 1) allows to understand the physical processes that take place. This sequence is a sequence of decreasing heating caused by the UV radiation field. Close to the star, the UV radiation field is very large, the temperature of the grains increases, and the [60]/[100] ratio increases. When the local energy density becomes larger than 1.65 eV cm^{-3}, the PAH are destroyed, and the [12]/[25] ratio decreases due to the disappearance of the 11.4 μm emission line of the PAH. Far from the star, the UV radiation field and the large grain temperature decrease. When the energy

Properties of dust model		
component	**IR emission**	**UV absorption**
macro molecules PAH (≈ 80 atoms) **micro grains** amorphous carbon, + impurities (O, Si)	**Unidentified IR bands** 6.25, 7.7, 8.6 and 11.4 μ	**Far UV extinction** ≤ 200 nm
Very Small grains graphite (size ≈ 2.5 nm)	**thermal emission** IRAS 25 and 60 μ	**217.5 nm bump**
normal grains silicate + graphite size ≈ 30nm	**thermal emission** IRAS 60 and 100 μ	**visible + UV extinction**

density becomes smaller than 1.65 eV cm^{-3}, the PAH remain stable and dominate the 12 μm emission and contribute to a large fraction to the 25 μm emission. The [12]/[25] ratio remains constant. The farthest points, where the UV radiation field is equal to the mean Interstellar Radiation Field (ISRF), the colors are very similar to the colors of the galactic cirrus.

3.2 Integrated infrared colors of galaxies

IRAS has produced a large database of integrated infrared colors of normal galaxies The first analysis has focused on asample selected according to their infrared properties. The pioneering work is the analysis by Helou (1986) of the Catalog of Galaxies and quasars observed by IRAS. He found that the galaxies are distributed in a narrow region in the color-color diagram (see fig. 1) His interpretation calls upon 2 components, a diffuse component, analog to the Galactic cirrus, and hot thermal emission regions associated with star forming regions. When the star formation rate increases, the ISRF increases and the proportion of the hot component increases; the representative point of the galaxy moves to the left of the diagram. In the Helou interpretation, the distribution of the galaxy colors corresponds to a sequence of increasing star formation rate. Several authors have elaborated on this scheme. Rowan-Robinson and Crawford (1989) have demonstrated that for active starburst the star forming regions are optically thick in the UV and proposed a model with 3 components, galactic cirrus, optically thick H_{II} regions and active nucleus. For normal galaxies, the results do not differ very much from the Helou results.

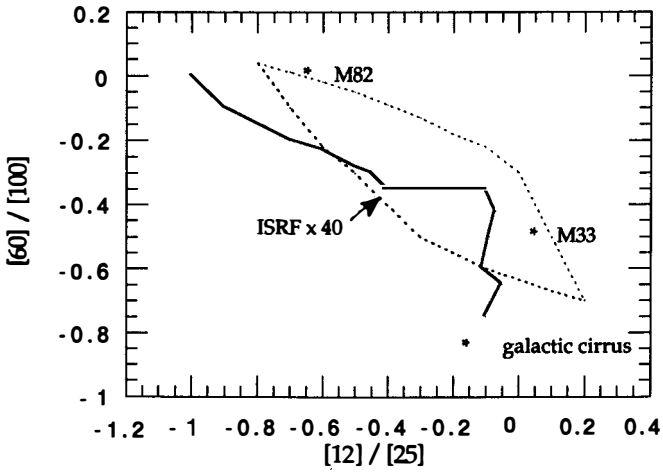

Figure 1: IRAS color color diagram

The log of the 60 μm to 100 μm ratio versus the log of the 12 μm to 25 μm ratio. When the dust temperature increases, the representative point moves up; when the PAH emission decreases, the point move to the left. Typical curves are given for a galactic nebula and for the envelope of integrated colors of normal galaxies.

Recently, Sauvage (1991), and Sauvage and Thuan (1992,a and b), have analyzed the infrared properties of a sample of galaxies selected according to their optical luminosity. The samples used by Helou, or Rowan-Robinson and Crawford were selected from infrared emissions. They were heavily biased toward late spirals or IR active galaxies. The Sauvage sample represents better what we call normal galaxies. He has analyzed the IRAS Faint Source Data Base and looked for correlations with the CFA catalog of galaxies. 1544 among 2445 of the CFA galaxies are detected by IRAS at least in 1 band. While all the galaxies fall on the normal Helou sequence, this works shows that there positions cannot be interpreted only in the framework of an increase of star formation rate. While there is a large dispersion of infrared colors among galaxies of the same morphological type, systematic variations of the infrared properties with type can be found. Some colors have monotonous variations with the morphological type, but some others have a peak for Sbc galaxies, and symmetrical variations towards elliptical on one side, and irregular galaxies on the other. In addition, IR luminosity is correlated with optical luminosity for the late type galaxies but not for early type. Sauvage and Thuan (1992,a) found a good correlation between $H\alpha$ and far infrared luminosity for spiral galaxies.

$$L_{H\alpha} \propto L_{FIR}^{0.7}$$

The non linearity is due to variation of the relative contribution of cold ISM (cirrus) and active star formation as a function of morphological type. The sequence from Irr to Sb is a sequence of increasing star formation efficiency, as was suggested by Helou. For early type galaxies, the analysis of Sauvage and Thuan (1992,b) shows that the sequence from Sb to E is a sequence of increased confinement of the dust near the galaxy center.

3.3 Spatially resolved galaxies

These interpretations are weakened because they rely on integrated properties. They should be confirmed by detailed infrared maps of galaxies with enough resolution to separate active star formation regions and diffuse emission, and to compare the IR emission regions to the optical emission profiles. The lack of spatial resolution has prevented IRAS from providing this information, except for some nearby galaxies, mainly from the local group.

Two nearby large spiral galaxies have been studied in detail, M33 (Rice et al, 1990), and NGC 6946 (Engargolia, 1991). In both of them, several components, diffuse emission, and star forming regions are clearly separated. Color maps show that all the regions of these 2 galaxies are spread along the Helou sequence, according to the local star formation rate. But, several points are surprising. In M33, 2 tracer of star formation, the far infrared emission and the 6 cm emission have different distributions. The scale length of far infrared emission is smaller than the scale length of the 6 cm. On small scale, the far infrared is more concentrated around star forming regions than non thermal radio emission. The origin of these differences is still unclear. The KAO observations of NGC 6946 have been made at 160 and 200 μm. They have revealed the presence of a cold dust component (15 - 25 K) distributed in an exponential disk. This disk was too cold to be seen by IRAS, and strengthen the need of observations at 200 μm to derive an accurate galaxy dust content.

Even for these large nearby galaxies, the IRAS resolution is hardly enough to resolve the star forming regions. This can be achieved only for the Magellanic Clouds. The first detailed analysis of infrared maps of the Magellanic Clouds was done by Schwering (1988). Two recent studies focused on correlation with other star formation tracers. Sauvage et al (1989) try to derive an ISRF indicator from the stellar population distribution and to link this indicator with the infrared colors. Due to scarcity of the stellar catalog, they get only a rough indicator of ISRF by computing the age of the younger stars in each pixel map. Although an accurate determination of local energy density is out of the possibility of this analysis, they found a stringent correlation between the ISRF indicator and the infrared colors. All the Magellanic Clouds points lie on the Helou sequence, and the younger regions, those with the largest ISRF, are located on the left part of the color color diagram. More precisely, there is a good correlation between age of the stellar population and infrared colors. The younger is the stellar population, the hotter are the large grains and the more deficient are the PAH. Stellar populations older than 2.10^7 years are not able to produce a significant ISRF

enhancement and the corresponding regions have the same infrared colors as the regions devoid of young stars. This analysis fully confirms the 2 component model, active star forming regions superposed to a diffuse cirrus like emission with a continuous transition between the 2 components according to the age of the last star forming event. With this decomposition, the star forming regions account for 60% of the far infrared emission. Xu et al (1992) try to correlate the far infrared emission with the radio continuum. By contrast to what is found in M33, the far infrared and the radio continuum have the same spatial extension. On small scales, as in M33, the far infrared and the radio continuum do not coincide. The more detailed maps of the Large Magellanic Cloud show that a large fraction of the far infrared emission comes from the interface region while the radio continuum emission comes from the whole star formation region. However, this last observation is at the margin of the capabilities of IRAS observations.

3.4 ISO observations

Concerning the observation of nearby normal galaxies, the advantages of ISO are twofolds, a better spatial resolution, and a better spectral resolution.

The better spatial resolution will be used to resolve this ambiguous superposition of radio continuum peak and far infrared peaks. It must be noticed that CO emission regions are not always associated with far infrared emission peaks, offsets are frequent, and CO peaks can be found without far infrared counterparts. While these tracers are linked with star formation process, the detailed mechanism is still unclear and will be solved by future ISO observations. The better spatial resolution will also be used to map more distant galaxies. We expect to obtain map as detailed as the IRAS maps of the Magellanic Clouds for galaxies up to 2 Mpc, and ISO will be able to resolve star forming regions from galaxies up to the distance of the Virgo cluster.

The better spectral resolution allows to map different species,

- ISOCAM can map the galaxies in most of the brightest PAH bands
- ISOCAM can image hot dust surrounding star forming regions with its 12 to 18 μm filter
- ISOPHOT can determine the cold dust content with its 100, and 200 μm filters, with a special emphasis on very cold dust, T < 30 K, which have escaped IRAS detection
- ionized gas can be imaged by ISOCAM in, Br_α, Ne_{II} (12.8 μm), and LWS in, O_I, 63 μm
- neutral gas can be imaged by LWS in, C_{II}, 157 μm.

According to these possibilities, a large fraction of the ISO central program is devoted to study of nearby galaxies. There is a joint study between ISOPHOT and ISOCAM of a complete sample of the Virgo cluster spiral galaxies, to determine their infrared spectrum. ISOPHOT will measure a large subsample of the Shapley

Ames galaxies. ISOCAM will obtain map of about 50 nearby galaxies, in continuum, and in PAH band, while LWS will provide the corresponding C_{II} maps.

4 Variation of 12 micron emission with metallicity

One of the most tantalizing observations is the maping of galaxies in the PAH bands. The IRAS observations have shown that systematic differences exist between the 12 μm emission and the 3 other far infrared bands. The Small Magellanic Cloud is more deficient in 12 μm than the Large Magellanic Cloud. This cannot be interpreted to an observationnal limitation, since they are at the same distance. The LMC, is itself deficient with respect to the galactic nebulae. Such a systematic trend, SMC, LMC, the Galaxy, reminds the abundance variation between those galaxies. Decreasing the abundance can explain the disappearance of the PAH by a larger ISRF due to the lower opacity of the interstellar medium. But, this effect can account marginally for the observed deficiency of 12 μm (Sauvage, 1991). More surprising, if one looks into a sample of blue compact and irregular galaxies with well established abundances and infrared colors (Sauvage et al, 1990), a clear correlation is found between the 12 μm / far infrared emission ratio and the metallicity (fig 2) as determined by the O/H abundance. It is not due to the decrease of dust/gas ratio with metallicity since the far infrared/blue luminosity ratio remains independent of abundance. This effect must be attributed to a low PAH emission relative to large grains in low metallicity galaxies.

A similar effect can be found in M33 where the 12 μm scale length is smaller than the far infrared one. When plotted against the radial variation of the O/H abundance (Zaritsky et al, 1990), the M33 points fall in the continuity of the irregular and blue compact galaxies points (see fig. 2).

Whatever the explanation, increase of UV ISRF density or true decrease of PAH/dust with metallicity, this result is in contradiction with what can be inferred from the UV extinction law. The smallest particles, and in particular the PAH, are responsible for the far UV extinction. From the observed decrease of PAH/dust ratio, one can deduce a lower extinction in the UV in the SMC, in the LMC, and then in the Galaxy. Observed UV extinction goes just the other way. Normalized to visible extinction, the UV extinction is the largest in the SMC, then in the LMC, and the smallest in the Galaxy.

The IRAS observations suffer from the unclear spectral signature of its 12 μm band. It contains PAH emission line but also continuum emission by hot dust. ISOCAM with its better spectral resolution will allow to know what is the origin of this 12 μm deficiency. A first sample of galaxies can be observed with the 5 to 8 μm filter which contains the main emission bands of PAH, and with the 12 to 18 μm filter which corresponds mainly to the thermal emission of hot dust. For the brightest galaxies, we can even make spectrophotometric maps with the CVF of

ISOCAM, to look for the relative variations of the dust and the PAH and look for correlations with the metallicicty and the local ISRF.

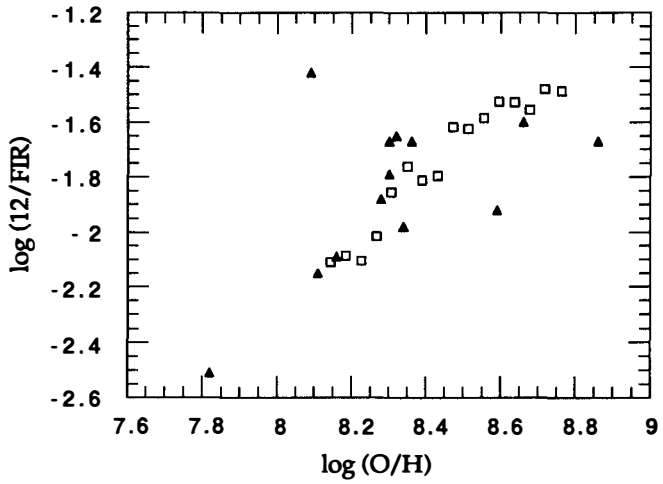

Fig. 3: Variation of log(12/(60 + 100)) infrared colors versus log(O/H) for Blue Compact and irregular galaxies (triangle) and M33 (square)

5. Far Infrared Lines

The following table summarizes the most important lines in the wavelength range of ISO.

Most of the studies so far have concentrated on the C^+ line. It is easily accessible from the KAO, and already 17 gas rich spiral galaxies have been mapped in C^+ (Stacey et al, 1991). The emission comes from photodissociation regions at interfaces between molecular clouds and ionized gas with $T \geq 200$ K and $n_{H2} \geq 10^3$ cm^{-3}. C^+ emission is the dominant cooling process of the interstellar matter. It accounts for 0.1 to 2% of the total far infrared emission. The C^+ emission increases strongly with the UV ISRF. Contrary to the continuum far infrared emission, CO and C^+ emission regions are well associated. Since C^+ is so well correlated to the ISRF, the C^+/CO ratio is a very good star formation indicator.

ion or atom	lines	location
O_I	63 μm	diffuse ISM + interfaces
	145 μm	
C_I	370 μm	
	609 μm	
C^+	158μm	interfaces
N^+	122 μm	HII regions
	205 μm	
N^{++}	57 μm	
O^+	52 μm	
	88 μm	

But comparison between the different far infrared emission lines shows contradictory results (Gry et al, 1992). COBE was able to measure the N^+ emission line at 205 μm in the galactic plane. It gives a C^+ / N^+ ratio of:

$$C^+ (158\ \mu m) / N^+ (205\ \mu m) \approx 0.1$$

But theoretical calculation shows that the expected ratio in H_{II} regions is:

$$C^+ (158\ \mu m) / N^+ (205\ \mu m) \approx 0.1 \quad (C/C_0) / (N/N_0)$$

With an ionization potential = 14.5 ev, N^+ is physically associated with HI regions, while with an ionization potential = 11.2 eV, smaller than the hydrogen ionization potential of 13.6 eV, C^+ is present in the H_{II} regions but also at the interfaces. Therefore, a C^+/N^+ ratio larger than the theoretical ratio for H_{II} regions was expected for the whole galaxy. There are several possibilities to explain this discrepancy, wrong atomic coefficients, C^+ optically thick, or C depleted in the dense ISM.

This question must be solved by detailed maps in some far infrared emission lines. In the galaxy, the distribution of C^+ can be obtained with the LWS on ISO. The optical thickness of CII can be determined by measuring $^{13}C^+$ (e.g., Stacey et al, 1991) with the KAO or later with SOFIA. This will solve the problem for our own Galaxy. Detailed maps of N_{II} and C_{II} in external galaxies must wait for FIRST.

6. Conclusions

The spectacular results of IRAS were the ultimate demonstration of the scientific capabilities of infrared space observatories. Analysis of these data have revealed a new world, starburst galaxies, ultra luminous galaxies, infrared quasars,... IRAS was an important step towards the comprehension of interstellar matter and star formation in normal galaxies. This review has shown that IRAS has open important new questions in this area. Future space observatories, in particular ISO, will have crucial problems to tackle, and we can predict that the scientific impact of these new generation observatories will be as significant as were the IRAS results

REFERENCES

Boulanger, F., Pérault, M., 1988, Ap.J., 330, 964
Désert, F.X., Boulanger,F., Puget,J.L., 1990, Astron. & Astrophys., 237, 215
Engargolia, G., 1991, Ap.J. supp., 76, 875
Helou,G., 1986, Ap.J. Let., 311, L33
Rice,W., Boulanger,F., Viallefond,F., Soifer,B.T., and Freedman,W.L., 1990, Ap.J., 358, 418
Rowan-Robinson,M., Crawford, J., 1989, MNRAS, 238, 523
Sauvage, M., 1991, these de spécialité, Université Paris VII.
Sauvage, M., Thuan, T. X., Vigroux, L., 1990, Astron. & Astrophys., 237, 296
Sauvage, M., Thuan, T.X., 1992, Ap.J., in press
Sauvage, M., Thuan, T.X, 1992, in prep.
Stacey, G.J., Townes, C.H., Poglitsch, A., Madden, S.C., Jackson, J.M., Herrmann, F., Genzel, R., and Geiss, N., 1991, Ap.J. Let., 382, L37
Stacey, G.J., Geiss, N., Genzel, R., Lutgen, J.B., Poglitsch, A., Sternberg, A., and Townes, C.H., 1991, Ap.J., 373, 423
Zaritsky, D., Elston, R., and Hill, J.M., 1990, Astron. J., 99, 1108

MULTI - POINT SPECTROSCOPY WITH OPTICAL FIBRES

Paul Felenbok
Observatoire Paris - Meudon
FRANCE

ABSTRACT

We present a review of multi- point spectroscopy as well on single objects in a large field as 2-D spectroscopy on extended objects. The technical problems related to optical fibres use, Focal Ratio Degradation and wavelength, are analyzed. A review of instruments planned or in operation in the major astronomical sites is given. The multi-object instrument (MEFOS) that our laboratory built for the 3.30m ESO telescope, is extensively described.

1. INTRODUCTION

We shall distinguish two types of multi-point spectroscopy : one is related to spread individual objects in a field and we will call this mode the MEDUSA mode and the other one related to point sampling in extended objects and we will call this mode the ARGUS mode. In the 2-D observations, the input fibres are packed together at the telescope focus and aligned at the output to form the entrance slit of the spectrograph. At

the detector, the spectrum of each fibre is individually identifyed giving a 2-D spectral information of the projected object.
Medusa type observations are possible also with slitlets or masks but this is limited to a small field on the sky, typically of the order of 10 arc minutes. The most recent instruments with this facility put in operation are the LDSS-2 at La Palma and the MOS/SIS at the CFHT. If larger fields are to be observed, only optical fibres could do it. This is why this solution is adopted for large surveys in one to three degrees fields.
For two dimension field spectroscopy, microlenses instruments can also be used but a special optical layout has to be implemented. This is the case for TIGRE, a visitor instrument in current operation at the CFHT.
For the multi-point spectrograph of the VLT, only optical fibres are foreseen for the Medusa and the Argus modes.

2. TECHNICAL ASPECTS OF OPTICAL FIBRES

Although optical fibres throughput improved impressively in the past few years, still some problems remain in the astronomical use of them, especially due to the fact that most of our applications are photon starving.

2.1 The chromatic transmission.

Traditional fibres have very good performances in the red part of the visible spectrum except around 720nm where the OH ions band is creating a deep absorption. Playing with the OH, it is possible to increase also the blue sensitivity and to get close to the Rayleigh limit of the material. By adding an hydrogen processing in the fibre manufacturing, it seems now possible to improve the blue performance with removing the OH absorption feature in the red . The new fibre from Polymicro has a smooth transmission starting at 60% at 350nm and reaching 87% at 500nm (for 25m length) and keeping this value to above 1μ. The length of the fibre has little impact in the red but counts very much in the blue. At 350nm, passing from 10m to 25m drops the transmission from 78% to 60%.

2.2 The focal ratio degradation (FRD)

When a light beam enters an optical fibre with a given aperture, at the exit of the fibre, this aperture is larger. This effect is increasing when the input beam is becoming smaller. This is due to geometrical imperfections of the fibre core and to micro bendings that are changing the symmetry of the internal total reflections at the core/cladding interface. This effect is artificially changing the projected sky scale and has to be minimized. This can be done by using large apertures for the input beam, as close as possible to the admittance fibre cone. in practice,

an input beam at F/2.5-3 is not suffering focal ratio degradation. This is the raison why focal reducers or microlenses are used to inject light to fibres.

3. 2-D INTEGRAL FIELD SPECTROSCOPY

To my knowledge, there are three sites where two dimensional spectroscopy with fibres is operated. The highest scientific output is coming from the CFHT.

3.1 SILFID at the 3.60m CFHT

The fibre system is made of 500 glass fibres, 397 for the object and the remaining ones for the sky. The fibres have a 100μm core with a 4μm cladding leading to an excellent packing ratio in an hexagonal shape covering 10 to 30 arc seconds on the sky, depending on the sampling chosen. This instrument is on a regular use at the Cass. focus of the 3.60m CFH telescope on QSO's, gravitational lenses, interacting galaxies, stellar jets, etc...

3.2 DENSEPAK at the 4m KPNO

This system is used at the RC focus of the 4m KPNO telescope. Its present configuration, called Dense Pak II, is a 7 x 7 matrix with 49 silica fibres with a 320μm core. At the telescope focus, the fibre cores subtend 2.1 arc seconds on the sky. The sampling is approximately 27 arc sec. giving the full array roughly a 16 x 19 arc sec. size. This instrument was used to search for intervening absorption lines systems along the line of sight to QSO's, the dynamic studies of Herbig-Haro objects and the gas shell surrounding the nova DQ Her.

3.3 HEXAFLEX at La Palma

This is a system of two bundles made of 61 fibres each. Each bundle has fibres of different fibre core diameter leading to different sampling scale on the sky. This device was used to observe the active galaxy NGC 4151.

4. MEDUSA MODE SPECTROSCOPY

4. 1 Plug boards.

The first observations made in Medusa mode where using a plug board. This is a metal plate placed in the telescope focal plane with drilled holes in the position of the objects to be observed. This technic, which is boring and expensive, is still the only one allowing a dense packing of

fibres and in fact, it is presently only used on dedicated telescopes for survey work. The following sites are equipped with this type of instruments :

ESO : OPTOPUS is implemented on the RC Cassegrain F/8 focus. It uses a 33 arc min. field with 50 independent fibres. To take in account the FRD of the fibre, the spectrograph collimator was replaced by an F/6 optics. This instrument is widely used and the large number of star plates to be precisely drilled is overflowing the mechanical shop capability. Its replacement by an automatic device is imminent.

AAO : FOCAP is implemented at the Cass. focus of the AAT. It was one of the first medusa type instrument in operation. It is now replaced by an automatic positioner, AUTOFIB, excepted for very special use.

KPNO : NESSIE is implement at the RC focus of the 4m telescope. It takes 40 objects in a field of 40 arc min. It is used in alternation with an automatic device, HYDRA, that is foreseen to replace it.

Mc Donald Observatory : This plugboard is implemented at the Ritchey - Chretien F/9 focus and uses 275 individual fibres in a field slightly above one square degree of sky. Two plugboards are used in alternation allowing rapid exchange at the telescope.

Las Campanas : This is the telescope with the larger field presently available for multi-object spectroscopy. It is a special optical design providing a two degree field at the Cass. F/7.5 focus of the 2.5m telescope with 50 independent fibres. This system is presently upgraded to accommodate up to 128 fibres.

DSS-NGC (Digital Sky Survey of the Galactic Northern Cup) : This is a project to build a 2.5m telescope with a 3 degrees field for galaxies red shift surveys. The plugboard is designed to handle 600 fibres that are feeding two spectrographs with a blue and a red camera each.

4.2 Automatic positioning

To avoid drilling focal plates and increase flexibility, automatic positioning systems are under current development in different sites. Two main systems are mainly in use : robot or arm systems.

4.2.1 Robot positioning.

The robot systems are based on a single positioning gripper travelling on X-Y slides. The optical fibres are stored around the focal

field and set at the object coordinates one after the other. The fibre buttons are locked in place by magnetic or pneumatic means are coupled to total reflection prisms that are bending the optical beam living the fibres in a radial display. This type of instrument is under construction or in use at the following sites :

AAO : AUTOFIB is taking over the plugboard device on the AAT. It addresses 64 objects in a 40 arc minutes field, at the Cassegrain. The locking mechanism is magnetic. There is an upgrading project, the two degrees field (2dF). The AAT will be provided with a two degrees corrector at the prime focus and a 200 fibres positioner will lock the fibres in place. Two spectrographs are used. To save configuration time, one focal board is processed when a other one is gathering object light.

KPNO : Hydra is implemented at the Cass. focus of the 4m telescope. It displays 100 fibres in a 40 arc minutes field.

Lick Observatory : There is a project to implement a one degree prime focus corrector to use with optical fibres. The coupled spectrograph is designed to accept up to 300 fibres.

4.2.2 Arm positioners

To save configuration time and to be able to correct fibre position in real time, some designs, called of the arm type, have been constructed. This instruments are made of a series of independent arms that are able to sweep a sector of the field. Each arm is fitted with one or two fibres hold permanently. Due to space occupancy, only a small number of fibres can be used in such a device. The arm positioners in operation at different sites are :

Steward observatory : MX works at the Cass. focus of the 2.3m telescope. It is the prototype of the arm positioners. It is made of 32 arms set like " fishermen around a pool " on a 45 arc minutes field.

CTIO : ARGUS is the first arm system implemented on a prime focus. It has 24 arms and works in 50 arc minutes field. The 4m prime focus is F/2.8 ideally suited for optical fibres light input.

ESO : MEFOS , that will be extensively described later, is implemented on the 3.60m ESO telescope prime focus at F/3.12. It has 29 arms for object spectroscopy and one for guiding.

5. MEFOS (MEUDON ESO FIBRE OPTICAL SYSTEM)

5.1 Introduction

Following the previous experiments conducted by J. Hill at Stewart Observatory and T.Ingerson at CTIO, we constructed an optical fibres actuator instrument of the arm type, MEFOS (Meudon-ESO Fibre Optical System). We choose the arm approach instead of the robot design because we wanted a real time control of all the device. This allows real time adjustment to compensate for atmospheric refraction or a fast exchange between object and sky fibres leading to a better sky subtraction. All 30 arms are moving together, saving set up time.

At the 3.60m telescope prime focus at ESO, using a triplet corrector, a field of one degree is available for faint objects spectroscopy with the B&C spectrograph located at the Cassegrain focus. This will be mainly used for extragalactic work due to the low spectral resolution available. For stellar work, the fibres will have to go to a bench spectrograph to be built in the next future. The prime focus F/3 input aperture is well suited for the best optical fibres performances as far as the focal ratio degradation is concerned. Of course, no front lenses are needed and different fibres cores can be used depending if point sources (QSOs) or extended sources (Galaxies) are observed.

5.2 The mechanical setup

The arm system is built to handle a one degree field at the ESO 3.60m telescope and this is a geometric area of 24cm in diameter. Only optical fibres are able to pick-up objects in such a big surface. We are using 30 arms set in a circle like "fishermen around a pool". Each arm is sweeping a triangular zone by rotation and translation. The prototype was built with step motors, as on MX or ARGUS. We found that this is a little dangerous because unexpected friction due to thermal effect or mechanical strain may result in step jumping, which drops the setting precision. To avoid this draw back, the final system uses DC motors and optical encoders. This instrument is fixed on the top of the triplet corrector with a tiltable interface for precise adjustment between the flat focal field and the fibres travelling surface.

5.3 The optical design

At the prime focus, with the triplet corrector, the focal ratio is F/3.12 and the scale is 52μm per arc second. With this aperture, optical fibres are used without focal ratio degradation and the spectrograph collimator is an F/3. A 100μm fibre is well suited for point like sources and for galaxies, 200μm fibres, are a better choice. We adopted 135μm

core Polymicro FBP type fibres, with a flat efficiency starting from 450nm. On the same tip as the spectrographical fibres is located an image conducting fibre bundle, 1.9mm x 1.9mm square, catching 36 arc sec. on the sky. When the arm is send to the object coordinates, it is the image bundle that goes to the object position. All the image bundles being projected to a CCD, after a short integration , the object position is precisely known on the image bundle once the CCD frame is analyzed. The positions between the single fibres and the bundle being fixed and known with precision, the correct offset is given to the arm for a perfect object fibre match. This procedure is applyed to every object located inside the image bundle area, so objects with coordinates poorly known, say 15 arcsec., could be used. The distance between the image bundle and the single fibre is of the order of few mm, and during the offset no additional error could occur. This means that in the first stage, once the object is located in the bundle, all the errors are taken into account. This is valid for mechanical bending and back lash, thermal expansion and optical aberrations.

5.4 The electronic design

The acquisition CCD camera for the object location in the image bundle uses a Thomson CCD with 1024 x1024 pixels of 19μm. The CCD is cooled with a two stages Peltier device.This is possible because the exposure time will never exceed few minutes and the readout noise will be small compared to the sky photon noise. A 14 bits A/D converter is used leading to a sufficient dynamical range and a fast readout.

The electronics driving the arms is based on a central master card located in a PC/AT computer and connected through an optical fiber to slaves cards located on the arms body. The master card is made around an 8 bits 80451 microcontroller and the slaves, all identical, are circuits made around a 80535microcontroller. Specifications given for electronic design of the arms are: time of positioning as shorter as possible, below 5 minutes, with a re-positioning accuracy of 10 μm. The PC/AT computes the right place of all fibres in the objects field, and transmits the coordinates to a master microcontroller located in the PC, and directly interfaced to the 8bits PC bus.

5.5 The software

The software that drives all the instrument is written in C language and is implemented on a PC/AT computer.It reads the object names and coordinates supplied on a floppy disk by the users community. The object arm assignment is made by software using the Hungarian algorithm for the best match and avoiding collisions.Once the arms are send in position to record the object in the image bundle, the software is processing the

CCD image to find the object position and sends the appropriate offset to each arm.

There is also an option that allows the observer to select the observing field of the instrument between the field generated by the object coordinates table on a graphic display.

5.6 The first test on telescope

The first test run at La Silla took place in February 91. MEFOS was in a 9 arms configuration and the B & C spectrograph was set with the F/3 collimator (1st Optopus version) and the F/2 blue dioptric camera. The Grating No. 15 (172 A/mm) and a thinned Tektronics CCD 512 x 512 with pixels of 27μm where used. At the beginning of the observations, the arms could not reach the proper field configuration because there was a bad scale factor introduced in the program and the field distortion was not included. This is now corrected.
Nevertheless, once the objects were inside the image fibres and analyzed with the acquisition program, the soft could send the spectral fibres to the objects with relatively good accuracy : less than 0.4". This error was difficult to estimate because of two factors : the spherical aberration produced by the misalignment of the triplet corrector and secondly because a telescope drift during the acquisition exposure time. In the laboratory, the same procedure yield a much better accuracy (less than 10 μm= 0.17" for the worst arm). Nevertheless, the same procedure applied at the telescope does not give the same result and this is due to the fact that during the CCD exposure time the telescope is not guided automatically but only is in tracking mode, so small image shifts can occur. This is fixed now by devoting one arm, the North one, to field recognition and permanent tracking.

The most significantly scientific exposure was a field of few galaxies with magnitudes between 17.5 and 19.9. This field was already observed before with Optopus (C. Balkowsky and R. Kraan). The spectra of a galaxy B = 18.6, z = 0.06, member of that field, taken in one hour reached a S/N of 50.
The next technical run in full configuration is scheduled in October 92 with a general, sheared risk use, in 93.

5.7 Acknowledgements

We are happy to thank G.Avila who supplied the test fibres and assisted us during observations, his advices where always very valuable.The design and construction of this instrument was done under the responsibility of André Collin and the mechanical shop of the CNRS at Bellevue.We are grateful to all colleagues that helped us during the test as well in Chile (A.Gillotte, M.Maugis, O.Lavin and W.Eckert) as in the preliminary data analysis(P.Focardi).

VII - THEORIES OF THE HUBBLE SEQUENCE

THE ORIGIN OF THE HUBBLE SEQUENCE

Richard B. Larson
Yale Astronomy Department
Box 6666
New Haven, Connecticut 06511
U.S.A.

ABSTRACT

A brief review is given of the aspects of galaxy formation and evolution that are relevant to understanding the origin of the Hubble sequence. The variation along the Hubble sequence of the gas content and related properties of galaxies is the result of a variation in the rate of galactic evolution that is probably controlled mainly by the underlying mass distribution, which is thus the most fundamental characteristic to be explained by theories of galaxy formation. Much recent theoretical work and observational evidence, including the fossil record for our Galaxy, support the view that most large galaxies are formed by the merging or accretion of smaller units. The structure of the resulting galaxy depends on the nature of the subunits: if they are mainly stellar, the result will be a bulge-dominated galaxy, while if they are mostly gaseous, the result may be a galaxy with a dominant disk. Star formation processes and mergers are both expected to proceed most rapidly in the densest parts of the universe, resulting in the formation of mostly bulge-dominated galaxies in these regions. This may account for the observed relation between morphology and environment, although continuing environmental effects including gas removal and the destruction of disks by interactions may also play an important role.

1. The Systematic Properties of Galaxies

Like all natural phenomena, galaxies exhibit a mixture of regularity and irregularity, or of order and chaos, in their properties. Hubble looked for the order among their properties, and noted several correlations that he adopted as the basis of his proposed classification scheme. As has been emphasized by Buta, Madore, and Gavazzi in this volume, galaxies may have a large number of measurable characteristics, but only a few parameters suffice to account for most of the variability in their properties. Principal component analysis shows that there are just two dominant parameters, and that they can be identified as 'scale' and 'form', or equivalently as luminosity and Hubble type (Whitmore 1984). This finding supports the utility of Hubble types as a predictor of other properties of galaxies, and also suggests that the Hubble classification scheme reflects important underlying regularities in the processes of galaxy formation and evolution.

Although the Hubble types and luminosities of galaxies are almost completely uncorrelated in the sample studied by Whitmore (1984), some correlation is found when a larger range of types is considered, the later-type galaxies generally being fainter (de Vaucouleurs 1977). Some authors have even suggested that the basic properties of galaxies are largely determined by a single parameter, which may be the total mass (Tully, Mould, and Aaronson 1982), the virial velocity (Lake and Carlberg 1988b), or just the bulge mass (Meisels and Ostriker 1984).

The classification sequence proposed by Hubble (1936) for spiral galaxies is based on three characteristics, all of which generally increase along the sequence: the disk-to-bulge ratio, the openness of the spiral pattern, and the resolution of the arms into bright knots. The resolution of the arms reflects the level of star formation activity, and this depends on the gas content, which also increases systematically along the sequence. As has been discussed by Eder in this volume, the S0 class introduced by Hubble as a transition between spirals and ellipticals can, with present data, be understood as forming a smooth extension of the spiral sequence to systems with weak or absent spiral structure and with little or no gas or present star formation. Weak disk components even appear to be present in some elliptical galaxies, which may thus constitute a further continuous extension of the sequence to systems that are almost pure bulge (Bender 1990).

The Hubble classification scheme does not, however, apply to dwarf galaxies, which differ fundamentally in several respects from the giant galaxies studied by Hubble; some of their properties have been reviewed by Ferguson in this volume. The dwarf galaxies do not exhibit distinct disk and bulge components, but they nevertheless vary greatly in their content of gas and young stars, and range from gas-poor dwarf ellipticals to gas-rich dwarf irregulars. The dwarf ellipticals and dwarf irregulars may in fact be

closely related, and may form a sequence of objects that differ mainly in gas content (Kormendy and Djorgovski 1989; Da Costa 1992).

It has been recognized since Hubble's time that the morphological properties of galaxies are correlated with their environment: spiral galaxies mainly inhabit low-density field regions, while ellipticals are concentrated in dense clusters. Several studies have shown that the mix of morphological types shifts steadily toward earlier types with increasing density of the environment (Oemler 1974; Dressler 1980; Postman and Geller 1984; Haynes 1987). A related finding is that the fraction of blue star-forming galaxies in clusters decreases with increasing cluster size (Oemler 1992). The 'morphology-density relation' clearly contains important clues about the formation and evolution of galaxies, but its interpretation has continued to be a subject of much discussion (*e.g.*, Dressler 1984; Salvador-Solé, Sanromà, and Jordana 1989; Whitmore and Gilmore 1991; Oemler 1992; see also the contributions of Salvador-Solé and Whitmore to this volume). The simplest and most obvious interpretation would be that the formation of disks is favored in low-density environments, while the formation of spheroids is favored in denser regions. However, environmental effects can also influence galactic morphology; for example, the galaxies in clusters may be gas-poor and typically of earlier Hubble types than field galaxies because of gas removal processes or because of interactions with other galaxies that have triggered enhanced star formation (Kenney 1990; Oemler 1992). The sweeping away of gas envelopes in dense environments might have a similar effect if gas infall is important for galactic evolution (Larson, Tinsley, and Caldwell 1980). It is even possible, as has been suggested by Whitmore in this volume, that the destruction of disks by violent interactions in forming clusters could account for the morphology-density relation by destroying most of the late-type galaxies in dense environments; in this case, the morphology-density relation might actually be telling us more about galaxy destruction than about galaxy formation.

The challenge is thus to account for the regularities embodied in the Hubble sequence and the morphology-density relation on the basis of an understanding of the processes of galaxy formation and evolution, and perhaps destruction. It will be argued in Section 2 that the variation of some of the properties of galaxies along the Hubble sequence results from a variation in the rate of galactic evolution that mainly depends on the underlying mass distribution. The most basic property of galaxies to be accounted for by theories of galaxy formation is then the internal mass distribution, as reflected for example in the disk-to-bulge ratio. Subsequent sections will discuss some current ideas about galaxy formation that are relevant to understanding the origin of the Hubble sequence, as well as some of the supporting evidence.

2. Galactic Evolution and the Hubble Sequence

Of the properties of galaxies that vary along the Hubble sequence, the gas content and related properties such as the star formation rate and the spiral arm structure may be regarded as secondary characteristics that depend only on the rate at which galaxies deplete their initial gas supply. The early-type galaxies have evidently evolved faster than the late-type galaxies in this respect, having consumed more of their gas because of higher past rates of star formation. Direct evidence that the timescale for gas depletion increases along the Hubble sequence is provided by the results of Donas *et al.* (1987) for the star formation rates and gas depletion times in a large sample of spiral and irregular galaxies, which show that at least along the later part of the sequence, the gas depletion time increases by roughly a factor of 4 from the Sbc galaxies to the irregular galaxies. This dependence of the timescale for galactic evolution on Hubble type is an important feature of the Hubble sequence that must be accounted for by any understanding of star formation processes and star formation rates in galaxies (Larson 1983). Here we summarize briefly why the timescale for gas depletion might be expected to depend on basic structural properties such as the disk-to-bulge ratio and the underlying mass distribution.

On the largest scales, star formation begins with the formation of giant molecular clouds and cloud complexes, and the star formation rate therefore depends on the rate of formation of these massive clouds and complexes. The formation of such large gas concentrations is almost certainly due primarily to the self-gravity of the interstellar medium in galaxies, and in this case the rates of cloud formation and star formation are controlled mainly by the timescale for gravitational accumulation of the gas (Larson 1987, 1988, 1992; Elmegreen 1990a,b). The gas layer in a galaxy is gravitationally unstable if the Toomre stability parameter $Q = c\kappa/\pi G\mu$ is smaller than unity, where c is the velocity dispersion of the gas, κ is the epicyclic frequency, and μ is the surface density; such gravitational instabilities may occur, for example, in irregular galaxies, and may be responsible for driving star formation in them. In spiral galaxies like our own, a true gravitational instability probably cannot occur because Q is actually somewhat larger than unity, but large density enhancements can still be generated by the closely related phenomenon of 'swing amplification', which is a kind of truncated instability (Toomre 1981, 1990). Evidence that swing amplification is responsible for driving much of the star formation in spiral galaxies is provided by the fact that star formation is observed to occur only where the surface density of gas exceeds a threshold that corresponds to a value for Q of about 1.8 (Kennicutt 1989), which is approximately the value of Q below which swing amplification becomes important; thus star formation is observed to turn on at just the same value of Q at which swing amplification turns on.

The timescale for gravitational instability or swing amplification effects is approximately $\tau \sim c/\pi G\mu$, and thus it depends on both the velocity dispersion c and the surface density μ of the gas. Two possible limiting cases have been considered by Larson (1988, 1992) in discussing the implied parameter dependences of the star formation rate. One possibility is that the velocity dispersion c is constant; in this case, the timescale for gas aggregation is inversely proportional to the gas surface density μ, and the resulting star formation rate per unit area is then proportional to μ^2, which is similar to the quadratic dependence on volume density originally proposed by Schmidt (1959). This prediction does not, however, provide any ready basis for understanding why the gas depletion timescale should increase along the Hubble sequence, since the average gas surface density does not vary much along this sequence. A second, perhaps more realistic assumption is that the stability parameter Q is constant, as is found to occur in numerical simulations of galactic disks where the value of Q is regulated dynamically at a value of about 1.7 (Carlberg 1987; Gunn 1987). The timescale for gas accumulation $\tau \sim c/\pi G\mu = Q/\kappa$ then becomes inversely proportional to κ, *i.e.* proportional to the epicyclic period, which in turn is approximately proportional to the galactic rotation period; thus the rotation period may be what sets the basic clock rate for the evolution of galaxies. Since galaxies with later Hubble types generally rotate more slowly than the earlier types (Rubin *et al.* 1985), they would then be expected also to consume their gas more slowly, as is observed. Quantitatively, since the typical rotation period increases by roughly a factor of 3 along the Hubble sequence, the gas depletion timescale would be expected to increase by about the same factor along the sequence, which is roughly consistent with the evidence noted above.

We can also understand the increase in the openness of the spiral pattern along the Hubble sequence in terms of the gas content and the rotational properties of galaxies. In gravitational theories of spiral structure, the spacing of the arms depends on the quantity $\lambda_{\rm crit} = 4\pi^2 G\mu/\kappa^2$, which is the maximum wavelength of unstable axisymmetric perturbations in a thin disk (Toomre 1964); it is also approximately the arm spacing for which swing amplification is most important (Toomre 1981, 1990; Carlberg and Freedman 1985; Carlberg 1987). A more open spiral pattern is therefore predicted if a galaxy has either a higher gas surface density or a lower epicyclic frequency; since the gas surface density does not vary strongly with Hubble type while the epicyclic frequency generally decreases along the Hubble sequence, the arm spacing is then predicted to increase along the sequence, just as is observed.

The variation of the gas content, star formation rate, and spiral arm properties of galaxies along the Hubble sequence can thus be understood as depending mainly on basic structural characteristics such as the mass distribution and the rotation rate. Galaxies that rotate faster are predicted to have lower fractional gas contents and more tightly

wound arms, so that two of the three defining characteristics of the Hubble sequence (the degree of resolution and the openness of the spiral arms) can be accounted for just in terms of the galactic rotation rate. If rotational shear is itself an important effect tending to drive star formation, a centrally condensed mass distribution might enhance the gas depletion rate and thus help to explain the correlation between gas content and disk-to-bulge ratio along the Hubble sequence (Larson 1983). It is clear in any case that the essential characteristic of galaxies that theories of galaxy formation should aim to account for is their internal mass distribution. To the extent that the morphology-density relation results from galaxy formation processes, it is necessary in particular to explain why galaxy formation in dense environments should produce systems with dominant bulges; also, to the extent that Hubble type correlates with mass, it is necessary to explain why bulge-dominated galaxies tend to be more massive than disk-dominated galaxies.

3. Protogalactic Collapse and the Hubble Sequence

According to the conventional view, galaxies like ours were formed by the collapse and simultaneous chemical enrichment of extended protogalactic gas clouds. Evidence suggesting that our Galaxy was formed by a collapse process was presented in an influential paper by Eggen, Lynden-Bell, and Sandage (1962), and a recent discussion of this evidence has been given by Sandage (1990). Inspired by this idea, many efforts have been made to model numerically the collapse of protogalaxies and to explain on this basis the basic properties with which galaxies are formed. In particular, much attention has been given to modeling the formation of disks and bulges and to trying to account for the variation of the disk-to-bulge ratio along the Hubble sequence. Collapse calculations yielding both bulges and disks have been made by Larson (1976a), Gott and Thuan (1976), Carlberg (1985), Lake and Carlberg (1988a), Burkert and Hensler (1988), and Katz (1992); reviews of the early work were given by Larson (1976b) and Gott (1977), and a more recent review of the subject has been given by Larson (1992).

Larson (1976a) and Gott and Thuan (1976) suggested that the disk-to-bulge ratio of a galaxy is determined primarily by the star formation rate in the initial protogalactic cloud: if star formation is sufficiently fast that most of the gas is turned into stars before the collapse is completed, the resulting galaxy will have a dominant spheroid, while if star formation is much slower or is delayed, most of the gas may settle into a disk before forming stars. Thus, an earlier Hubble type would be predicted to result when star formation proceeds more rapidly in relation to the collapse time. If the star formation rate depends on the gas density in accordance with the Schmidt law or a similar relation, then the ratio of the star formation timescale to the collapse

time decreases with increasing gas density, so that one might expect galaxies of earlier Hubble type to form in regions where the density is higher. This effect might account qualitatively for the observed morphology-density relation (Larson 1976b; Gott 1977), although the results of Larson (1976a) suggest that the magnitude of the effect is not quantitatively sufficient to account for the full observed range in disk-to-bulge ratio.

Larson (1976a) and Gott and Thuan (1976) also noted that star formation would be expected to proceed more rapidly in protogalaxies if their gas is strongly clumped. The clumpiness of a protogalaxy might then be important in determining the morphological type of the resulting galaxy. Clumping might also play an important role in the dynamics of the collapse through its effect in redistributing energy and angular momentum and thus allowing the formation of a dense and slowly rotating spheroid (Lake and Carlberg 1988a). Simulations of the collapse of systems of stars have in fact shown that gravitational interactions in a clumpy or inhomogeneous system tend quite generally to produce a structure like that of an elliptical galaxy or spiral bulge (*e.g.*, van Albada 1982; Villumsen 1984; Katz 1991). An extreme case of the effect of interactions on morphology is provided by galaxy mergers, in which the transfer of energy and angular momentum from the visible stars to the dark matter is found to be very effective in producing a centrally condensed and slowly rotating stellar system closely resembling an elliptical galaxy (Barnes 1988, 1989, 1990). The cosmological models and the observational evidence to be reviewed below make it appear very likely that interactions between subsystems are indeed involved in the formation of many elliptical galaxies and spiral bulges. Recent protogalaxy calculations based on current cosmological models will be discussed further in Section 5, following a brief review in Section 4 of the cosmological context of galaxy formation.

4. The Cosmological Context of Galaxy Formation

Most of the calculations mentioned above have adopted simple and idealized initial conditions for protogalaxies, but there has been much progress in recent years in understanding the structure and evolution of the universe and the likely initial conditions for galaxy formation. It is now recognized that the universe is inhomogeneous and hierarchical on a wide range of scales, and most current cosmological models assume that the universe was initially inhomogeneous on subgalactic scales as well. The presently observed galaxies and clusters of galaxies may then have been formed by the progressive merging of smaller structures into larger ones, and galaxies may simply be the smallest structures that have survived as discrete units (Peebles 1974, 1980; Press and Schechter 1974).

A number of surveys have shown that the large-scale structure of the universe is complex and intricate, consisting of a network of filaments, sheets, and voids of various sizes (*e.g.,* Maddox *et al.* 1990; Giovanelli and Haynes 1991). On scales larger than those of clusters of galaxies, this structure still reflects that of the pre-galactic universe, since there has not yet been time for gravitational clustering to erase the initial conditions on these scales; the observed density fluctuations are thus simply an amplified form of the initial fluctuations. On scales between about 5 and 50 Mpc, the observed galaxy distribution is found to be hierarchical and approximately self-similar, with a fractal dimension of about 2.2 (Einasto 1991; Guzzo *et al.* 1991); such a fractal dimension would be characteristic, for example, of an open filamentary network or sponge-like structure, which indeed is a good description of the observed appearance of the universe on these scales. In a fractal structure of dimension 2.2, a subunit of radius R has a mass proportional to $R^{2.2}$, a dependence similar to the approximate scaling law $M \propto R^2$ relating the masses and radii of giant galaxies. The corresponding relation between galactic mass and virial velocity, $M \propto V^4$, is essentially equivalent to both the Tully-Fisher (1977) relation observed for spirals and the Faber-Jackson (1976) relation for ellipticals. Thus these basic scaling laws for galaxies may be explainable if the pre-galactic universe was self-similar in structure with a fractal dimension of ~ 2 on scales down at least to those of individual galaxies.

Numerical simulations of the growth of structure in the universe, mostly based on the popular 'cold dark matter' (CDM) model, have successfully reproduced many aspects of the the large-scale distribution and clustering of galaxies, and even some of the gross properties of individual galaxies; for example, they predict approximately flat rotation curves, and can also account roughly for the Tully-Fisher and Faber-Jackson relations (*e.g.,* Frenk *et al.* 1985, 1988; Zurek, Quinn, and Salmon 1988; Carlberg 1988; Carlberg and Couchman 1989; Navarro and Benz 1991; Evrard, Summers, and Davis 1992). All of these simulations predict that in the densest parts of the universe, small concentrations of dark matter or dark halos rapidly merge to form larger ones. Gas condenses into these merging halos to form compact galaxy-like objects, which in the most detailed simulations (Evrard *et al.* 1992) are sometimes disks. These 'galaxies' also sometimes merge when their halos merge, but because of their smaller cross sections they experience less merging and thus tend to form groups or clusters of objects embedded in common dark halos. By contrast, merging is much less frequent in the low-density parts of the universe, and the dark halos and embedded galaxies that form in these regions grow only slowly by the accretion of diffuse matter. These results suggest that considerable early merging of smaller systems into larger ones may have occurred in the densest parts of the universe, while merging was much less important in low-density regions. Although the validity of the standard CDM model has been a subject of debate (*e.g.,* Peebles *et*

al. 1991), the qualitative results of these simulations do not depend critically on the details of the model but are generic to any cosmology in which structure develops in a bottom-up fashion (Efstathiou 1990).

These results may account for the morphology-density relation if the products of the mergers can be identified as elliptical galaxies and bulge-dominated spirals. The possible formation of elliptical galaxies by the merging of smaller systems, as suggested by Toomre (1977), is supported by considerable observational evidence (Schweizer 1990) and extensive numerical simulations (Barnes 1990), as again reviewed in this volume by Schweizer and Barnes. In the simulations reported here by Evrard, about half of the 'galaxies' in proto-cluster regions have experienced mergers with objects of comparable mass, while only about one-quarter of the objects in small groups have experienced such mergers and only about 15 percent of those in field regions have merged. These numbers are similar to the present fractions of elliptical galaxies in these different types of environments, suggesting that mergers may indeed be able to account for the correlation of morphology with environment. Because mergers also increase the sizes of galaxies, elliptical galaxies and early-type spirals would be expected to be more massive on the average than later-type galaxies; this prediction is again consistent with the available evidence (*e.g.,* Binggeli 1987), and might account for the correlation between Hubble type and luminosity noted in Section 1.

Environmental effects such as those mentioned in Section 1 may, of course, also play an important role in accounting for the observed morphology-density relation. Clarifying the relative importance of the various processes involved will be an important topic for further research.

5. Protogalactic Collapse Revisited

The most recent and detailed simulations of protogalactic collapse by Katz and Gunn (1991) and Katz (1992) have calculated the evolution of protogalaxies modeled as galaxy-sized pieces of a standard cold-dark-matter universe. As in the cosmological simulations discussed above, much small-scale structure is present during the early stages of evolution, and there is a chaotic period during which interactions and mergers between clumps build up an extended dark halo. Stars that have formed by gas condensation in the dense cores of these clumps are at the same time dispersed to form a stellar spheroid. The remaining gas then organizes itself more gradually into a disk in a process that is itself somewhat chaotic, since the disk is initially irregular and clumpy and retains a significant tilt with respect to the halo. These results illustrate that in reality it is probably not possible to draw a sharp distinction between the collapse and merger

pictures of galaxy formation, since elements of both are almost certainly involved in the formation of most large galaxies (Kormendy 1990; Larson 1990b).

A result of particular interest for the origin of the Hubble sequence is that random differences in the initial conditions can lead to substantial differences in the final disk-to-bulge ratio: protogalaxies that by chance contain more large clumps produce galaxies with larger spheroids. This result supports the earlier suggestions noted in Section 3 that the clumpiness of a protogalaxy may play an important role in determining the Hubble type of the resulting galaxy. Since this clumpiness is subject to statistical variations, the Hubble type of a galaxy might in part be of random origin, and this might account for some of the scatter in the correlations discussed in Section 1.

Another result found by Katz (1992) is that small satellite systems sometimes form during the initial chaotic stage of evolution, and they may survive as separate small galaxies for several orbits before merging with the main galaxy. The accretion of such satellite systems may account for the origin of the globular clusters in the outer halo of our Galaxy (Searle and Zinn 1978; Freeman 1990), a possibility that is strengthened by the evidence that these clusters have a significant age spread (see Section 7). Satellite accretion during the early stages of disk evolution might also account for the origin of the 'thick disk' component of our Galaxy (Freeman 1990, 1991; Katz 1992; Section 7).

6. Effects of Accretion and Interactions

While they appear to have many realistic features, the protogalaxy models described above are still simplified in that they include only the matter that was initially located inside an artificial spherical boundary. A real forming galaxy will be surrounded by additional matter that may continue to interact with and be accreted by it for an extended period of time. The infall of additional dark matter may build up the dark halos of galaxies (Gunn 1977), while the accretion of stars may build up galactic spheroids (Gott 1977) and the infall of gas may build up disks (Oort 1970; Larson 1972, 1976b; Gunn 1982, 1987). These authors all imagined the infalling matter to be diffuse and smoothly distributed; however, in an inhomogeneous and hierarchical universe like that described above, it seems more likely that much of this infalling matter will already have condensed into galaxies, in which case the accretion will take the form of captures or mergers. Evidence that elliptical galaxies grow by capturing smaller galaxies is provided by the frequent occurrence in their outer envelopes of shell-like features (Schweizer and Ford 1985; Prieur 1990) which are very similar to those predicted by numerical simulations of such captures (*e.g.*, Hernquist and Quinn 1989). The evidence that spiral galaxies also grow by accretion is less clear, but some of the disturbances observed in

the outer parts of spiral disks might be the result of accretion events (Larson 1976c; Binney 1990; Sancisi *et al.* 1990; Kamphuis and Briggs 1992; Sancisi, this volume).

The accretion of new material and the disturbances caused by interactions with surrounding galaxies may significantly influence the morphological types of galaxies. The acquisition of new gas may build up disks, but the effects of interactions are more likely in general to drive the morphology of galaxies toward earlier types by disrupting disks, removing gas, and building up spheroids. Such effects may help to explain the continuous shift in the morphology distribution of galaxies toward earlier types with increasing density of the environment (*e.g.*, Haynes 1987), especially if this shift is partly caused by effects acting over the entire lifetimes of galaxies, as suggested by Oemler (1992).

7. The Fossil Record for Our Galaxy

The above picture of galaxy formation by the merging and accretion of subunits can be tested for our Galaxy using the fossil record provided by the oldest stars and clusters, especially the globular clusters of the Galactic halo. Recent reviews of the evidence concerning the early evolution of our Galaxy have been given by van den Bergh (1990) and Larson (1990a, 1992). A central and much debated issue has been whether the globular clusters show a measurable age spread significantly exceeding 1 Gyr, since a smaller age spread would be consistent with the near free-fall protogalactic collapse proposed by Eggen, Lynden-Bell, and Sandage (1962), while a larger age spread would provide evidence for a more prolonged and chaotic process of galaxy formation, possibly involving the merging of smaller systems. The formation of the Galactic halo over a period of several Gyr by the accumulation of 'protogalactic fragments' was originally suggested by Searle (1977) and by Searle and Zinn (1978) to account for the chemical properties of the globular clusters, and also for the 'second parameter effect' (see below).

It is now generally accepted that at least a few of the globular clusters in the Galactic halo differ in age from others by several Gyr (VandenBerg, Bolte, and Stetson 1990; Sarajedini and Demarque 1990; Demarque, Deliyannis, and Sarajedini 1991; Da Costa, Armandroff, and Norris 1992). A brief summary of some recent age determinations has been given by Larson (1990a), and ages for larger samples of clusters have been given by Sarajedini and King (1989), Carney, Storm, and Jones (1992), and Chaboyer, Sarajedini, and Demarque (1992). The total spread in age indicated by these data is of the order of 5 Gyr, or about one-third of the Hubble time. There is a correlation between age and metallicity in the expected sense that the more metal-rich clusters tend to be younger, and there is also a suggestion that the inner Galactic halo experienced a more rapid rise in metallicity than the outer halo; however, these correlations are dominated

by a scatter that is at least as large as the trend, and is of the order of several Gyr at all metallicities.

An important result that is now seen for the first time in direct age determinations is that the age dispersion increases and the mean cluster age decreases with increasing distance from the Galactic center (Chaboyer *et al.* 1992). These trends had earlier been inferred from studies of the horizontal branch structure of globular clusters, which depends on metallicity and on a second parameter that is probably age (Rood and Iben 1968; Searle and Zinn 1978). If the second parameter is indeed age, as is supported by the recent work of Lee, Demarque, and Zinn (1988, 1990), it can be inferred that the clusters in the inner Galactic halo are all relatively old, while the clusters in the outer halo scatter increasingly toward younger ages with increasing Galactocentric distance. According to Lee (1992a,b), the typical age decreases from about 15 Gyr for clusters within 8 kpc of the Galactic center to only about 10 Gyr for clusters more than 24 kpc from the center. There is also evidence from the properties of the RR Lyrae stars in the Galactic bulge that the radial variation of the second parameter continues all the way into the central bulge, implying that the bulge contains stars that are about 1 Gyr older than even the oldest halo clusters (Lee 1992a,b).

The fossil record thus suggests that the halo of our Galaxy was built up from the inside out over a period of perhaps 5 Gyr or more. The central bulge appears to be the oldest part of the Galaxy, and it may therefore have served as a nucleus around which the rest of the Galaxy was built up by accretion. The evidence that the bulge contains the oldest Galactic stars does not necessarily conflict with the evidence discussed by Rich in this volume that most of the stars in the bulge are actually younger than the halo, since the continuing accretion of subsystems during the formation of our Galaxy would probably have deposited much new material into the bulge. Together with the evidence mentioned in Section 6 that many galaxies continue to grow by capturing smaller galaxies (see also Larson 1990b), these results make a strong case that typical large galaxies experience a prolonged formation process involving the continuing accumulation of smaller units. The youngest globular clusters in the Galactic halo, which are about 10 Gyr old, may date from the last major accretion event contributing to the formation of our Galaxy. This event may have strongly disturbed the still forming Galactic disk and thus created the 'thick disk', which appears to be a discrete Galactic component whose stars and clusters are all older than about 10 Gyr (Freeman 1991).

The 'thin disk', which contains the bulk of the Galactic disk mass, appears to have formed only after the chaotic phase of halo formation was over. Several indicators of the age of the local disk population all yield ages that are of the order of 10 Gyr or less; for example, the age inferred from the white dwarf luminosity function is between about 7 and 11 Gyr (Wood 1992), while the oldest known open cluster, NGC 6791, has an

age of about 7 to 9 Gyr (Demarque, Green, and Guenther 1992). The thick disk seems to be older than this, as noted above, and the 'disk globular clusters' that appear to belong to the thick disk population (Zinn 1990) have ages similar to those of the halo clusters; for example the best studied such cluster, 47 Tucanae, has an age of about 14 Gyr. However, since these disk globular clusters are strongly concentrated toward the Galactic center, this age may be more representative of the inner part of the disk than of the local region. If the inner disk is in fact older than the local region, both the halo and the disk of our Galaxy may then have been built up from the inside out, the disk forming mostly after the formation of the halo was completed at each radius. Since there is some evidence for chemical continuity between the halo and the disk, the disk may have been formed largely of material left over from, and chemically enriched by, the halo-forming subsystems (Larson 1991).

Current theoretical ideas about galaxy formation thus appear to receive strong support from the fossil record for our Galaxy. Not only is there evidence that the Galactic halo was formed from subsystems, but there is evidence that our Galaxy was built up from the inside out by the accretion of material from progressively greater distances. Thus, some additional support is given to the idea that the Hubble sequence can be understood as originating from the formation of galaxies from varying numbers and sizes of subunits.

8. Summary

The morphological characteristics of galaxies depend partly on the way in which they were formed, and partly on their subsequent evolution. Basic structural properties such as the disk-to-bulge ratio are determined mainly by the formation process, while more superficial features such as the gas content and the spiral arm characteristics depend on the internal dynamics and the evolutionary history of galaxies. It was suggested in Section 2 that these 'evolutionary' characteristics are themselves determined mainly by the galactic mass distribution through basic dynamical timescales such as the rotation period. Environmental effects can also influence the structures of galaxies by adding or removing material, and they may be difficult to separate from formation processes. Nevertheless, it is clear that the galactic mass distribution and the disk-to-bulge ratio are fundamental properties whose variation along the Hubble sequence must be explained by any understanding of galaxy formation processes.

Early attempts to model the formation of galaxies assuming homogeneous initial conditions concluded that the disk-to-bulge ratio is determined mainly by the star formation rate in the initial collapsing protogalaxy. It is now recognized, however, that the structure of the universe is inhomogeneous and hierarchical on a wide range of scales,

and it seems likely that it was initially inhomogeneous on subgalactic scales as well. Interactions and mergers among subunits must then have played an important role in the formation of most large galaxies, as suggested by Toomre (1977). Of particular importance for the origin of the Hubble sequence is the fact that the early merging of smaller systems into larger ones is expected to have occurred most frequently in the densest parts of the universe; if the products of the mergers are bulge-dominated galaxies, dense regions should then contain a relatively high proportion of such galaxies, as is in fact observed. Various environmental effects might also act to drive the morphology of galaxies toward earlier types in denser environments. Thus, the basic morphological properties of galaxies and their correlation with the environment might be accounted for at least qualitatively if inhomogeneities play an important role in their formation and if continuing interactions influence their subsequent evolution.

However, a fully quantitative understanding of the Hubble sequence is not yet in hand, since the structure of a galaxy formed by the merging of subunits will depend in detail on the nature of the subunits: if they consist mainly of stars, the result will be an elliptical galaxy or an early-type spiral, while if they are mainly gaseous, the resulting galaxy may have a dominant disk. It is therefore necessary to understand better the processes of star formation in protogalaxies, but star formation is still treated in a simple *ad hoc* manner even in the most detailed models. It is also important to treat carefully the physics of the gas, since some of the protogalactic gas may be heated by collisions and may thus form a hot diffuse medium that cannot directly participate in star formation. The feedback effects of star formation can also be important in heating the residual gas and thus inhibiting or delaying further star formation (Cole 1991; Navarro and Benz 1991; White and Frenk 1991). Since the thermal behavior of the gas depends strongly on its density, these effects might enhance the effective dependence of the protogalactic star formation rate on the gas density, for example by introducing a critical star formation rate such that the gas is efficiently heated and dispersed and further star formation is suppressed if this rate is exceeded (Larson 1974). If the result is that denser and more massive subsystems convert more of their gas into stars, as seems likely, then the size and density of the substructures from which a galaxy is formed may be the main factors determining the Hubble type of the galaxy.

In any case, it would appear that at least some of the processes responsible for the origin of the Hubble sequence have been identified, and we can look forward to further progress in understanding this subject as the various models and hypotheses that have been described are further refined and tested by comparison with the many relevant observations.

References

Barnes, J. E., 1988. *Astrophys. J.*, **331**, 699.

Barnes, J. E., 1989. *Nature*, **338**, 123.

Barnes, J., 1990. In *Dynamics and Interactions of Galaxies*, ed. R. Wielen, p. 186. Springer-Verlag, Berlin.

Bender, R., 1990. In *Dynamics and Interactions of Galaxies*, ed. R. Wielen, p. 232. Springer-Verlag, Berlin.

Binggeli, B., 1987. In *Nearly Normal Galaxies: From the Planck Time to the Present*, ed. S. M. Faber, p. 195. Springer-Verlag, New York.

Binney, J., 1990. In *Dynamics and Interactions of Galaxies*, ed. R. Wielen, p. 328. Springer-Verlag, Berlin.

Burkert, A., and Hensler, G., 1988. *Astron. Astrophys.*, **199**, 131.

Carlberg, R. G., 1985. In *The Milky Way Galaxy*, IAU Symposium No. 106, eds. H. van Woerden, R. J. Allen, and W. B. Burton, p. 615. Reidel, Dordrecht.

Carlberg, R. G., 1987. In *Nearly Normal Galaxies: From the Planck Time to the Present*, ed. S. M. Faber, p. 129. Springer-Verlag, New York.

Carlberg, R. G., 1988. *Astrophys. J.*, **332**, 26.

Carlberg, R. G., and Couchman, H. M. P., 1989. *Astrophys. J.*, **340**, 47.

Carlberg, R. G., and Freedman, W. L., 1985. *Astrophys. J.*, **298**, 486.

Carney, B. W., Storm, J., and Jones, R. V., 1992. *Astrophys. J.*, **386**, 663.

Chaboyer, B., Sarajedini, A., and Demarque, P., 1992. *Astrophys. J.*, **394**, in press.

Cole, S., 1991. *Astrophys. J.*, **367**, 45.

Da Costa, G. S., 1992. In *The Stellar Populations of Galaxies*, IAU Symposium No. 149, eds. B. Barbuy and A. Renzini, in press. Kluwer, Dordrecht.

Da Costa, G. S., Armandroff, T. E., and Norris, J. E., 1992. *Astron. J.*, **104**, in press.

Demarque, P., Deliyannis, C. P., and Sarajedini, A., 1991. In *Observational Tests of Cosmological Inflation*, eds. T. Shanks, A. J. Banday, R. S. Ellis, C. S. Frenk, and A. W. Wolfendale, p. 111. Kluwer, Dordrecht.

Demarque, P., Green, E. M., and Guenther, D. B., 1992. *Astron. J.*, **103**, 151.

de Vaucouleurs, G., 1977. In *The Evolution of Galaxies and Stellar Populations*, eds. B. M. Tinsley and R. B. Larson, p. 43. Yale University Observatory, New Haven.

Donas, J., Deharveng, J. M., Laget, M., Milliard, B., and Huguenin, D., 1987. *Astron. Astrophys.*, **180**, 12.

Dressler, A., 1980. *Astrophys. J.*, **236**, 351.

Dressler, A., 1984. *Ann. Rev. Astron. Astrophys.*, **22**, 185.

Efstathiou, G., 1990. In *Dynamics and Interactions of Galaxies*, ed. R. Wielen, p. 2. Springer-Verlag, Berlin.

Eggen, O. J., Lynden-Bell, D., and Sandage, A. R., 1962. *Astrophys. J.*, **136**, 748.

Einasto, M., 1991. *Mon. Not. Roy. Astron. Soc.*, **252**, 261.

Elmegreen, B. G., 1990a. In *The Evolution of the Interstellar Medium*, ed. L. Blitz, p. 247. Astronomical Society of the Pacific, San Francisco.

Elmegreen, B. G., 1990b. *Astrophys. J.*, **357**, 125.

Evrard, A. E, Summers, F. J., and Davis, M., 1992. *Nature*, in press.

Faber, S. M., and Jackson, R. E., 1976. *Astrophys. J.*, **204**, 668.

Freeman, K. C., 1990. In *Dynamics and Interactions of Galaxies*, ed. R. Wielen, p. 36. Springer-Verlag, Berlin.

Freeman, K. C., 1991. In *Dynamics of Disc Galaxies,* ed. B. Sundelius, p. 15. Department of Astronomy and Astrophysics, Göteborgs University, Göteborg.
Frenk, C. S., White, S. D. M., Efstathiou, G., and Davis. M., 1985. *Nature,* **317**, 595.
Frenk, C. S., White, S. D. M., Davis, M., and Efstathiou, G., 1988. *Astrophys. J.,* **327**, 507.
Giovanelli, R., and Haynes, M. P., 1991. *Ann. Rev. Astron. Astrophys.,* **29**, 499.
Gott, J. R., 1977. *Ann. Rev. Astron. Astrophys.,* **15**, 235.
Gott, J. R., and Thuan, T. X., 1976. *Astrophys. J.,* **204**, 649.
Gunn, J. E., 1977. *Astrophys. J.,* **218**, 592.
Gunn, J. E., 1982. In *Astrophysical Cosmology,* eds. H. A. Brück, G. V. Coyne, and M. S. Longair, p. 233. Specola Vaticana, Rome.
Gunn, J. E., 1987. In *The Galaxy,* eds. G. Gilmore and B. Carswell, p. 413. Reidel, Dordrecht.
Guzzo, L., Iovino, A., Chincarini, G., Giovanelli, R., and Haynes, M. P., 1991. *Astrophys. J.,* **382**, L5.
Haynes, M. P., 1987. In *Nearly Normal Galaxies: From the Planck Time to the Present,* ed. S. M. Faber, p. 220. Springer-Verlag, New York.
Hernquist, L., and Quinn, P. J., 1989. *Astrophys. J.,* **342**, 1.
Hubble, E., 1936. *The Realm of the Nebulae.* Yale University Press, New Haven.
Kamphuis, J., and Briggs, F., 1992. *Astron. Astrophys.,* **253**, 335.
Katz, N., 1991. *Astrophys. J.,* **368**, 325.
Katz, N., 1992. *Astrophys. J.,* **391**, in press.
Katz, N., and Gunn, J. E., 1991. *Astrophys. J.,* **377**, 365.
Kenney, J. D. P., 1990. In *The Interstellar Medium in Galaxies,* eds. H. A. Thronson and J. M. Shull, p. 151. Kluwer, Dordrecht.
Kennicutt, R. C., 1989. *Astrophys. J.,* **344**, 685.
Kormendy, J., 1990. In *Dynamics and Interactions of Galaxies,* ed. R. Wielen, p. 499. Springer-Verlag, Berlin.
Kormendy, J., and Djorgovski, S., 1989. *Ann. Rev. Astron. Astrophys.,* **27**, 235.
Lake, G., and Carlberg, R. G., 1988a. *Astron. J.,* **96**, 1581.
Lake, G., and Carlberg, R. G., 1988b. *Astron. J.,* **96**, 1587.
Larson, R. B., 1972. *Nature,* **236**, 21.
Larson, R. B., 1974. *Mon. Not. Roy. Astron. Soc.,* **169**, 229.
Larson, R. B., 1976a. *Mon. Not. Roy. Astron. Soc.,* **176**, 31.
Larson, R. B., 1976b. In *Galaxies,* Sixth Advanced Course of the Swiss Society of Astronomy and Astrophysics, eds. L. Martinet and M. Mayor, p. 67. Geneva Observatory, Sauverny.
Larson, R. B., 1976c. *Comments Astrophys.,* **6**, 139.
Larson, R. B., 1983. *Highlights Astron.,* **6**, 191.
Larson, R. B., 1987. In *Starbursts and Galaxy Evolution,* eds. T. X. Thuan, T. Montmerle, and J. Tran Thanh Van, p. 467. Editions Frontières, Gif sur Yvette.
Larson, R. B., 1988. In *Galactic and Extragalactic Star Formation,* eds. R. E. Pudritz and M. Fich, p. 459. Kluwer, Dordrecht.
Larson, R. B., 1990a. In *Dynamics and Interactions of Galaxies,* ed. R. Wielen, p. 48. Springer-Verlag, Berlin.
Larson, R. B., 1990b. *Publ. Astron. Soc. Pacific,* **102**, 709.
Larson, R. B., 1991. In *Frontiers of Stellar Evolution,* ed. D. L. Lambert, p. 571. Astronomical Society of the Pacific, San Francisco.

Larson, R. B., 1992. In *Star Formation in Stellar Systems,* eds. G. Tenorio-Tagle, M. Prieto, and F. Sanchez, in press. Cambridge University Press, Cambridge.
Larson, R. B., Tinsley, B. M., and Caldwell, C. N., 1980. *Astrophys. J.,* **237**, 692.
Lee, Y.-W., 1992a. In *The Stellar Populations of Galaxies,* IAU Symposium No. 149, eds. B. Barbuy and A. Renzini, in press. Kluwer, Dordrecht.
Lee, Y.-W., 1992b. In Proceedings of the First Hubble Symposium, Baltimore, 1991. *Publ. Astron. Soc. Pacific,* in press.
Lee, Y.-W., Demarque, P., and Zinn, R., 1988. In *Calibration of Stellar Ages,* ed. A. G. D. Philip, p. 149. L. Davis Press, Schenectady.
Lee, Y.-W., Demarque, P., and Zinn, R., 1990. *Astrophys. J.,* **350**, 155.
Maddox, S. J., Efstathiou, G., Sutherland, W. J., and Loveday, J., 1990. *Mon. Not. Roy. Astron. Soc.,* **242**, 43P.
Meisels, A., and Ostriker, J. P., 1984. *Astron. J.,* **89**, 1451.
Navarro, J. F., and Benz, W., 1991. *Astrophys. J.,* **380**, 320.
Oemler, A., 1974. *Astrophys. J.,* **194**, 1.
Oemler, A., 1992. In *Clusters and Superclusters of Galaxies,* ed. A. Fabian, in press. Kluwer, Dordrecht.
Oort, J. H., 1970. *Astron. Astrophys.,* **7**, 381.
Peebles, P. J. E., 1974. *Astrophys. J.,* **189**, L51.
Peebles, P. J. E., 1980. *The Large-Scale Structure of the Universe.* Princeton University Press, Princeton.
Peebles, P. J. E., Schramm, D. N., Turner, E. L., and Kron, R. G., 1991. *Nature,* **352**, 769.
Postman, M., and Geller, M. J., 1984. *Astrophys. J.,* **281**, 95.
Press, W. H., and Schechter, P., 1974. *Astrophys. J.,* **187**, 425.
Prieur, J.-L., 1990. In *Dynamics and Interactions of Galaxies,* ed. R. Wielen, p. 72. Springer-Verlag, Berlin.
Rood, R., and Iben, I., 1968. *Astrophys. J.,* **154**, 215.
Rubin, V. C., Burstein, D., Ford, W. K., and Thonnard, N., 1985. *Astrophys. J.,* **289**, 81.
Salvador-Solé, E., Sanromà, M., and Jordana, J. J. Rdz., 1989. *Astrophys. J.,* **337**, 636.
Sancisi, R., Broeils, A., Kamphuis, J., and van der Hulst, T., 1990. In *Dynamics and Interactions of Galaxies,* ed. R. Wielen, p. 304. Springer-Verlag, Berlin.
Sandage, A., 1990. *J. Roy. Astron. Soc. Canada,* **84**, 70.
Sarajedini, A., and Demarque, P., 1990. *Astrophys. J.,* **365**, 219.
Sarajedini, A., and King, C. R., 1989. *Astron. J.,* **98**, 1624.
Schmidt, M., 1959. *Astrophys. J.,* **129**, 243.
Schweizer, F., 1990. In *Dynamics and Interactions of Galaxies,* ed. R. Wielen, p. 60. Springer-Verlag, Berlin.
Schweizer, F., and Ford, W. K., 1985. In *New Aspects of Galaxy Photometry,* ed. J.-L. Nieto, p. 145. Springer-Verlag, Berlin.
Searle, L., 1977. In *The Evolution of Galaxies and Stellar Populations,* eds. B. M. Tinsley and R. B. Larson, p. 219. Yale University Observatory, New Haven.
Searle, L., and Zinn, R., 1978. *Astrophys. J.,* **225**, 357.
Toomre, A., 1964. *Astrophys. J.,* **139**, 1217.
Toomre, A., 1977. In *The Evolution of Galaxies and Stellar Populations,* eds. B. M. Tinsley and R. B. Larson, p. 401. Yale University Observatory, New Haven.

Toomre, A., 1981. In *The Structure and Evolution of Normal Galaxies,* eds. S. M. Fall and D. Lynden-Bell, p. 111. Cambridge University Press, Cambridge.
Toomre, A., 1990. In *Dynamics and Interactions of Galaxies,* ed. R. Wielen, p. 292. Springer-Verlag, Berlin.
Tully, R. B., and Fisher, J. R., 1977. *Astron. Astrophys.,* **54**, 661.
Tully, R. B., Mould, J. R., and Aaronson, M., 1982. *Astrophys. J.,* **257**, 527.
van Albada, T. S., 1982. *Mon. Not. Roy. Astron. Soc.,* **201**, 939.
VandenBerg, D. A., Bolte, M., and Stetson, P. B., 1990. *Astron. J.,* **100**, 445.
van den Bergh, S., 1990. *J. Roy. Astron. Soc. Canada,* **84**, 60.
Villumsen, J. V., 1984. *Astrophys. J.,* **284**, 75.
White, S. D. M., and Frenk, C. S., 1991. *Astrophys. J.,* **379**, 52.
Whitmore, B. C., 1984. *Astrophys. J.,* **278**, 61.
Whitmore, B. C., and Gilmore, D. M., 1991. *Astrophys. J.,* **367**, 64.
Wood, M. A., 1992. *Astrophys. J.,* **386**, 539.
Zinn, R., 1990. *J. Roy. Astron. Soc. Canada,* **84**, 89.
Zurek, W. H., Quinn, P. J., and Salmon, J. K., 1988. *Astrophys. J.,* **330**, 519.

DYNAMICS OF GALAXIES: NATURE OR NURTURE?

E. Athanassoula

Observatoire de Marseille, 2 Place Le Verrier,
F-13248 Marseille Cédex 4, France.

Abstract

I briefly list a number of structures often observed in galaxies and discuss their formation and maintenance, distinguishing between those that can be accounted for if the galaxy is considered as an "island universe", and those that are due to environmental influence. A score sheet of the above shows the importance of nurture in the evolution of galaxies.

1 Introduction

Galactic dynamics is too broad a subject to be reviewed in one hour, or in a few pages. I will therefore limit myself to listing a number of structures often observed in galaxies and then, in line with the subject of this conference, ask whether their formation and/or maintenance can be explained dynamically by considering each galaxy as an "island universe", or whether the effects of the environment have to be taken into account. One should distinguish two types of environmental influence: indirect, like the force exerted at a distance by a companion, and direct, when something actually hits the galaxy as in the case of infall.

I will first discuss disc galaxies (Section 2), and consider bridges and tails (2.1), spirals (2.2), bars (2.3), warps (2.4), the problem of disc thickness (2.5), rings in the galactic plane (2.6) and polar rings (2.7). I will then discuss structures in ellipticals (3.1), as well as different possibilities for their formation (3.2).

2 Disc galaxies

2.1 Bridges and tails

After the pioneering work of Toomre and Toomre (1972) and the many other studies that followed it (e.g. Barnes 1988) there is no more doubt that gravitational interactions are sufficient to account for the formation of bridges and tails, such as those observed in M51 (Rots *et al* 1990, Engström and Athanassoula 1992) or the antennae (NGC 4038/39; Arp 1966, Schweizer 1978, Toomre and Toomre 1972, Barnes 1988).

2.2 Spiral structure

More than one way has been proposed to make spirals. Some methods call for an instability of the disc, whereas others rely on external agents. We can briefly enumerate the following:

2.2.1 Modes

These are due either to feedback cycles and amplification at corotation, or to edge effects.

Two amplification schemes have been proposed so far. The WASER (Wave amplification via Stimulated Emission of Radiation; Toomre 1969, Mark 1976) involves an outgoing long trailing wave which stimulates the emission of two short trailing waves at corotation. One of them propagates outwards towards the outer Lindblad resonance while the other propagates inwards and is reflected at a Q barrier into a long trailing wave propagating outwards, which closes the cycle. Unfortunately the amplification thus achieved is very small, and negligible in the case of hot discs.

The second amplification scheme, the SWING (Toomre 1981) draws on the amplification a wave gets when it swings from leading to trailing (Goldreich and Lynden-Bell 1965, Julian and Toomre 1966, Toomre 1981). Thus the cycle involves an outwards traveling and swinging leading

wave, and two trailing waves, one traveling outwards from corotation to the outer Lindblad resonance and the other inwards. This cycle may be closed by a reflection of the inwards traveling trailing wave at a sharp edge or at the center of the galaxy (Bardeen 1975). The SWING amplifier is very powerful and can give important amplification rates. Several modes based on it have been found so far (e.g. Zang 1976, Toomre 1981, Bertin *et al* 1989).

Sharp gradients, edges (Toomre 1981, 1989) or grooves (Sellwood and Kahn 1991) can induce spirals. This is the result of two basic ingredients, the nonaxisymmetric instabilities of isolated thin rings (Maxwell 1856, Papaloizou and Lin 1989, Sellwood and Kahn 1991) and the response of the disc to such instabilities (Julian and Toomre 1966). The clumps produced by the instability rotate at the same angular velocity as the material in the ring and the disc responds to them as it does to giant molecular clouds.

2.2.2 Driving by bars

As can be seen both from observations and from simulations, bars can drive spiral patterns. This may be either at the same pattern speed as the bar (e.g. Sanders and Tubbs 1980, Athanassoula 1980, van Albada 1985), or at a different one (Tagger *et al* 1987, Sygnet *et al* 1988, Sellwood and Sparke 1988). The latter case can be explained if the corotation of the bar is at the same radius as the inner Lindblad resonance of the spiral. In such a case there could be a strong coupling of the two modes and of their beat wave. This, although very localised, is particularly strong because of the resonance overlap.

2.2.3 Tidal spirals

It is by now well established that companions can drive spirals. In the case of direct encounters one gets a two-armed spiral pattern, which, if it has an inner Lindblad resonance, is short lived, not exceeding a life time of the order of 10^9 years (Toomre 1969, 1981). A direct satellite can also drive two-armed spirals, now for much longer times, provided its orbit around the galaxy is appropriate (Goldreich and Tremaine 1979). On the other hand retrograde satellites may drive one armed leading spirals (Kalnajs 1974, Athanassoula 1978, Noguchi and Ishibashi 1986, Thomasson *et al* 1989).

2.2.4 Local responses

An orbiting massive clump in a galactic disc, such as a giant molecular cloud, drives a trailing spiral of mass much larger than its own (Julian and Toomre 1966). Toomre (1990) and Toomre and Kalnajs (1991) discussed this phenomenon in a shearing sheet N-body simulation, where each particle at the same time drives and is being driven, and which shows a kaleidoscope of transient streaky features, reminiscent of the late-type rather ragged spirals often observed in galactic discs.

2.3 Bars

Bars are the results of an instability of the disc, and as such can be fully attributed to nature. Even so, nurture may affect both their growth rates and pattern speeds. It is thus of interest to study the growth of the bar instability in galaxies with companions and the effect of companions on already developed bars.

The passage of a companion may either accelerate or slow down the growth of a bar. If the wave that will give rise to the bar has not had time to grow before the time of closest approach, then the passage will speed up bar formation (Noguchi 1987, Gerin *et al* 1990, Athanassoula 1991). On the other hand if the wave has developed a sizeable amplitude, then it will interact nonlinearly with the driving and the result may be an acceleration or a slowdown of the growth depending on the phases and pattern speeds of the two (Athanassoula 1991).

Another question is whether the angular velocity of the bar increases or decreases after the passage. Gerin *et al* (1990) showed that for large values of the perturbing mass the result depends on the relative phase at pericenter. If the bar is ahead of the companion at pericenter then it will slow down due to the interaction, the opposite being true if it is behind. Sundin and Sundelius (1991) extended this to include low mass perturbers and argued that the sign of the change will depend on the mass of the companion, as well as on the phase. Their figure 3 showed that the bar could slow down even if it is behind the companion, provided the mass of the companion is sufficiently low. Subsequent analysis showed that the perturbation had been introduced too early in the low mass cases, i.e. before the bar had evolved sufficiently (Sundelius priv. comm.). The corrected diagram, however, shows the same effect, but less pronounced (Sundin, Donner and Sundelius, in prep.).

2.4 Warps

Many theories have tried so far to explain the formation of warps. Discrete modes could be a solution if the density in the disc falls to zero unrealistically sharply at its edge (Hunter and Toomre 1969). A more plausible alternative would be that the halo is conveniently flattened (Sparke and Casertano 1988). However a complete analysis, treating in a selfconsistent way not only the disc but also the halo, is not an easy matter.

Continuum modes would Landau damp, and the main question is what the relevant time scale is. If this is short compared to a Hubble time one would need either to generate fresh waves regularly, or increase their lifetimes. A misaligned halo would be very helpful for the latter (Toomre 1983, Dekel and Shlosman 1983). As far as the origin of the warp is concerned there is no lack of possibilities. The disc formation simulations of Katz and Gunn (1991) show clearly that warps could come naturally with disc formation. They can also arise in a disc accreting a satellite, as can be seen in the simulations of Hernquist (1991). If this is the basic origin of warps, and since such events also cause the disc to thicken (cf. section 2.5), there should be a correlation between thick discs and the presence of warps. The existence of such a correlation could be checked with the help of CCD photometry of an appropriate sample of

edge-on disc galaxies. Finally warps could be tidally generated. Against this alternative it should be noted that a number of warped galaxies have no nearby companions. Of course this argument does not hold if the companions were composed solely of dark matter.

An interesting possibility, recently put forward (Binney 1991), is that warps are due to the continuous reorientation of the halo's angular momentum due to continuous cosmic infall. In such a case the outer halo would torque the inner one and the disc, and this could give rise to warps. A more direct contribution to the warp could come from the acquisition of freshly infallen gas. This scenario extends the previous ideas of misalignments between halos and discs from a once-in-a-lifetime case to a continuously evolving halo orientation. Fortunately cosmological numerical simulations (Warren and Salmon 1991, Zurek *et al* 1991) are approaching the point where such effects can be studied and the corresponding scenarios tested. Good recent reviews of the theories mentioned briefly above have been given by Binney (1991, 1992b).

2.5 Disc thickness

Thick discs have been observed in a number of edge-on galaxies (Tsikoudi 1979, 1980, Burstein 1979, van der Kruit and Searle 1981), as well as in our own galaxy (Gilmore and Reid 1983, Yoshii *et al* 1987). The latter is the only place where a thick disc can be studied in sufficient detail to reveal information about its rotation, age and metallicity (cf. Freeman 1991). The formation of this component, which is quite clear in some galaxies but far from ubiquitous, is not easy to understand. Some progress has been made recently when thick discs were ascribed to satellite accretion (Quinn and Goodman 1986, Tòth and Ostriker 1992).

As a satellite sinks in a galaxy it will lose its orbital energy via dynamical friction. Part of this can be converted into random motions of the disc stars. A rise of the radial component of the dispersion would result in higher values of the stability parameter Q (Toomre 1964), while an increase of the vertical component of the dispersion would result in a thicker disc. Thus this scenario can explain the formation of thick discs. Recently Tòth and Ostriker (1992) worried whether the thicknesses and Q values thus obtained could set a limit on the amount of accreted matter. They concluded that our Galaxy cannot have accreted within the last 5 10^9 years more than 4% of its mass within the solar radius. As long as the accreted mass stays within this limit, satellite accretion will give a scale height, Q value and shape of velocity ellipsoid similar to what is observed for old disc stars in the solar neighborhood. However, as they stress, this limit puts the standard cold dark matter model with $\Omega = 1$ in great difficulty since this model would predict an accreted mass of 28% within 5 10^9 years. On the other hand there would be no difficulty if the universe is open.

Given the importance of this estimate for cosmological scenarios, and the approximations necessary in deriving it analytically, Ivanio Puerari and I thought it useful to address this problem numerically, with the help of a tree code, and to compare with the analytical estimates. Although our investigation is still in a preliminary phase some discussion may be timely. It seems to us essential that in such simulations the companion, the halo and the disc of the galaxy

are responsive and their evolution is followed selfconsistently. This is very important for the following reasons: as the companion sinks inwards some of its mass can become unbound and stay with the halo. When it finally reaches the disc its mass will be less than at the beginning, the precise amount depending on how compact the companion was, and on its trajectory in the halo. For this reason all components need to be responsive, and any simulations in which the halo is absent or rigid, or in which the companion is rigid, can give erroneous estimates. Under this proviso one can make realistic estimates about how and how much the companion will heat the disc and compare with analytical estimates and with observations. However, one should be careful before setting strict limits to the amount of accreted mass. Indeed, we find that the amount of thickening depends on a number of factors other than the mass of the victim, like its compactness, its orbit in the halo, the extent, density and radial profile of the halo etc. Thus one would have to "convolve" the results of the simulations with information about the range and distribution of the parameters describing the above factors before being able to set a limit on the amount of accreted mass. In this we join the point of view expressed by Binney (1992a) in a recent discussion. Finally one might have to consider the result of the accretion in the framework of disc formation and evolution, since early accretion might form a thick disc component while the thin disc might form gradually after that.

In the case of barred spirals this infall has a further effect, namely that the bar becomes fatter in the disc plane (cf. Pfenniger 1991). This change in axial ratio, like the thickening of the disc, will depend on a number of parameters, and thus a quantitative discussion will necessitate a large number of simulations. Nevertheless the few simulations we have made so far argue that the existence of a thin well-developed bar in a galaxy can also set some interesting limits.

2.6 Rings in disc galaxies

Rings can often be observed in galactic discs, particularly those of barred galaxies. They can be divided into nuclear ones (around galactic nuclei), inner ones (with a radius roughly equal to the bar semimajor axis length) and outer ones (with a radius roughly 2.2 times larger than that of the inner one, when both are present). Their formation can be explained, at least in barred galaxies, which are the majority of cases, as due to the torque of the bar on the colliding gaseous clouds (Schwarz 1979, 1981), without having to invoke any external influences. However, it is less clear what provides the forcing in the non-barred galaxies and, in certain cases, a satellite could be an alternative (cf. Combes *et al* 1990, for nuclear spirals).

2.7 Polar rings

Several examples of polar rings have been so far observed around the disc of, generally, S0 galaxies. They are external to the disc with a size of the order of twice the disc radius. The plane of the ring makes an angle of roughly 90° with that of the disc, although deviations of up to 25° have been found (Schweizer *et al* 1983, Schechter *et al* 1984, Whitmore 1984). It is hard to envisage how the formation of two discs at nearly right angles can happen in a single collapse

event - thus polar rings must be due to a second event occurring after the formation epoch. One can consider the accretion of a companion galaxy, or mass transfer during encounters (Schweizer *et al* 1983). The formation and evolution of polar rings has been the object of many studies (see Casertano *et al* 1991 and references therein).

3 Elliptical galaxies

3.1 Structure in ellipticals

Fine structure in elliptical galaxies has always been linked with mergers or accretion events. Seitzer and Schweizer (1990) have looked for it in a sample of 74 nearby elliptical and S0 galaxies and have found it in more than half the cases. Schweizer *et al* (1990) introduced a " fine structure parameter", which is a measure of the amount of fine structure present in an elliptical, and found that its values correlate well with the strength of the nuclear H_β absorption line at any given magnitude and anticorrelates with the strengths of the CN and Mg_2 features. Similarly Schweizer and Seitzer (1992) find that the UBV colours become systematically bluer at any given luminosity as the amount of fine structure increases. They interpret these correlations as due to systematic variations in mean age and argue that they provide a rough ranking by date of the last major merger or accretion event.

3.1.1 Shells and ripples

Shells of low surface brightness have been found in many normal, or less normal, ellipticals, and even in a few disc galaxies (Malin and Carter 1980, 1983). Although a couple of suggestions that they are due to galactic winds have been put forward (Fabian *et al* 1980, Williams and Christiansen 1984), the prevalent view is that they can be explained as the results of the infall of a small companion of low velocity dispersion (Schweizer 1980; Quinn 1982, 1984; Dupraz 1984, Dupraz and Combes 1986, 1987; Hernquist and Quinn 1988, 1989), provided the companion has a sufficiently low orbital angular momentum. The shells are density waves or ridges moving outward with time, with a small phase velocity and "Pig-trough" dynamics (Lynden-Bell 1967) provides a useful analog for understanding the process. The interleaving of shells at opposite sides of the nucleus, the facts that the shells are aligned, concentric, and do not completely encircle the galaxy, and the consistency of the shell colours with those of disc stars are all natural consequences of this model.

3.1.2 Dust lanes with peculiar kinematics

Similarly a merger or accretion, now of a gas rich galaxy, seems to be the natural origin for the case of dust lanes which are kinematically decoupled from the stellar component of the elliptical galaxy in which they reside (e.g. Athanassoula and Bosma 1985, Bertola *et al* 1990, de Zeeuw 1990, Bettoni and Galletta 1991; and references therein).

3.1.3 Counter-rotating cores

Several elliptical galaxies are found to have counter-rotating cores, while their photometry shows no corresponding singular features (Franx and Illingworth 1988, Bender 1988, Jedrzejewski and Schechter 1988). Such kinematical behaviour can be understood in terms of a two-component galaxy, consisting of an extended component with a large velocity dispersion and slow rotation and a central counter-rotating component. This could arise if a small galaxy had fallen into the center of a big elliptical, as initially proposed by Kormendy (1984). Numerical simulations (Balcells and Quinn 1990) show that, for the ratio of masses explored, the infalling galaxy survives the tidal field and settles at the center of the remnant and that counter-rotation occurs only when the merging orbits are retrograde.

3.2 Formation

Although not strictly belonging to the topic of formation of structures in galaxies, let me, for the sake of completeness, say a few words about the formation of ellipticals. Two different scenarios have been proposed. On the one hand the dissipational or dissipationless collapse of a proto-galaxy or proto-cloud (van Albada 1982, May and van Albada 1984, Villumsen 1984, Aguilar 1988, Aguilar and Merritt 1990, Londrillo *et al* 1991, Larson 1976, Carlberg 1984, Carlberg *et al* 1986 etc), while on the other the merging of two or more elliptical or disc galaxies (Toomre 1977, White 1978, 1979, 1980, Miller and Smith 1980, Villumsen 1982, 1983, Barnes 1988, 1989, 1990, this volume, etc). Good arguments that at least some of the elliptical galaxies come from mergers come from the statistical arguments by Toomre (1977) and observations of merging systems (Schweizer 1990 and this volume; and references therein). Numerical simulations of both scenarios can, for appropriate initial conditions, give the proper forms (prolate, oblate or traxial) and radial density profiles which are $r^{1/4}$ in good agreement with the observations. The kinematical data of both merger remnants (Okumura *et al* 1991; Barnes, this volume) and collapse simulations (van Albada 1982) are also in good agreement with the observation. A more critical test might have to wait until a sufficiently large number of simulations have been made so that one can see if the global properties of the models exhibited the correlations, or, better, the fundamental plane found in the observations (Djorgovski and Davis 1987, Djorgovski *et al* 1988, Dressler *et al* 1987, Faber *et al* 1987, Lauer 1985). Finally, a mixed origin, i.e. some of the ellipticals coming from collapses and some from mergers, cannot be excluded. It is however clear that at least some of the ellipticals must have formed from mergers, for otherwise what (and where) are the merger remnants?

4 A score sheet

In the above I presented the effects and the relative importance of nature and nurture on the creation of various structures in galaxies. Instead of summarizing what has already been said I will end with a score sheet, showing the two influences. Table 1 lists the structures on the left

and "nature" and "nurture" in the second and third columns. A cross is put in a given column if that is the most likely, at least to my mind, agent for its formation. In some cases, either when both agents are important, or when it is still not clear which one dominates, there are crosses in both columns. Although one could argue that both agents are important, albeit to a different extent, this score sheet shows clearly the importance of the environment and of interactions and that there are many problems for which modeling the galaxies as "island universes" is not acceptable.

Table 1: Score sheet

	Nature	Nurture
DISCS		
Bridges and Tails		+
Spiral structure	+	+
Bars	+	
Warps	+	+
Thick discs		+
Rings	+	
Polar rings		+
ELLIPTICALS		
Shells		+
Kinematically decoupled dust lanes		+
Counter-rotating cores		+

Acknowledgements

I would like to thank Albert Bosma for many stimulating discussions.

References

Aguilar L. A., 1988 *Celest. Mech.*, **41**, 3

Aguilar L.A. and Merritt D.R., 1990 *Astrophys. J.* , **354**, 33

Arp H., 1966, *Atlas of Peculiar Galaxies*, Carnegie Institution of Washington

Athanassoula E., 1978 *Astron. and Astrophys.* , **69**, 395

Athanassoula E., 1980 *Astron. and Astrophys.* , **88**, 184

Athanassoula E., 1991 in *Dynamics of Galaxies and Molecular Cloud Distribution*, eds. F. Combes and F. Casoli, 1991, p. 274, Reidel pub.

Athanassoula E. and Bosma A., 1985 *Ann. Rev. Astron. Astrophys.* **23**, 147

Balcells and Quinn P.J., 1990 *Astrophys. J.* **361**, 381

Bardeen J.M., 1975 in *Dynamics of Stellar Systems*, ed. A. Hayli, p. 297, Reidel pub.

Barnes J.E., 1988 *Astrophys. J.* , **331**, 699

Barnes J.E., 1989 *Nature*, **338**, 123

Barnes J.E., 1990 in *Dynamics and Interactions of Galaxies*, ed. R. Wielen, p. 186, Springer-Verlag

Bender R., 1988 *Astron. and Astrophys.* **202**, L5

Bertin G., Lin C.C., Lowe S.A. and Thurstans R.P., 1989 *Astrophys. J.* **338**, 78 and 104

Bertola F., Bettoni D., Buson L.M. and Zeilinger W.W., 1990 in *Dynamics and Interactions of Galaxies*, ed. R. Wielen, p. 249, Springer Verlag

Bettoni D. and Galletta G., 1991 in *Dynamics of Disc Galaxies*, ed. B. Sundelius, p. 317, Göteborg

Binney J., 1991 in *Dynamics of Disc Galaxies*, ed. B. Sundelius, p. 297, Göteborg

Binney J., 1922a *Nature*, **358**, 104

Binney J., 1922b *Ann. Rev. Astron. Astrophys.* , in press

Burstein D. 1979 *Astrophys. J.* , **234**, 829

Carlberg R.G., 1984 *Astrophys. J.* , **286**, 403

Carlberg R.G., Lake G. and Norman C.A. 1986 *Astrophys. J.* , **300**, L1

Casertano S., Sackett P. and Briggs F. (Eds.), 1991 in *Warped disks and inclined rings around galaxies*, Cambridge University press

Combes F., Dupraz C. and Gerin M., 1990 in *Dynamics and Interactions of Galaxies*, ed. R. Wielen, p. 205, Springer Verlag

Dekel A. and Schlossman I., 1983 in *Internal Kinematics and Dynamics of Galaxies*, ed. E. Athanassoula, p. 187, Reidel pub.

de Zeeuw T. 1990 in *Dynamics and Interactions of Galaxies*, ed. R. Wielen, p. 263, Springer Verlag

Djorgovski S., Davis M., 1987 *Astrophys. J.* , **313**, 59

Djorgovski S., de Carvalho R., Han M.S., 1988 in *The Extragalactic Distance Scale*, ed. S. van den Bergh, C.J. Pritchet, p. 329, Astrom. Soc. of the Pac. Conf. Series

Dressler A., Lynden-Bell D., Burstein D., Davies R.L., Faber S.M., Terlevich R.J., Wegner G., 1987 *Astrophys. J.* , **313**, 42

Dupraz C., 1984 *These*, Universite de Paris VII

Dupraz C., and Combes F., 1986 *Astron. and Astrophys.* , **166**, 53

Dupraz C. and Combes F., 1987 *Astron. and Astrophys.* , **185**, L1

Engström S. and Athanassoula E., 1992 preprint

Faber S.M., Dressler A., Davies R.L., Burstein D., Lynden-Bell D., Terlevich R., Wegner G., 1987 in *Nearly Normal Galaxies*,ed. S.M. Faber, p. 175, Springer Verlag

Fabian A.C., Nulsen P.E.J., Stewart G.C., 1980 *Nature*, **287**, 613

Franx M., and Illingworth G., 1988 *Astrophys. J. Let.* , **327**, L55

Freeman K.C. 1991 in *Dynamics of Disc Galaxies*, ed. B. Sundelius, p. 15, Göteborg

Gerin M.Y., Combes F., Athanassoula E., 1990 *Astron. and Astrophys.* , **230**, 37

Gilmore G. and Reid N., 1983 *Monthly Notices of the Royal Astron. Society* **202**, 1025

Goldreich P. and Lynden-Bell D., 1965 *Monthly Notices of the Royal Astron. Society* **130**, 125

Goldreich P. and Tremaine S., 1979 *Astrophys. J.* **233**, 857

Hernquist L., 1991 in *Warped disks and inclined rings around galaxies*, eds. S. Casertano, P. Sacket, and F. Briggs, p. 96, Cambridge University press

Hernquist L. and Quinn P.J., 1988 *Astrophys. J.* , **331**, 682

Hernquist L. and Quinn P.J., 1989 *Astrophys. J.* , **342**, 1

Hunter C., and Toomre A., 1969 *Astrophys. J.* , **155**, 747

Jedrzejewski R. and Schechter P.L., 1988 *Astrophys. J. Let.* , **330**, L87
Julian W.H. and Toomre A., 1966 *Astrophys. J.* , **146**, 810
Kalnajs A.J., 1974 in *La dynamique des galaxies spirales*, ed. L. Weliachew, p. 103, editions CNRS
Katz N. and Gunn J.E., 1991 *Astrophys. J.* , **377**, 365
Kormendy J., 1984 *Astrophys. J.* , **287**, 577
Larson R.B. 1976 in *Galaxies*, Sixth Advanced Course of the Swiss Society of Astronomy and Astrophysics, eds. L. Martinet and M. Mayor, p. 67, Geneva Observatory; and references therein
Lauer T.R., 1985 *Astrophys. J.* , **292**, 104
Londrillo P., Messina A., Stiavelli M., 1991 *Monthly Notices of the Royal Astron. Society* , **250**, 54
Lynden-Bell D., 1967 *Monthly Notices of the Royal Astron. Society* , **136**, 101
Malin D.F. and Carter D., 1980 *Nature*, **285**, 643
Malin D.F. and Carter D., 1983 *Astrophys. J.* **274**, 534
Mark J. W.-K., 1976 *Astrophys. J.* , **205**, 363
Maxwell J.C., 1856 *Adams Prize Essay: On the stability of the Motion of Saturn's Rings* reprinted in *Scientific Papers of James Clerk Maxwell*, I, 288
May A. and van Albada T.S., 1984 *Monthly Notices of the Royal Astron. Society* , **209**, 15
Miller R.H. and Smith B., 1980 *Astrophys. J.* , **235**, 421
Noguchi M., 1987 *Monthly Notices of the Royal Astron. Society* , **228**, 635
Noguchi M. and Ishibashi S., 1986 *Monthly Notices of the Royal Astron. Society* , **219**, 305
Okumura S.K., Ebisuzaki T. and Makino J., 1991 *Publ. Astr. Soc. Jap.* , **43**, 781
Papaloizou J.C.B. and Lin D.N.C., 1989 *Astrophys. J.* , **344**, 645
Pfenniger D., 1991 in *Dynamics of Disc Galaxies*, ed. B. Sundelius, p. 191, Göteborg
Quinn P.J., 1982 *Ph. D. Thesis*, Australian National University
Quinn P.J., 1984 *Astrophys. J.* , **279**, 596
Quinn P.J. and Goodman J., 1986 *Astrophys. J.* , **309**, 472
Rots A.H., Bosma A., van der Hulst J.M., Athanassoula E., Crane P.C., 1990 *Astron. J.* , **100**, 387
Sanders R.H. and Tubbs A.D., 1980 *Astrophys. J.* , **235**, 803
Schwarz M.P., 1979 *Ph. D. Thesis*, Australian National University
Schwarz M.P., 1981 *Astrophys. J.* , **247**, 77
Schweizer F., 1978 in *Structure and Dynamics of Nearby galaxies*,eds. E. Berkhuijsen and R. Wielebinski, p. 279, Reidel pub.
Schweizer F., 1980 *Astrophys. J.* , **237**, 303
Schweizer F., 1990 in *Dynamics and Interactions of Galaxies*, ed. R. Wielen, p. 60, Springer Verlag
Schweizer F., Seitzer P., Faber S.M., Burstein D., Dalle Ore C.M. Gonzalez J.J., 1990 *Astrophys. J. Let.* , **364**, L33
Schweizer F. and Seitzer P., 1992 *Astron. J.* , in print
Schweizer F., Whitmore B.C. and Rubin V.C., 1983 *Astron. J.* , **88**, 909
Schechter P.L., Ulrich M.H., Boksenberg A., 1984 *Astrophys. J.* , **277**, 526
Schechter P.L., Sancisi R. van Woerden H. Lynds C.R., 1984 *Monthly Notices of the Royal Astron.*

Society , **208**, 111

Seitzer P. and Schweizer F., 1990 in *Dynamics and Interactions of Galaxies*, ed. R. Wielen, p. 270, Springer Verlag

Sellwood J.A. and Kahn F.D., 1991 *Monthly Notices of the Royal Astron. Society* , **250**, 278

Sellwood J.A. and Sparke L.S., 1988 *Monthly Notices of the Royal Astron. Society* , **231**, 25p

Sparke L.S. and Casertano S., 1988 *Monthly Notices of the Royal Astron. Society* , **234**, 873

Sundin M. and Sundelius B., 1991 *Astron. and Astrophys.* , **245**, L5

Sygnet J.F, Tagger M., Athanassoula E. and Pelat R., 1988 *Monthly Notices of the Royal Astron. Society* , **232**, 733

Tagger M., Sygnet J.F, Athanassoula E. and Pelat R., 1987 *Astrophys. J.* , **318**, L43

Thomasson M, Donner K.J., Sundelius B., Byrd G.G., Huang T.Y. Valtonen M.J., 1989 *Astron. and Astrophys.* , **211**, 25

Toomre A., 1964 *Astrophys. J.* , **139**, 1217

Toomre A., 1969 *Astrophys. J.* , **158**, 899

Toomre A., 1977 in *The Evolution of Galaxies and Stellar Populations*,eds. B.M. Tinsley and R.B. Larson, p. 401, Yale Univ. Obs.

Toomre A., 1981 in *The Structure and Evolution of Normal Galaxies*, eds. S.M. Fall and D. Lynden-Bell, p. 111, Cambridge University press

Toomre A., 1983 in *Internal Kinematics and Dynamics of Galaxies*, ed. E. Athanassoula, p. 177, Reidel pub.

Toomre A., 1989 in *Dynamics of Astrophysical discs*, ed. J.A. Sellwood, p. 153, Cambridge University press

Toomre A., 1990 in *Dynamics and Interactions of Galaxies*, ed. R. Wielen, p. 292, Springer Verlag

Toomre A. and Kalnajs A.J., 1991 in *Dynamics of Disc Galaxies*, ed. B. Sundelius, p. 341, Göteborg

Toomre A. and Toomre J., 1972 *Astrophys. J.* , **178**, 623

Tòth G. and Ostriker J.P., 1992 *Astrophys. J.* , **389**, 5

Tsikoudi V., 1979 *Astrophys. J.* , **234**, 842

Tsikoudi V., 1980 *Astrophys. J. Suppl.* , **43**, 365

van Albada G.D., 1985 *Astron. and Astrophys.* , **142**, 491

van Albada T.S., 1982 *Monthly Notices of the Royal Astron. Society* , **201**, 939

van der Kruit P.C. and Searle L., 1981 *Astron. and Astrophys.* , **95**, 105 and 116

Villumsen J.V., 1982 *Monthly Notices of the Royal Astron. Society* , **199**, 493

Villumsen J.V., 1983 *Monthly Notices of the Royal Astron. Society* , **204**, 219

Villumsen J.V., 1984 *Astrophys. J.* , **284**, 75

Warren M.S. and Salmon J.K., 1991 *Bulletin of the American Astron. Soc.* , **23**, 1345

White S.D.M., 1978 *Monthly Notices of the Royal Astron. Society* , **184**, 185

White S.D.M., 1979 *Monthly Notices of the Royal Astron. Society* , **189**, 831

White S.D.M., 1980 *Monthly Notices of the Royal Astron. Society* , **191**, 1P

Whitmore B.C., 1984 *Astron. J.* , **89**, 618

Williams R.E. and Christiansen W.A., 1985 *Astrophys. J.* , **291**, 80
Yoshii Y., Ishida K., Stobie R.S,. 1987 *Astron. J.* , **93**, 323
Zang T.A., 1976 *Ph. D. Thesis, MIT*
Zurek W.H., Warren M.S., Quinn P.J. and Salmon J.K., 1991 *Bulletin of the American Astron. Soc.* , **23**, 1345

DYNAMICS OF GALAXIES AND EVOLUTION ALONG THE HUBBLE SEQUENCE

Daniel Pfenniger
Geneva Observatory
CH-1290 Sauverny
Switzerland

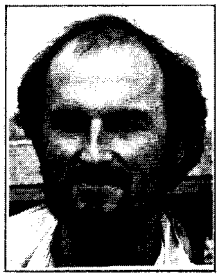

ABSTRACT

Dynamical studies such as N-body simulations, and energetics considerations show that disc galaxies have many occasions to undergo a change of Hubble type during 10^{10} y. Internal processes such as gravitational instabilities are sufficiently fast for creating and destroying a bar (SA $\leftrightarrow$ SB), for increasing the bulge-to-disc ratio (Sd $\rightarrow$ Sa), or for significantly changing the amount of gas, within time-scales smaller ($\simeq 10^9$ y) than the galaxy ages. These internal changes are triggered and accelerated by the dissipative components of the ISM and by star formation. Mergers and satellite encounters also contribute to speed up internal evolution. Consequently, the constraints of a secular evolution have to be taken into account in galaxy formation scenarios.

An important conclusion concerning the nature of dark matter is that if disc galaxies do evolve along the Hubble sequence in the sense Sd $\rightarrow$ Sa, then the observed decreasing M/L ratio suggests that most of the galactic dark matter must be in some form of primordial gas, in order to form stars later on.

1. ENERGETICS OF DISC GALAXIES

Paraphrasing Schweizer (this conference), most ($\approx 50-84\%$) of the stars in the Universe have never participated in a merger event. Therefore the understanding of the galaxy evolution driven only by internal processes is crucial.

At the simplest level of description, the global *equilibrium* of a physical system is described by a balance of *interacting energies* (virial theorem). The equilibrium of a galaxy is determined basically by gravitational energy and star kinetic energy, just because these energies *interact* and are much larger than the ISM energies. The amount of nuclear energy ($\lesssim 0.01\rho c^2$) is considerable but is generally locked; however, when released by star formation, it can disturb macroscopically the dynamical equilibrium (cf. superbubbles, HI holes), notably via massive stars. So while the ISM is a negligible component for determining the equilibrium, it is a decisive one for allowing nuclear energy to be released via star formation, and thus, for driving secular evolution.

At the simplest level of description, the *evolution* rate of a physical system close to equilibrium is characterised by the energy exchange rates, i.e. *powers*. The most significant energy output of a normal galaxy is in the form of visible and infrared light. Traditionally the nuclear energy output from stars has not been considered to be consequential for evolution, since galaxies were thought to be transparent. However recent works[1-3] have found that disc galaxies are instead semi-transparent. Roughly, half of the visible, and most of the UV photons are absorbed, which is consistent with the large far-infrared flux of normal spirals[4] which comes presumably from starlight thermalised in the ISM after various absorption processes. The ISM also absorbs the mechanical power of massive stars and supernovae. So the question is what is the typical mechanical power that a galaxy can deliver or absorb by large scale dynamical processes? If a self-gravitating system is near virial equilibrium ($GM = V^2R$), the gravitational power is of the order of the gravitational energy divided by the dynamical time, which gives a relation dependent only on the virial velocity V,

$$L_{\rm grav} = \left(GM^2/R\right) / \left(1/\sqrt{GM/R^3}\right) = V^5/G. \qquad (1)$$

For our Galaxy, with $V = 230\,{\rm km\,s^{-1}}$, $L_{\rm grav} \approx 10^{44}\,{\rm erg\,s^{-1}}$, which is coincidentally comparable to its luminosity. Kennicutt[5] and others (e.g. [6]) have convincingly argued that star formation in discs can be regulated by large scale gravitational instabilities. If luminosity is proportional to the amount of stars, which is proportional to the mechanical and thermal powers absorbed by the ISM, and this energy output is constantly regulated by gravitation, we can expect that a steady regime is attained when nuclear power ($L_\star$) is in balance with the gravitational power,

$$L_\star \sim L_{\rm grav} = V^5/G. \qquad (2)$$

Of course this order of magnitude relation ignores the light contribution of a not self-regulated component such as a bulge. Yet relation (2) is fairly close to the infrared Tully-Fisher relation for bulgeless (Scd-Sd) disc galaxies ($L_H \sim V^{4.9\pm0.3}$) [7-8] (Fig. 1)†.

† A constant M/L population in virial equilibrium has a luminosity-velocity-radius relation of the form $L \approx (M/L)^{-1}V^2R^1/G$ which seems to be the first order origin of the "fundamental plane" of ellipticals ($L \sim V^{2.12}R^{0.96}$ [9], and $L \sim V^{1.70}R^{0.73}$ [10]). Therefore it is not astonishing that the Tully-Fisher relation for galaxies with a superposition of a self-regulated disc and an older spheroidal population has exponents between 2 and 5 for V, and 0 and 1 for R.

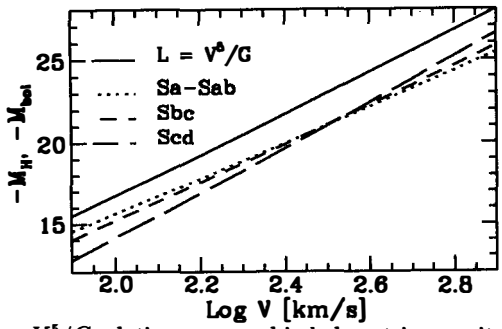

Fig. 1: The $L = V^5/G$ relation expressed in bolometric magnitude, and the infrared Tully-Fisher relation[7] for the uniform Hubble flow and different galaxy types, with the Hubble constant $H_0 = 80\,\mathrm{km\,s^{-1}\,Mpc^{-1}}$. The match in the zero-point would be better with $H_0 = 50\,\mathrm{km\,s^{-1}\,Mpc^{-1}}$.

As a consequence, it seems likely that the fundamental parameters of galaxies are determined principally by their "microscopic" physics, i.e. star and ISM physics, and weakly by the initial conditions in an early turbulent gas‡.

2. DISC FORMATION

From the virial theorem, we know that galaxies had to dissipate at least their present kinetic energy ($\approx \frac{1}{2}(200\,\mathrm{km\,s^{-1}})^2 = 2 \cdot 10^{14}\,\mathrm{erg\,g^{-1}} = 200\,\mathrm{eV/H}$) to reach their bound state. Dissipation is also a fundamental aspect for disc formation, since circular orbits are energy minima at constant specific angular momentum.

In a typical gaseous gravitational collapse where the pressure is not neglected, the free-fall time ($\tau_{\mathrm{ff}} = (G\rho_0)^{-1/2}$) characterises only the collapse time of the central region with density ρ_0. Rapidly, pressure *gradients* develop, and delay the infall of the outer parts for much longer than τ_{ff}. For a multiple of τ_{ff} a forming disc has turbulent, disorganised boundary conditions. Yet discs do form, as shown beautifully in numerical experiments (e.g. Evrard, this conference). Such studies show that irregular discs organise themselves in more *symmetric* shapes in a few rotational periods. Therefore, Im, Sm and Sd galaxies are dynamically young, i.e., they had to or will look different a few 10^8 y in the past or in the future. Yet self-gravitating discs with too much rotational energy are gravitationally unstable, therefore energy dissipation well conserving angular momentum leads inevitably to internal instabilities, in other words, to evolution.

If the amplitude of these instabilities saturates at a scale much smaller than a considered disc radius, an axisymmetric model with free boundary conditions is still reasonable. The extremisation of the total energy of a self-gravitating system purely supported by rotation and not constrained by boundary conditions restricts the allowed potentials Φ to the ones with *constant* rotation curve[11]:

$$E_{\mathrm{tot}} = 2\pi \int dz \int R\,dR \left(\tfrac{1}{2}\rho v_{\mathrm{circ}}^2 + \tfrac{1}{2}\rho\Phi\right), \quad \text{where} \quad \rho = \frac{\Delta\Phi}{4\pi G}, \quad v_{\mathrm{circ}}^2 = R\frac{\partial\Phi}{\partial R} \qquad (3)$$

then E_{tot} is a functional $E_{\mathrm{tot}}[\Phi]$ of the potential Φ only. Using the variational calculus,

‡ In analogy with stars, it would seem unwise to try to relate the fundamental parameters of stars to the initial fluctuation spectrum of molecular clouds!

$$\delta E_{\rm tot}[\Phi] = 0 \quad \Longrightarrow \quad \frac{\partial}{\partial R}\left(R\frac{\partial \Phi}{\partial R}\right) = 0 \quad \Longrightarrow \quad v_{\rm circ} = \text{const.} \tag{4}$$

Therefore, for continuous and at least twice differentiable Φ's, constant rotation curves extremise the total energy and can be viewed as a general property of self-gravitating discs, not necessarily restricted to galaxies¶.

However, finite sized instabilities can be comparable to some finite radii, therefore axisymmetry can be a poor approximation near the centre. Many N-body works have shown that typically large scale instabilities in a collisionless disc produce a rapidly rotating bar, within a time-scale of the order of 10^8 y. Stellar bars are stable over at least 10^{10} y [13] and represent a natural feature of disc galaxies. Other non-axisymmetric instabilities such as spiral arms typically fade away in less than 10^9 y. The stability of bars is explained by the existence of stable elongated orbits having shapes similar to the mass distribution. Bars have to rotate fast and can not be too eccentric[14–15].

In summary, the combination of dissipation and dynamical constraints leads naturally to view disc galaxies as having an evolution time-scale shorter than their age. On the long run dissipation triggers disc instabilities which, when small, tend to give a constant rotation curves, and which, when large, produce a bar in the inner stellar parts. The transformation from SA to SB galaxies is easy. In any case, the disc Hubble sequence can already be ordered according to the rotation velocity, the more rapidly rotating galaxies ($\approx 350\,\mathrm{km\,s^{-1}}$) having dissipated about 12 times more energy per nucleon than the slowly rotating ones ($\approx 100\,\mathrm{km\,s^{-1}}$). This difference could be ascribed to an age difference if the dissipative processes were roughly constant.

3. EFFECT OF A STELLAR BAR ON THE GAS AND THE DISC

From numerous works (e.g. [16–20]) the flow of gas inside a stellar bar is known to be constrained to move along the stable periodic orbits. Inside a strong bar a smooth flow is impossible because the periodic orbits self-intersect. Shocks develop, increase dissipation, which leads to three eventualities: 1) gas accretes toward the centre, 2) gas is expelled outside corotation, and 3) gas is transformed into stars. In the three cases, the bar region becomes depleted in gas after a time-scale that can hardly exceed 10^9 y.

Therefore the interaction of gas with a bar changes the star and gas mass ratio in a relatively short time-scale, a few rotational periods. Barred galaxies can be arranged in a time-sequence, even if the quantitative chronology depends strongly on the ISM physics, and is still approximate. For instance a gas rich bar in a SB galaxy with widely open bi-symmetric spiral arms is dynamically younger than a pure stellar bar not surrounded by spiral arms. The general trend suggested by hydrodynamics is that barred galaxies evolve in the sense SBd to SBa.

Bars are such major density perturbations of discs that the decomposition of a galaxy into disc, bulge and bar components has no *physical* meaning[21]. Indeed within a bar no circular orbits exist, angular momentum of particles is exchanged at a rate comparable to the orbital period[22], and the third dimension has to be taken into account, particularly when the distance from the centre is comparable to the galaxy thickness.

¶ The massive molecular disc around Cepheus A rotates at a nearly constant velocity of $1\,\mathrm{km\,s^{-1}}$ at a scale of the order of $0.2 - 0.4\,\mathrm{pc}$ [12].

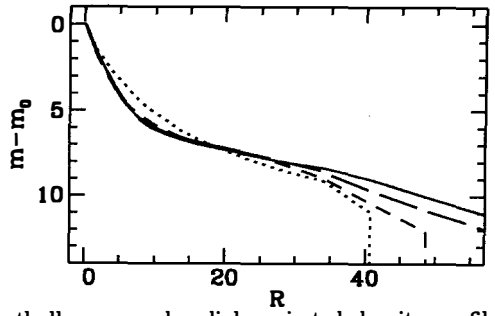

Fig. 2: Azimuthally averaged radial projected density profiles in magnitude of a disc N-body simulation. The initial model (dot), a truncated Miyamoto disc, is not particularly exponential, yet after 10 (short dash), 20 (long dash), and 40 (solid) rotational periods during which a bar instability has developed, the outer disc progressively tends from the inner to the outer parts toward an exponential profile, while the inner bar region ($R \lesssim 8$) takes rapidly a steeper, bulge-like profile.

An effect that was already clear in early 2D N-body simulations of stellar discs, pointed out by Hohl[23], yet mostly ignored later on but confirmed by more accurate 3D N-body simulations[13,22], is that the mixing of stellar orbits in a barred potential, a kind of mild relaxation, is sufficiently strong to redistribute the stars into both an outer exponential disc and an inner "bulge-bar" component with a steeper profile than the disc after a few rotational periods (Fig. 2). This orbit mixing tends to uniformise the colour of an old bar. If our Galaxy has a bar (e.g. [24]), we should expect it to generate a population of stars on chaotic orbits, similar to the "thick disc", that would diffuse back and forth from the inner bulge to radii larger than the Sun's orbit.

Another typical effect of a bar is that vertical instabilities, due to resonances exciting motion transversally to the galactic plane, are sufficiently strong to lift stellar orbits within the bar up to $1-2$ kpc from the plane, particularly if the central density profile is steep[25–26]. Since the centre is the bottom of the galactic potential where dissipating matter accumulates, a density spike easily develops there, and these vertical resonances are ineluctable. This leads to the proposition that bulges can be formed well *after* the formation of a disc, so bluish and metal rich bulges can naturally occur in this scenario (cf. Rich, this conference). Related to these vertical instabilities, a 2/1 resonance can trigger a global bending instability of the bar region which forms a box- or peanut-shaped bar-bulge[13,22,27–29] (Fig. 3).

All these processes have typical time-scales shorter than $\approx 10^9$ y. Therefore bars are important factors of galaxy secular evolution[30]. But the question remains: if stellar bars form easily and are robust, why aren't all disc galaxies already barred?

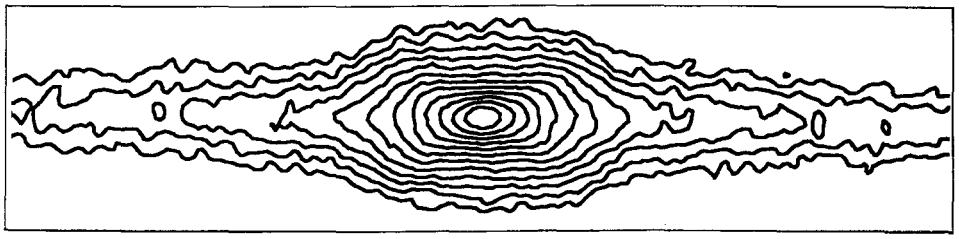

Fig. 3: A peanut-shaped bar-bulge seen edge-on in a 3D N-body disc simulation[22]. The isodensity contours are spaced by 0.5 mag.

4. EFFECT OF ACCRETION ON A BAR AND ON A STELLAR DISC

Since dissipation is a fundamental aspect of galaxy evolution, and that bars exchange angular momentum rapidly, the next logical step for understanding secular evolution is to examine the effect of accretion in the central region of a barred galaxy.

For a given dissipation rate, resonances amplify the effect of dissipation such as the accretion rate, or the "action" loss[26]. As a central mass concentration grows, the orbits supporting the bar are modified principally within the "inner Lindblad resonance" (ILR) region, where the stable orbits are perpendicular to the bar (Fig. 4). The distance at which an ILR exists is a rapidly increasing function of the central mass. At some point the ILR diameter is comparable with the original bar minor axis, and the bar must be destroyed[31]. Estimation with N-body runs show that only 1-3% of the galaxy mass accreted at the centre is sufficient to dissolve the bar[32]. The actual accretion mechanism is irrelevant, any central mass concentration increases the ILR radius. Gas accretion[33], but also the merging of small galaxy satellites[34] leads to the rapid dissolution of bars. Gas accretion within the ILR can lead to the formation of a secondary bar there, allowing angular momentum to be extracted and gas to accrete even deeper toward the centre (Martinet & Friedli, this conference). As a bar always develops strong resonances, a bar encourages its own destruction. The typical bar destruction time-scales are again short, $10^8 - 10^9$ y.

The final shape of a dissolved N-body bar is a hot, slightly triaxial and rotating spheroid. The overall aspect remarkably resembles early type galaxies having a hot central bulge with a steep density profile, surrounded by an exponential disc. In this respect M31 seems a good candidate to have dissolved a bar recently.

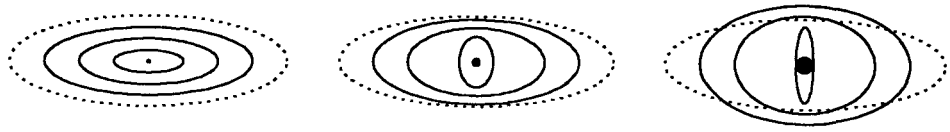

Fig. 4: Schematic evolution of stable periodic orbits (solid ellipses) in a bar model, outlined by a dotted ellipse, as a central mass concentration grows from left to right. The orbits in the right-hand side bar are not compatible with the mass distribution.

Fig. 5: Resulting edge-on views of an N-body disc heated for $4 \cdot 10^9$ y by ten satellites (point masses) of each 0.1% (left) and 1% (right) of the total mass. The initial velocity of the satellites is a pressure supported uniform distribution within a 60 kpc wide sphere. The smaller bulge on the left is entirely due to a bar and is nearly identical to the one resulting from an unperturbed simulation, while this bulge-bar is destroyed on the right because the satellites have all accumulated near the centre.

So accretion destroys bars easily, and bulges with dimensions comparable with the original bar result. However, bulges such as the one of M104, the Sombrero, are too big to be produced in this way. If ellipticals can result from violent mergers, intermediate sized mergers should produce big bulges. In a set of N-body simulations where 10 small satellites of the Magellanic class or smaller were perturbing a galactic disc on pressure supported orbits, we found that the threshold of accreted mass producing Sombrero type bulges lies between 1% and 10% of the galaxy mass. Therefore, discs can not absorb much mass at later times without heating stars considerably (see also [35]). Less mass in satellites does not form smaller bulges, but heats the whole discs more slowly.

5. DISC HUBBLE SEQUENCE EVOLUTION AND CONCLUSIONS

Several aspects of the properties of the disc Hubble sequence can be arranged in a causal evolutionary sequence. The virial theorem and the existence of dissipation already tell us that slowly rotating and less concentrated galaxies are energetically less evolved than rapidly rotating and dense ones. By loosing energy, self-gravitating systems must increase their rotation speed, and by loosing furthermore angular momentum, they must increase their central density. Thus the sense of evolution is from Sd's to Sa's.

Dynamics tells us that irregular and asymmetric galaxies have to change their morphology in less than 10^9 y, and that also only of the order of 10^9 y is required for taking an approximate disc shape and for winding up spiral arms. Galaxies appear today no longer as rigid and perennial objects, but as live and rapidly changing ones. Secularly bulges, including peanut-shaped bulges, can grow by internal processes such as bar and other instabilities, so galaxies with large bulges, more symmetric discs, and more wound up spiral arms are older than bulgeless, irregular, and widely open spiral arm galaxies. Again the sense of evolution is from Sd's to Sa's.

Star formation is also an irreversible process which secularly accumulates heavy elements and consumes gas, decreasing the M/L ratio. The star formation rates of many Sc's is too large to be sustained for more than 10^9 y, implying also an important modification of the galaxy type in the sense from Sd's to Sa's[36].

Erratically the evolution of a galaxy can be perturbed by merger events. Typically a satellite such as the LMC can easily excite a bar instability in a marginally stable disc[37]. The accretion of a satellite in the central region can also destroy a bar. Finally, several Magellanic sized mergers can heat discs to a larger scale than bars and produce the big bulges of some Sa, or S0 galaxies.

An important corollary of any evolution along the Hubble sequence from Sd's to Sa's that will have to be examined in the future, is that since the M/L ratio of the stellar regions of Sb-S0 galaxies can be explained essentially by known baryonic matter (cf. Freeman, this conference), the secular transformation of an Sd galaxy into an Sa one implies, unless an ad hoc mass segregation occurs, that dark matter in Sd's and in the outer parts of disc galaxies dominated by dark matter must be in some form of primordial gas, susceptible to be transformed into stars later on. The same conclusion could be drawn from the disc-halo conspiracy, where dark matter begins to predominate rotation curves precisely at the edge of the stellar disc, and the dark matter-gas ratio remains then constant[38]. Also, the systematic large gas mass in colliding galaxies (Combes, this conference), as if hidden gas were "revealed" by collisions, hints toward the existence of invisible matter in some form of primordial gas in quiescent galaxies. If the stellar mass in a disc increases with time, consistent with a steady star formation rate

during many 10^9 y, stars must be made from dark matter since the *estimated* amount of gas is insufficient by a factor of about 10, and the amount of gas accreted at later epoch must be a minor quantity for preserving the disc shapes[35].

In other words, the dark matter problem in galaxies could be simply solved if the mass estimate of the gas concomitant with HI in the outer discs, from which stars will eventually form, would be systematically too small by a factor $8 - 10$.

References

1. Disney, M.J., Davies, J., Phillips, S.: 1989, *M.N.R.A.S.* **239**, 939
2. Valentijn, E.A.: 1990, *Nature* **346**, 153
3. Peletier, R.F., Willner, S.P.: 1992, *A.J.* in press (June)
4. Takashi, I., Feigelson, E.D.: 1992, *Ap.J.Sup.* **79**, 197
5. Kennicutt, R.C.: 1989, *Ap.J.* **344**, 685
6. Quirk, W.J.: 1972, *Ap.J.* **176**, L9
7. Aaronson, M., Mould, J.: 1983, *Ap.J.* **265**, 1
8. Djorgovski, S., De Carvalho, R., Han, M.-S.: 1988, in *The Extragalactic Distance Scale*, eds. van den Bergh, S., Prichtet C.J., A.S.P. Conf. Ser. **4**, 329
9. Djorgovski, S., Davis, M.: 1987, *Ap.J.* **313**, 59
10. Dressler, A., Lynden-Bell, D., Burstein, D., Davies, et al.: 1987, *Ap.J.* **313**, 42
11. Pfenniger, D.: 1989, *Ap.J.* **343**, 142
12. Torrelles, J.M., Ho, P.T.P., Rodríguez, L.F., Cantó, J.: 1986, *Ap.J.* **305**, 721
13. Combes, F., Debbasch, F., Friedli, D., Pfenniger, D.: 1990, *A.A.* **233**, 82
14. Contopoulos, G., Papayannopoulos, Th.D.: 1980, *A.A.* **92**, 33
15. Athanassoula, E., Bienaymé, O., Martinet, L., Pfenniger, D.: 1983, *A.A.* **127**, 349
16. Roberts, W.W., Huntley, J.M., van Albada, G.D.: 1979, *Ap.J.* **233**, 67
17. Sanders, R.H., Tubbs, A.D.: 1980, *Ap.J.* **235**, 803
18. Schwarz, M.P.: 1981, *Ap.J.* **247**, 77
19. Athanassoula, E.: 1991, in *Dynamics of Disc Galaxies*, ed. B. Sundelius, Göteborg, 149
20. Friedli, D., Benz, W.: 1992, *A.A.* in press
21. Dubath, P., Jarvis, B.J., Martinet, L., Pfenniger, D.: 1991, in *Morphological and Physical Classification of Galaxies*, eds. Busarello, Capaccioli, Longo, (Kluwer: Dordrecht), 461
22. Pfenniger, D., Friedli, D.: 1991, *A.A.* **252**, 75
23. Hohl, F.: 1971, *Ap.J.* **168**, 343
24. Weinberg, M.D.: 1991, *Ap.J.* **384**, 81
25. Pfenniger, D.: 1984, *A.A.* **134**, 373, and 1985, *A.A.* **150**, 112
26. Pfenniger, D., Norman, C.: 1990, *Ap.J.* **363**, 391
27. Combes, F., Sanders, R.H.: 1981, *A.A.* **96**, 164
28. Friedli, D., Pfenniger, D.: 1990, in *Bulges of Galaxies*, ESO Conference and Workshop Proceedings No. 35, eds. B.J. Jarvis, D.M. Terndrup, 265
29. Raha, N., Sellwood, J.A., James, R.A., Kahn, F.D.: 1991, *Nature* **352**, 411
30. Kormendy, J.: 1979, *Ap.J.* **217**, 409
31. Hasan, H., Norman, C.: 1990, *Ap.J.* **361**, 69
32. Friedli, D., Pfenniger, D.: 1991, in *Dynamics of Galaxies and Molecular Clouds Distribution*, IAU Symp. No 146, eds. Casoli F., Combes, F., Dordrecht: Kluwer, 362
33. Friedli, D., Martinet, L.: 1992, *A.A.* in preparation
34. Pfenniger, D.: 1991, in *Dynamics of Disc Galaxies*, ed. B. Sundelius, Göteborg, 191
35. Toth, G., Ostriker, J.P.: 1992, preprint
36. Kennicutt, R.C.: 1990, in *Evolution of the Universe of Galaxies*, ed. R.G. Kron, A.S.P. Conf. Ser., **10**, 141
37. Noguchi, M.: 1987, *M.N.R.A.S.* **228**, 635
38. Bosma, A.: 1981, *A.J.* **86**, 1791, and 1825

BARS WITHIN BARS AND SECULAR EVOLUTION IN DISC GALAXIES

Daniel Friedli & Louis Martinet
Geneva Observatory
CH-1290 Sauverny, Switzerland

Presented by Louis Martinet

Abstract. Observations of some spiral or lenticular barred galaxies show either a misaligned secondary bar or triaxial bulge inside their primary bar. Some cases cannot be explained in terms of projection effects on two perpendicular bars. No favoured angle between the two stellar bars is found, suggesting time-dependent systems rotating with two different pattern speeds, whereas offsets between a stellar bar and a gaseous bar can be explained with identical pattern speeds under particular conditions. Bars within bars produced by self-consistent 3D N-body simulations with gas and stars are presented here and the necessary, very specific, conditions for them to be formed are given. In particular, the major role of dissipation is emphasised. The systems of embedded bars are stable over a few turns of the primary bar, and can transport amounts of gas to the galactic center. In an evolutionary sequence, the primary bar formation is followed by the secondary bar one, then by the dissolution of both bars induced by a broad and strong ILR. Disc galaxies can be viewed as time-dependent systems, where secular evolution due to dissipative effects is strongly transforming their morphology and their kinematics on less than a Hubble time.

1. OBSERVATIONAL EVIDENCES OF BARS WITHIN BARS

Observed morphologies in some SB galaxies suggest that "secondary" nuclear bars within "primary" bars could be more common than we think. We here establish a non-exhaustive list of objects displaying such a structure.

(a) Galaxies with mini-bar within the main bar. The prototype could be NGC 1291 (classified as SBa), already mentioned by de Vaucouleurs (1974). A bar within a bar with a mis-alignment of the major axis of 30° is clearly visible. Another one is the SBa galaxy NGC 1326 (de Vaucouleurs 1974). The SBb galaxy NGC 1433, mentioned by Sandage & Brucato (1979) and Buta (1984), has a small central lens internal to the main bar and inclined at 70° to it, and crossed by a small bar. NGC 1543 (SB0) has a very bright, well defined inner bar of 20" diameter tilted at about 70° to the main diffuse bar of 2' diameter (Sandage & Brucato 1979). Isophotes shown by Jarvis et al. (1988) effectively seem to suggest the existence of a secondary bar in this SB galaxy. Two prototypes of this class are presented in Fig. 1 which show isophotes extracted from CCD IR images in the Cousins I-band which have recently been obtained (January 1992) by P. Bratschi at the 70 cm Swiss Telescope at La Silla.

(b) Barred galaxies with an inner triaxial bulge. The prototype could be NGC 3945 (SB0) discussed by Kormendy (1979), which shows a spheroid distorted into a secondary bar of major strength. Other objects as NGC 2859, NGC 4340, NGC 4371, NGC 4754 and NGC 7743 are indicated as similar to NGC 3945 by the same author. Louis & Gerhard (1988) have outlined significant and various mis-alignments between the major axis of the bar and the inner flattened bulge in five galaxies: NGC 936, NGC 5020, NGC 5566, NGC 5905 and NGC 7479. These observations suggest that barred galaxies are genuinely time-dependent dynamical systems.

(c) Barred galaxies with an inner molecular bar. Kenney (1991) and Kenney et al. (1991) reported high resolution CO observations in the center of more or less strongly barred galaxies. These observations reveal the frequent presence of molecular bars. Typical objects are NGC 3351 (strong bar), NGC 3505 and 6951 (intermediate strength of bar), and M101 (weakly barred). A summary of some observed properties of such galaxies is given by Devereux et al. (1992).

(d) Galaxies with a nuclear ring eventually crossed by a secondary bar. The prototype could be NGC 3081, classified as a S0:r galaxy, but considered to be a weakly barred, early type ring galaxy by Buta (1990). A high resolution map (Fig. 6 of the Buta's paper) shows that a nuclear bar lies in the center. In projection, it is misaligned with

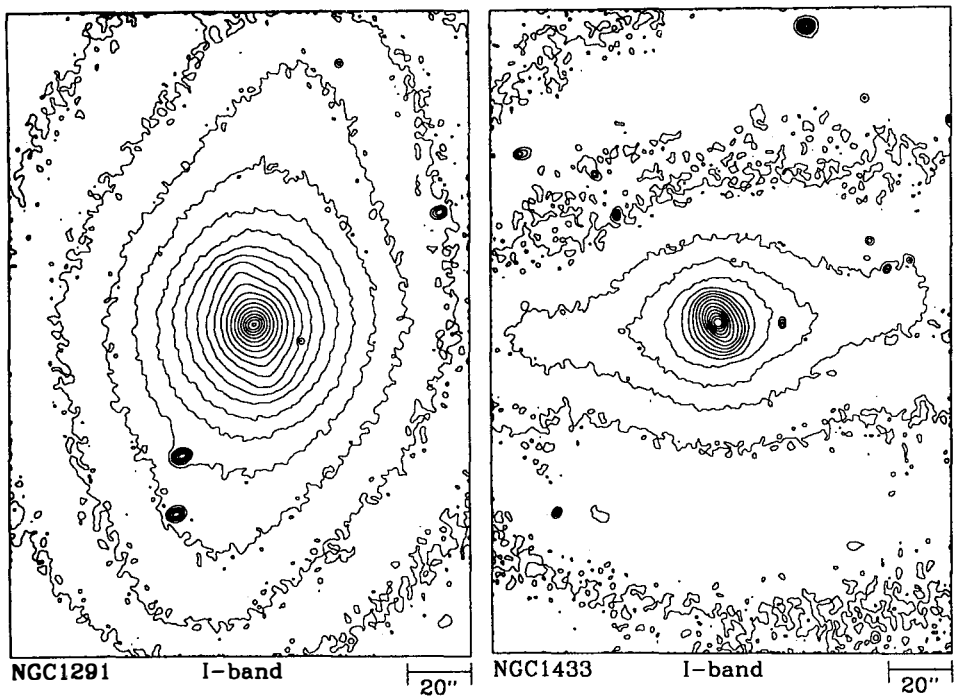

Fig. 1. Illustrative isophotes in I-band of two nearly face-on double-barred galaxy prototypes. The observed disc axis ratio is indicated in brackets. **Left** NGC 1291 (0.83). **Right** NGC 1433 (0.91).

the main bar by 50°. This case could be compared with NGC 1433 (see (a)) with respect to the strength of the primary bar. Secular dissolution of the primary bar, emphasised by Pfenniger & Norman (1990) and Friedli & Pfenniger (1991), could be occurring in NGC 3081. NGC 7702, also classified S0:r or $S0^+$, has bulge isophotes revealing the presence of a small oval in the 4" inner radius, which could indicate a nuclear bar of 1 kpc diameter (Buta 1991). A list of galaxies with nuclear rings, which could be similar either to NGC 3081 or to NGC 7702 has been given by Buta (1984). Candidates are: NGC 2781, NGC 2962, NGC 2997, NGC 3358, NGC 4429, NGC 4535, NGC 4553, NGC 5236, NGC 5248, NGC 5728, NGC 5850 and NGC 6753.

(e) Our Galaxy. Our Galaxy could be added to the list of candidates having two misaligned bars. Weinberg (1991) recently explored the disc structure by using AGB star tracers identified in the IRAS point source catalogue, and presented evidence of a strong stellar bar with a semi-major axis of about 5 kpc and a position angle of $-36° \pm 10°$ as seen from the Sun – Galactic center line. A non-axisymmetric component

at small radius (< 1 kpc) is not ruled out. The inner triaxial component inferred from Binney et al. (1991) and Blitz & Spergel (1992) seems to be dynamically distinct from the IRAS bar mentioned above, also suggesting for our Galaxy a double-bar feature.

The diversity of angles observed between major axis of primary and secondary bar cannot always be interpreted in terms of projection effects on two perpendicular bars. A series of simulations has shown that for example an angle of 30° between the two bars needs inclinations of more than 60°. As the inclination of NGC 1291, for instance, is of the order of 30°, the two bars cannot be perpendicular in this case. As the isophotes of Fig. 1 do not present any distortions or irregularities, it seems unlikely that the bars within bars phenomenon has to be related with galaxy interactions.

2. THEORETICAL ASPECTS

Global non-axisymmetric perturbations of galaxies (like bars) play a key role in collecting gas into the central regions, and they can be very efficient in transporting large amounts of angular momentum outwards (Combes 1988 and references therein). A detailed analysis of bar-driven fueling of galactic nuclei has been recently developed with the help of 3D N-body simulations of gas and stars by Friedli et al. (1991) and Friedli & Benz (1992). Moreover, bars within bars have been suggested by Shlosman et al. (1989, 1990) as a way to transport gas from the host galaxy (scale $\sim$ 10 kpc) to the nucleus (scale $\sim$ 10 pc). We below elaborate on different possibilities of bars within bars systems.

2.1 Systems with two stellar bars

We denote Ω_p as the primary bar pattern speed and Ω_s as the secondary bar pattern speed, and we define $\alpha = \Omega_s/\Omega_p$. Two main possibilities of systems in which one bar is embedded in another may be invoked:

(a) The two bars have the same pattern speed ($\alpha = 1$). The general case of two bars forming an arbitrary angle is not viable since the primary bar exerts a gravitational torque on the secondary bar and vice-versa and they will rapidly align. The case of two aligned bars will not concern us here as it corresponds simply to the case of one bar with a new density distribution. The particular case of two bars forming an angle of 90° is more interesting, but one expects that both bars survive only if the ILR is not too extended, and the mass of the secondary bar is small in comparison with that of the primary one.

(b) The two bars have different pattern speeds ($\alpha \neq 1$). The bases of theoretical

work concerning this case have been given by Louis & Gerhard (1988), who outlined that some galaxies may be in periodically time-dependent dynamical states, and as an example they spoke about the possibility that bar and triaxial bulge components of barred galaxies can rotate through each other. This is supported by observations of misaligned double barred systems. Some orbit computations of dissipative particles in double-barred potentials have also been done by Pfenniger & Norman (1990). Two bars with different pattern speeds such that $\alpha > 1$ seem to be an adequate system able to explain observations of misaligned stellar bars. Complete solid rotation seems unlikely and density fluctuations are especially expected near the secondary bar corotation (CR). It is important to emphasise that Sellwood & Sparke (1988) observed in their N-body simulations that the spiral arms and the bar have not the same pattern speed.

2.2 Systems with a stellar bar and a gaseous bar

Let us distinguish the two following cases:

(a) No ILR is present. In this case, the bar pattern speed is high and the gas will be trapped by the x_1 orbit family. As in the strong bar case, this family develops loops at a certain distance from the center, and the gas will only populate orbits close to the center. The small offsets between gaseous and stellar bars, noticed by Combes & Gerin (1985) and Barnes & Hernquist (1991), seem to be mainly a consequence of the viscous nature of the gas.

(b) An ILR is present. In this case, the gas can be trapped by the x_1 and the x_2 orbit families. If the x_1 develops loops, they start from regions approximately where the x_2 has disappeared. Some experiments by Sanders & Tubbs (1980) and Combes & Gerin (1985) revealed the possible mis-alignment of the gaseous and stellar bars provided that one has the CR far beyond the bar end and an ILR is present. They found that as the pattern speed is progressively decreased, the offset between the two bars increases to finally reach about 90°, with the gaseous bar leading the stellar one. However, if the mass of the secondary bar and the offset angle become important, the gravitational torque from both bars is significant and one can expect that the alignment of two bars will be a more favourable state. Moreover, large offsets need a CR far outside the bar. This seems unrealistic in the case of disc galaxies with rapidly rotating bars. Thus, it also appears necessary to invoke a system of two bars with different pattern speeds to explain large offsets between a gaseous bar and a stellar bar in a disc galaxy.

3. NUMERICAL SIMULATIONS

We tried to better understand the processes described in the previous section with the help of our self-consistent 3D simulations of galaxies, modeled as a mixture of a purely collisionless component (stars) and a dissipative one (gas). The complete code description is given in Pfenniger & Friedli (1991, 1992) for the gravitational part (Particle-Mesh method) and in Friedli & Benz (1992) for the hydrodynamical part (Smooth Particle Hydrodynamics technique).

Let us then consider the evolution of the angular momentum per unit mass as well as the variation of the derivative of this quantity, which corresponds to the angular momentum transfer rate per unit mass from the gas to the stars (Fig. 2a). A first loss of angular momentum in the gaseous component occurs with the quick formation of the primary bar in few dynamical time-scales. Later on a second loss occurs. It suggests the formation of a secondary bar structure in the inner region. This fact is confirmed by the aspect of "isophotes" presented in Fig. 3 together with the velocity field of the gaseous component. Persistence time scale of such a structure is of the order of a few 100 Myr. Figure 2b shows the evolution of the central gas mass concentration inside various radii, as well as the corresponding gas accretion rate. In parallel with angular momentum loss, an increase of gas in the center can be observed, first inside 1.0 kpc and then also inside 0.2 kpc. This confirms that bars are able to compress gas inside themselves to about one tenth of their scale length. The system of embedded bars can transport amounts of gas much closer to the galactic center, and such an accretion rate could be related to fueling of some starburst mechanism and/or active galactic nuclei as already suggested by Shlosman et al. (1989). Note that the minima of the transfer rate curve coincide with the maxima of the accretion rate curve.

Dissolution of the double-barred system into a weakly non-axisymmetric one occurs in less than one turn of the primary bar (about 100 Myr). The primary bar becomes a kind of lens and the secondary one a triaxial bulge. The galaxy looks like an SAB or an S with a triaxial bulge. Almost all the gas initially inside the primary bar region is now confined to the galaxy nucleus, inducing a broad ILR responsible for this morphological evolution. The latter needs a significant enough gaseous component (equal to about 10% of the total (gas plus stars) galaxy mass, or about 2% inside 1 kpc). If the mass of the gas is too small, it is insufficient to give rise to the decoupling between the central and the outer parts of the primary bar. If there is too much gas mass, the fueling is so significant that the primary bar will evaporate before the secondary bar can form. If a

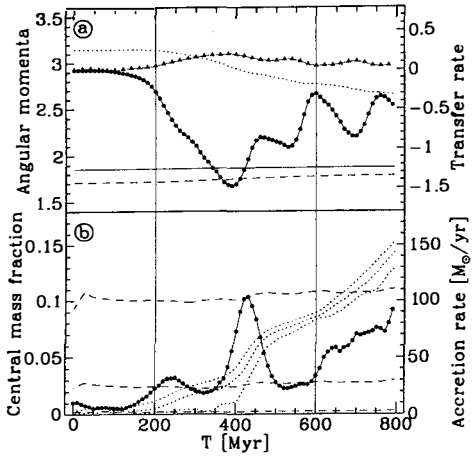

Figs. 2a and b. Time evolution: **a)** The angular momentum per unit mass for the gas (dotted), the stars (dashed), and the total (full). The derivatives of the gas curve (full circles) and of the star curve (full triangles) are superimposed. **b)** Central gas mass concentration inside 0.2, 0.5, and 1.0 kpc for the gas (dotted) and the stars (dashed). The derivative of the gas curve inside 1.0 kpc is superimposed (full circles). Vertical lines indicate approximately the appearance of the two bars.

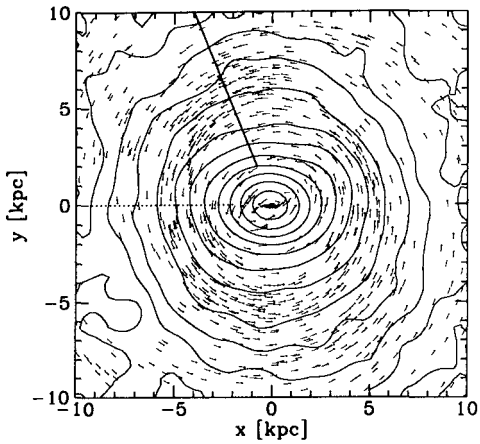

Fig. 3. Face-on view of the projected isodensity contour lines of the stellar component as well as the velocity field of the gaseous component at $t = 800$ Myr. Two misaligned bars can be observed. The approximate direction of bar major axis is indicated for the primary (full line) and the secondary (dotted line) bar. The angle between the two bars is about 70°. The high central gas concentration can also be observed.

secondary bar does form, its lifetime will be at best very short.

The decoupling between the central and the outer parts of the primary bar seems to require the formation of a primary bar ILR during time evolution, and consequently the presence of the anti-bar x_2 orbit family. The ongoing filling of these orbits by gaseous particles will trigger the decoupling mechanism. On the contrary, if a strong ILR is present from the beginning, the first bar cannot form, and if no ILR appears at all, the x_2 family does not exist and the decoupling is far less probable or does not happen.

4. CONCLUSIONS

Observations of bars within bars in a number of lenticular or spiral galaxies as well as connected theoretical aspects have been reviewed. No preferred angle between the two bars is found, and some cases cannot be explained in terms of projection effects on two perpendicular bars. Our simulations show that the appearance of misaligned bars within bars from an initially axisymmetric potential depends on the following points: 1) The stellar disc must obviously be bar unstable. As the two bars do not form simultaneously, a primary large bar has to be present to allow the secondary small bar to appear. 2)

A dissipative component has to be present so that material can accumulate onto the central part of the x_1 orbit family. 3) The mass of this component must be significant enough to give rise to the decoupling between the central and the outer parts of the primary bar; this decoupling can also be favoured by the torque of strong spiral arms. 4) The appearance of a primary bar ILR during time evolution allows for the presence of the x_2 orbit family, which is essential for triggering the decoupling.

The system of two bars is placed on an evolutionary sequence between a former phase of the primary bar formation and a latter phase of the two bar dissolution. The final central galaxy shape is similar to triaxial observed bulges, suggesting that some of them can be relics of destroyed bars. Disc galaxies can be viewed as time-dependent systems where secular evolution alters their morphology and kinematics on less than a Hubble time. Galaxies can thus change their Hubble type during their lifetimes.

References

Barnes, J., Hernquist, L., 1991, ApJ 370, L65
Binney, J., Gerhard, O.E., Stark, A.A., Bally, J., Uchida, K.I., 1991, MNRAS 252, 210
Blitz, L., Spergel, D.N., 1992, preprint
Buta, R., 1984, Ph. D. Thesis, University of Texas, Publication in Astronomy No. 23
Buta, R., 1990, ApJ 351, 62
Combes, F., 1988, in: Galactic and Extragalactic Star Formation, NATO ASI Series C No. 232, eds. R.E. Pudritz, M. Fich. Kluwer, Dordrecht, p. 475
Combes, F., Gerin, M., 1985, A&A 150, 327
de Vaucouleurs, G., 1974, in: Formation of Galaxies, IAU Symposium No. 58, ed. J.R. Shakeshaft. Reidel, Dordrecht, p. 335
Devereux, N.A., Kenney, J.D.P., Young, J.S., 1992, AJ 103, 784
Friedli, D., Pfenniger, D., 1991, in: Dynamics of Galaxies and their Molecular Cloud Distributions, IAU Symposium No. 146, eds. F. Combes, F. Casoli. Reidel, Dordrecht, p. 362
Friedli, D., Benz, W., Martinet, L., 1991, in: Dynamics of Disc Galaxies, Proceedings of Varberg Conference, ed. B. Sundelius. Göteborg, Sweden, p. 181
Friedli, D., Benz, W., 1992, A&A, (in preparation)
Jarvis, B., Dubath, P., Martinet, L., Bacon, R., 1988, A&AS 74, 513
Kenney J.D.P., 1991, in: Dynamics of Galaxies and their Molecular Cloud Distributions, IAU Symposium No. 146, eds. F. Combes, F. Casoli. Reidel, Dordrecht, p. 265
Kenney J.D.P., Scoville, N.Z., Wilson, C.D., 1991, ApJ 366, 432
Kormendy, J., 1979, ApJ 227, 714
Louis, P.D., Gerhard, O., 1988, MNRAS 233, 337
Pfenniger, D., Norman, C., 1990, ApJ 363, 391
Pfenniger, D., Friedli, D., 1991, A&A 252, 75
Pfenniger, D., Friedli, D., 1992, A&A, (submitted)
Sandage, A., Brucato, R., 1979, AJ 84, 472
Sanders, R.H., Tubbs, A.D., 1980, ApJ 235, 803
Sellwood, J., Sparke, L.S., 1988, MNRAS 231, 25p
Shlosman, I., Frank, J., Begelmann, M.C., 1989, Nature 338, 45
Shlosman, I., Begelmann, M.C., Frank, J., 1990, Nature 345, 679
Weinberg, M.D., 1991, ApJ 384, 81

AUTHORS INDEX

LIST OF PARTICIPANTS

AMRAM, P.	Observatoire de Marseille, France
ARSENAULT, R.	CFHT, Kamuela, USA
ATHANASSOULA, E.	Observatoire de Marseille, France
AURIERE, M.	Observatoire du Pic-du-Midi, France
BALKOWSKI, C.	Observatoire de Meudon, France
BARNES, J.E.	University of Hawaii, Honolulu, USA
BORNE, K.D.	STScI, Baltimore, USA
BUTA, R.	University of Alabama, Tuccaloosa, USA
COLLIN-SOUFFRIN, S.	Observatoire de Meudon, France
COMBES, F.	Observatoire de Meudon, France
COOPER, S.	Max Planck Institut für Physik, München, Germany
CRANE, P.	ESO, Garching, Germany
DAVIDSEN, A.F.	Johns Hopkins University, Baltimore, USA
DEEG, H.-J.	University of New Mexico, Albuquerque, USA
EDER, J.A.	Arecibo Observatory, Puerto Rico, USA
EVRARD, A.E.	University of Michigan, Ann Arbor, USA
FELENBOK, P.	Observatoire de Meudon, France
FERGUSON, H.C.	The Observatories, Cambridge, UK
FREEMAN, K.C.	Mt Stromlo Observatory, Weston Creek, Australia
FRITZE-v.ALVENSLEBEN, U.	Universitäts Sternwarte, Göttingen, Germany
GAVAZZI, G.	Osservatorio di Brera, Milan, Italy
GODLOWSKI, W.	Jagiellonian University, Krakow, Poland
HELD, H.	Osservatorio Astronomico, Bologne, Italy
HELLSTEN, U.	Niels Bohr Institute, Copenhagen, Denmark
JABLONKA, P.	Observatoire de Meudon, France
LARSON, R.B.	Yale Astronomy Department, New Haven, USA
LEITHERER, C.	STScI, Baltimore, USA
MADORE, B.F.	IPAC Caltech, Pasadena, USA
MAMON, G.A.	Observatoire de Meudon, France
MANRIQUE, A.	Facultad de Fisica di Barcelona, Spain
MARQUEZ, I.	Instituto de Astrofisica de Andalucia, Spain
MARTINET, L.	Observatoire de Genève, Sauverny, Switzerland
MOSCA, L.	CEN Saclay, Gif-sur-Yvette, France

PFENNIGER, D.	Observatoire de Genève, Sauverny, Switzerland
PIETSCH, W.	Max Planck Institut für Physik, Garching, Germany
RICH, R.M.	Columbia Astrophysics Laboratory, New York, USA
ROY, J.-R.	Université Laval, Québec, Canada
SALVADOR-SOLE, E.	Facultad de Fisica di Barcelona, Spain
SANCISI, R.	Kapteyn Laboratory, Groningen, Netherlands
SARAZIN, C.L.	University of Virginia, Charlottesville, USA
SCHWEIZER, F.	Carnegie Institution of Washington, USA
SOMMER-LARSEN, J.	Niels Bohr Institute, Copenhagen, Denmark
THUAN, T.X.	University of Virginia, Charlottesville, USA
VAN DRIEL, W.	University of Amsterdam, Netherlands
VERDES-MONTENEGRO, L	Instituto de Astrofisica de Andalucia, Spain
VIGROUX, L.	CEN Saclay, Gif-sur-Yvette, France
WHITMORE, B.C.	STScI, Baltimore, USA
YAHIL, A.	Observatoire de Meudon, France and Columbia University, New York, USA